

ERRATA

- p 110 line 2: "indicator" for "indictor"
- p 110 line 23: "[For" for "[for"
- p 110 line 24: "alkyl" for "Alkyl"
- p 114 line 9: "indicator" for "indictor"
- p 131 line 21: "our of" for "with through"
- p 141 line 12: "transporting" for "transport"
- p 141 line 13: "do" for "does"
- p 145 line 19: add "Mechanism of internal sizing by alkyl ketene dimers (AKD): The role of the spreading monolayer precursor and autophobicity." after "(2000)"
- p 148 line 16: "equipment" for "equipments"
- p 154 line 10: "because" for "because that"
- p 157 line 16: "rise" for "raise"
- p 175 last line: "to be" for "be"
- p 178 line 21: "permits" for "will permits"
- p 198 line 24: "one" for "on e"
- p 218 line 16: "countries" for "counties"



Low-Cost Microfluidic Diagnostics Based on Paper and Thread

**Thesis in the fulfillment of the requirement for the degree of
Doctor of Philosophy in Chemical Engineering**

by

Xu Li

Master of Science

**Department of Chemical Engineering
Faculty of Engineering
MONASH UNIVERSITY**

August 2011

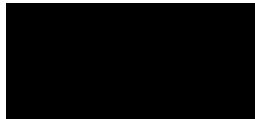
Dedicated to my parents and husband

Copyright Notice

Under the Copyright Act 1968, this thesis must be used only under the normal conditions of scholarly fair dealing. In particular no results or conclusions should be extracted from it, nor should it be copied or closely paraphrased in whole or in part without the written consent of the author. Proper written acknowledgement should be made for any assistance obtained from this thesis.

I certify that I have made all reasonable efforts to secure copyright permissions for third-party content included in this thesis and have not knowingly added copyright content to my work without the owner's permission.

Signed:



This page is intentionally blank

TABLE OF CONTENTS

	Page
Title Page	i
Table of Contents	iii
Summary	ix
General Declaration	xi
Acknowledgments	xiii
List of Publications, Patents and Awards	xv
List of Figures	xxii
List of Tables	xxx
List of Abbreviations	xxxix
List of Nomenclature	xxxiii

Chapter 1 Introduction and Literature Review

1.1 Introduction	2
1.2 Microfluidics	4
1.2.1 Overview of microfluidics	4
1.2.2 Requirements and challenges of diagnostics in the developing world	6
1.2.3 Microfluidic technologies for diagnostics in the developing world	8
1.3 Paper-Based Microfluidics	11
1.3.1 Paper as an analytical substrate	11
1.3.2 Surface modification of paper to control liquid and paper interaction	12
1.3.2.1 Paper sizing mechanisms	14
1.3.2.2 Plasma treatment	17
1.3.2.3 Ink jet printing	19
1.3.3 Development of paper-based microfluidics	21
1.3.3.1 Fabrication technologies	23
1.3.3.2 Detection methods and innovative applications	27
1.4 Thread-Based Microfluidics	37
1.4.1 General characteristics of thread	37
1.4.1.1 Cotton fibre	38
1.4.1.2 Polyester fibre	39
1.4.2 Medical applications of thread	40
1.4.3 Development of thread-based microfluidics	42

1.4.4 Blood grouping and existing blood grouping methods	44
1.5 Research Objectives and Aims	47
1.6 Thesis Outline	48
1.7 References	52

Part I Paper-Based Microfluidics

Chapter 2 Paper-Based Microfluidic Devices by Plasma Treatment	67
2.1 Abstract	71
2.2 Introduction	71
2.3 Experimental Section	72
2.4 Results and Discussion	74
2.4.1 Plasma Formed Patterns	74
2.4.2 Design of Sample Dosing and Detection Sites on Paper-Based Microfluidic Devices	75
2.4.3 Building Functional Elements on Paper-Based Microfluidic Systems	76
2.5 Conclusion	79
2.6 Acknowledgment	79
2.7 References	80
Chapter 3 Fabrication of Paper-Based Microfluidic Sensors by Printing	81
3.1 Abstract	85
3.2 Keywords	85
3.3 Introduction	86
3.4 Materials and Methods	87
3.4.1 Chemicals and Materials	87
3.4.2 Microfluidic Channel Formation on Paper	88
3.5 Results	89
3.5.1 Hydrophilic-Hydrophobic Contrast of Untreated and Treated Papers	89
3.5.2 Patterned De-Hydrophobization of Papers by Plasma Treatment	90
3.5.3 Patterned Hydrophobization of Papers by Ink Jet Printing	91
3.5.4 Characterization of Printed Microfluidic Channels in Paper	93
3.5.4.1 Hydrophilic Channel Resolution and Cross-Section	93
3.5.4.2 Liquid Penetration Behavior in a Printed Channel	95
3.5.5 Paper-Based Microfluidic Sensors with Incorporated Detection Chemistry	97

3.6 Discussion	99
3.7 Conclusion	100
3.8 Acknowledgment	101
3.9 References	102
Chapter 4 Quantitative Biomarker Assay with Microfluidic Paper-Based Analytical Devices	103
4.1 Abstract	107
4.2 Keywords	107
4.3 Introduction	108
4.4 Experimental Sections	110
4.4.1 Preparation of μ PADs	110
4.4.2 Preparation of Solutions	111
4.4.3 Running Assays on μ PADs	112
4.5 Results and Discussion	113
4.5.1 Patterning Paper as μ PADs	113
4.5.2 Calibration Curve for NO_2^-	114
4.5.3 Concentration Measurement of NO_2^- Sample	116
4.5.4 Concentration Measurement of UA Sample	118
4.6 Conclusion	120
4.7 Acknowledgment	120
4.8 References	121
Chapter 5 Progress in Patterned Paper Sizing for Fabrication of Paper-Based Microfluidic Sensors	123
5.1 Abstract	127
5.2 Keywords	127
5.3 Introduction	128
5.4 Experimental Section	131
5.4.1 Sizing Agents	131
5.4.2 Paper-Based Microfluidic Devices	131
5.4.3 Preparation of Liquid Samples	132
5.5 Results and Discussion	132
5.5.1 Hydrophilic-Hydrophobic Contrast of Untreated and Treated Papers	132
5.5.2 Fabrication of Paper-Based Microfluidic Devices	134

5.5.3 Printing Sensing Reagents or Biomolecules on Paper-Based Microfluidic Devices	136
5.5.4 Paper-Based Microfluidic Devices for Qualitative Multi-Analyte Detection and Quantitative Analysis	137
5.5.5 Functional Elements for Enhanced Sensing Capability	139
5.6 Discussion	140
5.7 Conclusion	142
5.8 Acknowledgment	143
5.9 References	144

Part II Thread-Based Microfluidics

Chapter 6 Thread as a Versatile Material for Low-Cost Microfluidic Diagnostics	149
6.1 Abstract	153
6.2 Keywords	153
6.3 Introduction	154
6.4 Experimental Section	155
6.5 Results and Discussion	158
6.6 Conclusions	165
6.7 Acknowledgment	166
6.8 References	167
Chapter 7 An Inexpensive Thread-Based System for Simple and Rapid Blood Grouping	169
7.1 Abstract	173
7.2 Keywords	174
7.3 Introduction	174
7.4 Experimental Section	176
7.4.1 Preparation of Antibody Impregnated Thread	176
7.4.2 Modification of Antibodies for Enhanced Detection	177
7.4.3 Blood Sample Tests Using the Thread-Based Platform	177
7.4.4 Confirmation of Donor Blood Type Using the Glass Slide Method	177
7.5 Results and Discussion	178
7.5.1 Separation of Agglutinated RBCs from Blood Serum on Thread	178

7.5.2 Effect of Adding Colouring Agents to Antibody Solutions	180
7.5.3 Low-Cost Dosing Device	183
7.5.4 Single-Step Prototype	184
7.5.5 Expiry Study	185
7.6 Conclusions	186
7.7 Acknowledgment	186
7.8 References	187
Chapter 8 Flow Control Concepts for Thread-Based Microfluidic Devices	189
8.1 Abstract	193
8.2 Introduction	194
8.3 Experimental Section	196
8.3.1 Threads and Textile	196
8.3.2 Measurement of Fluid Capillary Rise on Threads	197
8.3.3 Functional Elements on μ TADs for Flow Control	198
8.3.4 Testing Solutions	198
8.4 Results and Discussion	199
8.4.1 Fluid Penetration along Threads	199
8.4.2 Building Functional Elements on μ TADs for Controlled Fluid Transport	203
8.4.2.1 Binary Type (On/Off) Switches	204
8.4.2.2 Microselectors for Flow Control	206
8.4.2.3 Micromixers	208
8.5 Conclusions	211
8.6 Acknowledgment	212
8.7 References	213
Chapter 9 Conclusions and Future Work	215
Appendix I Papers Included in Each Chapter in Their Published Format	I-1
I (A) Paper-Based Microfluidic Devices by Plasma Treatment	I-3
I (B) Fabrication of Paper-Based Microfluidic Sensors by Printing	I-9
I (C) Quantitative Biomarker Assay with Microfluidic Paper-Based Analytical Devices	I-17

I (D) Progress in Patterned Paper Sizing for Fabrication of Paper-Based Microfluidic Sensors	I-25
I (E) Thread as a Versatile Material for Low-Cost Microfluidic Diagnostics	I-37
I (F) An Inexpensive Thread-Based System for Simple and Rapid Blood Grouping	I-43
I (G) Flow Control Concepts for Thread-Based Microfluidic Devices	I-51

Appendix II Related Co-Authored Papers Not Included in the Main Body of This Thesis

II (A) Printed Two-Dimensional Micro-Zone Plates for Chemical Analysis and ELISA	II-3
II (B) Capillary Driven Low-Cost V-groove Microfluidic Device with High Sample Transport Efficiency	II-11
II (C) Biosurface Engineering through Ink Jet Printing	II-19
II (D) Thermal Stability of Bioactive Enzymatic Papers	II-27
II (E) Porous Liquid Marble Shell Offers Possibilities for Gas Detection and Gas Reactions	II-35
II (F) Liquid Marble for Gas Sensing	II-43

Appendix III Patents Generated from This Thesis

III (A) Method of Fabricating Microfluidic Systems	III-3
III (B) Switches for Microfluidic Systems	III-23
III (C) Quantitative and Self-Calibrating Chemical Analysis Using Paper-Based Microfluidic Systems	III-43
III (D) Three-Dimensional Microfluidic Systems	III-57
III (E) Testing Device for Identifying Antigens and Antibodies in Biofluids	III-93

SUMMARY

The research reported in this thesis focuses on the development of a new class of microfluidic sensing devices for biomedical analysis. The distinctive aspect of these devices is that they are made of low-cost and universal materials, such as paper and thread. The intended applications of the low-cost microfluidic devices are predominantly for human healthcare, rapid disease detection and large scale disease screening in developing regions of the world where medical facilities and healthcare situations are much more challenging than in the developed world.

The potential of microfluidics in analytical and diagnostic fields has been demonstrated by a very large number of fundamental and application studies in the last couple of decades. However, most of highly sophisticated micro- and nano-fluidic diagnostic techniques are unable to meet the challenges of healthcare and disease screening in resource-limited developing regions in the world, as they are either too expensive or require trained personnel to operate. Since more than two-thirds of the world's population live in the developing countries and most of them are in resource-limited regions, there is an urgent need for low-cost, portable, rapid and electronically transmittable diagnostic methods and devices to be developed in order to significantly increase the accessibility of healthcare by people living in these regions.

This thesis has two parts, which separately present research work in paper-based and thread-based microfluidic devices. In the first part, research into paper-based microfluidics combines novel scientific ideas with traditional techniques and know-how in papermaking and printing. Liquid sample transport in these devices can be controlled by using channels chemically defined on paper via printing cellulose-reactive reagents. An interesting difference and novelty of this research compared with the research reported by other groups is that it uses well-known papermaking know-how (e.g. internal paper sizing) and ink jet printing technology, to create capillary-driven microfluidic devices. Biochemical detection chemistries can be printed into the designated detection zones of paper-based microfluidic devices. Another original concept explored by this thesis is the building of sample flow control switches and reactors on paper, enabling multi-step analyses to be performed on paper. Applications

of paper-based microfluidic systems for semi-quantitative and quantitative biochemical analyses are demonstrated in the thesis.

In the second part, innovations in using thread as a flexible and versatile material for microfluidic diagnostics are presented. Bioactivity can be relatively easily introduced onto threads; thread-based microfluidic devices can be simply fabricated by sewing bioactive threads onto suitable supporting materials using a household needle or a sewing machine. This part also demonstrates potential applications of the thread-based microfluidic devices not only in semiquantitative biochemical analysis, but more importantly, in real-life diagnostics such as blood grouping tests. This work shows that the bioactive thread-based microfluidic concept will serve as a platform that allows other healthcare diagnostic devices to be developed.

It is the sincere hope of the author that one day the findings presented in this thesis will be able to serve communities in the developing world by providing solutions to their problem with healthcare and disease control.

Monash University
Monash Research Graduate School

Declaration for thesis based or partially based on conjointly published or unpublished work

General Declaration

In accordance with Monash University Doctorate Regulation 17/ Doctor of Philosophy and Master of Philosophy (MPhil) regulations the following declarations are made:

I hereby declare that this thesis contains no material which has been accepted for the award of any other degree or diploma at any university or equivalent institution and that, to the best of my knowledge and belief, this thesis contains no material previously published or written by another person, except where due reference is made in the text of the thesis.

This thesis includes seven original papers published in peer reviewed journals. The core theme of the thesis is to explore novel fabrication concepts of low-cost microfluidic devices using paper and thread in order to provide affordable diagnostics for developing countries. The ideas, development and writing up of all the papers in the thesis were the principal responsibility of myself, the candidate, working within the Department of Chemical Engineering under the supervision of Assoc. Prof. Wei Shen and Prof. Gil Garnier.

The inclusion of co-authors reflects the fact that the work came from active collaboration between researchers and acknowledges input into team-based research.

In the case of the seven chapters listed below, my contribution to the work involved the following:

Thesis chapter	Publication title	Publication status	Nature and extent of candidate's contribution
2	Paper-Based Microfluidic Devices by Plasma Treatment	Published	Experimental design and conduct, writing
3	Fabrication of Paper-Based Microfluidic Sensors by Printing	Published	Experimental design and conduct, writing
4	Quantitative Biomarker Assay with Microfluidic Paper-Based Analytical Devices	Published	Experimental design and conduct, writing
5	Progress in Patterned Paper Sizing for Fabrication of Paper-Based Microfluidic Sensors	Published	Experimental design and conduct, writing
6	Thread as a Versatile Material for Low-Cost Microfluidic Diagnostics	Published	Experimental design and conduct, writing
7	An Inexpensive Thread-Based System for Simple and Rapid Blood Grouping	Published	Experimental design and conduct, writing
8	Flow Control Concepts for Thread-Based Microfluidic Devices	Published	Experimental design and conduct, writing

I have renumbered sections of published papers in order to generate a consistent presentation within the thesis.

Signed: 

Date: 02 / 08 / 2011

This page is intentionally blank

ACKNOWLEDGEMENTS

I would like to express my sincere gratitude and thanks to my supervisors Assoc. Prof. Wei Shen and Prof. Gil Garnier for their encouragement, patience and support throughout my entire candidature. I am most deeply grateful to my main supervisor Assoc. Prof. Wei Shen, for providing me the opportunity to start and complete this interesting project. He encouraged me to think out of the box, inspired me to try innovative ideas, trained me to do research efficiently, taught me to write great research articles and give attractive presentations, as well as provided me with a fun research environment. Most importantly, I have learnt from him how to be a good researcher and a wise teacher, which will benefit me in my future career and my life.

I gratefully acknowledge Monash University for providing me the research scholarships which have made my PhD work possible.

I would like to thank all the academic staff members at APPI and Department of Chemical Engineering at Monash University. Special thanks to Prof. Huanting Wang from Department of Chemical Engineering, Assoc. Prof. John Forsythe from Department of Materials Engineering at Monash University for their kind support and suggestions. I also acknowledge the support of the administrative staff and the technical staff at APPI and Department of Chemical Engineering, particularly Janette Anthony, Lilyanne Price, Jill Crisfield, Kim Phu, Ron Graham, Gamini Ganegoda, for their assistance throughout my candidature.

I acknowledge with gratitude the thesis editorial assistance given by Ms. Jane Moodie, the lecturer for research student academic support at Faculty of Engineering, and the thesis proofreading given by Dr. Emily Perkins and David Ballerini at Department of Chemical Engineering at Monash University.

I would like to acknowledge my primary and high school teachers, especially Mr. Fapeng Zhang, Mr. Suishun Zhang, Mr. Xiangtai Deng, for not only teaching me academic knowledge, but also helping me to develop conscience and morality. I also

acknowledge my lecturers and supervisors at Shandong University for the undergraduate and postgraduate education.

I would like to thank Junfei Tian, David Ballerini, Dr. Mohammad Mohidus Samad Khan, Dr. Lijing Wang, Dr. Thomas Gengenbach, Dr. Emily Perkins, Ying Ngo, Kai Wu, Ms. Lisa Collison and Thanh Nguyen for their support and help during the experimental work. I also would like to thank Tina Arbatan, Liyuan Zhang, Sharmiza Adnan, Galuh Yuliani, Sigappi Narayanan, Rosiana Lestiani, Scot Sharman, Henri Kröling, Dr. Ping Peng, Purim Jarujamrus, Lin Wang, Jielong Su, Matthew O'Connor, Dr. Wade Mosse, Dr. Mohammad Al-Tamimi and Khairunnisaa Abd Rasid at APPI for their friendship throughout my PhD study.

Last but most importantly, I would like to thank my parents and other family members for their lifetime support and encouragement. I would like to express my deepest gratitude to my husband Chao, for his love, support, understanding and patience throughout my entire PhD study.

LIST OF PUBLICATIONS, PATENTS AND AWARDS

Peer-Reviewed Journal Papers

The following published papers are included in this thesis as individual chapters. The sections of these published papers have been renumbered in order to generate a consistent presentation within the thesis. Papers in their published format are included in this thesis as Appendix I.

1. **Li, X.**, Ballerini, D., Shen, W., Flow Control Concepts for Thread-Based Microfluidic Devices, *Biomicrofluidics*, 2011, 5(1): p. 014105-13.
[**Impact:** Ranked seventh (March 2011), tenth (May 2011) and eighth (June 2011) in the most downloaded articles published in *Biomicrofluidics*]
2. **Li, X.**, Ballerini, D., Shen, W., An Inexpensive Thread-Based System for Simple and Rapid Blood Grouping, *Analytical and Bioanalytical Chemistry*, 2011, 399(5): p. 1869-1875.
[**Impact:** Contributed to the success of ARC Linkage proposal “Cellulose and Paper-Based Biosensors for Blood Analysis” (ARC LP110200973) by Monash University and Lateral Grifols (an Australian blood transfusion company) in 2011. Lateral Grifols commits AU\$ 2M cash input for five years]
3. **Li, X.**, Tian, J., Shen, W., Progress in Patterned Paper Sizing for Fabrication of Paper-Based Microfluidic Sensors, *Cellulose*, 2010, 17(3): p. 649-659.
4. **Li, X.**, Tian, J., Garnier, G., Shen, W., Fabrication of Paper-Based Microfluidic Sensors by Printing, *Colloids and Surfaces B: Biointerfaces*, 2010, 76(2): p. 564-570.
[**Impact:** 8 citations by 08/2011 according to Thomson Reuters Web of Knowledge]

5. **Li, X.**, Tian, J., Shen, W., Thread as a Versatile Material for Low-Cost Microfluidic Diagnostics, *ACS Applied Materials & Interfaces*, 2009, 2(1): p. 1-6.
[**Impact:** *American Chemical Society News Release*, 17/2/2010; Highlight in *Lab on a Chip* (2010, 10(4): p. 409-410); News in *The Age*, 10/5/2010; Highlight in *Science Daily*, 28/2/2010; UK-based *Science Radio & Science Podcasts*, 21/2/2010); *Monash University Newslines*, 26/2/2010; *Monash Memo*, 10/3/2010; *Monash Magazine*, 25/6/2010; Highlight in *Chemical Engineering*, 10/5/2010; more than 200 international and national web blogs, features and forums; ranked first (the first 3 months of 2010) and second (the whole year of 2010) in the most-accessed articles published in *ACS Applied Materials & Interfaces*]
6. **Li, X.**, Tian, J., Shen, W., Quantitative Biomarker Assay with Microfluidic Paper-Based Analytical Devices, *Analytical and Bioanalytical Chemistry*, 2010, 396(1): p. 495-501.
[**Impact:** 9 citations by 08/2011 according to Thomson Reuters Web of Knowledge]
7. **Li, X.**, Tian, J., Nguyen, T., Shen, W., Paper-Based Microfluidic Devices by Plasma Treatment, *Analytical Chemistry*, 2008, 80(23): p. 9131-9134.
[**Impact:** Highlight in *Lab on a Chip* (2009, 9(1): p. 15-16); 42 citations by 08/2011 according to Thomson Reuters Web of Knowledge]

The following co-authored papers have been published during this doctoral study. They are related to the main body of this thesis, and therefore are included in this thesis as Appendix II.

8. Tian, J., **Li, X.**, Shen, W., Printed Two-Dimensional Micro-Zone Plates for Chemical Analysis and ELISA, *Lab on a Chip*, 2011, 11(17): p. 2869-2875.
9. Tian, J., Kannangara, D., **Li, X.**, Shen, W., Capillary Driven Low-Cost V-groove Microfluidic Device with High Sample Transport Efficiency, *Lab on a Chip*, 2010, 10(17): p. 2258-2264.
10. Khan, M.S., Fon, D., **Li, X.**, Tian, J., Forsythe, J., Garnier, G., Shen, W., Biosurface Engineering through Ink Jet Printing, *Colloids and Surfaces B: Biointerfaces*, 2010, 75(2): p. 441-447.
[**Impact:** 9 citations by 08/2011 according to Thomson Reuters Web of Knowledge]
11. Khan, M.S., **Li, X.**, Shen, W., Garnier, G., Thermal Stability of Bioactive Enzymatic Papers, *Colloids and Surfaces B: Biointerfaces*, 2010, 75(1): p. 239-246.
12. Tian, J., Arbatan, T., **Li, X.**, Shen, W., Porous Liquid Marble Shell Offers Possibilities for Gas Detection and Gas Reactions, *Chemical Engineering Journal*, 2010, 165(1): p. 347-353.
[**Impact:** Journal front cover]
13. Tian, J., Arbatan, T., **Li, X.**, Shen, W., Liquid Marble for Gas Sensing, *Chemical Communications*, 2010, 46(26): p. 4734-4736.
[**Impact:** Highlighted in *Chemical Science* of RSC publishing; 10 citations by 08/2011 according to Thomson Reuters Web of Knowledge]

Conference Papers

The following conference papers have been presented by the author in international and national conferences during this doctoral study, but not included in this thesis.

1. **Li, X.**, Ballerini, D., Tian, J., Shen, W., Thread as a substrate for low-cost point-of-care diagnostics, *Sustainable Chemistry 2011*, Antwerp, Belgium, 2011.
2. **Li, X.**, Ballerini, D., Tian, J., Shen, W., Potential of low-cost thread-based microfluidic systems for point-of-care measurements, *Advances in Biodetection & Biosensors*, Hamburg, Germany, 2011
3. **Li, X.**, Tian, J., Shen, W., Microfluidic thread-based analytical devices for low-cost and low-volume diagnostics, *The Third Australia-China Joint Symposium on Science, Technology and Education*, Melbourne, Australia, 2010.
4. **Li, X.**, Tian, J., Shen, W., Microfluidic thread-based analytical devices for low-cost and low-volume diagnostics, *Chemeca*, Adelaide, Australia, 2010.
5. **Li, X.**, Tian, J., Shen, W., Progress in patterned paper sizing for fabrication of paper-based microfluidic sensors, *64th Appita Annual Conference & Exhibition*, Melbourne, Australia, 2010.
6. **Li, X.**, Tian, J., Shen, W., Paper as a low-cost base material for diagnostic and environmental sensing applications, *The 3rd Victorian Association of Chinese PhD students & scholars Research Workshop Proceedings*, Melbourne, Australia, 2009.
7. **Li, X.**, Tian, J., Shen, W., Paper as a low-cost base material for diagnostic and environmental sensing applications, *63rd Appita Annual Conference & Exhibition*, Melbourne, Australia, 2009.

The author has contributed to the following conference papers which have been or will be presented by the first author of each paper. These conferences papers are not included in this thesis.

8. Ballerini, D., **Li, X.**, Shen, W., Thread as a low-cost biodiagnostic substrate, *5th European Conference of the International Federation for Medical and Biological Engineering*, Budapest, Hungary, 2011.
9. Tian, J., **Li, X.**, Shen, W., A simple manufacturing process for paper-based microfluidics fabrication, *Chemeca*, Adelaide, Australia, 2010.
10. Khan, M.S., Tian, J., **Li, X.**, Shen, W., Garnier, G., Bioactive enzymatic papers, *14th Fundamental Research Symposium*, Oxford, 2009.
11. Khan, M.S., Fon, D., **Li, X.**, Forsythe, J., Thouas, G., Garnier, G., Shen, W., Printing biomolecules part-1: achieving total control of biomolecule delivery using ink jet printing, *Chemeca*, Newcastle, Australia, 2008.
12. Khan, M.S., Fon, D., **Li, X.**, Forsythe, J. S., Garnier, G., Shen, W., Ink jet printing of biomolecules on porous surfaces, *International Conference on Chemical Engineering (ICChE)*, Dhaka, Bangladesh, 2008.

Patents

The following patents have been generated during this doctoral study. The first five WO patents are included in this thesis as Appendix III, while the other two provisional patents are not included in this thesis.

1. Shen, W., **Li, X.**, Tian, J., Khan, M.S., Garnier, G., Method of fabricating microfluidic systems, Patent No.: WO/2010/003188.
2. Shen, W., **Li, X.**, Tian, J., Nguyen, T., Garnier, G., Switches for microfluidic systems, Patent No.: WO/2010/017578.
3. Shen, W., **Li, X.**, Tian, J., Garnier, G., Quantitative and self-calibrating chemical analysis using paper-based microfluidic systems, Patent No.: WO/2011/000047.
4. Shen, W., **Li, X.**, Ballerini, D., Tian, J., Three-dimensional microfluidic systems, Patent No.: WO/2011/009164.
5. Garnier, G., Shen, W., Khan, M.S., **Li, X.**, Thouas, G., Testing device for identifying antigens and antibodies in biofluids, Patent No.: WO/2011/035385.
6. Shen, W., Tian, J., **Li, X.**, Printed multi-zone microzone plates, Application No. 2010900564 (Provisional patent).
7. Shen, W., **Li, X.**, Ballerini, D., Method and system for detection of blood types, Application No. 20101223 (Provisional patent).

Awards

1. Postgraduate Publications Award (PPA), Round 2/2011, Monash Research Graduate School (MRGS)
(Prize: AU\$ 5,000, this award supports research students to write papers during the thesis examination)
2. Chinese Government Award for Outstanding Self-Financed Students Abroad (2010)
(Prize: US\$ 5,000, this award is sponsored by China Scholarship Council and is highly competitive; there were 35 awardees in Australia in 2010)
3. Winner of 63rd Australian and NZ Pulp and Paper Industry Technical Association (APPITA) Annual Conference and Exhibition New Speakers Contest (2009)
(Prize: AU\$ 4,000, this prize is sponsored by Appita and the Appita Asia Committee)

.

LIST OF FIGURES

Chapter 1

- Figure 1:** The proposed reaction mechanisms of AKD and ASA with cellulose (adapted with permission from ref [79]).
- Figure 2:** Examples of plasma-solid interactions including etching, activation and coating (with permission from ref [91]).
- Figure 3:** Different printing technologies: contact and non-contact printing (adapted with permission from ref [47]).
- Figure 4:** The first paper-based microfluidic channels created by impregnating paraffin on filter paper (with permission from ref [107]).
- Figure 5:** Colorimetric detections on μ PADs with different applications: (a) simultaneously glucose and protein tests (with permission from ref [4]); (b) concurrent active and deactivated enzyme detection; and (c) semiquantitative nitrite ion measurement.
- Figure 6:** Picture of three-electrode μ PAD. The hydrophilic area at the center of the device wicks sample into the three separate test zones where independent enzyme reactions occur. The silver electrodes and contact pads are made from Ag/AgCl paste with the black electrode portions being the Prussian Blue (PB)-modified carbon electrodes (device size is 4 cm \times 4 cm) (with permission from ref [135]).
- Figure 7:** Fabrication and operation of an ECL μ PAD. The individual μ PAD is filled with a 10 mM Ru(bpy)₃²⁺ solution before drying, and is then aligned and fixed onto the face of the SPE by laminating with transparent plastic. A drop of sample is introduced through a small aperture in the plastic at the base of the channel, and when the detection zone is fully wetted, the sensor is placed close to the lens of the camera phone, a potential of 1.25 V is applied, and the resulting emission is captured and analyzed (with permission from ref [119]).
- Figure 8:** 3D microfluidic device with control switch. Hydrophilic channels are formed on both the top and bottom sheets of papers. On the top paper sheet the hydrophilic channel is cut as shown so that they can be moved (S1). A hydrophobic medium in sheet or film form with a cut notch (or a hole, not shown) is sandwiched in between the two sheets. By aligning the channels on the paper sheets with the notch in the hydrophobic medium, a switch can be formed. The operation of the switch involves pushing the switch (S1) down to make contact with the hydrophilic channel in the bottom paper sheet through the notch in the hydrophobic film.
- Figure 9:** The structure formula of PET.

Chapter 2

Figure 1: Water penetration control of a plasma treated microfluidic channel using hydrophobized filter paper. (a) A hydrophobized filter paper sample immediately after the treatment and (b) the treated sample was exposed to water through the lower edge.

Figure 2: The performance of a paper-based microfluidic pattern fabricated by plasma treatment. Three active and three deactivated enzyme samples were introduced into detection ports of a six-channel pattern in alternation. A few drops of liquid substrate (BCIP/NBT) were introduced from the centre port. Liquid substrate penetrated into the detection ports, revealing the activity of the enzyme samples.

Figure 3: A simple and versatile design of a paper-based microfluidic separator. It can be activated by pulling the paper strip.

Figure 4: A filter made of silica coated matt ink jet paper was used to separate the magenta dye from a diluted ink jet ink solution.

Figure 5: A design of a simple paper-based microfluidic reactor consisting of two sample dosing sites (A1, A2), two switches (S1, S2) and a reaction site (B).

Figure 6: A microfluidic reactor in operation: (a) The reactor fabricated using plasma treatment. Phenolphthalein was deposited in the reaction site B. (b) Dosing of a NaOH solution via A1 and HCl solution via A2; (c) NaOH solution was allowed into the reaction site, triggering indicator color change; (d) HCl solution was allowed into the reaction site, causing indicator color fading; (e) Complete reversion of indicator color by HCl solution.

Chapter 3

Figure 1: The performance of a paper-based microfluidic pattern fabricated by plasma treatment. NaOH solution drops delivered to the central sample dosing zone penetrated through channels into the detection zones, causing color change of phenolphthalein indicator.

Figure 2: Ink jet printed paper-based microfluidic patterns have channels and zones defined by the hydrophilic–hydrophobic contrast (microfluidic patterns wetted with water).

Figure 3: Ink jet printed paper fluidic pattern of a Chinese paper cut. Four liquid feeding zones were added to the four corners of the pattern. Water penetration at an early stage (a) and at the final stage (b) is shown.

Figure 4: Microfluidic sensor patterns are printed on an A4 sized Whatman #4 filter paper. A colorless indicator for detection of NO_2^- was also printed into the circular detection zone. Five microlitres of 5 mM NO_2^- sample solution was introduced into the channel. As the sample solution reached the detection zones of the sensors, reproducible color changes were seen.

Figure 5: The cross-section of a channel with the design width of 500 μm . Water penetration in the channel shows a decrease and an increase in channel width on the top and the bottom sides of the paper respectively.

Figure 6: Micrographs of printed channels recorded using the transmission illumination mode. (a) Water was used as the wicking liquid to increase light transmission in paper for channel width measurement. The channel has an average width of around 300 μm ; (b) the penetration of a food dye solution reveals the integrity of the channel boundary. The channel very well defines the liquid wicking pathway and the amount of “leaking” does not present a problem to the liquid transport.

Figure 7: Experimental set up for water penetration rate measurements of a printed paper channel. The width of the channel was 1000 μm .

Figure 8: Water penetration distance in the printed channel as a function of the square root of time.

Figure 9: Ink jet printed paper microfluidic sensors. The fluidic pattern and the detection chemistries: (a) the indicator for NO_2^- was printed into the circular detection zone. Five microlitres of 5 mM NO_2^- sample solution was introduced into the channel. As the sample solution reached the detection zones of the sensors, reproducible color changes are seen; (b) alkaline phosphatase was printed into circular detection zone and the BCIP[®]/NBT liquid substrate solution was introduced at the sample dosing site. As the liquid substrate penetrated into the detection zone, the position and activity of the printed enzyme are revealed.

Figure 10: (a) The scanned image of the sensor using a desk-top scanner after the samples and indicator were introduced; (b) average color density of each detection zone was determined using PhotoShop and the whole calibration curve is obtained.

Figure 11: (a) The printed paper microfluidic patterns were subjected to a harsh bending/folding test; (b) the performance of the printed patterns showed no discernable deterioration after the test.

Chapter 4

Figure 1: Microfluidic patterns generated on paper using plasma treatment (a) and ink jet printing (b and c). The channels were wetted with water to visually show the patterns.

Figure 2: The scanned image of a six-channel μ PAD in which a series of standard NO_2^- solutions were used to construct a calibration curve. After reaction, color intensities can be visually detected.

Figure 3: The concentration calibration curve constructed using the grayscale intensity values converted from the image shown in Fig. 2.

Figure 4: The scanned image of a six-channel μ PAD in which a series of standard NO_2^- solutions were used to construct a calibration curve in a higher concentration range than that in Fig. 2. In this analysis, a sample solution of “unknown” NO_2^- concentration was also deposited in the device (*marked x*).

Figure 5: The concentration calibration curve constructed using the grayscale intensity values converted from the image shown in Fig. 4. The grayscale intensity for the sample of “unknown” concentration is shown by the *unfilled square*.

Figure 6: The scanned image of a six-channel μ PAD in which a series of standard UA solutions were used to construct a calibration curve. In this analysis, a sample solution of “unknown” UA concentration was also deposited in the device (*marked x*).

Figure 7: The concentration calibration curve constructed using the grayscale intensity values converted from the image shown in Fig. 6. The grayscale intensity for the sample of “unknown” concentration is shown by the *unfilled square*.

Chapter 5

Figure 1: Water wettability of a half-sized and half-unsized filter paper.

Figure 2: **a** Two identical metal masks for fabrication of paper-based microfluidic devices with plasma treatment; **b** A six-channel pattern fabricated using masks and plasma reactor (wetted with water).

Figure 3: **a** Computer-generated electronic pattern for ink jet printing of paper-based microfluidic device; **b** Ink jet printed microfluidic pattern on filter paper with borders defined by the hydrophilic-hydrophobic contrast (wetted with water).

Figure 4: The microscope image of a water wetted microfluidic channel on filter paper, showing the hydrophobic channel wall is strong enough to guide capillary penetration of water within the channel.

Figure 5: Qualitative multiple analytes detection with paper-based microfluidic devices

a The assay design: NO_2^- indicator and UA indicator were deposited in alternation into the six detection zones marked with N (for NO_2^-) and U (for UA); **b** Mix sample solution containing NO_2^- and UA was introduced from central inlet zone; the sample penetrated into different detection zones to trigger different colour changes (pink for NO_2^- and purple for UA).

Figure 6: Quantitative biological/chemical assay using paper-based microfluidic devices

a The assay design: NO_2^- standard solutions (0.5 μL) with different concentration from 0 to 1250 $\mu\text{mol/L}$ were deposited into detection zone 0 to zone 5 in sequence; **b** NO_2^- indicator solution was added into the device from central inlet zone and caused different colour changes in different detection zones; **c** Calibration curve created by colour density measurement using Adobe Photoshop of the scanned images of the tests. *Error bars* were obtained from six repeated measurements.

Figure 7: **a-c** A design of a simple paper-based microfluidic reactor consisting of two

sample dosing sites, two valves, and one central reaction site; **d-f** A paper-based microfluidic reactor based on this design was tested using acid–base neutralization reaction (**d** Phenolphthalein indicator solution was deposited onto the central reaction zone. NaOH and HCl solutions were added into reagent zones A and B, respectively; **e** NaOH solution was introduced into the reaction zone to trigger colour change; **f** HCl solution was introduced later into the reaction zone via valve B to neutralize NaOH in the reaction zone)..

Figure 8: **a** The paper-based microfluidic device was subjected to a harsh folding test;

b The performance of the device showed no deterioration after the test.

Chapter 6

Figure 1: (A) Three-dimensional microfluidic pattern fabricated by sewing threads

onto a translucent polymer film. (A1) Pattern sewed using hydrophilic cotton threads; (A2) introduction of liquids on threads; (A3) liquids wick throughout the thread pattern. Their stitches cross one another from above and below the polymer film and therefore do not mix. (B) Three-dimensional microfluidic channel of thread imbedded in plasticine. (B1) Imbedded hydrophilic cotton thread in plasticine; (B2) introduction of a liquid on the thread from one end; (B3) liquid wicks along the thread through plasticine.

Figure 2: (A, B) Twisted pair of an untreated and a plasma-treated cotton thread. When

the liquid is introduced onto the treated and hydrophilic thread, the liquid wicks only along the hydrophilic thread. (C) Sample mixing zone demonstrating the manipulation of liquid wicking along threads. The top and

the middle threads that transport cyan and yellow liquids are twisted and sleeved inside a heat shrink tube; the bottom thread that transports magenta liquid is not twisted with the other two threads and passes through the mixing zone from outside of the heat shrink tube.

Figure 3: Demonstration of a 3D thread-paper microfluidic sensor. (A) Fabrication of the sensor. (B) Front side and back side of the sensor. (C) Different color development on the front side (pink) and back side (purple) of the sensor when multianalyte test solution ($500\ \mu\text{M}\ \text{NO}_2^-$, $500\ \mu\text{M}\ \text{UA}$) was introduced from the central hole of the sensor onto the two threads and penetrated into paper discs (detection zones).

Figure 4: (A) Three parallel colorimetric measurements of serially diluted NO_2^- solution samples (0, 125, 250, 500, and $1000\ \mu\text{M}$) on the thread-based sensor. (B) NO_2^- concentration calibration curve established from thread stitches of six thread sensors using a desktop scanner and Adobe PhotoShop.

Figure 5: (A) Thread-paper microfluidic sensors using cotton thread as the liquid transport channel. (B) Colorimetric NO_2^- concentration series (0, 125, 250, 500, and $1000\ \mu\text{M}$) developed using a sensor array made of filter paper and cotton thread. (C) A NO_2^- concentration calibration curve established from six thread-paper microfluidic sensors using a desktop scanner and Adobe PhotoShop.

Chapter 7

Figure 1: Proof of concept testing with samples of whole blood of type A+, B+ and O− on antibody-treated polyester threads. *Columns* show results on threads A, B and D from *left to right*, whilst *rows* show the results for the different blood types as labelled on the left.

Figure 2: Graph of separation distance due to agglutination for positive reactions with the different antibody solutions: anti-A, anti-B and anti-D, including cyan and magenta ink jet ink modified anti-D solutions. *Error bars* represent one standard deviation from the arithmetic mean (ten repetitions).

Figure 3: Blood testing on threads CD, MD and D (for comparison) (a) A+ sample applied to thread CD, a light band can be seen between the RBCs and cyan antibody solution indicating separation of plasma and RBCs; (b) O− sample applied to thread CD, no separation visible. (c) A+ sample applied to thread MD; a positive result is indicated by a light band; (d) O− sample applied to thread MD, no separation visible. (e) a positive result on unmodified thread D for comparison; (f) a negative result on unmodified thread D for comparison.

Figure 4: Graph of penetration length on thread for blood samples dosed with micropipette and needle eye techniques.

Figure 5: A single-step blood grouping test prototype for proof of concept, composed of thread A, B and D wedged in a square of polymer film and sharing an intersecting sample delivery zone (a) the unused device with sample delivery zone indicated within a *red circle* (b) an enlargement of the *right-hand side* of the device after whole blood has been introduced into the delivery zone in the centre via needle eye. The separation occurring on thread A and D indicates that the blood is of type A+.

Chapter 8

Figure 1: A SEM image of a polyester thread, showing the individual fibres which comprise the overall structure. Capillary channels are formed by the gaps between fibres, enabling the thread to conduct flow.

Figure 2: A schematic of the apparatus employed for the fluid penetration measurements on thread. Threads were fixed to a polymer support film and wet with dye solutions from a fluid reservoir.

Figure 3: A graph of penetration distance vs the square root of time for (i) a single thread, (ii) twisted pair, or (iii) twisted triple. The graph highlights a linear relationship between penetration distance and the square root of time over the first minute ($\sim 8 \sqrt{s}$), concordant with the Washburn equation. After this the curve flattens out and reaches an ultimate penetration distance due to the effects of evaporation and gravity.

Figure 4: (a) The simplest of the “on/off” flow control switches is comprised of a thread which incorporates a knot and a loop with an adhesive-blocked segment, sliding the knot over the blocked segment in the loop enables flow to occur along the length of the thread. (a1) The knot device with the inlet fully wet by ink solution, the blockage caused by the glue is indicated by the red dashed line. (a2) The partially wetted device with the inlet in an ink reservoir, after being actuated by sliding the knot past the blocked region. (a3) The device after being removed from the reservoir after conducting flow from inlet to outlet. (b) The folding style switch makes use of a polymer film support material to function. (b1) The fold type switch in the open position with the inlet wet by ink. The fold line and blocked region are labelled. (b2) The folded device allowing flow from an ink reservoir at its inlet. (b3) The fully wetted device after being used to transport fluid (device having been reopened). (C) Folding style switches can be modified to be pull-tab actuated. (c1) The pull-tab switch with inlet connected to an ink reservoir. (c2) The pull-tab switch with tab removed, allowing flow across the device.

Figure 5: A microselector, with two inlets and a single outlet, allows a user to select between which one of two samples they wish to transport. Ink solutions are used for visualisation of the concept. (a) The unused selector switch set in the off position. The blocked region is indicated, and the inlets are connected to ink solution reservoirs. (b) The selector switch after sliding to the right, allowing flow of the yellow ink to the outlet. (c) The selector switch after sliding left, allowing flow of magenta ink.

Figure 6: The microselector allows a user to select between which analyte they wish to analyse. (a) The unused selector switch set in the off position. The blocked region is indicated by a red dashed line, and indicator locations are noted. (b) The selector switch allowing flow to the right, resulting in a colour change indicating the presence of protein. (c) The selector switch allowing flow to the left, the presence of glucose is indicated.

Figure 7: A micromixer device used to mix two coloured inks together. The green colour produced illustrates the efficacy of the device.

Figure 8: A micromixer used to neutralise acid and base solutions to demonstrate the possibility of high quality mixing. (a) The unused mixer with inlets on the left and outlet on the lower right. (b) The device in use, with one acid inlet (0.01M HCl), one base inlet (0.01M NaOH), and reservoirs. The device is held shut by bulldog clips. (c) pH paper showing measurements from the inlets (pH 2 and 12) and outlet (pH 6), suggesting that 99.99% of the acid was neutralised by the base.

LIST OF TABLES

Chapter 1

Table 1: An ideal POC test for low-resource settings: ASSURED criteria (adapted with permission from ref [27])

Table 2: Resources and capabilities at three infrastructure levels common in the developing world (adapted with permission from ref [27]).

Chapter 6

Table 1: Surface Atomic Concentration of C and O of Untreated and Treated Threads.

Chapter 7

Table 1: Results-matrix for aiding interpretation.

LIST OF ABBREVIATIONS

AKD	Alkyl ketene dimer
APPI	Australian Pulp and Paper Institute
ASA	Alkenyl succinic acid anhydride
AuNP	Gold nanoparticle
BioPRIA	Bioresource Processing Research Institute of Australia
BSA	Bovine serum albumin
CIJ	Continuous ink jet
CL	Chemiluminescence
DFA	Diagnostics for All
DNase I	Deoxyribonuclease I
DOD	Drop-on-demand
EAPap	Electro-active paper
EC	Electrochemical
ECL	Electrochemiluminescence
ELISA	Enzyme-linked immunosorbent assays
FLASH	Fast lithographic activation of sheets
FTIR	Fourier transform infrared spectroscopy
IC	Integrated circuits
ICS	Immunochromatographic strip
IPA	Isopropyl alcohol
Liquid AKD	Alkenyl ketene dimer
LOC	Lab-on-a-chip
MDT	Microfluidic diagnostic technology
NADH	Nicotinamide adenine dinucleotide
PB	Prussian Blue
PBT	Poly(butylene terephthalate)
PDMS	Polydimethylsiloxane
PEN	Poly(ethylene naphthalate)
PET	Poly(ethylene terephthalate)

PLA	Poly(lactic acid)
PMMA	Poly(methyl methacrylate)
POC	Point of care
PPT	Poly(propylene terephthalate)
PS	Polystyrene
RBCs	Red blood cells
SEM	Scanning electron microscopy
SERS	Surface-enhance Raman scattering
SPEs	Screen-printed electrodes
TA	Terephthalic acid
Thread A	Thread treated with anti-A reagent
Thread B	Thread treated with anti-B reagent
Thread D	Thread treated with anti-D/Rh reagent
Thread CD	Thread treated with cyan modified anti-D solution
Thread MD	Thread treated with magenta modified anti-D solution
UA	Uric acid
XPS	X-ray photoelectron spectroscopy
μPADs	Microfluidic paper-based analytical devices
3D μPADs	Three dimensional microfluidic paper-based analytical devices
μTADs	Microfluidic thread-based analytical devices
3D μTADs	Three dimensional microfluidic thread-based analytical devices
μTAS	Miniaturized total chemical analysis systems

LIST OF NOMENCLATURE

cSt	centistokes
eV	electronvolt
i.d.	Inner diameter
KDa	kilodalton
mbar	millibar
mM	millimolar
mN	millinewton
M	molar
nM	nanometre
pL	picolitre
μ L	microlitre
μ m	micrometre
μ M	micromolar
R^2	Coefficient of determination
s.d.	Standard deviation
W	watt
g	Gravitational constant
h	Fluid penetration distance along thread
l	Liquid penetration distance in paper
γ	Surface tension
η	Viscosity
ρ	Density
θ	Contact angle
r	Equivalent capillary pore radius
t	Penetration time
ΔP	Pressure
\varnothing	Diameter
$^{\circ}\text{C}$	Degree Celsius

This page is intentionally blank

Chapter 1: Introduction and Literature Review

1.1 Introduction

In recent years microfluidic diagnostic technology (MDT) has been used to provide point-of-care (POC) systems for less-industrialized countries. In microfluidics, the flow of samples and reagents can be controlled within microscale channels; thereby microfluidic devices require only a small amount of sample and reagent, and can test fluid samples quickly and efficiently [1-3]. A main challenge in MDT is to make microfluidic devices low cost, simple to use, and easy to fabricate so as to preferentially benefit the developing world.

When there is a need to develop new microfluidic platforms, the choice of materials and fabrication methods of the devices are the first issues to consider. The materials should be inexpensive to make the products affordable for users in under-developed countries; the fabrication methods should be as simple and efficient as possible to enable mass production and ease of use.

To achieve these aims, one option is to combine traditional well-developed industrial techniques and commonly-used cheap materials with innovative scientific ideas and engineering means. Using this approach, two novel low-cost microfluidic systems have been explored in this thesis: microfluidic paper-based analytical devices (μ PADs, presented in Part I of the thesis) and microfluidic thread-based analytical devices (μ TADs, presented in Part II of the thesis). The concept of using μ PADs for POC tests originated from the Whitesides group in 2007 [4]; however, this thesis, for the first time, through unrelated innovation, presents two inexpensive and easy ways (i.e. plasma treatment and ink jet printing) to create μ PADs. These fabrication methods adapt materials and manufacturing processes of the traditional papermaking and printing industries, thus enabling μ PADs to be fabricated at a potentially industrial scale. This thesis further proposes the concept of using thread as a versatile material to make μ TADs for semi-quantitative human biomarker analysis and easy blood grouping. The manufacture of μ TADs can easily be achieved through sewing or weaving threads by hands or a sewing machine, potentially allowing mass-scale manufacturing. Details of μ PADs and μ TADs innovations in device fabrication and in diagnostic applications will be discussed thoroughly in chapters 2 – 8.

The literature review chapter consists of three sections (Section 1.2, 1.3 and 1.4). It begins with a brief introduction to microfluidics, the diagnostic challenges in the developing world and the roles of microfluidics in POC diagnostics. Most importantly, this section outlines the urgent needs of exploring innovative low-cost microfluidic technologies to substantially improve healthcare and disease diagnosis situations in under-developed areas of the world. The second section presents an overview of the general properties of paper, the conventional analytical applications using paper, and the techniques for the modification of paper surfaces to control the liquid penetration behavior in paper. It also explains the feasibility of building μ PADs using the methods explored in this thesis. This section further summarizes the development of μ PADs (including other unrelated emerging fabrication technologies, detection methods and applications) and identifies the critical gaps in current approaches which must be addressed in order to progress the development in this field. The third section demonstrates the general properties of two types of threads (i.e. cotton and polyester thread) and the commercial applications of these threads in the medical textile industry. This section also introduces the innovative concept proposed in this thesis of fabricating μ TADs as low-cost POC diagnostic tools for the developing world, and the concurrent and later studies in this field reported by other groups. Due to the importance of the new thread-based blood grouping concept presented in this thesis, the fundamental and development of blood grouping are described at last in this section.

Section 1.5 presents the aims of the current research, and Section 1.6 outlines the structure of the thesis.

1.2 Microfluidics

1.2.1 Overview of microfluidics

Miniaturization is a recent powerful trend in life science and analytical chemistry. The miniaturization of fluid handling and fluid analysis has been emerging in the interdisciplinary research field of microfluidics which combines microfabrication techniques with chemistry and biology, a field that has been growing since the early 1990s [5]. Historically, microfluidic devices originated from the integrated circuits (IC) industry (the first IC was invented by Kilby in 1958 [6]).

In general, microfluidics can be defined as systems that use channels with dimensions of tens to hundreds of micrometers to process or manipulate minute amounts (10^{-9} to 10^{-18} L) of fluids [7]. In an engineering definition, microfluidics can be described as the study of flows that are simple or complex, mono- or multiphasic, which are circulating in artificial Microsystems [8].

Early microfluidic devices typically used silicon and glass, since the fabrication techniques using these materials were well-developed. However, these techniques are usually expensive and time-consuming, and they require access to specialized facilities. Therefore, these devices are only marginally useful in research requiring rapid evaluation of prototypes [9, 10]. Instead of microchannels being directly created in silicon and glass, polymers and elastomers are becoming more and more attractive for use in microfluidic devices, since microstructures can be inexpensively fabricated in them using several high throughput methods, such as injection molding, soft lithography, laser ablation, X-ray photolithography and hot embossing [11]. Among the commonly used polymers such as polydimethylsiloxane (PDMS) [9, 12-16], poly(methyl methacrylate) (PMMA) [11, 17, 18] and polystyrene (PS) [19, 20], PDMS is by far the dominant and preferred polymeric building material in microfluidics and has greatly accelerated microfluidics research since its introduction in the 1990s by Whitesides and others [12, 14].

Using microfluidics, processes (e.g. separation, isolation, and chemical/biological reactions) that typically demand laborious hours can be reduced to just a few minutes,

or even seconds. As sample volumes in microfluidic devices are in the range of pL to μL , microfluidic devices are ideal for accommodating precious, costly, toxic, or dangerous samples. Due to the numerous advantages of microfluidics, its applications have extended from its origin in analytical chemistry [5] to a wide range of chemical syntheses, biochemistry, cell biology, and point-of-care (POC).

The rapid expansion of the field of microfluidics seems to be driven in part by the possibility of integration. The ultimate goal is to create all-in-one microchips that are capable of all processes including transport, separation, reaction, and detection [21-23]. The domain of integrated microfluidic analysis systems has been designated as “miniaturized total chemical analysis systems” (μTAS), or “lab-on-a-chip” (LOC) systems (the two terms are essentially synonymous). MicroTAS, first defined in 1990 by Manz et al., emphasizes the analytical function of a microfluidic chip [5]. LOC is a term widely used for any kind of research with the goal of miniaturizing chemical and biological processes, although it is not a well-defined scientific term. LOC technologies include microfluidic chips as well as non-fluidic miniaturized systems such as sensors and arrays (the so-called biochips) [24]. The participation of researchers from a broad spectrum of disciplines, ranging from chemists, biologists, material scientists, physicists, chemical engineers, has tremendously benefited the research field of μTAS or LOC. Numerous large corporations have set up R&D divisions to explore commercialization opportunities in microfluidics [25].

Although PDMS and soft lithography have shown great success in microfluidics, researchers are continuing to explore new materials and fabrication methods for developing various innovative microfluidic systems that are required for an enormous range of different applications. One such application is the microfluidic-based diagnosis in the developing world.

1.2.2 Requirements and challenges of diagnostics in the developing world

The first step in effective prevention and treatment of disease is accurate diagnosis, but diagnostic tests that are a standard component of healthcare in high-income nations, are often unavailable, unreliable or unaffordable in the developing world. Therefore, it is difficult to control the spread of diseases before a major outbreak through rapid and reliable detection in under-developed regions where medical resources are limited. This problem leads to a huge health inequality issue between the developed and under-developed countries. The inequities are now the subject of intense global attention [26].

Since low-infrastructure sites serve most of the global population, lack of diagnostic tests at these sites will not provide the healthcare workers with the ability to identify potential patients who require treatment and, just as importantly, who should not be treated. In 2006 Yager et al. reported that of the world's 6.1 billion population, 3 billion lack basic sanitation, 2 billion do not have access to electricity, and more than 1 billion lack basic healthcare services and clean drinking water [1]. Increased access to the diagnostic products that could save lives in the developing world deserves attention from researchers and requires the development and deployment of new low-cost diagnostic tests that can be used in resource-limited settings, and preferably, by persons with little or no laboratory training [27].

However, commercial development of diagnostic tests designed specifically for low-resource settings has long been hindered by perceptions (and, frequently, realities) of a low return on investment and concerns regarding the challenges of implementation in regions with less-developed healthcare systems [26]. The commercial partners have shown limited willingness to engage in the development of new diagnostics for the developing world [28].

In order to improve health of the poorest people in the developing world and attract interest and investment from commercial partners, there is a need for researchers to explore the development and deployment of a variety of health innovations, including new drugs, vaccines, devices, and diagnostics, as well as new techniques in process engineering and manufacturing [29]. Luckily, changes have been seen in the last decade with increased efforts exerted that focus on the diagnostic technologies in the

developing world. In 2004, the Global Health Diagnostics Forum of the Bill & Melinda Gates Foundation began to study the potential for diagnostic tests to save lives in the developing world. In 2006, the Nature Publishing Group published a supplement of “Determining the Global Health Impact of Improved Diagnostic Technologies for the Developing World” [27, 30], with the aim to further the dissemination of current knowledge on global health diagnostic needs for the conditions that most severely affect the developing world [28].

It has been noticed that among the current diagnostic tools either commercially available or still under development for resource-limited settings, the potential utility of POC diagnostics becomes greater [31]. POC tests are considered as vanguard analytical systems in clinical analysis that provide onsite and reliable analytical results (qualitative and quantitative data) in a rapid and easy way. They constitute a type of testing implemented near the patient (e.g. home, emergency department of a hospital, bedside) in a remote and decentralized way when compared with the conventional diagnosis in a clinical laboratory. Their main purpose is to bring the clinical test results conveniently and immediately to the patient [32]. However, the realization of this potential is hampered by issues concerning test reliability, performance, cost, regulatory approval, documentation, and connectivity [12–16].

In 2003 WHO Sexually Transmitted Disease Diagnostics Initiative proposed a well-accepted ASSURED guideline (Table 1) which states the features a POC test should possess for its application in low-resource settings [33]. To develop POC tests that conform to the ASSURED guideline, long-term investment is required; however, it is probable to achieve short-term improvements in POC tests performance by adapting existing technologies such as microfluidic technology [34].

Table 1 An ideal POC test for low-resource settings: ASSURED criteria (adapted with permission from ref [27])

• Affordable
• Sensitive (avoid false negative results)
• Specific (avoid false positive results)
• User-friendly (simple to perform, uses non-invasive specimens)
• Rapid & robust
• Equipment-free
• Delivered (Accessible to end-users)

1.2.3 Microfluidic technologies for diagnostics in the developing world

In many ways, the intrinsic features of microfluidics are a natural fit for a POC diagnostics device including: low consumption of reagents and sample, miniaturization of device, integration of complex functions and short analysis time. All these characteristics enable microfluidic systems to move sophisticated diagnostic tools out of the developed-world laboratory [1]. Thus, it comes as no surprise that research on microfluidics for POC applications has increased markedly in recent years. The journal *Lab on a Chip* has launched a special issue in 2008 which captured some of the latest research areas of interest and technological approaches from leading researchers towards microfluidic-based POC diagnostics [35]. Thanks to an upsurge in interest in (and funding of) healthcare in the developing world, this new microfluidic diagnostic technology (MDT) may be adopted first for civilian healthcare within the next couple of years in the developing world [1].

However, unique and challenging design criteria must be met so that microfluidic diagnostic devices can be appropriate for their use in settings with limited infrastructure [36]. There are a number of key factors that will affect the introduction, acceptability and sustainability of MDT in the developing world, addressed by Yager et al. (Table 2) [1]. A microfluidic device for the developing world needs to be designed such that it can operate under the constraints of untrained workers, electricity shortage, limited laboratory supplies, and rough handling during transportation and storage [37].

One of the greatest challenges in deploying microfluidic diagnostic systems in the developing countries is to reduce the cost close to that of the most inexpensive current tests, namely the lateral flow or immunochromatographic strip (ICS) tests [1]. It is important to note that lateral-flow strip tests are, with few exceptions, the simplest and most commercialized type of POC tests on the market that have made a substantial impact in low-resource settings so far [26]. These tests are extensively being used to detect pregnancy, drugs, cholesterol, and cardiac markers [32, 38]. There are other successful POC diagnostic devices found on the market which employ an external reader for measuring and recording the signal when accurate tests are sought, such as the i-STAT[®] System [39] and Biosite Triage[®] Cardiac Panel [40].

Table 2 Resources and capabilities at three infrastructure levels common in the developing world (adapted with permission from ref [27])

	Health-care setting (personnel)	Summary of resources and capabilities
No laboratory infrastructure	In the community or home (possibly healthcare worker, pharmacist or family member)	No electricity or clean water available; no trained personnel; no laboratory space; cold storage not available; room temperature not controlled; venipuncture impossible; rapid answer required to prescribe treatment before patient leaves; no physician oversight.
Minimal laboratory infrastructure	Health clinics in Africa; rural health clinics in Latin America and Asia (nurse)	No reliable electricity and clean water; minimal trained personnel; no or minimal laboratory space; cold storage occasionally available; room temperature rarely controlled; venipuncture unlikely; rapid answer required to prescribe treatment before patients leave; no physician oversight.
Moderate to advanced laboratory infrastructure	Urban health clinics in Asia and Latin America; hospitals in Africa, Latin America and Asia (nurses, technicians and physicians)	Dependable electricity and clean water available; trained personnel available; dedicated laboratory space; cold storage available; room temperature sometimes controlled; venipuncture routine; time to answer usually less crucial with hospitalization patient, but still important for clinic patients; physician oversight routine.

In the literature, there are numerous studies showing a variety of microfluidic device prototypes that have potential to be applied in POC diagnostics. Different materials (e.g. metal, plastic) and methods (e.g. photolithography, electrochemical anodization) have been used to develop these devices [22], with some studies dedicating to exploring low-cost microfluidic devices for POC diagnostics. For example, Gervais et al. patterned PDMS by photolithography as a one-step POC chip and detected C-reactive protein (a general inflammation and cardiac marker) by measuring fluorescent signals [38]. Dimov et al. created a self-powered microfluidic blood analysis system using PDMS and glass microscope slides which integrates sample volume metering, whole-blood plasma separation, multiple immunoassays and flow propulsion [41]. These low-cost microfluidic devices have been recognized as promising POC devices to bring accurate and sensitive diagnostic tests to improve healthcare in the developing world as well as in high-income countries [31].

Although with all these endeavors and achievements, current microfluidic devices still generally require complex and somewhat expensive fabrication procedures using plastic or glass as substrates, thus severely limiting their affordability and availability in poor countries. Much progress needs to be made to further reduce the cost of microfluidic POC devices for their use in resource-limited settings [42]. Future development of new microfluidic diagnostic platforms may eventually benefit from materials with improved analytical performance, ease-of-fabrication as well as simplicity and cost-effectiveness to allow their wide utilization in the developing countries. Researchers need to think in innovative ways and to integrate disparate technologies to build these types of platforms. For this reason, the work reported in this thesis explores the feasibility of using cheap materials such as paper and thread to fabricate low-cost and easy-to-use microfluidic diagnostic devices for the developing world.

1.3 Paper-Based Microfluidics

1.3.1 Paper as an analytical substrate

Paper, as a cheap and universal material, has been used to produce a large range of products widely applied to a variety of areas, including printing, packaging, sanitation, and within the food industry. The applications of paper and paper-based products are virtually limitless. New paper-based specialty products are continually being developed [43].

Paper-based analytical products have been in the laboratory since the 19th century in the forms of filtration, chromatographic supports and litmus paper. The first paper-based bioassay was introduced in 1957 by Free et al. for the identification of glucose in urine [44]. Abnormal glucose levels can be indicated on the strip by the development of a blue color. By the mid-1960s, this analytical paper strip had been developed into a commercial product which can diagnose and manage diabetes [45]. Nowadays, 10-test dipsticks are commercially available and widely accepted as the inexpensive, convenient and rapid urinalysis test with a color-coded chart for diagnosis. In general, paper has been broadly used as an analytical substrate for qualitative spot tests which provide ‘yes/no’ detection of analytes with applications covering clinical diagnostics, organic and inorganic chemical analysis, environmental and geochemical analysis, and pharmaceutical and food chemistry. Such chemical detection systems offer several advantages such as ease of use, disposability, and low cost [46], but they are normally not capable of doing multiplex and quantitative analysis.

Apart from conventional analytical applications, paper has recently been physically or chemically modified to make smart products, such as bioactive paper, electro-active paper (EAPap), surface-enhanced Raman scattering (SERS)-active paper, for innovative analytical applications. Specifically, bioactive paper is a high value-added fibre-based product with an advanced biological functionality capable of identifying, capturing and/or inactivating specific target analytes [47]. SENTINEL (a Canadian bioactive paper organization) declared that the potential bioactive paper products include pathogen trapping paper, diagnostic paper and security paper [48]. The research on bioactive paper is booming and has attracted broad interest with many published

studies [49-60]. EAPap uses paper as a smart sensor and actuator material for many applications such as sensors, microelectro-mechanical systems, speakers, microphones, and transducers [61]. SERS-active paper uses commercially available photographic paper for black and white prints as a substrate for quantitative determination of organic compounds [62].

Even with all these traditional applications and new achievements of paper-based analytical products, it is still necessary to explore the capacity of the traditional papermaking industry in order to produce more functional innovative paper-based diagnostic and analytical products, especially for people living in the developing worlds. In this thesis, paper has been used as a low-cost substrate to fabricate a novel microfluidic analytical system – μ PAD, which combines the simplicity of paper strip tests and the complexity of the conventional microfluidic devices, holding a lot of potential for POC and on-site diagnostics. What is convenient about using paper as a microfluidic substrate is the fact that high speed surface sizing/coating and printing techniques have long been available for modifying paper substrates [63].

1.3.2 Surface modification of paper to control liquid and paper interaction

Paper allows water absorption, as the paper matrix is porous and hydrophilic. These properties allow a wetting liquid to penetrate and transport in paper. The kinetics of water penetration in paper has been studied by numerous groups in the context of printing and sanitary applications [64-71]. The Washburn equation has been used as the first order approximation to quantify the water absorption kinetics (equation (1)) [72]:

$$l = \sqrt{\frac{\gamma r \cos\theta}{2\eta} t} \quad (1)$$

Where l is the liquid penetration distance in paper, r is the equivalent capillary pore radius of paper, γ and η are the surface tension and viscosity of the liquid, θ is the contact angle and t is the time of penetration.

It has been shown that the experimentally observed water penetration rates in papers are usually 1 to 2 orders of magnitude lower than the theoretical rates calculated by the Washburn equation, suggesting that the mechanism of water transport in paper is more complicated than that via a single capillary tube, as described by the Washburn equation [73]. Three major factors may have contributed to the difference between the experimental and theoretical water penetration rates in paper.

- a) Pore sizes in paper are not uniform. The general modeling using pore size information obtained from Hg intrusion data may not be sufficient to reflect the penetration pathway for water in paper. Roberts et al. showed that water does not necessarily wick through larger pores, as suggested by the Washburn equation; instead, it preferentially penetrates along interfibre channels where there are less numbers of discontinuities [70].
- b) Cellulose fibres can be swollen by water and the fibre wall takes up a significant amount of water, leaving less free water to penetrate in the interfibre channels. The Washburn equation requires the penetrating liquid not to have chemical or physical reactions with the wall of the pores. Water penetration in paper violates this requirement. It is clear that such a violation of one of the fundamental requirements of the Washburn model contributes to the discrepancy between the theoretical and experimental observations.
- c) The pore size in paper will change after paper is wetted by water, because of the fibre swelling and the fibre matrix expansion. This point must be considered with higher order approximations when conducting modeling [74].

Despite these factors, the Washburn equation is still being used as a convenient semi-quantitative model for describing the general behavior of water penetration in paper.

The wettability of the fibre surface by the penetrating liquid significantly affects the rate of penetration. A widely used indicator of paper wettability is its apparent contact angle with the penetrating liquid [75]. This effect is shown in the Washburn equation, too. Many experimental studies have observed that the apparent contact angle of liquid on paper is a reliable indicator of its penetration rate in paper [71, 75]. Changing the liquid-paper contact angle has therefore been used as a convenient, effective and reliable way to control liquid penetration in paper.

Papermaking is a sequence of physical and chemical operations with the aim to produce papers that meet the increasing quality requirements and expectations of consumers [76]. Most grades of paper and board need to be resistant to wetting and penetration by liquids in a controlled manner. Patterned internal sizing treatments have been chosen in this thesis to fabricate μ PADs by defining hydrophilic microfluidic channels in paper with hydrophilic-hydrophobic contrast. The following subsections will provide a description of paper sizing mechanisms and the working principles of the two techniques (plasma treatment and ink jet printing) employed in this thesis to change the water wettability of paper on selected areas.

1.3.2.1 Paper sizing mechanisms

Paper hydrophobization can be achieved in the papermaking process using matured technologies such as “sizing”, and at industrial scales; there are many choices of hydrophobization or sizing agents for papermaking processes, such as alkyl ketene dimer (AKD), alkenyl succinic acid anhydride (ASA) and rosin. Highly hydrophobized papers show no difference to non-hydrophobized papers in terms of appearance and flexibility [77].

Paper hydrophobization treatments are chemical treatments to the cellulose fibre surface that aim to reduce the penetration rate of aqueous liquid into paper. Basically, sizing encompasses two ways to hydrophobize cellulose fibres during the papermaking process: introducing sizing agents to the fibre suspension (internal sizing) or applying a polymer or starch solution containing sizing agents to the paper web (surface sizing). Internal sizing results in the distribution of the sizing chemicals within the entire fibre matrix of the paper sheet and retards the spreading and penetration of the liquid through the pore system of paper and board [78]. Surface sizing involves the application of a sizing agent to at least one surface of a flat fibrous paper sheet, so that the sizing chemical is present on at least one of the two faces of the flat fibrous sheet, delivering the sizing effect to these surfaces. The internal fibre matrix of a surface sized paper may not be strongly hydrophobic. In general, sizing is recognized to confer a number of advantages (e.g. increase paper strength, resistance to picking and scuffing during printing), with perhaps, controlled resistance to the penetration of water and aqueous inks being of the utmost importance.

The commonly used synthetic sizing agents under neutral or slightly alkaline papermaking conditions are AKD, ASA and alkenyl ketene dimer (liquid AKD). Figure 1 shows the proposed reaction mechanisms of AKD and ASA with cellulose. AKD is a waxy material with a melting point of about 50°C, whereas liquid AKD and ASA are oily liquids at room temperature. The major difference between AKD and liquid AKD is that liquid AKD possesses a double bond in each of the two hydrocarbon chains; the double bond suppresses the melting point of these compounds. This principle is used to modify AKD from a solid wax into a liquid wax [79].

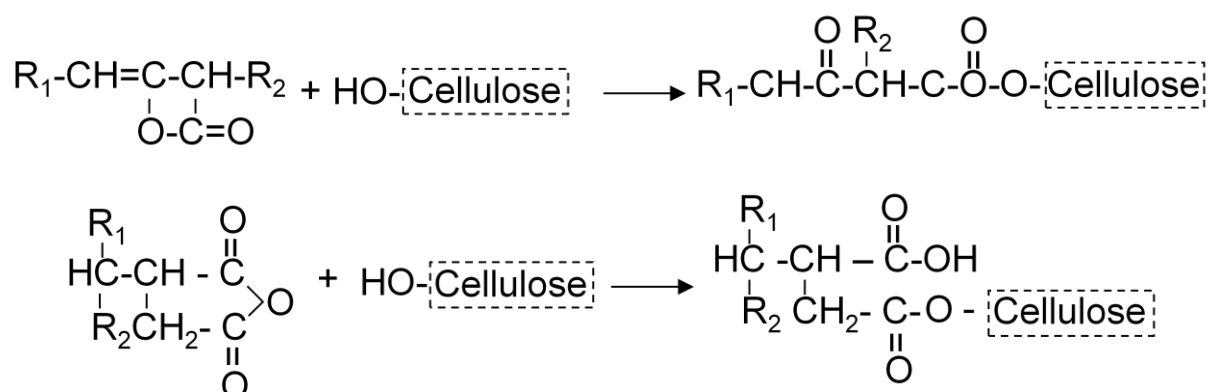


Figure 1: The proposed reaction mechanisms of AKD and ASA with cellulose (adapted with permission from ref [79]).

AKD is a product that had been developed by C. Weissgerber of Hercules Chemical Company in the 1950's. ASA was marketed as a sizing agent in the 1960's by O. Wurzburg and E. Mazzerella of the National Starch and Chemical Company, and gave papermakers a cheaper alternative to AKD. Both agents are applied to cellulose fibres in the form of a cationically stabilized emulsion in the fibre suspensions prior to forming. The two sizing agents have helped papermakers to make the transition from acid papermaking using clay as the primary pigment to neutral/alkaline papermaking using calcium carbonate [80]. The main difference between AKD and ASA is the much faster sizing development of ASA than AKD [81]. AKD sizing, on the other hand, develops more slowly, and the strong sizing effect takes place after the sized paper is cured or exposed to an elevated temperature which is typically between 100 and 120°C [82]. Unfortunately, a drawback of ASA is that it can undergo significantly faster hydrolysis that can considerably affect its performance, whereas AKD is much less

susceptible to hydrolysis [81]. AKD can be dissolved in organic solvents such as heptanes, toluene, and acetone; therefore it is possible to size paper with a solvent-based AKD solution. In this thesis, AKD and liquid AKD are chosen as the example sizing agents used to create hydrophilic-hydrophobic contrast on the paper surface for μ PADs fabrication. It is necessary to mention, however, that ASA is a potential alternative sizing chemical for the devices fabrication. A detailed sizing mechanism of ASA can be found in many literature articles [79, 80, 83], therefore will not be discussed in this literature review.

An AKD molecule contains a hydrophobic portion (two saturated hydrocarbon chains of C_{14} - C_{20}) that imparts the water resistance to paper, and an end group (four-membered lactone ring) that reacts with the hydroxyl group of cellulose to form β -keto ester [79, 82, 84, 85]. With the formation of a β -keto ester linkage under the influence of elevated temperature, the hydrophobic part of the molecule turns out from the surface, thus providing paper with hydrophobicity [77].

Cellulose is hydrophilic and has a low water contact angle. Kannangara et al. reported that the untreated cellulose has a contact angle of around 25° with water [64], whereas after AKD sizing, the hydrophobized filter paper samples are strongly hydrophobic and have an apparent contact angle of typically $110 - 125^\circ$ with water [75]. The Washburn Equation (Equation (1)) shows that if a paper surface sustains an apparent contact angle with a liquid of greater than 90° , then liquid penetration will not occur.

The new concept of creating microfluidic patterns on paper presented in this thesis is to generate the hydrophilic-hydrophobic contrast on the cellulose fibre surface by selectively hydrophobizing paper using sizing agents (here AKD and liquid AKD), rather than to build physical patterns using a polymer barrier reported by the Whitesides group [4]. Based on this concept, this work explores two novel μ PADs fabrication methods: 1) Treating the hydrophobized paper with plasma; 2) Printing sizing agents onto hydrophilic paper using an ink jet printer.

1.3.2.2 Plasma treatment

Plasma is an ionized gas with equal numbers of free positive and negative charges; the term, plasma, was first used by Lewi Tonks and Irving Langmuir in 1929 [86]. As a distinct fourth state of matter, plasma is the most abundant and common state of matter in the universe; but in the Earth's atmosphere plasma can be seen only under abnormal conditions (e.g. lightning). In spite of this, people can still create plasma in the laboratory or in an industrial environment by applying a high voltage to a gas.

The plasma process started to be applied for surface modification of materials in the 1970's, in the fields of microelectronics and semiconductors [87]. Since then, plasma processes have permeated to various scientific areas and industrial fields for traditional or innovative applications in polymers, textiles, microfluidics, paper, packaging, and so on. Plasma treatment affects surface properties such as wettability, adhesion and friction, as well as modifying molecular properties of only the outermost surface layers, and meanwhile preserving the beneficial physical chemistry characteristics of the bulk material [88].

Typically, in plasma processing, organic gases or vapors are partially ionized by an electric discharge even at room temperatures, which results in the creation of highly reactive species; otherwise those species can only be obtained at high temperatures through thermal excitation. Generation of reactive species at low temperatures is a significant advantage when treating paper fibres which will decompose at high temperatures [89].

There are two common types of plasma treatments available: vacuum (used in this thesis) and atmospheric plasma treatments. Vacuum plasma treatment requires the sample to be treated under low pressure in a chamber. A bleed gas is then introduced and ionized. The resulting surface changes depend on the composition of the surface and the gas used. Various gases have been used including oxygen, nitrogen, argon and air, with each producing a unique plasma composition and resulting in different surface properties [90].

Plasma-solid interactions can be generally divided into three groups: 1) Etching, by which material is removed from the solid surface; 2) Activation, by which the solid surface can be chemically and/or physically modified by species existing in the plasma; 3) Coating, by which material is deposited as a thin form on the solid surface (Figure 2) [91]. In this thesis, plasma etching and activation are used as the two modification techniques. Plasma etching employs a glow discharge to generate active species such as atoms or free radicals from molecular gases. These species diffuse to the substrate where they react with the surface molecules to produce volatile reaction products. Plasma etching is a well-mastered technique for patterning features larger than $0.2\ \mu\text{m}$, and for aspect ratio below 5 [92]. Plasma activation is a process where surface functional groups are replaced with different atoms or chemical groups from the plasma.

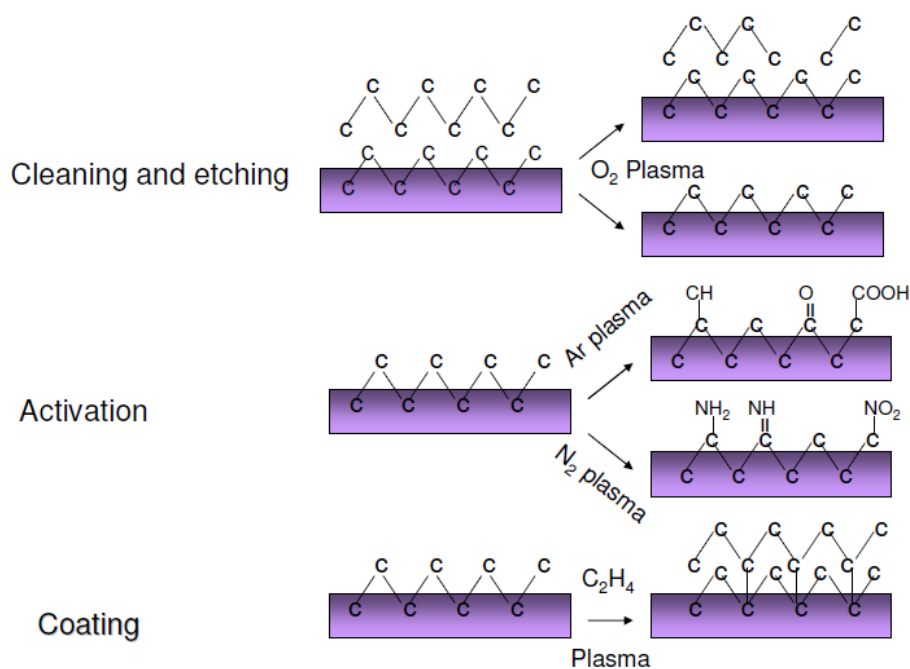


Figure 2: Examples of plasma-solid interactions including etching, activation and coating (with permission from ref [91]).

One advantage of plasma over the traditional wet chemistry treatments is that plasma is a dry, solventless and environmentally friendly process technology, producing an extremely low-level of industrial by-products [86]. Balamurali found that the popularity of using plasma-based technologies for cellulose treatment has been increasing exponentially in the last decades, based on his searching results of a large number of publications containing the terms “plasma” and “cellulose” (from ISI Web of Science

report) [89]. It needs to be noticed that, in the paper industry, atmospheric plasma and corona treatments have been applied at an industrial scale to change surface properties of papers in terms of wettability, surface energy and adhesion [93].

Several studies have reported the effects of low-pressure plasma on paper properties, summarized by Pykönen in a recent work [91]. These studies proved that hydrogen plasma can reduce the wettability of cellulose filter paper; oxygen plasma can oxidize the surface and increase the wettability of cellulose filter paper; both argon and oxygen low-pressure plasma can create oxygen-containing groups on cellulose filter paper, and the power and pressure of the treatment has a significant influence on the types of molecule groups created [91]. Vesel et al. (2007) showed that by exposing paper samples which contain ~10% of AKD to oxygen plasma, paper became strongly hydrophilic after only a one second treatment [94]. There was no significant degradation in the paper surface hydrophilicity after one month. They believe AKD degrades when it reacts with activated species in plasma, causing an increased hydrophilicity of paper.

1.3.2.3 Ink jet printing

To easily fabricate low-cost μ PADs, a suitable high-speed and mass-production manufacturing process is necessary. In addition, if this process can incorporate bioagents into the μ PADs during the fabrication of the devices, a fully-functionalized paper-based sensor can be created in a straightforward manner. The printing technology has been regarded as a suitable choice for delivering hydrophobization agents and bioagents onto paper surfaces in this thesis. Printing technology is generally divided into two groups: contact printing and non-contact printing, for each group there are various printing methods. Figure 3 lists a few representative methods in each group that have been used for bio- and functional-printing applications [47]. The non-contact printing methods favor a cleaner deposition process for the agents, reducing contamination risks and mechanical impact. Among different non-contact printing methods, ink jet printing technology has certain unique advantages in delivering bioactive reagent solutions onto a range of solid substrates, including small deposition volume (1 pL), fast speed, accurate placement, electronic pattern manipulation and high spatial resolution.

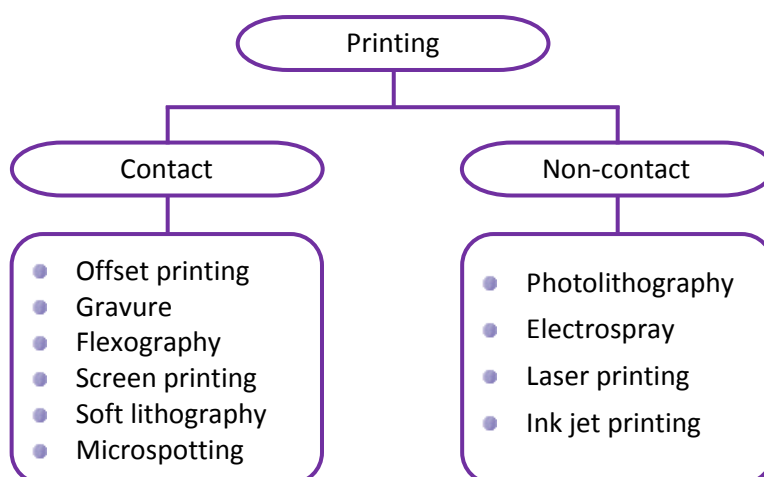


Figure 3: Different printing technologies: contact and non-contact printing (adapted with permission from ref [47]).

Based on different ink delivery and management concepts, there are two major ink jet printing technologies, continuous ink jet (CIJ) technology and drop-on-demand (DOD) technology [95]. In CIJ, ink droplets are continuously generated and ejected out of a nozzle; the desired printing pattern on a substrate is obtained by controlling, for example, an electric field in the ink droplet pathway. A droplet is allowed to pass the field and is deposited onto the substrate to form the printed pattern, or deflected into a gutter if it is not required. In DOD, the digital page data is fed to the nozzle so that an ink droplet is generated when it is required. Most office ink jet printers and laboratory ink jet printers are based on the DOD design.

The working mechanisms of DOD ink jet printers are based on either a thermal or a piezoelectric element driven by current or voltage signals to eject small ink droplets out of micro nozzles [95]. In thermal (or bubble) inkjet printing, resistive microheaters rapidly evaporate a small volume of ink which then drives a droplet of ink through a nozzle. Piezoelectric printers use voltage-controlled crystal deformation of piezoelectric actuators to dispense droplets [96].

Numerous studies have shown that different types of cheap office ink jet printers can be modified to dispense a variety of biomolecule solutions instead of ink [58, 97-99]. Meanwhile, many studies have proved that biomolecules (e.g. DNA, enzymes) or cells

can be printed without thermal degradation using a thermal ink jet printer [58, 98, 100-103]. Therefore, the study reported in this thesis selects the use of office thermal ink jet printers which are reconstructed to fabricate μ PADs. The reconstructed printer inherits the frugal ink management feature and fast printing speed of normal printers and is capable of depositing hydrophobization agents as well as the bioagents onto the paper surface, providing a cost-effective solution for fabricating μ PADs and paper-based sensors at a pilot scale.

1.3.3 Development of paper-based microfluidics

Paper has been used as low-cost chromatographic substrates since 1850 [104]. The development of diagnostics and biodetections based on paper strips started in 1950s which was driven by the fact that paper strip tests of biologically relevant species (e.g. glucose in urine) were as simple as pH paper test [105]. In the last decades, paper and other fibrous non-woven materials have been widely used as substrates for POC diagnostics [106]. Many paper strip tests are commercially available for POC diagnostics such as pregnancy tests. Although these strip tests are simple and low cost, they are not sufficient to operate multiple and quantitative analyses. In 2007, the Whitesides group introduced a new concept of fabricating μ PADs to simultaneously detect multiple analytes in a liquid sample [4].

The origins of the currently ascendant research on μ PADs can be traced back to 1949 when Müller et al. first created confined channels on paper for conducting preferential elution of pigments mixture within the channel. They patterned the filter paper by impregnating a paraffin barrier on it using a heated metal die; the resulting channel pattern on the paper restricted the flow of the sample within the channel (Figure 4) [107]. The authors observed that the confined channel sped up the diffusion process and reduced the sample consumption to smaller quantities.

However, this paper patterning concept has not been expanded until the Whitesides group reported the μ PADs as low-cost POC diagnostic tools. Compared with conventional microfluidic devices, μ PADs have advantages in that: 1) the device is sufficiently cheap and therefore disposable; 2) the sample transport within microfluidic channels does not need any external equipment owing to capillary action; 3) the device

is easy-to-use and can potentially be developed into devices operated by untrained users [4]. This new research area of creating μ PADs for simple, low-cost and low-volume bio/chemical/medical/environmental detections is currently flourishing with more than 80 research and review articles being published in high-impact authoritative journals up to January 2011. In general, these published works focus on: 1) Inventing novel, simpler and cheaper μ PADs fabrication concepts and methods; 2) Exploring efficient detection methods for μ PADs; 3) Finding new applications of μ PADs. The following reviews will mainly focus on these topics.

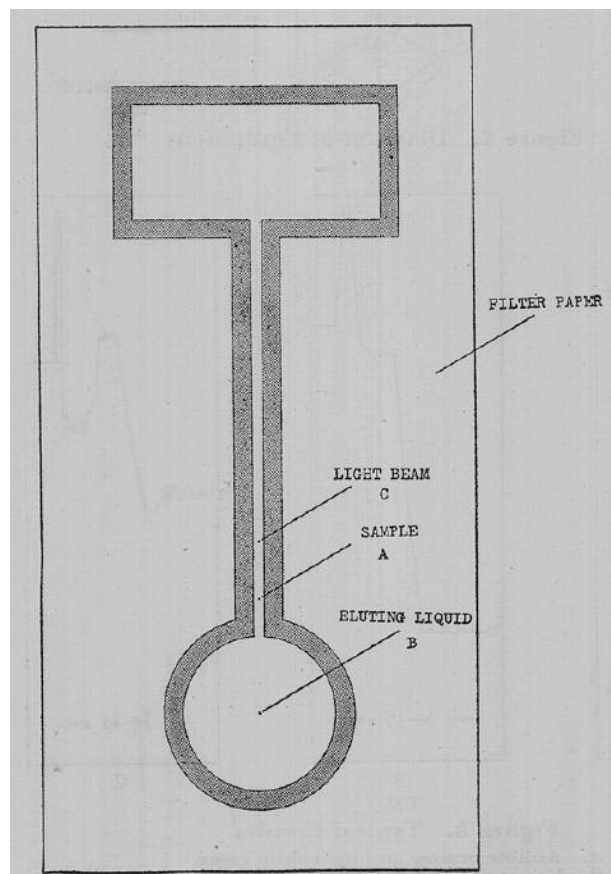


Figure 4: The first paper-based microfluidic channels created by impregnating paraffin on filter paper (with permission from ref [107]).

1.3.3.1 Fabrication technologies

A variety of μ PADs have been developed by researchers around the world. Basically, there are nine methods reported so far to fabricate μ PADs, including two methods firstly proposed in this thesis (i.e. plasma treatment and ink jet printing). All the methods have their own advantages and limitations; therefore, to choose the proper method, researchers and manufacturers should consider all the factors including equipment available to them, material costs, fabrication simplicity and future applications of μ PADs. In the author's personal opinion, the AKD ink jet printing and wax printing at present are the most promising methods for industrial-scale μ PADs manufacture due to the low cost of hydrophobization agents and easy and rapid fabrication process (both methods require only a single print and heat cycle to produce multiple μ PADs on an A4 sized piece of paper within 10 minutes). Though the resolution of channels built with these two methods is not as high as the photolithography method, the patterns are adequately well-defined for most applications of μ PADs. Besides, both methods have the potential to be upgraded to pilot or even larger scale processes by which paper could first go through an ink jet printer (or wax printer), then through an oven for heat treatment, and finally through other ink jet printers which can print detection reagents for assays or other applications. It can be envisaged that new fabrication methods will continuously emerge since this new research area continues to attract more and more interest. The subsequent parts review the nine fabrication methods reported so far, following the chronological sequence of their publication.

- Photolithography

The first μ PADs fabrication method proposed by Martinez et al. is demarcating barriers of photoresist on filter paper using photolithography [4]. The width of hydrophilic channels on paper can be achieved as narrow as 200 μ m reported from their following studies [108]. The μ PADs can efficiently guide the capillary penetration of liquids and, by incorporating indicators, can detect multiple chemical components simultaneous in a liquid sample. But there are some draw-backs of this patterning method as follows.

- a) Photolithography technology requires standard cleanroom, expensive materials and equipments. This method is therefore restricted to researchers who have access to such infrastructures.
- b) The photoresist SU-8 is much less flexible than paper, making μ PADs easily damaged by bending or folding [109].
- c) The patterning process is complex which includes several steps of baking, exposing, washing. Besides, an extra oxygen plasma treatment is required due to the altered wettability of paper affected by patterning. Therefore, other μ PADs fabrication methods are requisite to simplify the manufacturing process.

Using photolithography, 3D μ PADs have been built by stacking μ PADs and double-sided adhesive tapes [110]. 3D μ PADs, with complex microfluidic channels, expand the capabilities of low-cost paper-based analytical systems. 3D μ PADs can wick fluids and distribute microliter volumes of samples from single inlet points into arrays of detection zones (e.g., up to 1,024 detection zones if distribute 400 μ L of dye solutions).

The Whitesides group later introduced a fast lithographic activation of sheets (FLASH) method for prototyping μ PADs. This method is still based on photolithography, but eliminates the reliance on cleanroom or other specialized facilities [108]. More recently, Klasner et al. reported using a novel polymer blend to fabricate μ PADs through photolithography. This new polymer is cheaper than SU-8 and, shortens fabrication time and eliminates the additional plasma oxidation step [111].

- **Printing PDMS with x,y-plotter**

Bruzewicz et al. used a modified x,y-plotter to create barrier pattern by printing the “ink” of PDMS diluted in hexanes onto paper [109]. When PDMS penetrates into paper, it forms hydrophobic wall which defines the hydrophilic channels in paper. They chose PDMS instead of photoresist for the following reasons: PDMS is much cheaper than SU-8; it is an elastomer, which is more flexible than conventional photoresist. Different patterns have been created with the minimum resolution of ~ 1 mm of channel width. This method undeniably solved some problems existing in the photolithography method, but it also has shortcomings and brings new inconvenience for fabricating μ PADs.

- a) PDMS solution penetrates into paper easily due to the low surface tension of PDMS and its solvent. Paper is not a uniform porous material; the penetration cannot be well controlled after printing, causing deteriorated barrier definition.
- b) This patterning method cannot be readily or economically applied to high-throughput production to meet the requirement of large-scale and high-speed manufacturing.

- Etching polystyrene-modified paper

Abe et al. took a polystyrene (PS) solution impregnation approach to introduce hydrophobicity into the paper matrix. After paper was impregnated with PS, they used a microdrop dispensing device to print solvent (toluene) onto the impregnated paper to selectively dissolve PS and form fine liquid penetration channels. These authors also printed chemical sensing agents into μ PADs to form a functional device for biomedical detection [112]. This fabrication concept is similar to the above-mentioned barrier concept, since it relies on cellulose fibres in paper to be physically covered by a layer of hydrophobic polymer. A severe limitation of this method is that microfluidic channel could only be created after 10 times of printing of toluene, making this method impractical for large scale μ PADs fabrication.

- Plasma treatment

This thesis firstly reported the use of traditional paper sizing agents (e.g. AKD) to fabricate μ PADs with two steps: hydrophobizing paper with AKD and followed by the patterned dehydrophobization of paper using plasma [113]. Traditional papermaking technology has been introduced for the first time in this thesis to produce μ PADs; it, therefore, reveals a possibility to develop mass production methods using traditional and economic knowhow in paper industry. These commonly used paper sizing agents, compared with photoresist and other toners, dramatically reduces the fabrication cost of μ PADs. However, it has been noticed that for creating different patterns of μ PADs, different mask needs to be manufactured for plasma processing. Therefore, ink jet printing method was proposed in a later study of this thesis to reduce inconvenience of mask-making and simplify fabrication process [114]. The plasma treatment method is described in detail in Chapter 2.

- **Cutting**

Fenton et al. fabricated paper-based and nitrocellulose-based lateral flow devices using a computer-controlled X-Y knife plotter which shapes devices in two dimensions [45]. The shaped paper can readily be used in the assays, but usually it needs to be encased in tape to produce laminar composite. This cutting method has been used by Wang et al. in a more recent study [115].

- **Wax printing**

Wax printing is considered as a simple and inexpensive method for fabricating μ PADs. The commercially available wax printer prints the pattern of solid wax onto paper surface and the hot plate melts wax to form complete hydrophobic barriers. Lu et al. firstly demonstrated using this method to form well-defined millimeter-sized channels on hydrophilic papers [116]. Printed wax is initially only on the paper surface facing inkjet cartridge, therefore an additional heating step is needed. Wax will penetrate through the paper and diffuse laterally outward of the printed wax line when heated, thus the resulting channel width will become thinner than the original channel width. Carrilho et al. reported a similar work of printing μ PADs with wax, showing more complex designs such as 384-zone paper plates and 3D μ PADs [117]. This method has also been used by Leung et al. in a more recent work [118]. Wax printing is a simple fabrication process with fast production speed (5-10 min). In principle, the patterned paper can be produced in massive quantity using this method. The cost of the wax ink is claimed to be $\sim \$0.0001/\text{cm}^2$ of paper assuming 20% ink coverage.

- **AKD ink jet printing**

The study in this thesis firstly reported the combination of traditional papermaking technique with well-developed ink jet printing technology for fabricating μ PADs. This method prints the cellulose reactive AKD onto paper surface, followed by a brief heat treatment to cure AKD on paper. The pattern can be easily designed using computer with software such as Microsoft Word or Powerpoint. The reagents for bio/chemical assays can also be easily deposited onto μ PADs using ink jet printing. The color printer can deposit different inks onto different areas of paper, thus the modified printer is able to deposit a variety of reagents into sample transport channels and detection zones of μ PADs [114]. This method has been used by Delaney et al. in a latest study [119]. Chapter 3 presents this fabrication method in detail.

- **Flexography**

Olkkonen et al. reported using flexographic printing to print a solvent solution of polystyrene on paper to form liquid-guiding boundaries [120]. This method allows direct roll-to-roll production of liquid guiding barrier into paper substrates in existing printing houses and avoids the heat treatment of printed patterns. However, to obtain leaky-free channels, two prints of polystyrene solution on paper are required. Because different printing plates are required for different patterns, it is more difficult and time consuming of using flexographic printing to produce microfluidic patterns than using ink jet printing. A further draw-back of flexography is the print quality which relies on the smoothness of the paper surface. But excess smoothness treatment to paper surface may negatively influence fluid absorption.

- **Laser printing**

Laser treatment was used to selectively modify the surface structure and property of paper through hydrophobic surface coating from a most recent report. This method, although being claimed as a single step process, still requires paper to be hydrophobic before laser treatment, which uses similar fabrication principle as the plasma treatment method reported in this thesis, i.e. selective dehydrophobization. One advantage of this method is the high resolution ($62 \pm 1 \mu\text{m}$), but microchannels built using this method do not allow lateral diffusion/flow of aqueous reagents and have to be coated with silica microparticles for liquid transport, making the fabrication process complicated [121].

Other paper-based microfluidic systems include glue-bonded devices which diffuse glue into the cut-through paper and use gaps between the bonded-paper and glass (or PMMA) as 2D or 3D microchannels. Paper modified in this way is not used as liquid transport channels but as device fabrication templates [122].

1.3.3.2 Detection methods and innovative applications

Most work on μPADs is based on colorimetric detection chemistries which are related to enzymatic or chemical color-change reactions; alternative detection methods are also proposed in the literature, such as electrochemical or electrochemiluminescent-based detection. Referring to the ASSURED guideline (discussed in Section 1.2.2), the

preferred detection systems for μ PADs are those that give a visible indication and do not require expensive or complex instruments for detection and interpretation of results.

- Colorimetric detection

Colorimetric assays comprise of a robust category of readout methods requiring no instruments. In most cases, the analysis of results can be visually assessed by the unaided eye [123]. The colorimetric detection based on visual detection systems is adequate when a yes/no answer or semiquantitative detection is sufficient for diagnosis [124].

Martinez et al. first reported a rapid method of using μ PADs to simultaneously detect glucose and protein in an artificial urine sample (5 μ L) with established color reactions. Their work shows the feasibility and sensitivity of using μ PADs as POC diagnostic devices (Figure 5a) [4]. The bioassay results can be semiquantified by visually comparing the intensity of the color developed in different reaction spots. Matching color and color intensity can be achieved either by the unaided eye or by recording results with a camera or scanner and then analyzing color intensity with certain software (e.g. Adobe Photoshop, ImageJ) to generate a calibration curve. This colorimetric method of glucose and protein analysis has been used in many of the following studies to verify the practicability of new μ PADs fabrication methods and to show more new applications of μ PADs [45, 109-112, 116, 125-128].

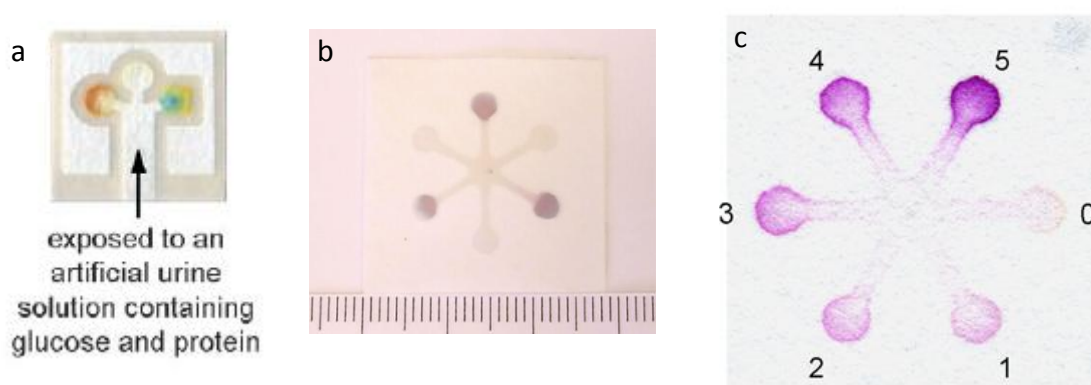


Figure 5: Colorimetric detections on μ PADs with different applications: (a) simultaneously glucose and protein tests (with permission from ref [4]); (b) concurrent active and deactivated enzyme detection; and (c) semiquantitative nitrite ion measurement.

The concept of combining colorimetric detection on μ PADs with mobile phone technology proposed by the Whitesides group can potentially make expert diagnosis available even in remote areas, through the realization of on-site detection and off-site diagnosis [125]. This concept takes advantage of the rapid increase in telecommunications and in the global mobile phone coverage. Most modern mobile phones have a built-in camera and email function, enabling patients to snap a photograph and send it to specialists who are equipped to analyze the results and transmit medical instructions back to patient [129]. This new diagnostic concept also encourages further development of mobile phone software to interpret colorimetric and other diagnostic signals.

In a more recent study, the Whitesides group used an inexpensive hand-held colorimeter to quantify signals generated on μ PADs [128]. They claimed that this transmission-based color detection was more sensitive in quantifying analytes present in the low micro- to picomolar concentration compared with the reflectance-based detection [128]. However, they admitted that the detection cannot work well in a dusty climate. Besides, Pelton pointed out that the ultimate goal for paper-based sensor research is to develop entities free of electronics [130].

This thesis firstly demonstrates the concurrent detection of active and deactivated enzyme (e.g. alkaline phosphatase) on μ PADs (Figure 5b) and the semiquantitative detection of uric acid and nitrite ions on μ PADs (Figure 5c) [113, 114, 131], all via colorimetric detection. Both uric acid and nitrite are important biomarkers for human disease [132]. Due to the influence of variations in lighting condition and paper surface brightness on colorimetric measurements, this thesis proposes an original concept of generating self-calibration curve for the analyte on one μ PAD, thus minimizing errors from external factors [131]. These studies will be presented in detail in Chapters 2 – 5.

Wang et al. integrated a self-calibration to μ PADs in order to collect sample and standard solution information at the same time. They used the integrated standard bovine serum albumin (BSA) solution to semiquantitatively detect an unknown concentration. The greatest advantage of this self-calibration strategy is that the standard reference gives users direct judgment without handling any standard solution [115]. However, the shelf-life data of the device has not been reported in their study. If

the color development of a standard reference changed after the device was stored over a long time, the unknown concentration measurement may be not accurate.

One problem of the traditional colorimetric readout is that the sensitivity is limited. Several studies on bioactive paper have proposed a few promising ideas to overcome this problem. One proposal is combining assay reagents with sol-gel materials to immobilize reagents on paper to enhance the detection sensitivity [51, 54, 55]. In this way, Hossain et al. developed a paper-based sensor which can detect organophosphate pesticides of nanomolar quantities in milk or lettuce by color changing [54]. Another proposal is using gold nanoparticle (AuNP) based colorimetric detection which can dramatically improve both the sensitivity and the specificity of detection [133]. Zhao et al. applied a AuNP colorimetric probe to paper-based assays for Deoxyribonuclease I (DNase I) and adenosine detection [53]. All these developments in improving the detection sensitivity and selectivity will make colorimetric assays more effective for μ PADs.

- **Electrochemical detection**

Electrochemical (EC) detection is one of the most widely used LOC techniques, which allows direct measurement of electrical signals from solutions, with minimal pretreatment of analytes. The sensitivity of EC detection is high, resulting from low interference from background noise and low limit of detection (LOD), enabling the successful detection and quantification in nM range. There are three main detection modes in EC techniques, amperometry, potentiometry and conductimetry; among them amperometric detection is the most widely applied method [123]. EC detection is simple and miniaturizable as demonstrated by glucose sensing systems that currently dominate the market. Electrochemistry – unlike colorimetry and spectrophotometry – is insensitive to local lighting conditions, therefore is less prone to interference from certain types of contaminants (suspended solids, colored materials) present in the samples [134]. Besides, the technology for the high volume production of inexpensive screen-printed electrodes (SPEs) is also very well advanced; many different designs are available commercially [119].

Dungchai et al. first reported the detection of glucose, lactate and uric acid in biological samples using μ PADs with EC detection [135]. They printed electrodes onto μ PADs

using screen printing; one single electrode type is adequate for multiple species detection (Figure 6). EC detection provides high sensitivity and selectivity to analyses on μ PADs, which is particularly necessary when analytes are of low levels.

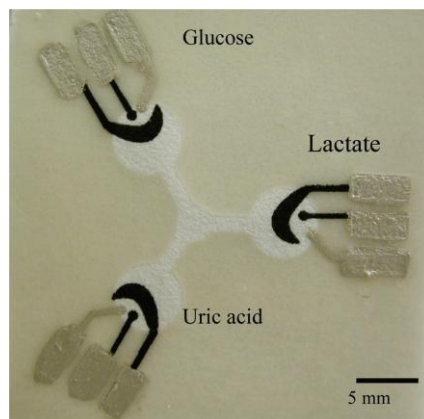


Figure 6: Picture of three-electrode μ PAD. The hydrophilic area at the center of the device wicks sample into the three separate test zones where independent enzyme reactions occur. The silver electrodes and contact pads are made from Ag/AgCl paste with the black electrode portions being the Prussian Blue (PB)-modified carbon electrodes (device size is 4 cm \times 4 cm) (with permission from ref [135]).

Nie et al. combined EC μ PADs with commercially available hand-held glucometers to conduct rapid and quantitative EC analysis of metabolites such as glucose, cholesterol and lactate. Using glucometers as readers for EC μ PADs increases the applications of μ PADs in resource-limited settings [134].

Tan et al. demonstrated a one-step, quantitative trace Pb(II) detection on EC μ PADs [136]. They prestored the internal standard on a filter paper disk, thus avoiding the need to dispense liquid reagents into a test cartridge before or during processing of the assay and to run a series of standard measurements for calibration purposes. The μ PADs can be brought to the field for Pb(II) level detection with a portable voltammetric analyzer.

Apilux et al. reported the use of μ PADs for determining Au(III) in industrial (gold refining) waste solutions by combining EC detection with colorimetric detection. Fe(III) is the only metal that interferes the EC detection of Au(III) when present above a 2.5-fold excess concentration to that of the Au(III), therefore a colorimetric detection was used to detect Fe(III) in order to eliminate this interference [137].

- Electrochemiluminescence detection

Fluorescence, chemiluminescence (CL) and electrochemiluminescence (ECL) are the most common optical detection methods in microfluidics. Among them, ECL is attractive; it combines advantages of luminescence and EC techniques, and provides added selectivity. Typically, ECL relies on luminescence from excited molecules generated by EC redox reactions [123]. Unlike colorimetric detection, ECL is performed in the dark and is independent of ambient light.

Delaney et al. reported the first approach of conducting ECL detection on μ PADs. SPEs were integrated into μ PADs to create cheap and disposable ECL sensors. The sensing mechanism is based on the bright orange luminescence generated from the ECL reaction of tris (2,2'-bipyridyl) ruthenium (II) (the best known ECL reagent) with certain analytes such as nicotinamide adenine dinucleotide (NADH). NADH is an important biological compound and is found in over 250 biological pathways [119]. These ECL sensors can be read with a conventional photodetector or a mobile camera phone (Figure 7).

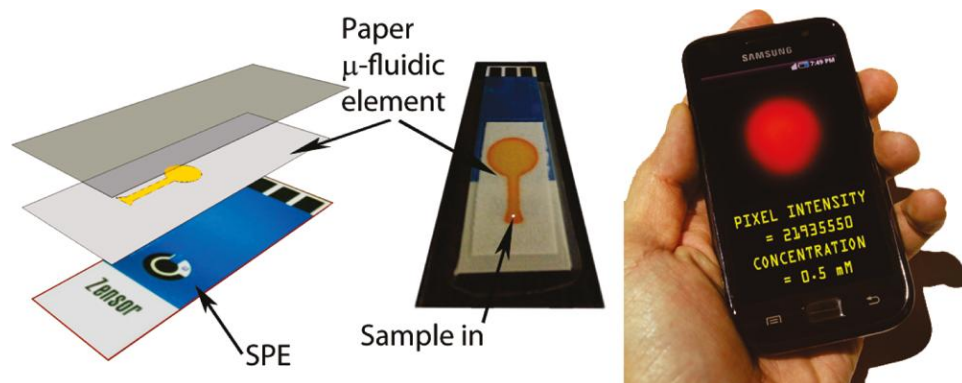


Figure 7: Fabrication and operation of an ECL μ PAD. The individual μ PAD is filled with a 10 mM $\text{Ru}(\text{bpy})_3^{2+}$ solution before drying, and is then aligned and fixed onto the face of the SPE by laminating with transparent plastic. A drop of sample is introduced through a small aperture in the plastic at the base of the channel, and when the detection zone is fully wetted, the sensor is placed close to the lens of the camera phone, a potential of 1.25 V is applied, and the resulting emission is captured and analyzed (with permission from ref [119]).

- **Streaming potential measurement**

Leung et al. reported the use of streaming potential measurement for monitoring the adsorption of charged molecules onto hydrophilic channels in μ PADs. Their work showed that the polarity and magnitude of the measured potentials are sensitive to the presence of charged polymers adsorbed on the surfaces of the hydrophilic channels. They predicted that the streaming potential measurement could provide an electrical interface for μ PADs and the binding of biological targets to receptors conjugated to the cellulose surface could be detected using this method [118].

- **Functional elements on μ PADs**

Simple analyte-detection μ PADs can be used for many applications, but more complex devices are required where there are multiple steps involved in the analysis/diagnosis, such as the premixing of chemicals before the final reaction. In these cases, functional elements can be incorporated into μ PADs to expand the device functions.

1) Paper-based separators

This thesis proposes the use of μ PADs as separation/filter devices by coating additional agents onto the separation strip in μ PADs. Different chemical components in the sample solution can be separated using these paper-based separators [113]. This innovative concept has been highlighted in the journal *Lab on a Chip* [138]. The detailed description of this study can be found in Chapter 2.

In a later study, Carvalhal et al. demonstrated the simultaneous separation and quantification of electroactive compounds such as ascorbic acid and uric acids from aqueous mixtures on microfluidic paper-based separation devices (μ PSDs) by combining paper chromatography with EC detection. The ionic strength of the eluent buffer has a strong effect on the peak height of analytes, and therefore it needs control to achieve the measurement repeatability. The integration of gold electrodes to μ PSDs for EC detection will certainly increase the device cost, which may compromise the distinguishing features of μ PADs such as low cost [139].

2) Paper-based switches and reactors

The concept of building switches and reactors into μ PADs is firstly introduced in this thesis in order to enhance the capabilities of μ PADs by giving analytes enough reaction

time in multi-step reactions [113]. Many colorimetric assays used in the clinic require sequential mixing of reagents with analyte and require defined incubation time at each step. The paper-based switch concept will help the conduction of multi-step assays on μ PADs without increasing the device cost. One design shown in a WO patent generated from this work is using paper/film/paper composite to build a control switch (Figure 8) [140].

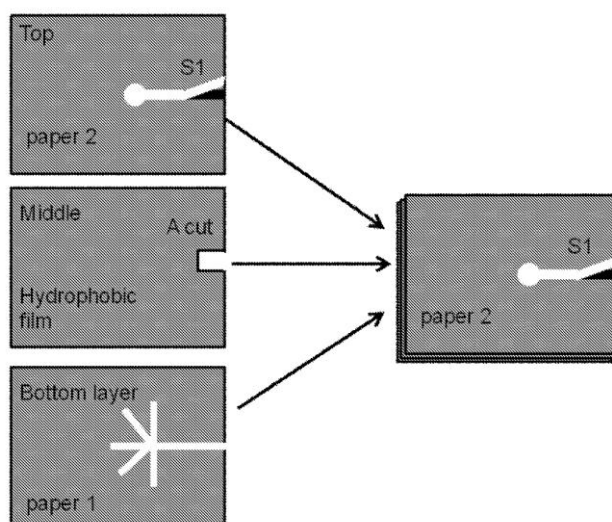


Figure 8: 3D microfluidic device with control switch. Hydrophilic channels are formed on both the top and bottom sheets of papers. On the top paper sheet the hydrophilic channel is cut as shown so that they can be moved (S1). A hydrophobic medium in sheet or film form with a cut notch (or a hole, not shown) is sandwiched in between the two sheets. By aligning the channels on the paper sheets with the notch in the hydrophobic medium, a switch can be formed. The operation of the switch involves pushing the switch (S1) down to make contact with the hydrophilic channel in the bottom paper sheet through the notch in the hydrophobic film.

Martinez et al. reported a programmable 3D μ PADs made from paper and tape [141]. These μ PADs are programmed by pressing single-use ‘on’ buttons, using a stylus or a ballpoint pen to generate multiple patterns of flow through them. Pressing a button closes a small gap between two vertically aligned microfluidic channels, allowing fluids to wick from one channel to the other. These μ PADs, with the similar fluid flow control concept, i.e. paper-based switches proposed in this thesis, provide an alternative way to control the fluids movement in paper-based microfluidic channels.

The research group led by Paul Yager has executed comprehensive studies on the characterization of fluid flow in paper-based microfluidic channels and on controlled liquid sample transport [142-145]. The group led by Scott Phillips described one method to control when and how quickly a fluid is distributed into detection zones by integrating paraffin wax into μ PADs as fluidic timers [146, 147].

- Other innovative applications of μ PADs

MicroPADs have been used as a template for fabricating thin materials such as films of ionotropic hydrogels [148-151]. The thin structures of ionotropic hydrogels are used in drug delivery, for encapsulation of cells and as sorbents for toxic metals in wound dressings. MicroPADs have also been used as a stamp for the contact printing of biochemicals such as reagents, antigens, proteins and DNA onto planar substrates [152]. Another interesting application of μ PADs is using them as a flexible substrate for rapidly prototyping PDMS microdevices. This method could simplify the operation procedures and reduce the fabrication cost of PDMS microdevices [153].

The μ PADs fabrication technique has been used for fabricating paper-based microzone plates (e.g. 96-microzone plates) which could serve as alternatives to plastic microtiter plates. [46]. Paper-based microzone plates are made by patterning a sheet of paper into an array of circular or square test zones with the same dimensions and distribution as the wells in a plastic plate. They can be used to perform enzyme-linked immunosorbent assays (ELISA) [154, 155]. Compared with conventional ELISA, paper-based ELISA is faster and less expensive, though less sensitive.

Currently there are several organizations that aim to develop and commercialize paper-based diagnostic technologies in order to facilitate this rising field of innovation. A few representatives include the US-based Diagnostics for All (DFA), the Canadian government sponsored SENTINEL Bioactive Paper Network, the Finland's VTT Technical Research Centre Bioactive Paper project, and the recent established Bioresource Processing Research Institute of Australia (BioPRIA) which is a part of the Australian Pulp and Paper Institute (APPI) [156].

It needs, however, to be pointed out that, like any other new technologies, paper-based microfluidic technology also has some limitations. These limitations are related to either the material properties of paper or the fabrication technologies of μ PADs. Specifically, these limitations include the following: 1) The poor wet strength makes μ PADs easily break after being wetted by aqueous samples and reagents; 2) Some hydrophobization agents for creating μ PADs cannot build the hydrophobic barriers strong enough to withstand samples of extreme low surface tension; 3) The 3D μ PADs fabrication method reported so far requires a complicated process involving the stacking layers of μ PADs and tapes. These limitations inspire the author to explore other cheap materials and fabrication methods for creating new types of low-cost microfluidic systems; one such system is the thread-based microfluidic system presented in this thesis.

1.4 Thread-Based Microfluidics

1.4.1 General characteristics of thread

In the textile industry the term “thread” refers to a fine cord of twisted fibres used in sewing and weaving. Fibres can be either natural or synthetic (i.e. man-made). Commonly used natural fibres include raw cotton, wool, silk, etc., while synthetic fibres include polyester, nylon, polyacrylic and others made from natural polymers or derived from synthesized polymers [157].

This thesis, for the first time, reported the use of thread for fabricating low-cost microfluidic thread-based analytical devices (μ TADs). MicroTADs have great potential to be used for applications such as biomarker detection and blood grouping due to the excellent characteristics of thread. Some of those desirable characteristics are as follows: 1) Thread is very cheap, universal and physically flexible; it can be manufactured and manipulated almost all over the world. This provides the potential for fabricating μ TADs in massive quantities; 2) Gaps between thread fibres provide capillary channels for liquid transport along thread, thus avoiding the requirement of external power sources or pumps. For threads which are not hydrophilic enough for liquid wicking, they can be treated using industrial-scale plasma treatment or mercerization to become more hydrophilic; 3) Thread-based microfluidic channels do not rely on hydrophobic boundaries; therefore less sophisticated equipments are required to fabricate μ TADs and 3D μ TADs compared with μ PADs; 4) Thread fibres are usually white and can be stained, presenting a suitable background for color display. 5) Thread can be functionalized using established chemistries, providing more functional devices for chemical/biomedical/environmental analyses; 6) Thread has higher wet strength compared with paper, making it resistant to breakage when conducting the flow of aqueous solutions under certain conditions; 7) Thread is lightweight, and therefore can be easily transported and stored; 8) Thread fibres are combustible, making μ TADs disposable by incineration.

In this thesis, cotton and polyester threads have been chosen to fabricate μ TADs as they are made from the most important and broadly used natural and synthetic fibres –

cotton and polyester fibres. The following parts will depict the general properties of both cotton and polyester fibres as well as their medical applications.

1.4.1.1 Cotton fibre

The use of cotton predates recorded history. Cotton is grown in about 80 countries and it was reported that in 2004 developing countries accounted for about 75% of the global production [158]. Cotton fibre is the most important natural vegetable textile fibre used in spinning to produce apparel, home furnishings and industrial products [159]. In 2009, cotton fibre consumption accounted for ~36% of the textile fibres consumed worldwide [160]. The prime position of cotton fibre among textile fibres is due to its capacity to withstand chemical damage during processing.

Cotton fibre is a single and complete biological cell that develops in the epidermis of the seed coat around the time the flower opens. The width and length of cotton fibre are typically 15-24 μm and 12-60 mm, respectively. The mature cotton fibre is a dead, hollow, dried cell wall. In the dried out fibre, the tubular structure is collapsed, shriveled, and twisted, giving cotton fibre convolutions which differentiate cotton fibre from all other forms of seed hairs and are partially responsible for several distinctive characteristics of cotton fibre, for example, the natural interlocking of fibres in a thread during spinning.

Raw cotton fibre after ginning and mechanical cleaning is composed almost entirely (95%) of the polysaccharide cellulose which is a 1-4 linked linear polymer of β -D-glucopyranose. The chains of cellulose molecules associate with each other to form microfibrils by forming intermolecular hydrogen bonds and hydrophobic bonds. Microfibrils organize into macrofibrils (60-300 nm wide), which are further arranged into fibres with a complex, reversing, helical organization. The noncellulosic constituents of raw cotton fibre are mainly located in the primary wall. These constituents consist mostly of waxes, pectinaceous substances, and nitrogenous matter (mainly protein) [158]. Cotton wax provides a protective barrier to water penetration and microbial degradation of the underlying polysaccharides; it also serves as a lubricant in manufacturing. After spinning and weaving or knitting, wax is removed by scouring and bleaching in preparation for dyeing and finishing.

Mercerization, as one commercial treatment, improves cotton thread properties such as dye affinity, chemical reactivity, tensile strength, luster, and smoothness of the cotton fabrics produced. Another useful surface treatment of cotton cellulose is plasma treatment which increases water absorbency and strength of cotton fabric. Light microscopy shows a smoother surface of cotton fabric after low pressure plasma treatment, while SEM (scanning electron microscopy) shows no change from native cotton. FTIR (Fourier transform infrared spectroscopy) analysis shows some oxidation of the treated cotton, with a decreased carbon/oxygen ratio [159].

Cotton thread is dyeable with an extensive number of dye classes; it also can be colored with pigments [158]. These properties make cotton thread as a suitable substrate to display color changes for colorimetric detections.

1.4.1.2 Polyester fibre

Polyester fibre is the largest volume synthetic fibre produced in the world. The total volume of synthetic fibres produced worldwide in 2009 was around 40.3 million metric tons, while polyester fibre production accounted for 79% in the total production [160]. The fibre-forming substance in polyester fibre is any long-chain synthetic polymer composed of at least 85 wt % of an ester of a dihydric alcohol (HOROH) and terephthalic acid (TA, p -HOOC C_6H_4 COOH). Polyester fibre is smooth, crisp and resilient. The most widely used polyester fibre is made from linear poly(ethylene terephthalate) (PET) (Figure 9).

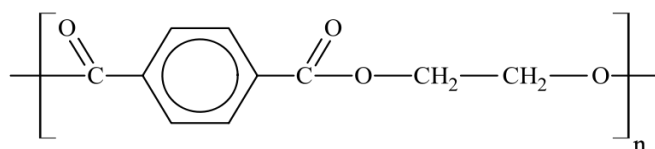


Figure 9: The structure formula of PET.

Other polyesters which are commercially produced in fibre form, including poly(ethylene naphthalate) (PEN), poly(butylene terephthalate) (PBT), poly(propylene terephthalate) (PPT), poly(lactic acid) (PLA), are of insignificant volume compared to PET [158]. Reasons for the dominating success of PET fibre are: 1) low cost, 2)

convenient processability, 3) high strength, and 4) excellent and tailorable performance. PET is chemically stable and virtually nonbiodegradable. In comparison between in vitro toxicity and in vivo fibrinogenicity for various polymer and mineral dusts, PET exhibits the lowest effects [157]. It is likely that PET will continue to dominate as the synthetic fibre of choice in future.

The development of PET fibre began with the pioneering work on condensation polymers led by W.H. Carothers of Dupont in the 1930s. Commercialization of PET was rapid after World War II with the introduction of Terylene in Great Britain by ICI and the introduction of Dacron in the United States [158]. PET is the condensation product of TA and ethylene glycol. The preferred PET synthesis method is the direct esterification of TA. The development of low-cost and pure TA from mixed xylenes by Amoco Company in the mid-20th century enabled the cost-effective polymerization of PET. Ethylene glycol is a material of major commercial significance. The large-scale production of both monomers assures low-cost PET and makes competition from new compositions of fibre-forming polymers very difficult [158].

Polyester fibres can be used for a great number of purposes; the major applications include the following three areas: (i) apparel: every form of clothing; (ii) home furnishings: carpets, curtains, draperies, sheets; (iii) other uses: hoses, power belting, ropes and nets, surgeon's gowns, fibrous prostheses [161].

1.4.2 Medical applications of thread

Apart from general uses (e.g. apparel, household products) of textiles made from fibres, medical textile, as an important technical textile, has been used in the medical field for a long time, though the term has been coined only very recently [162]. The first recorded use of fibres in medicine was in the form of “surgical papyrus” nearly 4000 years ago. As more research has been completed, constant improvements and innovations in textile technology and medical procedures have resulted in recent decades witnessing major development in medical textile production.

All fibres used for medical purposes must be non-allergenic, non-carcinogenic, non-toxic, and antistatic in nature with optimum fatigue endurance and bio-compatibility, as

well as being flame-proof. In general, medical fibres are used as both non-implantable and implantable materials, with the specific applications of each having been summarized by Rigby et al [163]. The non-implantable materials are used for external applications on the body and may or may not make contact with skin. The implantable materials are used in body repair for wound closure or replacement surgery. Fibres have also been widely used to produce healthcare/hygiene products, such as bedding, clothing, surgical gowns, cloths, wipes. Some types of fibres can even be applied to build extracorporeal devices which are mechanical organs (e.g. artificial kidney, liver and medical lung) used for blood purification. Among all available medical fibres, cotton is a commonly used natural fibre in non-implantable materials and healthcare/hygiene products. While polyester is a commonly used synthetic fibre for a wide variety of products and specific applications [163].

During the last few years, novel medical textile products, for example sensor embedded fabrics, have been developed as diagnostic and health monitoring tools for healthcare applications [164]. The integration of textile with biomedical sensors and mobile telecommunication devices represents a great opportunity for research, healthcare and health provision as it possesses high market potential. Such “sensitive” fabrics and garments containing sensors and conductive fibres are usually termed as “wearable electronics” or “intelligent textiles”. They can be interfaced with microprocessors for noninvasively monitoring physiological, biochemical, emotional and physical parameters. These intelligent wearable systems provide the possibility of making daily life healthier, safer and more comfortable [165-170].

Medical textiles have attracted considerable attention; a variety of fibre/thread-based intelligent systems have been developed for improving human health. Researchers should continue to explore more diagnostic applications of textile fibres and threads. For this reason, the study reported in this thesis investigates the use of thread (cotton and polyester threads) for fabricating new microfluidic diagnostic devices which have the potential to benefit people, especially those from the developing world, by improving their healthcare conditions, as well as to stimulate the development of traditional textile industry.

1.4.3 Development of thread-based microfluidics

The physical and liquid transport properties, as well as the color display property make thread intuitively suitable for making microfluidic sensors. Besides these intrinsic properties, thread does not require any physical or chemical barrier to act as a liquid transport channel, making it a much more convenient material to make 3D microfluidic systems than paper. In addition, compared to the pore structures in paper, pores in thread are generated by interfibre gaps. These gaps, like fibres, are in a helical form going along the thread; meaning liquid transport in thread faces fewer obstacles and therefore requires a lower number of changes between channels compared with liquid transport in paper. As a result, liquid transport in thread may be more efficient than in paper.

Liquid transport in multi-filament threads has been investigated by a number of research groups. Perwuelz et al. reported that the Washburn model can provide a general first order description to liquid penetration behavior along threads [171]. Ferrero studied liquid penetration using the capillary rise approach. He considered the gravity influence and showed that the Washburn model can be used to predict liquid transport behavior [172]. Wang et al. considered the helical nature of the interfibre gaps in a multi-filament thread and showed that the general trend of liquid penetration along a thread follows trend predicted by the Washburn model [173].

Like liquid penetration in paper, liquid penetration along thread is also sensitively affected by the apparent contact angle between the penetrating liquid and thread. The measurement of the apparent liquid contact angle with thread is much more difficult than that with paper, due to the small size of thread. In this thesis, the method reported by Aspler and later by Nisbet et al. [174] is employed to measure the wettability of a thread by a liquid. This method is based on the matching of the liquid surface tension to the surface free energy of the thread. In situations where the liquid surface tension is greater than the surface free energy of the thread, penetration will not occur. Conversely, if the liquid surface tension is lower than the surface free energy of the thread, penetration will proceed. A more detailed experimental methodology will be presented in Chapter 6.

Safavieh et al. reported the possibility of creating complex microfluidic circuits with hydrophilic, hydrophobic and selectively coated cotton yarns in 2009 [175]. This thesis concurrently reported the use of threads to fabricate microfluidic devices (see Chapter 6). Compared with the work of Safavieh et al. which only shows the liquid (food dye solutions in their work) transport properties on the thread, this thesis, for the first time, presents the analytical and diagnostic capabilities of thread-based microfluidic devices.

In this thesis, low-cost and easy-to-use μ TADs and 3D μ TADs have firstly been fabricated using cotton and polyester threads and been applied to perform bioassays, for example, semiquantitative detection of biomarkers such as nitrite ions [176]. Furthermore, μ TADs have been used as a diagnostic tool for easy and rapid blood grouping which only requires a small amount of whole blood (e.g. 2 μ L is sufficient for ABO and Rh blood typing) from a pricked finger without handling any buffer or reagent solution (Chapter 7) [177]. Due to the significance of this application, the principle of blood grouping and existing blood grouping methods are discussed in the following subsection (1.4.4). Moreover, the liquid penetration behavior along single or twined threads and the building of functional elements (e.g. microswitches, microselectors, micromixers) on μ TADs have been investigated thoroughly in this thesis. These studies provide a better understanding on thread-based microfluidic networks and offer innovative design concepts to μ TADs, enabling them to have more functions and applications [178].

The Whitesides group also reported the application of μ TADs in bioassays [179], which followed the similar detection concept shown in Chapter 6 in this thesis, and therefore will not be discussed in detail here.

1.4.4 Blood grouping and existing blood grouping methods

As mentioned above, blood grouping on μ TADs is a unique and important diagnostic application of μ TADs proposed in this thesis. Therefore, the history, principle and importance of blood grouping are discussed in this subsection.

Blood is a sophisticated and highly specialized fluid used by the body to transport nutrients to and wastes from cells. Though comprised of numerous components, blood can be simply described as being cells suspended in a liquid called blood serum or plasma. The cells can be separated into red and white cells, and blood platelets, with red cells transporting oxygen and carbon dioxide during respiration, white cells providing immunological resistance to infectious diseases and platelets being cell fragments which contribute to the clotting of blood from damaged blood vessels [180]. These and a myriad of other functions performed by blood make it vital to human life, and for this reason blood is constantly needed across the globe, with millions requiring life saving transfusions every year [181].

The correct grouping of human blood is important for a variety of reasons, most importantly for transfusion compatibility. The term “blood group” or “blood type” is a classification of an individual’s blood based upon the inherent presence or absence of antigens on the surface of their red blood cells (RBCs) [182]. An antigen is any substance to which the immune system can respond [180]. “Self” antigens, naturally produced by a person’s body, are tolerated by the immune system of this person. In blood plasma, antibodies are formed against foreign antigens to protect the body from perceived threats. This reciprocal relationship is known as Landsteiner’s Law, the consequence of which is that individuals who lack an RBC antigen possess the corresponding serum antibody, whilst those who possess the antigen must not [183].

Blood transfusion has been attempted since the 17th century, but the poor understanding of blood and its immunological functions prevented successful and safe transfusion. It was not until the discovery of blood agglutinins and hence the ABO blood group system (the root of which is the A and B antigens) in 1901 by Karl

Landsteiner that blood transfusions became relatively safe [184]. Landsteiner noticed that mixing the blood of two individuals often caused agglutination, and identified that this was caused specifically by contact with the blood serum. He recognized three groups of blood: A, B and C (later renamed O), and found that between members of the same group no agglutination occurred upon mixing [185]. The AB group was identified in the following year [186]. Further work by Landsteiner et al. in 1940 yielded the discovery of the Rh blood system (a complex system involving many antigens but primarily governed by the D antigen), also significant in evaluating transfusion compatibility and for preventing hemolytic disease of the newborn [187]. It was these works that led to the first safe transfusion of blood between humans, and eventually to the development of the “blood banks”.

To date there have been 30 discrete blood type systems recognized by the ISBT Committee on Terminology for Red Cell Surface Antigens [188], with the most commonly known being the ABO and Rh systems. These two systems are of primary importance when transfusing blood to a patient, as the transfusion of incompatible blood is likely to cause a potentially fatal hemolytic reaction [180]. Hemolytic reactions are caused by the recipient’s own serum antibodies destroying the foreign donor RBCs being transfused into their body. Without ABO compatibility testing, around one-third of unscreened blood transfusions would be expected to cause a hemolytic transfusion reaction [188]. For these reasons, the correct ABO and Rh grouping of blood is imperative before a blood transfusion is performed. Most techniques applied for ABO and Rh blood grouping are based upon the principle of hemagglutination reactions between RBCs and serum antibodies. The absence of agglutination indicates no hemagglutination reaction [189].

Commonly used blood grouping tests in hospitals and laboratories include the slide test [190], tube test [191], micro plate method [192-194], and the column agglutination system [195, 196]. These tests, as they either require specific antibody to be added during test, or need to be performed by well-trained personnel with centrifugation, are difficult to carry out away from the central laboratory or hospital setting, and therefore, are not suitable for field use in resource-limited areas or for emergency blood typing. Commercially available blood typing systems such as lateral flow devices [197] and

bedside test cards [198], though rapid and without the need for expensive equipment, always require the pre-treatment of the blood sample or the reconstitution of antibodies with water or saline. A recent study which performed blood typing on antibody-coated paper strips avoids the pre-treatment of the blood sample, but with the blood sample required for ABO and Rh grouping being 20 μL , venipuncture is still necessary [199]. In order to overcome limitations in these blood grouping methods, this thesis proposes a new blood grouping platform, by virtue of the porous nature of threads, to determine blood groups in a simpler and more inexpensive way as well as with low sample consumptions.

1.5 Research Objectives and Aims

The overall objective of this research is to use cheap and universal materials to develop low-cost and easy-to-use microfluidic POC devices, with which health monitoring and disease screening can be performed for people living in the developing world with limited resources who cannot afford expensive microfluidic devices.

In particular, the specific objectives of this study are:

1. To explore novel concepts for building novel low-cost microfluidic devices as POC testing tools for people in the developing world and resource limited areas;
2. To investigate new fabrication technologies of μ PADs by adapting the existing papermaking techniques and investigate more diagnostic applications of μ PADs;
3. To explore the capability of using thread as the base material to create μ TADs and evaluate the practicability of using μ TADs as low-cost analytical devices;
4. To investigate more diagnostic applications of μ TADs as POC testing tools for people in the developing countries;
5. To analyze the liquid penetration behavior on threads to give a better understanding of the thread-based microfluidic networks; and
6. To integrate functional elements (e.g. switches, selectors, separators) onto μ PADs and μ TADs to build devices with more functions for more applications such as multistep analysis.

1.6 Thesis Outline

This thesis reports the development of two low-cost microfluidic systems for providing people living in the developing world with cheap and easy-to-use diagnostic tools to improve their state of health and the quality of life. The two systems are presented in two individual parts. Part I which is reported in Chapters 2-5 focuses on the investigation of microfluidic paper-based analytical devices (μ PADs); and Part II which is reported in Chapters 6-8 illustrates the development of microfluidic thread-based analytical devices (μ TADs).

This thesis is presented in the format of “Thesis by Publication” based on the Monash University Handbook for Doctoral and MPhil Degrees 2011 [200] and the Thesis by Published and Unpublished papers (Monash Research Graduate School) [201]. Part I consists of four published studies with one publication presented in each chapter, while Part II has three published studies with one publication presented in each chapter. As the thesis is submitted in this way, all published papers are reformatted to generate a consistent presentation within the thesis, whilst the content remains unchanged. The original publications are given in Appendix I.

Part I Paper-Based Microfluidics

Chapter 2: Paper-Based Microfluidic Devices by Plasma Treatment

(Published in *Analytical Chemistry*)

This chapter reports an innovation in which plasma treatment technology is used for fabricating μ PADs. This new fabrication concept combines the conventional AKD sizing technique with plasma treatment technology to produce μ PADs in only two steps. First paper samples are hydrophobized by AKD sizing and then paper samples are selectively dehydrophobized by plasma treatment. This fabrication concept not only enables μ PADs to be easily fabricated at low cost, but also allows μ PADs to retain the flexibility of paper. A major advantage of μ PADs produced using this fabrication concept is that simple functional elements such as control switches and separators can be built into μ PADs. These elements are important for multiple-step chemical tests.

Chapter 3: Fabrication of Paper-Based Microfluidic Sensors by Printing

(Published in *Colloids and Surfaces B: Biointerfaces*)

This chapter reports an innovation in which ink jet printing technology is used for fabricating μ PADs. This novel fabrication concept produces μ PADs in just one step, where paper samples are selectively hydrophobized by printing paper sizing agents “ink” onto the paper surface using a modified ink jet printer. One advantage of this fabrication method is that it allows a variety of microfluidic patterns to be created by designing digital patterns using conventional computer software. Another advantage of this method is that it can be scaled up by using high speed, high volume and low cost commercial printing technology. This chapter further reports that by printing bioagents “ink” onto μ PADs in a second printing step, complete paper-based microfluidic sensors are easily produced which include both microfluidic patterns and detection chemistries. Such microfluidic sensors can be directly used for diagnostics.

Chapter 4: Quantitative Biomarker Assay with Microfluidic Paper-Based Analytical Devices

(Published in *Analytical and Bioanalytical Chemistry*)

This chapter describes the use of a single μ PAD which has multiple detection zones to perform semiquantitative and quantitative diagnostic tests. In the test, the first step is to individually deposit a series of standard solutions and the unknown sample into each detection zone, and the second step is to introduce an indicator solution from the μ PAD inlet to each detection zone. As a result of the colorimetric reaction in each zone, the color changes can be correlated to the biomarker concentration of the standard solutions and the unknown sample. A calibration curve is generated by plotting the color intensity versus the biomarker concentration of standard solutions. This calibration curve is used for establishing the biomarker concentration of the unknown sample. A key advantage of this test principle is that it reduces errors introduced from different background colors of different μ PADs and from color measurement devices, because all the solutions are simultaneously assayed on the same μ PAD.

Chapter 5: Progress in Patterned Paper Sizing for Fabrication of Paper-Based Microfluidic Sensors

(Published in *Cellulose*)

This chapter reports the progress in using paper sizing chemistry to fabricate μ PADs for chemical and biological sensing applications. This chapter first outlines the fundamental principle underlying the fabrication concepts of the two μ PADs, i.e. plasma treatment and ink jet printing proposed in Chapter 2 and 3. This common principle is that the hydrophilic-hydrophobic contrast is created on a paper surface using paper sizing agents to form microfluidic channels on the paper. This chapter further compares the different fabrication processes in plasma treatment and ink jet printing, and outlines the unique characters of μ PADs fabricated using these two processes. Moreover, this chapter summarizes a variety of analytical and diagnostic applications of μ PADs. Finally, this chapter compares the material cost of producing μ PADs with different fabrication methods, including the two methods proposed in this thesis and methods reported by other groups, showing the advantage of the fabrication concepts in this thesis over other concepts.

Part II Thread-Based Microfluidics

Chapter 6: Thread as a Versatile Material for Low-Cost Microfluidic Diagnostics

(Published in *ACS Applied Materials & Interfaces*)

This chapter describes a novel concept of using threads for fabricating low-cost and easy-to-use microfluidic devices, i.e. μ TADs. These devices provide an alternative platform for rapid diagnostic tests such as multi-biomarker detection and semiquantitative biomarker analysis. In addition, the devices require lower sample consumption compared with μ PADs. The unique properties of threads including liquid capillary wicking and flexibility make threads particularly suitable for the fabrication of 3D μ TADs which provide μ TADs with more functions. The fabrication process of 3D μ TADs is much simpler than that of the 3D μ PADs reported by other groups. Due to the simplicity of fabricating μ TADs, the reliance on modern equipment is reduced, thus enabling the potential production of μ TADs in developing countries.

Chapter 7: An Inexpensive Thread-Based System for Simple and Rapid Blood Grouping

(Published in *Analytical and Bioanalytical Chemistry*)

This chapter reports an investigation of a novel blood grouping concept which uses thread-based microfluidic systems as a diagnostic platform. Threads are coated with different antibody solutions in advance to serve as both the reaction site and the result display zone. Compared with most existing blood grouping methods, this new test concept uses a different mechanism for separating the agglutinated red blood cells (RBCs) and the blood serum phase. The principle of this chromatographic separation is explained by adding suitable dyes to antibody solutions, through which the visual detection of the separation is enhanced between the agglutinated RBCs and the blood serum phase. Using this test concept, the ABO and Rh groups are determined in 1 minute on μ TADs with only 2 μ L of the whole blood sample from a pricked finger tip. The test neither requires any pre-treatment of the blood sample nor handles any antibody solutions.

Chapter 8: Flow Control Concepts for Thread-Based Microfluidic Devices

(Published in *Biomicrofluidics*)

This chapter reports an investigation of the liquid penetration behavior along threads and a variety of mechanisms for controlling the flow of reagents and samples in μ TADs. The study of fluid penetration, particularly ultimate penetration distance and flow velocity, in single threads and in twined threads provides the fundamental understanding necessary for designing μ TADs. The flow control mechanisms proposed in this chapter allow more functionalized μ TADs to be fabricated. One approach for controlling fluid flow on μ TADs is building functional elements such as microswitches and microselectors on μ TADs, by using plastic films and household adhesive. These functionalized μ TADs, which incorporate more complex detection chemistries whilst maintaining low production cost and simplicity of construction, will provide more applications for μ TADs in diagnostics.

1.7 References

1. Yager, P., Edwards, T., Fu, E., Helton, K., Nelson, K., Tam, M.R., Weigl, B.H., Microfluidic Diagnostic Technologies for Global Public Health, *Nature*, 2006, 442(7101): p. 412-418.
2. Hansen, C., Quake, S.R., Microfluidics in Structural Biology: Smaller, Faster... Better, *Current Opinion in Structural Biology*, 2003, 13(5): p. 538-544.
3. Weigl, B., Domingo, G., LaBarre, P., Gerlach, J., Towards Non- and Minimally Instrumented, Microfluidics-Based Diagnostic Devices, *Lab on a Chip*, 2008, 8(12): p. 1999-2014.
4. Martinez, A.W., Phillips, S.T., Butte, M.J., Whitesides, G.M., Patterned Paper as a Platform for Inexpensive, Low-Volume, Portable Bioassays, *Angewandte Chemie International Edition*, 2007, 46(8): p. 1318-1320.
5. Manz, A., Graber, N., Widmer, H.M., Miniaturized Total Chemical Analysis Systems: A Novel Concept for Chemical Sensing, *Sensors and Actuators B: Chemical*, 1990, 1(1-6): p. 244-248.
6. Kilby, J.S., The Integrated Circuit's Early History, *Proceedings of the IEEE*, 2000, 88(1): p. 109-111.
7. Whitesides, G.M., The Origins and the Future of Microfluidics, *Nature*, 2006, 442(7101): p. 368-373.
8. Tabeling, P., *Introduction to Microfluidics*. 2005, New York: Oxford University Press.
9. McDonald, J.C., Whitesides, G.M., Poly(Dimethylsiloxane) as a Material for Fabricating Microfluidic Devices, *Accounts of Chemical Research*, 2002, 35(7): p. 491-499.
10. Vyawahare, S., Griffiths, A.D., Merten, C.A., Miniaturization and Parallelization of Biological And chemical Assays in Microfluidic Devices, *Chemistry & Biology*, 2010, 17(10): p. 1052-1065.
11. Brown, L., Koerner, T., Horton, J.H., Oleschuk, R.D., Fabrication and Characterization of Poly(Methylmethacrylate) Microfluidic Devices Bonded Using Surface Modifications and Solvents, *Lab on a Chip*, 2006, 6(1): p. 66-73.
12. Duffy, D.C., McDonald, J.C., Schueller, O.J.A., Whitesides, G.M., Rapid Prototyping of Microfluidic Systems in Poly(Dimethylsiloxane), *Analytical Chemistry*, 1998, 70(23): p. 4974-4984.
13. Sia, S.K., Whitesides, G.M., Microfluidic Devices Fabricated in Poly(Dimethylsiloxane) for Biological Studies, *Electrophoresis*, 2003, 24(21): p. 3563-3576.
14. Zhou, J., Ellis, A.V., Voelcker, N.H., Recent Developments in Pdms Surface Modification for Microfluidic Devices, *Electrophoresis*, 2010, 31(1): p. 2-16.
15. Zhou, F., Lu, M., Wang, W., Bian, Z.-P., Zhang, J.-R., Zhu, J.-J., Electrochemical Immunosensor for Simultaneous Detection of Dual Cardiac Markers Based on a Poly(Dimethylsiloxane)-Gold Nanoparticles Composite Microfluidic Chip: A Proof of Principle, *Clinical Chemistry*, 2010, 56(11): p. 1701-1707.
16. Zhang, M., Wu, J., Wang, L., Xiao, K., Wen, W., A Simple Method for Fabricating Multi-Layer Pdms Structures for 3d Microfluidic Chips, *Lab on a Chip*, 2010, 10(9): p. 1199-1203.

17. Piruska, A., Nikcevic, I., Lee, S.H., Ahn, C., Heineman, W.R., Limbach, P.A., Seliskar, C.J., The Autofluorescence of Plastic Materials and Chips Measured under Laser Irradiation, *Lab on a Chip*, 2005, 5(12): p. 1348-1354.
18. Li, S.W., et al., Low-Temperature Bonding of Poly-(Methyl Methacrylate) Microfluidic Devices under an Ultrasonic Field, *Journal of Micromechanics and Microengineering*, 2009, 19(1): p. 015035.
19. Young, E.W.K., Berthier, E., Guckenberger, D.J., Sackmann, E., Lamers, C., Meyvantsson, I., Huttenlocher, A., Beebe, D.J., Rapid Prototyping of Arrayed Microfluidic Systems in Polystyrene for Cell-Based Assays, *Analytical Chemistry*, 2011, 83(4): p. 1408-1417.
20. Mehta, G., Lee, J., Cha, W., Tung, Y.-C., Linderman, J.J., Takayama, S., Hard Top Soft Bottom Microfluidic Devices for Cell Culture and Chemical Analysis, *Analytical Chemistry*, 2009, 81(10): p. 3714-3722.
21. Dittrich, P.S., Tachikawa, K., Manz, A., Micro Total Analysis Systems. Latest Advancements and Trends, *Analytical Chemistry*, 2006, 78(12): p. 3887-3908.
22. West, J., Becker, M., Tombrink, S., Manz, A., Micro Total Analysis Systems: Latest Achievements, *Analytical Chemistry*, 2008, 80(12): p. 4403-4419.
23. Arora, A., Simone, G., Salieb-Beugelaar, G.B., Kim, J.T., Manz, A., Latest Developments in Micro Total Analysis Systems, *Analytical Chemistry*, 2010, 82(12): p. 4830-4847.
24. Dittrich, P.S., Manz, A., Lab-on-a-Chip: Microfluidics in Drug Discovery, *Nature Reviews Drug Discovery*, 2006, 5(3): p. 210-218.
25. Tian, W., Finehout, E., *Current and Future Trends in Microfluidics within Biotechnology Research*, in *Microfluidics for Biological Applications*. 2009, Springer US. p. 385-411.
26. Weigl, B., Boyle, D., Santos, T.d.l., Peck, R., Steele, M., Simplicity of Use: A Critical Feature for Widespread Adoption of Diagnostic Technologies in Low-Resource Settings, *Expert Review of Medical Devices*, 2009, 6(5): p. 461-464.
27. Urdea, M., Penny, L.A., Olmsted, S.S., Giovanni, M.Y., Kaspar, P., Shepherd, A., Wilson, P., Dahl, C.A., Buchsbaum, S., Moeller, G., Hay Burgess, D.C., Requirements for High Impact Diagnostics in the Developing World, *Nature*, 2006, 444: p. 73-79.
28. Hay Burgess, D.C., Wasserman, J., Dahl, C.A., Global Health Diagnostics, *Nature*, 2006, 444: p. 1-2.
29. Morel, C.M., Acharya, T., Broun, D., Dangi, A., Elias, C., Ganguly, N.K., Gardner, C.A., Gupta, R.K., Haycock, J., Heher, A.D., Hotez, P.J., Kettler, H.E., Keusch, G.T., Krattiger, A.F., Kreutz, F.T., Lall, S., Lee, K., Mahoney, R., Martinez-Palomo, A., Mashelkar, R.A., Matlin, S.A., Mzimba, M., Oehler, J., Ridley, R.G., Senanayake, P., Singer, P., Yun, M., Health Innovation Networks to Help Developing Countries Address Neglected Diseases, *Science*, 2005, 309(5733): p. 401-404.
30. Girosi, F., Olmsted, S.S., Keeler, E., Hay Burgess, D.C., Lim, Y.-W., Aledort, J.E., Rafael, M.E., Ricci, K.A., Boer, R., Hilborne, L., Derosé, K.P., Shea, M.V., Beighley, C.M., Dahl, C.A., Wasserman, J., Developing and Interpreting Models to Improve Diagnostics in Developing Countries, *Nature*, 2006, 444: p. 3-8.
31. Yager, P., Domingo, G.J., Gerdes, J., Point-of-Care Diagnostics for Global Health, *Annual Review of Biomedical Engineering*, 2008, 10(1): p. 107-144.
32. Aguilera-Herrador, E., Cruz-Vera, M., Valcarcel, M., Analytical Connotations of Point-of-Care Testing, *Analyst*, 2010, 135(9): p. 2220-2232.

33. Kettler, H., White, K., Hawkes, S., *Mapping the Landscape of Diagnostics for Sexually Transmitted Infections*. 2003, WHO/TDR: Geneva.
34. Mabey, D., Peeling, R.W., Ustianowski, A., Perkins, M.D., Tropical Infectious Diseases: Diagnostics for the Developing World, *Nature Reviews Microbiology*, 2004, 2(3): p. 231-240.
35. Sia, S.K., Kricka, L.J., Microfluidics and Point-of-Care Testing, *Lab on a Chip*, 2008, 8(12): p. 1982-1983.
36. Laksanasopin, T., Chin, C.D., Moore, H., Wang, J., Yuk Kee, C., Sia, S.K. *Microfluidic Point-of-Care Diagnostics for Resource-Poor Environments*. in *Engineering in Medicine and Biology Society, Annual International Conference of the IEEE*. 2009.
37. Chin, C.D., Linder, V., Sia, S.K., Lab-on-a-Chip Devices for Global Health: Past Studies and Future Opportunities, *Lab on a Chip*, 2007, 7(1): p. 41-57.
38. Gervais, L., Delamarche, E., Toward One-Step Point-of-Care Immunodiagnostics Using Capillary-Driven Microfluidics and Pdms Substrates, *Lab on a Chip*, 2009, 9(23): p. 3330-3337.
39. Abbott Point of Care Products and Services. Available from: <http://www.abbottpointofcare.com/testing-products.aspx>.
40. Triage® Cardiac Panel. Available from: <http://www.biosite.com/products/cardiac.aspx>.
41. Dimov, I.K., Basabe-Desmonts, L., Garcia-Cordero, J.L., Ross, B.M., Ricco, A.J., Lee, L.P., Stand-Alone Self-Powered Integrated Microfluidic Blood Analysis System (Simbas), *Lab on a Chip*, 2011.
42. Lee, W.G., Kim, Y.-G., Chung, B.G., Demirci, U., Khademhosseini, A., Nano/Microfluidics for Diagnosis of Infectious Diseases in Developing Countries, *Advanced Drug Delivery Reviews*, 2010, 62(4-5): p. 449-457.
43. Smook, G.A., *Handbook for Pulp & Paper Technologists*. 3rd edition 2002, Vancouver: Angus Wilde Publications Inc.
44. Free, A.H., Adams, E.C., Kercher, M.L., Free, H.M., Cook, M.H., Simple Specific Test for Urine Glucose, *Clinical Chemistry*, 1957, 3(3): p. 163-168.
45. Fenton, E.M., Mascarenas, M.R., López, G.P., Sibbett, S.S., Multiplex Lateral-Flow Test Strips Fabricated by Two-Dimensional Shaping, *ACS Applied Materials & Interfaces*, 2008, 1(1): p. 124-129.
46. Martinez, A.W., Phillips, S.T., Whitesides, G.M., Carrilho, E., Diagnostics for the Developing World: Microfluidic Paper-Based Analytical Devices, *Analytical Chemistry*, 2009, 82(1): p. 3-10.
47. Di Risio, S., Yan, N., Bioactive Paper through Inkjet Printing, *Journal of Adhesion Science and Technology*, 2010, 24(3): p. 661-684.
48. Sentinel - the Bioactive Paper Network. Available from: www.bioactivepaper.com.
49. Su, S., Ali, M.M., Filipe, C.D.M., Li, Y., Pelton, R., Microgel-Based Inks for Paper-Supported Biosensing Applications, *Biomacromolecules*, 2008, 9(3): p. 935-941.
50. Ali, M.M., Aguirre, S.D., Xu, Y., Filipe, C.D.M., Pelton, R., Li, Y., Detection of DNA Using Bioactive Paper Strips, *Chemical Communications*, 2009(43): p. 6640-6642.
51. Hossain, S.M.Z., Luckham, R.E., Smith, A.M., Lebert, J.M., Davies, L.M., Pelton, R.H., Filipe, C.D.M., Brennan, J.D., Development of a Bioactive Paper Sensor for Detection of Neurotoxins Using Piezoelectric Inkjet Printing of Sol-Gel-Derived Bioinks, *Analytical Chemistry*, 2009, 81(13): p. 5474-5483.

52. Pelton, R., Bioactive Paper Provides a Low-Cost Platform for Diagnostics, *TrAC Trends in Analytical Chemistry*, 2009, 28(8): p. 925-942.
53. Zhao, W., Ali, M.M., Aguirre, S.D., Brook, M.A., Li, Y., Paper-Based Bioassays Using Gold Nanoparticle Colorimetric Probes, *Analytical Chemistry*, 2008, 80(22): p. 8431-8437.
54. Hossain, S.M.Z., Luckham, R.E., McFadden, M.J., Brennan, J.D., Reagentless Bidirectional Lateral Flow Bioactive Paper Sensors for Detection of Pesticides in Beverage and Food Samples, *Analytical Chemistry*, 2009, 81(21): p. 9055-9064.
55. Luckham, R.E., Brennan, J.D., Bioactive Paper Dipstick Sensors for Acetylcholinesterase Inhibitors Based on Sol-Gel/Enzyme/Gold Nanoparticle Composites, *Analyst*, 2010, 135(8): p. 2028-2035.
56. Krska, R., Molinelli, A., Rapid Test Strips for Analysis of Mycotoxins in Food and Feed, *Analytical and Bioanalytical Chemistry*, 2009, 393(1): p. 67-71.
57. Struss, A., Pasini, P., Ensor, C.M., Raut, N., Daunert, S., Paper Strip Whole Cell Biosensors: A Portable Test for the Semiquantitative Detection of Bacterial Quorum Signaling Molecules, *Analytical Chemistry*, 2010, 82(11): p. 4457-4463.
58. Khan, M.S., Fon, D., Li, X., Tian, J., Forsythe, J., Garnier, G., Shen, W., Biosurface Engineering through Ink Jet Printing, *Colloids and Surfaces B: Biointerfaces*, 2010, 75(2): p. 441-447.
59. Khan, M.S., Haniffa, S.B.M., Slater, A., Garnier, G., Effect of Polymers on the Retention and Aging of Enzyme on Bioactive Papers, *Colloids and Surfaces B: Biointerfaces*, 2010, 79(1): p. 88-96.
60. Khan, M.S., Li, X., Shen, W., Garnier, G., Thermal Stability of Bioactive Enzymatic Papers, *Colloids and Surfaces B: Biointerfaces*, 2010, 75(1): p. 239-246.
61. Yun, S., Kim, J., Lee, K.-S., Evaluation of Cellulose Electro-Active Paper Made by Tape Casting and Zone Stretching Methods, *International Journal of Precision Engineering and Manufacturing*, 2010, 11(6): p. 987-990.
62. Gliemann, H., Nickel, U., Schneider, S., Application of Photographic Paper as a Substrate for Surface-Enhanced Raman Spectroscopy, *Journal of Raman Spectroscopy*, 1998, 29(12): p. 1041-1046.
63. Zhao, W., van den berg, A., Lab on Paper, *Lab on a Chip*, 2008, 8(12): p. 1988-1991.
64. Kannangara, D., Zhang, H., Shen, W., Liquid-Paper Interactions During Liquid Drop Impact and Recoil on Paper Surfaces, *Colloids and Surfaces A: Physicochemical and Engineering Aspects*, 2006, 280(1-3): p. 203-215.
65. Modaressi, H., Garnier, G., Mechanism of Wetting and Absorption of Water Droplets on Sized Paper: Effects of Chemical and Physical Heterogeneity, *Langmuir*, 2002, 18(3): p. 642-649.
66. Takahashi, A., auml, ggkvist, M., Li, T.-Q., Capillary Penetration in Fibrous Matrices Studied by Dynamic Spiral Magnetic Resonance Imaging, *Physical Review E*, 1997, 56(2): p. 2035.
67. Daniel, R.C., Berg, J.C., Spreading on and Penetration into Thin, Permeable Print Media: Application to Ink-Jet Printing, *Advances in Colloid and Interface Science*, 2006, 123-126: p. 439-469.
68. Lee, K.S., Ivanova, N., Starov, V.M., Hilal, N., Dutschk, V., Kinetics of Wetting and Spreading by Aqueous Surfactant Solutions, *Advances in Colloid and Interface Science*, 2008, 144(1-2): p. 54-65.

69. Kannangara, D., Khan, M.S., Shen, W. *An Analysis of Effects of Internal and Surface Sizing on Ink Jet Printing Quality*. in *63rd Appita Annual Conference and Exhibition*. 2009. Melbourne.
70. Roberts, R.J., Senden, T.J., Knackstedt, M.A., Lyne, M.B., Spreading of Aqueous Liquids in Unsized Papers Is by Film Flow, *Journal of Pulp and Paper Science*, 2003, 29(4): p. 123-131.
71. Roberts, R.J., Senden, T.J., Knackstedt, M.A., Lyne, M.B., Schrof, W. *3d Imaging of the Spreading and Penetration of Aqueous Liquids into Unsized and Sized Papers*. 2003.
72. Hodgson, K.T., Berg, J.C., The Effect of Surfactants on Wicking Flow in Fiber Networks, *Journal of Colloid and Interface Science*, 1988, 121(1): p. 22-31.
73. Tian, J., Kannangara, D., Li, X., Shen, W., Capillary Driven Low-Cost V-Groove Microfluidic Device with High Sample Transport Efficiency, *Lab on a Chip*, 2010, 10(17): p. 2258-2264.
74. Yamazaki, H., Munakata, U., *A Liquid Absorption Model*. in *Proceedings of the 10th Fundamental Research Symposium*. 1993: Oxford.
75. Shen, W., Filonanko, Y., Truong, Y., Parker, I.H., Brack, N., Pigram, P., Liesegang, J., Contact Angle Measurement and Surface Energetics of Sized and Unsized Paper, *Colloids and Surfaces A: Physicochemical and Engineering Aspects*, 2000, 173(1-3): p. 117-126.
76. Ferreira, P.J., Gamelas, J.A., Moutinho, I.M., Ferreira, A.G., Gómez, N., Molleda, C., Figueiredo, M.M., Application of Ft-Ir-Atr Spectroscopy to Evaluate the Penetration of Surface Sizing Agents into the Paper Structure, *Industrial & Engineering Chemistry Research*, 2009, 48(8): p. 3867-3872.
77. Neimo, L., Andersson, T., *Papermaking Chemistry*. Papermaking Science and Technology, ed. L. Neimo. 1999, Helsinki: Fapet Oy.
78. Kannangara, D., *Phenomena of Liquid Drop Impact on Solid Surfaces in Very Early Stages*, PhD Thesis in *Department of Chemical Engineering*. 2007, Monash University: Melbourne.
79. Zhang, H., Kannangara, D., Hilder, M., Ettl, R., Shen, W., The Role of Vapour Deposition in the Hydrophobization Treatment of Cellulose Fibres Using Alkyl Ketene Dimers and Alkenyl Succinic Acid Anhydrides, *Colloids and Surfaces A: Physicochemical and Engineering Aspects*, 2007, 297(1-3): p. 203-210.
80. Gess, J.M., Rende, D.S., Alkenyl Succinic Anhydride (Asa), *Tappi Journal*, 2005, 4(9): p. 6.
81. Hutton, B.H., Parker, I.H., A Surface Study of Cellulose Fibres Impregnated with Alkyl Ketene Dimers Via Subcritical and Supercritical Carbon Dioxide, *Colloids and Surfaces A: Physicochemical and Engineering Aspects*, 2009, 334(1-3): p. 59-65.
82. Shen, W., Parker, I.H., A Preliminary Study of the Spreading of Akd in the Presence of Capillary Structures, *Journal of Colloid and Interface Science*, 2001, 240(1): p. 172-181.
83. Lindfors, J., Salmi, J., Laine, J., Stenius, P., Akd and Asa Model Surfaces: Preparation and Characterization, *Bioresources*, 2007, 2(4): p. 9.
84. Ek, M., Gellerstedt, G., Henriksson, G., *Paper Chemistry and Technology*. 2009, Berlin: Walter de Gruyter GmbH & Co. KG.
85. Isogai, A., Sizing Mechanism of Paper by Alkylketene Dimers, *Journal of Pulp and Paper Science* 1999, 25(7): p. 6.
86. Rauscher, H., Perucca, M., Buyle, G., *Plasma Technology for Hyperfunctional Surfaces*. 2010: Wiley-VCH.

87. Manos, D.M., Flamm, D.L., *Plasma Etching an Introduction*. Plasma-Materials Interactions, ed. O. Auciello and D.L. Flamm. 1988: Academic Press, INC.
88. Sapieha, S., Wrobel, A.M., Wertheimer, M.R., Plasma-Assisted Etching of Paper, *Plasma Chemistry and Plasma Processing*, 1988, 8(3): p. 331-346.
89. Balu, B., *Plasma Processing of Cellulose Surfaces and Their Interactions with Fluids*, in *School of Chemical & Biomolecular Engineering*. 2009, Georgia Institute of Technology: Atlanta.
90. Mukhopadhyay, S.M., et al., Plasma Assisted Hydrophobic Coatings on Porous Materials: Influence of Plasma Parameters, *Journal of Physics D: Applied Physics*, 2002, 35(16): p. 1927.
91. Pykönen, M., *Influence of Plasma Modification on Surface Properties and Offset Printability of Coated Paper*, PhD Thesis in Chemical Engineering. 2010, Åbo Akademi University: Turku.
92. Cardinaud, C., Peignon, M.-C., Tessier, P.-Y., Plasma Etching: Principles, Mechanisms, Application to Micro- and Nano-Technologies, *Applied Surface Science*, 2000, 164(1-4): p. 72-83.
93. Mittal, K.L., Pizzi, A., *Adhesion Promotion Techniques : Technological Applications* 1999, New York Marcel Dekker.
94. Vesel, A., et al., Modification of Ink-Jet Paper by Oxygen-Plasma Treatment, *Journal of Physics D: Applied Physics*, 2007, 40(12): p. 3689.
95. Le, H.P., Progress and Trends in Ink-Jet Printing Technology, *Journal of Imaging Science and Technology*, 1998, 42(1): p. 14.
96. Barbulovic-Nad, I., Lucente, M., Sun, Y., Zhang, M., Wheeler, A.R., Bussmann, M., Bio-Microarray Fabrication Techniques—a Review, *Critical Reviews in Biotechnology*, 2006, 26(4): p. 237-259.
97. Allain, L., Askari, M., Stokes, D., Vo-Dinh, T., Microarray Sampling-Platform Fabrication Using Bubble-Jet Technology for a Biochip System, *Fresenius' Journal of Analytical Chemistry*, 2001, 371(2): p. 146-150.
98. Xu, T., Jin, J., Gregory, C., Hickman, J.J., Boland, T., Inkjet Printing of Viable Mammalian Cells, *Biomaterials*, 2005, 26(1): p. 93-99.
99. Roda, A., Guardigli, M., Russo, C., Pasini, P., Baraldini, M., Protein Microdeposition Using a Conventional Ink-Jet Printer *BioTechniques*, 2000, 28(3): p. 5.
100. Okamoto, T., Suzuki, T., Yamamoto, N., Microarray Fabrication with Covalent Attachment of DNA Using Bubble Jet Technology, *Nature Biotechnology*, 2000, 18(4): p. 438-441.
101. Setti, L., Fraleoni-Morgera, A., Ballarin, B., Filippini, A., Frascaro, D., Piana, C., An Amperometric Glucose Biosensor Prototype Fabricated by Thermal Inkjet Printing, *Biosensors and Bioelectronics*, 2005, 20(10): p. 2019-2026.
102. Setti, L., Fraleoni-Morgera, A., Mencarelli, I., Filippini, A., Ballarin, B., Di Biase, M., An Hrp-Based Amperometric Biosensor Fabricated by Thermal Inkjet Printing, *Sensors and Actuators B: Chemical*, 2007, 126(1): p. 252-257.
103. Boland, T., Xu, T., Damon, B., Cui, X., Application of Inkjet Printing to Tissue Engineering, *Biotechnology Journal*, 2006, 1(9): p. 910-917.
104. Braithwaite, A., Smith, F.J., *Chromatographic Methods*. 5th edition. 1996, Glasgow: Chapman & Hall.
105. Comer, J.P., Semiquantitative Specific Test Paper for Glucose in Urine, *Analytical Chemistry*, 1956, 28(11): p. 1748-1750.

106. von Lode, P., Point-of-Care Immunotesting: Approaching the Analytical Performance of Central Laboratory Methods, *Clinical Biochemistry*, 2005, 38(7): p. 591-606.
107. Müller, R.H., Clegg, D.L., Automatic Paper Chromatography, *Analytical Chemistry*, 1949, 21(9): p. 1123-1125.
108. Martinez, A.W., Phillips, S.T., Wiley, B.J., Gupta, M., Whitesides, G.M., Flash: A Rapid Method for Prototyping Paper-Based Microfluidic Devices, *Lab on a Chip*, 2008, 8(12): p. 2146-2150.
109. Bruzewicz, D.A., Reches, M., Whitesides, G.M., Low-Cost Printing of Poly(Dimethylsiloxane) Barriers to Define Microchannels in Paper, *Analytical Chemistry*, 2008, 80(9): p. 3387-3392.
110. Martinez, A.W., Phillips, S.T., Whitesides, G.M., Three-Dimensional Microfluidic Devices Fabricated in Layered Paper and Tape, *Proceedings of the National Academy of Sciences*, 2008, 105(50): p. 19606-19611.
111. Klasner, S., Price, A., Hoeman, K., Wilson, R., Bell, K., Culbertson, C., Paper-Based Microfluidic Devices for Analysis of Clinically Relevant Analytes Present in Urine and Saliva, *Analytical and Bioanalytical Chemistry*, 2010, 397(5): p. 1821-1829.
112. Abe, K., Suzuki, K., Citterio, D., Inkjet-Printed Microfluidic Multianalyte Chemical Sensing Paper, *Analytical Chemistry*, 2008, 80(18): p. 6928-6934.
113. Li, X., Tian, J., Nguyen, T., Shen, W., Paper-Based Microfluidic Devices by Plasma Treatment, *Analytical Chemistry*, 2008, 80(23): p. 9131-9134.
114. Li, X., Tian, J., Garnier, G., Shen, W., Fabrication of Paper-Based Microfluidic Sensors by Printing, *Colloids and Surfaces B: Biointerfaces*, 2010, 76(2): p. 564-570.
115. Wang, W., Wu, W.-Y., Zhu, J.-J., Tree-Shaped Paper Strip for Semiquantitative Colorimetric Detection of Protein with Self-Calibration, *Journal of Chromatography A*, 2010, 1217(24): p. 3896-3899.
116. Lu, Y., Shi, W., Jiang, L., Qin, J., Lin, B., Rapid Prototyping of Paper-Based Microfluidics with Wax for Low-Cost, Portable Bioassay, *Electrophoresis*, 2009, 30(9): p. 1497-1500.
117. Carrilho, E., Martinez, A.W., Whitesides, G.M., Understanding Wax Printing: A Simple Micropatterning Process for Paper-Based Microfluidics, *Analytical Chemistry*, 2009, 81(16): p. 7091-7095.
118. Leung, V., Shehata, A.-A.M., Filipe, C.D.M., Pelton, R., Streaming Potential Sensing in Paper-Based Microfluidic Channels, *Colloids and Surfaces A: Physicochemical and Engineering Aspects*, 2010, 364(1-3): p. 16-18.
119. Delaney, J.L., Hogan, C.F., Tian, J., Shen, W., Electrogenerated Chemiluminescence Detection in Paper-Based Microfluidic Sensors, *Analytical Chemistry*, 2011, 83(4): p. 1300-1306.
120. Olkkonen, J., Lehtinen, K., Erho, T., Flexographically Printed Fluidic Structures in Paper, *Analytical Chemistry*, 2010, 82(24): p. 10246-10250.
121. Chitnis, G., Ding, Z., Chang, C.-L., Savran, C.A., Ziaie, B., Laser-Treated Hydrophobic Paper: An Inexpensive Microfluidic Platform, *Lab on a Chip*, 2011, 11(6): p. 1161-1165.
122. Yi, X., Kodzius, R., Gong, X., Xiao, K., Wen, W., A Simple Method of Fabricating Mask-Free Microfluidic Devices for Biological Analysis, *Biomicrofluidics*, 2010, 4(3): p. 036503-8.

123. Liu, Y., Sun, Y., Sun, K., Song, L., Jiang, X., Recent Developments Employing New Materials for Readout in Lab-on-a-Chip, *Journal of Materials Chemistry*, 2010, 20(35): p. 7305-7311.
124. Carvalhal, R.F., Carrilho, E., Kubota, L.T., The Potential and Application of Microfluidic Paper-Based Separation Devices, *Bioanalysis*, 2010, 2(10): p. 1663-1665.
125. Martinez, A.W., Phillips, S.T., Carrilho, E., Thomas, S.W., Sindi, H., Whitesides, G.M., Simple Telemedicine for Developing Regions: Camera Phones and Paper-Based Microfluidic Devices for Real-Time, Off-Site Diagnosis, *Analytical Chemistry*, 2008, 80(10): p. 3699-3707.
126. Abe, K., Kotera, K., Suzuki, K., Citterio, D., Inkjet-Printed Paperfluidic Immuno-Chemical Sensing Device, *Analytical and Bioanalytical Chemistry*, 2010, 398(2): p. 885-893.
127. Dungchai, W., Chailapakul, O., Henry, C.S., Use of Multiple Colorimetric Indicators for Paper-Based Microfluidic Devices, *Analytica Chimica Acta*, 2010, 674(2): p. 227-233.
128. Ellerbee, A.K., Phillips, S.T., Siegel, A.C., Mirica, K.A., Martinez, A.W., Striehl, P., Jain, N., Prentiss, M., Whitesides, G.M., Quantifying Colorimetric Assays in Paper-Based Microfluidic Devices by Measuring the Transmission of Light through Paper, *Analytical Chemistry*, 2009, 81(20): p. 8447-8452.
129. *World Telecommunication/Ict Development Report* 2010, International telecommunications Union Place des Nations: Geneva.
130. Mukhopadhyay, R., Cheap, Handheld Colorimeter to Read Paper-Based Diagnostic Devices, *Analytical Chemistry*, 2009, 81(21): p. 8659-8659.
131. Li, X., Tian, J., Shen, W., Quantitative Biomarker Assay with Microfluidic Paper-Based Analytical Devices, *Analytical and Bioanalytical Chemistry*, 2010, 396(1): p. 495-501.
132. Blicharz, T.M., Rissin, D.M., Bowden, M., Hayman, R.B., DiCesare, C., Bhatia, J.S., Grand-Pierre, N., Siqueira, W.L., Helmerhorst, E.J., Loscalzo, J., Oppenheim, F.G., Walt, D.R., Use of Colorimetric Test Strips for Monitoring the Effect of Hemodialysis on Salivary Nitrite and Uric Acid in Patients with End-Stage Renal Disease: A Proof of Principle, *Clinical Chemistry*, 2008, 54(9): p. 1473-1480.
133. Zhao, W., Brook, M.A., Li, Y., Design of Gold Nanoparticle-Based Colorimetric Biosensing Assays, *ChemBioChem*, 2008, 9(15): p. 2363-2371.
134. Nie, Z., Deiss, F., Liu, X., Akbulut, O., Whitesides, G.M., Integration of Paper-Based Microfluidic Devices with Commercial Electrochemical Readers, *Lab on a Chip*, 2010, 10(22): p. 3163-3169.
135. Dungchai, W., Chailapakul, O., Henry, C.S., Electrochemical Detection for Paper-Based Microfluidics, *Analytical Chemistry*, 2009, 81(14): p. 5821-5826.
136. Tan, S.N., Ge, L., Wang, W., Paper Disk on Screen Printed Electrode for One-Step Sensing with an Internal Standard, *Analytical Chemistry*, 2010, 82(21): p. 8844-8847.
137. Apilux, A., Dungchai, W., Siangproh, W., Praphairaksit, N., Henry, C.S., Chailapakul, O., Lab-on-Paper with Dual Electrochemical/Colorimetric Detection for Simultaneous Determination of Gold and Iron, *Analytical Chemistry*, 2010, 82(5): p. 1727-1732.
138. Dittrich, P.S., Research Highlights, *Lab on a Chip*, 2009, 9(1): p. 15-16.

139. Carvalho, R.F., Simão Kfour, M., de Oliveira Piazzetta, M.H., Gobbi, A.L., Kubota, L.T., Electrochemical Detection in a Paper-Based Separation Device, *Analytical Chemistry*, 2010, 82(3): p. 1162-1165.
140. Shen, W., Li, X., Tian, J., Nguyen, T.H., Garnier, G., *Switches for Microfluidic Systems*, Patent No.: WO/2010/017578.
141. Martinez, A.W., Phillips, S.T., Nie, Z., Cheng, C.-M., Carrilho, E., Wiley, B.J., Whitesides, G.M., Programmable Diagnostic Devices Made from Paper and Tape, *Lab on a Chip*, 2010, 10(19): p. 2499-2504.
142. Fu, E., Lutz, B., Kauffman, P., Yager, P., Controlled Reagent Transport in Disposable 2d Paper Networks, *Lab on a Chip*, 2010, 10(7): p. 918-920.
143. Kauffman, P., Fu, E., Lutz, B., Yager, P., Visualization and Measurement of Flow in Two-Dimensional Paper Networks, *Lab on a Chip*, 2010, 10(19): p. 2614-2617.
144. Fu, E., Ramsey, S., Kauffman, P., Lutz, B., Yager, P., Transport in Two-Dimensional Paper Networks, *Microfluidics and Nanofluidics*, 2010: p. 1-7.
145. Fu, E., Kauffman, P., Lutz, B., Yager, P., Chemical Signal Amplification in Two-Dimensional Paper Networks, *Sensors and Actuators B: Chemical*, 2010, 149(1): p. 325-328.
146. Noh, H., Phillips, S.T., Metering the Capillary-Driven Flow of Fluids in Paper-Based Microfluidic Devices, *Analytical Chemistry*, 2010, 82(10): p. 4181-4187.
147. Noh, H., Phillips, S.T., Fluidic Timers for Time-Dependent, Point-of-Care Assays on Paper, *Analytical Chemistry*, 2010, 82(19): p. 8071-8078.
148. Bracher, P.J., Gupta, M., Mack, E.T., Whitesides, G.M., Heterogeneous Films of Ionotropic Hydrogels Fabricated from Delivery Templates of Patterned Paper, *ACS Applied Materials & Interfaces*, 2009, 1(8): p. 1807-1812.
149. Bracher, P.J., Gupta, M., Whitesides, G.M., Patterned Paper as a Template for the Delivery of Reactants in the Fabrication of Planar Materials, *Soft Matter*, 2010, 6(18): p. 4303-4309.
150. Bracher, P.J., Gupta, M., Whitesides, G.M., Patterning Precipitates of Reactions in Paper, *Journal of Materials Chemistry*, 2010, 20(24): p. 5117-5122.
151. Bracher, P.J., Gupta, M., Whitesides, G.M., Shaped Films of Ionotropic Hydrogels Fabricated Using Templates of Patterned Paper, *Advanced Materials*, 2009, 21(4): p. 445-450.
152. Cheng, C.-M., Mazzeo, A.D., Gong, J., Martinez, A.W., Phillips, S.T., Jain, N., Whitesides, G.M., Millimeter-Scale Contact Printing of Aqueous Solutions Using a Stamp Made out of Paper and Tape, *Lab on a Chip*, 2010, 10(23): p. 3201-3205.
153. Lu, Y., Lin, B., Qin, J., Patterned Paper as a Low-Cost, Flexible Substrate for Rapid Prototyping of Pdms Microdevices Via "Liquid Molding", *Analytical Chemistry*, 2011, 83(5): p. 1830-1835.
154. Carrilho, E., Phillips, S.T., Vella, S.J., Martinez, A.W., Whitesides, G.M., Paper Microzone Plates, *Analytical Chemistry*, 2009, 81(15): p. 5990-5998.
155. Cheng, C.-M., Martinez, A.W., Gong, J., Mace, C.R., Phillips, S.T., Carrilho, E., Mirica, K.A., Whitesides, G.M., Paper-Based Elisa, *Angewandte Chemie International Edition*, 2010, 49(28): p. 4771-4774.
156. Mukhopadhyay, R., *Paper-Based Diagnostics*. 2010, Chemistry World.
157. Grayson, M., ed. *Encyclopedia of Textiles, Fibers, and Nonwoven Fabrics*. Encyclopedia Reprint Series, ed. M. Grayson. 1984, John Wiley & Sons, Inc.: Toronto.

158. Lewin, M., *Handbook of Fiber Chemistry*. 3rd edition. in *International Fibre Science and Technology Series*, 2006, Taylor & Francis Group: Boca Raton.
159. Wakelyn, P.J., *Cotton*. Kirk-Othmer Encyclopedia of Chemical Technology. 2000: John Wiley & Sons, Inc.
160. Babacan, T., *The Fiber Year 2009/10 a World Survey on Textile and Non-Wovens Industry*. 2010, Oerlikon Corporation AG.
161. Albrecht, W., Fuchs, H., Kittelmann, W., *Nonwoven Fabrics*. 2002, WILEY-VCH: Weinheim.
162. Czajka, R., Development of Medical Textile Market, *Fibers & Textiles in Eastern Europe*, 2005, 13(1): p. 3.
163. Horrocks, A.R., Anand, S.C., *Handbook of Technical Textiles*. 2000, Woodhead Publishing Ltd and CRC Press LLC: Cambridge.
164. Papaspyrides, C.D., Pavlidou, S., Vouyiouka, S.N., Development of Advanced Textile Materials: Natural Fibre Composites, Anti-Microbial, and Flame-Retardant Fabrics, *Proceedings of the Institution of Mechanical Engineers, Part L: Journal of Materials: Design and Applications* 2009, 223: p. 12.
165. Lymberis, A., Intelligent Wearable Systems Achievements, Challenges and Perspectives, *Advances in Science and Technology*, 2008, 57: p. 7.
166. Tao, X., ed. *Wearable Electronics and Photonics*. 2005, Woodhead Publishing Ltd: Cambridge.
167. Sungmee, P., Jayaraman, S., Smart Textile-Based Wearable Biomedical Systems: A Transition Plan for Research to Reality, *Information Technology in Biomedicine, IEEE Transactions on*, 2010, 14(1): p. 86-92.
168. Bonato, P., Wearable Sensors/Systems and Their Impact on Biomedical Engineering, *Engineering in Medicine and Biology Magazine, IEEE*, 2003, 22(3): p. 18-20.
169. Lam Po Tang, S., Recent Developments in Flexible Wearable Electronics for Monitoring Applications, *Transactions of the Institute of Measurement and Control*, 2007, 29(3-4): p. 283-300.
170. Luprano, J., Bio-Sensing Textile for Medical Monitoring Applications, *Advances in Science and Technology*, 2008, 57: p. 10.
171. Perwuelz, A., Casetta, M., Caze, C., Liquid Organisation During Capillary Rise in Yarns--Influence of Yarn Torsion, *Polymer Testing*, 2001, 20(5): p. 553-561.
172. Ferrero, F., Wettability Measurements on Plasma Treated Synthetic Fabrics by Capillary Rise Method, *Polymer Testing*, 2003, 22(5): p. 571-578.
173. Wang, N., Zha, A., Wang, J., Study on the Wicking Property of Polyester Filament Yarns, *Fibers and Polymers*, 2008, 9(1): p. 97-100.
174. Nisbet, D.R., Pattanawong, S., Ritchie, N.E., Shen, W., Finkelstein, D.I., Horne, M.K., Forsythe, J.S., Interaction of Embryonic Cortical Neurons on Nanofibrous Scaffolds for Neural Tissue Engineering, *Journal of Neural Engineering*, 2007, 4(2): p. 35.
175. Safavieh, R., Mirzaei, M., Qasaimeh, M.A., Juncker, D. *Yarn Based Microfluidics: From Basic Elements to Complex Circuits*. in *Thirteenth International Conference on Miniaturized Systems for Chemistry and Life Sciences*. 2009. Jeju, Korea.
176. Li, X., Tian, J., Shen, W., Thread as a Versatile Material for Low-Cost Microfluidic Diagnostics, *ACS Applied Materials & Interfaces*, 2010, 2(1): p. 1-6.

177. Ballerini, D., Li, X., Shen, W., An Inexpensive Thread-Based System for Simple and Rapid Blood Grouping, *Analytical and Bioanalytical Chemistry*, 2011, 399(5): p. 1869-1875.
178. Ballerini, D.R., Li, X., Shen, W., Flow Control Concepts for Thread-Based Microfluidic Devices, *Biomicrofluidics*, 2011, 5(1): p. 014105-13.
179. Reches, M., Mirica, K.A., Dasgupta, R., Dickey, M.D., Butte, M.J., Whitesides, G.M., Thread as a Matrix for Biomedical Assays, *ACS Applied Materials & Interfaces*, 2010, 2(6): p. 1722-1728.
180. Dean, L., *Blood Groups and Red Cell Antigens*. 2005, Bethesda (MD): National Center for Biotechnology Information (US)
181. 10 Facts on Blood, World Health Organization. Available from: http://www.who.int/features/factfiles/blood_transfusion/en/index.html.
182. Daniels, G., Bromilow, I., *Essential Guide to Blood Groups*. 2010: Wiley-Blackwell.
183. Joshi, V.D., Nandedkar, A.N., Mendhruwar, S.S., *Anatomy and Physiology for Nursing and Health Care*. 2006, New Delhi: BI Publications Pvt Ltd.
184. Watkins, W.M., The Abo Blood Group System: Historical Background, *Transfusion Medicine*, 2001, 11(4): p. 243-265.
185. Landsteiner, K., Zur Kenntnis Antifermentativen, Lytis-Chen Und Agglutinierenden Wirkungen Des Blutserums Und Der Lymphe, *Zbl Bakt*, 1900, 27: p. 357-362.
186. von Decastello, A., Struli, A., Ueber Die Isoagglutinine Im Serum Gesunder Und Kranker Menschen, *Mfinch med Wschr*, 1902, 49: p. 1090-1095.
187. Landsteiner, K., Wiener, A., An Agglutinable Factor in Human Blood Recognized by Immune Sera for Rhesus Blood, *Proceedings of the Society for Experimental Biology and Medicine*, 1940, 43: p. 223-224.
188. Daniels, G., Reid, M.E., Blood Groups: The Past 50 Years, *Transfusion*, 2010, 50(2): p. 281-289.
189. Malomgré, W., Neumeister, B., Recent and Future Trends in Blood Group Typing, *Analytical and Bioanalytical Chemistry*, 2009, 393(5): p. 1443-1451.
190. Pramanik, D., *Principles of Physiology*. 2010, Kolkata: Academic Publishers.
191. Estridge, B.H., Reynolds, A.P., Walters, N.J., *Basic Medical Laboratory Techniques*. 2000, New York: Delmar Cengage Learning.
192. Llopis, F., Carbonell-Uberos, F., Montero, M.C., Bonanad, S., Planelles, M.D., Plasencia, I., Riol, C., Planells, T., Carrillo, C., De Miguel, A., A New Method for Phenotyping Red Blood Cells Using Microplates, *Vox Sanguinis*, 1999, 77(3): p. 143-148.
193. Llopis, F., Carbonell-Uberos, F., Planelles, M.D., Montero, M., Puig, N., Atienza, T., Alba, E., Montoro, J.A., A Monolayer Coagglutination Microplate Technique for Typing Red Blood Cells, *Vox Sanguinis*, 1997, 72(1): p. 26-30.
194. Spindler, J.H., Klüter, H., Kerowgan, M., A Novel Microplate Agglutination Method for Blood Grouping and Reverse Typing without the Need for Centrifugation, *Transfusion*, 2001, 41(5): p. 627-632.
195. Langston, M.M., Procter, J.L., Cipolone, K.M., Stroncek, D.F., Evaluation of the Gel System for Abo Grouping and D Typing, *Transfusion*, 1999, 39(3): p. 300-305.
196. Lapierre, Y., Rigal, D., Adam, J., Josef, D., Meyer, F., Greber, S., Drot, C., The Gel Test: A New Way to Detect Red Cell Antigen-Antibody Reactions, *Transfusion*, 1990, 30(2): p. 109-113.

197. Plapp, F., Rachel, J., Sinor, L., Dipsticks for Determining Abo Blood Groups, *The Lancet*, 1986, 327(8496): p. 1465-1466.
198. Giebel, F., Picker, S.M., Gathof, B.S., Evaluation of Four Bedside Test Systems for Card Performance, Handling and Safety, *Transfusion Medicine and Hemotherapy*, 2008, 35(1): p. 33-36.
199. Khan, M.S., Thouas, G., Shen, W., Whyte, G., Garnier, G., Paper Diagnostic for Instantaneous Blood Typing, *Analytical Chemistry*, 2010, 82(10): p. 4158-4164.
200. Handbook for Doctoral and Mphil Degrees. Available from: http://www.mrgs.monash.edu.au/research/doctoral/archive/handbook_cd_2011/handbook/index.html.
201. Thesis by Published and Unpublished Papers. Available from: <http://www.mrgs.monash.edu.au/research/examination/thesis-by-publication/index.html>.

This page is intentionally blank

Part I: Paper-Based Microfluidics

Paper-based microfluidics is a platform for low-cost, rapid diagnostics and environmental sensing. The foundation of this platform is the ability to control the liquid penetration in paper. Paper made of cellulose fibres is hydrophilic and allows rapid penetration of aqueous liquids. Paper can also be treated to acquire hydrophobicity to retard liquid penetration, and such treatment is a central technology in papermaking, known as paper sizing. Paper-based microfluidic systems require precise control of liquid penetration; such a requirement can be realized by creating patterns of hydrophilic-hydrophobic contrast in paper.

The first part of this thesis presents novel concepts and methods for creating hydrophilic-hydrophobic contrast in paper by combining paper sizing chemistry and patterned plasma treatment or digital ink jet printing. The combination of these technologies has successfully generated paper-based microfluidics capable for diagnostic applications. The fabrication concepts presented in this thesis are uniquely based on papermaking and printing technology framework and have realistic potential to be scaled up.

This part of the thesis also presented novel concepts of semiquantitative chemical analysis using paper-based microfluidics. The use of self-calibration curve significantly increases the reliability of the analytical results.

Furthermore, this part of the thesis has, for the first time, asked and answered the question of building into the paper-based microfluidic systems control elements, such as valves, to enable microfluidic control by the operator. This new concept lays the ground for fabricating reactors on paper, capable of multi-step, operator controllable diagnostic and chemical analysis.

Chapter 2: Paper-Based Microfluidic Devices by Plasma Treatment

This page is intentionally blank

Monash University Declaration for Thesis Chapter 2

Declaration by candidate

In the case of Chapter 2, the nature and extent of my contribution to the work was the following:

Nature of contribution	Extent of contribution (%)
Experimental design and conduct, paper writing	60

The following co-authors contributed to the work. Co-authors who are students at Monash University must also indicate the extent of their contribution in percentage terms:

Name	Nature of contribution	Extent of contribution (%) for student co-authors only
Junfei Tian	Experimental design, assisted in experimentation, corrected manuscript	20
Thanh Nguyen	Assisted in experimentation, corrected manuscript	10
Wei Shen	Experimental design, corrected manuscript	Supervisor

Candidate's
Signature

	Date 04/08/2011
---	--------------------

Declaration by co-authors

The undersigned hereby certify that:

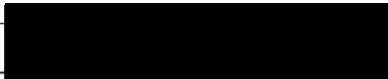
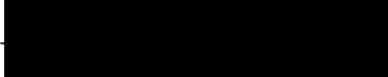

- (1) the above declaration correctly reflects the nature and extent of the candidate's contribution to this work, and the nature of the contribution of each of the co-authors.
- (2) they meet the criteria for authorship in that they have participated in the conception, execution, or interpretation, of at least that part of the publication in their field of expertise;
- (3) they take public responsibility for their part of the publication, except for the responsible author who accepts overall responsibility for the publication;
- (4) there are no other authors of the publication according to these criteria;
- (5) potential conflicts of interest have been disclosed to (a) granting bodies, (b) the editor or publisher of journals or other publications, and (c) the head of the responsible academic unit; and
- (6) the original data are stored at the following location(s) and will be held for at least five years from the date indicated below:

Location(s)	Australian Pulp and Paper Institute (APPI), Department of Chemical Engineering, Monash University, Clayton, VIC 3800, Australia
-------------	---

Signature 1

Signature 2

Signature 3

	Date 04/08/2011
	04/08/11
	4/8/11

This page is intentionally blank

Paper-Based Microfluidic Devices by Plasma Treatment

Xu Li, Junfei Tian, Thanh Nguyen and Wei Shen*

*Australian Pulp and Paper Institute, Department of Chemical Engineering,
Monash University. Wellington Road, Clayton, Victoria 3800, Australia*

**Corresponding Author: Email: wei.shen@eng.monash.edu.au*

Phone: +61 3 99053447; Fax: +61 3 99053413

2.1 ABSTRACT

Paper-based microfluidic patterns have been demonstrated in recent literature to have a significant potential in developing low-cost analytical devices for telemedicine and general health monitoring. This study reports a new method for making microfluidic patterns on a paper surface using plasma treatment. Paper was first hydrophobized and then treated using plasma in conjunction with a mask. This formed well defined hydrophilic channels on the paper. Paper-based microfluidic systems produced in this way retained the flexibility of paper and a variety of patterns could be formed. A major advantage of this system is that simple functional elements such as switches and filters can be built into the patterns. Examples of these elements are given in this study.

2.2 INTRODUCTION

This article reports on a novel method of creating patterns in paper to control the transport of liquid for pathological testing and environmental monitoring. Nonwoven fibrous materials such as paper have very good potential as low-cost base materials for diagnostic devices for such applications. Cellulose-based papers have been used as chromatographic substrates since 1850.^{1,2} A number of testing devices, such as paper-based indicators³ and “dip stick” test assays are made of paper. Recently, Martinez et

al.⁴⁻⁶ used paper as a base material to create barrier patterns with photolithographic techniques. The photoresist patterns they produced guide the capillary penetration of liquids and, with the appropriate indicators, can detect chemical components in a liquid sample. This type of paper-based detector, when used with modern communication tools such as camera phones, can provide powerful real-time and off-site diagnostic devices for telemedicine with great potential to be developed into a low-cost health monitoring system.⁵ The drawback of conventional photoresist is that it is much less flexible than paper and the device can be easily damaged by bending and folding.⁷

More recently, Bruzewicz et al.⁷ used a modified plotter to create a barrier pattern by printing Polydimethylsiloxane (PDMS) onto paper. When PDMS penetrated into paper, it formed a barrier pattern and could be used to control the penetration of liquid in channels defined by the barrier pattern. Since PDMS is an elastomer, it is more flexible than conventional photoresist and is less susceptible to mechanical damage. However, because of the low surface tension of the solvent used, the PDMS solution penetrates into paper rather easily. Since paper is not a uniform porous material, the penetration of PDMS cannot be well controlled, resulting in the wall of the barrier pattern not being straight.

The novel method of the present study enables patterns to be created on paper surfaces without affecting their flexibility or surface topography. The major advantage of this novel method over previously reported paper-based microfluidic devices is that it allows not only sample testing but also building of simple functional components such as control switches, microfilters and microreactors, which are important elements for multiple-step chemical tests. Several examples of these functional elements are presented in this work.

2.3 EXPERIMENTAL SECTION

Alkyl ketene dimer (AKD) (Wax 88 konz, BASF) was used as the cellulose hydrophobization agent. Analytical grade *n*-heptane (Aldrich) was used as the solvent

for AKD. Whatman filter paper was selected as the paper substrate. MilliQ water was used to prepare all liquid samples required for testing the performance of the device.

The filter paper was hydrophobized using an AKD–heptane solution (0.6 g/L). The filter paper samples were dipped in this solution and immediately removed and placed in a fume cupboard to allow evaporation of the heptane. The filter paper samples were then heated in an oven at 100 °C for 45 min to cure the AKD. The treated filter paper samples are strongly hydrophobic and have contact angles of typically 110–125° with water.⁹ Therefore, water shows no penetration into the paper hydrophobized with AKD.

Hydrophilic patterns were formed on paper samples using plasma treatment. The paper samples were sandwiched between metal masks having the desired patterns and then placed into a vacuum plasma reactor (K1050X plasma asher (Quorum Emitech, U.K.)) for 15 sec at the intensity of 15 W. Metal masks were made by mechanically cutting patterns through stainless steel sheets. Four screws were used to secure the alignments of the masks. The vacuum level for the treatment was 6×10^{-1} mbar. The plasma treatment left no visible mark on the samples, which retained its original flexibility. The plasma treated areas were strongly wettable by water or aqueous solutions and allowed the transport of aqueous solutions along and within the plasma treated channels via capillary penetration.⁸

A color change reaction for the evaluation of enzyme activity was used to test the device. Alkaline phosphatase enzyme solution was prepared using alkaline phosphatase (lyophilized powder, from bovine intestinal mucosa, 10–30 DEA units/mg solid) from Sigma-Aldrich. Phosphatase solution (1 mg/ml) was prepared in the buffer solution (pH = 9.8) which contains 1.0 M diethanolamine ($\geq 98\%$, Sigma Aldrich) and 0.5 mM $\text{MgCl}_2 \cdot 6\text{H}_2\text{O}$ ($\geq 99\%$, Sigma-Aldrich). The phosphatase enzyme solution was divided into two parts; one part was heated at $>70^\circ\text{C}$ for 10 min to purposely deactivate the enzyme. A BCIP/NBT substrate system (Sigma-Aldrich) was used with the phosphatase enzyme to indicate the activity of the enzyme via color change. A phenolphthalein–ethanol solution was used as the color indicator for testing the performance of a paper-based microfluidic reactor. It was prepared using phenolphthalein (BDH) and ethanol (AR, BDH).

2.4 RESULTS AND DISCUSSION

2.4.1 Plasma Formed Patterns

Parts a and b of Figure 1 show a filter paper sample immediately after treatment and after being exposed to water. Water penetration demonstrated that the plasma treated channel has well-defined borders; the width of the channel can be reasonably well controlled. The channel in Figure 1b was made using a 1 mm wide mask, and a channel < 1.5 mm in width was uniformly penetrated by water.

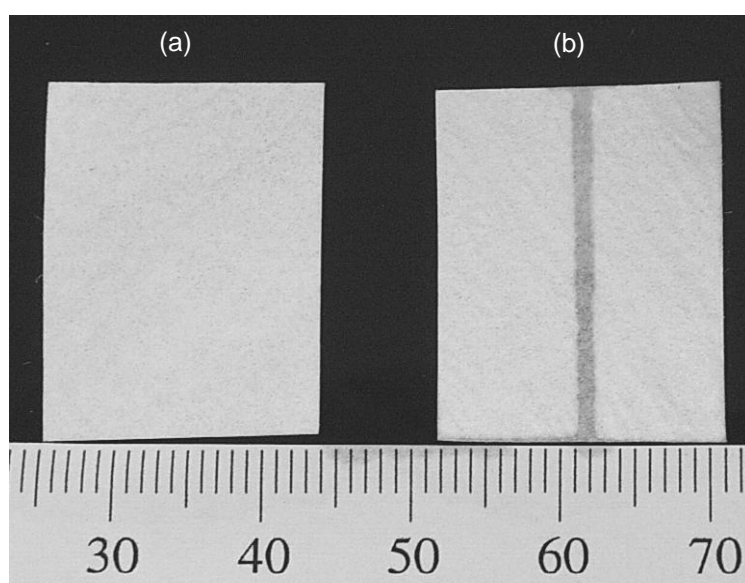


Figure 1. Water penetration control of a plasma treated microfluidic channel using hydrophobized filter paper. (a) A hydrophobized filter paper sample immediately after the treatment and (b) the treated sample was exposed to water through the lower edge.

Hot electrons and other energetic particles generated in vacuum plasma have long mean free paths. Overetching of the substrate under a mask is a known problem for plasma treatment, causing the treated pattern to be slightly bigger than the mask. However, overetching could be controlled by optimizing the treatment intensity and time. When the treatment intensity and time were fixed, the channel width was found very reproducible.

2.4.2 Design of Sample Dosing and Detection Sites on Paper-Based Microfluidic Devices

An important application of paper-based microfluidic devices is to analyze chemical components in a liquid sample by means of color indicators.⁴⁻⁷ The research group in Harvard University was the first to explore this application.⁴⁻⁷ In their approaches, the concept of a capillary channel barrier was used to confine the liquid penetration path from sample dosing zone(s) to sample detection zones. In our approach, plasma generated hydrophilic patterns in a hydrophobized paper can control the capillary flow path of liquids and can be designed to have one or more detection zones. Figure 2 shows a test of a plasma generated pattern. Small quantities (2 μ L) of three active and three deactivated enzyme samples were introduced in alternation into detection ports of a six-channel pattern. A few drops of liquid substrate (BCIP/NBT) were introduced from the centre port of the pattern. A few drops of liquid substrate (BCIP/NBT) were introduced from the centre port of the pattern. Three samples with active enzyme show color change and three deactivated enzyme samples show no color change. This microfluidic system created by plasma treated paper is capable of performing analytical tests proposed by other researchers.⁴⁻⁷

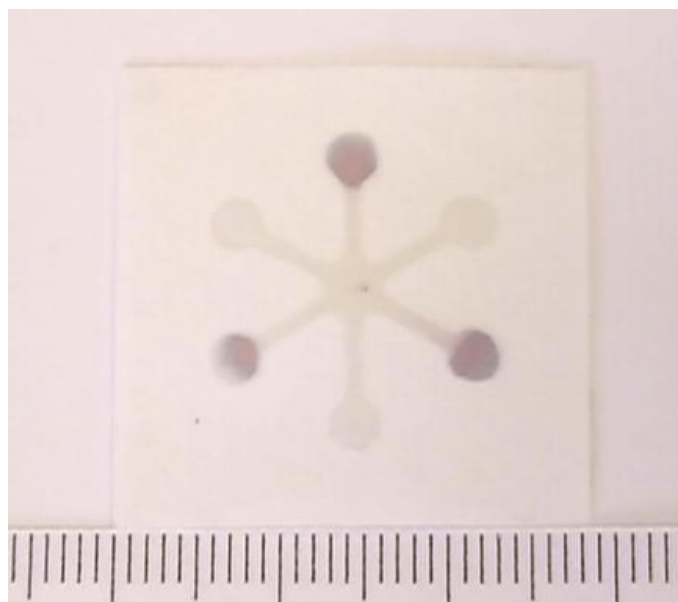


Figure 2. The performance of a paper-based microfluidic pattern fabricated by plasma treatment. Three active and three deactivated enzyme samples were introduced into detection ports of a six-channel pattern in alternation. A few drops of liquid substrate (BCIP/NBT) were introduced from the centre port. Liquid substrate penetrated into the detection ports, revealing the activity of the enzyme samples.

2.4.3 Building Functional Elements on Paper-Based Microfluidic Systems

Functional elements such as switches, filters, and separators can be easily built into microfluidic devices made by plasma treatment of paper. An advantage of plasma treated paper is that the untreated areas remain hydrophobic and do not allow capillary penetration of sample liquids. Such structure allows simple switches to be built so as to connect and disconnect the microfluidic channels. Several of many possible mechanical designs can be found in the Supporting Information. Simple switch design can be found below (Figures 5 and 6). It is possible that such switches can be activated by some other means such as by electrostatic or electromagnetic forces, etc.

A filter or a separator can also be easily designed for paper-based microfluidic systems. With dependence on the requirement of the analytical task, ion-exchange resins, high surface area functionalized nano- or microparticles or cationic polymer-coated mineral fillers can be deposited on the surface of the mechanical switches. When the switch is in the connected state, the sample liquid can be filtered to remove solid particles when penetrating through the filter. Also, certain molecular species can be separated from the sample liquid chromatographically as the sample penetrates through a separator.

Figure 3 shows an even simpler and versatile design of a paper-based chromatographic separator. A strip of paper or other flexible material with a patch of coating, as shown in Figure 3, can be used to form the separation element. The separator is activated by pulling the strip as illustrated in Figure 3. To demonstrate the operation and effectiveness of this type of separator, a strip of matt ink-jet printing paper with a silica coating layer was used to separate a diluted ink-jet ink solution (Figure 4). The diluted ink was deposited on the right side of the microfluidic channel; as the solution passed through the separator and reached the left side channel, dye in the solution was retained by the ink jet paper separator. Figure 4 indicates that this separator performed satisfactorily.

With the functional components shown above, a controllable microfluidic reactor can be built on paper or other suitable nonwoven materials. Figure 5 shows the concept of a simple reactor consisting of two sample dosing sites (A_1 and A_2), which are connected

to a reaction site (B) via two switches (S_1 and S_2). Two liquid reactants can be placed in each of the dosing sites; they can be controlled to enter the reactor by the switches.

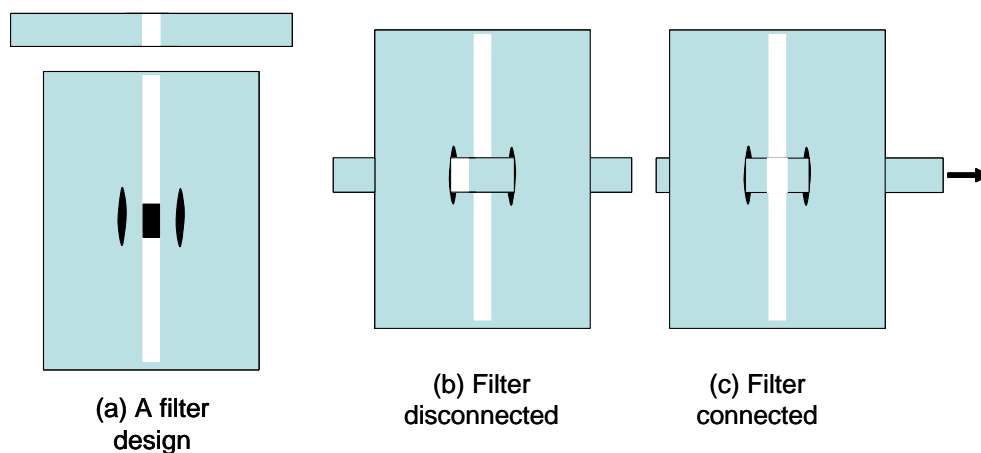


Figure 3. A simple and versatile design of a paper-based microfluidic separator. It can be activated by pulling the paper strip.

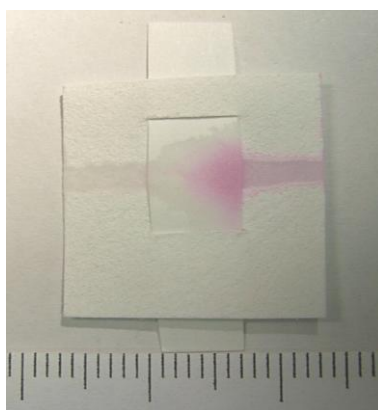


Figure 4. A filter made of silica coated matt ink jet paper was used to separate the magenta dye from a diluted ink jet ink solution.

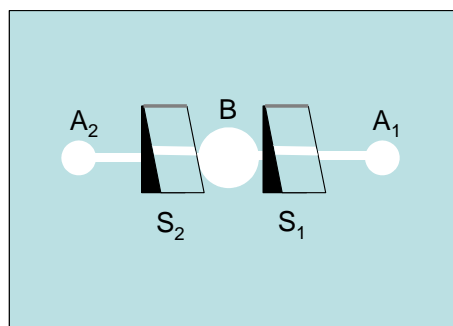


Figure 5. A design of a simple paper-based microfluidic reactor consisting of two sample dosing sites (A_1 , A_2), two switches (S_1 , S_2) and a reaction site (B).

Figure 6 shows a microfluidic reactor (Figure 6a) in operation. A small quantity of phenolphthalein indicator was placed into the reaction zone (B) to demonstrate an acid–base neutralization reaction. A NaOH and a HCl solution were introduced into sample dosing zones A_1 and A_2 , respectively (Figure 6b). Both switches were in the disconnected position. Switch S_1 was then switched on to allow the NaOH solution to enter the reaction zone. As the NaOH solution entered the reaction zone, the change of indicator color was observed (Figure 6c). Then S_2 was switched on to allow the HCl solution to enter the reaction zone (Figure 6d). As the HCl solution entered the reaction zone, the neutralization reaction occurred. Figure 6e shows the expected fading of indicator color as the neutralization reaction completed.

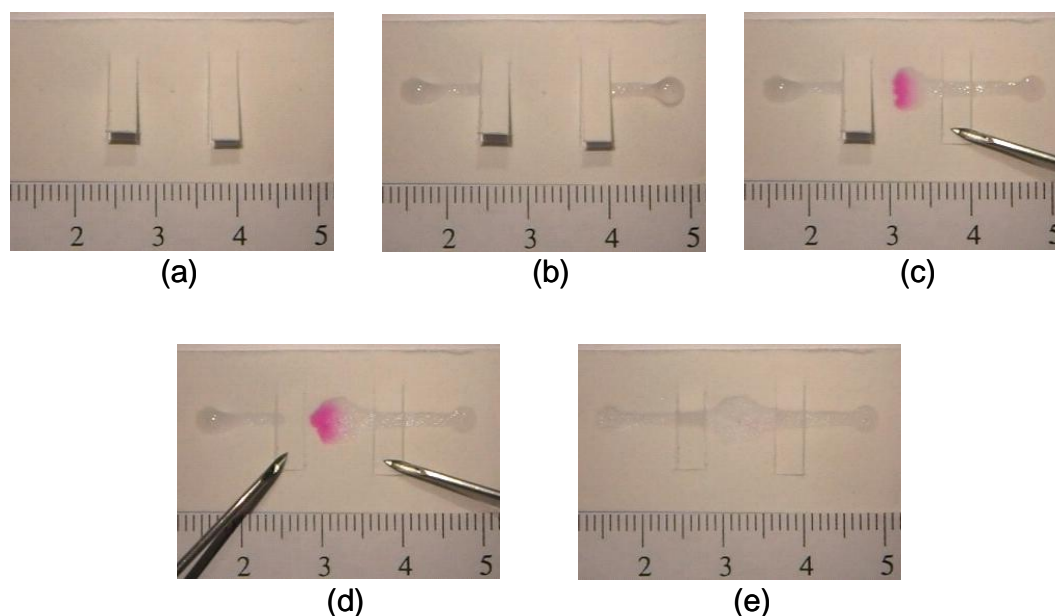


Figure 6. A microfluidic reactor in operation: (a) The reactor fabricated using plasma treatment. Phenolphthalein was deposited in the reaction site B. (b) Dosing of a NaOH solution via A_1 and HCl solution via A_2 ; (c) NaOH solution was allowed into the reaction site, triggering indicator color change; (d) HCl solution was allowed into the reaction site, causing indicator color fading; (e) Complete reversion of indicator color by HCl solution.

Paper-based microfluidic systems fabricated using plasma treatment are capable of allowing single- and multi-step tests, as well as reactions to be performed. Plasma treatment allows the paper to retain its original flexibility. Since the treatment does not change the color of the paper, diagnostic devices made using this method allow easy color identification.

2.5 CONCLUSION

A new method of making paper-based microfluidic patterns by plasma treatment was developed. Microfluidic devices made using this method have the same capability of transferring and analyzing liquid samples as similar devices reported previously, but the paper devices made using plasma treatment have an advantage over the barrier design in that simple functional elements such as switches, filters, and separators can be easily built in the microfluidic system. This advantage will be further explored to build more advanced paper-based microfluidic devices.

2.6 ACKNOWLEDGEMENT

The authors would like to gratefully acknowledge Monash University and Australian Research Council for their scholarships (X.L. and T.N.). The authors would also like to thank Dr. N. Cowieson of Monash Centre for Synchrotron Science for valuable discussions.

2.7 REFERENCES

- (1) Stock, R.; Rice, C. B. F. *Chromatographic Methods*, 3rd ed.; John Wiley & Sons: New York, 1974; p 106.
- (2) Atkins, P.; Jones, L. *Chemistry—Molecules, Matter, and Change*, 3rd ed.; W.H. Freeman & Company: New York, 1997; p 26.
- (3) Umland, J. B. *General Chemistry*; West Publishing Company: St. Paul, MN, 1993; p 592.
- (4) Martinez, A. W.; Phillips, S. T.; Buttle, M. J.; Whitesides, G. M. *Angew. Chem., Int. Ed.* 2007, 46, 1318–1320.
- (5) Martinez, A. W.; Phillips, S. T.; Carrilho, E.; Thomas, S. W., III; Sindi, H.; Whitesides, G. M. *Anal. Chem.* 2008, 80, 3699–3707.
- (6) Martinez, A. W.; Phillips, S. T.; Wiley, B. J.; Gupta, M. J.; Whitesides, G. M. *Lab Chip* 2008, 8, 2146–2150.
- (7) Bruzewicz, D. A.; Reches, M.; and Whitesides, G. M. *Anal. Chem.* 2008, 80, 3387–3392.
- (8) Shen, W.; Tian, J.; Li, X.; Garnier, G. Australian Provisional Patent No. 2008903553, July 11, 2008.
- (9) Shen, W.; Filonanko, Y.; Truong, Y.; Parker, I. H.; Brack, N.; Pigram, P.; Liesegang, J. *Colloid Surf. A* 2000, 173, 117–126.

Chapter 3: Fabrication of Paper-Based Microfluidic Sensors by Printing

This page is intentionally blank

Monash University
Declaration for Thesis Chapter 3

Declaration by candidate

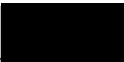
In the case of Chapter 3, the nature and extent of my contribution to the work was the following:

Nature of contribution	Extent of contribution (%)
Experimental design and conduct, paper writing	50

The following co-authors contributed to the work. Co-authors who are students at Monash University must also indicate the extent of their contribution in percentage terms:

Name	Nature of contribution	Extent of contribution (%) for student co-authors only
Junfei Tian	Experimental design, assisted in experimentation	40
Gil Garnier	Corrected manuscript	Co-supervisor
Wei Shen	Experimental design, corrected manuscript	Co-supervisor

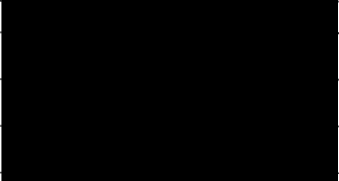
Candidate's Signature

	Date 04/08/2011
---	---------------------------

Declaration by co-authors

The undersigned hereby certify that:

- (1) the above declaration correctly reflects the nature and extent of the candidate's contribution to this work, and the nature of the contribution of each of the co-authors.
- (2) they meet the criteria for authorship in that they have participated in the conception, execution, or interpretation, of at least that part of the publication in their field of expertise;
- (3) they take public responsibility for their part of the publication, except for the responsible author who accepts overall responsibility for the publication;
- (4) there are no other authors of the publication according to these criteria;
- (5) potential conflicts of interest have been disclosed to (a) granting bodies, (b) the editor or publisher of journals or other publications, and (c) the head of the responsible academic unit; and
- (6) the original data are stored at the following location(s) and will be held for at least five years from the date indicated below:

Location(s)	Australian Pulp and Paper Institute (APPI), Department of Chemical Engineering, Monash University, Clayton, VIC 3800, Australia	
Signature 1		Date 04/08/2011
Signature 2		05/08/2011
Signature 3		4/8/11

This page is intentionally blank

Fabrication of Paper-Based Microfluidic Sensors by Printing

Xu Li, Junfei Tian, Gil Garnier, Wei Shen*

*Australian Pulp and Paper Institute, Department of Chemical Engineering,
Monash University, Clayton Campus, PO Box 69M, Melbourne, Vic. 3800, Australia*

**Corresponding Author: Email: [REDACTED]*

Tel: [REDACTED] Fax: [REDACTED]

3.1 ABSTRACT

A novel method for the fabrication of paper-based microfluidic diagnostic devices is reported; it consists of selectively hydrophobizing paper using cellulose reactive hydrophobization agents. The hydrophilic–hydrophobic contrast of patterns so created has excellent ability to control capillary penetration of aqueous liquids in paper channels. Incorporating this idea with digital ink jet printing techniques, a new fabrication method of paper-based microfluidic devices is established. Ink jet printing can deliver biomolecules and indicator reagents with precision into the microfluidic patterns to form bio-chemical sensing zones within the device. This method thus allows the complete sensor, i.e. channel patterns and the detecting chemistries, to be fabricated only by two printing steps. This fabrication method can be scaled up and adapted to use high speed, high volume and low cost commercial printing technology. Sensors can be fabricated for specific tests, or they can be made as general devices to perform on-demand quantitative analytical tasks by incorporating the required detection chemistries for the required tasks.

3.2 KEYWORDS

Microfluidic system, Ink jet printing, Paper, Sizing

3.3 INTRODUCTION

Paper made of cellulose fibres is naturally hydrophilic and allows penetration of aqueous liquids within its fibre matrix. This property provides the foundation for using paper to fabricate microfluidic systems [1]. It has been reported that paper-based microfluidic devices can be built by demarcating hydrophilic paper by walls of hydrophobic polymers [2]. Following this principle, Martinez et al. [2, 3] explored the use of a photolithography method to create microfluidic channels in paper by making hydrophobic barrier walls in the paper matrix. Hydrophobic photoresist polymers provide a very good physical barrier, which defines the liquid penetration pathways into paper. A liquid sample can be directed into multiple detection zones where indicators have been deposited. This device demonstrates the possibility of the simultaneous detection of multiple analytes in a liquid sample. The barrier-design microfluidic systems are well suited for making health care and telemedicine devices. However, this fabrication method has two potential deficiencies: first, the hardened photoresist barrier is susceptible to the damage from bending and folding. Second, photolithography requires expensive equipment and the fabrication process has multiple steps. There is a need for alternative and more efficient fabrication methods.

Bruzewicz et al. [4] used a modified plotter to create a barrier pattern by printing polydimethylsiloxane (PDMS) onto paper. This method overcame the problem of physical inflexibility of devices made using photolithography. However, the quality of the barrier definition deteriorated, since the penetration of PDMS in paper could not be very well controlled, resulting in the wall of the barrier not being straight. This method is also limited to producing devices on an up-graded scale and at a high speed.

Abe et al. [5] took a polymer (polystyrene) solution impregnation approach to introduce hydrophobicity into the paper matrix. They then used a microdrop dispensing device to print solvent onto the impregnated paper to dissolve the polymer and to form fine liquid penetration channels. These researchers also printed chemical sensing agents into their pattern to form a functional device for biomedical detection. Lu et al. [6] used a wax printer to generate microfluidic patterns in paper. The pattern was then heated to allow wax diffusion into paper and to form the barriers for microfluidic channels. These

fabrication concepts are similar to the barrier concept, since they rely on cellulose fibres in paper to be physically covered by a layer of hydrophobic materials.

The motivation of this work is to present a new concept of creating microfluidic patterns and channels by generating a hydrophilic–hydrophobic contrast on the paper surface, forming liquid penetration channels, rather than building patterns using a physical polymer barrier. Building barriers in paper to define channels is a limiting process to the speed and cost of large scale fabrication, as it usually involves multiple steps including polymer impregnation and pattern development. The ink jet printing approach reported in this study can fabricate paper-based microfluidic patterns in a single printing step. This concept, therefore, has a clear potential to enable the fabrication of paper-based microfluidic sensors, i.e. patterns and incorporated sensing chemistries, by continuous high-speed and large-volume industrial printing processes. Such efficiencies enable the ultimate practical use of these sensors for health care and environmental applications. Since printed paper retains its original flexibility, the new method also overcomes the problem of channel damage by folding and bending. Also, simple and functional elements, such as switches and micro-reactors, can be easily built into the devices made by this approach [7].

3.4 MATERIALS AND METHODS

3.4.1 Chemicals and Materials

Alkyl ketene dimer (Wax 88 konz, BASF) and alkenyl ketene dimer (Precis 900, Hercules Australia Pty. Ltd.) were used as the cellulose hydrophobization (or sizing) agents. Both dimers have two hydrocarbon chains of C_{16} – C_{20} . Alkenyl ketene dimer, however, has one $-C=C-$ in each of its two hydrocarbon chains [8]. Analytical grade n-heptane (Sigma–Aldrich) was used as the solvent to make solutions of both dimers. A4 size Whatman filter paper (No. 4) with the pore size of 20–25 μm (Sigma–Aldrich specification) was used as the paper substrate for printing. MilliQ water was used for all aqueous sample dilutions.

Alkaline phosphatase (lyophilized powder, from bovine intestinal mucosa, 10–30 DEA units/mg solid) was obtained from Sigma–Aldrich. One milligram per milliliter phosphatase solution was prepared in the buffer solution (pH 9.8) which contains 1.0 M diethanolamine ($\geq 98\%$, Sigma–Aldrich) and 0.5 mM $\text{MgCl}_2 \cdot 6\text{H}_2\text{O}$ ($\geq 99\%$, Sigma–Aldrich). A BCIP[®]/NBT substrate system (Sigma–Aldrich) was used to indicate the activity of the enzyme through color change.

NaNO_2 ($\geq 99\%$) was obtained from Sigma–Aldrich. The indicator solution for NO_2^- contains 50 mmol/L sulfanilamide ($\geq 99\%$, Sigma–Aldrich), 330 mmol/L citric acid ($\geq 99.5\%$, Sigma–Aldrich), and 10 mmol/L N-(1-naphthyl)ethylenediamine, ($\geq 98\%$, Sigma–Aldrich).

3.4.2 Microfluidic Channel Formation on Paper

In the first approach, patterned de-hydrophobization of paper was used to generate hydrophilic channels on paper. Filter paper samples were first hydrophobized by dipping in and quickly removing out of an alkyl ketene dimer–heptane solution (0.6 g/L) to allow evaporation of heptane. Filter paper samples were then heated in an oven at 100 °C for 5 min to facilitate the curing of alkyl ketene dimer on cellulose fibres. The hydrophobized samples were sandwiched between metal masks and then treated with a vacuum plasma reactor (Quorum Emitech, UK) for 15 s at an intensity of 15 W. The vacuum level for the treatment was 6×10^{-1} mbar. Metal masks were made by mechanically cutting the desired patterns out of stainless steel sheets. Four screws were used to align the masks. The treated paper samples retained their original flexibility without visible marks.

In the second approach, patterned hydrophobization of paper was used to generate hydrophilic channels on paper. Hydrophilic filter papers were printed using a reconstructed commercial digital ink jet printer (Canon Pixma ip4500) with electronically generated patterns of an alkenyl ketene dimer–heptane solution (5%, v/v). The modification of the printer involved replacing the ink in cartridge with the alkenyl ketene dimer–heptane solution. This solution is printable by the Canon printer chosen for this work. Solvents of strong dissolving power, such as chloroform and toluene, are

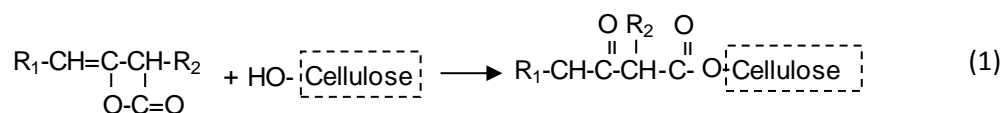
not suitable, as they may chemically attack certain parts of the printer. Printing did not leave any visible mark on paper samples which retain their original flexibility. The printed filter paper samples were then heated in an oven at 100 °C for 8 min to cure alkenyl ketene dimer onto the cellulose fibres. A stop watch, ruler, video camera, and optical microscope were used for the characterization of liquid penetration inside paper microfluidic channels.

Paper sheets with hydrophobized patterns were then printed with detection reagents to form complete sensors. Two printed chemistries were used to visually demonstrate the applications of the sensors. First, a 1 mg/mL alkaline phosphatase enzyme solution was printed into the detection zone of a sensor. The BCIP[®]/NBT liquid substrate was introduced into the sensor via its sample introduction zone. The liquid substrate penetrated through the channel, reaching the detection zone, and lead to the color change that confirms the presence and the activity of the enzyme. Second, a colorimetric reaction for NO₂⁻ detection was employed. An indicator solution for colorimetric detection of NO₂⁻ (an aqueous solution of citric acid, sulfanilamide and N-(1-naphthyl)-ethylenediamine [9]) was printed onto the sheet with same patterns and into the detection zones of all sensors. Five microlitres of NO₂⁻ sample solution (5 mM) was manually introduced into the microfluidic channels of all sensors and allowed to penetrate into the detection zones, showing a color change.

3.5 RESULTS

3.5.1 Hydrophilic-Hydrophobic Contrast of Untreated and Treated Papers

Alkyl and alkenyl ketene dimers are reactive cellulose hydrophobization agents. Their common reactive functional group is the four-member lactone ring, which is connected to two long hydrocarbon chains (C₁₆–C₂₀). Once alkyl and alkenyl ketene dimers are immobilized on fibre surfaces via the (esterification) reaction with –OH groups of cellulose, the two hydrocarbon chains impart hydrophobicity to the cellulose fibre surface [10]:



The hydrophobized filter paper samples are strongly hydrophobic and have contact angles of typically 110–125° with water [10], whereas untreated cellulose has a contact angle of only 25° [11]. The Washburn equation has been used as a first order approximation to study the penetration of liquids in paper (Eq. (2)) [12]:

$$l = \sqrt{\frac{\gamma \cos \theta}{2\eta} t} \quad (2)$$

Where l is the liquid penetration distance in paper, r is the equivalent capillary pore radius of paper, γ and η are the surface tension and viscosity of the liquid, θ is the contact angle and t is the time of penetration. Eq. (2) shows that if a paper surface sustains an apparent contact angle with a liquid of greater than 90°, then liquid penetration will not occur. This phenomenon is the basis of our study of using patterned hydrophilic–hydrophobic contrast to fabricate paper-based microfluidic sensors. Plasma treatment and printing are intuitively two of the simplest ways to generate patterns of hydrophilic–hydrophobic contrast on paper.

3.5.2 Patterned De-Hydrophobization of Papers by Plasma Treatment

Plasma treatment was used to prove the principle of using hydrophilic–hydrophobic contrast for the fabrication of paper-based microfluidic devices. Plasma treatment of hydrophobic paper with patterned masks provides an easy method to selectively introduce hydrophilic patterns to hydrophobic paper. Fig. 1 shows a six-channel pattern created in a hydrophobic paper by plasma treatment. The channel width on the masks was 1 mm and that on the treated paper was around 1.5 mm. A NaOH solution was introduced into the pattern through the central sample dosing site and simultaneously penetrated along all channels into the detection zones where a phenolphthalein–ethanol solution was deposited after plasma treatment. The plasma treated channels have well-defined borders; the indicator color change in all detection zones demonstrated that the

device is capable of performing similar analytical tasks as demonstrated in previous studies [2-5].

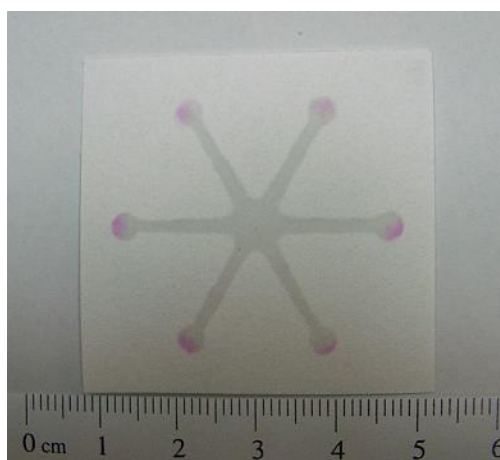


Fig. 1. The performance of a paper-based microfluidic pattern fabricated by plasma treatment. NaOH solution drops delivered to the central sample dosing zone penetrated through channels into the detection zones, causing color change of phenolphthalein indicator.

Hot electrons and other energetic particles generated in vacuum plasma have long mean free paths. Over-etching of the substrate under a mask is a known problem for plasma treatment, causing the treated pattern to be slightly bigger than the mask. However, over-etching could be controlled by optimizing the treatment intensity and time. When the treatment intensity and time were fixed, channels of very reproducible width were achieved. The plasma treated areas were highly wettable by water or aqueous solutions and allowed the transport of aqueous solutions along and within the plasma treated channels via capillary penetration [7].

3.5.3 Patterned Hydrophobization of Papers by Ink Jet Printing

A reconstructed ink jet printer was used to print the alkenyl ketene dimer–heptane solution onto an untreated filter paper. After curing, the printed area became strongly hydrophobic and the non-printed area remained hydrophilic. The printed area sustained water contact angle of greater than 110° . Printed hydrophobic patterns are invisible to the eye and printed papers retain their original flexibility. Fig. 2 shows a printed pattern on a filter paper; water was allowed to wick into the pattern starting from circular zones

at the end of the channels to reveal the printed hydrophobic and non-printed hydrophilic areas.

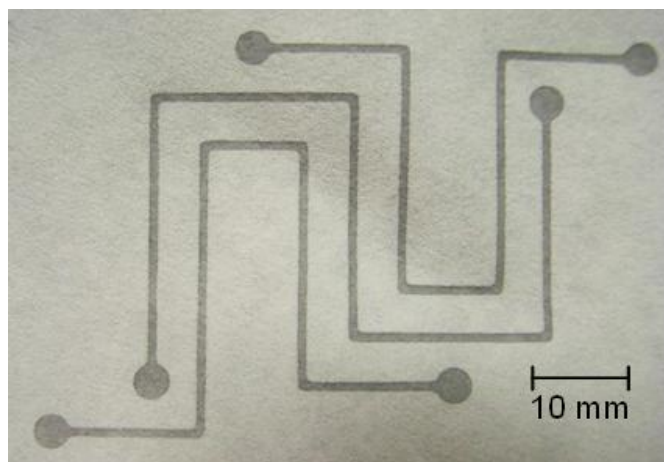


Fig. 2. Ink jet printed paper-based microfluidic patterns have channels and zones defined by the hydrophilic–hydrophobic contrast (microfluidic patterns wetted with water).

Current commercial digital ink jet printers are capable of issuing small droplets of a few picolitres and use a small volume of ink for generating an electronically created image. The reconstructed printer also inherits this frugal ink management feature. Heptane is a fast evaporating solvent; its fast evaporation after printing limits the penetration of the solution into the paper matrix. This allows the hydrophilic channels on paper surface created by a single-step printing to have a well-defined hydrophilic–hydrophobic border (Fig. 2). Ink jet printing has the advantage of easily varying the printed pattern electronically on demand. We used ink jet printing to print a traditional Chinese paper cut pattern of a dragon to demonstrate this advantage; four liquid dosing ports were added to the four corners of the pattern. Fig. 3(a) shows an early stage of water penetration from the four ports; Fig. 3(b) shows the complete penetration of the pattern by water. Fig. 4 shows the microfluidic sensor patterns printed on an A4 size filter paper sheet; it consists of the fluidic channels, detection zones and the indicator for NO_2^- . A 5 μL aliquot of NO_2^- solution (5.0 mM) was introduced into each sensor on the sheet to reveal the color change in sensors and show the uniformity of the printed sensors. Fig. 3 and 4 thus demonstrate the possibility of using our concept to mass produce paper-based microfluidic sensors with easy and simple electronic pattern variations.

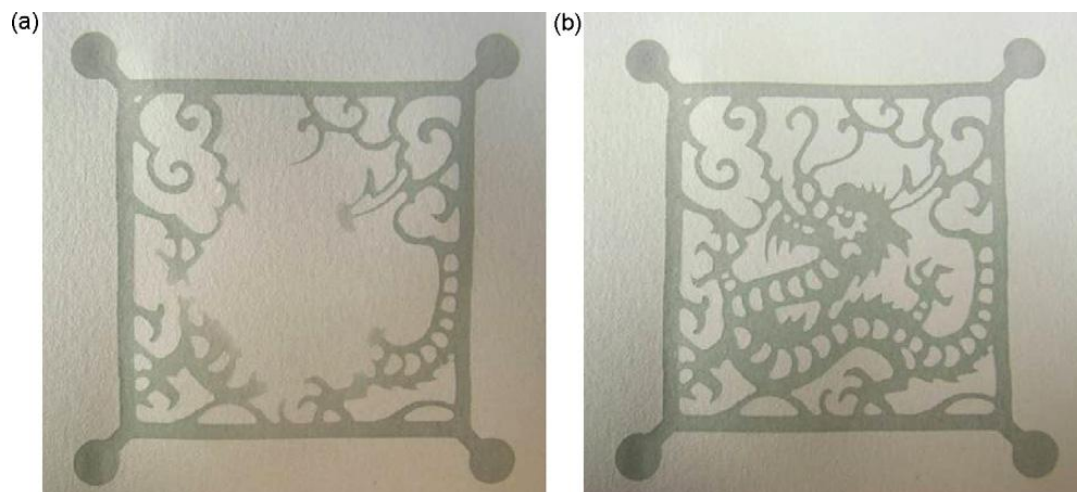


Fig. 3. Ink jet printed paper fluidic pattern of a Chinese paper cut. Four liquid feeding zones were added to the four corners of the pattern. Water penetration at an early stage (a) and at the final stage (b) is shown.



Fig. 4. Microfluidic sensor patterns are printed on an A4 sized Whatman #4 filter paper. A colorless indicator for detection of NO_2^- was also printed into the circular detection zone. Five microlitres of 5 mM NO_2^- sample solution was introduced into the channel. As the sample solution reached the detection zones of the sensors, reproducible color changes were seen.

3.5.4 Characterization of Printed Microfluidic Channels in Paper

3.5.4.1 Hydrophilic Channel Resolution and Cross-Section

The ink jet printer prints the hydrophobization “ink” only on one surface of the paper, and the ink undergoes free penetration into the paper structure. The ink jet printer

issues only a small amount of ink; thus, the penetration distance of the ink into the paper is small. The quick evaporation of the hydrocarbon solvent further reduces the ink penetration distance. A paper-based device with the single-channel pattern was cut with a razor blade; the channel was then fed with water to allow visualization of the cross-section of a water-wetted channel. The cross-section of the wetted paper channel therefore illustrates water transportation in the paper channel, and shows that the cross-section of the channel is not perfectly rectangular (Fig. 5). The printing of a designed 500 μm channel resulted in a printed channel with the top side of 475 μm and a somewhat larger bottom side of 667 μm . The decreased width of the top side of the channel is due to the horizontal penetration of the hydrophobization ink and the increased width of the bottom side of the channel is due to the shorter z -direction of penetration of the hydrophobization ink at the edge of the pattern. Although the cross-section of the hydrophilic channel formed by printing is not perfectly rectangular, it is, however, adequate for its intended use of transporting liquid samples in the paper-based microfluidic pattern. Using ink jet printing, finer channels of 300 μm can be easily printed which was wetted with water (Fig. 6(a)). A rose-pink food dye solution was introduced into a hydrophilic channel of 600 μm ; the penetration of the dye solution along the channel shows that the hydrophilic–hydrophobic contrast at the channel boundary maintains a good level of channel integrity and the amount of solution “leaking” does not present a problem to the liquid transport in the channel (Fig. 6(b)).

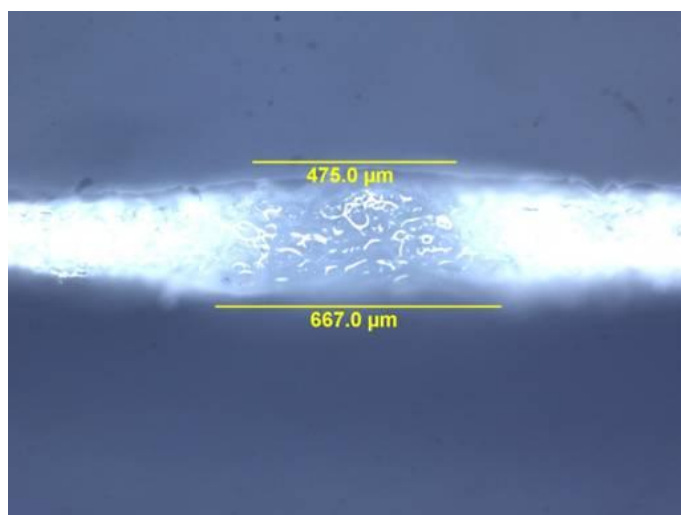


Fig. 5. The cross-section of a channel with the design width of 500 μm . Water penetration in the channel shows a decrease and an increase in channel width on the top and the bottom sides of the paper respectively.

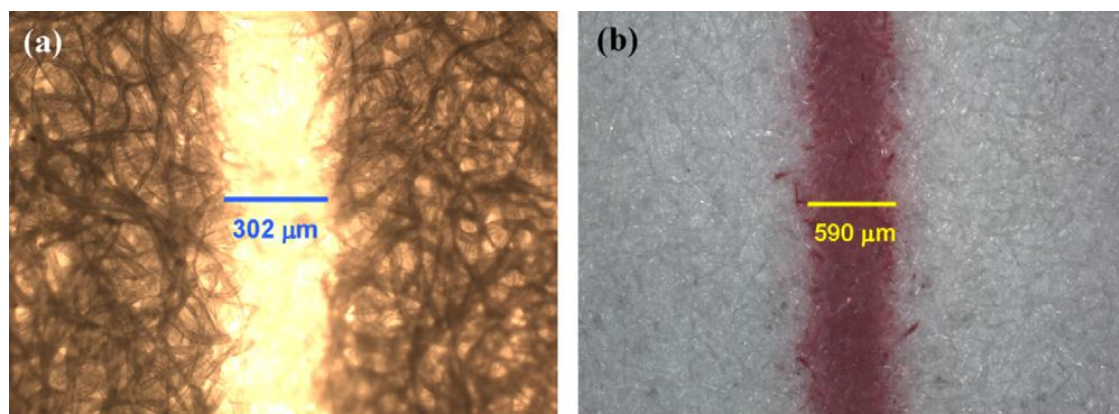


Fig. 6. Micrographs of printed channels recorded using the transmission illumination mode. (a) Water was used as the wicking liquid to increase light transmission in paper for channel width measurement. The channel has an average width of around 300 μm ; (b) the penetration of a food dye solution reveals the integrity of the channel boundary. The channel very well defines the liquid wicking pathway and the amount of “leaking” does not present a problem to the liquid transport.

3.5.4.2 Liquid Penetration Behavior in a Printed Channel

Fabricating microfluidic channels by ink jet printing requires only one of the paper surfaces to be printed. Water penetration in a 1000 μm hydrophilic channel printed on paper was studied using a ruler, stop watch and video camera (Fig. 7). Measurement of water penetration distance against the square root of time shows that the penetration in paper channel agrees reasonably well with the Washburn model (Eq. (2)) (Fig. 8). The noticeable deviation of the data from the linear trend line at longer penetration times is likely to be caused by the loss of driving force. A possible reason may be fibre swelling. Fibre swelling absorbs liquid into the fibre wall, leaving less amount of the free liquid to transport in inter fibre capillary channels. Fibre swelling may also restrict the capillary pores in paper, making the liquid penetration slower. Another minor contribution to the deviation may be the gravity. The original Washburn model does not consider the liquid absorption by the capillary wall nor the gravity factor. The linear regime of the penetration data is useful for the estimation of the penetration rate of water in the channel for sensor design purposes.

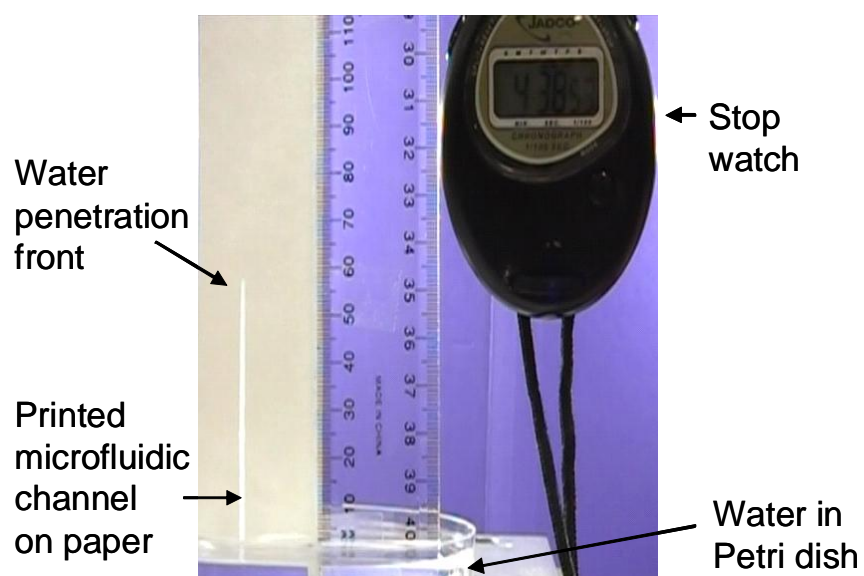


Fig. 7. Experimental set up for water penetration rate measurements of a printed paper channel. The width of the channel was 1000 μm .

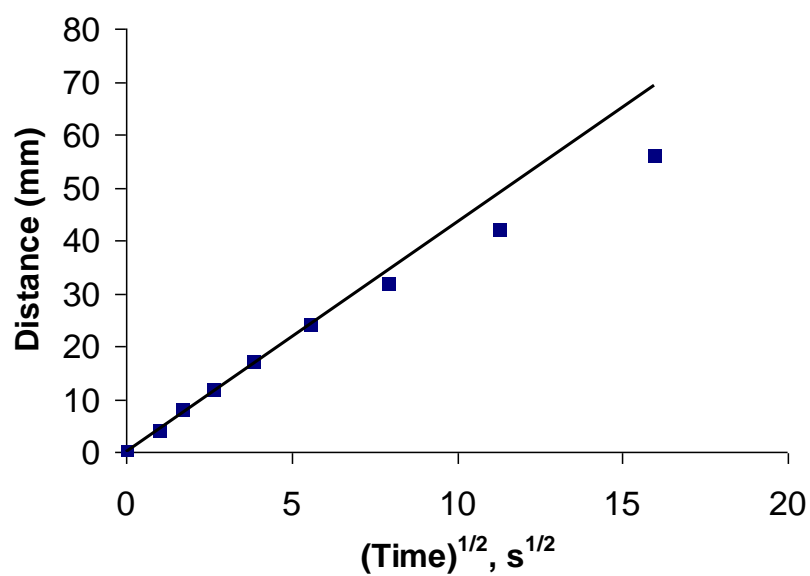


Fig. 8. Water penetration distance in the printed channel as a function of the square root of time.

3.5.5 Paper-Based Microfluidic Sensors with Incorporated Detection Chemistry

Ink jet printing of biomolecules has been reported previously by many research groups [13, 14]. Ink jet printing is a non-contact printing process, which offers a unique advantage of minimizing cross-sample contamination. By combining printing of biomolecules and the printing of capillary channel patterns together, an efficient approach for fabrication of microfluidic sensors using paper is formed. Fig. 9 shows an ink jet printed paper microfluidic sensor; the fluidic pattern and the alkaline phosphatase solution were printed using two cartridges in two steps. The introduction of the liquid substrate onto the printed sensor shows the printed pattern of the enzyme and confirms its activity after printing. Printing is, therefore, a highly efficient way to fabricate paper-based microfluidic sensors. In commercial printing, up to 8 inks can be printed on a substrate in one printing process [15]. It is, therefore, realistic to use commercial printing processes to fabricate paper-based microfluidic sensors at low cost. Commercial printing processes can easily offer drying and heating treatment in between two steps of printing [15].

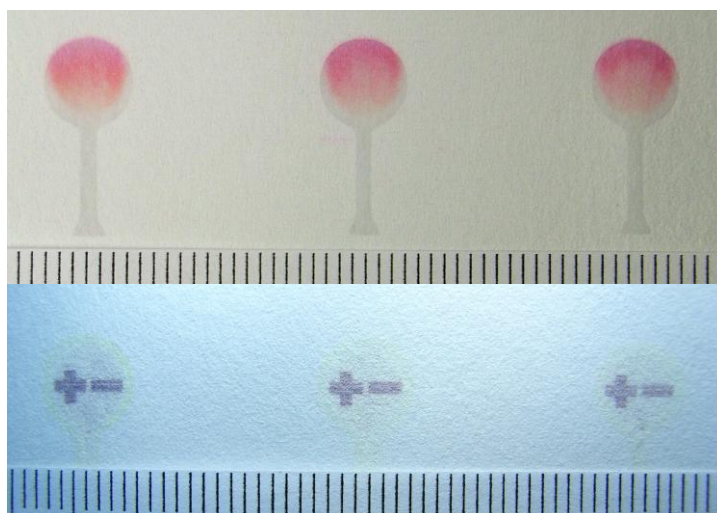


Fig. 9. Ink jet printed paper microfluidic sensors. The fluidic pattern and the detection chemistries: (a) the indicator for NO_2^- was printed into the circular detection zone. Five microlitres of 5 mM NO_2^- sample solution was introduced into the channel. As the sample solution reached the detection zones of the sensors, reproducible color changes are seen; (b) alkaline phosphatase was printed into circular detection zone and the BCIP[®]/NBT liquid substrate solution was introduced at the sample dosing site. As the liquid substrate penetrated into the detection zone, the position and activity of the printed enzyme are revealed.

Whilst sensors for specific purposes can be fabricated by printing both the microfluidic patterns and the specific detection chemical reagents, sensors for general purpose can be fabricated by only printing the microfluidic patterns with the desirable sample handling features. Detection chemistry can be introduced in an “on demand” manner, depending on the analytical task. Fig. 10 shows a general purpose of paper-based microfluidic pattern that can be used for qualitative and quantitative analytical purposes.

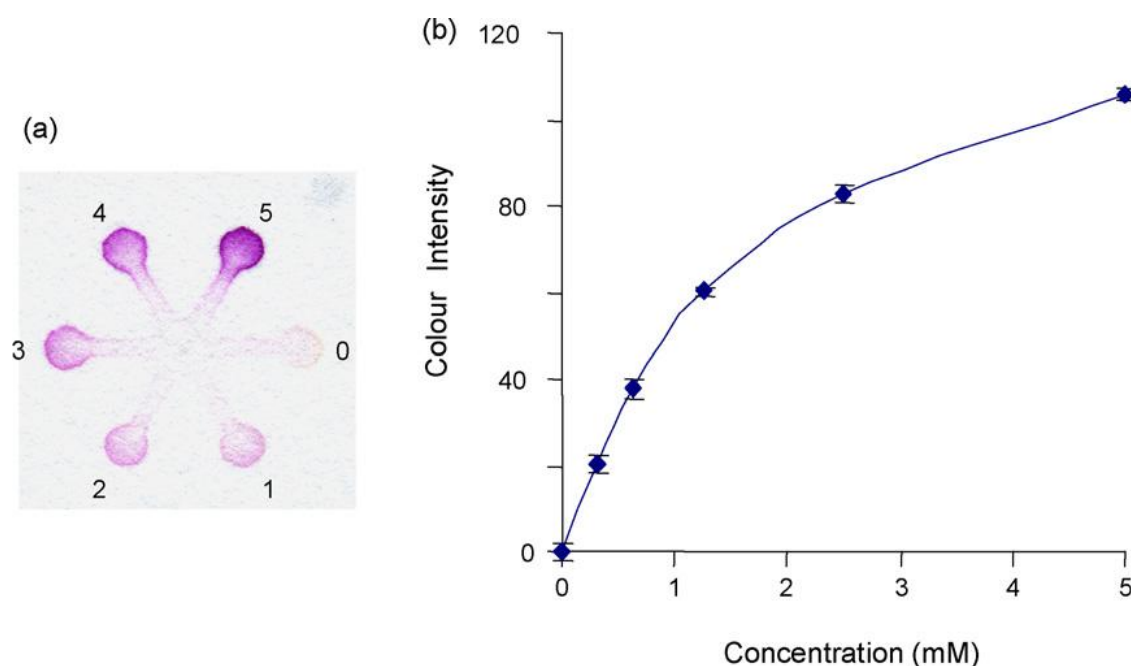


Fig. 10. (a) The scanned image of the sensor using a desk-top scanner after the samples and indicator were introduced; (b) average color density of each detection zone was determined using PhotoShop and the whole calibration curve is obtained.

To demonstrate its use for quantitative analysis, a colorimetric reaction for detecting NO_2^- was used in conjunction with the paper-based microfluidic pattern. NO_2^- is a bio-marker present in the saliva of renal disease sufferers; [9] rapid and quantitative detection of the species is thus useful for monitoring a patient's condition. A standard calibration curve of NO_2^- is highly desirable for its quantitative determination. The calibration curve can be obtained by adding a series of standard solutions of NO_2^- (0–5 mmol/L) into a sensor with six detection zones (Fig. 10(a)). An indicator is added to the central zone; the indicator rapidly penetrates through the channels into the detection zones, causing corresponding color changes. The paper sensor can then be scanned using a desk-top scanner and the average color density values determined by

PhotoShop can be used to construct the calibration curve. Five independent measurements were taken from the five paper-based microfluidic devices to give the average values \pm standard deviation. Small error bars of the five measurements indicate good reproducibility. Detailed quantitative aspects and application of this method was reported elsewhere [16].

3.6 DISCUSSION

Compared with the previous physical barrier fabrication methods, the new fabrication method reported in this study enables the manufacturing of paper-based microfluidic devices at commercial scales and very low cost. Price is a very sensitive factor for paper-based microfluidic sensors; the material cost for making these sensors is, therefore, an important point of consideration [3]. The whole sale prices of AKD from European manufacturers are 3–4 euro/kg, and the AKD usage in paper sizing is typically less than 5 kg/ton of dry fibre. If the basis weight of the paper is 92 g/m² (Whatman quality control information, <http://www.whatman.com>) and the area of each paper-based microfluidic sensor is 25 cm² (i.e. 5 cm \times 5 cm), the cost of AKD on each device will only be 0.000005 euro. In the lab-scale fabrication, each A4 size filter paper can produce 20 sensors; using the printing method reported in this work and taking ink consumption for printing each A4 sheet as 400 μ L, the AKD cost of each sensor (25 cm²) will be 0.000002 euro, significantly cheaper than the barrier material costs of barrier-based paper sensors reported previously which were \$0.025 for photoresist SU-8 and \$0.0025 for PDMS [4, 17]. The creation of the hydrophilic–hydrophobic contrast is a simpler approach to define liquid penetration channels in paper than the physical barrier approach. Several cellulose hydrophobization chemistry systems have been used in commercial papermaking processes [10]; these chemistry systems can also be modified for the purpose of printing paper-based microfluidic sensors.

The use of digital printing technology to selectively deliver cellulose hydrophobization chemicals on paper surfaces to form the hydrophilic–hydrophobic contrast has several additional advantages. Digital printing offers electronic pattern variation which allows fast change over between the fabrications of different devices. Since the hydrophilic–

hydrophobic contrast fabrication concept can retain the original flexibility of the paper, it offers natural bending and folding resistance, which fundamentally overcomes the poor bending and folding resistance often encountered with devices fabricated by other methods [18]. Fig. 11 shows an example of a harsh bending and folding test. The performance of the ink jet printed patterns shows no discernable deterioration after the bending test.

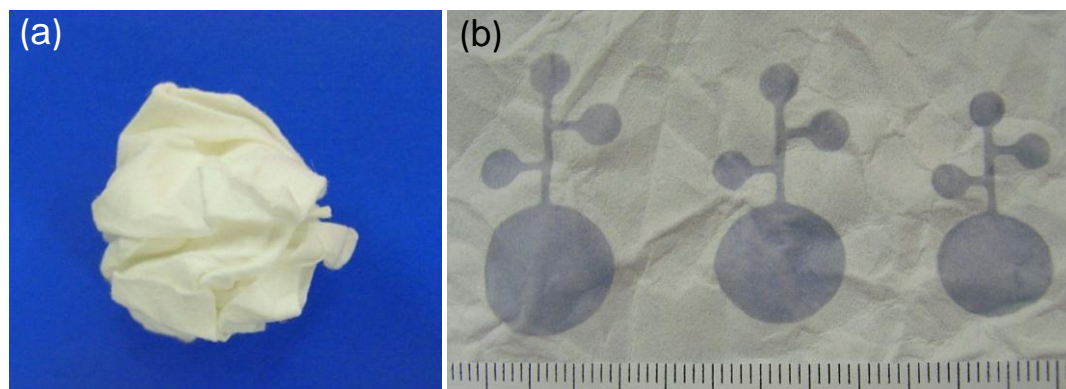


Fig. 11. (a) The printed paper microfluidic patterns were subjected to a harsh bending/folding test; (b) the performance of the printed patterns showed no discernable deterioration after the test.

The concept of hydrophilic–hydrophobic contrast allows simple yet functional elements such as switches to be built into devices [7]. Reactor systems are possible by combining channels, switches and filters. Multi-step diagnostic tests can also be achieved with switches. Commercial printing can easily build simple switches on paper by die-cutting operations. By printing hydrophilic–hydrophobic contrast on papers, a plethora of flexible microfluidic sensors can be fabricated and their production scaled up.

3.7 CONCLUSION

The concept of printing hydrophilic–hydrophobic contrast to fabricate paper-based microfluidic sensors was investigated. Hydrophobized filter paper shows strong wetting resistance compared to the untreated filter paper. Combining this concept with plasma treatment and ink jet printing, well-defined microfluidic channels can be created on

paper. Ink jet printing can also print (bio) chemical sensing agents in the microfluidic patterns with precision, which allows complete paper-based microfluidic sensors to be fabricated in one printing process consisting of two printing steps. The printing method provides potential for the mass production of microfluidic sensors at low cost as well as for laboratory research use where pattern variability is likely to be required. Qualitative and quantitative analyses can easily be achieved with different types of paper-based microfluidic sensors.

Paper-based microfluidic sensors fabricated using the hydrophilic–hydrophobic contrast concept retain the original paper flexibility. This allows simple and functional elements, such as switches and filters/separators, to be built into the sensors. With these functional elements, more advanced paper-based sensors can be designed and fabricated for more sophisticated tests.

3.8 ACKNOWLEDGEMENT

The research scholarships of Monash University and the Department of Chemical Engineering are gratefully acknowledged. BASF and Hercules Australia are thanked for providing the hydrophobization agents. The authors would like to specially thank Dr. E. Perkins of the Department of Chemical Engineering, Monash University for proof reading the manuscript.

3.9 REFERENCES

- [1] R. Stock, C.B.F. Rice, *Chromatographic Methods*, 3rd ed., John Wiley & Sons, New York, 1974, p. 106.
- [2] A.W. Martinez, S. T. Phillips, M. J. Butte, G.M. Whitesides, *Angew. Chem., Int. Ed.* 46 (2007) 1318–1320.
- [3] A.W. Martinez, S. T. Phillips, E.Carrilho, S.W. Thomas III, H. Sindi, G.M. Whitesides, *Anal. Chem.* 80 (2008) 3699–3707.
- [4] D.A. Bruzewicz, M. Reches, G.M. Whitesides, *Anal. Chem.* 80 (2008) 3387–3392.
- [5] K. Abe, K. Suzuki, D. Citterio, *Anal. Chem.* 80 (2008) 6928–6934.
- [6] Y. Lu, W. Shi, L. Jiang, J. Qin, B. Lin, *Electrophoresis* 30 (2009) 1497–1500.
- [7] X. Li, J. Tian, T. Nguyen, W. Shen, *Anal. Chem.* 80 (2008) 9131–9134.
- [8] L. Qiao, Q. Gu, H.N. Cheng, *Carbohydr. Polym.* 66 (2006) 135–140.
- [9] T.M. Blicharz, D.M. Rissin, M. Bowden, R.B. Hayman, C. DiCesare, J.S. Bhatia, N. Grand-Pierre, W.L. Siqueira, E.J. Helmerhorst, J. Loscalzo, F.G. Oppenheim, D.R. Walt, *Clin. Chem.* 54 (2008) 1473–1480.
- [10] W. Shen, Y. Filonanko, Y. Truong, I.H. Parker, N. Brack, P. Pigram, J. Liesegang, *Colloids Surf. A* 173 (2000) 117–126.
- [11] D. Kannangara, H. Zhang, W. Shen, *Colloids Surf. A* 280 (2006) 203–215.
- [12] K.T. Hodgson, J.C. Berg, *J. Colloid Interface Sci.* 121 (1988) 22–31.
- [13] V. Vauvreau, G. Laroche, *Bioconjugate Chem.* 16 (2005) 1088–1097.
- [14] S.D. Risio, N. Yan, *Macromol. Rapid Commun.* 28 (2007) 1934–1940.
- [15] H. Kipphan, *Hand Book of Printing Media*, Springer-Verlag, Berlin, Germany, 2001, p. 55.
- [16] X. Li, J. Tian, W. Shen, *Anal. Bioanal. Chem.* 396 (2010) 495–501.
- [17] A.W. Martinez, S.T. Phillips, B.J. Wiley, M. Gupta, G.M. Whitesides, *Lab Chip* 8 (2008) 2146–2150.
- [18] P.S. Dittrich, *Lab Chip* 9 (2009) 15–16.

Chapter 4: Quantitative Biomarker Assay with Microfluidic Paper-Based Analytical Devices

This page is intentionally blank

Monash University Declaration for Thesis Chapter 4

Declaration by candidate

In the case of Chapter 4, the nature and extent of my contribution to the work was the following:

Nature of contribution	Extent of contribution (%)
Experimental design and conduct, paper writing	65

The following co-authors contributed to the work. Co-authors who are students at Monash University must also indicate the extent of their contribution in percentage terms:

Name	Nature of contribution	Extent of contribution (%) for student co-authors only
Junfei Tian	Experimental design, assisted in experimentation	25
Wei Shen	Experimental design, corrected manuscript	Supervisor

Candidate's
Signature

	Date 02/08/2011
---	--------------------

Declaration by co-authors


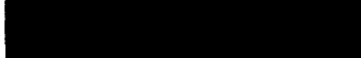
The undersigned hereby certify that:

- (1) the above declaration correctly reflects the nature and extent of the candidate's contribution to this work, and the nature of the contribution of each of the co-authors.
- (2) they meet the criteria for authorship in that they have participated in the conception, execution, or interpretation, of at least that part of the publication in their field of expertise;
- (3) they take public responsibility for their part of the publication, except for the responsible author who accepts overall responsibility for the publication;
- (4) there are no other authors of the publication according to these criteria;
- (5) potential conflicts of interest have been disclosed to (a) granting bodies, (b) the editor or publisher of journals or other publications, and (c) the head of the responsible academic unit; and
- (6) the original data are stored at the following location(s) and will be held for at least five years from the date indicated below:

Location(s)	Australian Pulp and Paper Institute (APPI), Department of Chemical Engineering, Monash University, Clayton, VIC 3800, Australia
-------------	---

Signature 1

Signature 2


	Date 02/08/2011
	4/8/11

This page is intentionally blank

Quantitative Biomarker Assay with Microfluidic Paper-Based Analytical Devices

Xu Li, Junfei Tian and Wei Shen*

*Australian Pulp and Paper Institute, Department of Chemical Engineering,
Monash University, Clayton, Melbourne 3800, Victoria, Australia*

**Corresponding Author: Email:* 

4.1 ABSTRACT

This article describes the use of microfluidic paper-based analytical devices (μ PADs) to perform quantitative chemical assays with internal standards. MicroPADs are well-suited for colorimetric biochemical assays; however, errors can be introduced from the background color of the paper due to batch difference and age, and from color measurement devices. To reduce errors from these sources, a series of standard analyte solutions and the sample solution are assayed on a single device with multiple detection zones simultaneously; an analyte concentration calibration curve can thus be established from the standards. Since the μ PAD design allows the colorimetric measurements of the standards and the sample to be conducted simultaneously and under the same condition, errors from the above sources can be minimized. The analytical approach reported in this work shows that μ PADs can perform quantitative chemical analysis at very low cost.

4.2 KEYWORDS

Quantitative assay, Paper, Microfluidic devices, Biomarkers

4.3 INTRODUCTION

The concept of microfluidic paper-based analytical devices (μ PADs) was recently proposed by a research group from Harvard University in 2007 [1]. They used the photolithography technique to selectively build hydrophobic barrier in filter paper with photoresist. The hydrophilic paper channels demarcated by walls of hydrophobic photoresist can control the transport of aqueous solutions by capillary action in porous paper matrix without the need of external pumping. This new concept has led to the rising of the new research area of patterning paper as low-cost, portable microfluidic platform for bio/chemical/medical application [2]. In this work, different but simpler methods (plasma treatment and ink jet printing) were used to fabricate μ PADs with cellulose reactive hydrophobization agents such as alkyl ketene dimer (AKD) and alkenyl succinic acid anhydride (ASA). Since these two methods do not require the building of polymer barriers in the paper sheet, devices made using these methods retain the original flexibility of the paper [3, 4]. The flexible patterned paper allows the construction of switches, separators and multi-component reactors in paper; these functional elements can significantly increase the functions of μ PADs [5].

The analytical applications of μ PADs have been pursued by several research groups. Patterned μ PADs were shown to be capable of performing qualitative [3] and semi-quantitative [2] colorimetric analyses. Low-cost desktop scanners and image analysis software have been used to measure analytical results as colorimetric changes in μ PADs [2, 3, 6]. Since scanner digitizes colorimetric results, electronic transmission of such results between laboratories has been shown feasible [2]. The μ PAD is superior to traditional colorimetric analytical methods such as UV–Vis spectrophotometry in terms of the small quantity of sample required for an analysis and the device portability. MicroPAD can also potentially reach the analytical accuracy of UV–Vis spectrophotometry, satisfying the analytical requirements of a range of rapid and routine biochemical analyses that need to be performed in field or in non-laboratory facilities.

A point that requires special emphasis is the analytical accuracy and precision. Analytical errors using μ PADs can be easily introduced through slightly different

measurement conditions as well as small batch variations of paper qualities. Errors can be effectively reduced if an internal calibration can be provided within the device. Among a variety of applications with μ PADs, two general principles can be perceived. In the first principle, a μ PAD can be designed for a specific (single- or multi-compound) measurement, e.g., urine glucose and protein tests. In these tests, the detection chemistries can be introduced into the detection zones of μ PADs when the devices are fabricated [2]; such devices are ready to use. Each μ PAD can be used to measure a single datum for each compound the device is designed to measure. A concentration calibration curve of a compound (i.e., glucose or protein) can be obtained by analyzing several standard solutions of the compound of known concentrations using the same number of μ PADs, provided that the quality variation between μ PADs is well controlled and the measurement conditions are the same. In the second principle, a μ PAD can be designed for on-demand analyses. The μ PAD only provides a microfluidic pattern without any specific detection chemistry; the detection chemistry can be introduced into the device prior to a test. In such applications, it is possible that a series of analyte solutions of known concentration be introduced into one μ PAD to generate a calibration curve. Better still, in a quantitative analysis, if the sample (of unknown concentration) can be introduced into the same μ PAD together with the series of calibration standards and exposed to the same detection reagent(s) simultaneously, errors due to paper quality variation and different scanning conditions can be significantly reduced. Inter-laboratory transmission of colorimetric results using μ PADs with the self-calibration curves is therefore expected to be more reliable.

The purpose of this study is to demonstrate quantitative analysis potential of μ PADs. Two simple fabrication methods of μ PADs will be described. A μ PAD pattern was selected to explore the above-mentioned second principle of using μ PADs for quantitative chemical analysis. Two clinical analyses, i.e., the analyses of nitrite ion (NO_2^-) and uric acid (UA), are used to demonstrate the principle. Both NO_2^- and UA are present in human body and are biomarkers for human renal and lung diseases and can be detected with colorimetric methods. Recently, Blicharz et al. [7] and Nagler [8] used the colorimetric methods to detect these biomarkers in saliva by paper strips and have reported that these methods are efficient for monitoring the effect of dialysis in patients with end-stage renal disease. The results reported in this work show that when these two detection methods are used in conjunction with μ PADs, tedious paper strips

preparation can be avoided. Standards and sample solutions can be introduced into one μ PAD directly and the subsequent introduction of the indicator allows the sample and standards to develop color changes simultaneously for colorimetric analysis.

The results of this study show that μ PADs can be used as an analytical device to easily and rapidly quantify colorimetrically detectable analytes at very low cost. Moreover, this method requires less than 1 μ L of the standard or sample solutions and less than 10 μ L of indicators, which are much lower than the volume needed for a paper strip analysis [7, 8] and conventional UV–Vis analysis. With the new strategy, it is possible to use μ PADs to provide quantitative results with the accuracy approaching to that of conventional methods such as UV–Vis spectrophotometry and at a greatly reduced cost. The method is particularly useful in remote and developing regions where analytical and medical infrastructure is limited.

4.4 EXPERIMENTAL SECTIONS

4.4.1 Preparation of μ PADs

Alkyl ketene dimer (Wax 88 konz, BASF) and Alkenyl ketene dimer (Precis 900, Hercules Australia Pty Ltd) were used as the cellulose hydrophobization reagents. Analytical grade *n*-heptane (Sigma-Aldrich) was used as the solvent for the dimers. Whatman filter paper (No. 4) was selected as the substrate to fabricate μ PADs. Two methods were used for μ PADs fabrication – plasma treatment and ink jet printing. In the plasma treatment method, a vacuum plasma reactor (K1050X plasma asher, Quorum Emitech, UK) and metal masks bearing the sensor pattern were used to selectively dehydrophobize filter papers which have already been hydrophobized by alkyl ketene dimer beforehand. [The preparation of the hydrophobic filter paper involves dipping the paper into a 0.6 g/L alkyl ketene dimer–heptane solution. After the evaporation of heptane, the filter paper was heat-treated in an oven at 105 °C for 45 min to allow the development of paper hydrophobicity] In the ink jet printing method, a commercial desktop ink jet printer (Canon Pixma ip4500) was used to print computer-generated patterns onto the filter paper with the ink solution of alkenyl ketene dimer–heptane (3%, v/v). The kinematic viscosity and the surface tension of the ink solution at

25 °C are 0.506 cSt and 19.90 mN/m, respectively. These values are in the low end of the printable liquids [9]; ink solution can be successfully and accurately printed. The printed filter paper was then heat-treated in an oven to allow hydrophobicity of the printed area on paper to fully develop. The detailed fabrication process can be found elsewhere [3, 4]. In this article, the μ PADs were fabricated with a pattern consisting of six detection zones and one central fluid inlet zone.

4.4.2 Preparation of Solutions

Millipore-purified water was used to prepare all liquid samples required for testing the performance of μ PADs.

The stock solution of NO_2^- (10.0 mmol/L) was prepared by dissolving 69.0 mg sodium nitrite ($\geq 99\%$, Sigma-Aldrich) in 100 mL water. Then this stock solution was diluted with water to get serially diluted NO_2^- standard solutions with the concentrations of 2,500, 1,250, 625, 312, 156 and 78 $\mu\text{mol/L}$. The standard solution (625 $\mu\text{mol/L}$) was used to prepare the assumed “unknown” NO_2^- sample solution (500 $\mu\text{mol/L}$).

The UA stock solution (12.8 mmol/L) was prepared with dissolving 215.0 mg uric acid ($\geq 99\%$, Sigma-Aldrich) in 100 mL sodium hydroxide solution (0.2 mol/L). The serially diluted UA standard solutions were prepared by diluting the stock solution with 0.2 mol/L NaOH to have different concentrations of 1,600, 800, 400, 200 and 100 $\mu\text{mol/L}$. Then the standard solution (800 $\mu\text{mol/L}$) was diluted to prepare the “unknown” UA sample solution (500 $\mu\text{mol/L}$).

The indicator solution for NO_2^- contains 50 mmol/L sulfanilamide ($\geq 99\%$, Sigma-Aldrich), 330 mmol/L citric acid ($\geq 99.5\%$, Sigma-Aldrich), and 10 mmol/L *N*-(1-naphthyl) ethylenediamine ($\geq 98\%$, Sigma-Aldrich) [7].

The indicator solution for UA consists of the 1:1 mixture of solution A (2.56% (w/v) 2,2'-biquinoline-4,4'-dicarboxylic acid disodium salt hydrate, $\geq 98\%$, Sigma-Aldrich) and solution B (20 mmol/L sodium citrate and 0.08% (w/v) copper (II) sulfate, $\geq 99\%$, Sigma-Aldrich) [7].

4.4.3 Running Assays on μ PADs

For creating NO_2^- calibration curve, one blank control (water, 0.5 μL) and five serially diluted NO_2^- standard solution samples (with concentration ranging from 78 $\mu\text{mol/L}$ to 1,250 $\mu\text{mol/L}$, 0.5 μL) were deposited into six detection zones in sequence using a micro pipette (Eppendorf research[®] 0.1-2.5 μL).

A NO_2^- solution (500 $\mu\text{mol/L}$ NO_2^-) was prepared and used as the sample solution with “unknown” concentration. The “unknown” sample solution (0.5 μL) was deposited into one detection zone along side with the serially diluted NO_2^- standard solutions on the same device. In this assay, water (0.5 μL) was added into the central inlet zone as the blank control.

For UA assay, a UA solution (500 $\mu\text{mol/L}$ UA) was assumed as an unknown sample solution and successively loaded with five serially diluted UA standard solution samples (100 $\mu\text{mol/L}$ to 1600 $\mu\text{mol/L}$) into each detection zone of the μPAD . NaOH solution (0.2 mol/L) was used as the blank control in this assay.

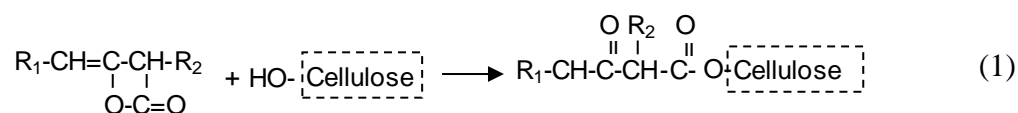
In all the above assays, corresponding indicator solutions (5 μL) were introduced into the central inlet zone with the Eppendorf research[®] pipette (0.5–10 μL); indicator solutions rapidly penetrated into all detection zones. Color changes of all standards and the unknown sample developed simultaneously as the indicator solution reached the detection zones. For each assay, six independent measurements have been taken using six μPADs made from the same sheet of filter paper (paper batch variation was assumed to be irrelevant).

The results of the colorimetric assays were imaged with a desktop scanner (Epson Perfection 2450, color photo setting, 1200 dpi resolution), then imported into Adobe Photoshop and converted into grayscale mode. The mean grayscale intensities were quantified using the histogram function of Adobe Photoshop. The ultimate mean intensity value of each detection zone was obtained by subtracting the measured average detection zone intensity from the mean intensity of the blank control; the average intensity data were then transferred to Microsoft Excel to obtain calibration curve data.

4.5 RESULTS AND DISCUSSION

4.5.1 Patterning Paper as μ PADs

The principle of paper-sizing chemistry is used to fabricate μ PADs used in this study. Alkyl ketene dimer and alkenyl ketene dimer have two long hydrocarbon chains (C_{14} – C_{18}) which impart to the cellulose surface with water-repellence once the dimers react with $-OH$ groups of cellulose (1). The hydrophobized part of filter paper has typical apparent contact angles of 110 – 125° with water [10], whereas unhydrophobized part of paper is hydrophilic and has a contact angle typically around 25° [11]. A μ PAD patterned with the alkyl or alkenyl ketene dimers therefore forms a patterned hydrophilic–hydrophobic contrast which guides the penetration of aqueous samples.



When the hydrophobized filter paper is exposed to plasma treatment under a mask, the unmasked area becomes hydrophilic and highly wettable by water, thus allowing aqueous liquids to penetrate within the hydrophilic channels of μ PADs. Figure 1a shows a water-wetted six-channel pattern generated using plasma treatment. The channel width of this pattern is around 1 mm, and the diameter of each testing zone is ~ 2.5 mm.

When using the ink jet printing method to fabricate μ PADs, computer-generated pattern is printed on paper using “inks” of the heptane solution of alkenyl ketene dimer. This method has the advantage of electronic pattern design, easy pattern variation, and high-speed production of a large number of μ PADs. Figure 1b and c are several different patterns generated with commercial desktop ink jet printer.

To demonstrate the feasibility of using μ PAD as a quantitative analyzing device, μ PAD with six-channel pattern (Fig. 1a) was chosen as the device design to perform all assays. This design allows the quantitative concentration measurement of an analyte based on a

six-point calibration curve simultaneously developed on the same μ PAD and under the same condition.

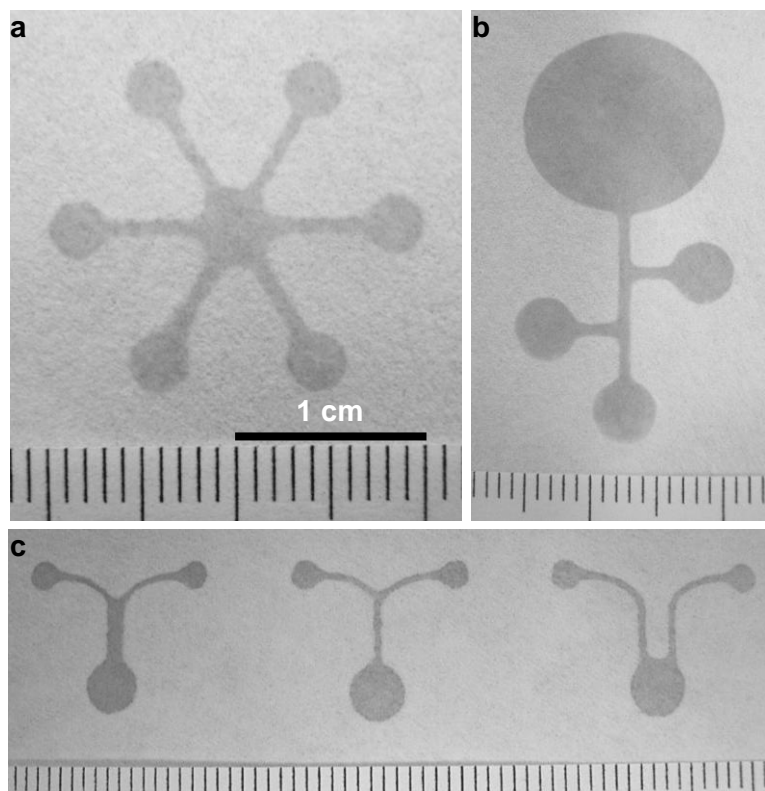


Fig. 1 Microfluidic patterns generated on paper using plasma treatment (a) and ink jet printing (b and c). The channels were wetted with water to visually show the patterns

4.5.2 Calibration Curve for NO_2^-

The colorimetric detection of NO_2^- is based on the principle of the Griess reaction which is a common quantification method for NO_2^- [12]. In this assay, 0.5 μL of serially diluted NO_2^- standard solutions (78, 156, 312, 625, 1,250 $\mu\text{mol/L}$) were transferred using a micro pipette into each detection zones 1–5 in sequence, while the blank control solution was spotted on the detection zone 0. Then, the indicator solution (5 μL) for NO_2^- was introduced into the device via the inlet zone. When the indicator solution penetrated into testing zones (<3 s) by capillary action and contacted with the analyte, the citric acid within the indicator solution converted NO_2^- to HNO_2 . The nitrous acid then transformed sulfanilamide into diazotized sulfanilamide which

coupled with *N*-(1-naphthyl)-ethylenediamine to form a pink azo compound (full color developed within 5 s). The resulting color developed in each detection zone changes from almost colorless (zone 0) to pink (zone 5) due to the different concentration of standard solution samples (Fig. 2). The measurement was repeated six times using six μ PADs; the average grayscale intensity and the error bar (relative standard deviation) for each standard NO_2^- solution were determined (Fig. 3). Linear least-squares fitting of the NO_2^- data gave coefficient of determination (R^2) of 0.9902. The mean color intensity is proportional to the NO_2^- concentration. This assay confirms that μ PAD can be used to create calibration curves for quantitative analysis.

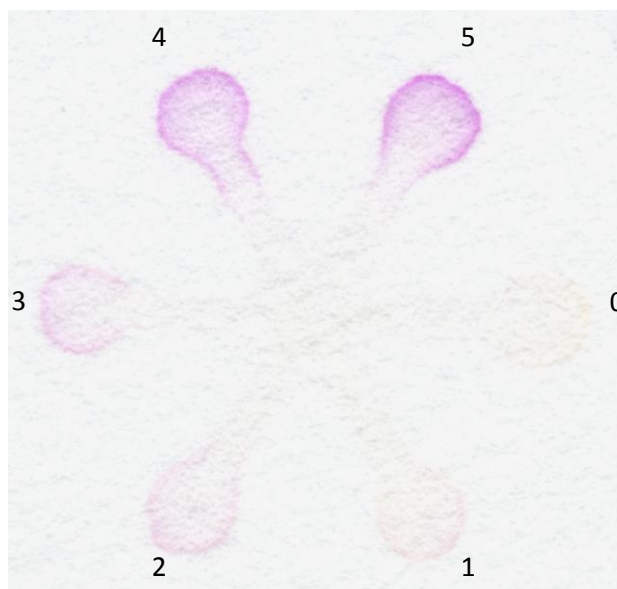


Fig. 2 The scanned image of a six-channel μ PAD in which a series of standard NO_2^- solutions were used to construct a calibration curve. After reaction, color intensities can be visually detected

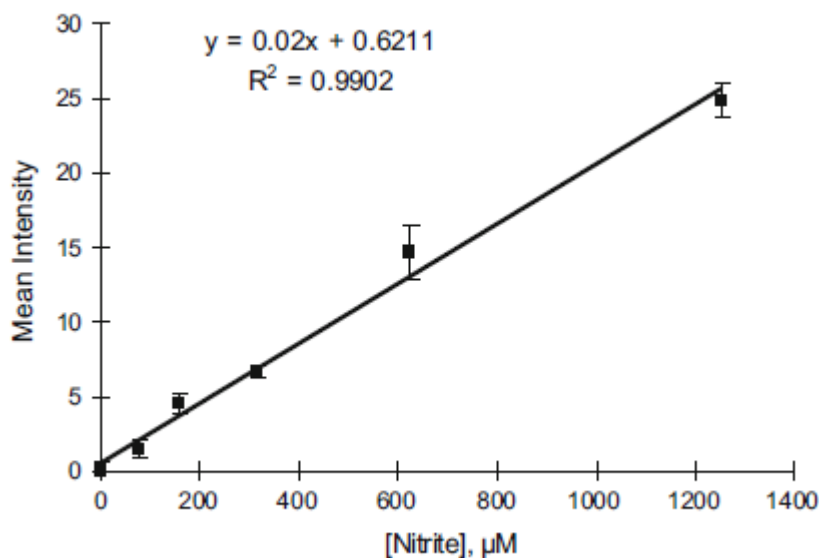


Fig. 3 The concentration calibration curve constructed using the grayscale intensity values converted from the image shown in Fig. 2

4.5.3 Concentration Measurement of NO_2^- Sample

To demonstrate the quantification of the NO_2^- concentration in sample solution, we prepared a blank control solution (0 $\mu\text{mol/L}$ NO_2^- , deposited on zone 0), five standard solutions (156, 312, 625, 1,250, 2,500 $\mu\text{mol/L}$ NO_2^- , deposited on zones 1–5), and a 500 $\mu\text{mol/L}$ NO_2^- solution (deposited on zone x) which was used as an “unknown” sample solution (Fig. 4). It should be noted that the calibration curve in this assay covered a wider concentration range than the calibration curve in Fig. 3. The indicator solution was still introduced into the device from central inlet zone (0). As the indicator solution penetrated into the detection zones (1–5 and x), NO_2^- in these zones caused color change (Fig. 4). To demonstrate the reproducibility of this assay, the measurement was repeated six times using six μPADs made from the same sheet of filter paper (paper batch variation was assumed to be irrelevant). The average grayscale intensity and the error bar (relative standard deviation) for each standard NO_2^- solution were determined (Fig. 5). The calibration curve obtained was not linear, but was quadratic. Grayscale analysis shows that the average intensity for the “unknown sample” was 12.684. Accordingly, the NO_2^- concentration of the unknown sample quantified using the calculation curve was 507 $\mu\text{mol/L}$. This leads to a relative error of 1.4% compared with the concentration of 500 $\mu\text{mol/L}$.

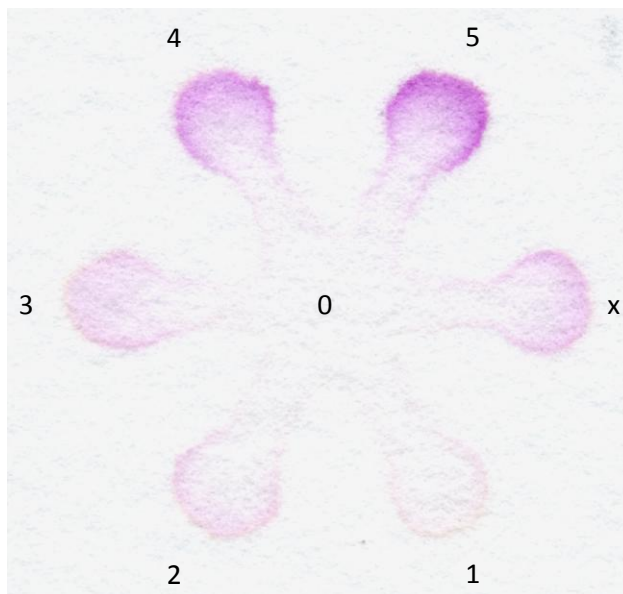


Fig. 4 The scanned image of a six-channel μ PAD in which a series of standard NO_2^- solutions were used to construct a calibration curve in a higher concentration range than that in Fig. 2. In this analysis, a sample solution of “unknown” NO_2^- concentration was also deposited in the device (*marked x*)

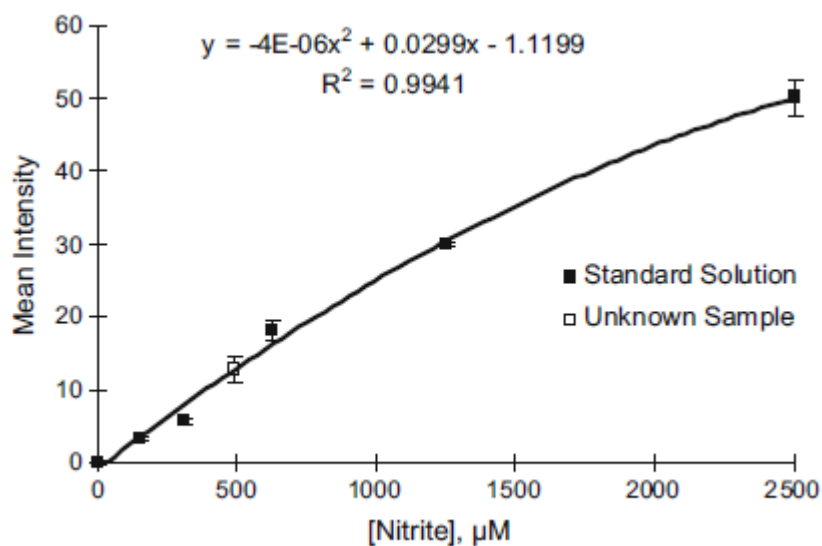


Fig. 5 The concentration calibration curve constructed using the grayscale intensity values converted from the image shown in Fig. 4. The grayscale intensity for the sample of “unknown” concentration is shown by the *unfilled square*

4.5.4 Concentration Measurement of UA Sample

The colorimetric assay of UA was based on a bicinchoninate chelate method [13]. When the indicator solution for UA penetrates into the detection zone, Cu (II) in the indicator solution was reduced to Cu (I) by UA, which was deposited into the detection zone beforehand. The cuprous ion then formed a purple chelate product with bicinchoninate ion. A calibration curve was established by depositing 0.5 μL of serially diluted standard UA solutions (0, 100, 200, 400, 800, 1,600 $\mu\text{mol/L}$) into detection zones 0–5. A 500 $\mu\text{mol/L}$ UA solution was used as the “unknown” sample and was deposited in detection zone x (Fig. 6). The indicator solution (5 μL) was introduced to μPAD from zone 0 and was allowed to penetrate into all detection zones via hydrophilic channels. The resulting color developed in detection zones 0–5 can be observed ranging from light purple to purple, corresponding to the different UA concentrations of the standard UA solutions (Fig. 6). To show the reproducibility of this assay, the measurement was also repeated six times using six μPADs made from the same sheet of filter paper; the average grayscale intensity and the error bar (relative standard deviation) for each standard UA solution were determined (Fig. 7). Following the same procedure, the average grayscale density of the “unknown” sample was measured to be 12.492. The average concentration of the “unknown” sample calculated from six independent measurements using the regression equation was 502 $\mu\text{mol/L}$, corresponding to a relative error of 0.4% when compared with the concentration of 500 $\mu\text{mol/L}$.

The above assays demonstrate the potential of using μPADs to perform rapid quantitative chemical analysis at a low cost and low sample volume requirement. By selecting suitable patterns, μPADs are capable of simultaneously presenting the detection results of a calibration curve and unknown samples. The colorimetric data of all calibration points and unknown samples can be recorded using a scanner (or any recording device such as a camera phone) under the same condition and at the same age. Since the colorimetric data of all calibration points and unknown samples are developed on the same μPAD , colorimetric error resulted from paper batch variation can be eliminated. Work reported in this study shows that μPADs can be fabricated

using very simple methods and μ PADs can deliver reasonably good analytical accuracy rapidly and at very low cost.

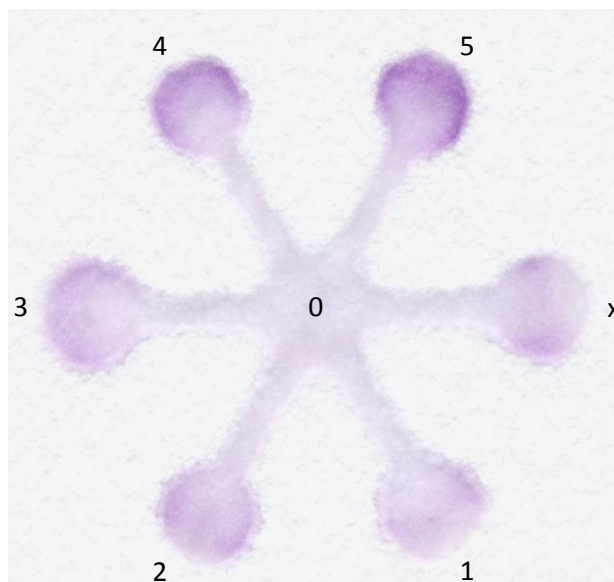


Fig. 6 The scanned image of a six-channel μ PAD in which a series of standard UA solutions were used to construct a calibration curve. In this analysis, a sample solution of “unknown” UA concentration was also deposited in the device (*marked x*)

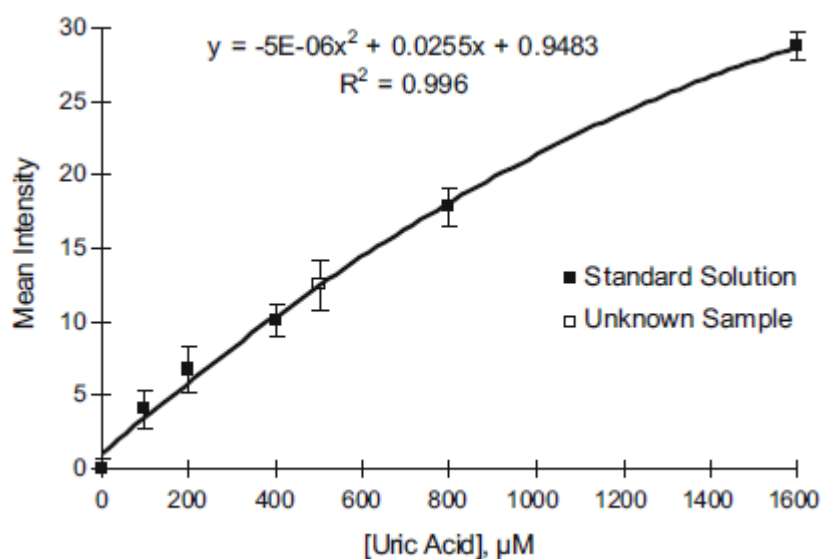


Fig. 7 The concentration calibration curve constructed using the grayscale intensity values converted from the image shown in Fig. 6. The grayscale intensity for the sample of “unknown” concentration is shown by the *unfilled square*

4.6 CONCLUSIONS

Microfluidic paper-based analytical devices, combined with the colorimetric reaction of analyte and the existing computer software (e.g., Adobe Photoshop), can provide a cheap and easy-to-use tool for the quantitative detection of unknown sample concentration. The raw material for μ PADs - paper - is relatively cheap and the fabrication methods of μ PADs are quite simple. Therefore, the μ PAD can be a useful tool when measurements need to be performed in less-industrialized area or remote region where analytical infrastructure is limited. Moreover, this analysis method substantially reduces the sample volume, which is an important advantage when the obtainable sample amount is limited (e.g., the biological sample from patients).

4.7 ACKNOWLEDGEMENT

The research scholarships of Monash University and the Department of Chemical Engineering are gratefully acknowledged. BASF and Hercules Australia are thanked for providing the hydrophobization agents.

4.8 REFERENCES

1. Martinez AW, Phillips ST, Butte M, Whitesides GM (2007) *Angew Chem Int Ed* 46:1318-1320
2. Martinez AW, Phillips ST, Carrilho E, Thomas III SW, Sindi H, Whitesides GM (2008) *Anal Chem* 80:3699-3707
3. Li X, Tian J, Nguyen T, Shen W (2008) *Anal Chem* 80:9131- 9134
4. Shen W, Tian J, Li X, Khan MS, Garnier G (2009) *Method of Fabricating Microfluidic Systems* PCT/AU2009/000889
5. Dittrich PS (2009) *Lab Chip* 9:15-16
6. Abe K, Suzuki K, Citterio D (2008) *Anal Chem* 80:6928-6934
7. Blicharz TM, Rissin DM, Bowden M, Hayman RB, DiCesare C, Bhatia JS, Grand-Pierre N, Siqueira WL, Helmerhorst EJ, Loscalzo J, Oppenheim FG, Walt DR (2008) *Clin Chem* 54:1473-1480
8. Nagler RM (2008) *Clin Chem* 54:1415-1417
9. Khan MS, Fon D, Li X, Forsythe J, Thouas G, Garnier G, Shen W (2008) *Chemeca 2008: Towards a Sustainable Australasia* 744-753
10. Shen W, Filonanko Y, Truong Y, Parker IH (2000) *Colloid and Surface A: Phys Eng Asp* 173:117-126
11. Kannangara D, Zhang H, Shen W (2006) *Colloid and Surface A: Phys Eng Asp* 280:203-215
12. Sun J, Zhang X, Broderick M, Fein H (2003) *Sensors* 3:276-284
13. Gindler EM (1970) *Clin Chem* 16:536

This page is intentionally blank

Chapter 5: Progress in Patterned Paper Sizing for Fabrication of Paper-Based Microfluidic Sensors

This page is intentionally blank

Monash University
Declaration for Thesis Chapter 5

Declaration by candidate

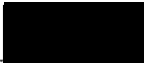
In the case of Chapter 5, the nature and extent of my contribution to the work was the following:

Nature of contribution	Extent of contribution (%)
Experimental design and conduct, paper writing	65

The following co-authors contributed to the work. Co-authors who are students at Monash University must also indicate the extent of their contribution in percentage terms:

Name	Nature of contribution	Extent of contribution (%) for student co-authors only
Junfei Tian	Experimental design, assisted in experimentation	25
Wei Shen	Experimental design, corrected manuscript	Supervisor

Candidate's Signature

	Date 04/08/2011
---	---------------------------

Declaration by co-authors

The undersigned hereby certify that:

- (1) the above declaration correctly reflects the nature and extent of the candidate's contribution to this work, and the nature of the contribution of each of the co-authors.
- (2) they meet the criteria for authorship in that they have participated in the conception, execution, or interpretation, of at least that part of the publication in their field of expertise;
- (3) they take public responsibility for their part of the publication, except for the responsible author who accepts overall responsibility for the publication;
- (4) there are no other authors of the publication according to these criteria;
- (5) potential conflicts of interest have been disclosed to (a) granting bodies, (b) the editor or publisher of journals or other publications, and (c) the head of the responsible academic unit; and
- (6) the original data are stored at the following location(s) and will be held for at least five years from the date indicated below:

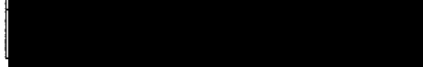
Location(s)	Australian Pulp and Paper Institute (APPI), Department of Chemical Engineering, Monash University, Clayton, VIC 3800, Australia
--------------------	---

Signature 1



Date 04/08/2011

Signature 2




4/8/11

This page is intentionally blank

Progress in Patterned Paper Sizing for Fabrication of Paper-Based Microfluidic Sensors

Xu Li, Junfei Tian, Wei Shen*

*Department of Chemical Engineering, Australian Pulp and Paper Institute,
Monash University, Clayton Campus, Melbourne, VIC 3800, Australia*

* Corresponding Author: Email: 

5.1 ABSTRACT

In this paper, we report the progress in using paper sizing chemistry to fabricate patterned paper for chemical and biological sensing applications. Patterned paper sizing uses paper sizing agents to selectively hydrophobize certain area of a sheet. The hydrophilic-hydrophobic contrast of the pattern so created has an excellent ability to control capillary penetration of aqueous liquids in channels of the pattern. Incorporating this idea with digital ink jet printing technique, a new fabrication method of paper-based microfluidic devices is established. Ink jet printing can deliver biomolecules and chemicals with precision into the microfluidic patterns to form biological/chemical sensing sites within the patterns, forming the complete sensing devices. This study shows the potential of combining paper sizing chemistry and ink jet printing to produce paper-based sensors at low cost and at commercial volume.

5.2 KEYWORDS

Paper microfluidics, Ink jet printing, Paper sizing, Low-cost sensors

5.3 INTRODUCTION

The applications of microfluidic technology in chemical and biochemical analysis, as well as in point-of-care (POC) diagnostics, are expanding rapidly, since microfluidic technology has the ability to control and direct small quantities (10^{-9} to 10^{-18} L) of liquid samples to produce rapid analysis (Whitesides 2006). The term *lab on a chip* (LOC) describes the current status of microfluidic analytical sensors. Although LOC devices have demonstrated clear advantages over many conventional analytical instruments in their high analytical sensitivity and resolution, the cost of these devices and the skills required to operate some of those devices make them not readily accessible to average users in developing countries (Zhao and van der Berg 2008). Microfluidic devices made using inexpensive materials such as paper therefore provide a new platform for low-cost, low-volume and portable bioassays (Martinez et al. 2007). Paper-based microfluidic devices can be made more accessible to population in developing regions because of their low cost; they are particularly suitable for obtaining semi-quantitative disease and health information from populations in remote area and developing countries.

Recent research on paper-based microfluidic devices has shown that paper has great potential for making low-cost diagnostic devices for health care and environmental monitoring purposes (Abe et al. 2008; Bruzewicz et al. 2008; Carrilho et al. 2009; Dungchai et al. 2009; Hossain et al. 2009; Li et al. 2008; Lu et al. 2009; Martinez et al. 2007, 2008a, b). Cellulose paper is naturally hydrophilic and allows fast penetration of aqueous liquids. This property provides the foundation for using paper to fabricate microfluidic systems (Stock and Rice 1974). To use paper to fabricate microfluidic devices for practical purposes, several technical issues need to be resolved. First, the device must be able to very well control the penetration of liquid sample in paper; this requires the liquid penetration pathways to be defined either physically or chemically within the paper matrix. Second, efficient fabrication methods must be developed so that such devices can be fabricated using modern high-speed and high-volume processes at low cost. Third, paper-based microfluidic systems must be able to withstand handling by field personnel and untrained patients. Additional fabrication challenge is that the resolution of the liquid sample channels in such devices must be

high enough to meet the analytical requirements. Furthermore, building valves in devices to control liquid penetration for multi-step tests can enhance the capability of the devices for intelligent applications.

It has been demonstrated that paper-based microfluidic devices can be built by demarcating hydrophilic paper by walls of hydrophobic polymers (Martinez et al. 2007). Following this principle, Martinez et al. (2007, 2008a, b) explored the use of photolithography method to create microfluidic channels in paper by making hydrophobic barrier walls in paper matrix. Hydrophobic photoresist polymers provide very good physical barrier, which defines liquid penetration pathways into paper. A liquid sample can be directed into multiple detection zones where indicators were deposited. This device demonstrates the possibility of the simultaneous detection of multiple analytes in a liquid sample. The barrier-design microfluidic systems are well suited for making health care and telemedicine devices (Martinez et al. 2008a, b). However, this fabrication method (photolithography) suffers from two major deficiencies: first, the hardened photoresist barrier is susceptible to bending and folding damages (Bruzewicz et al. 2008); second, photolithography requires expensive equipment and the fabrication process is slow and needs multiple steps (Lu et al. 2009).

Bruzewicz et al. (2008) used a modified plotter to create a barrier pattern by printing polydimethylsiloxane (PDMS) onto paper. This method overcame the problem of physical inflexibility of devices made using photolithography. However, barrier definition deteriorated, since the penetration of PDMS in paper could not be very well controlled, resulting in the wall of the barrier not being straight. This method is unable to produce devices in massive scale and at high speed.

Abe et al. (2008) took a polymer (polystyrene) solution impregnation approach to introduce hydrophobicity into the paper matrix. They then used a specialty micro drop dispensing system to print solvent onto the impregnated paper to dissolve the polymer and form fine liquid penetration channels. These authors also printed chemical sensing agents into their pattern to form a functional device for biomedical detection. Lu et al. (2009) used a wax laser printer to generate microfluidic patterns on paper. The pattern was then heated to allow wax diffusion into paper and form a barrier for microfluidic channels. These fabrication concepts are similar to the barrier concept, since they rely

on cellulose fibres in paper to be physically covered by a layer of hydrophobic materials.

Our recent work (Li et al. 2008, 2010a) reported new methods of using paper sizing chemistry to generate patterns of hydrophilic-hydrophobic contrast in paper to form microfluidic devices. We successfully performed qualitative and quantitative chemical/biological analyses using patterned paper devices fabricated by AKD sizing.

In this paper, we report the progress in using paper sizing chemistry to create paper-based microfluidic sensors. We also present the qualitative and quantitative analysis capabilities of the sensors so fabricated, and comment on the potential of using sizing chemistry and printing technology to upscale paper-based sensors production.

There are three significant advantages of using paper sizing chemistry to fabricate paper-based microfluidic sensors. First, papermakers are very familiar with paper sizing chemistry; the representative paper sizing agents are alkyl ketene dimer (AKD), alkenyl ketene dimer (liquid AKD) and alkenyl succinic acid anhydride (ASA). These sizing agents are widely and globally used in papermaking industry. Second, AKD and ASA are the cheapest paper patterning materials among all patterning materials so far reported for fabrication of paper-based diagnostic devices. Since price is a very sensitive factor for paper-based microfluidic diagnostic devices, material cost for making these devices is therefore an important point of consideration (Bruzewicz et al. 2008). A detailed cost analysis can be found in the discussion section. Third, by combining paper sizing chemistry and printing technology, it is possible to upscale the fabrication of paper-based microfluidic devices. Making physical hydrophobic barriers to build channels in paper is a limiting step to the speed and cost of large scale fabrication. The physical barrier approaches usually involve polymer impregnation followed by pattern developing. The approach reported in this study potentially enables the fabrication of paper-based microfluidic devices, i.e. pattern and incorporated sensing chemistries, with continuous high-speed and large-volume industrial printing processes, enabling the ultimate practical use of the devices for health care and environmental purposes. Since printed paper retains its original flexibility, the new method fundamentally overcomes the problem of channel damage by folding and

bending. Furthermore, simple and functional elements, such as valve-controlled reactor, can be easily built into paper-based microfluidic devices made by this novel approach.

5.4 EXPERIMENTAL SECTION

5.4.1 Sizing Agents

Alkyl ketene dimer (Wax 88 konz, BASF) and alkenyl ketene dimer (Precis 900, Hercules Australia Pty Ltd) were used as the cellulose hydrophobization (or sizing) agents. Both dimers have two hydrocarbon chains of C₁₆–C₂₀. Alkenyl ketene dimer, however, has one –C = C– in each of its two hydrocarbon chains (Qiao et al. 2006). Analytical grade *n*-heptane (Sigma-Aldrich) was used as the solvent to make solutions of both dimers.

5.4.2 Paper-Based Microfluidic Devices

Whatman filter paper (No. 4) was used as the paper substrate. In the first concept-proving approach, filter papers were sized and then treated with plasma to generate hydrophilic patterns. Filter paper samples were dipped in and shortly removed out of an alkyl ketene dimer – heptane solution (0.6 g/L) to allow evaporation of heptane. Filter paper samples were then heated in an oven at 100 °C for 5 min to facilitate the curing of alkyl ketene dimer on cellulose fibres. The hydrophobized samples were sandwiched between metal masks and then treated with a vacuum plasma reactor (K1050X plasma asher (Quorum Emitech, UK)) for 15 s at the intensity of 15 W. The vacuum level for the treatment was 6×10^{-1} mbar. Metal masks were made by mechanically cutting the desired patterns out of stainless steel sheets. The treated paper samples retained their original flexibility without visible marks.

In the second approach, filter papers were printed using a reconstructed commercial digital ink jet printer (Canon Pixma ip4500) with electronically generated patterns of an alkenyl ketene dimer – heptane solution (2%, v/v). Printing does not leave any visible mark on paper samples which retained their original flexibility. The printed filter paper

samples were then heated in an oven at 100 °C for 8 min to cure alkenyl ketene dimer onto cellulose fibres. Printing of water-based sizing emulsion is also possible, it will be a separate topic discussed elsewhere.

5.4.3 Preparation of Liquid Samples

Millipore purified water was used to prepare all liquid samples. The stock solution of NO_2^- (10.0 mmol/L) was prepared by dissolving 69.0 mg sodium nitrite ($\geq 99\%$, Sigma–Aldrich) in 100 mL water. The indicator solution for NO_2^- contains 50 mmol/L sulfanilamide ($\geq 99\%$, Sigma–Aldrich), 330 mmol/L citric acid ($\geq 99.5\%$, Sigma–Aldrich), and 10 mmol/L N-(1-naphthyl) ethylenediamine ($\geq 98\%$, Sigma–Aldrich) (Blicharz et al. 2008).

The UA stock solution (12.8 mmol/L) was prepared with dissolving 215.0 mg uric acid ($\geq 99\%$, Sigma–Aldrich) in 100 mL sodium hydroxide solution (0.2 mol/L). The indicator solution for UA consists of the 1:1 mixture of solution A (2.56% (w/v) 2,2'-biquinoline-4,4'-dicarboxylic acid disodium salt hydrate, $\geq 98\%$, Sigma–Aldrich) and solution B (20 mmol/L sodium citrate and 0.08% (w/v) copper (II) sulfate, $\geq 99\%$, Sigma–Aldrich) (Blicharz et al. 2008).

The mixed sample solution (625 $\mu\text{mol/L}$ NO_2^- , 800 $\mu\text{mol/L}$ UA) was prepared using NO_2^- and UA stock solutions.

5.5 RESULTS AND DISCUSSION

5.5.1 Hydrophilic-Hydrophobic Contrast of Untreated and Treated Papers

The common reactive functional group of alkyl and alkenyl ketene dimers is the four-member lactone ring. It is connected to two long hydrocarbon chains. Once alkyl and alkenyl ketene dimers are immobilized on fibre surface via the (esterification) reaction with $-\text{OH}$ groups of cellulose, the two hydrocarbon chains impart hydrophobicity to cellulose fibre surface (Shen et al. 2000).

The sized filter paper samples are strongly hydrophobic and have contact angles of typically 110–125° with water (Shen et al. 2000), whereas unsized cellulose has a contact angle of only 25° with water (Kannangara et al. 2006). The Washburn equation has been used as the first order approximation to study the penetration of liquids in paper (Eq. (1)) (Hodgson and Berg 1988):

$$l = \sqrt{\frac{\gamma r \cos \theta}{2\eta} t} \quad (1)$$

Where l is the liquid penetration distance in paper, r is the equivalent capillary pore radius of paper, γ and η are the surface tension and viscosity of the liquid, θ is the contact angle and t is the time of penetration. Equation (1) shows that if a paper surface sustains an apparent contact angle with a liquid of greater than 90°, then liquid penetration will not occur. Figure 1 shows the hydrophilic-hydrophobic contrast of a half-sized and half-unsized filter paper when exposed to water. This phenomenon motivated us to investigate the use of the hydrophilic-hydrophobic contrast to fabricate microfluidic patterns in paper.

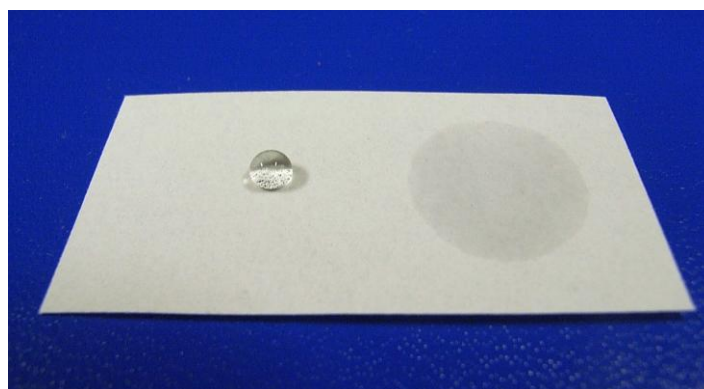
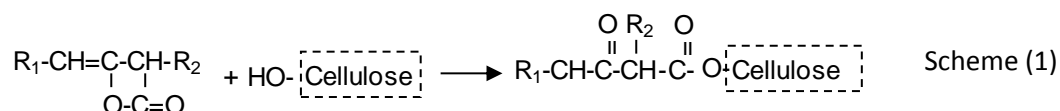


Fig. 1 Water wettability of a half-sized and half-unsized filter paper

AKD sizing required the AKD to first spread over the fibre surface in paper. As AKD in paper is subjected to moderate heat for curing treatment, it redistributes in the fibre matrix via several possible mechanisms: capillary wicking along fibre gaps (Shen and Parker 2001); vaporization and re-deposition (Zhang et al. 2007); fibre wetting by AKD via autophobic precursor (Seppanen et al. 2000; Shen and Parker 2001); low-

temperature spreading after curing treatment (Shen et al. 2003). Among those mechanisms, the capillary wicking and vapour re-deposition are fast redistribution mechanisms, whereas the autophobic precursor and low temperature spreading after curing treatment are very slow mechanisms. Zhang et al. (2007) investigated the chemical composition of “AKD vapour” and have found that “AKD vapour” is dominantly fatty acids which do not provide strong sizing to paper. Therefore, the only fast AKD redistribution mechanism is likely to be capillary wicking of AKD along inter- and intra- fibre gaps. If the amount of AKD applied to paper can be well controlled, the capillary wicking distance of AKD in fibre gaps can also be controlled. Therefore, the spreading of AKD in paper can be controlled; and the use of sizing to create hydrophilic-hydrophobic contrast is possible. After spreading, AKD reacts with the cellulose in paper following Scheme (1).



There have been controversies regarding the mechanism and the degree of AKD-cellulose reaction during sizing. The details of AKD-cellulose chemical reaction mechanism, however, are outside of the scope of this study.

5.5.2 Fabrication of Paper-Based Microfluidic Devices

Plasma treatment was used to prove the principle of using hydrophilic-hydrophobic contrast for the fabrication of paper-based microfluidic devices. Plasma treatment of hydrophobic paper with patterned masks provides an easy method to selectively introduce hydrophilic patterns to hydrophobic paper. Figure 2 shows the masks with desired pattern and a six-channel pattern created on the sized filter paper surface with these two masks by plasma treatment. Water was introduced from the central inlet zone and penetrated within the channels via capillary penetration.

A reconstructed ink jet printer was used to print the alkenyl ketene dimer–heptane ink solution onto an untreated filter paper. After curing, the printed area became strongly hydrophobic and the non-printed area remained hydrophilic. The printed area sustained water contact angle of greater than 110°. Printed paper-based microfluidic devices

retain their original flexibility. Figure 3 shows a computer-generated electronic pattern (blue area was the intended printing (sized) area while white area was the non-printing (unsized) hydrophilic area) and the microfluidic pattern on filter paper. Water was introduced to reveal the printed and sized area as well as the non-printed hydrophilic area.

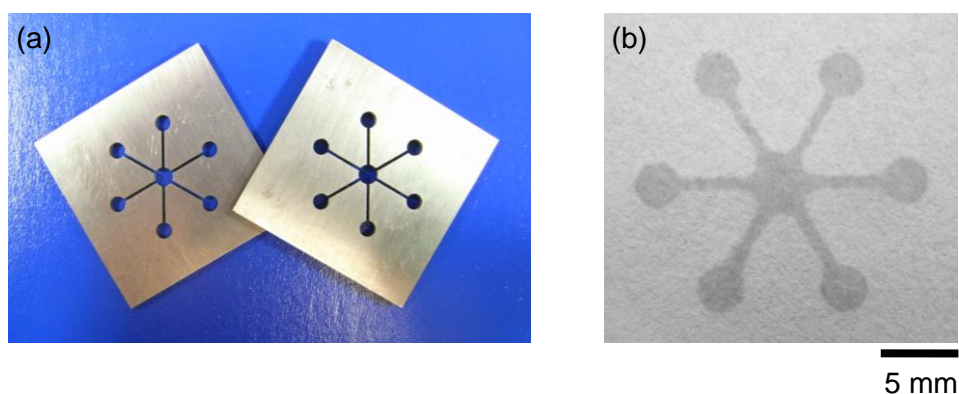


Fig. 2 **a** Two identical metal masks for fabrication of paper-based microfluidic devices with plasma treatment; **b** A six-channel pattern fabricated using masks and plasma reactor (wetted with water)

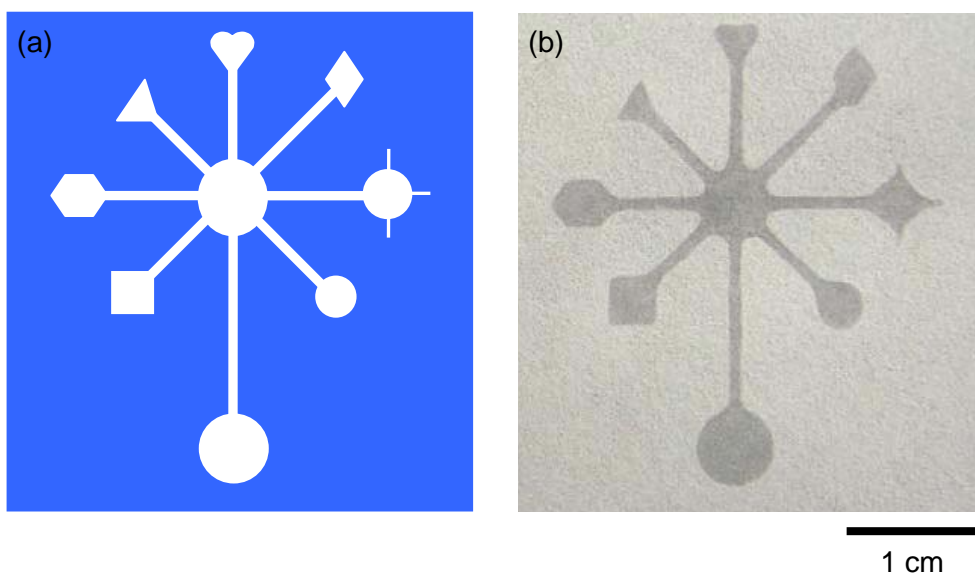


Fig. 3 **a** Computer-generated electronic pattern for ink jet printing of paper-based microfluidic device; **b** Ink jet printed microfluidic pattern on filter paper with borders defined by the hydrophilic-hydrophobic contrast (wetted with water)

Current commercial digital ink jet printers are capable of issuing small droplets of a few picolitres and small amount of ink for generating patterns on paper. The

reconstructed printer also inherits this frugal ink management feature. Heptane is a fast evaporating solvent; its fast evaporation after printing limits the penetration of the solution into the paper matrix. This allows the hydrophilic channels on paper surface created by printing to have a well-defined hydrophilic-hydrophobic border. Figure 4 shows a micrograph of a water wetted paper channel fabricated by printing. The channel wall defined by the hydrophilic-hydrophobic contrast is able to guide liquid capillary flow in the channel. It can be envisaged that with the web-based ink jet printing facilities, high speed printing of sensors is possible.

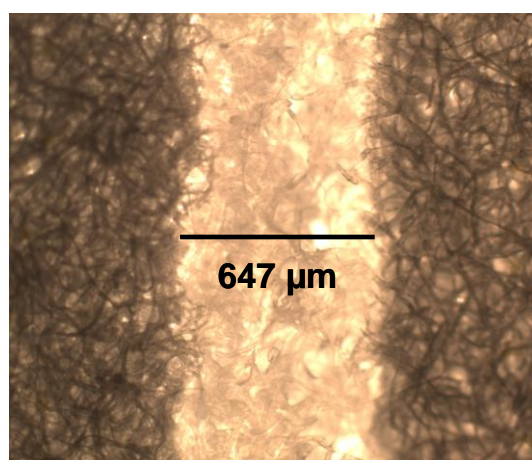


Fig. 4 The microscope image of a water wetted microfluidic channel on filter paper, showing the hydrophobic channel wall is strong enough to guide capillary penetration of water within the channel

5.5.3 Printing Sensing Reagents or Biomolecules on Paper-Based Microfluidic Devices

Ink jet printing of biomolecules has been reported previously by many research groups (Vauvreau and Laroche 2005; Risio and Yan 2007). Ink jet printing is a non-contact printing process, which offers a unique advantage of minimizing cross-sample contamination. The printing of the sizing agents on paper to build the microfluidic channels has added a new capability to ink jet printing for device fabrication; the multiple printing cartridges of ink jet printers can be used to print different materials. By combining printing of sensing reagents or biomolecules and the printing of sizing agents together, a new approach for fabrication of paper-based microfluidic sensors is formed.

5.5.4 Paper-Based Microfluidic Devices for Qualitative Multi-Analyte Detection and Quantitative Analysis

To illustrate the use of paper-based microfluidic devices for multiple analytes measurement, NO_2^- and UA were used as two example analytes, since they are two important biomarkers for a number of human health conditions (Nagler 2008). In this test, the NO_2^- and UA indicator solution (0.5 μL) has been deposited onto detection zones N (for NO_2^-) and U (for UA) separately as shown in Fig. 5a. Then the mixed sample solution (625 $\mu\text{mol/L}$ NO_2^- , 800 $\mu\text{mol/L}$ UA) was introduced from the central sample inlet zone; the sample solution penetrated into each and every detection zone within 2 s. Different detection zones showed different colour development, indicating positive detections of NO_2^- (pink) and UA (purple), respectively (Fig. 5b). This test shows that sized paper sensors are capable of detecting multiple chemical species in unknown samples.

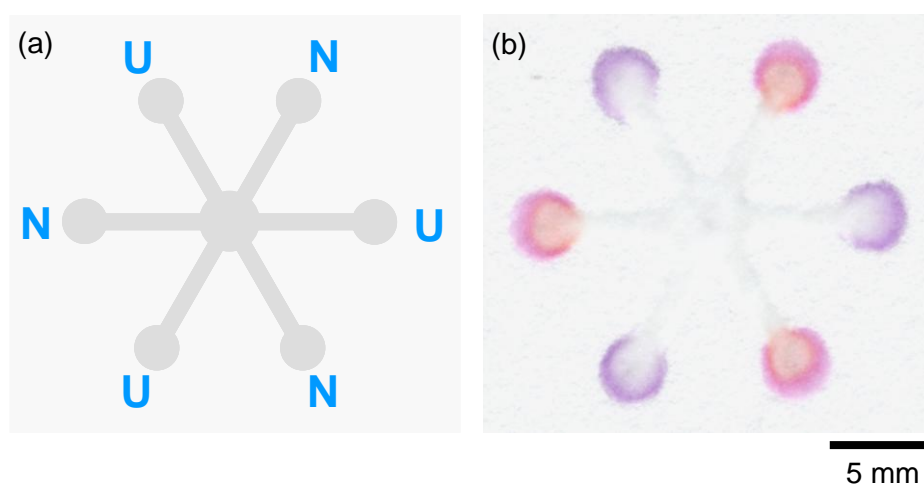


Fig. 5 Qualitative multiple analytes detection with paper-based microfluidic devices **a** The assay design: NO_2^- indicator and UA indicator were deposited in alternation into the six detection zones marked with N (for NO_2^-) and U (for UA); **b** Mix sample solution containing NO_2^- and UA was introduced from central inlet zone; the sample penetrated into different detection zones to trigger different colour changes (pink for NO_2^- and purple for UA)

Paper-based microfluidic devices can also be utilized for quantitative biological or chemical analyses, such as creating calibration curve, measuring sample concentration. Compared with the traditional UV-vis spectrophotometry method, the paper sensor method is a much cheaper and easier analytical approach, and requires lower sample

volumes ($< 1\ \mu\text{L}$). To show this capability of paper-based devices, six serially diluted NO_2^- standard solutions (0, 78, 156, 312, 625 and 1250 $\mu\text{mol/L}$, 0.5 μL) prepared using NO_2^- stock solution were deposited into six different detection zones of a blank paper-based microfluidic device from zone 0 to 5 (Fig. 6a). After that, NO_2^- indicator solution (5 μL) was added from the central inlet zone and penetrated into different detection zones to give different colour development from nearly colorless to strong pink (Fig. 6b). Then we used a desktop scanner (Epson Perfection 2450, colour photo setting, 1,200 dpi resolution) to capture the image and the histogram function of Adobe Photoshop to measure the colour intensity in different detection zones. Six independent measurements were operated with six paper-based microfluidic devices. The NO_2^- calibration curve obtained in this test (Fig. 6c) shows that sized patterned paper-based devices have great potential to conduct quantitative assays at very low cost. In our previous work reported elsewhere, we have successfully applied the quantitative analysis approach using sized paper sensors to analyze unknown NO_2^- and UA samples with high accuracy which was comparable to that of UV-vis spectroscopy method (Li et al. 2010a).

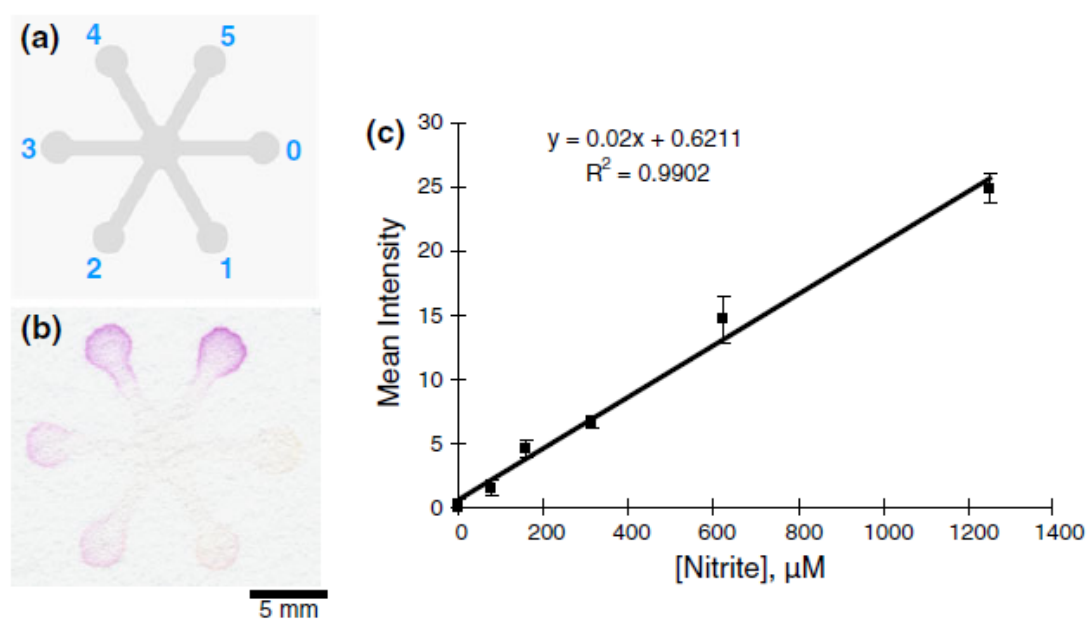


Fig. 6 Quantitative biological/chemical assay using paper-based microfluidic devices **a** The assay design: NO_2^- standard solutions (0.5 μL) with different concentration from 0 to 1250 $\mu\text{mol/L}$ were deposited into detection zone 0 to zone 5 in sequence; **b** NO_2^- indicator solution was added into the device from central inlet zone and caused different colour changes in different detection zones; **c** Calibration curve created by colour density measurement using Adobe Photoshop of the scanned images of the tests. *Error bars* were obtained from six repeated measurements

5.5.5 Functional Elements for Enhanced Sensing Capability

Functional elements can be easily built in paper-based microfluidic devices to provide cheap and easy-to-use functional devices (e.g., switches, separators (Li et al. 2008)) for various applications. A simple valve-controlled reactor design was presented in this study to demonstrate the possibility of creating functional components on paper-based microfluidic devices. Figure 7a-c shows the concept of a reactor design on paper, in which different reagents can be introduced into the reactor at different time controlled by two valves. An acid–base neutralization reaction was used to illustrate the feasibility.

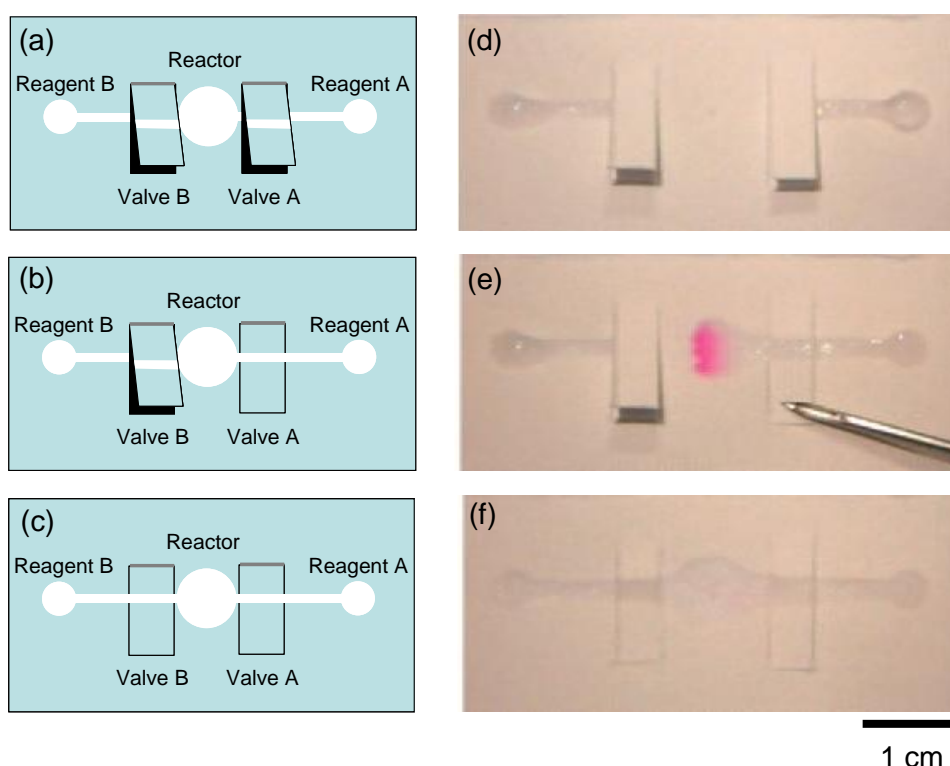


Fig. 7 **a-c** A design of a simple paper-based microfluidic reactor consisting of two sample dosing sites, two valves, and one central reaction site; **d-f** A paper-based microfluidic reactor based on this design was tested using acid–base neutralization reaction (**d** Phenolphthalein indicator solution was deposited onto the central reaction zone. NaOH and HCl solutions were added into reagent zones A and B, respectively; **e** NaOH solution was introduced into the reaction zone to trigger colour change; **f** HCl solution was introduced later into the reaction zone via valve B to neutralize NaOH in the reaction zone)

NaOH and HCl solutions were added into reagent A and B zones respectively. A small amount of phenolphthalein indicator solution was deposited onto the central reaction zone (Fig. 7d). The NaOH solution was firstly introduced into the reaction zone to

trigger the colour change (Fig. 7e), and then the HCl solution was introduced into the reaction zone via valve B to neutralize NaOH in the reaction zone. The completion of the reaction is indicated by the fading of pink colour (Fig. 7f). The simple reactors such as the one shown in Fig. 7 are useful for multi-step chemical and biological assays.

5.6 DISCUSSION

Compared with the previous barrier fabrication method, the new fabrication concept enables the manufacturing of paper-based microfluidic devices by simpler process and at low cost. Creation of hydrophilic-hydrophobic contrast is a simpler approach to define aqueous liquid penetration channels in paper than the barrier approach. Several major commercial paper sizing chemistry systems are suitable for paper-based microfluidic devices fabrication. It is expected that ink jet, flexo and gravure may be the most suitable processes to print sizing agents on paper surface. The requirement of curing of the AKD and ASA chemistries presents a challenge to the continuous production of paper-based diagnostic devices. However, it is possible to add a roller-nip heating station between the printing stations for pattern and for sensing reagents printing. Among these processes, ink jet printing has a further advantage of non-contact liquid delivery, which is highly desirable for printing detection chemistries into the devices. With the advance of web ink jet printers, continuous production of paper-based microfluidic diagnostic sensors will become a reality in future.

The use of digital printing technology to selectively deliver paper sizing chemicals on paper surface to form the hydrophilic-hydrophobic contrast has another advantage. Digital printing offers electronic pattern variation which allows fast change over for fabrication of different devices. Since the hydrophilic-hydrophobic contrast fabrication concept can retain the original flexibility of the paper, it offers natural bending and folding resistance to the paper-based microfluidic devices, which fundamentally overcomes the poor bending and folding resistance often encountered with some other techniques. Figure 8 shows an example of a bending and folding test. The performance of the ink jet printed patterns shows no discernable deterioration after the test.

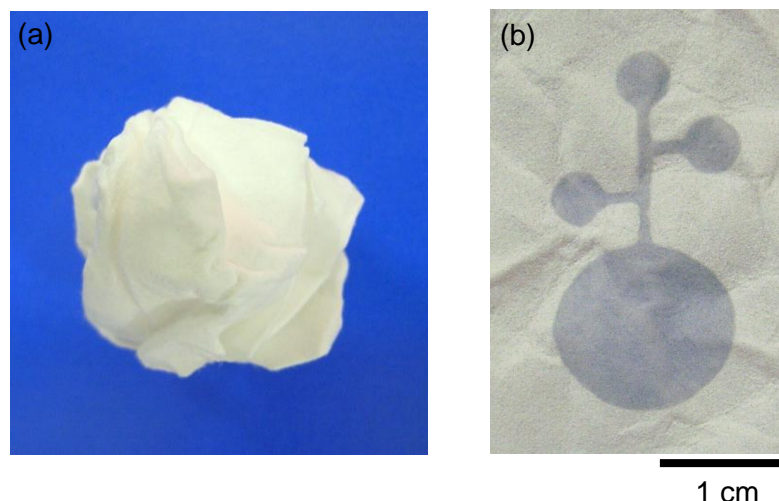


Fig. 8 a The paper-based microfluidic device was subjected to a harsh folding test; **b** The performance of the device showed no deterioration after the test

The concept of hydrophilic-hydrophobic contrast in paper allows simple yet functional elements such as valves to be built into devices. Reactor systems are possible by combining valves, channels and reservoir. Multi-step diagnostic tests can also be achieved with reactors. Valve can also be built in 3D paper-based microfluidic devices having paper-film-paper structure; a liquid sample can be directed from one sheet of paper to the other by activating a valve. Commercial printing can easily build simple valves on paper by die-cutting operations. By printing hydrophilic-hydrophobic contrast on papers, a plethora of flexible microfluidic devices can be fabricated and their production is able to be scaled up.

Since AKD and ASA sized paper does not resist the penetration of oil or low surface tension aqueous liquids, sized paper-based microfluidic channels are likely to widen when transport these samples (surface tension <35 mN/m). In these circumstances, sensors made of cotton thread can be used (Li et al. 2010b). Thread-based sensors do not rely on the barrier or the hydrophilic-hydrophobic contrast to define the liquid passageway, they therefore can transport oil and surfactant solutions effectively. Alternatively, sensors made using fluorocarbon-based sizing agents or barriers that can resist oil or surfactant solutions can be used.

As mentioned earlier, AKD and ASA are the cheapest paper patterning materials among all patterning materials so far reported for fabrication of paper-based diagnostic

devices. Taking AKD for example, the whole sale prices of AKD from European manufacturers are 3–4 euro per kilogram, whereas the cost of ASA is even lower. The AKD usage in paper sizing is typically less than 5 kg per ton of dry fibre. If the basis weight of the paper is 92 g/m^2 and the area of each paper microfluidic sensor is 25 cm^2 (i.e. $5 \text{ cm} \times 5 \text{ cm}$), the cost of AKD on each device will only be 0.000005 euro. In laboratory scale fabrication, each A4 sheet of paper can produce 20 devices; using the printing method reported in this work and taking ink consumption for printing each A4 sheet as $400 \text{ }\mu\text{L}$, the AKD cost of each device (25 cm^2) will be 0.000002 euro, significantly cheaper than the non-paper material costs of all fabrication methods reported to date. The barrier material costs of each barrier-based paper sensor reported previously were \$0.025 for photoresist SU-8 (Martinez et al. 2008a, b) and \$0.0025 for PDMS (Bruzewicz et al. 2008).

The qualitative and, in particular, quantitative analysis with the use of self calibration standards make paper-based microfluidic sensors cost-competitive devices for health care and environment monitoring applications. Some future improvements of paper-based devices identified in our research are to further reduce the sampling amount to match those microfluidic analytical devices made using expensive technologies, to significantly increase sample delivering efficiency so as to allow paper-based microfluidic devices to handle low concentration biological and environmental samples and, to make paper-based diagnostics as a reliable means to perform mass analytical tasks such as population screening for certain health threats.

5.7 CONCLUSION

This article reports the progress of using patterned sizing and printing method to fabricate paper-based microfluidic devices. Sized paper shows strong wetting contrast to the unsized paper. Combining this hydrophilic-hydrophobic contrast concept with ink jet printing, well-defined microfluidic channels can be created into paper. Ink jet printing can also print required detection chemistries or biomolecules into the pattern to form complete paper-based microfluidic sensors. This fabrication concept provides potential for the mass production of paper-based sensing devices at very low cost.

Paper-based microfluidic devices fabricated using the hydrophilic-hydrophobic contrast concept retain the original flexibility of paper. It allows simple and functional elements, such as valves and reactors, to be built into the devices. With these functional elements, more advanced paper-based devices can be designed and fabricated.

The analytical capability of paper-based sensors fabricated using patterned AKD sizing shows that paper-based sensors have the potential to change the way of some analytical chemistries are performed.

5.8 ACKNOWLEDGEMENT

The research scholarships of Monash University and the Department of Chemical Engineering are gratefully acknowledged. BASF and Hercules Australia are thanked for kindly providing paper sizing agents.

5.9 REFERENCES

- Abe K, Suzuki K, Citterio D (2008) Inkjet-printed microfluidic multianalyte chemical sensing paper. *Anal Chem* 80:6928-6934
- Blicharz TM, Rissin DM, Bowden M, Hayman RB, DiCesare C, Bhatia JS, Grand-Pierre N, Siqueira WL, Helmerhorst EJ, Loscalzo J, Oppenheim FG, Walt DR (2008) Use of colorimetric test strips for monitoring the effect of hemodialysis on salivary nitrite and uric acid in patients with end-stage renal disease: a proof of principle. *Clin Chem* 54:1473-1480
- Bruzewicz DA, Reches M, Whitesides GM (2008) Low-cost printing of poly(dimethylsiloxane) barriers to define microchannels in paper. *Anal Chem* 80:3387-3392
- Carrilho E, Martinez AW, Whitesides GM (2009) Understanding wax printing: a simple micropatterning process for paper-based microfluidics. *Anal Chem* 81:7091-7095
- Dungchai W, Chailapakul O, Henry CS (2009) Electrochemical detection for paper-based Microfluidics. *Anal Chem* 81:5821-5826
- Hodgson KT, Berg JCJ (1988) The effect of surfactants on wicking flow in fiber networks. *Colloid Interface Sci* 121:22-31
- Hossain SMZ, Luckham RE, McFadden MJ, Brennan JD (2009) Reagentless bidirectional lateral flow bioactive paper sensors for detection of pesticides in beverage and food samples. *Anal Chem* 81:9055-9064
- Kannangara D, Zhang H, Shen W (2006) Liquid-paper interactions during liquid drop impact and recoil on paper surfaces. *Colloid Surf A-Physiochem Eng Asp* 280:203-215
- Li X, Tian J, Nguyen T, Shen W (2008) Paper-based microfluidic devices by plasma treatment. *Anal Chem* 80:9131-9134
- Li X, Tian J, Shen W (2010a) Quantitative biomarker assay with microfluidic paper-based analytical devices. *Anal Bioanal Chem* 396:495-501
- Li X, Tian J, Shen W (2010b) Thread as a versatile material for low-cost microfluidic diagnostics. *ACS Appl Mater Interface* 1:1-6
- Lu Y, Shi W, Jiang L, Qin J, Lin B (2009) Rapid prototyping of paper-based

- microfluidics with wax for low-cost, portable bioassay. *Electrophoresis* 30:1497-1500
- Martinez AW, Phillips ST, Butte MJ, Whitesides GM (2007) Patterned paper as a platform for inexpensive, low-volume, portable bioassays. *Angew Chem Int Ed* 46:1318-1320
- Martinez AW, Phillips ST, Carrilho E, Thomas III SW, Sindi H, Whitesides GM (2008a) Simple telemedicine for developing regions: camera phones and paper-based microfluidic devices for real-time, off-site diagnosis. *Anal Chem* 80:3699-3707
- Martinez AW, Phillips S T, Wiley BJ, Gupta M, Whitesides GM (2008b) FLASH: A rapid method for prototyping paper-based microfluidic devices. *Lab Chip* 8:2146-2150
- Nagler RM (2008) Saliva analysis for monitoring dialysis and renal function 54:1415-1417
- Qiao L, Gu QM, Cheng HN (2006) Enzyme-catalyzed synthesis of hydrophobically modified starch. *Carbohydr Polym* 66:135-140
- Risio SD, Yan N (2007) Piezoelectric ink-jet printing of horseradish peroxidase: effect of ink viscosity modifiers on activity. *Macromol Rapid Commun* 28:1934-1940
- Seppanen R, Tiberg F, Valignat MP (2000) Mechanism of internal sizing by alkyl ketene dimers (AKD): The role of the spreading monolayer precursor and autophobicity. *Nord Pulp Paper Res* 15:452-458
- Shen W, Parker IH (2001) A preliminary study of the spreading of AKD in the presence of capillary structures. *J Colloid Interface Sci* 240:172-181
- Shen W, Filonanko Y, Truong Y, Parker IH, Brack N, Pigram P, Liesegang J (2000) Contact angle measurement and surface energetics of sized and unsized paper. *Colloid Surf A-Physiochem Eng Asp* 173:117-126
- Shen W, Xu F, and Parker IH (2003) An experimental investigation of the redistribution behaviour of alkyl ketene dimers and their corresponding ketones. *Colloid Surf A*, 212:197-209
- Stock R, Rice CBF (1974) *Chromatographic methods*, 3rd edn. Chapman and Hall, London, pp 106
- Vauvreau V, Laroche G (2005) Micropattern printing of adhesion, spreading, and

migration peptides on poly(tetrafluoroethylene) films to promote endothelialization. *Bioconjugate Chem* 16:1088-1097

Whitesides GM (2006) The origin and future of microfluidics. *Nature*, 442:368-373

Zhang H, Kannangara D, Hilder M, Ettl R and Shen W (2007) The role of vapour deposition in the hydrophobization treatment of cellulose fibres using alkyl ketene dimers and alkenyl succinic acid anhydrides, *Colloid and Surf A*, 297:203-210

Zhao W, van der Berg A, (2008) Lab on Paper. *Lab Chip*, 8:1988-1991

Part II: Thread-Based Microfluidics

The second part of this thesis presents an innovation on using multi-filament threads to build low-cost and disposable microfluidic diagnostics. This innovation was initially driven by our quest of finding simple ways to build 3D microfluidic systems using low-cost materials. Although 3D microfluidic systems can be built using paper plus sticky tape and cellulose powder, we believe other low-cost materials do exist and thread is one of those materials that can make simple 3D microfluidic systems.

This part of the thesis consists of three papers detailing the prove-of-concept study of thread-based microfluidic system, new concepts of building operator-controlled valves, mixers and reactors, and a real-life diagnosis study on human blood grouping using thread-based device. It was discovered in three studies that thread has certain interesting advantages over paper as the basic materials for building microfluidic systems. These advantages are discussed in detail in the chapters.

Our vision developed from the study of thread-based microfluidic analytical devices has the following two points. First, the fabrication methods of thread-based microfluidic systems are easier than those for fabricating paper-based microfluidic systems. They are less reliant on high-capital equipment. Therefore it may be possible that some thread-based analytical devices can be made by the skilled textile work force in developing countries. Second, we believe that, apart from thread, there must be other low-cost materials that can be used for making low-cost microfluidic analytical devices. This point is supported by the work presented in Appendix B to which the author has contributed as an assistant researcher.

Chapter 6: Thread as a Versatile Material for Low-Cost Microfluidic Diagnostics

This page is intentionally blank

Monash University
Declaration for Thesis Chapter 6

Declaration by candidate

In the case of Chapter 6, the nature and extent of my contribution to the work was the following:

Nature of contribution	Extent of contribution (%)
Experimental design and conduct, paper writing	70

The following co-authors contributed to the work. Co-authors who are students at Monash University must also indicate the extent of their contribution in percentage terms:

Name	Nature of contribution	Extent of contribution (%) for student co-authors only
Junfei Tian	Experimental design, assisted in experimentation	20
Wei Shen	Experimental design, corrected manuscript	Supervisor

Candidate's Signature

	Date 02/08/2011
---	---------------------------

Declaration by co-authors

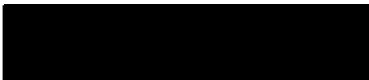

The undersigned hereby certify that:

- (1) the above declaration correctly reflects the nature and extent of the candidate's contribution to this work, and the nature of the contribution of each of the co-authors.
- (2) they meet the criteria for authorship in that they have participated in the conception, execution, or interpretation, of at least that part of the publication in their field of expertise;
- (3) they take public responsibility for their part of the publication, except for the responsible author who accepts overall responsibility for the publication;
- (4) there are no other authors of the publication according to these criteria;
- (5) potential conflicts of interest have been disclosed to (a) granting bodies, (b) the editor or publisher of journals or other publications, and (c) the head of the responsible academic unit; and
- (6) the original data are stored at the following location(s) and will be held for at least five years from the date indicated below:

Location(s)	Australian Pulp and Paper Institute (APPI), Department of Chemical Engineering, Monash University, Clayton, VIC 3800, Australia
--------------------	---

Signature 1

Signature 2

	Date 02/08/2011
	4/8/11

This page is intentionally blank

Thread as a Versatile Material for Low-Cost Microfluidic Diagnostics

Xu Li, Junfei Tian, Wei Shen*

*Australian Pulp and Paper Institute, Department of Chemical Engineering,
Monash University, Clayton Campus, VIC 3800 Australia*

*Corresponding Author: Email: [REDACTED]

Tel: [REDACTED] Fax: [REDACTED]

6.1 ABSTRACT

This paper describes a new and simple concept for fabricating low-cost, low-volume, easy-to-use microfluidic devices using threads. A thread can transport liquid via capillary wicking without the need of a barrier; as it is stainable, it is also a desirable material for displaying colorimetric results. When used in sewing, threads have 3D passageways in sewed materials. The wicking property and flexibility of thread make it particularly suitable to fabricate 3D microfluidic devices. Threads can also be used with other materials (e.g., paper) to make microfluidic devices for rapid qualitative or semiquantitative analysis. These thread-based and thread-paper-based devices have potential applications in human health diagnostics, environmental monitoring, and food safety analysis, and are particularly appropriate for the developing world or remote areas, because of their relatively low fabrication costs.

6.2 KEYWORDS

Thread, Paper, Diagnostics, 3D microfluidics, Low-cost sensors.

6.3 INTRODUCTION

New concepts and applications of low-cost, portable and field-based diagnostic technologies have become an area attracting a lot of research interest (1). The potential of these technologies in providing affordable healthcare and environmental monitoring to remote and developing regions strongly drives the continuous developments of these technologies. The recent rise of paper-based microfluidic devices (2-5) once again shows the attraction of low-cost and field-based technologies.

Cotton thread as an ancient material in civilization is also an attractive material for the fabrication of low-cost and low-volume microfluidic diagnostic devices for healthcare and environmental assays. This is because the gaps between fibers provide capillary channels for liquids to wick along the thread. Thread has been used for sensor fabrication, but only for purposes other than building microfluidic sensors. The idea of using electronic threads for human health monitoring has been reported in many studies (6-9). The electronic threads are usually metal-based threads (7) or threads made by carbon nanotubes coated with polyelectrolytes (8, 9). To the best of our knowledge, there has been no work reported using cotton or other multifilament threads for fabricating simple and low-cost microfluidic analytical devices.

In this study, cotton thread is used to fabricate microfluidic devices with 3D structures by sewing it onto other materials (e.g., polymer film). In this way, we show the possibility to fabricate high density thread microfluidic channels to enable the transportation of several liquids through the structure without mixing. Threads with different wettability can also be used to manipulate liquid wicking and mixing. These capabilities further enable us to fabricate 3D thread-based microfluidic devices which encompass complicated microfluidic channels compared to lateral flow systems (5). The fabrication of thread-based microfluidic devices is simple and relatively low-cost, because it requires only sewing needles or household sewing machines, which are commonly used and affordable, even in some of the under-developed world. Liquids can penetrate from thread into other hydrophilic porous materials; therefore, thread can be used with other materials (e.g., paper) to form microfluidic devices with enhanced sample delivering efficiency. In this work, thread-based and thread-paper-based

microfluidic sensors are fabricated with the incorporated colorimetric indicators for two important biomarkers for several human medical conditions, nitrite ion (NO_2^-) and uric acid (UA) (10-12). The potential of using thread and thread-paper microfluidic sensors to provide low-cost, low-volume, semiquantitative and multispecies analysis is shown through the detection and measurement of these species. Our results demonstrate that thread is a suitable material for fabricating microfluidic diagnostic devices for monitoring human health, environment and food safety; especially for the population in less-industrialized areas or remote regions (13, 14).

6.4 EXPERIMENTAL SECTION

Cotton thread was kindly provided by the School of Fashion and Textiles, RMIT University, Melbourne, Australia. The average diameter of the thread was measured using a microscope (Olympus, BX-60) which was interfaced to a PC to allow object size measurement. The cotton thread was found to have an average thickness of $244 \pm 41 \mu\text{m}$. Natural cotton thread is not wettable by aqueous liquids; this is because natural cotton fibers have wax on their surface and in the fiber wall. Therefore, natural cotton thread needs to be dewaxed or surface treated to allow the wicking of aqueous liquids (15). In this study, to obtain hydrophilic cotton thread, we used a vacuum plasma reactor (K1050X plasma asher (Quorum Emitech, UK)) to treat cotton thread for 1 min at an intensity of 50 W. The vacuum level for the treatment was 6×10^{-1} mbar.

The treated and untreated thread samples were analyzed using XPS to show the effect of the plasma treatment on their surface chemistry and wettability differences. XPS analysis was conducted using an AXIS HSI spectrometer (Kratos) with monochromatized Al $K\alpha$ radiation. The photoelectron emission angle was 90° with respect to the sample surface. This corresponds to a maximum sampling depth of ca. 10 nm. Thread samples were wound around a sample holder to form a closely packed mesh providing the necessary area for the X-ray beam, which was about 2 mm in diameter. Table 1 lists the changes in surface atomic concentration of C and O before and after plasma treatment. Filter paper was used as the control for cellulose. The presence of C (1+2) on filter paper surface was most likely due to surface

contamination during the production and packaging processes. Plasma treatment may have two effects on the thread surface modification: First, the surface was substantially oxidized; this is indicated by the increase in surface concentration of C species with binding energies of 288.3 and 289.2 eV, which correspond to the generation of surface O–C–O, C=O and O–C=O groups. Second, the increase in surface concentration of C–O (286.8 eV) may mean that the plasma treatment also partially removed wax and exposed the underlying cellulose. These combined changes significantly increased the surface oxygen concentration (Table 1) and therefore increased surface polarity. The increased water wettability after plasma treatment is consistent with the surface chemistry changes revealed by XPS. After treatment water can readily wet and wick along the cotton thread.

Table 1. Surface Atomic Concentration of C and O of Untreated and Treated Threads

sample	filter paper (cellulose)	thread (untreated)	thread (plasma treated)	binding energy (eV)	assignment
C (1+2)	0.215	0.784	0.562	285.0, 285.5	C–C, C–H
C (3)	0.605	0.163	0.261	286.8	C–O
C (4)	0.180	0.032	0.107	288.3	O–C–O, C=O
C (5)		0.021	0.069	289.2	O–C=O
O	0.596	0.139	0.574	533.2	

To characterize the hydrophobic and hydrophilic contrast between threads, we prepared a series of water–isopropyl alcohol (IPA) (HPLC grade, EMD Chemicals Inc.) solutions with different IPA mass percentages (14, 16, 18, 20, 22, and 24%) as a means to measure the onset of wicking of water–IPA solutions in untreated cotton thread. Because the surface tension values of the water–IPA system are known (16), it can be used as a convenient measure to characterize the wicking property of the thread. Aspler et al. (17) and Nisbet et al. (18) have shown that the polar liquid wicking in a porous material occurs when the surface tension of the liquid is lowered to a critical value. The wicking onset, in the porous material, can be identified by testing the wicking speed of a series of liquids with different surface tension values. Although high surface tension liquids do not wick (zero speed) in the material, liquids that have a certain surface tension value start to wick in the material at an observable speed. Aspler et al. (17)

referred this surface tension value as the critical wicking surface tension. Liquids that have a surface tension lower than this value can all wick in the material. This method was used to identify the liquid wicking onset of untreated cotton thread.

Millipore-purified water was used to prepare all aqueous samples required for testing the performance of threads. The ink solutions (cyan, magenta, blank and yellow) used in the liquid wicking experiments were prepared by diluting commercial Canon ink jet inks (CLI Y-M-C-BK, PGBK (<http://www.canon.com.au/>)) with water. The red ink solution was prepared by mixing magenta and yellow ink solutions. The green ink solution was a mixture of cyan and yellow ink solutions. The density values of the ink solutions were measured using a Mettler Toledo Densito 30Px (Switzerland). The surface tension of the ink solutions were measured by the capillary rise method (19) using a cathetometer. Glass capillary tubes were first washed with laboratory detergent (RBS 35 detergent, Chemical products, Belgium), followed by rinsing with ample amounts of water. The capillary tubes were dried under ambient temperature, followed by 60 °C oven drying. Finally, the tubes were plasma treated to ensure complete wetting. The tube diameter was determined by measuring the capillary rise of n-hexadecane (Aldrich, >99%) of known surface tension.

The stock solution of NO_2^- (10.0 mmol/L) was prepared by dissolving 69.0 mg sodium nitrite ($\geq 99\%$, Sigma-Aldrich) in 100 mL water. This stock solution was then diluted with water to get serially diluted NO_2^- standard solutions with concentrations of 1000, 500, 250, 125 and 0 $\mu\text{mol/L}$. The indicator solution for NO_2^- contained 50 mmol/L sulfanilamide ($\geq 99\%$, Sigma-Aldrich), 330 mmol/L citric acid ($\geq 99.5\%$, Sigma-Aldrich), and 10 mmol/L N-(1-naphthyl) ethylenediamine ($\geq 98\%$, Sigma-Aldrich) (10).

The UA stock solution (10.0 mmol/L) was prepared by dissolving 168.1 mg uric acid ($\geq 99\%$, Sigma-Aldrich) in 100 mL NaOH solution (0.2 mol/L). The UA sample solution (1000 $\mu\text{mol/L}$) was prepared by further diluting the stock solution with NaOH solution. The indicator solution for UA consisted of a 1:1 ratio mixture of solution A (2.56% (w/v) 2,2'-biquinoline-4,4'-dicarboxylic acid disodium salt hydrate, $\geq 98\%$, Sigma-Aldrich) and solution B (20 mmol/L sodium citrate and 0.08% (w/v) copper (II) sulfate, $\geq 99\%$, Sigma-Aldrich) (10).

6.5 RESULTS AND DISCUSSION

Gaps between fibers of cotton threads provide capillary channels for liquids to wick along threads without the need of an external pump. Panels A and B in Figure 1 show two examples of using plasma-treated hydrophilic threads to form 3D structures. In Figure 1A, a 3D microfluidic pattern was fabricated by sewing threads through a polymer film. A translucent polymer film was chosen to visually demonstrate the liquid wicking passageways. In this pattern, the stitches of the threads pass one another from above and below the polymer film, and therefore, do not have contact. Ink solutions of different colors wick along the threads and cross one another without mixing. Thus, threads allow complex continuous 3D microfluidic channels to be built without the need of patterned barriers to define the liquid wicking passageways. High-density thread circuitries can be built in a relatively small space that is suitable for miniaturization. Fabrication of such 3D microfluidic structures with threads requires only some basic tools such as a sewing needle or a household sewing machine, and is therefore less reliant on sophisticated equipment required for patterned paper devices. Figure 1B shows ink solution transport through a cotton thread embedded in plasticine. The ink solution can wick through tortuous passageways, even if the solid material enclosing the thread is not wettable by the wicking liquid. Therefore, when thread is used to provide the capillary driving force for liquid transport, the wetting property of the support material will no longer be a design restriction.

Thread has other interesting properties that can be used to control liquid wicking along it. First, liquid wicking along a thread is controlled by the liquid wettability of thread. The hydrophilic–hydrophobic contrast of the treated and untreated thread provides a convenient option to manipulate liquid transport. The wicking onset characterization using the water-IPA solution series showed that solutions of less than 20% IPA (w/w) form bead on the surface of untreated thread and do not wick along the thread. The surface tension value of this solution is 31.2 mN/m at 20 °C (16). IPA solutions of higher concentrations than 20% can wick along the untreated thread. Therefore, aqueous solutions with a surface tension higher than 31.2 mN/m can only wick along the treated thread, but not along untreated thread.

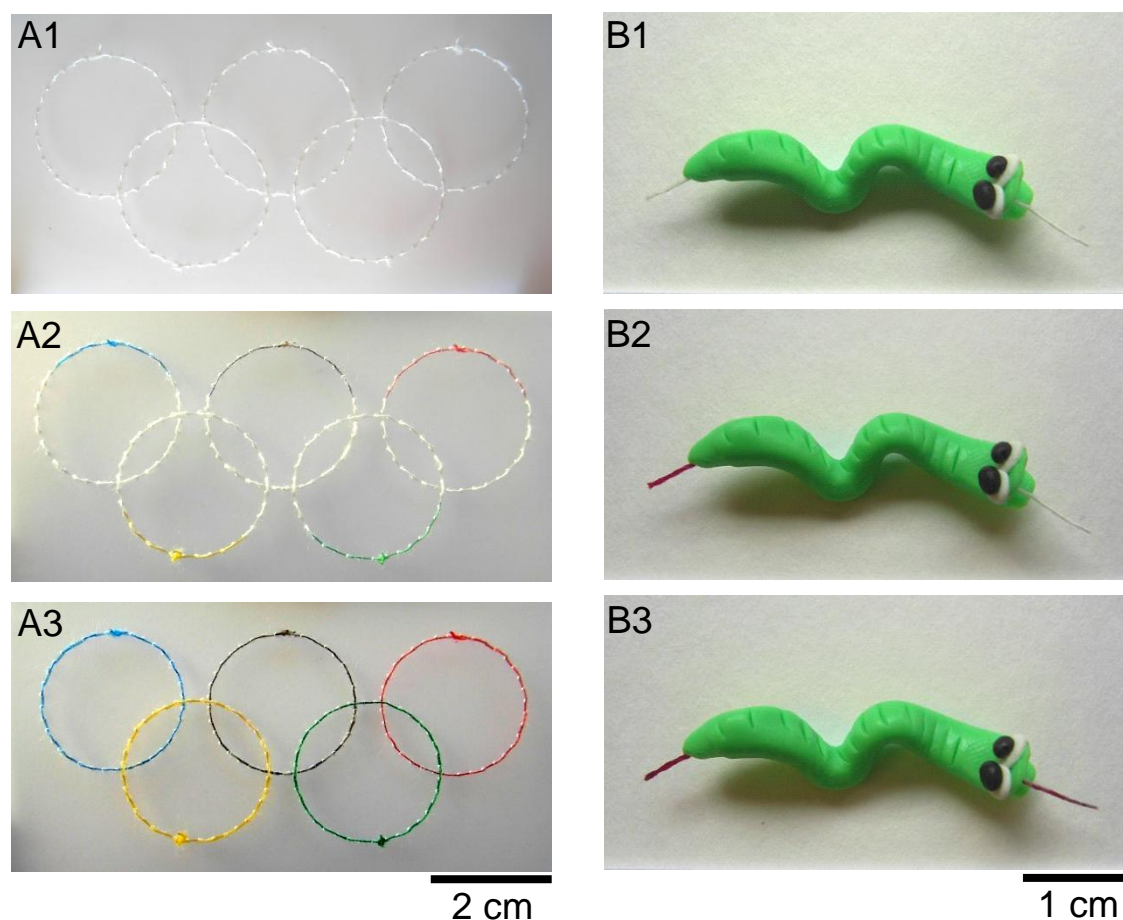


FIGURE 1. (A) Three-dimensional microfluidic pattern fabricated by sewing threads onto a translucent polymer film. (A1) Pattern sewed using hydrophilic cotton threads; (A2) introduction of liquids on threads; (A3) liquids wick throughout the thread pattern. Their stitches cross one another from above and below the polymer film and therefore do not mix. (B) Three-dimensional microfluidic channel of thread imbedded in plasticine. (B1) Imbedded hydrophilic cotton thread in plasticine; (B2) introduction of a liquid on the thread from one end; (B3) liquid wicks along the thread through plasticine.

The sensitivity of liquid wicking to the surface condition of a thread can be used as a convenient option for designing a thread network to facilitate and control liquid transport. Panels A and B in Figure 2 show a twisted pair of cotton threads, one untreated and the other plasma-treated. The cyan ink solution was introduced onto the treated hydrophilic thread and wicked only along this thread. The surface tension values of all the diluted ink solutions were higher than the critical wicking surface tension of the untreated thread (e.g., the cyan ink solution (10%, v/v) was 37.4 mN/m at 20 °C with the density of 1.022 g/mL). Therefore, the ink solutions can only wick along the treated thread, but not along the untreated thread. Second, liquid wicking can be

relayed from a hydrophilic thread to another hydrophilic thread or a hydrophilic porous material. This property of thread makes it possible to use thread with other porous materials to form more sophisticated microfluidic systems. If two hydrophilic threads are twisted together, and a different liquid solution is introduced to each of the thread, the two solutions will mix when the two threads meet. Figure 2C demonstrates a simple mixing zone in a thread device. Three threads pass through a liquid mixing zone, restrained by a tube of sticky tape. The top and the middle threads that transport cyan and yellow ink solutions are twisted and sleeved inside a heat shrink tube; the bottom thread that transports magenta ink solution is not twisted with the other two threads and passes through the mixing zone from outside of the heat shrink tube. The magenta ink solution therefore does not mix with other solutions. The ability to manipulate liquid transport and mixing offers the possibility of using threads to fabricate more sophisticated microfluidic patterns.

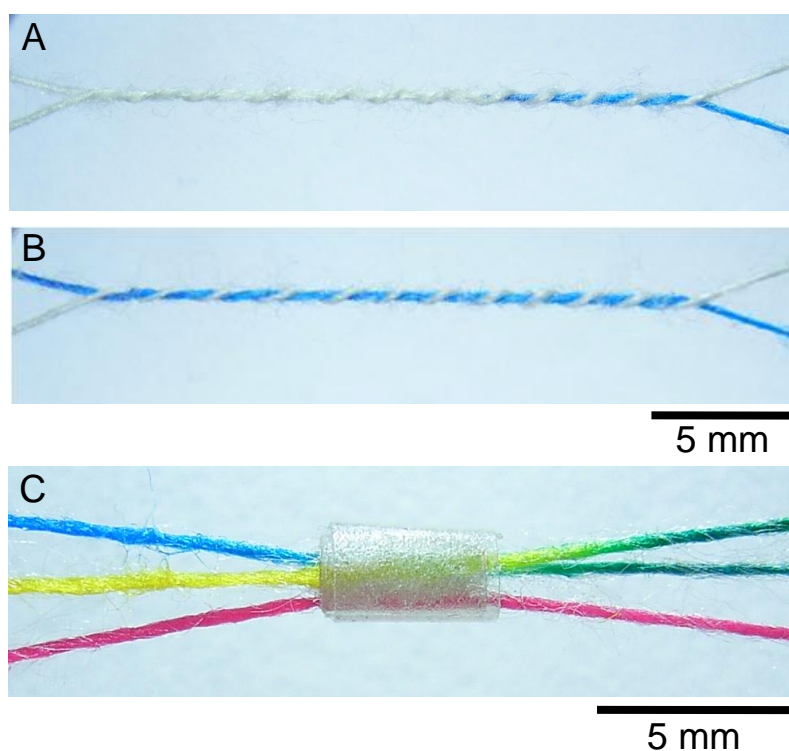


FIGURE 2. (A, B) Twisted pair of an untreated and a plasma-treated cotton thread. When the liquid is introduced onto the treated and hydrophilic thread, the liquid wicks only along the hydrophilic thread. (C) Sample mixing zone demonstrating the manipulation of liquid wicking along threads. The top and the middle threads that transport cyan and yellow liquids are twisted and sleeved inside a heat shrink tube; the bottom thread that transports magenta liquid is not twisted with the other two threads and passes through the mixing zone from outside of the heat shrink tube.

Liquids wicking on two twisted hydrophilic threads can mix surprisingly well (Figure 2C). This phenomenon may be related to the good alignment of closely packed long fibers in a thread in a helical arrangement. The fiber gaps, therefore, also have good alignment in the thread. When two threads are twisted together for a number of turns, fiber gaps in one thread are in contact with all fiber gaps of the other thread, and these contacts form new gaps for the liquid to wick. We think the full contact of all fiber gaps between the two twisted threads is responsible for the good liquid mixing result.

Combining the thread properties shown in Figures 1 and 2, multianalyte and 3D microfluidic devices can be easily designed. The combination of thread and filter paper provides a proof-of-concept design for 3D microfluidic devices (Figure 3). Circular paper discs ($\varnothing = 2$ mm) were produced from Whatman No.4 filter paper using a disk punching device (Facit 4070, Sweden) to make thread-paper sensors. Paper discs were immersed either in the NO_2^- or the UA indicator solution respectively to full saturation and were then dried in an oven at 60 °C for ~ 5 min. Two hydrophilic cotton threads (~2 cm) were sewed through an opaque polymer film (2.5 cm \times 2.5 cm), with half the length left on the front side and the other half on the back side of film. The ends of the two threads on the front side were made to contact the two paper discs treated with NO_2^- indicator solution; the other ends of the two threads on the back side were made to contact the paper discs treated with UA indicator solution. Single-sided sticky tape was used to fix the paper discs and threads onto the film (panels A and B in Figure 3). A test solution containing 500 $\mu\text{mol/L}$ NO_2^- and 500 $\mu\text{mol/L}$ UA was prepared by mixing equal volumes of 1000 $\mu\text{mol/L}$ NO_2^- and 1000 $\mu\text{mol/L}$ UA solutions. A 3 μL test solution was introduced onto the threads from the central film hole with a micro pipet (eppendorf research[®] 1.0–10 μL); the test solution rapidly wicked along the threads and reached paper discs. Paper discs treated with NO_2^- indicator on the front side of the film rapidly developed a pink color, confirming the detection of NO_2^- , whereas paper discs treated with UA indicator on the back side of the film developed a purple color, confirming the detection of UA (Figure 3C). The fabrication process of this kind of thread-paper 3D microfluidic devices is simpler than that reported for 3D microfluidic devices fabricated by stacking layers of paper and tape (20).

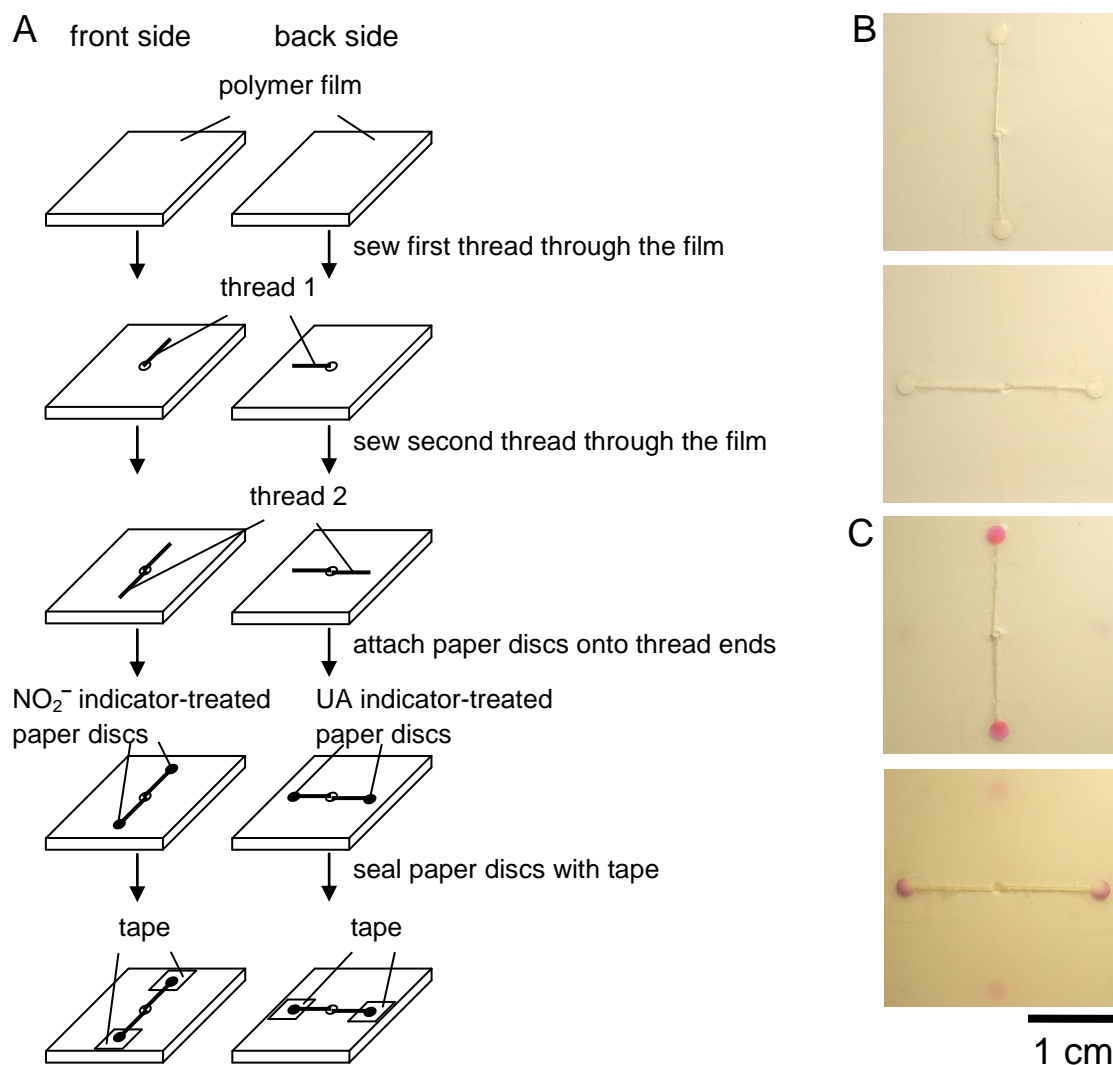


FIGURE 3. Demonstration of a 3D thread-paper microfluidic sensor. (A) Fabrication of the sensor. (B) Front side and back side of the sensor. (C) Different color development on the front side (pink) and back side (purple) of the sensor when multianalyte test solution (500 μM NO_2^- , 500 μM UA) was introduced from the central hole of the sensor onto the two threads and penetrated into paper discs (detection zones).

Thread can be used by itself for semiquantitative colorimetric assay. Cotton thread is white which provides a desirable reference background for colorimetric detections. An aqueous liquid (0.1 μL) wicks for a length of ~ 6 mm on a plasma-treated household sewing cotton thread which is about the length of two stitches. A thread-based microfluidic device can be made by simply sewing thread onto a support material such as polymer film. For creating NO_2^- calibration curve with thread-based devices, hydrophilic thread was immersed in the NO_2^- indicator solution and was then dried in an oven at 60°C for ~ 5 min. Five short threads cut from the indicator-treated thread were sewed onto an opaque polymer sheet with one stitch (~ 3 mm) exposing at the top side of the sheet as the detection zone. Five serially diluted NO_2^- standard solution samples (0.1 μL , 1000, 500, 250, 125 and 0 $\mu\text{mol/L}$) were deposited onto the five sewed threads separately with a micro pipet (eppendorf research[®] 0.1-2.5 μL). Colorimetric change on each stitch can be clearly seen. The extra amount of solution continues to wick along the thread to the other side of the polymer film and cannot be seen. The color development can be recorded by a digital camera for visual appraisal. Figure 4A shows a photo of three repeated measurements of the same serially diluted NO_2^- solutions samples. The results of the colorimetric assays can also be recorded for data analysis with a desktop scanner (Epson Perfection 2450 PHOTO) using the color photo setting and 4800 dpi resolution. It is noted that for the image scanning, the orientation of the stitches should be positioned parallel to the scanning direction of the light bar in the scanner to avoid the shadowing effect caused by the protruding stitches on the polymer film surface. The recorded color image data can then be imported into Adobe Photoshop and converted into grayscale mode. A fixed area is applied to all detection zones. The mean grayscale intensities can be quantified using the histogram function of Adobe Photoshop. The ultimate mean intensity value of each detection zone can be obtained by subtracting the measured average detection zone intensity from the mean intensity of the 0 $\mu\text{mol/L}$ NO_2^- solution; the average intensity data can then be transferred to Microsoft Excel to obtain calibration curve data (Figure 4B). In this work, six independent measurements were taken using six thread-based devices made from the same indicator-treated thread. Data points are the average values \pm s.d. ($n = 6$). Thread, therefore, offers a new design concept for low-cost and low-volume healthcare and diagnostic sensors. The low material cost of such sensors will make them very useful in the developing and remote regions where well-equipped medical services are lacking.

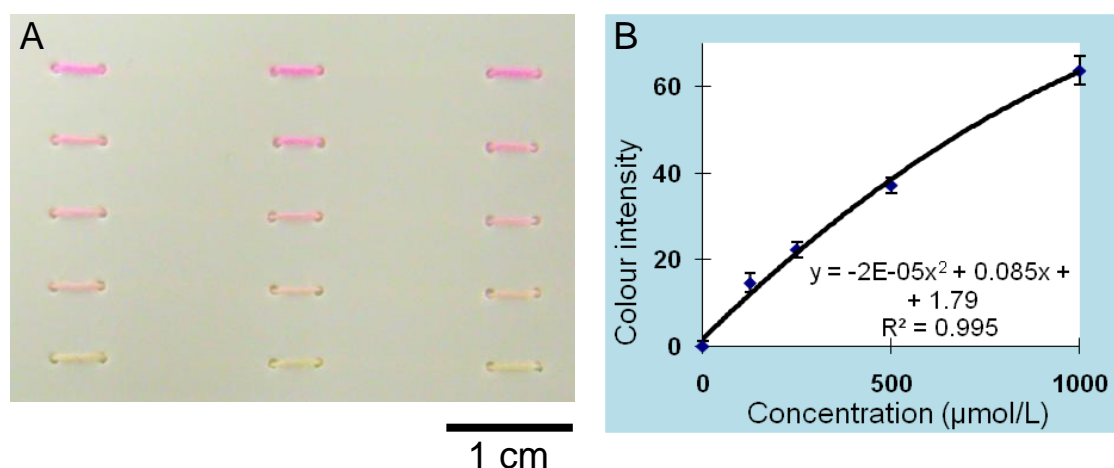


FIGURE 4. (A) Three parallel colorimetric measurements of serially diluted NO_2^- solution samples (0, 125, 250, 500, and 1000 μM) on the thread-based sensor. (B) NO_2^- concentration calibration curve established from thread stitches of six thread sensors using a desktop scanner and Adobe PhotoShop.

Thread can also be used with other porous materials such as paper for semiquantitative colorimetric assay. Figure 5 shows a thread-paper microfluidic sensor array of a separate-sample-inlet design. Five NO_2^- indicator-treated paper discs were first laid onto a single-sided sticky tape in a line. Five hydrophilic cotton threads were then laid onto the sticky tape, each touching one of the five separate paper discs. A white opaque polymer film was finally pressed onto the sticky tape, forming the whole sensor. It is worth noting that using polymer film and sticky tape to form a sensor has an advantage of reducing sensor contamination and sample evaporation. NO_2^- solutions (0.8 μL) of a series of concentrations (0, 125, 250, 500, and 1000 $\mu\text{mol/L}$) were introduced in sequence using the micro pipet to the free end of each thread. The sample solutions rapidly penetrated along the threads and reached the paper discs in less than 2 s and triggered full color changes within 5 s. The fully developed colors were recorded by the digital camera for visual appraisal (Figure 5B) and by the desktop scanner for data analysis. The NO_2^- concentration calibration curve was established following the procedure mentioned earlier for thread-based sensors (Figure 5C). The circular area enclosing the entire paper disk was selected for color analysis, and six independent measurements were taken from the six thread-paper sensors to give the average values \pm s.d..

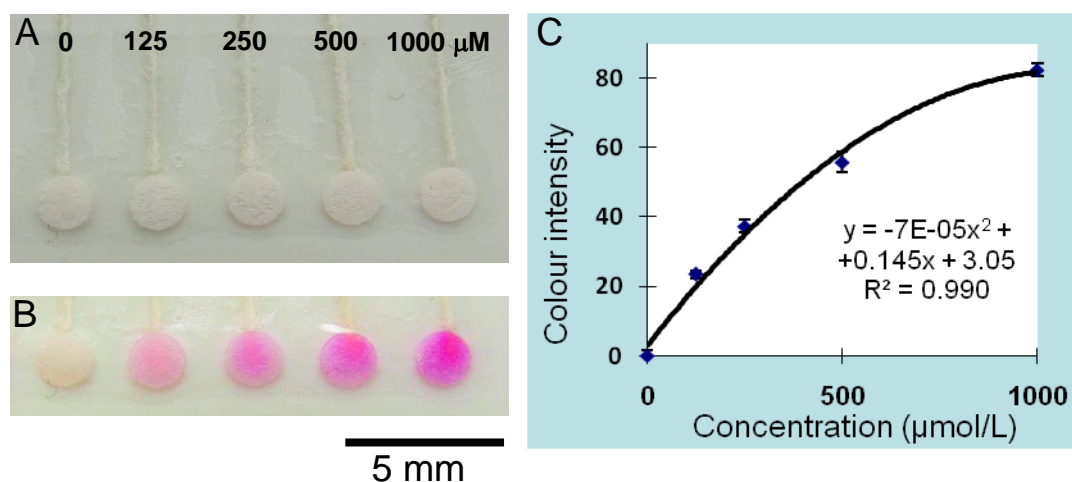


FIGURE 5. (A) Thread-paper microfluidic sensors using cotton thread as the liquid transport channel. (B) Colorimetric NO_2^- concentration series (0, 125, 250, 500, and 1000 μM) developed using a sensor array made of filter paper and cotton thread. (C) A NO_2^- concentration calibration curve established from six thread-paper microfluidic sensors using a desktop scanner and Adobe PhotoShop.

6.6 CONCLUSIONS

Thread has been used to fabricate 3D and semiquantitative microfluidic analytical devices. An advantage of using thread as the liquid transporting channels is that it does not need patterned barriers. Another advantage of using thread or thread with other porous materials such as paper to fabricate microfluidic devices is that these devices can be fabricated with basic tools; the reliance on modern equipment is reduced. Certain simple devices may even be fabricated by a skilled work force within the textile industry in developing regions. It can be envisaged that thread, either alone or with other materials, can be used to fabricate a family of microfluidic diagnostic devices suitable for colorimetric, electrochemical, chemiluminescent, electrochemiluminescent assays and electrophoresis. The low-cost, flexible and versatile nature of thread will allow this ancient material to have new applications in disposable microfluidic devices, advanced textile and personal care products, healthcare and environmental sensors.

6.7 ACKNOWLEDGMENT

The research scholarships of Monash University and the Department of Chemical Engineering are gratefully acknowledged. The authors would like to thank Dr. L. Wang of the School of Fashion and Textiles, RMIT University, for kindly providing us with the cotton thread sample, and Dr. T. Gengenbach of CSIRO Molecular and Health Technologies for taking XPS measurements of the thread samples. The authors specially thank Dr. E. Perkins of the Department of Chemical Engineering, Monash University, for proofreading the manuscript.

6.8 REFERENCES

- (1) Weigl, B.; Domingo, G.; LaBarre, P.; Gerlach, J. *Lab on a Chip* **2008**, 8, 1999-2014.
- (2) Martinez, A. W.; Phillips, S. T.; Butte, M. J.; Whitesides, G. M. *Angew. Chem., Int. Ed.* **2007**, 46, 1318-1320.
- (3) Abe, K.; Suzuki, K.; Citterio, D. *Anal. Chem.* **2008**, 80, 6928-6934.
- (4) Li, X.; Tian, J.; Nguyen, T.; Shen, W. *Anal. Chem.* **2008**, 80, 9131-9134.
- (5) Fenton, E. M.; Mascarenas, M. R.; Lo'pez, G. P.; Sibbett, S. S. *ACS Appl. Mater. Interfaces* **2009**, 1, 124-129.
- (6) Carpi, F.; Rossi, D. D. *IEEE Trans. Inf. Technol. Biomed.* **2005**, 9, 295-318.
- (7) Paradiso, R.; Loriga, G.; Taccini, N. *IEEE Trans. Inf. Technol. Biomed.* **2005**, 9, 337-344.
- (8) Shim, B. S.; Chen, W.; Doty, C.; Xu, C.; Kotov, N. A. *Nano Lett.* **2008**, 8, 4151-4157.
- (9) Zhang, M.; Atkinson, K. R.; Baughman, R. H. *Science* **2004**, 306, 1358-1361.
- (10) Blicharz, T. M.; Rissin, D. M.; Bowden, M.; Hayman, R. B.; DiCesare, C.; Bhatia, J. S.; Grand-Pierre, N.; Siqueira, W. L.; Helmerhorst, E. J.; Loscalzo, J.; Oppenheim, F. G.; Walt, D. R. *Clin. Chem.* **2008**, 54, 1473-1480.
- (11) Nagler, R. M. *Clin. Chem.* **2008**, 54, 1415-1417.
- (12) Wink, D. A.; Kasprzak, K. S.; Maragos, C. M.; Elespuru, R. K.; Misara, M.; Dunams, T. M.; Cebula, T. A.; Koch, W. H.; Andrews, A. W.; Allen, J. S.; Keefer, L. K. *Science* **1991**, 254, 1001-1003.
- (13) Yager, P.; Domingo, G. J.; Gerdes, J. *Annu. Rev. Biomed. Eng.* **2008**, 10, 107-144.
- (14) Mabey, D.; Peeling, R. W.; Ustianowski, A.; Perkins, M. D. *Nat. Rev. Microbiol.* **2004**, 2, 231-240.
- (15) Hown-Grant, M. in *Encyclopedia of Chemical Technology*, 4th ed.; Wiley-Interscience: New York, 1993, Vol. 7, p.633.
- (16) Vázquez, G.; Alvarez, E.; Navaza, J. M. *J. Chem. Eng. Data* **1995**, 40, 611-614.
- (17) Aspler, J. S.; Davis, S.; Lyne, M. B. *J. Pulp Paper Sci.* **1987**, 13, 55-60.
- (18) Nisbet, D. R.; Pattanawong, S.; Ritchie, N. E.; Shen, W.; Finkelstein, D. I.; Horne, M. K.; Forsythe, J. *J. Neural Eng.* **2007**, 4, 1-7.

- (19) Shaw, D. J. *Introduction to Colloid and Surface Chemistry*, 4th ed.; Butterworth, Oxford, UK, 1992, p.71.
- (20) Martinez, A. W.; Phillips, S. T.; Whitesides, G. M. *Proc. Natl. Acad. Sci. U. S. A.* **2008**, 105, 19606-19611.

Chapter 7: An Inexpensive Thread-Based System for Simple and Rapid Blood Grouping

This page is intentionally blank

Monash University
Declaration for Thesis Chapter 7

Declaration by candidate

In the case of Chapter 7, the nature and extent of my contribution to the work was the following:

Nature of contribution	Extent of contribution (%)
Experimental design and conduct, paper writing	45

The following co-authors contributed to the work. Co-authors who are students at Monash University must also indicate the extent of their contribution in percentage terms:

Name	Nature of contribution	Extent of contribution (%) for student co-authors only
David Ballerini	Experimental design and conduct, paper writing	45
Wei Shen	Experimental design, corrected manuscript	Supervisor

Candidate's Signature

	Date 02/08/2011
---	---------------------------

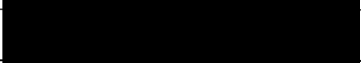
Declaration by co-authors

The undersigned hereby certify that:

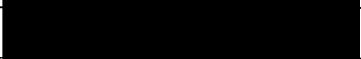
- (1) the above declaration correctly reflects the nature and extent of the candidate's contribution to this work, and the nature of the contribution of each of the co-authors.
- (2) they meet the criteria for authorship in that they have participated in the conception, execution, or interpretation, of at least that part of the publication in their field of expertise;
- (3) they take public responsibility for their part of the publication, except for the responsible author who accepts overall responsibility for the publication;
- (4) there are no other authors of the publication according to these criteria;
- (5) potential conflicts of interest have been disclosed to (a) granting bodies, (b) the editor or publisher of journals or other publications, and (c) the head of the responsible academic unit; and
- (6) the original data are stored at the following location(s) and will be held for at least five years from the date indicated below:

Location(s)	Australian Pulp and Paper Institute (APPI), Department of Chemical Engineering, Monash University, Clayton, VIC 3800, Australia
--------------------	---

Signature 1

	Date 2/8/2011
---	----------------------

Signature 2

	4/8/11
---	--------

This page is intentionally blank

An Inexpensive Thread-Based System for Simple and Rapid Blood Grouping

Xu Li¹, David R. Ballerini¹, Wei Shen*

*Department of Chemical Engineering, Monash University, Clayton Campus, Melbourne, VIC 3800,
Australia*

I D. R. Ballerini and X. Li contributed equally as co-first authors.

**Corresponding Author: Email:* [REDACTED]

7.1 ABSTRACT

This study investigates the use of thread as a flexible and low-cost substrate for the rapid grouping of blood. The use of a capillary substrate such as thread for blood grouping utilises the sensitivity of the flow resistance of large particles in narrow capillary channels to separate agglutinated red blood cells (RBCs) from plasma. Large and discrete particles formed in a continuous liquid phase do not provide capillary wicking driving force and fall behind the capillary wicking front, leading to their separation from the wicking liquid. The capillary substrate therefore provides a very promising but different mechanism for the separation of the agglutinated RBCs and the blood serum phase compared to most existing blood grouping methods. The principle of chromatographic separation is also exploited in this study via the use of suitable dyes to enhance the visual detection of the agglutinated RBCs and the serum phase; surprising and encouraging outcomes are obtained. Using a thread-based device, the ABO and Rh groups can be successfully determined with only 2 μL of whole blood from a pricked finger tip within 1 min and without pre-treatment of the blood sample. It is hoped that a new, inexpensive, rapid and simple method may provide an easy-to-use blood grouping platform well suited to those in developing or remote regions of the world.

7.2 KEYWORDS

Blood typing, Thread-based, Point of care, Microfluidic, Low-cost, Developing regions

7.3 INTRODUCTION

Correct grouping of human blood is imperative for numerous reasons; among them transfusion compatibility is paramount. The term “blood group” is a classification of an individual’s blood based upon the inherent presence or absence of antigens on the surface of their red blood cells (RBCs) [1]. In the blood plasma, antibodies exist which are formed against foreign antigens to protect the body from perceived threats. This reciprocal relationship, Landsteiner’s Law, means that individuals who lack a RBC antigen (A, B or D for example) will possess the corresponding serum antibody, whilst those who possess the antigen must not [2]. There are 30 discrete blood type systems recognised by the ISBT Committee on Terminology for Red Cell Surface Antigens [3]. Among these the ABO and Rh systems are of primary importance when transfusing blood, as incompatibility may lead to an acute haemolytic reaction with catastrophic results such as shock and renal failure leading to death [4]. Without ABO compatibility testing, around one-third of unscreened blood transfusions would be expected to cause a haemolytic reaction [3]. For this reason the ability to quickly and cheaply identify blood type is highly valued, and may lead to the saving of many lives.

The vast majority of techniques for ABO and Rh grouping of blood to date have been based upon the principle of haemagglutination reactions between RBCs and serum antibodies. The absence of agglutination indicates no haemagglutination reaction [5]. An exception to this is the technique of gene-sequencing, which analyses DNA to precisely determine blood type, albeit at considerable cost [6].

Commonly used methods include the slide test [7], tube test [8], micro plate method [9-11], and the column agglutination system [12,13]. These methods require specific antiserum addition during testing or well-trained personnel to perform centrifugation, and are therefore difficult away from the laboratory setting. Disposable systems such as

lateral flow devices [14] and bedside test cards [15], though rapid and without the need of expensive equipment, always require the pre-treatment of blood samples or reconstitution of antibody.

All of the techniques mentioned suffer from shortcomings such as (1) high cost (2) necessity of trained personnel (3) sample pre-treatment (4) additional reagent handling or (5) large sample volume requirements. This limits use in developing regions and emergency situations where medical facilities are unavailable. A recent study performed blood typing on paper strips coated with antibody eliminating the pre-treatment of blood samples, but with the sample volume required for each test being 20 μL , venipuncture is necessary [16]. This study provides a new testing platform utilising the porous nature of thread which avoids these limitations whilst being simple, rapid and inexpensive with low sample volume requirements.

Recent research into the use of thread as a substrate for biomedical and environmental diagnostics has shown the material to be excellent for use in microfluidic devices due to its “ready-made” channel structure [17]. Thread is able to wick liquids through capillary motion due to the capillary structure formed by spaces between fibres comprising the thread. Cotton and polyester threads are inexpensive and globally ubiquitous. They have excellent colour display properties, physical strength and wettability. By impregnating thread with serum antibodies, agglutination of RBCs will occur upon the addition of whole blood to the dried thread. This reaction occurring between RBC surface antigens and serum antibodies results in separation of the RBCs and plasma, resulting in three distinct, visible regions when the test is positive. When no interaction occurs, the test is negative and no separation is visible.

The chromatographic separation principle, when used for blood typing with a porous substrate such as thread, offers an unexpected advantage for the identification of haemagglutination. It was found that adding suitable dyes to antibodies significantly enhanced the clarity of results. Having low affinity to cellulose and polyester fibre surfaces, the dyes are eluted by the serum phase remaining at the wicking front, generating a visible gap between the dye and agglutinated RBCs. Another focus of this study is to prove the concept of a simple, recyclable blood sample handling tool. This tool allows the required volume of blood sample to be extracted from a finger pricked

with a conventional lancet device safely and adequately for testing, increasing the ease of the procedure.

The restrictive requirements of existing techniques render them less suitable for point-of-care monitoring and treatment, especially for use in under-developed areas, emergency situations, and general field use. Although this new platform is not expected to replace current methods practiced in the developed world, it is hoped that it may find use in remote and developing regions where access to laboratories or hospitals is unavailable.

7.4 EXPERIMENTAL SECTION

7.4.1 Preparation of Antibody Impregnated Thread

Polyester thread was obtained from the School of Fashion and Textiles, RMIT University, Melbourne, Australia. The selection of polyester thread as the substrate was due to its excellent colour display properties, which aid in the identification of the separation of sample components in capillary channels. The thread used was given an initial plasma treatment as described by Li et al. to remove surface contaminants which greatly increased its ability to be wetted [17]. EpicloneTM anti-A, anti-B and anti-D monoclonal grouping reagents were sourced from CSL Australia. Anti-A and anti-B are a transparent cyan and a yellow solution respectively, whilst anti-D is a clear solution. Threads were treated with antibody via soaking in the grouping reagent followed by blotting with standard blotting paper (Drink Coaster Blotting, 280 gm⁻²) to remove any surplus of antibody solution from the thread. After drying under a fume hood for 10 min, treated threads were ready to be used for ABO and Rh blood typing. In this work, “thread A”, “thread B” and “thread D” are used as abbreviations for the three types of thread, treated with anti-A, anti-B and anti-D/Rh respectively.

7.4.2 Modification of Antibodies for Enhanced Detection

It was found that the addition of strongly water-soluble dyes to antibody solutions can significantly assist in the visual detection of the agglutination of RBCs. In this study, water-soluble dyes were added to the clear anti-D solution to achieve this enhancement to result interpretation. Ink solutions (cyan and magenta) for visual indication of successful separation were prepared by diluting commercial Canon ink jet inks (CLI Y-M-C-BK, PGBK (<http://www.canon.com.au>)) with Millipore filtered water. Diluted inks were then mixed with antibody solution in the ratio of 1:25 (V: V) ink to antibody solution. Thread was soaked in the coloured anti-D solutions and then dried under a fume hood. Abbreviations of “thread MD” and “thread CD” were adopted for threads treated with magenta and cyan modified anti-D solutions.

7.4.3 Blood Sample Tests Using the Thread-Based Platform

Blood samples (A+, B+ and O–) were sourced from donors of known blood type, with samples being drawn by a trained nurse, and stored in Vacutainer[®] test tubes containing lithium-heparin anticoagulant. All blood samples were stored at 4 °C, and used within 5 days of withdrawal. For the primary investigation of the feasibility of using antibody-treated thread as a blood typing system, three treated threads (thread A, B, D) were immobilised in folded polypropylene films with lodging slits to aid testing, and a micropipette (Eppendorf research[®] 0.1–2.5 µL) was used to dose a 1 µL blood sample onto each thread. Threads MD and CD were tested in a similar fashion to evaluate whether coloured anti-D enhanced the visibility of separation. For positive results showing separation of agglutinated RBCs and serum, the separation distance between the edge of RBCs and serum was measured using a Vernier calliper.

7.4.4 Confirmation of Donor Blood Type Using the Glass Slide Method

Donor blood types were confirmed using the conventional glass slide technique to provide a control for the thread-based platform. Testing procedure was provided by CSL, Australia. This established method was also used to confirm that the dyes added to anti-D solutions did not affect the results by inhibiting agglutination (in the positive

case where the blood contains the corresponding antigen) or by causing agglutination when none should occur (by mixing ink solution and blood with no antibody present).

7.5 RESULTS AND DISCUSSION

7.5.1 Separation of Agglutinated RBCs from Blood Serum on Thread

Identifying the agglutination of RBCs using porous media has a unique advantage: large and discrete particles in a suspension system undergo a phase separation from the continuous liquid phase in the capillary channels. As the whole-blood sample wicks through the inter-fibre gaps of the antibody treated threads, blood serum will dissolve the antibody molecules deposited on the surface of the fibres. Therefore, if RBC agglutination occurs as a result of a haemagglutination reaction it is expected to take place at the blood wicking front first. Haemagglutination reactions occur when antibodies (immunoglobulin molecules, IgG and IgM) bond to the specific binding sites on the antigens of adjacent RBCs [1]. The aggregation of the RBCs by the antibody molecules leads to the formation of significantly larger particles that cannot be stably suspended in the serum phase. As the sample wicks along the thread, the size of the agglutinated particles increases. Since the agglutinated RBCs form discrete particles, they cannot contribute to the capillary driving force required for the blood sample to continue wicking forward. Instead, the agglutinated RBC particles can only be carried by the serum to move forward. In this situation agglutinated particles will be gradually left behind from the serum wicking front. Furthermore, the agglutinated particles in the inter-fibre channels may act as a “filter” which permits serum to pass, but prevents other agglutinated RBC particles from passing. This causes the separation of the agglutinated RBCs from the serum phase. This reaction is visually identifiable by the appearance of a pale pink coloured band between the RBCs and dry antibody residue, as seen in Fig. 1(a, c, e, f). In the case where the deposited antibody does not react with the antigens of the RBCs, no separation is visually detectable (as seen for type O–blood in Fig. 1g–i).

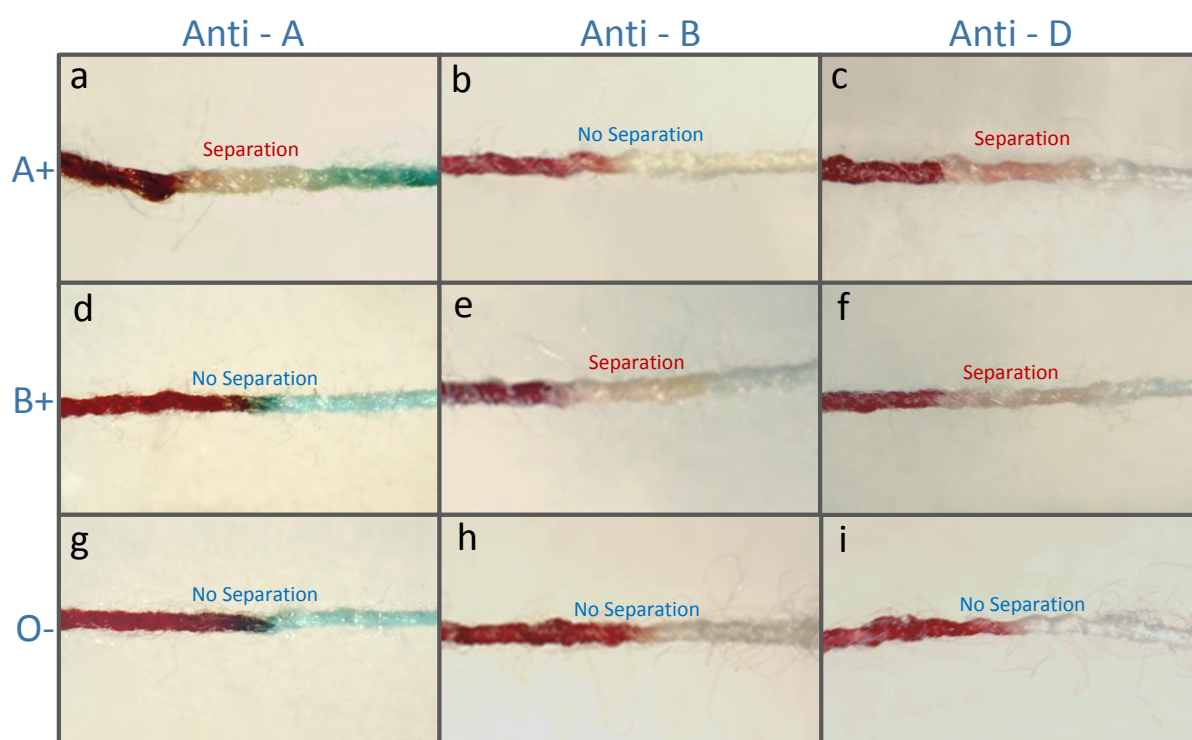


Fig.1 Proof of concept testing with samples of whole blood of type A+, B+ and O– on antibody-treated polyester threads. *Columns* show results on threads A, B and D from *left to right*, whilst *rows* show the results for the different blood types as labelled on the left

Figure 2 displays collected data quantifying the average length of separation distance for different types of antibody-treated thread. Although there is a small difference in separation distance between differing antibodies, a distance of approximately 3 mm was typical and easily visible by the human eye, being of similar length to a standard “stitch” found on a shirt cuff. Typically, results became easily visible within 1 min of sample dosing, making the test quite rapid compared to existing techniques.

Identifying a person’s ABO and Rh blood type requires three tests, two for the A and B antigens to determine ABO grouping, and a further test for the D antigen to determine Rh grouping. A results-matrix is shown in Table 1 which aids in the interpretation of results. Due to the serious consequences of blood transfusion incompatibility, it is recommended that a serum cross check be performed to ensure a safe transfusion, as is standard with all existing blood grouping methods.

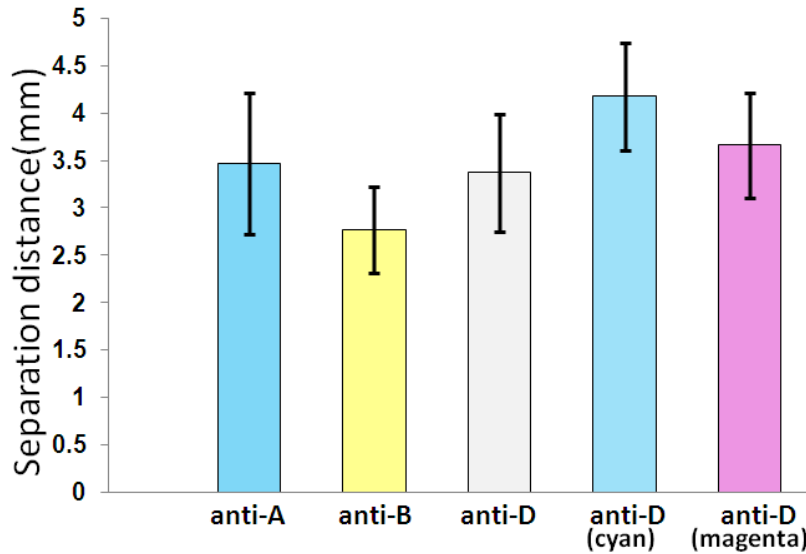


Fig.2 Graph of separation distance due to agglutination for positive reactions with the different antibody solutions: anti-A, anti-B and anti-D, including cyan and magenta ink jet ink modified anti-D solutions. *Error bars* represent one standard deviation from the arithmetic mean (ten repetitions)

Table 1 Results-matrix for aiding interpretation.

Anti - A	✓	✓	✓	✓	×	×	×	×
Anti - B	✓	✓	×	×	✓	✓	×	×
Anti - D	✓	×	✓	×	✓	×	✓	×
	AB+	AB-	A+	A-	B+	B-	O+	O-

[Ticks indicate a positive result (separation has occurred) whilst crosses indicate a negative result (no separation). The user simply identifies which column matches their result to find their blood type]

7.5.2 Effect of Adding Colouring Agents to Antibody Solutions

As the detection of separation is performed visually, it is more difficult to identify the separation of the blood components on thread B and D compared to thread A, due to the similar colour of the anti-B and anti-D solutions and the blood plasma on thread. The addition of dyes to the antibody solutions can assist interpretation of such results. The antibodies purchased are coloured for the purpose of identification, with anti-A being cyan coloured, anti-B, light yellow whilst anti-D/Rh is colourless. It is from this colouring that the enhancement effect was first noticed on thread, with positive results for thread A being much easier to interpret due to the presence of a light coloured band

formed between the agglutinated RBCs and the cyan antibody solution. This band is caused by the migration of the blood plasma.

The cyan and yellow dyes in the commercial anti-A and anti-B solutions are patent blue V and tartrazine, respectively. Patent blue V is an acid dye with two sulphonic groups; it dissociates in aqueous solutions and is negatively charged. This dye therefore has a weak affinity towards cellulose and polyester fibre surfaces, which also carry a weak negative charge in aqueous solutions [19]. Tartrazine is an azo dye with three dissociable acidic groups – two sulphonic and one carboxylic. Its negatively charged character in aqueous solutions indicates that it also has weak affinity towards cellulose and polyester. When these dyes are deposited onto thread together with antibodies, they can be readily dissolved and carried forward along the thread by the wicking blood sample. When anti-A binds the RBCs and causes their agglutination, the agglutinated RBCs will be left further and further behind the wicking front of the plasma. The dissolved dye molecules, in contrast to RBCs, will be carried by the plasma and remain in the wicking front of the plasma phase until it stops. The different migration behaviour of the agglutinated RBCs and these dyes allows a gap to develop between the RBCs and the dye as the plasma wicks along the antibody-treated thread. This gap results in the formation of a band of very light colour in contrast to the agglutinated RBCs and the colour of the dye in the plasma wicking front. The length of the band is comparable to the separation length previously mentioned for unmodified anti D (Fig. 2), but the contrasting colours make separation more easily visible, enhancing the ability of the user to detect agglutination. This effect is minimal for the Tartrazine doped anti-B due to its light yellow colouring which is similar to that of plasma. In situations where agglutination does not occur, this band does not develop.

In this study, diluted ink jet printing inks were used as colouring agents to modify antibody solutions. Despite detailed information about the dyes used in the ink formulations being unavailable, it is expected that the dyes must have excellent solubility in aqueous solutions (a basic requirement for ink-formulation dyes) [18]. Since all dyes for ink jet ink-formulation carry negative charges for reasons of safety [18] (positively charged dyes may possess mutagenic properties), ink jet ink dyes also have a poor affinity with the fibres used. Although this poor affinity has a well-known

and unwanted effect upon ink jet printing [18], it makes these ink solutions well suited for the doping of antibody solutions.

The enhanced visual identification effect can be achieved for threads B and D by adding ink to the antibody solution before thread treatment. Figure 3 illustrates the effect, showing threads (CD and MD) which have been treated with anti-D solution modified to include cyan and magenta inkjet inks. When compared to earlier results for thread D, one can see that the separation of plasma and RBCs is much clearer with the modified antibody. Figure 2 shows the mean separation distance between agglutinated RBCs and serum on threads CD and MD from ten repeated measurements to be 4.2 and 3.6 mm, respectively. It is expected that the use of suitable dyes to enhance visual identification of blood typing results is applicable for other porous substrates.

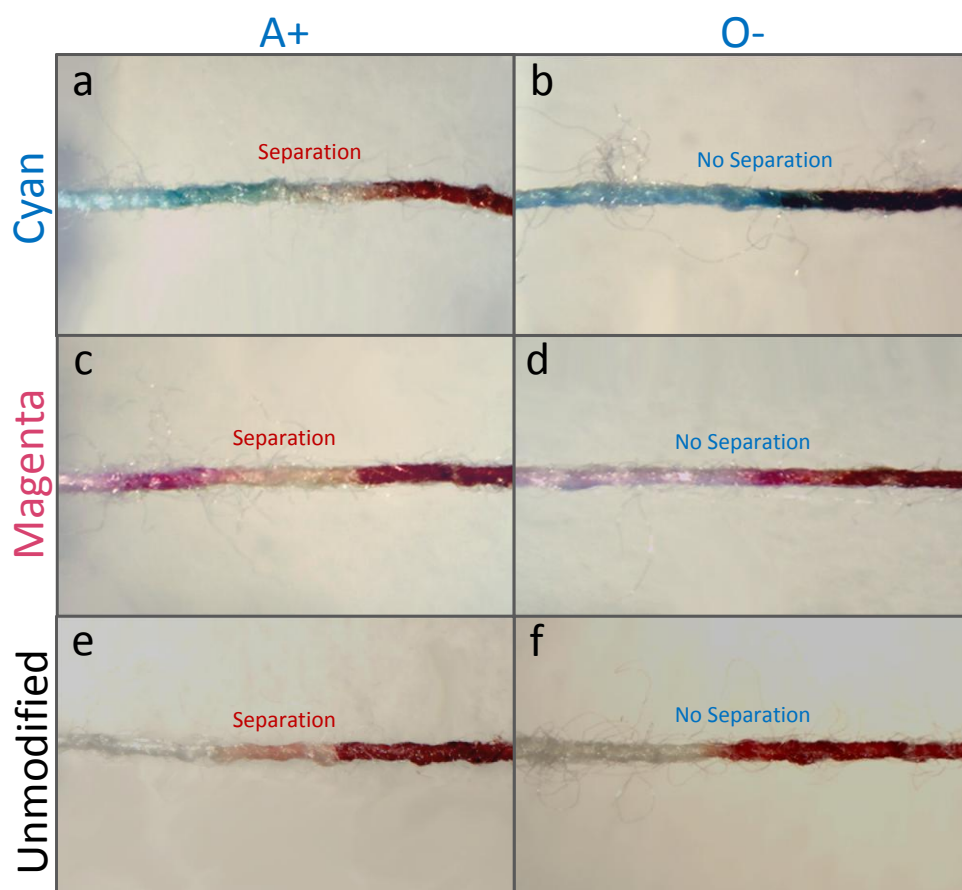


Fig.3 Blood testing on threads CD, MD and D (for comparison) (a) A+ sample applied to thread CD, a light band can be seen between the RBCs and cyan antibody solution indicating separation of plasma and RBCs; (b) O- sample applied to thread CD, no separation visible. (c) A+ sample applied to thread MD; a positive result is indicated by a light band; (d) O- sample applied to thread MD, no separation visible. (e) a positive result on unmodified thread D for comparison; (f) a negative result on unmodified thread D for comparison

7.5.3 Low-Cost Dosing Device

Blood samples of 1 μL were deposited by micropipette for the previously discussed study. However, no necessity exists for maintaining the sample volume at exactly 1 μL to achieve accurate results. Blood samples (A+) of different volume (0.6, 1, 2 and 4 μL) were deposited onto portions of thread A (six repetitions per volume) to validate this. All threads showed positive results, with separation of agglutinated RBCs and plasma occurring. This result indicates that the use of a simple and low-cost dosing device to deliver blood samples is feasible if sample volumes fall within the range of 0.6 to 4 μL . Various tools for dosing blood into the thread-based system were investigated, with cost, consistency of sample volume delivered and disposability/recyclability being of primary importance. These tools remove the requirement for more precise and expensive tools (e.g. micropipettes) which are not universally available in under-developed areas or for general users.

Among these tools, the use of a sewing needle eye for sample dosing was exemplary as it was (1) able to deliver relatively consistent whole-blood sample volumes (2) easily cleaned and sterilised using a flame (3) inexpensive to obtain (4) easily transported and extremely portable and (5) commonplace globally. The procedure simply involves dipping the needle eye into a drop of whole blood from a pricked finger. Blood is drawn into the needle eye and can then be transferred by pressing the needle eye to the thread, which has finer capillary channels and therefore stronger liquid absorption ability.

The repeatability of this technique was assessed by measuring whole-blood penetration length into untreated thread. If the thread is considered relatively uniform then penetration distance is proportional to delivered sample volume. Samples were dosed using a needle eye (of aperture dimensions 0.6 mm \times 4.1 mm) yielding an average penetration of 15.1 mm with a standard deviation (s.d.) of 1.1 mm from six repetitions. In comparison, the micropipette yielded 16.0 \pm 0.5 mm (average \pm s.d.) for 1 μL blood sample and 14.6 \pm 0.5 mm for 0.6 μL (see Fig. 4). This result suggests that although the needle eye method does not achieve consistency of the same degree as the expensive micropipette, it is still capable of delivering samples within the range necessary for the test. Although the metal needles used are recyclable and easily sanitised, a disposable

plastic device could be made which operates upon the same principal, albeit at lower cost.

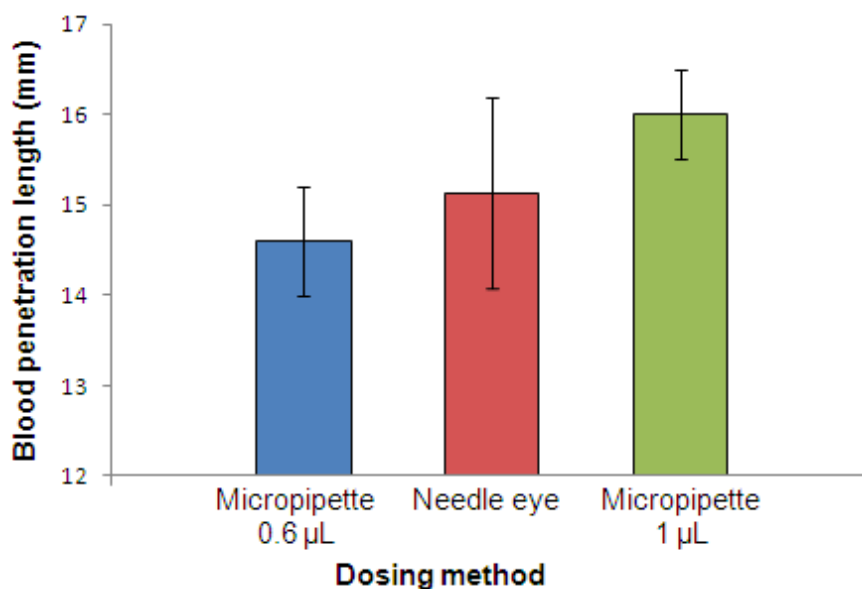


Fig.4 Graph of penetration length on thread for blood samples dosed with micropipette and needle eye techniques

7.5.4 Single-Step Prototype

In order to further simplify the testing process a single-step device was investigated which can perform the three different antibody tests simultaneously. By immobilising a sample of threads A, B and D in a small square of polymer film in a criss-cross arrangement, it is possible to determine a person's ABO and Rh blood groups with a single dose of whole-blood. A sample of 2 μL was proven to be sufficient for the test, and could easily be delivered using the needle eye technique previously described (albeit with a larger needle eye) to the centre of the device where the threads intersect. As the sample wicks along each thread, antibody is chromatographically eluted along the length of the threads and away from their intersection much quicker than between different threads; hence any migration of antibody between threads is greatly reduced preventing interference to correct grouping. Figure 5 displays one possible prototype; Fig. 5b is an enlarged image of the right half of the device, the separation achieved indicates the sample is of type A+. The prototype shown in Fig. 5a was constructed simply by wedging the threads in small slits in the polymer film, but it should be noted

that a sturdier device could easily be constructed by sewing or gluing the threads to the film. This device is simple to use and produce, compact and portable. A generous cost estimate of only \$0.009 USD per device suggests suitability for use in regions which are economically under-developed.

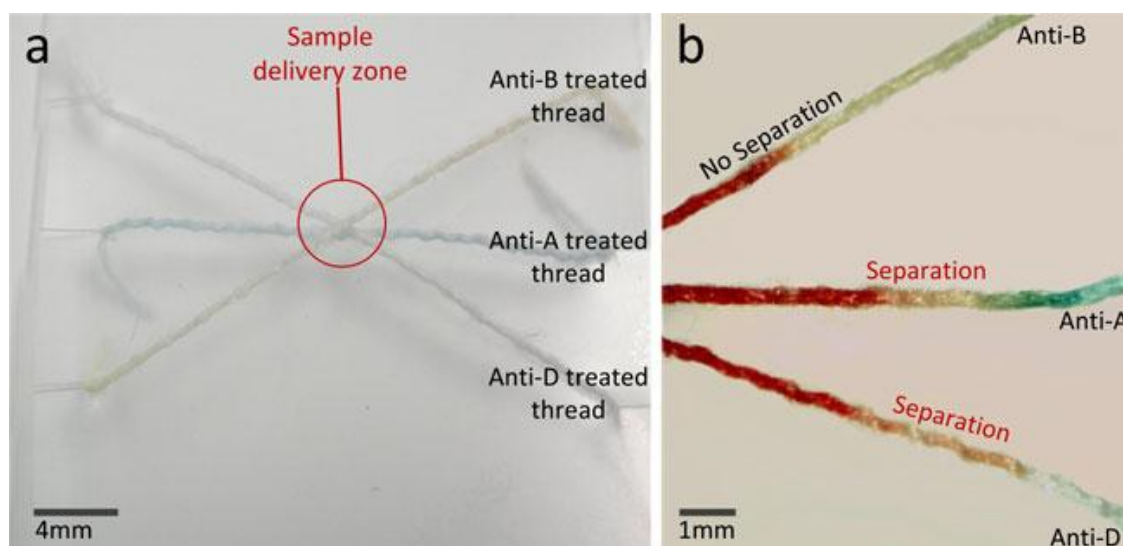


Fig.5 A single-step blood grouping test prototype for proof of concept, composed of thread A, B and D wedged in a square of polymer film and sharing an intersecting sample delivery zone **(a)** the unused device with sample delivery zone indicated within a *red circle* **(b)** an enlargement of the *right-hand side* of the device after whole blood has been introduced into the delivery zone in the centre via needle eye. The separation occurring on thread A and D indicates that the blood is of type A+

7.5.5 Expiry Study

A study was performed investigating the efficacy of the thread-based platform after a 4-week storage period. Two sets of samples were stored in micro-tubes wrapped in foil; one at 4 °C the other at ambient temperature. After storage testing gave good results for all antibody-treated thread types, suggesting that the devices could be transported and stored for a moderate period of time without degrading if sealed in airtight and light-proof packaging.

7.6 CONCLUSIONS

The results of this study show that the use of thread as a porous substrate for ABO and Rh blood typing is viable; and reduces the volume of blood required (to ~2 μL) compared to conventional methods. The technique is rapid, requires only whole blood and eliminates the need for the end user to either handle other testing reagents or perform sample dilutions. The addition of dye to the antibody solution chromatographically enhances the visibility of the separation of agglutinated RBCs and plasma, making it easier for the user to identify a positive reaction. The simple and recyclable (or disposable) metering device explored enhances the simplicity of the test and further reduces the need for complicated or expensive equipment.

Although only ABO and Rh/D blood groups were tested in this study, it is expected that the platform could easily be extended to identify other groups of interest that follow similar antibody/antigen interactions.

The thread-based blood grouping device prototyped is simple and robust enough to be employed by the end user without assistance. It is portable, disposable, can be easily preserved and maintains a low cost of construction, making it attractive for diagnostics and point of care testing especially in remote and developing regions.

7.7 ACKNOWLEDGEMENT

This work is supported by the Australian Research Council Grant (DP1094179). The authors would like to thank the kind blood donors; Mr. Scot Sharman, Mr. Henri Kröling and Mr. Junfei Tian whose donations have made this work possible as well as Ms. Lisa Collison of the Monash University Health Service for collecting blood donations. The authors also thank Dr. Lijing Wang of the School of Fashion and Textiles, RMIT University, for kindly providing thread and textile samples. The research scholarships of Monash University and the Department of Chemical Engineering are gratefully acknowledged.

7.8 REFERENCES

1. Daniels G, Bromilow I (2007) Essential guide to blood groups. Blackwell Publishing Ltd., Oxford, UK
2. Joshi et al VDJ (2006) Anatomy and physiology for nursing and health care. BI Publications,
3. Daniels G, Reid ME (2010) Transfusion 50 (2):281-289
4. Dean L (2005) Blood groups and red cell antigens. National Center for Biotechnology Information (NCBI), Bethesda, MD, US
5. Malomgré W, Neumeister B (2009) Anal Bioanal Chem 393 (5):1443-1451
6. Storry JR, Olsson ML, Reid ME (2007) Transfusion 47:73S-78S
7. Pramanik D (2010) Principles of physiology. Third edn. Academic Publishers, Kolkata
8. Estridge BH, Reynolds AP, Walters NJ (2000) Basic medical laboratory techniques. Delmar Cengage Learning, Albany, NY, USA
9. Llopis F, Carbonell-Uberos F, Montero MC, Bonanad S, Planelles MD, Plasencia I, Riols C, Planells T, Carrillo C, De Miguel A (1999) Vox Sang 77 (3):143-148
10. Llopis F, Carbonell-Uberos F, Planelles M, Montero M, Puig N, Atienza T, Alba E, Montoro J (1997) Vox Sang 72 (1):26-30
11. Spindler JH, Kl, ter H, Kerowgan M (2001) Transfusion 41:627-632
12. Langston MM, Procter JL, Cipolone KM, Stroncek DF (1999) Transfusion 39 (3):300-305
13. Lapierre Y, Rigal D, Adam J, Josef D, Meyer F, Greber S, Drot C (1990) Transfusion 30 (2305438):109-113
14. Plapp F, Rachel J, Sinor L (1986) Lancet 327 (8496):1465-1466
15. Giebel F, Picker SM, Gathof BS (2008) Transfus Med Hemoth 35 (1):33-36
16. Khan MS, Thouas G, Shen W, Whyte G, Garnier G (2010) Anal Chem 82 (10):4158-4164
17. Li X, Tian J, Shen W (2009) ACS Appl Mater Interfaces 2 (1):1-6
18. Gregory P (1991) High-technology applications of organic colorants. Plenum Publishing Corporation, New York, NY, USA
19. Scott WE (1996) Principles of wet end chemistry. TAPPI Press, Atlanta, GA, USA

This page is intentionally blank

Chapter 8: Flow Control Concepts for Thread-Based Microfluidic Devices

This page is intentionally blank

Monash University
Declaration for Thesis Chapter 8

Declaration by candidate

In the case of Chapter 8, the nature and extent of my contribution to the work was the following:

Nature of contribution	Extent of contribution (%)
Experimental design and conduct, paper writing	45

The following co-authors contributed to the work. Co-authors who are students at Monash University must also indicate the extent of their contribution in percentage terms:

Name	Nature of contribution	Extent of contribution (%) for student co-authors only
David Ballerini	Experimental design and conduct, paper writing	45
Wei Shen	Experimental design, corrected manuscript	Supervisor

Candidate's Signature

	Date 02/08/2011
---	---------------------------

Declaration by co-authors


The undersigned hereby certify that:

- (1) the above declaration correctly reflects the nature and extent of the candidate's contribution to this work, and the nature of the contribution of each of the co-authors.
- (2) they meet the criteria for authorship in that they have participated in the conception, execution, or interpretation, of at least that part of the publication in their field of expertise;
- (3) they take public responsibility for their part of the publication, except for the responsible author who accepts overall responsibility for the publication;
- (4) there are no other authors of the publication according to these criteria;
- (5) potential conflicts of interest have been disclosed to (a) granting bodies, (b) the editor or publisher of journals or other publications, and (c) the head of the responsible academic unit; and
- (6) the original data are stored at the following location(s) and will be held for at least five years from the date indicated below:

Location(s)

Australian Pulp and Paper Institute (APPI), Department of Chemical Engineering, Monash University, Clayton, VIC 3800, Australia

Signature 1

	Date 2/8/2011
Signature 2	4/11/2011

This page is intentionally blank

Flow Control Concepts for Thread-Based Microfluidic Devices

Xu Li¹, David R. Ballerini¹, Wei Shen*

*Australian Pulp and Paper Institute, Department of Chemical Engineering,
Monash University, Clayton Campus, PO Box 69M, Melbourne, Vic. 3800, Australia*

¹ *D. R. Ballerini and X. Li contributed equally as co-first authors*

**Corresponding Author: Email: [REDACTED]*

Tel: [REDACTED] Fax: [REDACTED]

8.1 ABSTRACT

The emerging concept of thread-based microfluidics has shown great promise for application to inexpensive disease detection and environmental monitoring. To allow the creation of more sophisticated and functional thread-based sensor designs, the ability to better control and understand the flow of fluids in the devices is required. To meet this end, various mechanisms for controlling the flow of reagents and samples in thread-based microfluidic devices are investigated in this study. A study of fluid penetration in single threads and in twined threads provides greater practical understanding of fluid velocity and ultimate penetration for the design of devices. “Switches” which control when or where flow can occur, or allow the mixing of multiple fluids, have been successfully prototyped from multifilament threads, plastic films and household adhesive. This advancement allows the fabrication of more functional sensory devices which can incorporate more complex detection chemistries, whilst maintaining low production cost and simplicity of construction.

8.2 INTRODUCTION

Developments in field-based diagnostic technologies have garnered great interest for their potential application to medical and environmental sensing, particularly in impoverished regions where specialist laboratory access is unavailable¹⁻⁵. A demand for simple, inexpensive diagnostic devices has been publicized by a significant amount of research interest being displayed in microfluidic paper-based analytical devices (μ PADs)⁶⁻¹⁶. A strong demand exists for sensors which can detect biomarkers of disease in blood or urine or environmental contaminants in waterways but are also inexpensive and disposable.

Recent studies from our group and others have further shown that multifilament threads are a viable and inexpensive alternative for the production of low-cost microfluidic devices¹⁷⁻¹⁹. These microfluidic thread-based analytical devices (μ TADs) can be produced by relatively unskilled persons quickly and cheaply using simple tools. These devices have shown great potential for use as medical and environmental sensors. Three dimensional μ TADs can also be easily fabricated due to the flexibility and strength of thread.

The flow of the fluid along thread is driven by capillarity without the need of external forces, following the analogous concept of fluid flow in μ PADs. Although the chemical nature of thread and paper is the same, many other material properties are significantly different. These differences include the length of the fibres, the inter-fibre bonding, as well as differences in the characteristic porous channel structures. Recent research has highlighted a necessity for characterizing fluid flow in low-cost microfluidic sensors, beginning with μ PADs in order to expand their diagnostic capabilities^{9, 13, 20-23}. It is therefore logical that the next step in the progression of thread-based sensors is an investigation of liquid transport and control on μ TADs to optimise device design and functionality.

In order to design μ TADs which have a reasonable result-reporting time under ambient conditions, it is necessary to characterize the fluid penetration along the thread to estimate the time required for sample fluid transportation. In particular, the ultimate

distance of the fluid penetration and the linear range (i.e., distance versus square root of time) of fluid penetration with no external intervention are important parameters to assist device design. Another desirable feature for μ TADs is the ability to control the fluid penetration in a thread by means of external intervention. This involves the design of mechanisms using thread and other low-cost materials to enable control of the timing or the direction of the fluid penetration in μ TADs. The research on these mechanisms, at its preliminary stage, allows the user to design devices which can control the flow of fluids and the timing of reactions in an on/off fashion by designing switches. The on/off switches can be used to develop microselectors to selectively direct flow to a desired location, or micromixers to mix multiple fluids together.

The SEM image in Figure 1 shows that a polyester thread is formed by many fibres; the gaps between fibres form capillary channels which enable the penetration of a wetting fluid. In μ TADs, threads must function as fluid transport channels and detection sites. It is possible to divide a piece of thread into different segments, making these segments fulfil different functions. Such division can be made by applying liquid adhesive or wax onto the thread to occupy the interfibre gaps in a thread, eliminating the capillary channels. In such a way, a piece of thread can be divided into a fluid transport channel and a detection site. Sample fluid in the transport channel cannot enter the detection site without external intervention (i.e., activation by a switch). In many applications, the detection zone requires treatment with indicators that should be localized within the detection zone¹⁷. Segmenting a piece of thread into a transporting channel and detection zone is therefore a necessary fabrication consideration. The sample transporting channel and the detection zone can only be connected when an on/off switch is activated and the two segments are bridged to enable sample flow across the blockage.

Other control mechanisms can further enhance the functions of μ TADs. For example, microselectors can be built into μ TADs which allow users to direct the samples or reagents they desire to a specific location given multiple options. Moreover, μ TADs can be used as controllable micromixers which are useful when a requirement to mix samples and reagents together at a specific time exists. Micro-TADs incorporating all of these new and simple mechanisms are inexpensive and easily fabricated without specialist equipment, and therefore suitable for use in underdeveloped areas, remote regions or potentially as point-of-care products globally. We expect that by

understanding fluid penetration distance and flow rate as well as exploiting a variety of mechanisms for flow control on μ TADs, we have provided a means to create more sophisticated and functional μ TADs, allowing their further development and expansion of their potential applications.

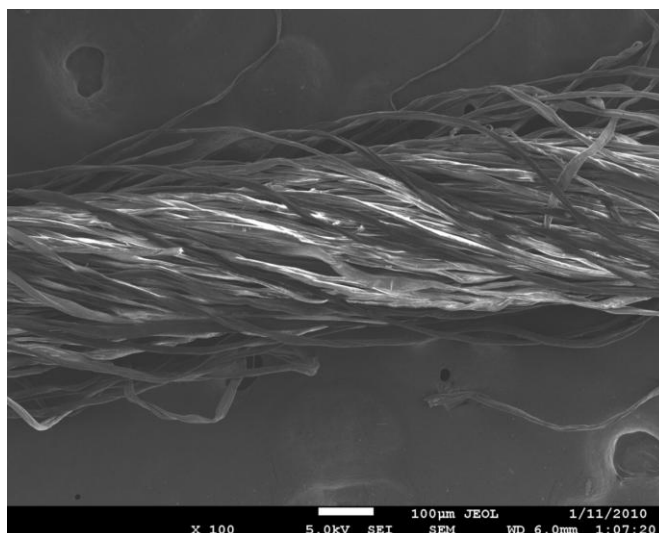


FIG. 1. A SEM image of a polyester thread, showing the individual fibres which comprise the overall structure. Capillary channels are formed by the gaps between fibres, enabling the thread to conduct flow.

8.3 EXPERIMENTAL SECTION

8.3.1 Threads and Textile

Polyester thread was kindly provided by the School of Fashion and Textiles, RMIT University, Melbourne, Australia. Untreated polyester thread can be wetted by aqueous solutions, albeit with a slow penetration rate. Plasma oxidation was used to improve fluid penetration along the polyester thread, since such treatment increases the fibre surface polarity by removing surface contamination by low surface energy materials and also oxidizing the fibre surface. Our previous study showed that cotton thread is also a suitable material for fabricating μ TADs¹⁷.

8.3.2 Measurement of Fluid Capillary Rise on Threads

Synthetic food dye solution (Queen Food Colouring, Pillar box red) was used to track the penetration of fluids within thread. The surface tension of the dye solution was measured by the capillary rise method²⁴ using a glass capillary (i.d.=0.9 mm) and cathetometer. The kinematic viscosity of the solution was measured with a U-tube viscometer (BS/U tube) using Millipore-purified water as the standard solution. Measurement was conducted in a water bath with temperature held at $30 \pm 0.1^\circ\text{C}$.

A schematic of the apparatus for measurement of fluid penetration on threads is shown in Figure 2. A laboratory jack was used to hoist the fluid reservoir containing the dye solution to the appropriate height; a ruler was used to measure the fluid penetration distance on thread. The surface tension and kinematic viscosity of the food dye solution in the reservoir (i.e., beaker) were 65.1 mN/m and 0.883 cSt, respectively (at 30°C). Fluid penetration was recorded using a camcorder (JVC GZ-MG530) and a snapshot program was used to record time-lapse images. Data acquisition began when threads were dipped into the penetration fluid, with penetration distance recorded for 15 min. Each measurement was repeated six times to give the average penetration distance and standard deviation data. Contact between polymer film and the threads was restricted by bending the film and fixing only the two ends of the thread to the film, which also served to eliminate the untwisting of the threads.

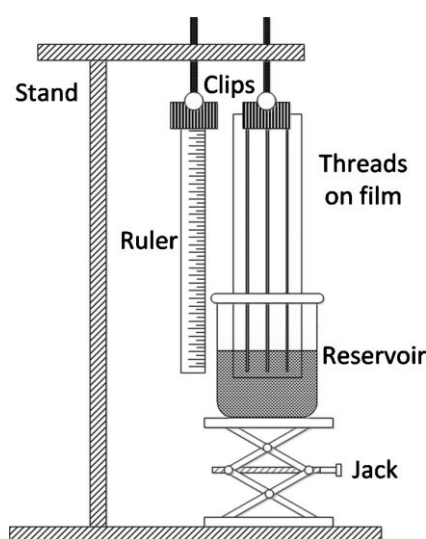


FIG. 2. A schematic of the apparatus employed for the fluid penetration measurements on thread. Threads were fixed to a polymer support film and wet with dye solutions from a fluid reservoir.

8.3.3 Functional Elements on μ TADs for Flow Control

In order to selectively inhibit fluid flow along the thread, inter-fibre channels were blocked using commercially available cyanoacrylate-based fast acting adhesive (Selleys Quick Fix Supa Glue). With the application of glue (0.5 μ L, 10 min cure under fume hood), no fluid penetration past the glue-sealed segment is possible, suggesting the complete blockage of the interfibre channels within the thread. Glue can also be employed to fix thread onto polymer film for support. These blocking and adhesive characteristics provide the opportunity to build functional elements into μ TADs for more sophisticated fluid flow control.

The first functional element demonstrated for thread-based microfluidics is the binary (on/off) fluid flow control switch. One simple concept is a “knot style” switch built with only thread itself and glue. The device was made by tying an overhand knot in a polyester thread, and then a small segment of the thread located on the loop is completely blocked to stop fluid flow using glue. Polymer film was also incorporated for some other on/off flow control designs, polypropylene polymer was selected as the film material due to its hydrophobic nature which eliminates any flow from occurring in the small gap between the thread and film surface.

The second functional element is the flow selector. The proof-of-concept design shown consists of two inlets (one thread was separated into two parts by blocking the middle part with glue) and one outlet (one thread was capable of being dragged along the first thread to select the flow from the two inlets).

The third functional element is the micromixer; it is composed of two binary switches which are activated at the same time, enabling a μ TAD to mix two solutions from two separate inlets into one outlet by twisting the inlet threads.

8.3.4 Testing Solutions

Millipore-purified water was used to prepare all aqueous samples required. Ink solutions (cyan, magenta and yellow) for visual indication of successful flow control

used during experiments were prepared by diluting commercial Canon ink jet inks (CLI Y-M-C-BK, PGBK (<http://www.canon.com.au>)) with water.

Sample solutions containing analytes of glucose and protein (bovine serum albumin, BSA, ~66 KDa) were prepared with the artificial urine. Sample solution 1 was a solution of 30 μ M BSA and 10 mM glucose in artificial urine²⁵. The glucose and protein indicator solutions were prepared and applied to the thread using micropipette²⁵. All reagents were purchased from Sigma-Aldrich.

Sample solutions for micromixer mixing effect tests were HCl (0.01 M, solution 2) and NaOH (0.01 M, solution 3) solutions which were introduced into two inlets of the micromixer and mixed within a common outlet after folding the μ TADs. The commercial pH paper (Advantec, whole range pH test paper) was used to test the pH values of the two inlets and one outlet to show the mixing effect by means of a neutralization reaction.

8.4 RESULTS AND DISCUSSION

8.4.1 Fluid Penetration along Threads

The fluid penetration distance along threads as a function of time was investigated experimentally by observation of the capillary rise of the testing fluid against gravity. In general modelling of fluid penetration within a porous media, the Washburn equation is used. In the present study, however, since the capillary rising of fluid in threads was investigated against gravity, the capillary driving force must be reconsidered to include gravity²⁶. The capillary rising model in the literature was adapted in this study to provide an understanding of fluid penetration along threads. Another factor under ambient conditions is fluid evaporation, which will also be discussed qualitatively below.

Wang et al.²⁶ studied the vertical capillary rise and made a derivation using Hagen-Poiseuille's law (Eq. (1)). In this derivation the authors assumed that the cross section

of the interfibre channels in a yarn has an equivalent radius r and the capillary driving force comprises two opposite pressures, the Laplace pressure and the hydraulic pressure due to gravity (Eq.(2)).

$$\frac{dh}{dt} = \frac{r^2 \Delta P}{8\eta h} \quad (1)$$

$$\Delta P = \frac{2\gamma \cos \theta}{r} - \rho g h \quad (2)$$

where h is the fluid penetration distance along the thread, γ , η and ρ are the fluid surface tension, viscosity and density, ΔP is the pressure that provides the fluid penetration driving force and g is the gravitational constant.

Since the helical nature of the interfibre channels (Figure 1) is not considered, this model will provide a qualitative trend-prediction of the capillary rise in a thread. The helical pathways of the channels have greater length than the actual length of the thread, therefore the fluid rising rate observed experimentally along the thread would be lower than the modelling prediction. Despite this, the qualitative understanding will still provide practical information of fluid penetration along a thread, which is useful for the design of μ TADs.

In the original Washburn derivation²⁷ horizontal capillaries were considered and the driving force comprised of only the Laplace pressure. By substituting the Laplace pressure into Eq. (1), the original form of the Washburn equation can be obtained (Eq.(3)):

$$\frac{dh}{dt} = \frac{\gamma \cos \theta}{4\eta h} = \frac{r^2}{8\eta h} \left(\frac{2\gamma \cos \theta}{r} \right) \quad (3)$$

Integrating equation (3) with the initial condition of $h = 0$ at $t = 0$ will yield the Washburn equation²⁷:

$$h = \sqrt{\frac{\gamma \cos \theta}{2\eta}} t \quad (4)$$

When the capillary height is plotted against square root of time, a straight line will be obtained.

However, when a vertical capillary is modelled, the gravitational force needs to be considered (Eq.(2)). The fluid penetration kinetics can be written as follows²⁷:

$$\frac{dh}{dt} = \frac{r^2}{8\eta h} \left(\frac{2\gamma \cos\theta}{r} - \rho g h \right) \quad (5)$$

Comparing equations (3) and (5), the capillary driving force (bracketed section) in the case of vertical capillary rise decreases as the height of capillary rise increases. Such a height-dependent loss of driving force will cause the plot of capillary rise height against the square root of time to deviate from the straight line of the horizontal capillary penetration model (Eq. (4)) at longer penetration time. This study provides the basic experimental data and understanding which will be used as general guidance for the design of functional elements.

Our experimental data of capillary rise height and the square root of time show a linear relation when the height is relatively small (Figure 3), but gradually deviates from this linear trend as the time of wetting exceeds ~1 min. Such fluid penetration behaviour is in an apparent agreement with the loss of capillary driving force (partially) due to gravity. It can be expected that this deviation from linearity would be delayed if threads were orientated horizontally.

Another factor that causes the loss of capillary force is fluid evaporation during the penetration process. This factor is not considered in the modelling above, but is likely to have a dominant effect over longer times, since fluid evaporation will become more and more substantial as the time and the area of fluid on the thread surface exposed to air increase. Fluid evaporation leaves less free fluid in the capillary channels between fibres, reducing the driving force for the fluid flow through fluid starvation. The complete halting of the fluid penetration front as the penetration distance reached 5.4 cm along a single thread is most likely due to the establishment of an equilibrium between fluid evaporation from the wetted thread surface and the capillary fluid uptake

from the reservoir. This conclusion is supported by a further observation that the equilibrium height of capillary rise in a single thread is higher if fluid evaporation is reduced by covering the thread with a film. The understanding of fluid penetration behaviour along a single thread enables a basic degree of prediction which can be used in the design of μ TADs.

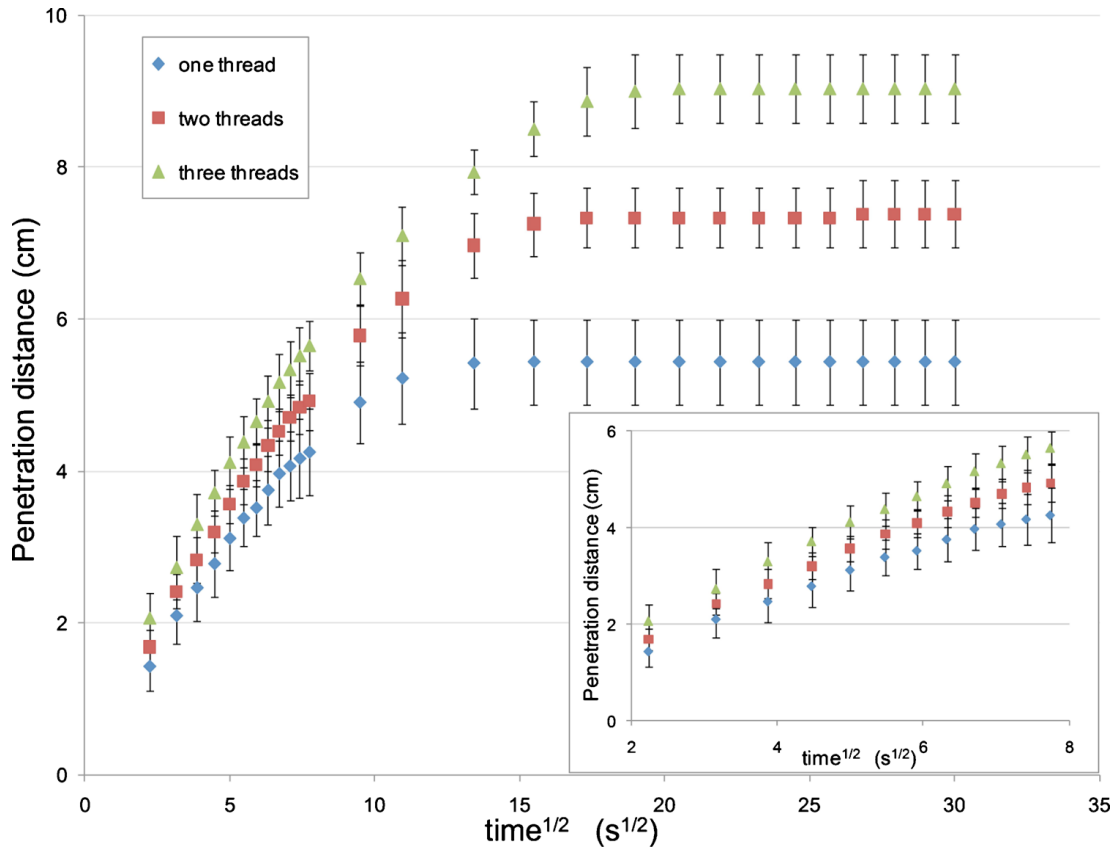


FIG. 3. A graph of penetration distance vs the square root of time for (i) a single thread, (ii) twisted pair, or (iii) twisted triple. The graph highlights a linear relationship between penetration distance and the square root of time over the first minute ($\sim 8 \sqrt{s}$), concordant with the Washburn equation. After this the curve flattens out and reaches an ultimate penetration distance due to the effects of evaporation and gravity.

The effect of twisting multiple threads together was investigated by comparing the fluid penetration on a single thread, double-twisted threads and triple-twisted threads (the twisting frequency is around 200 twists/m). The major geometric feature of the twisted threads is the generation of inter-thread gaps; these gaps are much larger than inter-fibre gaps in a thread. The shape of an inter-thread gap may be crudely viewed as

analogous to a “V-groove”. Rye et al.²⁸ modelled fluid flow in a V-groove driven by capillary force and found that fluid penetration rate in a V-groove driven by capillary force can be described by a pseudo Washburn relationship (i.e. penetration distance \propto square root of time). These authors also showed that fluid penetration rate in V-grooves is proportional to the cross sectional width of the groove, and is sensitive to the groove apex angle (the angle between the two walls of the V-groove). Our experimental data show that fluid penetration rates along double-twisted threads are greater than that of a single thread. The fluid shows even higher penetration rate along triple-twisted threads than double-twisted threads, since the former have more inter-thread gaps. These observations agree with the general trend of the V-groove model and this model can be used to provide a qualitative description of the twisted threads. Furthermore, a gravitational and fluid evaporation effects can also be seen from the penetration results for twisted threads. Since the inter-thread V-grooves increase fluid uptake from the reservoir, the equilibrium of the fluid uptake and fluid evaporation occurs at a higher capillary rise (Figure 3).

The experimental study of fluid penetration along threads mentioned above suggests that only moderate lengths are appropriate for building functional elements for control of fluid transport. Also, twisted threads can be used for the design of a fluid splitter or a mixer where a sufficient fluid supply needs to be provided to suffice two split flows and *vice versa*. Moreover, variation of fluid flow rate on μ TADs can be easily achieved by twisting threads together, useful knowledge for the design of devices.

8.4.2 Building Functional Elements on μ TADs for Controlled Fluid Transport

For traditional microfluidic devices, some useful features such as flow control microvalves and fluid micromixers, have been successfully built into devices for sophisticated fluid control. However, similar techniques are still unavailable for μ TADs. It is expected that achieving better control over flow connection/disconnection, fluid selection and mixing on μ TADs will accelerate the development of μ TADs and widen the applicability of thread-based microfluidics.

8.4.2.1 Binary Type (On/Off) Switches

The binary type switch works on the principle of using a blocking point to disable fluid transport between two segments of a piece of thread (off), but enable fluid transport when activated by by-passing the blocking point (on). As mentioned earlier, the isolation of the detection zone from the sample introduction channel is necessary for the device fabrication and function. Another desired feature in some analyses is to stop the back flow of the indicator from the detection zone to the channel after the sample delivery¹⁷. With the switch, this can be done by “turning off” the switch after the sample introduction. The advantage of using glue to form blocking points in thread over using reactive chemical hydrophobisation methods is that the blocking points can be formed over a short stretch of thread, and even withstand surfactant solutions with a depressed surface tension as the capillary channels have been effectively eliminated over the range of the blockage.

The simplest of the designs presented here uses a knot in a single piece of thread to create a basic on/off flow control mechanism, as shown in Figure 4a. Diluted inkjet magenta ink was used to examine the on/off flow along the knotted switch. An overhand knot with a draw loop²⁹ was tied loosely in a thread such that it could slide along the length of the thread. A section of the draw loop was then blocked against fluid flow using glue, and the knot slid and placed over this blocked region so that the switch was in the “off” position and the ink was unable to penetrate through this region (Figure 4a1). After sliding the knot away from the blocked region, the ink can flow across the knot and through the length of the thread (Figure 4a2), while the blocked region remains unwet by the fluid.

When polymer film is used as a supporting material for μ TADs design, on/off flow control can be easily achieved in a variety of ways. In this study, we demonstrated different mechanisms of on/off control in μ TADs. These mechanisms included folding the polymer film or removing a temporary obstruction such as a pull-tab.

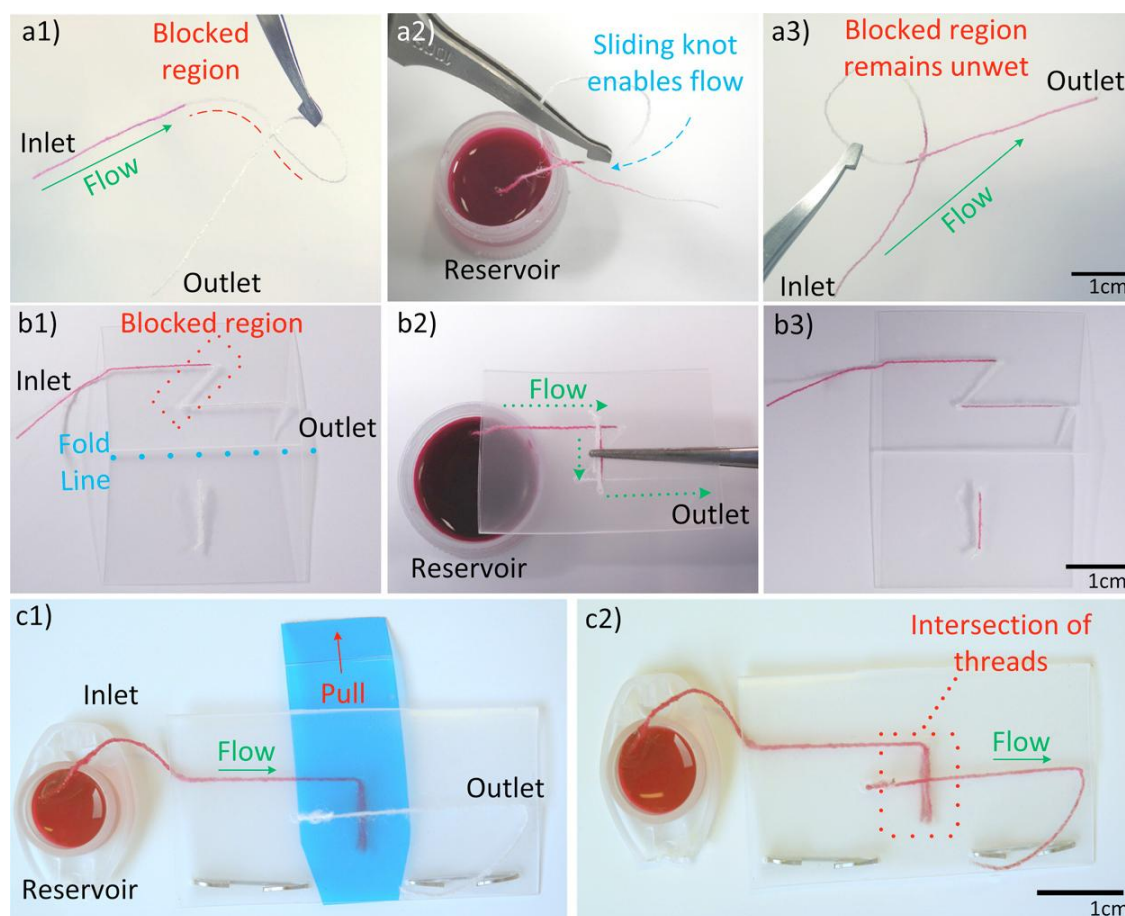


FIG. 4. (a) The simplest of the “on/off” flow control switches is comprised of a thread which incorporates a knot and a loop with an adhesive-blocked segment, sliding the knot over the blocked segment in the loop enables flow to occur along the length of the thread. (a1) The knot device with the inlet fully wet by ink solution, the blockage caused by the glue is indicated by the red dashed line. (a2) The partially wetted device with the inlet in an ink reservoir, after being actuated by sliding the knot past the blocked region. (a3) The device after being removed from the reservoir after conducting flow from inlet to outlet. (b) The folding style switch makes use of a polymer film support material to function. (b1) The fold type switch in the open position with the inlet wet by ink. The fold line and blocked region are labelled. (b2) The folded device allowing flow from an ink reservoir at its inlet. (b3) The fully wetted device after being used to transport fluid (device having been reopened). (C) Folding style switches can be modified to be pull-tab actuated. (c1) The pull-tab switch with inlet connected to an ink reservoir. (c2) The pull-tab switch with tab removed, allowing flow across the device.

A simple folding style switch is shown in Figure 4B. The device was constructed by folding polymer film into two smaller rectangles of equal area. On one side of the fold, a thread was stitched into the film running parallel with the crease line of the fold, but with a “z” shaped kink in the centre. The diagonal section of the “z” shape was then blocked using adhesive to prevent the flow. On the opposing side of the film, a small bridge was sewn which was perpendicular to the fold line and directly opposite the centre of the “z” shape. The device is activated by folding the film and bringing threads on opposing sides into contact with each other. The small thread section on the left acts as a bridge allowing flow to jump between different sections of the partially blocked thread on the right. Additionally, other porous materials such as textile and paper can be used to act as bridges to allow on/off flow control on thread.

In a pull-tab activated on/off flow control mechanism, a small removable section of polymer film (blue film in Figure 4C) was inserted into the device to form a barrier to flow between opposing threads sewn to the top and bottom film of the device. When the tab is removed by the user pulling upon it, threads on opposing sides of the device are brought into contact with each other and the switch is activated. An advantage of this actuation method is its ease of use, as it eliminates the need for users to hold the device folded shut, and minimizes user contact with the internals of the device. Should an application require the incorporation of hazardous reagents, designers could enclose them entirely within plastic films, reducing the risk of user contact.

An important future application of on-off switches will be to fabricate thread-based microreactors, which allow different reagents to be introduced into reaction zones simultaneously or separately in multistep reactions, or provide controllable reaction time for detection chemistries which require multiple steps, e. g. in blood and urine testing, an analyte may need to be converted into a more detectable form using an enzyme before final detection.

8.4.2.2 Microselectors for Flow Control

The two-way microselector device shown in Figure 5 allows a user to choose between samples or reagents (magenta and yellow inks as example solutions here) at two inlets and direct flow down a particular outlet channel at the time the user desires.

Alternatively the device can function in reverse, with a single sample or reagent directed to a desired outlet selected from 2 or more options. Such a device could be useful in complex systems which possess multiple reaction or detection sites, enabling users to selectively perform different types of analyses with the same device.

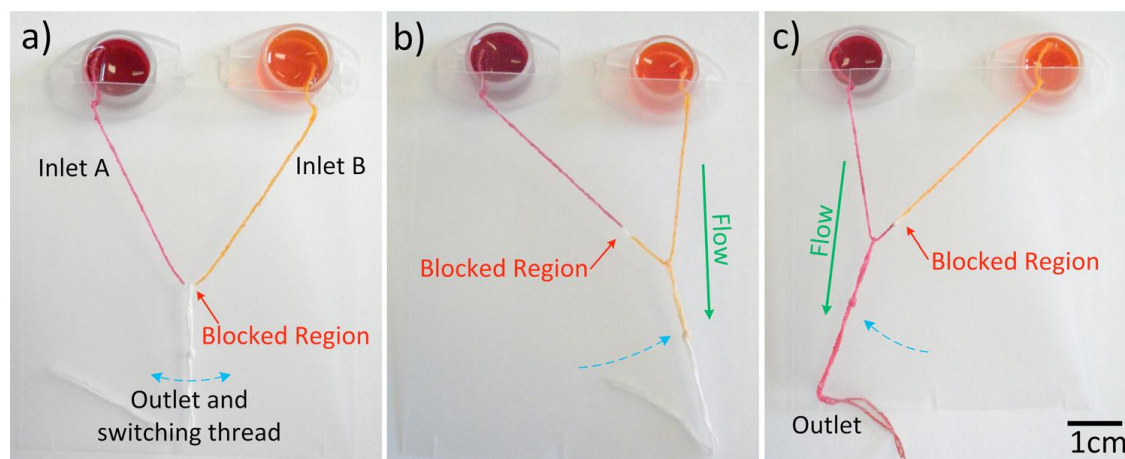


FIG. 5. A microselector, with two inlets and a single outlet, allows a user to select between which one of two samples they wish to transport. Ink solutions are used for visualisation of the concept. (a) The unused selector switch set in the off position. The blocked region is indicated, and the inlets are connected to ink solution reservoirs. (b) The selector switch after sliding to the right, allowing flow of the yellow ink to the outlet. (c) The selector switch after sliding left, allowing flow of magenta ink.

To illustrate the thread-based microselector applicability to bioassays, a sample solution containing both glucose and protein (sample solution 1) was used to show one possibility for directing sample flow into different outlet channels (Figure 6). The glucose and protein indicators (0.1 μL) were deposited onto the upper left and right threads (i.e., the left and right outlet channels) respectively. The indicators were then allowed to dry under ambient conditions for 15 min. The sample solution was introduced from the lower thread (i.e., the inlet channel). When the sample solution was selected to flow into the right outlet channel by moving the loop to the right, the color change of protein indicator from yellow to blue-green showed that the sample solution had arrived at the desired channel. The loop was then moved to the left to direct the sample flow into the left outlet channel, which was shown by the development of a yellowish brown colour caused by the glucose indicator present. The results showed

that the transport of multiple fluid flows can be controlled with the sequential delivery of fluids within μ TADs, thus extending the capabilities and performance of μ TADs while still at low manufacturing cost.

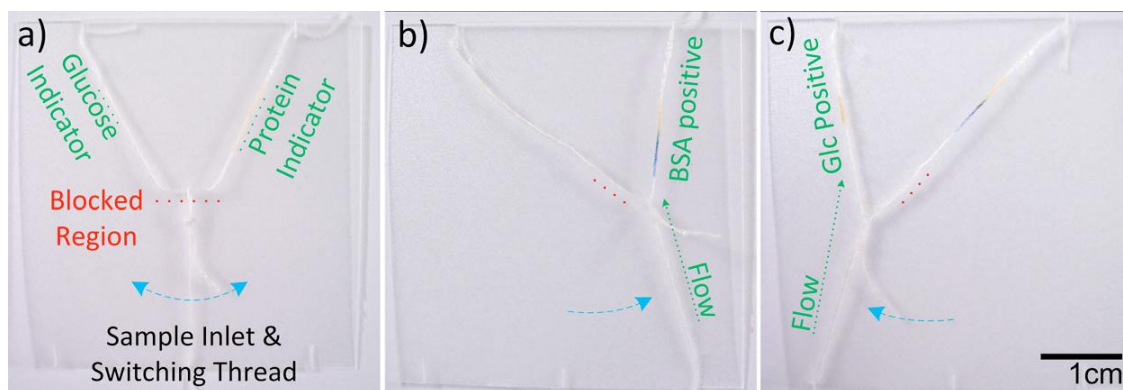


FIG. 6. The microselector allows a user to select between which analyte they wish to analyse. (a) The unused selector switch set in the off position. The blocked region is indicated by a red dashed line, and indicator locations are noted. (b) The selector switch allowing flow to the right, resulting in a colour change indicating the presence of protein. (c) The selector switch allowing flow to the left, the presence of glucose is indicated.

8.4.2.3 Micromixers

Mixing is an important feature in microfluidic devices, required for various chemical functions. The ability to mix reagents and samples gives a designer of μ TADs access to a suite of detection chemistries not available when using only “single step” functionality. This could include sensing systems where an analyte can only be detected after it has been chemically converted to a different form or instances where a colorimetric indicator compound requires a second reaction to produce its visual effect. The flexibility of thread makes it a suitable material for mixing fluids, simply by twisting threads together (i.e. coupling multiple inlets to a single outlet). High twist level maximizes the contact areas between threads (two or more) and therefore increases the diffusion interface and enables fluid mixing. The device shown in Figure 7 achieved the desired mixing of two coloured inks when the device was folded to bring the two wet thread sections in contact with a mixing zone. Thread-based micromixers can also be fabricated with “pull tab” activation mechanisms.

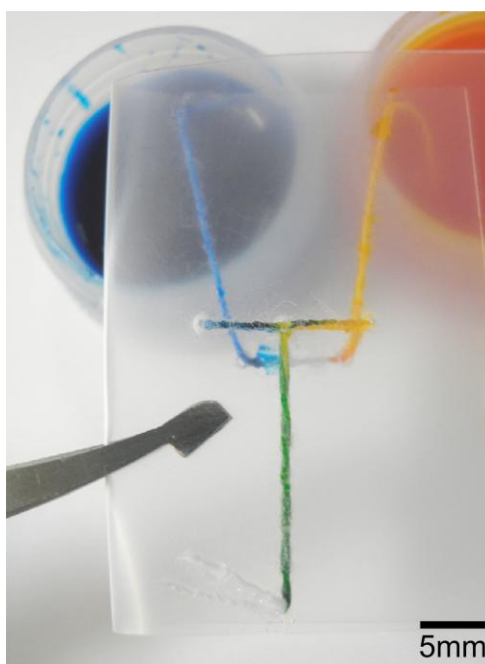


FIG. 7. A micromixer device used to mix two coloured inks together. The green colour produced illustrates the efficacy of the device.

The efficacy of the thread-based micromixer was shown by testing an acid-base neutralization reaction (Figure 8). HCl and NaOH solutions (solution 2 and 3) with equivalent molarity (0.01 M) were used as sample solutions in this test. The ends of two inlets of the μ TAD were immersed into two reservoirs filled with solution 2 and 3 respectively. After the solutions had fully wet the two inlets, the device was folded (by hand, tweezers or clippers) to direct two solutions into the twisted threads simultaneously for mixing (Figure 8b). Universal pH test paper was used to test the pH values for three points: (i) middle of inlet transporting solution 2, (ii) middle of inlet transporting solution 3, and (iii) 1 cm from the intersection of the twisted threads (outlet) (Figure 8c). The theoretical pH values of solution 2 and 3 are 2 and 12, respectively, which are concordant with the testing values of the first and second test points (at the inlets) from the 12 repeated measurements. For the third test point (i.e. the outlet or reaction product point), readings were recorded at 1 and 3 min after the device being folded. All measurements were repeated 12 times and the results showed that for this test point, the pH value varied between 6 and 8. Compared with the theoretically expected pH value of 7 for the reaction product, the measured values indicated that the

unneutralized reagent concentration is at most 10^{-6} M, (i.e. $\geq 99.99\%$ conversion), showing the intended neutralization and hence mixing capability of the thread-based micromixer.

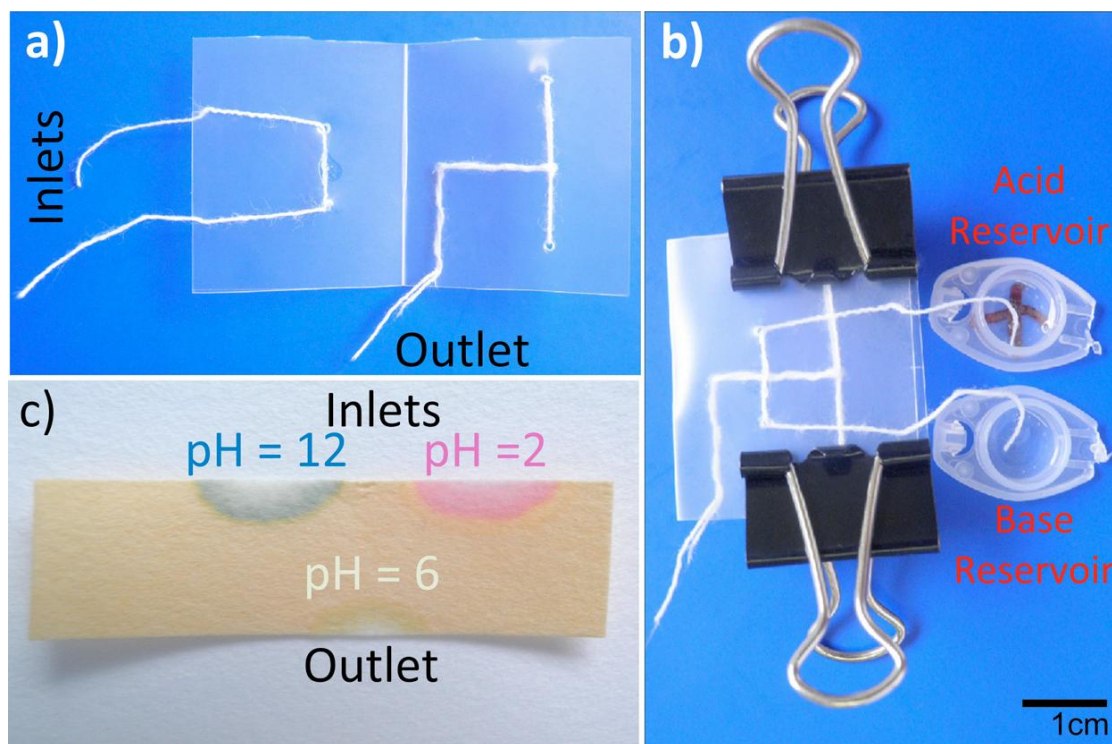


FIG. 8. A micromixer used to neutralise acid and base solutions to demonstrate the possibility of high quality mixing. (a) The unused mixer with inlets on the left and outlet on the lower right. (b) The device in use, with one acid inlet (0.01M HCl), one base inlet (0.01M NaOH), and reservoirs. The device is held shut by bulldog clips. (c) pH paper showing measurements from the inlets (pH 2 and 12) and outlet (pH 6), suggesting that 99.99% of the acid was neutralised by the base.

The concept of building thread-based functional elements (e.g. switches, microselectors and micromixers) into low-cost μ TADs is valuable for more advanced fluid flow control and provides possibilities for performing multi-step reactions on μ TADs without compromising the low fabrication cost and ease of use.

8.5 CONCLUSIONS

This study shows that the ability to control flow on thread allows for more sophisticated functions to be built into μ TADs. The measurement of fluid penetration distances and flow rates on thread is an important consideration for the design of μ TADs and understanding fluid transport in these devices. The capacity to mix and select between reagents enables the user to create devices with higher functionality, and facilitates the incorporation of more complex chemistries. The results of this work show that such devices can be made simply and cheaply by relatively unskilled persons using inexpensive materials.

Various mechanisms of flow control (i.e. functional elements) have been demonstrated in this study, with the most basic being the binary on/off style switch which is useful for controlling the timing of fluid introduction to reactors or other channels. More sophisticated designs included microselectors which give the user the ability to direct flow to one specific outlet given multiple choices. It was also shown that microselectors could function in reverse, with the user selecting one of several samples to be directed into a single outlet. Micromixers which could effectively mix multiple fluids together at a desired time were also developed, allowing the inclusion of multiple-step chemistries into thread-based microfluidics. For these functional elements of thread microfluidic systems, actuation can also be achieved by incorporating external elements (e.g., magnetic or electronic elements) to trigger folding or tab pulling and prolonged closure of the devices.

Concepts presented in this study have provided more flexibility for the design of μ TADs by giving designers new mechanisms for the control of fluid flows without compromising the distinctive properties of μ TADs, such as low cost and ease of use. It is hoped that this addition to knowledge in the field can be utilized to create more functional devices for the detection of disease, environmental contamination or other novel applications.

8.6 ACKNOWLEDGMENTS

The research scholarships of Monash University and the Department of Chemical Engineering are gratefully acknowledged. The authors thank Dr. L. Wang of the School of Fashion and Textiles, RMIT University, for kindly providing us with thread and textile samples, Ms. Y.H. Ngo for assistance in obtaining SEM images, and Mr. K. Wu for assistance in generating fluid penetration data.

8.7 REFERENCES

- 1 D. Mabey, R. W. Peeling, A. Ustianowski, M. D. Perkins, *Nat Rev Micro.* **2**, 231 (2004).
- 2 P. von Lode, *Clinical Biochemistry.* **38**, 591 (2005).
- 3 W. G. Lee, Y.-G. Kim, B. G. Chung, U. Demirci, A. Khademhosseini, *Advanced Drug Delivery Reviews.* **62**, 449 (2010).
- 4 P. Yager, G. J. Domingo, J. Gerdes, *Annual Review of Biomedical Engineering.* **10**, 107 (2008).
- 5 P. Yager, T. Edwards, E. Fu, K. Helton, K. Nelson, M. R. Tam, B. H. Weigl, *Nature.* **442**, 412 (2006).
- 6 E. M. Fenton, M. R. Mascarenas, G. P. López, S. S. Sibbett, *ACS Applied Materials & Interfaces.* **1**, 124 (2008).
- 7 X. Li, J. Tian, G. Garnier, W. Shen, *Colloids and Surfaces B: Biointerfaces.* **76**, 564 (2010).
- 8 A. W. Martinez, S. T. Phillips, G. M. Whitesides, E. Carrilho, *Analytical chemistry.* **82**, 3 (2009).
- 9 X. Li, J. Tian, T. Nguyen, W. Shen, *Analytical chemistry.* **80**, 9131 (2008).
- 10 A. Qi, L. Yeo, J. Friend, J. Ho, *Lab on a Chip.* **10**, 470 (2010).
- 11 Y. Lu, W. Shi, L. Jiang, J. Qin, B. Lin, *ELECTROPHORESIS.* **30**, 1497 (2009).
- 12 K. Abe, K. Suzuki, D. Citterio, *Analytical chemistry.* **80**, 6928 (2008).
- 13 H. Noh, S. T. Phillips, *Analytical chemistry.* **82**, 4181 (2010).
- 14 R. Pelton, *TrAC Trends in Analytical Chemistry.* **28**, 925 (2009).
- 15 M. S. Khan, G. Thouas, W. Shen, G. Whyte, G. Garnier, *Analytical chemistry.* **82**, 4158 (2010).
- 16 Andres W. Martinez, Scott T. Phillips, Manish J. Butte, George M. Whitesides, *Angewandte Chemie International Edition.* **46**, 1318 (2007).
- 17 X. Li, J. Tian, W. Shen, *ACS Applied Materials & Interfaces.* **2**, 1 (2009).
- 18 R. Safavieh, M. Mirzaei, M. A. Qasaimeh, D. Juncker, *Proceedings of MicroTAS 2009, The thirteenth International Conference on Miniaturized Systems for Chemistry and Life Sciences*, Jeju, South Korea November 1st -5th, 2009 (The Chemical and Biological Microsystems Society, 2009).

- 19 M. Reches, K. A. Mirica, R. Dasgupta, M. D. Dickey, M. J. Butte, G. M. Whitesides, *ACS Applied Materials & Interfaces*. **2**, 1722 (2010).
- 20 J. L. Osborn, B. Lutz, E. Fu, P. Kauffman, D. Y. Stevens, P. Yager, *Lab on a Chip*. **10**, 2659 (2010).
- 21 E. Fu, S. Ramsey, P. Kauffman, B. Lutz, P. Yager, *Microfluidics and Nanofluidics*. **10**, 29 (2011).
- 22 E. Fu, B. Lutz, P. Kauffman, P. Yager, *Lab on a Chip*. **10**, 918 (2010).
- 23 E. Fu, P. Kauffman, B. Lutz, P. Yager, *Sensors and Actuators B: Chemical*. **149**, 325 (2010).
- 24 D. J. Shaw, *Introduction to Colloid and Surface Chemistry* (Butterworth-Heinemann, Ann Arbor, 1992).
- 25 A. W. Martinez, S. T. Phillips, G. M. Whitesides, *Proceedings of the National Academy of Sciences*. **105**, 19606 (2008).
- 26 N. Wang, A. Zha, J. Wang, *Fibers and Polymers*. **9**, 97 (2008).
- 27 E. W. Washburn, *Physical Review*. **17**, 273 (1921).
- 28 R. R. Rye, F. G. Yost, J. A. Mann, *Langmuir*. **12**, 4625 (1996).
- 29 G. Budworth, *Essential knots & basic ropework* (Lorenz Books, New York City, 2000).



Chapter 9: Conclusions and Future Work

CONCLUSIONS AND FUTURE WORK

This thesis reported a series of major developments in a new and rising diagnostic platform technology –paper-based microfluidic diagnostics. Work published from this research encompasses novel fabrication methods of microfluidic paper-based analytical devices (μ PADs), new concepts for building microfluidic control elements in μ PADs, and self-calibrated semi-quantitative and quantitative analytical methods. These innovations have enriched this rapidly expanding platform and contributed to the breadth of the fabrication and application prospects of paper-based microfluidic diagnostics.

A distinctive point of difference of the μ PADs developed in this research is that they are fabricated using traditional paper hydrophobization (or sizing) chemistry and printing and surface treatment techniques. Fabrication methods reported in this thesis significantly reduced the reliance on high-capital equipment in the early days of the development of this platform.

At the time when the articles in this thesis were published, they addressed serious problems of existing μ PADs such as the poor bending resistance of devices, and significantly simplified fabrication processes. The concept of using the self-calibration approach in μ PADs proposed in this thesis allowed μ PADs to have quantitative potential.

Another significant achievement of this thesis is that it realized certain weaknesses of paper substrates and started to explore other low-cost materials and systems. The major weaknesses of paper-based microfluidic systems are the complexity required to make 3D μ PADs, and the sample loss through the chromatographic effect during liquid transportation in paper-based microfluidic channels. This thesis has therefore explored the use of thread for low-cost diagnostics.

Thread, as a flexible, versatile and low-cost material, has been used to fabricate 3D microfluidics without the need of building physical or chemical barriers to control liquid flow. The fabrication of thread-based analytical devices (μ TADs) requires only

sewing needles or household sewing machines, which are commonly used and affordable even in under-developed regions. Thread-based microfluidics is another platform for low-cost diagnostics.

The real-life diagnostic potential of μ TADs is demonstrated through the blood group analysis studies. It has been discovered that thread has a major advantage over paper in that thread requires a far lower amount of sample to make an analysis. Acquiring blood samples from humans is a culturally sensitive issue, but finger pricking seems to be an acceptable practice by many cultures. Blood grouping can be performed using μ TADs with finger pricking.

The use of thread or other cheap materials for fabricating microfluidic devices will greatly enrich the research and applications of low-cost diagnostics, laying the ground for future research as a direction.

The μ PADs and μ TADs reported in this thesis not only overcome some drawbacks of conventional microfluidic devices, but also extend bioassays from simple 1D lateral flow systems which are used in paper strip tests to more complex systems. With these novel devices, 1) multiple biomarkers can be simultaneously detected; 2) biomarkers can be quantitatively and semiquantitatively monitored; 3) antibody-antigen reaction can be conducted for diagnostic analyses. Using paper and/or thread as the substrate ensures the devices can be operated without external pumps or forces. Downsizing the reaction zones and fluidic channels minimizes the consumption of precious reagents and limited samples. Therefore, these devices provide a new microfluidic platform with potential applications in POC diagnostics, such as disease screening and healthcare monitoring. This disruptive concept is expected to extensively benefit people with improved healthcare, especially those living in the developing world where they cannot afford expensive diagnostic technologies.

It should be noted that some limitations on sensitivity or selectivity should be accepted in POC testing when using μ PADs and μ TADs for rapid diagnosis. MicroPADs and/or μ TADs should be considered as a valuable alternative rather than as a competitor to precise lab-based analytical devices and methodologies. In fact, using μ PADs and μ TADs for rapid screening a large number of samples may speed up proper decision-

making by the clinician, while conventional lab-based diagnostic techniques can be used subsequently for the better characterization of analytes.

MicroPADs and μ TADs have great potential to be used for and adapted to a number of assays. This has been shown by a multitude of studies reported in this thesis and by other research groups. Currently the most popular trend is using μ PADs and μ TADs as low-cost POC diagnostic devices. Nevertheless, these low-cost devices will open up the possibility of a plethora of analytical tests such as the detection of environmental pollutants and foodborne pathogens. These tests are usually expensive to conduct in the developing world by using conventional microfluidic devices.

This thesis also presented promising ways of making traditional engineering industries accommodate high-tech industries. Researchers should operate across the boundaries of traditional and high-tech industry sectors, and combine existing cheap materials and easy fabrication technologies with the scientific innovation. The fabrication methods (especially for μ TADs) and basic materials proposed in this thesis are easily accessed by developing countries. Therefore, these devices can even be fabricated in developing countries. This is a great advantage since developing countries also play an increasingly important role in manufacturing health products to meet global healthcare requirements.

Future work in research and development may need to address the following:

- a) Further the innovation in device fabrication concepts and techniques using paper and/or thread. Further the innovation in device detection mechanisms and device applications.
- b) Fully explore the strength of papermaking and printing technologies; increase the liquid transport and biochemical detection capabilities of μ PADs through applying the state-of-art paper sheet formation know-how and building new liquid transport control feature.
- c) Further understand the differences in pore structures between thread and paper. Take full advantages of thread in liquid transport in order to fabricate μ TADs which can conduct certain analyses that cannot be efficiently performed by μ PADs.

- d) Identify the weaknesses of μ PADs and μ TADs through their applications and innovate using other low-cost materials for rapid diagnosis and environmental sensing.

People living in developing countries or remote regions cannot be helped unless academic research, publications, and patents are turned into tangible products or improved practices and policies. Other future work will be to commercialize these low-cost microfluidic devices. Although the potential of mass-production of μ PADs and μ TADs have been illustrated, many obstacles will still arise when attempting to go further. The successful realization of a technology requires the advances in fundamental and engineering sciences and the integration of multiple building blocks of technologies and expertise. Although there is still a long way to go for practically applying μ PADs and μ TADs in the developing world, these devices are believed to eventually become one of the strongest candidates for the real world.

This page is intentionally blank



Appendix I: Papers Included in Each Chapter in Their Published Format

This page is intentionally blank

Article

Paper-Based Microfluidic Devices by Plasma Treatment

Xu Li, Junfei Tian, Thanh Nguyen, and Wei Shen

Anal. Chem., **2008**, 80 (23), 9131-9134 • Publication Date (Web): 01 November 2008

Downloaded from <http://pubs.acs.org> on December 1, 2008

More About This Article

Additional resources and features associated with this article are available within the HTML version:

- Supporting Information
- Access to high resolution figures
- Links to articles and content related to this article
- Copyright permission to reproduce figures and/or text from this article

[View the Full Text HTML](#)



ACS Publications
High quality. High impact.

Analytical Chemistry is published by the American Chemical Society, 1155
Sixteenth Street N.W., Washington, DC 20036

Paper-Based Microfluidic Devices by Plasma Treatment

Xu Li, Junfei Tian, Thanh Nguyen, and Wei Shen*

Australian Pulp and Paper Institute, Department of Chemical Engineering, Monash University, Wellington Road, Clayton, Victoria 3800, Australia

Paper-based microfluidic patterns have been demonstrated in recent literature to have a significant potential in developing low-cost analytical devices for telemedicine and general health monitoring. This study reports a new method for making microfluidic patterns on a paper surface using plasma treatment. Paper was first hydrophobized and then treated using plasma in conjunction with a mask. This formed well defined hydrophilic channels on the paper. Paper-based microfluidic systems produced in this way retained the flexibility of paper and a variety of patterns could be formed. A major advantage of this system is that simple functional elements such as switches and filters can be built into the patterns. Examples of these elements are given in this study.

This article reports on a novel method of creating patterns in paper to control the transport of liquid for pathological testing and environmental monitoring. Nonwoven fibrous materials such as paper have very good potential as low-cost base materials for diagnostic devices for such applications. Cellulose-based papers have been used as chromatographic substrates since 1850.^{1,2} A number of testing devices, such as paper-based indicators³ and “dip stick” test assays are made of paper. Recently, Martinez et al.^{4–6} used paper as a base material to create barrier patterns with photolithographic techniques. The photoresist patterns they produced guide the capillary penetration of liquids and, with the appropriate indicators, can detect chemical components in a liquid sample. This type of paper-based detector, when used with modern communication tools such as camera phones, can provide powerful real-time and off-site diagnostic devices for telemedicine with great potential to be developed into a low-cost health monitoring system.⁵ The drawback of conventional photoresist

is that it is much less flexible than paper, and the device can be easily damaged by bending and folding.⁷

More recently, Bruzewicz et al.⁷ used a modified plotter to create a barrier pattern by printing polydimethylsiloxane (PDMS) onto paper. When PDMS penetrated into paper, it formed a barrier pattern and could be used to control the penetration of liquid in channels defined by the barrier pattern. Since PDMS is an elastomer, it is more flexible than conventional photoresist and is less susceptible to mechanical damage. However, because of the low surface tension of the solvent used, the PDMS solution penetrates into paper rather easily. Since paper is not a uniform porous material, the penetration of PDMS cannot be well controlled, resulting in the wall of the barrier pattern not being straight.

The novel method of the present study enables patterns to be created on paper surfaces without affecting their flexibility or surface topography. The major advantage of this novel method over previously reported paper-based microfluidic devices is that it allows not only sample testing but also building of simple functional components such as control switches, microfilters, and microreactors, which are important elements for multiple-step chemical tests. Several examples of these functional elements are presented in this work.

EXPERIMENTAL SECTION

Alkyl ketene dimer (AKD) (Wax 88 konz, BASF) was used as the cellulose hydrophobization agent. Analytical grade *n*-heptane (Aldrich) was used as the solvent for AKD. Whatman filter paper was selected as the paper substrate. MilliQ water was used to prepare all liquid samples required for testing the performance of the device.

The filter paper was hydrophobized using an AKD–heptane solution (0.6 g/L). The filter paper samples were dipped in this solution and immediately removed and placed in a fume cupboard to allow evaporation of the heptane. The filter paper samples were then heated in an oven at 100 °C for 45 min to cure the AKD. The treated filter paper samples are strongly hydrophobic and have contact angles of typically 110–125° with water.⁹ Therefore, water shows no penetration into the paper hydrophobized with AKD.

* Corresponding author. E-mail: wei.shen@eng.monash.edu.au. Phone: +61 3 99053447. Fax: +61 3 99053413.

- (1) Stock, R.; Rice, C. B. F. *Chromatographic Methods*, 3rd ed.; John Wiley & Sons: New York, 1974; p 106.
- (2) Atkins, P.; Jones, L. *Chemistry-Molecules, Matter, and Change*, 3rd ed.; W.H. Freeman & Company: New York, 1997; p 26.
- (3) Umland, J. B. *General Chemistry*; West Publishing Company: St. Paul, MN, 1993; p 592.
- (4) Martinez, A. W.; Phillips, S. T.; Buttle, M. J.; Whitesides, G. M. *Angew. Chem., Int. Ed.* **2007**, *46*, 1318–1320.
- (5) Martinez, A. W.; Phillips, S. T.; Carrilho, E.; Thomas, S. W., III; Sindi, H.; Whitesides, G. M. *Anal. Chem.* **2008**, *80*, 3699–3707.
- (6) Martinez, A. W.; Phillips, S. T.; Wiley, B. J.; Gupta, M. J.; Whitesides, G. M. *Lab Chip* **2008**, DOI: 10.1039/b811135a.

(7) Bruzewicz, D. A.; Reches, M.; Whitesides, G. M. *Anal. Chem.* **2008**, *80*, 3387–3392.

(8) Shen, W.; Tian, J.; Li, X.; Garnier, G. Australian Provisional Patent No. 2008903553, July 11, 2008.

(9) Shen, W.; Filonanko, Y.; Truong, Y.; Parker, I. H.; Brack, N.; Pigram, P.; Liesegang, J. *Colloids Surf., A* **2000**, *173*, 117–126.

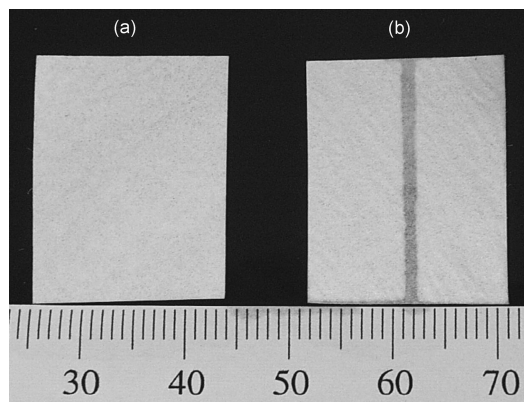


Figure 1. Water penetration control of a plasma treated microfluidic channel using hydrophobized filter paper. (a) A hydrophobized filter paper sample immediately after the treatment and (b) the treated sample was exposed to water through the lower edge.

Hydrophilic patterns were formed on paper samples using plasma treatment. The paper samples were sandwiched between metal masks having the desired patterns and then placed into a vacuum plasma reactor (K1050X plasma asher (Quorum Emitech, U.K.)) for 15 sec at the intensity of 15 W. Metal masks were made by mechanically cutting patterns through stainless steel sheets. Four screws were used to secure the alignments of the masks. The vacuum level for the treatment was 6×10^{-1} mbar. The plasma treatment left no visible mark on the samples, which retained its original flexibility. The plasma treated areas were strongly wettable by water or aqueous solutions and allowed the transport of aqueous solutions along and within the plasma treated channels via capillary penetration.⁸

A color change reaction for the evaluation of enzyme activity was used to test the device. Alkaline phosphatase enzyme solution was prepared using alkaline phosphatase (lyophilized powder, from bovine intestinal mucosa, 10–30 DEA units/mg of solid) from Sigma-Aldrich. Phosphatase solution (1 mg/mL) was prepared in the buffer solution (pH = 9.8) which contains 1.0 M diethanolamine ($\geq 98\%$, Sigma Aldrich) and 0.5 mM $\text{MgCl}_2 \cdot 6\text{H}_2\text{O}$ ($\geq 99\%$, Sigma-Aldrich). The phosphatase enzyme solution was divided into two parts; one part was heated at $>70^\circ\text{C}$ for 10 min to purposely deactivate the enzyme. A BCIP/NBT substrate system (Sigma-Aldrich) was used with the phosphatase enzyme to indicate the activity of the enzyme via color change. A phenolphthalein–ethanol solution was used as the color indicator for testing the performance of a paper-based microfluidic reactor. It was prepared using phenolphthalein (BDH) and ethanol (AR, BDH).

RESULTS AND DISCUSSION

Plasma Formed Patterns. Parts a and b of Figure 1 show a filter paper sample immediately after treatment and after being exposed to water. Water penetration demonstrated that the plasma treated channel has well-defined borders; the width of the channel can be reasonably well controlled. The channel in Figure 1b was made using a 1 mm wide mask, and a channel <1.5 mm in width was uniformly penetrated by water.

Hot electrons and other energetic particles generated in vacuum plasma have long mean free paths. Overetching of the substrate under a mask is a known problem for plasma treatment,

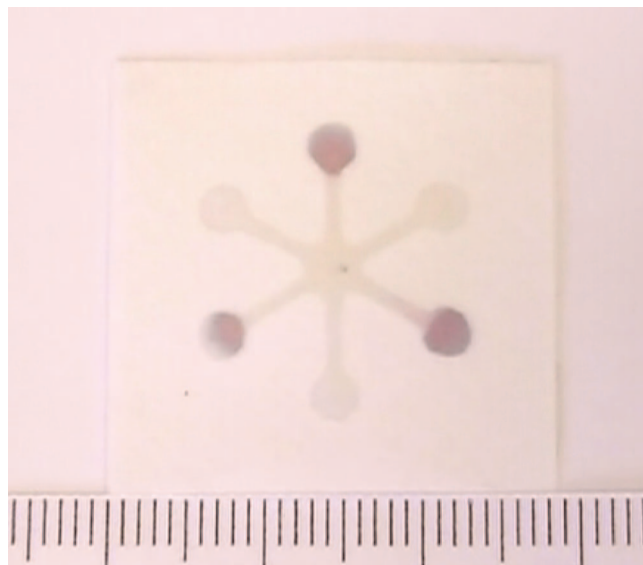


Figure 2. The performance of a paper-based microfluidic pattern fabricated by plasma treatment. Three active and three deactivated enzyme samples were introduced into detection ports of a six-channel pattern in alternation. A few drops of liquid substrate (BCIP/NBT) were introduced from the center port. Liquid substrate penetrated into the detection ports, revealing the activity of the enzyme samples.

causing the treated pattern to be slightly bigger than the mask. However, overetching could be controlled by optimizing the treatment intensity and time. When the treatment intensity and time were fixed, the channel width was found very reproducible.

Design of Sample Dosing and Detection Sites on Paper-Based Microfluidic Devices. An important application of paper-based microfluidic devices is to analyze chemical components in a liquid sample by means of color indicators.^{4–7} The research group in Harvard University was the first to explore this application.^{4–7} In their approaches, the concept of a capillary channel barrier was used to confine the liquid penetration path from sample dosing zone(s) to sample detection zones. In our approach, plasma generated hydrophilic patterns in a hydrophobized paper can control the capillary flow path of liquids and can be designed to have one or more detection zones. Figure 2 shows a test of a plasma generated pattern. Small quantities ($2\ \mu\text{L}$) of three active and three deactivated enzyme samples were introduced in alternation into detection ports of a six-channel pattern. A few drops of liquid substrate (BCIP/NBT) were introduced from the center port of the pattern. Three samples with active enzyme show a color change, and three deactivated enzyme samples show no color change. This microfluidic system created by plasma treated paper is capable of performing analytical tests proposed by other researchers.^{4–7}

Building Functional Elements on Paper-Based Microfluidic Systems. Functional elements such as switches, filters, and separators can be easily built into microfluidic devices made by plasma treatment of paper. An advantage of plasma treated paper is that the untreated areas remain hydrophobic and do not allow capillary penetration of sample liquids. Such structure allows simple switches to be built so as to connect and disconnect the microfluidic channels. Several of many possible mechanical designs can be found in the Supporting Information. Simple switch

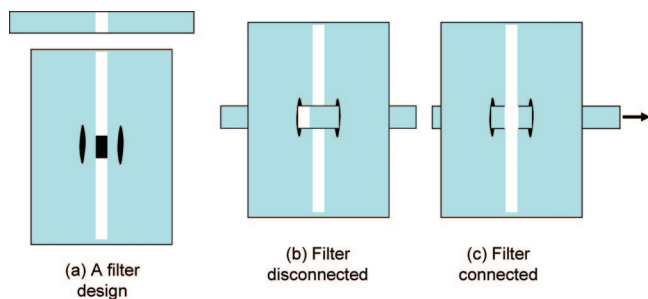


Figure 3. A simple and versatile design of a paper-based microfluidic separator. It can be activated by pulling the paper strip.

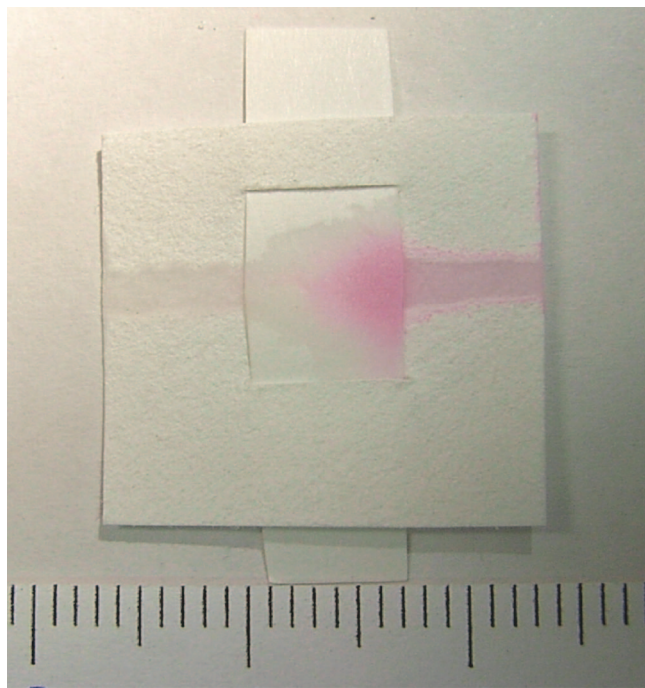


Figure 4. A filter made of silica coated matt ink jet paper was used to separate the magenta dye from a diluted ink jet ink solution.

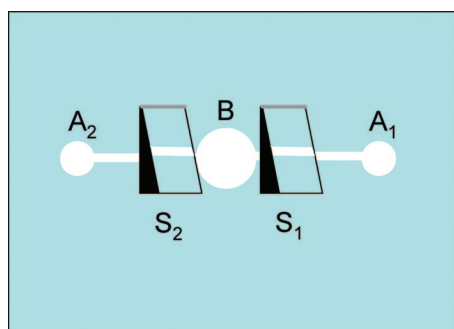


Figure 5. A design of a simple paper-based microfluidic reactor consisting of two sample dosing sites (A_1 , A_2), two switches (S_1 , S_2), and a reaction site (B).

design can be found below (Figures 5 and 6). It is possible that such switches can be activated by some other means such as by electrostatic or electromagnetic forces, etc.

A filter or a separator can also be easily designed for paper-based microfluidic systems. With dependence on the requirement of the analytical task, ion-exchange resins, high surface area functionalized nano- or microparticles or cationic polymer-coated mineral fillers can be deposited on the surface of the mechanical

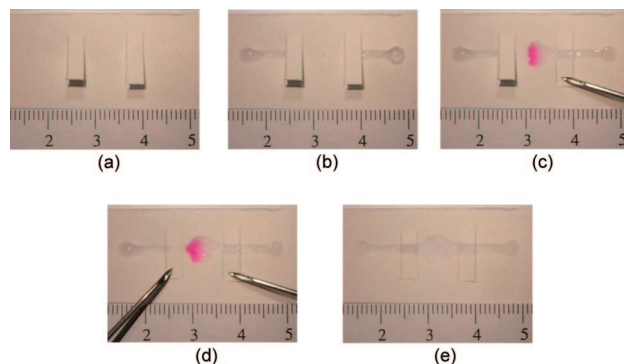


Figure 6. A microfluidic reactor in operation: (a) The reactor fabricated using plasma treatment. Phenolphthalein was deposited in the reaction site B. (b) Dosing of a NaOH solution via A_1 and HCl solution via A_2 ; (c) NaOH solution was allowed into the reaction site, triggering indicator color change; (d) HCl solution was allowed into the reaction site, causing indicator color fading; (e) complete reversion of indicator color by HCl solution.

switches. When the switch is in the connected state, the sample liquid can be filtered to remove solid particles when penetrating through the filter. Also, certain molecular species can be separated from the sample liquid chromatographically as the sample penetrates through a separator.

Figure 3 shows an even simpler and versatile design of a paper-based chromatographic separator. A strip of paper or other flexible material with a patch of coating, as shown in Figure 3, can be used to form the separation element. The separator is activated by pulling the strip as illustrated in Figure 3. To demonstrate the operation and effectiveness of this type of separator, a strip of matt ink-jet printing paper with a silica coating layer was used to separate a diluted ink-jet ink solution (Figure 4). The diluted ink was deposited on the right side of the microfluidic channel; as the solution passed through the separator and reached the left side channel, dye in the solution was retained by the ink jet paper separator. Figure 4 indicates that this separator performed satisfactorily.

With the functional components shown above, a controllable microfluidic reactor can be built on paper or other suitable nonwoven materials. Figure 5 shows the concept of a simple reactor consisting of two sample dosing sites (A_1 and A_2), which are connected to a reaction site (B) via two switches (S_1 and S_2). Two liquid reactants can be placed in each of the dosing sites; they can be controlled to enter the reactor by the switches.

Figure 6 shows a microfluidic reactor (Figure 6a) in operation. A small quantity of phenolphthalein indicator was placed into the reaction zone (B) to demonstrate an acid–base neutralization reaction. A NaOH and a HCl solution were introduced into sample dosing zones A_1 and A_2 , respectively (Figure 6b). Both switches were in the disconnected position. Switch S_1 was then switched on to allow the NaOH solution to enter the reaction zone. As the NaOH solution entered the reaction zone, the change of indicator color was observed (Figure 6c). Then S_2 was switched on to allow the HCl solution to enter the reaction zone (Figure 6d). As the HCl solution entered the reaction zone, the neutralization reaction occurred. Figure 6e shows the expected fading of indicator color as the neutralization reaction completed.

Paper-based microfluidic systems fabricated using plasma treatment are capable of allowing single- and multi-step tests, as

well as reactions to be performed. Plasma treatment allows the paper to retain its original flexibility. Since the treatment does not change the color of the paper, diagnostic devices made using this method allow easy color identification.

CONCLUSION

A new method of making paper-based microfluidic patterns by plasma treatment was developed. Microfluidic devices made using this method have the same capability of transferring and analyzing liquid samples as similar devices reported previously, but the paper devices made using plasma treatment have an advantage over the barrier design in that simple functional elements such as switches, filters, and separators can be easily built in the microfluidic system. This advantage will be further explored to build more advanced paper-based microfluidic devices.

ACKNOWLEDGMENT

The authors would like to gratefully acknowledge Monash University and Australian Research Council for their scholarships (X.L. and T.N.). The authors would also like to thank Dr. N. Cowieson of Monash Centre for Synchrotron Science for valuable discussions.

SUPPORTING INFORMATION AVAILABLE

Additional information as noted in text. This material is available free of charge via the Internet at <http://pubs.acs.org>.

Received for review August 18, 2008. Accepted October 8, 2008.

AC801729T



Fabrication of paper-based microfluidic sensors by printing

Xu Li, Junfei Tian, Gil Garnier, Wei Shen*

Australian Pulp and Paper Institute, Department of Chemical Engineering, Monash University, Clayton Campus, Vic. 3800, Australia

ARTICLE INFO

Article history:

Received 14 August 2009

Received in revised form

21 December 2009

Accepted 28 December 2009

Available online 13 January 2010

Keywords:

Microfluidic system

Ink jet printing

Paper

Sizing

ABSTRACT

A novel method for the fabrication of paper-based microfluidic diagnostic devices is reported; it consists of selectively hydrophobizing paper using cellulose reactive hydrophobization agents. The hydrophilic–hydrophobic contrast of patterns so created has excellent ability to control capillary penetration of aqueous liquids in paper channels. Incorporating this idea with digital ink jet printing techniques, a new fabrication method of paper-based microfluidic devices is established. Ink jet printing can deliver biomolecules and indicator reagents with precision into the microfluidic patterns to form bio-chemical sensing zones within the device. This method thus allows the complete sensor, i.e. channel patterns and the detecting chemistries, to be fabricated only by two printing steps. This fabrication method can be scaled up and adapted to use high speed, high volume and low cost commercial printing technology. Sensors can be fabricated for specific tests, or they can be made as general devices to perform on-demand quantitative analytical tasks by incorporating the required detection chemistries for the required tasks.

© 2010 Elsevier B.V. All rights reserved.

1. Introduction

Paper made of cellulose fibres is naturally hydrophilic and allows penetration of aqueous liquids within its fibre matrix. This property provides the foundation for using paper to fabricate microfluidic systems [1]. It has been reported that paper-based microfluidic devices can be built by demarcating hydrophilic paper by walls of hydrophobic polymers [2]. Following this principle, Martinez et al. [2,3] explored the use of a photolithography method to create microfluidic channels in paper by making hydrophobic barrier walls in the paper matrix. Hydrophobic photoresist polymers provide a very good physical barrier, which defines the liquid penetration pathways into paper. A liquid sample can be directed into multiple detection zones where indicators have been deposited. This device demonstrates the possibility of the simultaneous detection of multiple analytes in a liquid sample. The barrier-design microfluidic systems are well suited for making health care and telemedicine devices. However, this fabrication method has two potential deficiencies: first, the hardened photoresist barrier is susceptible to the damage from bending and folding. Second, photolithography requires expensive equipment and the fabrication process has multiple steps. There is a need for alternative and more efficient fabrication methods.

Bruzewicz et al. [4] used a modified plotter to create a barrier pattern by printing polydimethylsiloxane (PDMS) onto paper. This method overcame the problem of physical inflexibility of devices made using photolithography. However, the quality of the barrier definition deteriorated, since the penetration of PDMS in paper could not be very well controlled, resulting in the wall of the barrier not being straight. This method is also limited to producing devices on an up-graded scale and at a high speed.

Abe et al. [5] took a polymer (polystyrene) solution impregnation approach to introduce hydrophobicity into the paper matrix. They then used a microdrop dispensing device to print solvent onto the impregnated paper to dissolve the polymer and to form fine liquid penetration channels. These researchers also printed chemical sensing agents into their pattern to form a functional device for biomedical detection. Lu et al. [6] used a wax printer to generate microfluidic patterns in paper. The pattern was then heated to allow wax diffusion into paper and to form the barriers for microfluidic channels. These fabrication concepts are similar to the barrier concept, since they rely on cellulose fibres in paper to be physically covered by a layer of hydrophobic materials.

The motivation of this work is to present a new concept of creating microfluidic patterns and channels by generating a hydrophilic–hydrophobic contrast on the paper surface, forming liquid penetration channels, rather than building patterns using a physical polymer barrier. Building barriers in paper to define channels is a limiting process to the speed and cost of large scale fabrication, as it usually involves multiple steps including polymer impregnation and pattern development. The ink jet printing approach reported in this study can fabricate paper-based microfluidic patterns in a single printing step. This concept, therefore, has a

* Corresponding author at: Australian Pulp and Paper Institute, Department of Chemical Engineering, Monash University, Clayton Campus, PO Box 69M, Melbourne, Vic. 3800, Australia. Tel.: +61 3 9905 3447; fax: +61 3 99053413.

E-mail address: Wei.shen@eng.monash.edu.au (W. Shen).

clear potential to enable the fabrication of paper-based microfluidic sensors, i.e. patterns and incorporated sensing chemistries, by continuous high-speed and large-volume industrial printing processes. Such efficiencies enable the ultimate practical use of these sensors for health care and environmental applications. Since printed paper retains its original flexibility, the new method also overcomes the problem of channel damage by folding and bending. Also, simple and functional elements, such as switches and micro-reactors, can be easily built into the devices made by this approach [7].

2. Materials and methods

2.1. Chemicals and materials

Alkyl ketene dimer (Wax 88 konz, BASF) and alkenyl ketene dimer (Precis 900, Hercules Australia Pty. Ltd.) were used as the cellulose hydrophobization (or sizing) agents. Both dimers have two hydrocarbon chains of C_{16} – C_{20} . Alkenyl ketene dimer, however, has one $-C=C-$ in each of its two hydrocarbon chains [8]. Analytical grade *n*-heptane (Sigma–Aldrich) was used as the solvent to make solutions of both dimers. A4 size Whatman filter paper (No. 4) with the pore size of 20–25 μm (Sigma–Aldrich specification) was used as the paper substrate for printing. MilliQ water was used for all aqueous sample dilutions.

Alkaline phosphatase (lyophilized powder, from bovine intestinal mucosa, 10–30 DEA units/mg solid) was obtained from Sigma–Aldrich. One milligram per millilitre phosphatase solution was prepared in the buffer solution (pH 9.8) which contains 1.0 M diethanolamine ($\geq 98\%$, Sigma–Aldrich) and 0.5 mM $\text{MgCl}_2 \cdot 6\text{H}_2\text{O}$ ($\geq 99\%$, Sigma–Aldrich). A BCIP®/NBT substrate system (Sigma–Aldrich) was used to indicate the activity of the enzyme through color change.

NaNO_2 ($\geq 99\%$) was obtained from Sigma–Aldrich. The indicator solution for NO_2^- contains 50 mmol/L sulfanilamide ($\geq 99\%$, Sigma–Aldrich), 330 mmol/L citric acid ($\geq 99.5\%$, Sigma–Aldrich), and 10 mmol/L *N*-(1-naphthyl)ethylenediamine ($\geq 98\%$, Sigma–Aldrich).

2.2. Microfluidic channel formation on paper

In the first approach, patterned de-hydrophobization of paper was used to generate hydrophilic channels on paper. Filter paper samples were first hydrophobized by dipping in and quickly removing out of an alkyl ketene dimer–heptane solution (0.6 g/L) to allow evaporation of heptane. Filter paper samples were then heated in an oven at 100°C for 5 min to facilitate the curing of alkyl ketene dimer on cellulose fibres. The hydrophobized samples were sandwiched between metal masks and then treated with a vacuum plasma reactor (Quorum Emitech, UK) for 15 s at an intensity of 15 W. The vacuum level for the treatment was 6×10^{-1} mbar. Metal masks were made by mechanically cutting the desired patterns out of stainless steel sheets. Four screws were used to align the masks. The treated paper samples retained their original flexibility without visible marks.

In the second approach, patterned hydrophobization of paper was used to generate hydrophilic channels on paper. Hydrophilic filter papers were printed using a reconstructed commercial digital ink jet printer (Canon Pixma ip4500) with electronically generated patterns of an alkenyl ketene dimer–heptane solution (5%, v/v). The modification of the printer involved replacing the ink in cartridge with the alkenyl ketene dimer–heptane solution. This solution is printable by the Canon printer chosen for this work. Solvents of strong dissolving power, such as chloroform and toluene, are not suitable, as they may chemically attack certain parts of the printer. Printing did not leave any visible mark on paper samples which

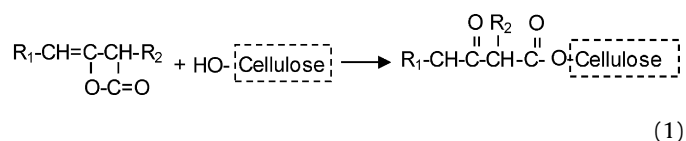
retain their original flexibility. The printed filter paper samples were then heated in an oven at 100°C for 8 min to cure alkenyl ketene dimer onto the cellulose fibres. A stop watch, ruler, video camera, and optical microscope were used for the characterization of liquid penetration inside paper microfluidic channels.

Paper sheets with hydrophobized patterns were then printed with detection reagents to form complete sensors. Two printed chemistries were used to visually demonstrate the applications of the sensors. First, a 1 mg/mL alkaline phosphatase enzyme solution was printed into the detection zone of a sensor. The BCIP®/NBT liquid substrate was introduced into the sensor via its sample introduction zone. The liquid substrate penetrated through the channel, reaching the detection zone, and lead to the color change that confirms the presence and the activity of the enzyme. Second, a colorimetric reaction for NO_2^- detection was employed. An indicator solution for colorimetric detection of NO_2^- (an aqueous solution of citric acid, sulfanilamide and *N*-(1-naphthyl)ethylenediamine [9]) was printed onto the sheet with same patterns and into the detection zones of all sensors. Five microlitres of NO_2^- sample solution (5 mM) was manually introduced into the microfluidic channels of all sensors and allowed to penetrate into the detection zones, showing a color change.

3. Results

3.1. Hydrophilic–hydrophobic contrast of untreated and treated papers

Alkyl and alkenyl ketene dimers are reactive cellulose hydrophobization agents. Their common reactive functional group is the four-member lactone ring, which is connected to two long hydrocarbon chains (C_{16} – C_{20}). Once alkyl and alkenyl ketene dimers are immobilized on fibre surfaces via the (esterification) reaction with $-OH$ groups of cellulose, the two hydrocarbon chains impart hydrophobicity to the cellulose fibre surface [10]:



The hydrophobized filter paper samples are strongly hydrophobic and have contact angles of typically 110 – 125° with water [10], whereas untreated cellulose has a contact angle of only 25° [11]. The Washburn equation has been used as a first order approximation to study the penetration of liquids in paper (Eq. (2)) [12]:

$$l = \sqrt{\frac{\gamma r \cos \theta}{2\eta}} t \quad (2)$$

where l is the liquid penetration distance in paper, r is the equivalent capillary pore radius of paper, γ and η are the surface tension and viscosity of the liquid, θ is the contact angle and t is the time of penetration. Eq. (2) shows that if a paper surface sustains an apparent contact angle with a liquid of greater than 90° , then liquid penetration will not occur. This phenomenon is the basis of our study of using patterned hydrophilic–hydrophobic contrast to fabricate paper-based microfluidic sensors. Plasma treatment and printing are intuitively two of the simplest ways to generate patterns of hydrophilic–hydrophobic contrast on paper.

3.2. Patterned de-hydrophobization of papers by plasma treatment

Plasma treatment was used to prove the principle of using hydrophilic–hydrophobic contrast for the fabrication of paper-based microfluidic devices. Plasma treatment of hydrophobic paper

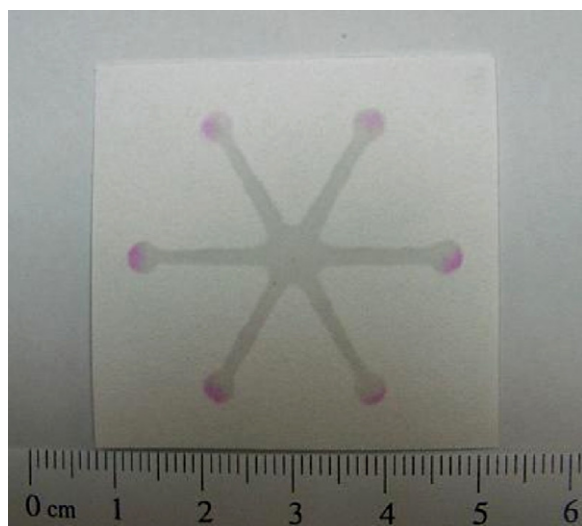


Fig. 1. The performance of a paper-based microfluidic pattern fabricated by plasma treatment. NaOH solution drops delivered to the central sample dosing zone penetrated through channels into the detection zones, causing color change of phenolphthalein indicator.

with patterned masks provides an easy method to selectively introduce hydrophilic patterns to hydrophobic paper. Fig. 1 shows a six-channel pattern created in a hydrophobic paper by plasma treatment. The channel width on the masks was 1 mm and that on the treated paper was around 1.5 mm. A NaOH solution was introduced into the pattern through the central sample dosing site and simultaneously penetrated along all channels into the detection zones where a phenolphthalein–ethanol solution was deposited after plasma treatment. The plasma treated channels have well-defined borders; the indicator color change in all detection zones demonstrated that the device is capable of performing similar analytical tasks as demonstrated in previous studies [2–5].

Hot electrons and other energetic particles generated in vacuum plasma have long mean free paths. Over-etching of the substrate under a mask is a known problem for plasma treatment, causing the treated pattern to be slightly bigger than the mask. However, over-etching could be controlled by optimizing the treatment intensity and time. When the treatment intensity and time were fixed, channels of very reproducible width were achieved. The plasma treated areas were highly wettable by water or aqueous solutions and allowed the transport of aqueous solutions along and within the plasma treated channels via capillary penetration [7].

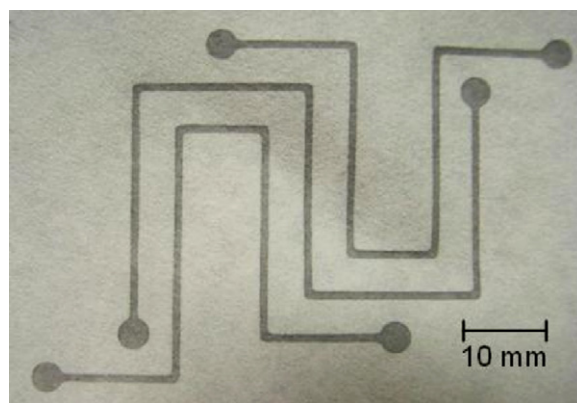


Fig. 2. Ink jet printed paper-based microfluidic patterns have channels and zones defined by the hydrophilic–hydrophobic contrast (microfluidic patterns wetted with water).

3.3. Patterned hydrophobization of papers by ink jet printing

A reconstructed ink jet printer was used to print the alkenyl ketene dimer–heptane solution onto an untreated filter paper. After curing, the printed area became strongly hydrophobic and the non-printed area remained hydrophilic. The printed area sustained water contact angle of greater than 110° . Printed hydrophobic patterns are invisible to the eye and printed papers retain their original flexibility. Fig. 2 shows a printed pattern on a filter paper; water was allowed to wick into the pattern starting from circular zones at the end of the channels to reveal the printed hydrophobic and non-printed hydrophilic areas.

Current commercial digital ink jet printers are capable of issuing small droplets of a few picolitres and use a small volume of ink for generating an electronically created image. The reconstructed printer also inherits this frugal ink management feature. Heptane is a fast evaporating solvent; its fast evaporation after printing limits the penetration of the solution into the paper matrix. This allows the hydrophilic channels on paper surface created by a single-step printing to have a well-defined hydrophilic–hydrophobic border (Fig. 2). Ink jet printing has the advantage of easily varying the printed pattern electronically on demand. We used ink jet printing to print a traditional Chinese paper cut pattern of a dragon to demonstrate this advantage; four liquid dosing ports were added to the four corners of the pattern. Fig. 3(a) shows an early stage of water penetration from the four ports; Fig. 3(b) shows the complete penetration of the pattern by water. Fig. 4 shows the microfluidic

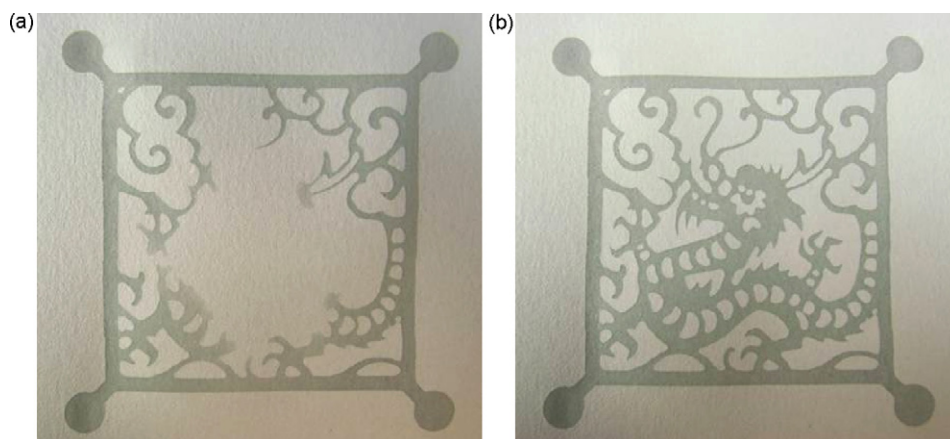


Fig. 3. Ink jet printed paper fluidic pattern of a Chinese paper cut. Four liquid feeding zones were added to the four corners of the pattern. Water penetration at an early stage (a) and at the final stage (b) is shown.

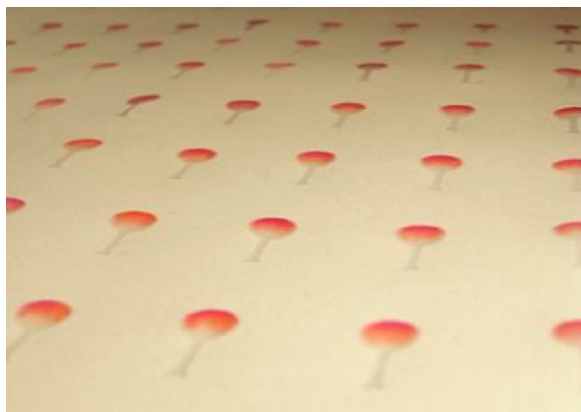


Fig. 4. Microfluidic sensor patterns are printed on an A4 sized Whatman #4 filter paper. A colorless indicator for detection of NO_2^- was also printed into the circular detection zone. Five microlitres of 5 mM NO_2^- sample solution was introduced into the channel. As the sample solution reached the detection zones of the sensors, reproducible color changes were seen.

sensor patterns printed on an A4 size filter paper sheet; it consists of the fluidic channels, detection zones and the indicator for NO_2^- . A 5 μL aliquot of NO_2^- solution (5.0 mM) was introduced into each sensor on the sheet to reveal the color change in sensors and show the uniformity of the printed sensors. Figs. 3 and 4 thus demonstrate the possibility of using our concept to mass produce paper-based microfluidic sensors with easy and simple electronic pattern variations.

3.4. Characterization of printed microfluidic channels in paper

3.4.1. Hydrophilic channel resolution and cross-section

The ink jet printer prints the hydrophobization “ink” only on one surface of the paper, and the ink undergoes free penetration into the paper structure. The ink jet printer issues only a small amount of ink; thus, the penetration distance of the ink into the paper is small. The quick evaporation of the hydrocarbon solvent further reduces the ink penetration distance. A paper-based device with the single-channel pattern was cut with a razor blade; the channel was then fed with water to allow visualization of the cross-section of a water-wetted channel. The cross-section of the wetted paper channel therefore illustrates water transportation in the paper channel, and shows that the cross-section of the channel is not perfectly rectangular (Fig. 5). The printing of a designed 500 μm channel resulted in a printed channel with the top side of 475 μm and a somewhat larger bottom side of 667 μm . The decreased width of the top side of the channel is due to the horizontal penetration of the hydrophobization ink and the increased width of the bottom

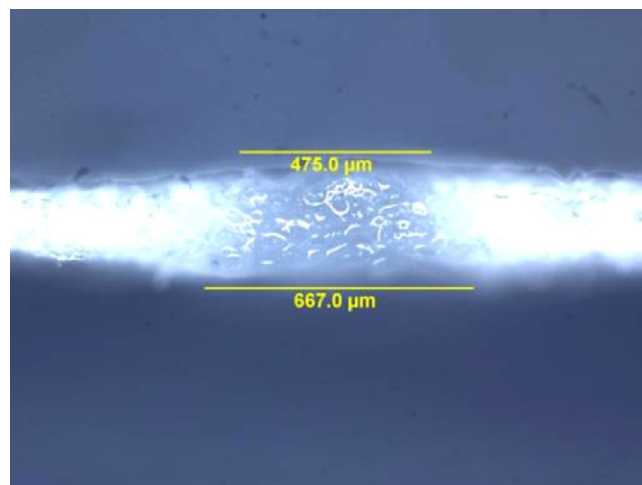


Fig. 5. The cross-section of a channel with the design width of 500 μm . Water penetration in the channel shows a decrease and an increase in channel width on the top and the bottom sides of the paper respectively.

side of the channel is due to the shorter z-direction of penetration of the hydrophobization ink at the edge of the pattern. Although the cross-section of the hydrophilic channel formed by printing is not perfectly rectangular, it is, however, adequate for its intended use of transporting liquid samples in the paper-based microfluidic pattern. Using ink jet printing, finer channels of 300 μm can be easily printed which was wetted with water (Fig. 6(a)). A rose-pink food dye solution was introduced into a hydrophilic channel of 600 μm ; the penetration of the dye solution along the channel shows that the hydrophilic–hydrophobic contrast at the channel boundary maintains a good level of channel integrity and the amount of solution “leaking” does not present a problem to the liquid transport in the channel (Fig. 6(b)).

3.4.2. Liquid penetration behavior in a printed channel

Fabricating microfluidic channels by ink jet printing requires only one of the paper surfaces to be printed. Water penetration in a 1000 μm hydrophilic channel printed on paper was studied using a ruler, stop watch and video camera (Fig. 7). Measurement of water penetration distance against the square root of time shows that the penetration in paper channel agrees reasonably well with the Washburn model (Eq. (2)) (Fig. 8). The noticeable deviation of the data from the linear trend line at longer penetration times is likely to be caused by the loss of driving force. A possible reason may be fibre swelling. Fibre swelling absorbs liquid into the fibre wall, leaving less amount of the free liquid to transport in inter

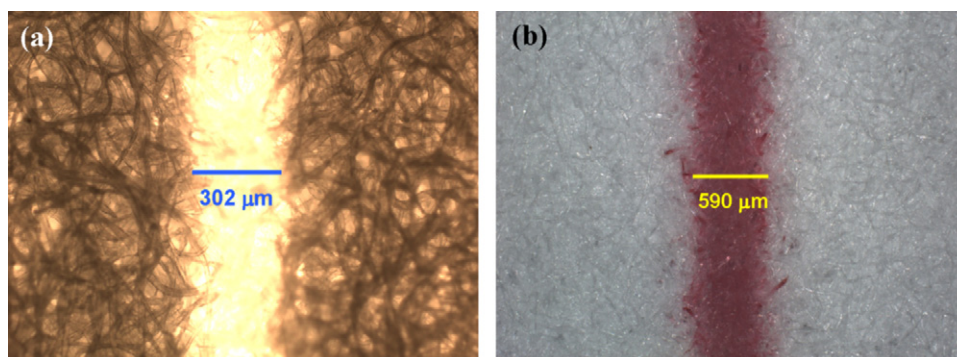


Fig. 6. Micrographs of printed channels recorded using the transmission illumination mode. (a) Water was used as the wicking liquid to increase light transmission in paper for channel width measurement. The channel has an average width of around 300 μm ; (b) the penetration of a food dye solution reveals the integrity of the channel boundary. The channel very well defines the liquid wicking pathway and the amount of “leaking” does not present a problem to the liquid transport.

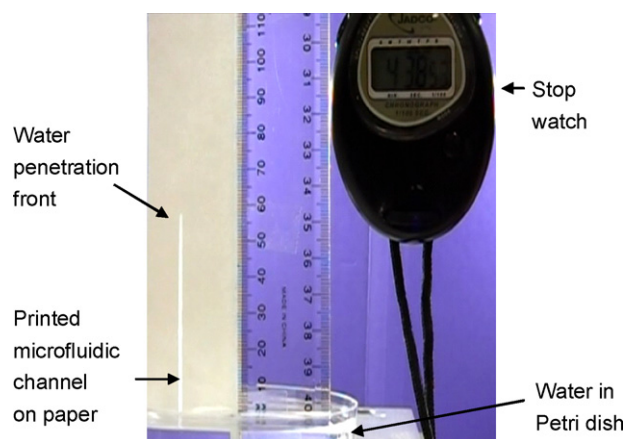


Fig. 7. Experimental set up for water penetration rate measurements of a printed paper channel. The width of the channel was 1000 μm .

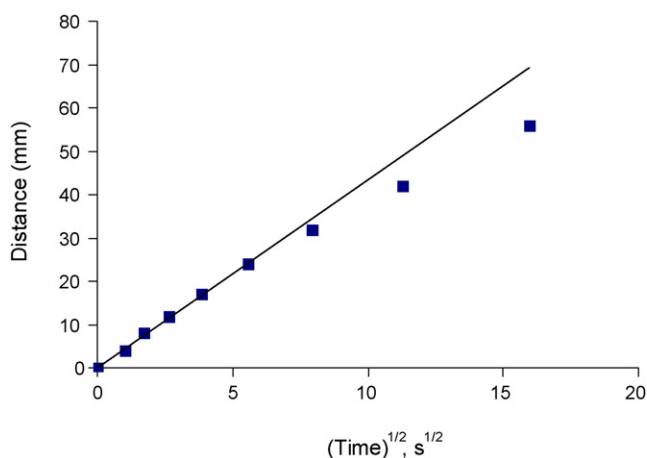


Fig. 8. Water penetration distance in the printed channel as a function of the square root of time.

fibre capillary channels. Fibre swelling may also restrict the capillary pores in paper, making the liquid penetration slower. Another minor contribution to the deviation may be the gravity. The original Washburn model does not consider the liquid absorption by the capillary wall nor the gravity factor. The linear regime of the

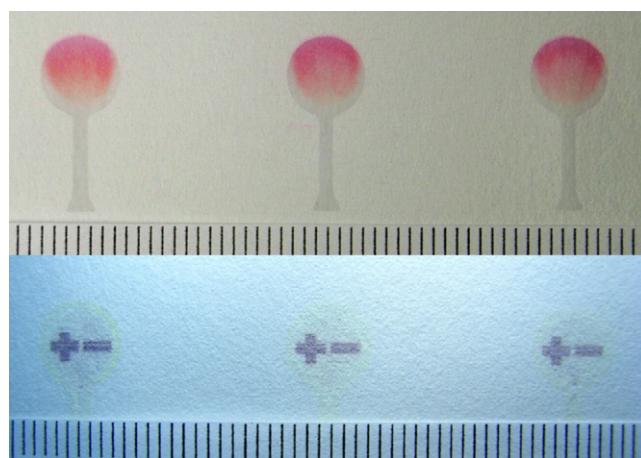


Fig. 9. Ink jet printed paper microfluidic sensors. The fluidic pattern and the detection chemistries: (a) the indicator for NO_2^- was printed into the circular detection zone. Five microlitres of 5 mM NO_2^- sample solution was introduced into the channel. As the sample solution reached the detection zones of the sensors, reproducible color changes are seen; (b) alkaline phosphatase was printed into circular detection zone and the BCIP[®]/NBT liquid substrate solution was introduced at the sample dosing site. As the liquid substrate penetrated into the detection zone, the position and activity of the printed enzyme are revealed.

penetration data is useful for the estimation of the penetration rate of water in the channel for sensor design purposes.

3.5. Paper-based microfluidic sensors with incorporated detection chemistry

Ink jet printing of biomolecules has been reported previously by many research groups [13,14]. Ink jet printing is a non-contact printing process, which offers a unique advantage of minimizing cross-sample contamination. By combining printing of biomolecules and the printing of capillary channel patterns together, an efficient approach for fabrication of microfluidic sensors using paper is formed. Fig. 9 shows an ink jet printed paper microfluidic sensor; the fluidic pattern and the alkaline phosphatase solution were printed using two cartridges in two steps. The introduction of the liquid substrate onto the printed sensor shows the printed pattern of the enzyme and confirms its activity after printing. Printing is, therefore, a highly efficient way to fabricate paper-based microfluidic sensors. In commercial printing, up

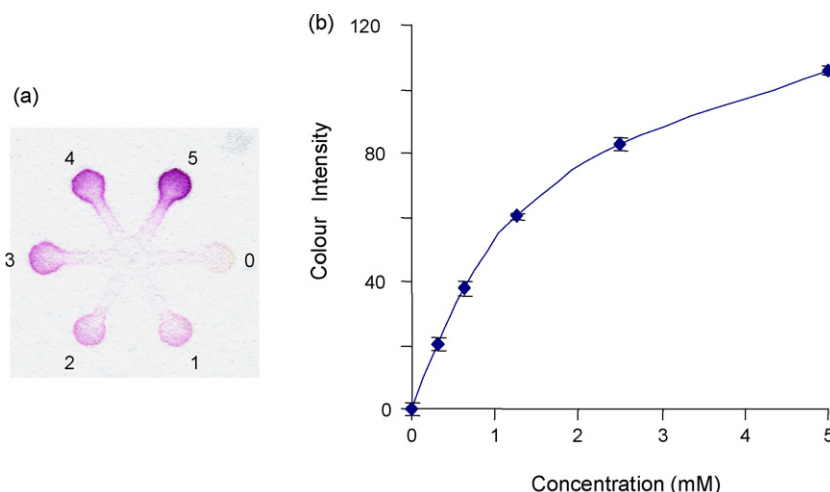


Fig. 10. (a) The scanned image of the sensor using a desk-top scanner after the samples and indicator were introduced; (b) average colour density of each detection zone was determined using PhotoShop and the whole calibration curve is obtained.

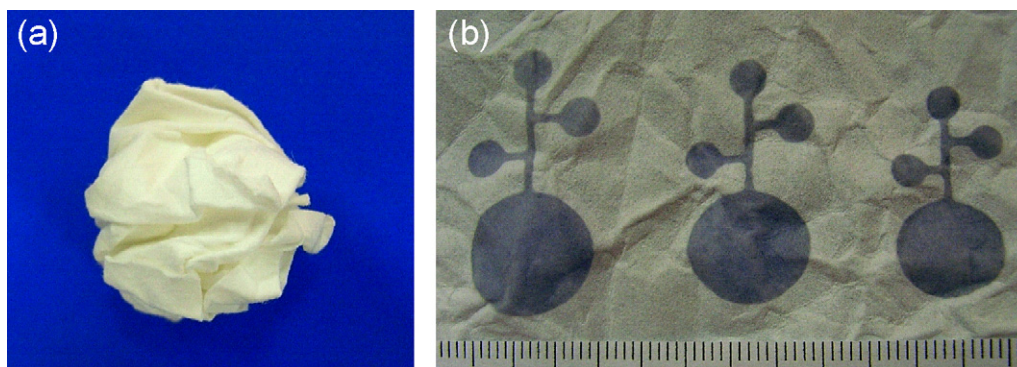


Fig. 11. (a) The printed paper microfluidic patterns were subjected to a harsh bending/folding test; (b) the performance of the printed patterns showed no discernable deterioration after the test.

to 8 inks can be printed on a substrate in one printing process [15]. It is, therefore, realistic to use commercial printing processes to fabricate paper-based microfluidic sensors at low cost. Commercial printing processes can easily offer drying and heating treatment in between two steps of printing [15].

Whilst sensors for specific purposes can be fabricated by printing both the microfluidic patterns and the specific detection chemical reagents, sensors for general purpose can be fabricated by only printing the microfluidic patterns with the desirable sample handling features. Detection chemistry can be introduced in an “on-demand” manner, depending on the analytical task. Fig. 10 shows a general purpose of paper-based microfluidic pattern that can be used for qualitative and quantitative analytical purposes.

To demonstrate its use for quantitative analysis, a colorimetric reaction for detecting NO_2^- was used in conjunction with the paper-based microfluidic pattern. NO_2^- is a bio-marker present in the saliva of renal disease sufferers [9]; rapid and quantitative detection of the species is thus useful for monitoring a patient's condition. A standard calibration curve of NO_2^- is highly desirable for its quantitative determination. The calibration curve can be obtained by adding a series of standard solutions of NO_2^- (0–5 mmol/L) into a sensor with six detection zones (Fig. 10(a)). An indicator is added to the central zone; the indicator rapidly penetrates through the channels into the detection zones, causing corresponding color changes. The paper sensor can then be scanned using a desk-top scanner and the average color density values determined by PhotoShop can be used to construct the calibration curve. Five independent measurements were taken from the five paper-based microfluidic devices to give the average values \pm standard deviation. Small error bars of the five measurements indicate good reproducibility. Detailed quantitative aspects and application of this method was reported elsewhere [16].

4. Discussion

Compared with the previous physical barrier fabrication methods, the new fabrication method reported in this study enables the manufacturing of paper-based microfluidic devices at commercial scales and very low cost. Price is a very sensitive factor for paper-based microfluidic sensors; the material cost for making these sensors is, therefore, an important point of consideration [3]. The whole sale prices of AKD from European manufacturers are 3–4 euro/kg, and the AKD usage in paper sizing is typically less than 5 kg/ton of dry fibre. If the basis weight of the paper is 92 g/m² (Whatman quality control information, <http://www.whatman.com>) and the area of each paper-based microfluidic sensor is 25 cm² (i.e. 5 cm \times 5 cm), the cost of AKD on each device will only be 0.000005 euro. In the lab-scale fabrication, each A4 size filter paper can produce 20 sensors; using the printing method reported in this work and taking ink con-

sumption for printing each A4 sheet as 400 μL , the AKD cost of each sensor (25 cm²) will be 0.000002 euro, significantly cheaper than the barrier material costs of barrier-based paper sensors reported previously which were \$0.025 for photoresist SU-8 and \$0.0025 for PDMS [4,17]. The creation of the hydrophilic–hydrophobic contrast is a simpler approach to define liquid penetration channels in paper than the physical barrier approach. Several cellulose hydrophobization chemistry systems have been used in commercial papermaking processes [10]; these chemistry systems can also be modified for the purpose of printing paper-based microfluidic sensors.

The use of digital printing technology to selectively deliver cellulose hydrophobization chemicals on paper surfaces to form the hydrophilic–hydrophobic contrast has several additional advantages. Digital printing offers electronic pattern variation which allows fast change over between the fabrications of different devices. Since the hydrophilic–hydrophobic contrast fabrication concept can retain the original flexibility of the paper, it offers natural bending and folding resistance, which fundamentally overcomes the poor bending and folding resistance often encountered with devices fabricated by other methods [18]. Fig. 11 shows an example of a harsh bending and folding test. The performance of the ink jet printed patterns shows no discernable deterioration after the bending test.

The concept of hydrophilic–hydrophobic contrast allows simple yet functional elements such as switches to be built into devices [7]. Reactor systems are possible by combining channels, switches and filters. Multi-step diagnostic tests can also be achieved with switches. Commercial printing can easily build simple switches on paper by die-cutting operations. By printing hydrophilic–hydrophobic contrast on papers, a plethora of flexible microfluidic sensors can be fabricated and their production scaled up.

5. Conclusions

The concept of printing hydrophilic–hydrophobic contrast to fabricate paper-based microfluidic sensors was investigated. Hydrophobized filter paper shows strong wetting resistance compared to the untreated filter paper. Combining this concept with plasma treatment and ink jet printing, well-defined microfluidic channels can be created on paper. Ink jet printing can also print (bio) chemical sensing agents in the microfluidic patterns with precision, which allows complete paper-based microfluidic sensors to be fabricated in one printing process consisting of two printing steps. The printing method provides potential for the mass production of microfluidic sensors at low cost as well as for laboratory research use where pattern variability is likely to be required. Qualitative and quantitative analyses can easily be achieved with different types of paper-based microfluidic sensors.

Paper-based microfluidic sensors fabricated using the hydrophilic–hydrophobic contrast concept retain the original paper flexibility. This allows simple and functional elements, such as switches and filters/separators, to be built into the sensors. With these functional elements, more advanced paper-based sensors can be designed and fabricated for more sophisticated tests.

Acknowledgements

The research scholarships of Monash University and the Department of Chemical Engineering are gratefully acknowledged. BASF and Hercules Australia are thanked for providing the hydrophobization agents. The authors would like to specially thank Dr. E. Perkins of the Department of Chemical Engineering, Monash University for proof reading the manuscript.

References

- [1] R. Stock, C.B.F. Rice, *Chromatographic Methods*, 3rd ed., John Wiley & Sons, New York, 1974, p. 106.
- [2] A.W. Martinez, S.T. Phillips, M.J. Butte, G.M. Whitesides, *Angew. Chem. Int. Ed.* 46 (2007) 1318–1320.
- [3] A.W. Martinez, S.T. Phillips, E. Carrilho, S.W. Thomas III, H. Sindi, G.M. Whitesides, *Anal. Chem.* 80 (2008) 3699–3707.
- [4] D.A. Bruzewicz, M. Reches, G.M. Whitesides, *Anal. Chem.* 80 (2008) 3387–3392.
- [5] K. Abe, K. Suzuki, D. Citterio, *Anal. Chem.* 80 (2008) 6928–6934.
- [6] Y. Lu, W. Shi, L. Jiang, J. Qin, B. Lin, *Electrophoresis* 30 (2009) 1497–1500.
- [7] X. Li, J. Tian, T. Nguyen, W. Shen, *Anal. Chem.* 80 (2008) 9131–9134.
- [8] L. Qiao, Q. Gu, H.N. Cheng, *Carbohydr. Polym.* 66 (2006) 135–140.
- [9] T.M. Blicharz, D.M. Rissin, M. Bowden, R.B. Hayman, C. DiCesare, J.S. Bhatia, N. Grand-Pierre, W.L. Siqueira, E.J. Helmerhorst, J. Loscalzo, F.G. Oppenheim, D.R. Walt, *Clin. Chem.* 54 (2008) 1473–1480.
- [10] W. Shen, Y. Filonanko, Y. Truong, I.H. Parker, N. Brack, P. Pigram, J. Liesegang, *Colloids Surf. A* 173 (2000) 117–126.
- [11] D. Kannangara, H. Zhang, W. Shen, *Colloids Surf. A* 280 (2006) 203–215.
- [12] K.T. Hodgson, J.C. Berg, *J. Colloid Interface Sci.* 121 (1988) 22–31.
- [13] V. Vauvreau, G. Laroche, *Bioconj. Chem.* 16 (2005) 1088–1097.
- [14] S.D. Risio, N. Yan, *Macromol. Rapid Commun.* 28 (2007) 1934–1940.
- [15] H. Kipphan, *Hand Book of Printing Media*, Springer-Verlag, Berlin, Germany, 2001, p. 55.
- [16] X. Li, J. Tian, W. Shen, *Anal. Bioanal. Chem.* 396 (2010) 495–501.
- [17] A.W. Martinez, S.T. Phillips, B.J. Wiley, M. Gupta, G.M. Whitesides, *Lab Chip* 8 (2008) 2146–2150.
- [18] P.S. Dittrich, *Lab Chip* 9 (2009) 15–16.

Quantitative biomarker assay with microfluidic paper-based analytical devices

Xu Li · Junfei Tian · Wei Shen

Received: 24 July 2009 / Revised: 25 September 2009 / Accepted: 25 September 2009 / Published online: 18 October 2009
© Springer-Verlag 2009

Abstract This article describes the use of microfluidic paper-based analytical devices (μ PADs) to perform quantitative chemical assays with internal standards. MicroPADs are well-suited for colorimetric biochemical assays; however, errors can be introduced from the background color of the paper due to batch difference and age, and from color measurement devices. To reduce errors from these sources, a series of standard analyte solutions and the sample solution are assayed on a single device with multiple detection zones simultaneously; an analyte concentration calibration curve can thus be established from the standards. Since the μ PAD design allows the colorimetric measurements of the standards and the sample to be conducted simultaneously and under the same condition, errors from the above sources can be minimized. The analytical approach reported in this work shows that μ PADs can perform quantitative chemical analysis at very low cost.

Keywords Quantitative assay · Paper · Microfluidic devices · Biomarkers

Introduction

The concept of microfluidic paper-based analytical devices (μ PADs) was recently proposed by a research group from Harvard University in 2007 [1]. They used the photolithography technique to selectively build hydrophobic barrier in filter paper with photoresist. The hydrophilic paper channels

demarcated by walls of hydrophobic photoresist can control the transport of aqueous solutions by capillary action in porous paper matrix without the need of external pumping. This new concept has led to the rising of the new research area of patterning paper as low-cost, portable microfluidic platform for bio/chemical/medical application [2]. In this work, different but simpler methods (plasma treatment and ink jet printing) were used to fabricate μ PADs with cellulose reactive hydrophobization agents such as alkyl ketene dimer and succinic acid anhydride. Since these two methods do not require the building of polymer barriers in the paper sheet, devices made using these methods retain the original flexibility of the paper [3, 4]. The flexible patterned paper allows the construction of switches, separators, and multi-component reactors in paper; these functional elements can significantly increase the functions of μ PADs [5].

The analytical applications of μ PADs have been pursued by several research groups. Patterned μ PADs were shown to be capable of performing qualitative [3] and semi-quantitative [2] colorimetric analyses. Low-cost desktop scanners and image analysis software have been used to measure analytical results as colorimetric changes in μ PADs [2, 3, 6]. Since scanner digitizes colorimetric results, electronic transmission of such results between laboratories has been shown feasible [2]. The μ PAD is superior to traditional colorimetric analytical methods such as UV–Vis spectrophotometry in terms of the small quantity of sample required for an analysis and the device portability. MicroPAD can also potentially reach the analytical accuracy of UV–Vis spectrophotometry, satisfying the analytical requirements of a range of rapid and routine biochemical analyses that need to be performed in field or in non-laboratory facilities.

A point that requires special emphasis is the analytical accuracy and precision. Analytical errors using μ PADs can be

X. Li · J. Tian · W. Shen (✉)
Australian Pulp and Paper Institute,
Department of Chemical Engineering,
Monash University, Clayton,
Melbourne 3800, Victoria, Australia
e-mail: wei.shen@eng.monash.edu.au

easily introduced through slightly different measurement conditions as well as small batch variations of paper qualities. Errors can be effectively reduced if an internal calibration can be provided within the device. Among a variety of applications with μ PADs, two general principles can be perceived. In the first principle, a μ PAD can be designed for a specific (single- or multi-compound) measurement, e.g., urine glucose and protein tests. In these tests, the detection chemistries can be introduced into the detection zones of μ PADs when the devices are fabricated [2]; such devices are ready to use. Each μ PAD can be used to measure a single datum for each compound the device is designed to measure. A concentration calibration curve of a compound (i.e., glucose or protein) can be obtained by analyzing several standard solutions of the compound of known concentrations using the same number of μ PADs, provided that the quality variation between μ PADs is well controlled and the measurement conditions are the same. In the second principle, a μ PAD can be designed for on-demand analyses. The μ PAD only provides a microfluidic pattern without any specific detection chemistry; the detection chemistry can be introduced into the device prior to a test. In such applications, it is possible that a series of analyte solutions of known concentration be introduced into one μ PAD to generate a calibration curve. Better still, in a quantitative analysis, if the sample (of unknown concentration) can be introduced into the same μ PAD together with the series of calibration standards and exposed to the same detection reagent(s) simultaneously, errors due to paper quality variation and different scanning conditions can be significantly reduced. Inter-laboratory transmission of colorimetric results using μ PADs with the self-calibration curves is therefore expected to be more reliable.

The purpose of this study is to demonstrate quantitative analysis potential of μ PADs. Two simple fabrication methods of μ PADs will be described. A μ PAD pattern was selected to explore the above-mentioned second principle of using μ PADs for quantitative chemical analysis. Two clinical analyses, i.e., the analyses of nitrite ion (NO_2^-) and uric acid (UA), are used to demonstrate the principle. Both NO_2^- and UA are present in human body and are biomarkers for human renal and lung diseases and can be detected with colorimetric methods. Recently, Blicharz et al. [7] and Nagler [8] used the colorimetric methods to detect these biomarkers in saliva by paper strips and have reported that these methods are efficient for monitoring the effect of dialysis in patients with end-stage renal disease. The results reported in this work show that when these two detection methods are used in conjunction with μ PADs, tedious paper strips preparation can be avoided. Standards and sample solutions can be introduced into one μ PAD directly and the subsequent introduction of the indicator allows the sample and standards to develop color changes simultaneously for colorimetric analysis.

The results of this study show that μ PADs can be used as an analytical device to easily and rapidly quantify colorimetrically detectable analytes at very low cost. Moreover, this method requires less than 1 μL of the standard or sample solutions and less than 10 μL of indicators, which are much lower than the volume needed for a paper strip analysis [7, 8] and conventional UV–Vis analysis. With the new strategy, it is possible to use μ PADs to provide quantitative results with the accuracy approaching to that of conventional methods such as UV–Vis spectrophotometry and at a greatly reduced cost. The method is particularly useful in remote and developing regions where analytical and medical infrastructure is limited.

Experimental sections

Preparation of μ PADs

Alkyl ketene dimer (Wax 88 konz, BASF) and alkenyl ketene dimer (Precis 900, Hercules Australia Pty Ltd) were used as the cellulose hydrophobization reagents. Analytical-grade *n*-heptane (Sigma-Aldrich) was used as the solvent for the dimers. Whatman filter paper (No. 4) was selected as the substrate to fabricate μ PADs. Two methods were used for μ PADs fabrication—plasma treatment and ink jet printing. In the plasma treatment method, a vacuum plasma reactor (K1050X plasma asher, Quorum Emitech, UK) and metal masks bearing the sensor pattern were used to selectively dehydrophobize filter papers which have already been hydrophobized by alkyl ketene dimer beforehand. [the preparation of the hydrophobic filter paper involves dipping the paper into a 0.6 g/L alkyl ketene dimer–heptane solution. After the evaporation of heptane, the filter paper was heat-treated in an oven at 105°C for 45 min to allow the development of paper hydrophobicity] In the ink jet printing method, a reconstructed commercial desktop ink jet printer (Canon Pixma ip4500) was used to print computer-generated patterns onto the filter paper with the ink solution of alkenyl ketene dimer–heptane (3%, *v/v*). The kinematic viscosity and the surface tension of the ink solution at 25°C are 0.506 cSt and 19.90 mN/m, respectively. These values are in the low end of the printable liquids [9]; ink solution can be successfully and accurately printed. The printed filter paper was then heat-treated in an oven to allow hydrophobicity of the printed area on paper to fully develop. The detailed fabrication process can be found elsewhere [3, 4]. In this article, the μ PADs were fabricated with a pattern consisting of six detection zones and one central fluid inlet zone.

Preparation of solutions

Millipore-purified water was used to prepare all liquid samples required for testing the performance of μ PADs.

The stock solution of NO_2^- (10.0 mmol/L) was prepared by dissolving 69.0 mg sodium nitrite ($\geq 99\%$, Sigma-Aldrich) in 100 mL water. Then, this stock solution was diluted with water to get serially diluted NO_2^- standard solutions with the concentrations of 2,500, 1,250, 625, 312, 156, and 78 $\mu\text{mol/L}$. The standard solution (625 $\mu\text{mol/L}$) was used to prepare the assumed “unknown” NO_2^- sample solution (500 $\mu\text{mol/L}$).

The UA stock solution (12.8 mmol/L) was prepared with dissolving 215.0 mg uric acid ($\geq 99\%$, Sigma-Aldrich) in 100 mL sodium hydroxide solution (0.2 mol/L). The serially diluted UA standard solutions were prepared by diluting the stock solution with 0.2 mol/L NaOH to have different concentrations of 1,600, 800, 400, 200 and 100 $\mu\text{mol/L}$. Then the standard solution (800 $\mu\text{mol/L}$) was diluted to prepare the “unknown” UA sample solution (500 $\mu\text{mol/L}$).

The indicator solution for NO_2^- contains 50 mmol/L sulfanilamide ($\geq 99\%$, Sigma-Aldrich), 330 mmol/L citric acid ($\geq 99.5\%$, Sigma-Aldrich), and 10 mmol/L *N*-(1-naphthyl) ethylenediamine ($\geq 98\%$, Sigma-Aldrich) [7].

The indicator solution for UA consists of the 1:1 mixture of solution A (2.56% (w/v) 2,2'-biquinoline-4,4'-dicarboxylic acid disodium salt hydrate, $\geq 98\%$, Sigma-Aldrich) and solution B (20 mmol/L sodium citrate and 0.08% (w/v) copper (II) sulfate, $\geq 99\%$, Sigma-Aldrich) [7].

Running assays on μ PADs

For creating NO_2^- calibration curve, one blank control (water, 0.5 μL) and five serially diluted NO_2^- standard solution samples (with concentration ranging from 78 $\mu\text{mol/L}$ to 1,250 $\mu\text{mol/L}$, 0.5 μL) were deposited into six detection zones in sequence using a micro pipette (Eppendorf Research® 0.1–2.5 μL).

A NO_2^- solution (500 $\mu\text{mol/L}$ NO_2^-) was prepared and used as the sample solution with “unknown” concentration. The “unknown” sample solution (0.5 μL) was deposited into one detection zone along side with the serially diluted NO_2^- standard solutions on the same device. In this assay, water (0.5 μL) was added into the central inlet zone as the blank control.

For UA assay, a UA solution (500 $\mu\text{mol/L}$ UA) was assumed as an unknown sample solution and successively

loaded with five serially diluted UA standard solution samples (100 $\mu\text{mol/L}$ to 1600 $\mu\text{mol/L}$) into each detection zone of the μ PAD. NaOH solution (0.2 mol/L) was used as the blank control in this assay.

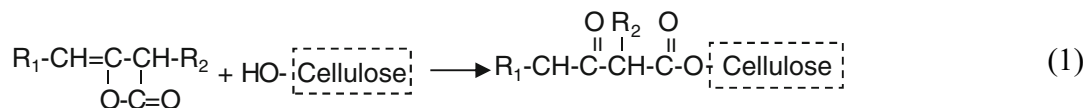
In all the above assays, corresponding indicator solutions (5 μL) were introduced into the central inlet zone with the Eppendorf Research® pipette (0.5–10 μL); indicator solutions rapidly penetrated into all detection zones. Color changes of all standards and the unknown sample developed simultaneously as the indicator solution reached the detection zones. For each assay, six independent measurements have been taken using six μ PADs made from the same sheet of filter paper (paper batch variation was assumed to be irrelevant).

The results of the colorimetric assays were imaged with a desktop scanner (Epson Perfection 2450, color photo setting, 1200 dpi resolution), then imported into Adobe Photoshop and converted into grayscale mode. The mean grayscale intensities were quantified using the histogram function of Adobe Photoshop. The ultimate mean intensity value of each detection zone was obtained by subtracting the measured average detection zone intensity from the mean intensity of the blank control; the average intensity data were then transferred to Microsoft Excel to obtain calibration curve data.

Results and discussion

Patterning paper as μ PADs

The principle of paper-sizing chemistry is used to fabricate μ PADs used in this study. Alkyl ketene dimer and alkenyl ketene dimer have two long hydrocarbon chains (C_{14} – C_{18}) which impart to the cellulose surface with water-repellence once the dimers react with $-\text{OH}$ groups of cellulose (1). The hydrophobized part of filter paper has typical apparent contact angles of 110 – 125° with water [10], whereas unhydrophobized part of paper is hydrophilic and has a contact angle typically around 25° [11]. A μ PAD patterned with the alkyl or alkenyl ketene dimers therefore forms a patterned hydrophilic–hydrophobic contrast which guides the penetration of aqueous samples.



When the hydrophobized filter paper is exposed to plasma treatment under a mask, the unmasked area

becomes hydrophilic and highly wettable by water, thus allowing aqueous liquids to penetrate within the hydrophil-

ic channels of μ PADs. Figure 1a shows a water-wetted six-channel pattern generated using plasma treatment. The channel width of this pattern is around 1 mm, and the diameter of each testing zone is ~ 2.5 mm.

When using the ink jet printing method to fabricate μ PADs, computer-generated pattern is printed on paper using “inks” of the heptane solution of alkenyl ketene dimer. This method has the advantage of electronic pattern design, easy pattern variation, and high-speed production of a large number of μ PADs. Figure 1b and c are several different patterns generated with the reconstructed commercial desktop ink jet printer.

To demonstrate the feasibility of using μ PAD as a quantitative analyzing device, μ PAD with six-channel pattern (Fig. 1a) was chosen as the device design to perform all assays. This design allows the quantitative concentration measurement of an analyte based on a six-point calibration curve simultaneously developed on the same μ PAD and under the same condition.

Calibration curve for NO_2^-

The colorimetric detection of NO_2^- is based on the principle of the Griess reaction which is a common

quantification method for NO_2^- [12]. In this assay, 0.5 μL of serially diluted NO_2^- standard solutions (78, 156, 312, 625, 1,250 $\mu\text{mol/L}$) were transferred using a micro pipette into detection zones 1–5 in sequence, while the blank control solution was spotted on the detection zone 0. Then, the indicator solution (5 μL) for NO_2^- was introduced into the device via the inlet zone. When the indicator solution penetrated into testing zones (<3 s) by capillary action and contacted with the analyte, the citric acid within the indicator solution converted NO_2^- to HNO_2 . The nitrous acid then transformed sulfanilamide into diazotized sulfanilamide which coupled with *N*-(1-naphthyl)-ethylenediamine to form a pink azo compound (full color developed within 5 s). The resulting color developed in each detection zone changes from almost colorless (zone 0) to pink (zone 5) due to the different concentration of standard solution samples (Fig. 2). The measurement was repeated six times using six μ PADs; the average grayscale intensity and the error bar (relative standard deviation) for each standard NO_2^- solution were determined (Fig. 3). Linear least-squares fitting of the NO_2^- data gave coefficient of determination (R^2) of 0.9902. The mean color intensity is proportional to the NO_2^- concentration. This assay confirms that μ PAD can

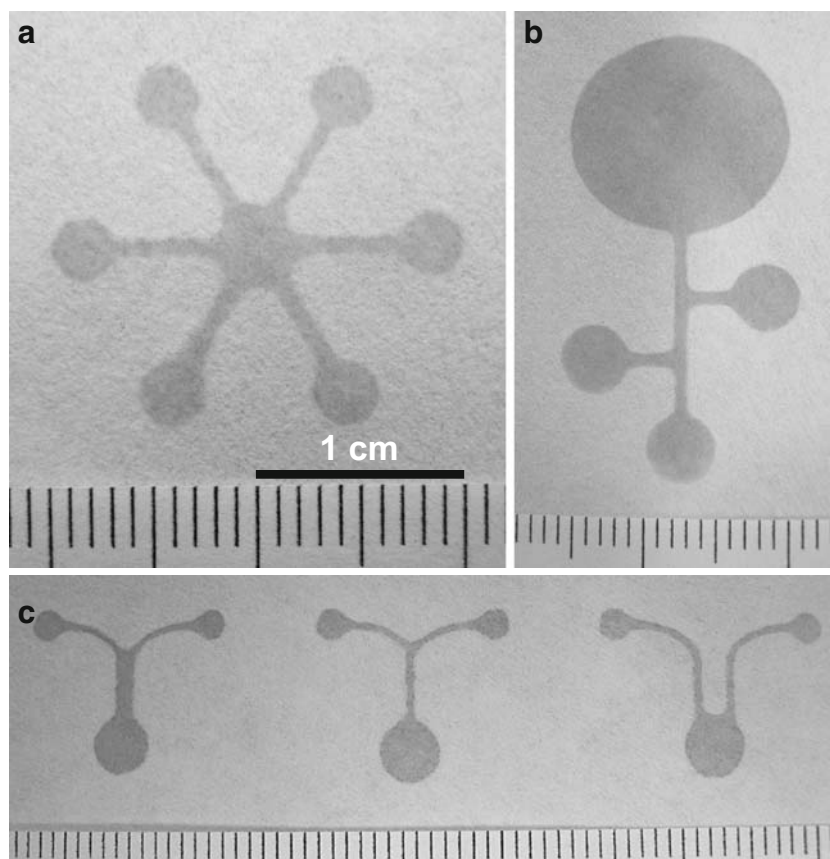


Fig. 1 Microfluidic patterns generated on paper using plasma treatment (a) and ink jet printing (b and c). The channels were wetted with water to visually show the patterns

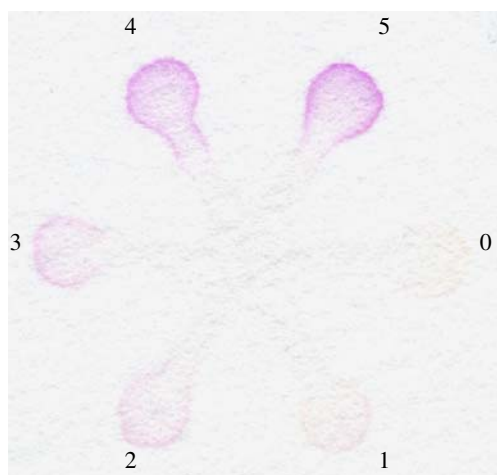


Fig. 2 The scanned image of a six-channel μ PAD in which a series of standard NO_2^- solutions were used to construct a calibration curve. After reaction, color intensities can be visually detected

be used to create calibration curves for quantitative analysis.

Concentration measurement of NO_2^- sample

To demonstrate the quantification of the NO_2^- concentration in sample solution, we prepared a blank control solution (0 $\mu\text{mol/L}$ NO_2^- , deposited on zone 0), five standard solutions (156, 312, 625, 1,250, 2,500 $\mu\text{mol/L}$ NO_2^- , deposited on zones 1–5), and a 500 $\mu\text{mol/L}$ NO_2^- solution (deposited on zone x) which was used as an “unknown” sample solution (Fig. 4). It should be noted that the calibration curve in this assay covered a wider concentration range than the calibration curve in Fig. 3. The indicator solution was still introduced into the device from central inlet zone (0). As the indicator solution

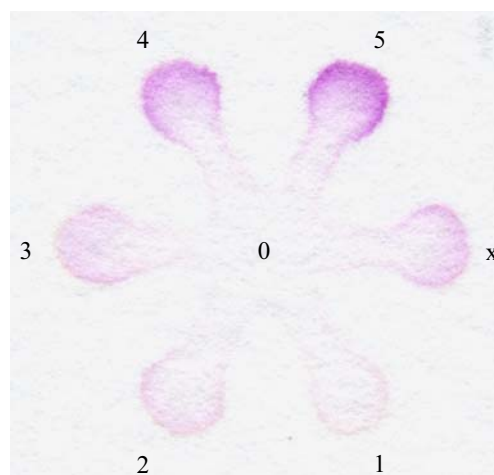


Fig. 4 The scanned image of a six-channel μ PAD in which a series of standard NO_2^- solutions were used to construct a calibration curve in a higher concentration range than that in Fig. 2. In this analysis, a sample solution of “unknown” NO_2^- concentration was also deposited in the device (marked x)

penetrated into the detection zones (1–5 and x), NO_2^- in these zones caused color change (Fig. 4). To demonstrate the reproducibility of this assay, the measurement was repeated six times using six μ PADs made from the same sheet of filter paper (paper batch variation was assumed to be irrelevant). The average grayscale intensity and the error bar (relative standard deviation) for each standard NO_2^- solution were determined (Fig. 5). The calibration curve obtained was not linear, but was quadratic. Grayscale analysis shows that the average intensity for the “unknown sample” was 12.684. Accordingly, the NO_2^- concentration of the unknown sample quantified using the calculation curve was 507 $\mu\text{mol/L}$. This leads to a relative error of 1.4% compared with the concentration of 500 $\mu\text{mol/L}$.

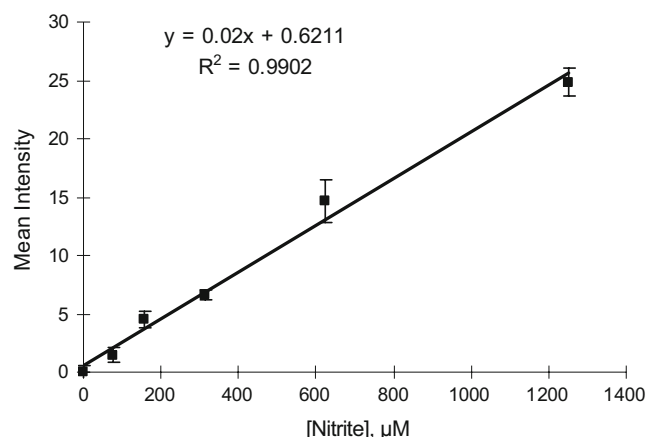


Fig. 3 The concentration calibration curve constructed using the grayscale intensity values converted from the image shown in Fig. 2

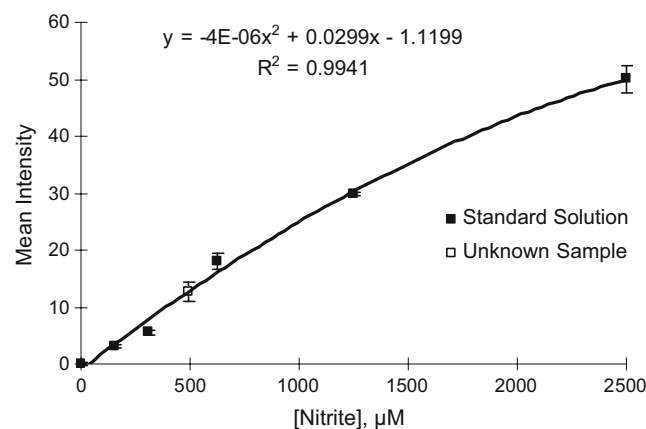


Fig. 5 The concentration calibration curve constructed using the grayscale intensity values converted from the image shown in Fig. 4. The grayscale intensity for the sample of “unknown” concentration is shown by the unfilled square

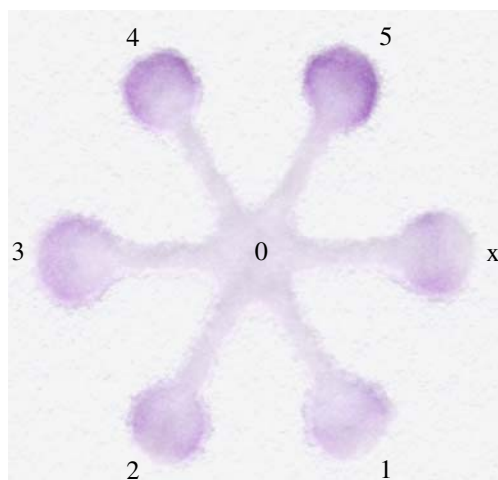


Fig. 6 The scanned image of a six-channel μ PAD in which a series of standard UA solutions were used to construct a calibration curve. In this analysis, a sample solution of “unknown” UA concentration was also deposited in the device (marked x)

Concentration measurement of UA sample

The colorimetric assay of UA was based on a bicinchoninate chelate method [13]. When the indicator solution for UA penetrates into the detection zone, Cu (II) in the indicator solution was reduced to Cu (I) by UA, which was deposited into the detection zone beforehand. The cuprous ion then formed a purple chelate product with bicinchoninate ion. A calibration curve was established by depositing 0.5 μ L of serially diluted standard UA solutions (0, 100, 200, 400, 800, 1,600 μ mol/L) into detection zones 0–5. A 500 μ mol/L UA solution was used as the “unknown” sample and was deposited in detection zone x (Fig. 6). The indicator solution (5 μ L) was introduced to μ PAD from zone 0 and was allowed to penetrate into all detections zones via hydrophilic channels. The resulting color developed in detection zones 0–5 can be observed ranging from light purple to purple, corresponding to the different UA concentrations of the standard UA solutions (Fig. 6). To show the reproducibility of this assay, the measurement was also repeated six times using six μ PADs made from the same sheet of filter paper; the average grayscale intensity and the error bar (relative standard deviation) for each standard UA solution were determined (Fig. 7). Following the same procedure, the average grayscale density of the “unknown” sample was measured to be 12.492. The average concentration of the “unknown” sample calculated from six independent measurements using the regression equation was 502 μ mol/L, corresponding to a relative error of 0.4% when compared with the concentration of 500 μ mol/L.

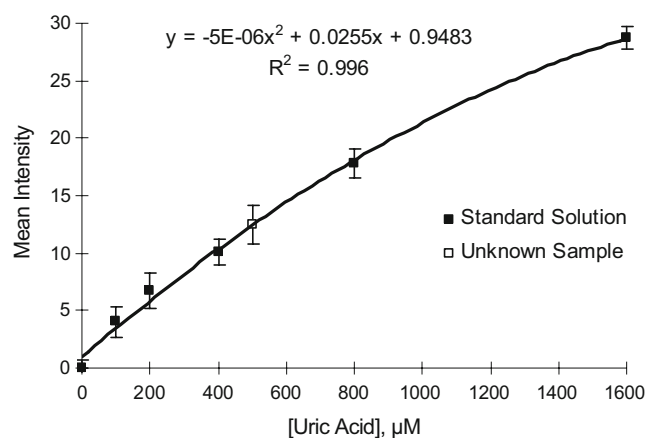


Fig. 7 The concentration calibration curve constructed using the grayscale intensity values converted from the image shown in Fig. 6. The grayscale intensity for the sample of “unknown” concentration is shown by the unfilled square

The above assays demonstrate the potential of using μ PADs to perform rapid quantitative chemical analysis at a low cost and low sample volume requirement. By selecting suitable patterns, μ PADs are capable of simultaneously presenting the detection results of a calibration curve and unknown samples. The colorimetric data of all calibration points and unknown samples can be recorded using a scanner (or any recording device such as a camera phone) under the same condition and at the same age. Since the colorimetric data of all calibration points and unknown samples are developed on the same μ PAD, colorimetric error resulted from paper batch variation can be eliminated. Work reported in this study shows that μ PADs can be fabricated using very simple methods and μ PADs can deliver reasonably good analytical accuracy rapidly and at very low cost.

Conclusions

Microfluidic paper-based analytical devices, combined with the colorimetric reaction of analyte and the existing computer software (e.g., Adobe Photoshop), can provide a cheap and easy-to-use tool for the quantitative detection of unknown sample concentration. The raw material for μ PADs - paper - is relatively cheap and the fabrication methods of μ PADs are quite simple. Therefore, the μ PAD can be a useful tool when measurements need to be performed in less-industrialized area or remote region where analytical infrastructure is limited. Moreover, this analysis method substantially reduces the

sample volume, which is an important advantage when the obtainable sample amount is limited (e.g., the biological sample from patients).

Acknowledgments The research scholarships of Monash University and the Department of Chemical Engineering are gratefully acknowledged. BASF and Hercules Australia are thanked for providing the hydrophobization agents.

References

1. Martinez AW, Phillips ST, Butte M, Whitesides GM (2007) *Angew Chem Int Ed* 46:1318–1320
2. Martinez AW, Phillips ST, Carrilho E, Thomas SW III, Sindi H, Whitesides GM (2008) *Anal Chem* 80:3699–3707
3. Li X, Tian J, Nguyen T, Shen W (2008) *Anal Chem* 80:9131–9134
4. Shen W, Tian J, Li X, Khan MS, Garnier G (2009) Method of fabricating microfluidic systems PCT/AU2009/000889
5. Dittrich PS (2009) *Lab Chip* 9:15–16
6. Abe K, Suzuki K, Citterio D (2008) *Anal Chem* 80:6928–6934
7. Blicharz TM, Rissin DM, Bowden M, Hayman RB, DiCesare C, Bhatia JS, Grand-Pierre N, Siqueira WL, Helmerhorst EJ, Loscalzo J, Oppenheim FG, Walt DR (2008) *Clin Chem* 54:1473–1480
8. Nagler RM (2008) *Clin Chem* 54:1415–1417
9. Khan MS, Fon D, Li X, Forsythe J, Thouas G, Garnier G, Shen W (2008) *Chemeca 2008: Towards a Sustainable Australasia* 744–753
10. Shen W, Filonanko Y, Truong Y, Parker IH (2000) *Colloid and Surface A: Phys Eng Asp* 173:117–126
11. Kannangara D, Zhang H, Shen W (2006) *Colloid and Surface A: Phys Eng Asp* 280:203–215
12. Sun J, Zhang X, Broderick M, Fein H (2003) *Sensors* 3:276–284
13. Gindler EM (1970) *Clin Chem* 16:536

Progress in patterned paper sizing for fabrication of paper-based microfluidic sensors

Xu Li · Junfei Tian · Wei Shen

Received: 30 October 2009 / Accepted: 12 January 2010 / Published online: 27 January 2010
© Springer Science+Business Media B.V. 2010

Abstract In this paper, we report the progress in using paper sizing chemistry to fabricate patterned paper for chemical and biological sensing applications. Patterned paper sizing uses paper sizing agents to selectively hydrophobize certain area of a sheet. The hydrophilic-hydrophobic contrast of the pattern so created has an excellent ability to control capillary penetration of aqueous liquids in channels of the pattern. Incorporating this idea with digital ink jet printing technique, a new fabrication method of paper-based microfluidic devices is established. Ink jet printing can deliver biomolecules and chemicals with precision into the microfluidic patterns to form biological/chemical sensing sites within the patterns, forming the complete sensing devices. This study shows the potential of combining paper sizing chemistry and ink jet printing to produce paper-based sensors at low cost and at commercial volume.

Keywords Paper microfluidics · Ink jet printing · Paper sizing · Low-cost sensors

Introduction

The applications of microfluidic technology in chemical and biochemical analysis, as well as in point-of-care (POC) diagnostics, are expanding rapidly, since microfluidic technology has the ability to control and direct small quantities (10^{-9} to 10^{-18} L) of liquid samples to produce rapid analysis (Whitesides 2006). The term *lab on a chip* (LOC) describes the current status of microfluidic analytical sensors. Although LOC devices have demonstrated clear advantages over many conventional analytical instruments in their high analytical sensitivity and resolution, the cost of these devices and the skills required to operate some of those devices make them not readily accessible to average users in developing countries (Zhao and van der Berg 2008). Microfluidic devices made using inexpensive materials such as paper therefore provide a new platform for low-cost, low-volume and portable bioassays (Martinez et al. 2007). Paper-based microfluidic devices can be made more accessible to population in developing regions because of their low cost; they are particularly suitable for obtaining semi-quantitative disease and health information from populations in remote area and developing countries.

Recent research on paper-based microfluidic devices has shown that paper has great potential for making low-cost diagnostic devices for health care and environmental monitoring purposes (Abe et al. 2008; Bruzewicz et al. 2008; Carrilho et al. 2009;

X. Li · J. Tian · W. Shen (✉)
Department of Chemical Engineering,
Australian Pulp and Paper Institute, Monash University,
Clayton Campus, Melbourne, VIC 3800, Australia
e-mail: wei.shen@eng.monash.edu.au

Dungchai et al. 2009; Hossain et al. 2009; Li et al. 2008; Lu et al. 2009; Martinez et al. 2007, 2008a, b). Cellulose paper is naturally hydrophilic and allows fast penetration of aqueous liquids. This property provides the foundation for using paper to fabricate microfluidic systems (Stock and Rice 1974). To use paper to fabricate microfluidic devices for practical purposes, several technical issues need to be resolved. First, the device must be able to very well control the penetration of liquid sample in paper; this requires the liquid penetration pathways to be defined either physically or chemically within the paper matrix. Second, efficient fabrication methods must be developed so that such devices can be fabricated using modern high-speed and high-volume processes at low cost. Third, paper-based microfluidic systems must be able to withstand handling by field personnel and untrained patients. Additional fabrication challenge is that the resolution of the liquid sample channels in such devices must be high enough to meet the analytical requirements. Furthermore, building valves in devices to control liquid penetration for multi-step tests can enhance the capability of the devices for intelligent applications.

It has been demonstrated that paper-based microfluidic devices can be built by demarcating hydrophilic paper by walls of hydrophobic polymers (Martinez et al. 2007). Following this principle, Martinez et al. (2007, 2008a, b) explored the use of photolithography method to create microfluidic channels in paper by making hydrophobic barrier walls in paper matrix. Hydrophobic photoresist polymers provide very good physical barrier, which defines liquid penetration pathways into paper. A liquid sample can be directed into multiple detection zones where indicators were deposited. This device demonstrates the possibility of the simultaneous detection of multiple analytes in a liquid sample. The barrier-design microfluidic systems are well suited for making health care and telemedicine devices (Martinez et al. 2008a, b). However, this fabrication method (photolithography) suffers from two major deficiencies: first, the hardened photoresist barrier is susceptible to bending and folding damages (Bruzewicz et al. 2008); second, photolithography requires expensive equipment and the fabrication process is slow and needs multiple steps (Lu et al. 2009).

Bruzewicz et al. (2008) used a modified plotter to create a barrier pattern by printing polydimethylsiloxane

(PDMS) onto paper. This method overcame the problem of physical inflexibility of devices made using photolithography. However, barrier definition deteriorated, since the penetration of PDMS in paper could not be very well controlled, resulting in the wall of the barrier not being straight. This method is unable to produce devices in massive scale and at high speed.

Abe et al. (2008) took a polymer (polystyrene) solution impregnation approach to introduce hydrophobicity into the paper matrix. They then used a specialty micro drop dispensing system to print solvent onto the impregnated paper to dissolve the polymer and form fine liquid penetration channels. These authors also printed chemical sensing agents into their pattern to form a functional device for biomedical detection. Lu et al. (2009) used a wax laser printer to generate microfluidic patterns on paper. The pattern was then heated to allow wax diffusion into paper and form a barrier for microfluidic channels. These fabrication concepts are similar to the barrier concept, since they rely on cellulose fibres in paper to be physically covered by a layer of hydrophobic materials.

Our recent work (Li et al. 2008, 2010) reported new methods of using paper sizing chemistry to generate patterns of hydrophilic-hydrophobic contrast in paper to form microfluidic devices. We successfully performed qualitative and quantitative chemical/biological analyses using patterned paper devices fabricated by AKD sizing.

In this paper, we report the progress in using paper sizing chemistry to create paper-based microfluidic sensors. We also present the qualitative and quantitative analysis capabilities of the sensors so fabricated, and comment on the potential of using sizing chemistry and printing technology to upscale paper-based sensors production.

There are three significant advantages of using paper sizing chemistry to fabricate paper-based microfluidic sensors. First, papermakers are very familiar with paper sizing chemistry; the representative paper sizing agents are alkyl ketene dimer (AKD), alkenyl ketene dimer (liquid AKD) and alkenyl succinic acid anhydrate (ASA). These sizing agents are widely and globally used in papermaking industry. Second, AKD and ASA are the cheapest paper patterning materials among all patterning materials so far reported for fabrication of paper-based diagnostic devices. Since price is a very

sensitive factor for paper-based microfluidic diagnostic devices, material cost for making these devices is therefore an important point of consideration (Bruzewicz et al. 2008). A detailed cost analysis can be found in the discussion section. Third, by combining paper sizing chemistry and printing technology, it is possible to upscale the fabrication of paper-based microfluidic devices. Making physical hydrophobic barriers to build channels in paper is a limiting step to the speed and cost of large scale fabrication. The physical barrier approaches usually involve polymer impregnation followed by pattern developing. The approach reported in this study potentially enables the fabrication of paper-based microfluidic devices, i.e. pattern and incorporated sensing chemistries, with continuous high-speed and large-volume industrial printing processes, enabling the ultimate practical use of the devices for health care and environmental purposes. Since printed paper retains its original flexibility, the new method fundamentally overcomes the problem of channel damage by folding and bending. Furthermore, simple and functional elements, such as valve-controlled reactor, can be easily built into paper-based microfluidic devices made by this novel approach.

Experimental section

Sizing agents

Alkyl ketene dimer (Wax 88 konz, BASF) and alkenyl ketene dimer (Precis 900, Hercules Australia Pty Ltd) were used as the cellulose hydrophobization (or sizing) agents. Both dimers have two hydrocarbon chains of C_{16} – C_{20} . Alkenyl ketene dimer, however, has one $-C=C-$ in each of its two hydrocarbon chains (Qiao et al. 2006). Analytical grade *n*-heptane (Sigma–Aldrich) was used as the solvent to make solutions of both dimers.

Paper-based microfluidic devices

Whatman filter paper (No. 4) was used as the paper substrate. In the first concept-proving approach, filter papers were sized and then treated with plasma to generate hydrophilic patterns. Filter paper samples were dipped in and shortly removed out of an alkyl ketene dimer - heptane solution (0.6 g/L) to allow

evaporation of heptane. Filter paper samples were then heated in an oven at 100 °C for 5 min to facilitate the curing of alkyl ketene dimer on cellulose fibres. The hydrophobized samples were sandwiched between metal masks and then treated with a vacuum plasma reactor (K1050X plasma asher (Quorum Emitech, UK)) for 15 s at the intensity of 15 W. The vacuum level for the treatment was 6×10^{-1} mbar. Metal masks were made by mechanically cutting the desired patterns with through stainless steel sheets. The treated paper samples retained their original flexibility without visible marks.

In the second approach, filter papers were printed using a reconstructed commercial digital ink jet printer (Canon Pixma ip4500) with electronically generated patterns of an alkenyl ketene dimer–heptane solution (2%, v/v). Printing does not leave any visible mark on paper samples which retained their original flexibility. The printed filter paper samples were then heated in an oven at 100 °C for 8 min to cure alkenyl ketene dimer onto cellulose fibres. Printing of water-based sizing emulsion is also possible, it will be a separate topic discussed elsewhere.

Preparation of liquid samples

Millipore purified water was used to prepare all liquid samples. The stock solution of NO_2^- (10.0 mmol/L) was prepared by dissolving 69.0 mg sodium nitrite ($\geq 99\%$, Sigma–Aldrich) in 100 mL water. The indicator solution for NO_2^- contains 50 mmol/L sulfanilamide ($\geq 99\%$, Sigma–Aldrich), 330 mmol/L citric acid ($\geq 99.5\%$, Sigma–Aldrich), and 10 mmol/L *N*-(1-naphthyl) ethylenediamine ($\geq 98\%$, Sigma–Aldrich) (Blicharz et al. 2008).

The UA stock solution (12.8 mmol/L) was prepared with dissolving 215.0 mg uric acid ($\geq 99\%$, Sigma–Aldrich) in 100 mL sodium hydroxide solution (0.2 mol/L). The indicator solution for UA consists of the 1:1 mixture of solution A (2.56% (w/v) 2,2'-biquinoline-4,4'-dicarboxylic acid disodium salt hydrate, $\geq 98\%$, Sigma–Aldrich) and solution B (20 mmol/L sodium citrate and 0.08% (w/v) copper (II) sulfate, $\geq 99\%$, Sigma–Aldrich) (Blicharz et al. 2008).

The mixed sample solution (625 μ mol/L NO_2^- , 800 μ mol/L UA) was prepared using NO_2^- and UA stock solutions.

Results and discussion

Hydrophilic-hydrophobic contrast of untreated and treated papers

The common reactive functional group of alkyl and alkenyl ketene dimers is the four-member lactone ring. It is connected to two long hydrocarbon chains. Once alkyl and alkenyl ketene dimers are immobilized on fibre surface via the (esterification) reaction with $-OH$ groups of cellulose, the two hydrocarbon chains impart hydrophobicity to cellulose fibre surface (Shen et al. 2000).

The sized filter paper samples are strongly hydrophobic and have contact angles of typically 110 – 125° with water (Shen et al. 2000), whereas unsized cellulose has a contact angle of only 25° with water (Kannangara et al. 2006). The Washburn equation has been used as the first order approximation to study the penetration of liquids in paper (Eq. (1)) (Hodgson and Berg 1988):

$$l = \sqrt{\frac{\gamma r \cos \theta}{2\eta} t} \quad (1)$$

Where l is the liquid penetration distance in paper, r is the equivalent capillary pore radius of paper, γ and η are the surface tension and viscosity of the liquid, θ is the contact angle and t is the time of penetration. Equation (1) shows that if a paper surface sustains an apparent contact angle with a liquid of greater than 90° , then liquid penetration will

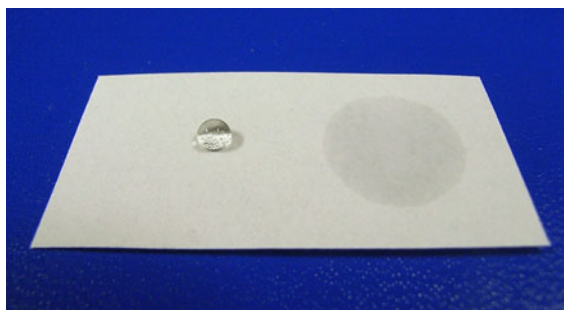
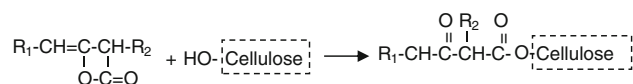


Fig. 1 Water wettability of a half-sized and half-unsized filter paper

Scheme 1



not occur. Figure 1 shows the hydrophilic-hydrophobic contrast of a half-sized and half-unsized filter paper when exposed to water. This phenomenon motivated us to investigate the use of the hydrophilic-hydrophobic contrast to fabricate microfluidic patterns in paper.

AKD sizing required the AKD to first spread over the fibre surface in paper. As AKD in paper is subjected to moderate heat for curing treatment, it redistributes in the fibre matrix via several possible mechanisms: capillary wicking along fibre gaps (Shen and Parker 2001); vaporization and re-deposition (Zhang et al. 2007); fibre wetting by AKD via autophobic precursor (Seppanen et al. 2000; Shen and Parker 2001); low-temperature spreading after curing treatment (Shen et al. 2003). Among those mechanisms, the capillary wicking and vapour re-deposition are fast redistribution mechanisms, whereas the autophobic precursor and low temperature spreading after curing treatment are very slow mechanisms. Zhang et al. (2007) investigated the chemical composition of “AKD vapour” and have found that “AKD vapour” is dominantly fatty acids which do not provide strong sizing to paper. Therefore, the only fast AKD redistribution mechanism is likely to be capillary wicking of AKD along inter- and intra- fibre gaps. If the amount of AKD applied to paper can be well controlled, the capillary wicking distance of AKD in fibre gaps can also be controlled. Therefore, the spreading of AKD in paper can be controlled; and the use of sizing to create hydrophilic-hydrophobic contrast is possible. After spreading, AKD reacts with the cellulose in paper following Scheme (1).

There have been controversies regarding the mechanism and the degree of AKD-cellulose reaction during sizing. The details of AKD-cellulose chemical reaction mechanism, however, are outside of the scope of this study.

Fabrication of paper-based microfluidic devices

Plasma treatment was used to prove the principle of using hydrophilic-hydrophobic contrast for the fabrication of paper-based microfluidic devices. Plasma treatment of hydrophobic paper with patterned masks

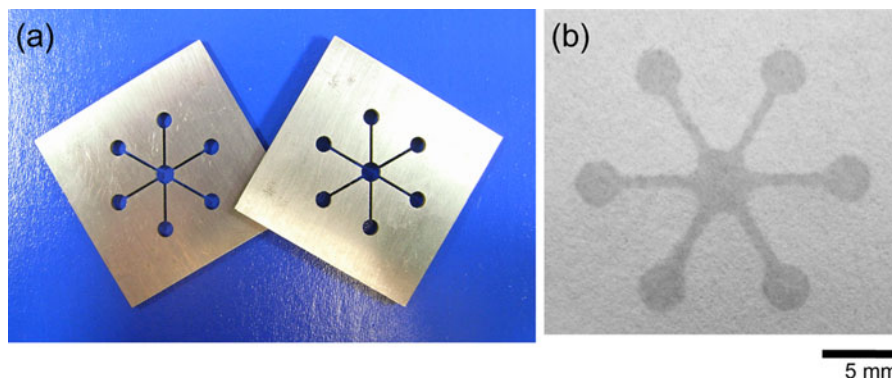


Fig. 2 **a** Two identical metal masks for fabrication of paper-based microfluidic devices with plasma treatment; **b** A six-channel pattern fabricated using masks and plasma reactor (wetted with water)

provides an easy method to selectively introduce hydrophilic patterns to hydrophobic paper. Figure 2 shows the masks with desired pattern and a six-channel pattern created on the sized filter paper surface with these two masks by plasma treatment. Water was introduced from the central inlet zone and penetrated within the channels via capillary penetration.

A reconstructed ink jet printer was used to print the alkenyl ketene dimer–heptane ink solution onto an untreated filter paper. After curing, the printed area became strongly hydrophobic and the non-printed area remained hydrophilic. The printed area sustained water contact angle of greater than 110° .

Printed paper-based microfluidic devices retain their original flexibility. Figure 3 shows a computer-generated electronic pattern (blue area was the intended printing (sized) area while white area was the non-printing (unsized) hydrophilic area) and the microfluidic pattern on filter paper. Water was introduced to reveal the printed and sized area as well as the non-printed hydrophilic area.

Current commercial digital ink jet printers are capable of issuing small droplets of a few picolitres and small amount of ink for generating patterns on paper. The reconstructed printer also inherits this frugal ink management feature. Heptane is a fast evaporating solvent; its fast evaporation after printing

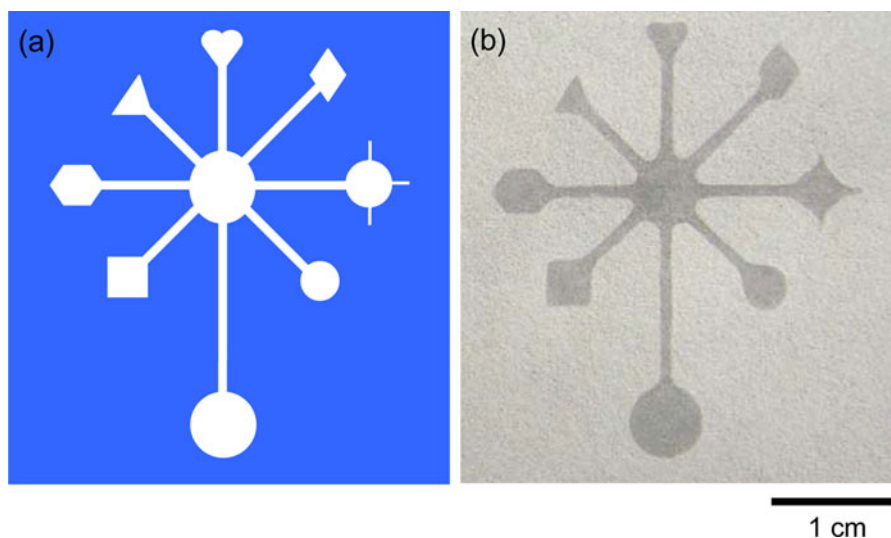


Fig. 3 **a** Computer-generated electronic pattern for ink jet printing of paper-based microfluidic device; **b** Ink jet printed microfluidic pattern on filter paper with borders defined by the hydrophilic-hydrophobic contrast (wetted with water)

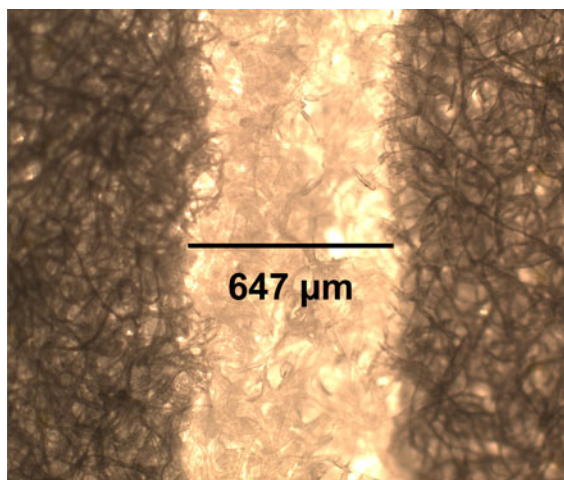


Fig. 4 The microscope image of a water wetted microfluidic channel on filter paper, showing the hydrophobic channel wall is strong enough to guide capillary penetration of water within the channel

limits the penetration of the solution into the paper matrix. This allows the hydrophilic channels on paper surface created by printing to have a well-defined hydrophilic-hydrophobic border. Figure 4 shows a micrograph of a water wetted paper channel fabricated by printing. The channel wall defined by the hydrophilic-hydrophobic contrast is able to guide liquid capillary flow in the channel. It can be envisaged that with the web-based ink jet printing facilities, high speed printing of sensors is possible.

Printing sensing reagents or biomolecules on paper-based microfluidic devices

Ink jet printing of biomolecules has been reported previously by many research groups (Vauvreau and Laroche 2005; Risio and Yan 2007). Ink jet printing is a non-contact printing process, which offers a unique advantage of minimizing cross-sample contamination. The printing of the sizing agents on paper to build the microfluidic channels has added a new capability to ink jet printing for device fabrication; the multiple printing cartridges of ink jet printers can be used to print different materials. By combining printing of sensing reagents or biomolecules and the printing of sizing agents together, a new approach for fabrication of paper-based microfluidic sensors is formed.

Paper-based microfluidic devices for qualitative multi-analyte detection and quantitative analysis

To illustrate the use of paper-based microfluidic devices for multiple analytes measurement, NO_2^- and UA were used as two example analytes, since they are two important biomarkers for a number of human health conditions (Nagler 2008). In this test, the NO_2^- and UA indicator solution (0.5 μL) has been deposited onto detection zones N (for NO_2^-) and U (for UA) separately as shown in Fig. 5a. Then

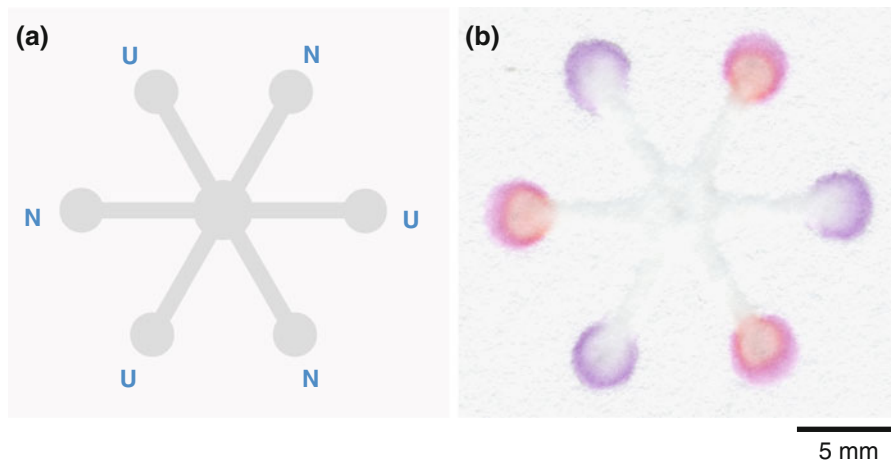


Fig. 5 Qualitative multiple analytes detection with paper-based microfluidic devices **a** The assay design: NO_2^- indicator and UA indicator were deposited in alternation into the six detection zones marked with N (for NO_2^-) and U (for UA);

b Mixed sample solution containing NO_2^- and UA was introduced from central inlet zone; the sample penetrated into different detection zones to trigger different colour changes (pink for NO_2^- and purple for UA)

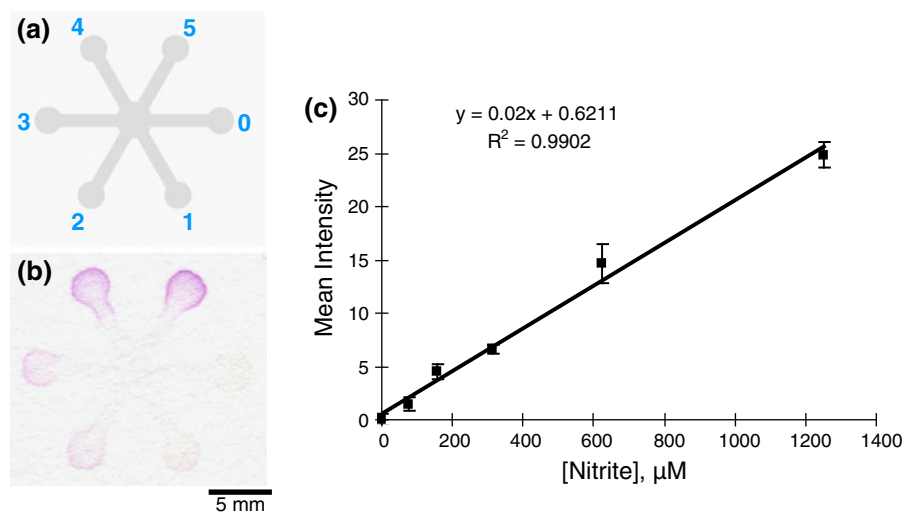


Fig. 6 Quantitative biological/chemical assay using paper-based microfluidic devices **a** The assay design: NO_2^- standard solutions ($0.5 \mu\text{L}$) with different concentration from 0 to $1250 \mu\text{mol/L}$ were deposited into detection zone 0 to zone 5 in sequence; **b** NO_2^- indicator solution was added into the device

the mixed sample solution ($625 \mu\text{mol/L NO}_2^-$, $800 \mu\text{mol/L UA}$) was introduced from the central sample inlet zone; the sample solution penetrated into each and every detection zone within 2 s. Different detection zones showed different colour development, indicating positive detections of NO_2^- (pink) and UA (purple), respectively (Fig. 5b). This test shows that sized paper sensors are capable of detecting multiple chemical species in unknown samples.

Paper-based microfluidic devices can also be utilized for quantitative biological or chemical analyses, such as creating calibration curve, measuring sample concentration. Compared with the traditional UV–vis spectrophotometry method, the paper sensor method is a much cheaper and easier analytical approach, and requires lower sample volumes ($<1 \mu\text{L}$). To show this capability of paper-based devices, six serially diluted NO_2^- standard solutions (0, 78, 156, 312, 625 and $1250 \mu\text{mol/L}$, $0.5 \mu\text{L}$) prepared using NO_2^- stock solution were deposited into six different detection zones of a blank paper-based microfluidic device from zone 0 to 5 (Fig. 6a). After that, NO_2^- indicator solution ($5 \mu\text{L}$) was added from the central inlet zone and penetrated into different detection zones to give different colour development from nearly colorless to strong pink (Fig. 6b). Then we used a desktop scanner (Epson

from central inlet zone and caused different colour changes in different detection zones; **c** Calibration curve created by colour density measurement using Adobe Photoshop of the scanned images of the tests. Error bars were obtained from six repeated measurements

Perfection 2450, colour photo setting, 1,200 dpi resolution) to capture the image and the histogram function of Adobe Photoshop to measure the colour intensity in different detection zones. Six independent measurements were operated with six paper-based microfluidic devices. The NO_2^- calibration curve obtained in this test (Fig. 6c) shows that sized patterned paper-based devices have great potential to conduct quantitative assays at very low cost. In our previous work reported elsewhere, we have successfully applied the quantitative analysis approach using sized paper sensors to analyze unknown NO_2^- and UA samples with high accuracy which was comparable to that of UV–vis spectroscopy method (Li et al. 2010).

Functional elements for enhanced sensing capability

Functional elements can be easily built in paper-based microfluidic devices to provide cheap and easy-to-use functional devices (e.g., switches, separators (Li et al. 2008)) for various applications. A simple valve-controlled reactor design was presented in this study to demonstrate the possibility of creating functional components on paper-based microfluidic devices. Figure 7a–c shows the concept of a reactor design on paper, in which different reagents can be

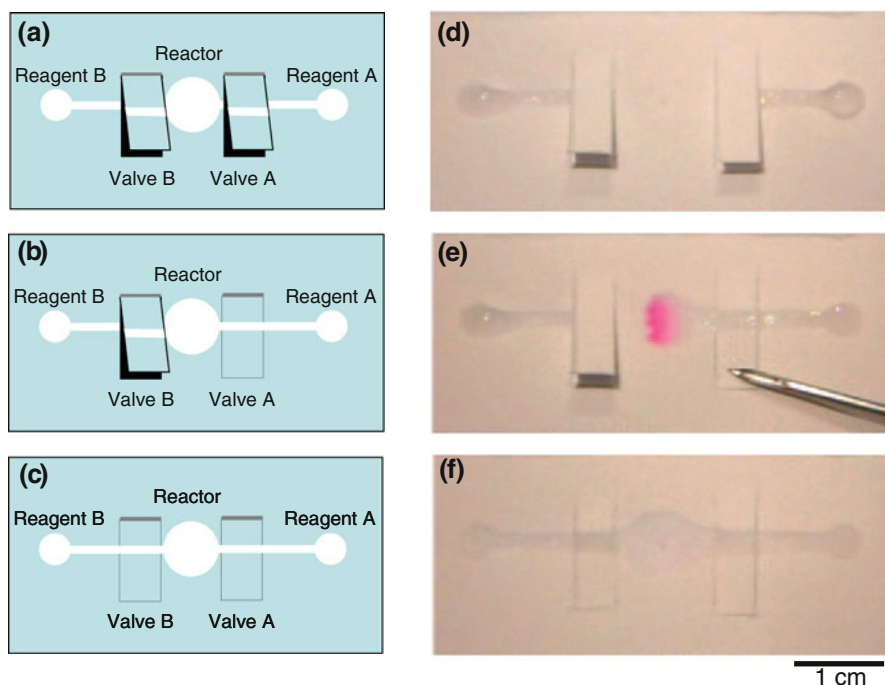


Fig. 7 **a–c** A design of a simple paper-based microfluidic reactor consisting of two sample dosing sites, two valves, and one central reaction site; **d–f** A paper-based microfluidic reactor based on this design was tested using acid–base neutralization reaction (**d** Phenolphthalein indicator solution was deposited onto the central reaction zone. NaOH and HCl

solutions were added into reagent zones A and B, respectively; **e** NaOH solution was introduced into the reaction zone to trigger colour change; **f** HCl solution was introduced later into the reaction zone via valve B to neutralize NaOH in the reaction zone)

introduced into the reactor at different time controlled by two valves. An acid–base neutralization reaction was used to illustrate the feasibility. NaOH and HCl solutions were added into reagent A and B zones, respectively. A small amount of phenolphthalein indicator solution was deposited onto the central reaction zone (Fig. 7d). The NaOH solution was firstly introduced into the reaction zone to trigger the colour change (Fig. 7e), and then the HCl solution was introduced into the reaction zone via valve B to neutralize NaOH in the reaction zone. The completion of the reaction is indicated by the fading of pink colour (Fig. 7f). The simple reactors such as the one shown in Fig. 7 are useful for multi-step chemical and biological assays.

Discussion

Compared with the previous barrier fabrication method, the new fabrication concept enables the

manufacturing of paper-based microfluidic devices by simpler process and at low cost. Creation of hydrophilic–hydrophobic contrast is a simpler approach to define aqueous liquid penetration channels in paper than the barrier approach. Several major commercial paper sizing chemistry systems are suitable for paper-based microfluidic devices fabrication. It is expected that ink jet, flexo and gravure may be the most suitable processes to print sizing agents on paper surface. The requirement of curing of the AKD and ASA chemistries presents a challenge to the continuous production of paper-based diagnostic devices. However, it is possible to add a roller-nip heating station between the printing stations for pattern and for sensing reagents printing. Among these processes, ink jet printing has a further advantage of non-contact liquid delivery, which is highly desirable for printing detection chemistries into the devices. With the advance of web ink jet printers, continuous production of paper-based microfluidic diagnostic sensors will become a reality in future.

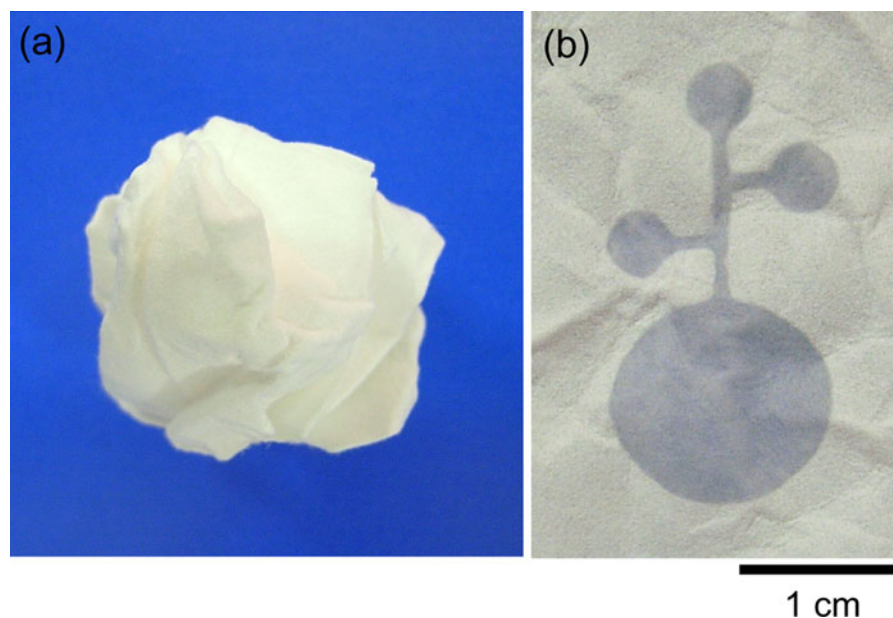


Fig. 8 **a** The paper-based microfluidic device was subjected to a harsh folding test; **b** The performance of the device showed no deterioration after the test

The use of digital printing technology to selectively deliver paper sizing chemicals on paper surface to form the hydrophilic-hydrophobic contrast has another advantage. Digital printing offers electronic pattern variation which allows fast change over for fabrication of different devices. Since the hydrophilic-hydrophobic contrast fabrication concept can retain the original flexibility of the paper, it offers natural bending and folding resistance to the paper-based microfluidic devices, which fundamentally overcomes the poor bending and folding resistance often encountered with some other techniques. Figure 8 shows an example of a bending and folding test. The performance of the ink jet printed patterns shows no discernable deterioration after the test.

The concept of hydrophilic-hydrophobic contrast in paper allows simple yet functional elements such as valves to be built into devices. Reactor systems are possible by combining valves, channels and reservoir. Multi-step diagnostic tests can also be achieved with reactors. Valve can also be built in 3D paper-based microfluidic devices having paper-film-paper structure; a liquid sample can be directed from one sheet of paper to the other by activating a valve. Commercial printing can easily build simple valves on paper by die-cutting operations. By printing hydrophilic-hydrophobic contrast on papers, a plethora of flexible

microfluidic devices can be fabricated and their production is able to be scaled up.

Since AKD and ASA sized paper does not resist the penetration of oil or low surface tension aqueous liquids, sized paper-based microfluidic channels are likely to widen when transport these samples (surface tension <35 mN/m). In these circumstances, sensors made of cotton thread can be used (Li et al. *in press*). Thread-based sensors does not rely on the barrier or the hydrophilic-hydrophobic contrast to define the liquid passageway, they therefore can transport oil and surfactant solutions effectively. Alternatively, sensors made using fluorocarbon-based sizing agents or barriers that can resist oil or surfactant solutions can be used.

As mentioned earlier, AKD and ASA are the cheapest paper patterning materials among all patterning materials so far reported for fabrication of paper-based diagnostic devices. Taking AKD for example, the whole sale prices of AKD from European manufacturers are 3–4 euro per kilogram, whereas the cost of ASA is even lower. The AKD usage in paper sizing is typically less than 5 kg per ton of dry fibre. If the basis weight of the paper is 92 g/m^2 and the area of each paper microfluidic sensor is 25 cm^2 (i.e. $5 \text{ cm} \times 5 \text{ cm}$), the cost of AKD on each device will only be 0.000005 euro. In

laboratory scale fabrication, each A4 sheet of paper can produce 20 devices; using the printing method reported in this work and taking ink consumption for printing each A4 sheet as 400 μL , the AKD cost of each device (25 cm^2) will be 0.000002 euro, significantly cheaper than the non-paper material costs of all fabrication methods reported to date. The barrier material costs of each barrier-based paper sensor reported previously were \$0.025 for photoresist SU-8 (Martinez et al. 2008a, b) and \$0.0025 for PDMS (Bruzewicz et al. 2008).

The qualitative and, in particular, quantitative analysis with the use of self calibration standards make paper-based microfluidic sensors cost-competitive devices for health care and environment monitoring applications. Some future improvements of paper-based devices identified in our research are to further reduce the sampling amount to match those microfluidic analytical devices made using expensive technologies, to significantly increase sample delivering efficiency so as to allow paper-based microfluidic devices to handle low concentration biological and environmental samples and, to make paper-based diagnostics as a reliable means to perform mass analytical tasks such as population screening for certain health threats.

Conclusion

This article reports the progress of using patterned sizing and printing method to fabricate paper-based microfluidic devices. Sized paper shows strong wetting contrast to the unsized paper. Combining this hydrophilic-hydrophobic contrast concept with ink jet printing, well-defined microfluidic channels can be created into paper. Ink jet printing can also print required detection chemistries or biomolecules into the pattern to form complete paper-based microfluidic sensors. This fabrication concept provides potential for the mass production of paper-based sensing devices at very low cost.

Paper-based microfluidic devices fabricated using the hydrophilic-hydrophobic contrast concept retain the original flexibility of paper. It allows simple and functional elements, such as valves and reactors, to be built into the devices. With these functional elements, more advanced paper-based devices can be designed and fabricated.

The analytical capability of paper-based sensors fabricated using patterned AKD sizing shows that paper-based sensors have the potential to change the way of some analytical chemistries are performed.

Acknowledgments The research scholarships of Monash University and the Department of Chemical Engineering are gratefully acknowledged. BASF and Hercules Australia are thanked for kindly providing paper sizing agents.

References

- Abe K, Suzuki K, Citterio D (2008) Inkjet-printed microfluidic multianalyte chemical sensing paper. *Anal Chem* 80:6928–6934
- Blicharz TM, Rissin DM, Bowden M, Hayman RB, DiCesare C, Bhatia JS, Grand-Pierre N, Siqueira WL, Helmerhorst EJ, Loscalzo J, Oppenheim FG, Walt DR (2008) Use of colorimetric test strips for monitoring the effect of hemodialysis on salivary nitrite and uric acid in patients with end-stage renal disease: a proof of principle. *Clin Chem* 54:1473–1480
- Bruzewicz DA, Reches M, Whitesides GM (2008) Low-cost printing of poly(dimethylsiloxane) barriers to define microchannels in paper. *Anal Chem* 80:3387–3392
- Carrilho E, Martinez AW, Whitesides GM (2009) Understanding wax printing: a simple micropatterning process for paper-based microfluidics. *Anal Chem* 81:7091–7095
- Dungchai W, Chailapakul O, Henry CS (2009) Electrochemical detection for paper-based Microfluidics. *Anal Chem* 81:5821–5826
- Hodgson KT, Berg JCJ (1988) The effect of surfactants on wicking flow in fiber networks. *Colloid Interface Sci* 121:22–31
- Hossain SMZ, Luckham RE, McFadden MJ, Brennan JD (2009) Reagentless bidirectional lateral flow bioactive paper sensors for detection of pesticides in beverage and food samples. *Anal Chem* 81:9055–9064
- Kannangara D, Zhang H, Shen W (2006) Liquid-paper interactions during liquid drop impact and recoil on paper surfaces. *Colloid Surf A-Physiochem Eng Asp* 280:203–215
- Li X, Tian J, Nguyen T, Shen W (2008) Paper-based microfluidic devices by plasma treatment. *Anal Chem* 80:9131–9134
- Li X, Tian J, Shen W (2010) Quantitative biomarker assay with microfluidic paper-based analytical devices. *Anal Bioanal Chem* 396:495–501
- Li X, Tian J, Shen W (in press) Thread as a Versatile Material for Low-Cost Microfluidic Diagnostics. *ACS Appl Mater Interface* doi: 10.1021/am9006148
- Lu Y, Shi W, Jiang L, Qin J, Lin B (2009) Rapid prototyping of paper-based microfluidics with wax for low-cost, portable bioassay. *Electrophoresis* 30:1497–1500
- Martinez AW, Phillips ST, Butte MJ, Whitesides GM (2007) Patterned paper as a platform for inexpensive, low-volume, portable bioassays. *Angew Chem Int Ed* 46:1318–1320

- Martinez AW, Phillips ST, Carrilho E, SW ThomasIII, Sindi H, Whitesides GM (2008a) Simple telemedicine for developing regions: camera phones and paper-based microfluidic devices for real-time, off-site diagnosis. *Anal Chem* 80:3699–3707
- Martinez AW, Phillips ST, Wiley BJ, Gupta M, Whitesides GM (2008b) Flash: a rapid method for prototyping paper-based microfluidic devices. *Lab Chip* 8:2146–2150
- Nagler RM (2008) Saliva analysis for monitoring dialysis and renal function. *Clin Chem* 54:1415–1417
- Qiao L, Gu QM, Cheng HN (2006) Enzyme-catalyzed synthesis of hydrophobically modified starch. *Carbohydr Polym* 66:135–140
- Risio SD, Yan N (2007) Piezoelectric ink-jet printing of horseradish peroxidase: effect of ink viscosity modifiers on activity. *Macromol Rapid Commun* 28:1934–1940
- Seppanen R, Tiberg F, Valignat MP (2000) *Nord Pulp Paper Res* 15:452–458
- Shen W, Parker IH (2001) A preliminary study of the spreading of AKD in the presence of capillary structures. *J Colloid Interface Sci* 240:172–181
- Shen W, Filonanko Y, Truong Y, Parker IH, Brack N, Pigram P, Liesegang J (2000) Contact angle measurement and surface energetics of sized and unsized paper. *Colloid Surf A-Physiochem Eng Asp* 173:117–126
- Shen W, Xu F, Parker IH (2003) An experimental investigation of the redistribution behaviour of alkyl ketene dimers and their corresponding ketones. *Colloid Surf A* 212:197–209
- Stock R, Rice CBF (1974) *Chromatographic methods*, 3rd edn. Chapman and Hall, London, p 106
- Vauvreau V, Laroche G (2005) Micropattern printing of adhesion, spreading, and migration peptides on poly(tetrafluoroethylene) films to promote endothelialization. *Bioconjugate Chem* 16:1088–1097
- Whitesides GM (2006) The origin and future of microfluidics. *Nature* 442:368–373
- Zhang H, Kannangara D, Hilder M, Ettl R, Shen W (2007) The role of vapour deposition in the hydrophobization treatment of cellulose fibres using alkyl ketene dimers and alkenyl succinic acid anhydrides. *Colloid Surf A* 297:203–210
- Zhao W, van der Berg A (2008) Lab on Paper. *Lab Chip* 8:1988–1991

Thread as a Versatile Material for Low-Cost Microfluidic Diagnostics

Xu Li, Junfei Tian, and Wei Shen*

Australian Pulp and Paper Institute, Department of Chemical Engineering, Monash University, Clayton Campus, VIC 3800 Australia

ABSTRACT This paper describes a new and simple concept for fabricating low-cost, low-volume, easy-to-use microfluidic devices using threads. A thread can transport liquid via capillary wicking without the need of a barrier; as it is stainable, it is also a desirable material for displaying colorimetric results. When used in sewing, threads have 3D passageways in sewed materials. The wicking property and flexibility of thread make it particularly suitable to fabricate 3D microfluidic devices. Threads can also be used with other materials (e.g., paper) to make microfluidic devices for rapid qualitative or semiquantitative analysis. These thread-based and thread-paper-based devices have potential applications in human health diagnostics, environmental monitoring, and food safety analysis, and are particularly appropriate for the developing world or remote areas, because of their relatively low fabrication costs.

KEYWORDS: thread • paper • diagnostics • 3D microfluidics • low-cost sensors.

New concepts and applications of low-cost, portable, and field-based diagnostic technologies have become an area attracting a lot of research interest (1). The potential of these technologies in providing affordable healthcare and environmental monitoring to remote and developing regions strongly drives the continuous developments of these technologies. The recent rise of paper-based microfluidic devices (2–5) once again shows the attraction of low-cost and field-based technologies.

Cotton thread as an ancient material in civilization is also an attractive material for the fabrication of low-cost and low-volume microfluidic diagnostic devices for healthcare and environmental assays. This is because that the gaps between fibers provide capillary channels for liquids to wick along the thread. Thread has been used for sensor fabrication, but only for purposes other than building microfluidic sensors. The idea of using electronic threads for human health monitoring has been reported in many studies (6–9). The electronic threads are usually metal-based threads (7) or threads made by carbon nanotubes coated with polyelectrolytes (8, 9). To the best of our knowledge, there has been no work reported using cotton or other multifilament threads for fabricating simple and low-cost microfluidic analytical devices.

In this study, cotton thread is used to fabricate microfluidic devices with 3D structures by sewing it onto other materials (e.g., polymer film). In this way, we show the possibility to fabricate high density thread microfluidic channels to enable the transportation of several liquids through the structure without mixing. Threads with different wettability can also be used to manipulate liquid wicking and mixing. These capabilities further enable us to fabricate 3D

thread-based microfluidic devices which encompass complicated microfluidic channels compared to lateral flow systems (5). The fabrication of thread-based microfluidic devices is simple and relatively low-cost, because it requires only sewing needles or household sewing machines, which are commonly used and affordable, even in some of the under-developed regions. Liquids can penetrate from thread into other hydrophilic porous materials; therefore, thread can be used with other materials (e.g., paper) to form microfluidic devices with enhanced sample delivering efficiency. In this work, thread-based and thread-paper-based microfluidic sensors are fabricated with the incorporated colorimetric indicators for two important biomarkers for several human medical conditions, nitrite ion (NO_2^-) and uric acid (UA) (10–12). The potential of using thread and thread-paper microfluidic sensors to provide low-cost, low-volume, semiquantitative, and multispecies analysis is shown through the detection and measurement of these species. Our results demonstrate that thread is a suitable material for fabricating microfluidic diagnostic devices for monitoring human health, environment and food safety; especially for the population in less-industrialized areas or remote regions (13, 14).

Experimental Section. Cotton thread was kindly provided by the School of Fashion and Textiles, RMIT University, Melbourne, Australia. The average diameter of the thread was measured using a microscope (Olympus, BX-60) that was interfaced to a PC to allow object size measurement. The cotton thread was found to have an average thickness of $244 \pm 41 \mu\text{m}$. Natural cotton thread is not wettable by aqueous liquids; this is because natural cotton fibers have wax on their surface and in the fiber wall. Therefore, natural cotton thread needs to be dewaxed or surface treated to allow the wicking of aqueous liquids (15). In this study, to obtain hydrophilic cotton thread, we used a vacuum plasma reactor (K1050X plasma asher (Quorum

* Corresponding author. Tel: +61 3 99053447. Fax: +61 3 99053413. E-mail: wei.shen@eng.monash.edu.au.

Received for review September 11, 2009 and accepted November 27, 2009

DOI: 10.1021/am9006148

© 2010 American Chemical Society

Table 1. Surface Atomic Concentration of C and O of Untreated and Treated Threads

sample	filter paper (cellulose)	thread (untreated)	thread (plasma treated)	binding energy (eV)	assignment
C (1 + 2)	0.215	0.784	0.562	285.0, 285.5	C—C, C—H
C (3)	0.605	0.163	0.261	286.8	C—O
C (4)	0.180	0.032	0.107	288.3	O—C—O, C=O
C (5)		0.021	0.069	289.2	O—C=O
O	0.596	0.139	0.574	533.2	

Emitech, UK)) to treat cotton thread for 1 min at an intensity of 50 W. The vacuum level for the treatment was 6×10^{-1} mbar.

The treated and untreated thread samples were analyzed using XPS to show the effect of the plasma treatment on their surface chemistry and wettability differences. XPS analysis was conducted using an AXIS HSI spectrometer (Kratos) with monochromatized Al K α radiation. The photoelectron emission angle was 90° with respect to the sample surface. This corresponds to a maximum sampling depth of ca. 10 nm. Thread samples were wound around a sample holder to form a closely packed mesh providing the necessary area for the X-ray beam, which was about 2 mm in diameter. Table 1 lists the changes in surface atomic concentration of C and O before and after plasma treatment. Filter paper was used as the control for cellulose. The presence of C (1 + 2) on filter paper surface was most likely due to surface contamination during the production and packaging processes. Plasma treatment may have two effects on the thread surface modification: First, the surface was substantially oxidized; this is indicated by the increase in surface concentration of C species with binding energies of 288.3 and 289.2 eV, which correspond to the generation of surface O—C—O, C=O and O—C=O groups. Second, the increase in surface concentration of C—O (286.8 eV) may mean that the plasma treatment also partially removed wax and exposed the underlying cellulose. These combined changes significantly increased the surface oxygen concentration (Table 1) and therefore increased surface polarity. The increased water wettability after plasma treatment is consistent with the surface chemistry changes revealed by XPS. After treatment, water can readily wet and wick along the cotton thread.

To characterize the hydrophobic and hydrophilic contrast between threads, we prepared a series of water–isopropyl alcohol (IPA) (HPLC grade, EMD Chemicals Inc.) solutions with different IPA mass percentages (14, 16, 18, 20, 22, and 24%) as a means to measure the onset of wicking of water–IPA solutions in untreated cotton thread. Because the surface tension values of the water–IPA system are known (16), it can be used as a convenient measure to characterize the wicking property of the thread. Aspler et al. (17) and Nisbet et al. (18) have shown that the polar liquid wicking in a porous material occurs when the surface tension of the liquid is lowered to a critical value. The wicking onset, in the porous material, can be identified by testing the wicking speed of a series of liquids with different surface tension values. Although high surface tension liquids do not wick (zero speed) in the material, liquids that have a certain surface tension value start to wick in the material at an

observable speed. Aspler et al. (17) referred this surface tension value as the critical wicking surface tension. Liquids that have a surface tension lower than this value can all wick in the material. This method was used to identify the liquid wicking onset of untreated cotton thread.

Millipore-purified water was used to prepare all aqueous samples required for testing the performance of threads. The ink solutions (cyan, magenta, blank and yellow) used in the liquid wicking experiments were prepared by diluting commercial Canon ink jet inks (CLI Y-M-C-BK, PGBK (<http://www.canon.com.au/>)) with water. The red ink solution was prepared by mixing magenta and yellow ink solutions. The green ink solution was a mixture of cyan and yellow ink solutions. The density values of the ink solutions were measured using a Mettler Toledo Densito 30Px (Switzerland). The surface tension of the ink solutions were measured by the capillary rise method (19) using a cathetometer. Glass capillary tubes were first washed with laboratory detergent (RBS 35 detergent, Chemical Products, Belgium), followed by rinsing with ample amounts of water. The capillary tubes were dried under ambient temperature, followed by 60 °C oven drying. Finally, the tubes were plasma treated to ensure complete wetting. The tube diameter was determined by measuring the capillary raise of n-hexadecane (Aldrich, >99%) of known surface tension.

The stock solution of NO $_2^-$ (10.0 mmol/L) was prepared by dissolving 69.0 mg of sodium nitrite ($\geq 99\%$, Sigma-Aldrich) in 100 mL water. This stock solution was then diluted with water to get serially diluted NO $_2^-$ standard solutions with concentrations of 1000, 500, 250, 125, and 0 μ mol/L. The indicator solution for NO $_2^-$ contained 50 mmol/L sulfanilamide ($\geq 99\%$, Sigma-Aldrich), 330 mmol/L citric acid ($\geq 99.5\%$, Sigma-Aldrich), and 10 mmol/L N-(1-naphthyl) ethylenediamine ($\geq 98\%$, Sigma-Aldrich) (10).

The UA stock solution (10.0 mmol/L) was prepared by dissolving 168.1 mg of uric acid ($\geq 99\%$, Sigma-Aldrich) in 100 mL of NaOH solution (0.2 mol/L). The UA sample solution (1000 μ mol/L) was prepared by further diluting the stock solution with NaOH solution. The indicator solution for UA consisted of a 1:1 ratio mixture of solution A (2.56% (w/v) 2,2'-biquinoline-4,4'-dicarboxylic acid disodium salt hydrate, $\geq 98\%$, Sigma-Aldrich) and solution B (20 mmol/L sodium citrate and 0.08% (w/v) copper(II) sulfate, $\geq 99\%$, Sigma-Aldrich) (10).

Results and Discussion. Gaps between fibers of cotton threads provide capillary channels for liquids to wick along threads without the need of an external pump. Panels A and B in Figure 1 show two examples of using plasma-treated hydrophilic threads to form 3D structures. In Figure

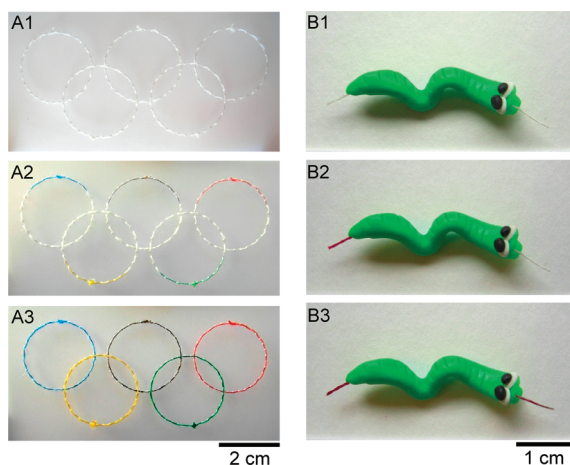


FIGURE 1. (A) Three-dimensional microfluidic pattern fabricated by sewing threads onto a translucent polymer film. (A1) Pattern sewed using hydrophilic cotton threads; (A2) introduction of liquids on threads; (A3) liquids wick throughout the thread pattern. Their stitches cross one another from above and below the polymer film and therefore do not mix. (B) Three-dimensional microfluidic channel of thread imbedded in plasticine. (B1) Imbedded hydrophilic cotton thread in plasticine; (B2) introduction of a liquid on the thread from one end; (B3) liquid wicks along the thread through plasticine.

1A, a 3D microfluidic pattern was fabricated by sewing threads through a polymer film. A translucent polymer film was chosen to visually demonstrate the liquid wicking passageways. In this pattern, the stitches of the threads pass one another from above and below the polymer film, and therefore, do not have contact. Ink solutions of different colors wick along the threads and cross one another without mixing. Thus, threads allow complex continuous 3D microfluidic channels to be built without the need of patterned barriers to define the liquid wicking passageways. High-density thread circuitries can be built in a relatively small space that is suitable for miniaturization. Fabrication of such 3D microfluidic structures with threads requires only some basic tools such as a sewing needle or a household sewing machine, and is therefore less reliant on sophisticated equipment required for patterned paper devices. Figure 1B shows ink solution transport through a cotton thread embedded in plasticine. The ink solution can wick through tortuous passageways, even if the solid material enclosing the thread is not wettable by the wicking liquid. Therefore, when thread is used to provide the capillary driving force for liquid transport, the wetting property of the support material will no longer be a design restriction.

Thread has other interesting properties that can be used to control liquid wicking along it. First, liquid wicking along a thread is controlled by the liquid wettability of thread. The hydrophilic–hydrophobic contrast of the treated and untreated thread provides a convenient option to manipulate liquid transport. The wicking onset characterization using the water-IPA solution series showed that solutions of less than 20% IPA (w/w) form bead on the surface of untreated thread and do not wick along the thread. The surface tension value of this solution is 31.2 mN/m at 20 °C (16). IPA solutions of higher concentrations than 20% can wick along the untreated thread. Therefore, aqueous solutions with a surface

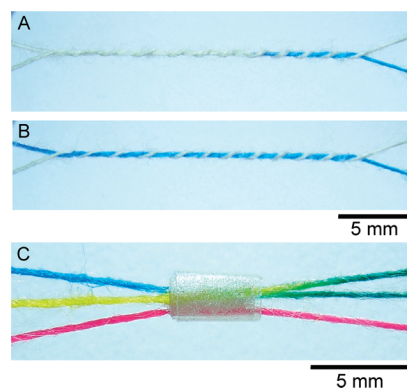


FIGURE 2. (A, B) Twisted pair of an untreated and a plasma-treated cotton thread. When the liquid is introduced onto the treated and hydrophilic thread, the liquid wicks only along the hydrophilic thread. (C) Sample mixing zone demonstrating the manipulation of liquid wicking along threads. The top and the middle threads that transport cyan and yellow liquids are twisted and sleeved inside a heat shrink tube; the bottom thread that transports magenta liquid is not twisted with the other two threads and passes through the mixing zone from outside of the heat shrink tube.

tension higher than 31.2 mN/m can wick only along the treated thread, but not along untreated thread.

The sensitivity of liquid wicking to the surface condition of a thread can be used as a convenient option for designing a thread network to facilitate and control liquid transport. Panels A and B in Figure 2 show a twisted pair of cotton threads, one untreated and the other plasma-treated. The cyan ink solution was introduced onto the treated hydrophilic thread and wicked only along this thread. The surface tension values of all the diluted ink solutions were higher than the critical wicking surface tension of the untreated thread (e.g., the cyan ink solution (10%, v/v) was 37.4 mN/m at 20 °C with the density of 1.022 g/mL). Therefore, the ink solutions can only wick along the treated thread, but not along the untreated thread. Second, liquid wicking can be relayed from a hydrophilic thread to another hydrophilic thread or a hydrophilic porous material. This property of thread makes it possible to use thread with other porous materials to form more sophisticated microfluidic systems. If two hydrophilic threads are twisted together, and a different liquid solution is introduced to each of the thread, the two solutions will mix when the two threads meet. Figure 2C demonstrates a simple mixing zone in a thread device. Three threads pass through a liquid mixing zone, restrained by a tube of sticky tape. The top and the middle threads that transport cyan and yellow ink solutions are twisted and sleeved inside a heat shrink tube; the bottom thread that transports magenta ink solution is not twisted with the other two threads and passes through the mixing zone from outside of the heat shrink tube. The magenta ink solution therefore does not mix with other solutions. The ability to manipulate liquid transport and mixing offers the possibility of using threads to fabricate more sophisticated microfluidic patterns.

Liquids wicking on two twisted hydrophilic threads can mix surprisingly well (Figure 2C). This phenomenon may be related to the good alignment of closely packed long fibres in a thread in a helical arrangement. The fiber gaps, there-

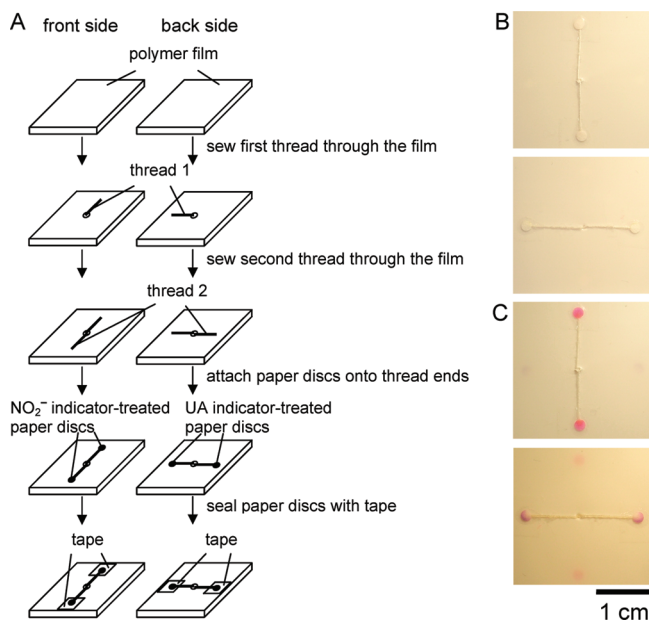


FIGURE 3. Demonstration of a 3D thread-paper microfluidic sensor. (A) Fabrication of the sensor. (B) Front side and back side of the sensor. (C) Different color development on the front side (pink) and back side (purple) of the sensor when multianalyte test solution (500 μM NO_2^- , 500 μM UA) was introduced from the central hole of the sensor onto the two threads and penetrated into paper discs (detection zones).

fore, also have good alignment in the thread. When two threads are twisted together for a number of turns, fiber gaps in one thread are in contact with all fiber gaps of the other thread, and these contacts form new gaps for the liquid to wick. We think the full contact of all fiber gaps between the two twisted threads is responsible for the good liquid mixing result.

Combining the thread properties shown in Figures 1 and 2, multianalyte and 3D microfluidic devices can be easily designed. The combination of thread and filter paper provides a proof-of-concept design for 3D microfluidic devices (Figure 3). Circular paper discs ($\varnothing = 2$ mm) were produced from Whatman No.4 filter paper using a disk punching device (Facit 4070, Sweden) to make thread-paper sensors. Paper discs were immersed either in the NO_2^- or the UA indicator solution respectively to full saturation and were then dried in an oven at 60 $^\circ\text{C}$ for ~ 5 min. Two hydrophilic cotton threads (~ 2 cm) were sewed through an opaque polymer film (2.5 cm \times 2.5 cm), with half the length left on the front side and the other half on the back side of film. The ends of the two threads on the front side were made to contact the two paper discs treated with NO_2^- indicator solution; the other ends of the two threads on the back side were made to contact the paper discs treated with UA indicator solution. Single-sided sticky tape was used to fix the paper discs and threads onto the film (panels A and B in Figure 3). A test solution containing 500 $\mu\text{mol/L}$ NO_2^- and 500 $\mu\text{mol/L}$ UA was prepared by mixing equal volumes of 1000 $\mu\text{mol/L}$ NO_2^- and 1000 $\mu\text{mol/L}$ UA solutions. A 3 μL test solution was introduced onto the threads from the central film hole with a micro pipet (eppendorf research 1.0–10 μL); the test solution rapidly wicked along the threads and

reached paper discs. Paper discs treated with NO_2^- indicator on the front side of the film rapidly developed a pink color, confirming the detection of NO_2^- , whereas paper discs treated with UA indicator on the back side of the film developed a purple color, confirming the detection of UA (Figure 3C). The fabrication process of this kind of thread-paper 3D microfluidic devices is simpler than that reported for 3D microfluidic devices fabricated by stacking layers of paper and tape (20).

Thread can be used by itself for semiquantitative colorimetric assay. Cotton thread is white which provides a desirable reference background for colorimetric detections. An aqueous liquid (0.1 μL) wicks for a length of ~ 6 mm on a plasma-treated household sewing cotton thread which is about the length of two stitches. A thread-based microfluidic device can be made by simply sewing thread onto a support material such as polymer film. For creating NO_2^- calibration curve with thread-based devices, hydrophilic thread was immersed in the NO_2^- indicator solution and was then dried in an oven at 60 $^\circ\text{C}$ for ~ 5 min. Five short threads cut from the indicator-treated thread were sewed onto an opaque polymer sheet with one stitch (~ 3 mm) exposing at the top side of the sheet as the detection zone. Five serially diluted NO_2^- standard solution samples (0.1 μL , 1000, 500, 250, 125, and 0 $\mu\text{mol/L}$) were deposited onto the five sewed threads separately with a micro pipet (eppendorf research 0.1–2.5 μL). Colorimetric change on each stitch can be clearly seen. The extra amount of solution continues to wick along the thread to the other side of the polymer film and cannot be seen. The color development can be recorded by a digital camera for visual appraisal. Figure 4A shows a photo of three repeated measurements of the same serially diluted NO_2^- solution samples. The results of the colorimetric assays can also be recorded for data analysis with a desktop scanner (Epson Perfection 2450 PHOTO) using the color photo setting and 4800 dpi resolution. It is noted that for the image scanning, the orientation of the stitches should be positioned parallel to the scanning direction of the light bar in the scanner to avoid the shadowing effect caused by the protruding stitches on the polymer film surface. The recorded color image data can then be imported into Adobe Photoshop and converted into grayscale mode. A fixed area is applied to all detection zones. The mean grayscale intensities can be quantified using the histogram function of Adobe Photoshop. The ultimate mean intensity value of each detection zone can be obtained by subtracting the measured average detection zone intensity from the mean intensity of the 0 $\mu\text{mol/L}$ NO_2^- solution; the average intensity data can then be transferred to Microsoft Excel to obtain calibration curve data (Figure 4B). In this work, six independent measurements were taken using six thread-based devices made from the same indicator-treated thread. Data points are the average values \pm s.d. ($n = 6$). Thread, therefore, offers a new design concept for low-cost and low-volume healthcare and diagnostic sensors. The low material cost of such sensors will make them very useful in the developing and remote regions where well-equipped medical services are lacking.

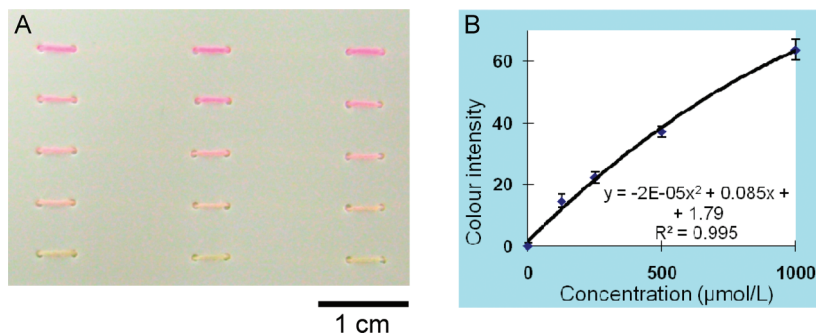


FIGURE 4. (A) Three parallel colorimetric measurements of serially diluted NO_2^- solution samples (0, 125, 250, 500, and 1000 μM) on the thread-based sensor. (B) NO_2^- concentration calibration curve established from thread stitches of six thread sensors using a desktop scanner and Adobe PhotoShop.

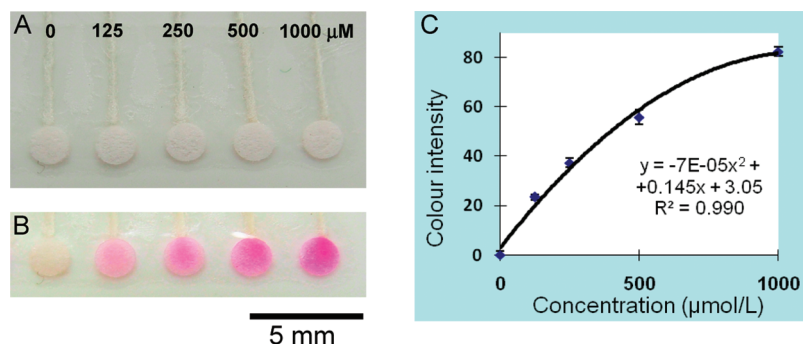


FIGURE 5. (A) Thread-paper microfluidic sensors using cotton thread as the liquid transport channel. (B) Colorimetric NO_2^- concentration series (0, 125, 250, 500, and 1000 μM) developed using a sensor array made of filter paper and cotton thread. (C) NO_2^- concentration calibration curve established from six thread-paper microfluidic sensors using a desktop scanner and Adobe PhotoShop.

Thread can also be used with other porous materials such as paper for semiquantitative colorimetric assay. Figure 5 shows a thread-paper microfluidic sensor array of a separate-sample-inlet design. Five NO_2^- indicator-treated paper discs were first laid onto a single-sided sticky tape in a line. Five hydrophilic cotton threads were then laid onto the sticky tape, each touching one of the five separate paper discs. A white opaque polymer film was finally pressed onto the sticky tape, forming the whole sensor. It is worth noting that using polymer film and sticky tape to form a sensor has an advantage of reducing sensor contamination and sample evaporation. NO_2^- solutions (0.8 μL) of a series of concentrations (0, 125, 250, 500, and 1000 $\mu\text{mol/L}$) were introduced in sequence using the micro pipet to the free end of each thread. The sample solutions rapidly penetrated along the threads and reached the paper discs in less than 2 s and triggered full color changes within 5 s. The fully developed colors were recorded by the digital camera for visual appraisal (Figure 5B) and by the desktop scanner for data analysis. The NO_2^- concentration calibration curve was established following the procedure mentioned earlier for thread-based sensors (Figure 5C). The circular area enclosing the entire paper disk was selected for color analysis, and six independent measurements were taken from the six thread-paper sensors to give the average values \pm s.d.

Conclusions. Thread has been used to fabricate 3D and semiquantitative microfluidic analytical devices. An advantage of using thread as the liquid transporting channels is that it does not need patterned barriers. Another advantage of using thread or thread with other porous materials such

as paper to fabricate microfluidic devices is that these devices can be fabricated with basic tools; the reliance on modern equipment is reduced. Certain simple devices may even be fabricated by a skilled work force within the textile industry in developing regions. It can be envisaged that thread, either alone or with other materials, can be used to fabricate a family of microfluidic diagnostic devices suitable for colorimetric, electrochemical, chemiluminescent, electrochemiluminescent assays and electrophoresis. The low-cost, flexible, and versatile nature of thread will allow this ancient material to have new applications in disposable microfluidic devices, advanced textile and personal care products, healthcare, and environmental sensors.

Acknowledgment. The research scholarships of Monash University and the Department of Chemical Engineering are gratefully acknowledged. The authors thank Dr. L. Wang of the School of Fashion and Textiles, RMIT University, for kindly providing us with the cotton thread sample, and Dr. T. Gengenbach of CSIRO Molecular and Health Technologies for taking XPS measurements of the thread samples. The authors specially thank Dr. E. Perkins of the Department of Chemical Engineering, Monash University, for proofreading the manuscript.

REFERENCES AND NOTES

- (1) Weigl, B.; Domingo, G.; LaBarre, P.; Gerlach, J. *Lab Chip* **2008**, *8*, 1999–2014.
- (2) Martinez, A. W.; Phillips, S. T.; Butte, M. J.; Whitesides, G. M. *Angew. Chem., Int. Ed.* **2007**, *46*, 1318–1320.
- (3) Abe, K.; Suzuki, K.; Citterio, D. *Anal. Chem.* **2008**, *80*, 6928–6934.
- (4) Li, X.; Tian, J.; Nguyen, T.; Shen, W. *Anal. Chem.* **2008**, *80*, 9131–9134.

- (5) Fenton, E. M.; Mascarenas, M. R.; Lo'pez, G. P.; Sibbett, S. S. *ACS Appl. Mater. Interfaces* **2009**, *1*, 124–129.
- (6) Carpi, F.; Rossi, D. D. *IEEE Trans. Inf. Technol. Biomed.* **2005**, *9*, 295–318.
- (7) Paradiso, R.; Loriga, G.; Taccini, N. *IEEE Trans. Inf. Technol. Biomed.* **2005**, *9*, 337–344.
- (8) Shim, B. S.; Chen, W.; Doty, C.; Xu, C.; Kotov, N. A. *Nano Lett.* **2008**, *8*, 4151–4157.
- (9) Zhang, M.; Atkinson, K. R.; Baughman, R. H. *Science* **2004**, *306*, 1358–1361.
- (10) Blicharz, T. M.; Rissin, D. M.; Bowden, M.; Hayman, R. B.; DiCesare, C.; Bhatia, J. S.; Grand-Pierre, N.; Siqueira, W. L.; Helmerhorst, E. J.; Loscalzo, J.; Oppenheim, F. G.; Walt, D. R. *Clin. Chem.* **2008**, *54*, 1473–1480.
- (11) Nagler, R. M. *Clin. Chem.* **2008**, *54*, 1415–1417.
- (12) Wink, D. A.; Kasprzak, K. S.; Maragos, C. M.; Elespuru, R. K.; Misara, M.; Dunams, T. M.; Cebula, T. A.; Koch, W. H.; Andrews, A. W.; Allen, J. S.; Keefer, L. K. *Science* **1991**, *254*, 1001–1003.
- (13) Yager, P.; Domingo, G. J.; Gerdes, J. *Annu. Rev. Biomed. Eng.* **2008**, *10*, 107–144.
- (14) Mabey, D.; Peeling, R. W.; Ustianowski, A.; Perkins, M. D. *Nat. Rev. Microbiol.* **2004**, *2*, 231–240.
- (15) Hown-Grant, M. In *Encyclopedia of Chemical Technology*, 4th ed.; Wiley-Interscience: New York, 1993; Vol. 7, p 633.
- (16) Vázquez, G.; Alvarez, E.; Navaza, J. M. *J. Chem. Eng. Data* **1995**, *40*, 611–614.
- (17) Aspler, J. S.; Davis, S.; Lyne, M. B. *J. Pulp Paper Sci.* **1987**, *13*, 55–60.
- (18) Nisbet, D. R.; Pattanawong, S.; Ritchie, N. E.; Shen, W.; Finkelstein, D. I.; Horne, M. K.; Forsythe, J. *J. Neural Eng.* **2007**, *4*, 1–7.
- (19) Shaw, D. J. *Introduction to Colloid and Surface Chemistry*, 4th ed.; Butterworth: Oxford, U.K., 1992, p 71.
- (20) Martinez, A. W.; Phillips, S. T.; Whitesides, G. M. *Proc. Natl. Acad. Sci. U.S.A.* **2008**, *105*, 19606–19611.

AM9006148

An inexpensive thread-based system for simple and rapid blood grouping

David R. Ballerini · Xu Li · Wei Shen

Received: 15 September 2010 / Revised: 4 November 2010 / Accepted: 8 December 2010 / Published online: 10 January 2011
© Springer-Verlag 2011

Abstract This study investigates the use of thread as a flexible and low-cost substrate for the rapid grouping of blood. The use of a capillary substrate such as thread for blood grouping utilises the sensitivity of the flow resistance of large particles in narrow capillary channels to separate agglutinated red blood cells (RBCs) from plasma. Large and discrete particles formed in a continuous liquid phase do not provide capillary wicking driving force and fall behind the capillary wicking front, leading to their separation from the wicking liquid. The capillary substrate therefore provides a very promising but different mechanism for the separation of the agglutinated RBCs and the blood serum phase compared to most existing blood grouping methods. The principle of chromatographic separation is also exploited in this study via the use of suitable dyes to enhance the visual detection of the agglutinated RBCs and the serum phase; surprising and encouraging outcomes are obtained. Using a thread-based device, the ABO and Rh groups can be successfully determined with only 2 μ L of whole blood from a pricked finger tip within 1 min and without pre-treatment of the blood sample. It is hoped that a new, inexpensive, rapid and simple method may provide an easy-to-use blood grouping platform well suited to those in developing or remote regions of the world.

Keywords Blood typing · Thread-based · Point of care · Microfluidic · Low-cost · Developing regions

Introduction

Correct grouping of human blood is imperative for numerous reasons; among them transfusion compatibility is paramount. The term “blood group” is a classification of an individual’s blood based upon the inherent presence or absence of antigens on the surface of their red blood cells (RBCs) [1]. In the blood plasma, antibodies exist which are formed against foreign antigens to protect the body from perceived threats. This reciprocal relationship, Landsteiner’s Law, means that individuals who lack a RBC antigen (A, B or D for example) will possess the corresponding serum antibody, whilst those who possess the antigen must not [2]. There are 30 discrete blood type systems recognised by the ISBT Committee on Terminology for Red Cell Surface Antigens [3]. Among these the ABO and Rh systems are of primary importance when transfusing blood, as incompatibility may lead to an acute haemolytic reaction with catastrophic results such as shock and renal failure leading to death [4]. Without ABO compatibility testing, around one-third of unscreened blood transfusions would be expected to cause a haemolytic reaction [3]. For this reason the ability to quickly and cheaply identify blood type is highly valued, and may lead to the saving of many lives.

The vast majority of techniques for ABO and Rh grouping of blood to date have been based upon the principle of haemagglutination reactions between RBCs and serum antibodies. The absence of agglutination indicates no haemagglutination reaction [5]. An exception to this is the technique of gene-sequencing, which analyses DNA to precisely determine blood type, albeit at considerable cost [6].

Commonly used methods include the slide test [7], tube test [8], micro plate method [9–11], and the column agglutination system [12, 13]. These methods require specific antiserum addition during testing or well-trained personnel to perform

D. R. Ballerini and X. Li contributed equally as co-first authors.

D. R. Ballerini · X. Li · W. Shen (✉)
Department of Chemical Engineering, Monash University,
Clayton Campus,
Melbourne, VIC 3800, Australia
e-mail: wei.shen@eng.monash.edu.au

centrifugation, and are therefore difficult away from the laboratory setting. Disposable systems such as lateral flow devices [14] and bedside test cards [15], though rapid and without the need of expensive equipment, always require the pre-treatment of blood samples or reconstitution of antibody.

All of the techniques mentioned suffer from shortcomings such as (1) high cost (2) necessity of trained personnel (3) sample pre-treatment (4) additional reagent handling or (5) large sample volume requirements. This limits use in developing regions and emergency situations where medical facilities are unavailable. A recent study performed blood typing on paper strips coated with antibody eliminating the pre-treatment of blood samples, but with the sample volume required for each test being 20 μL , venipuncture is necessary [16]. This study provides a new testing platform utilising the porous nature of thread which avoids these limitations whilst being simple, rapid and inexpensive with low sample volume requirements.

Recent research into the use of thread as a substrate for biomedical and environmental diagnostics has shown the material to be excellent for use in microfluidic devices due to its “ready-made” channel structure [17]. Thread is able to wick liquids through capillary motion due to the capillary structure formed by spaces between fibres comprising the thread. Cotton and polyester threads are inexpensive and globally ubiquitous. They have excellent colour display properties, physical strength and wettability. By impregnating thread with serum antibodies, agglutination of RBCs will occur upon the addition of whole blood to the dried thread. This reaction occurring between RBC surface antigens and serum antibodies results in separation of the RBCs and plasma, resulting in three distinct, visible regions when the test is positive. When no interaction occurs, the test is negative and no separation is visible.

The chromatographic separation principle, when used for blood typing with a porous substrate such as thread, offers an unexpected advantage for the identification of haemagglutination. It was found that adding suitable dyes to antibodies significantly enhanced the clarity of results. Having low affinity to cellulose and polyester fibre surfaces, the dyes are eluted by the serum phase remaining at the wicking front, generating a visible gap between the dye and agglutinated RBCs. Another focus of this study is to prove the concept of a simple, recyclable blood sample handling tool. This tool allows the required volume of blood sample be extracted from a finger pricked with a conventional lancet device safely and adequately for testing, increasing the ease of the procedure.

The restrictive requirements of existing techniques render them less suitable for point-of-care monitoring and treatment, especially for use in under-developed areas, emergency situations, and general field use. Although this new platform is not expected to replace current methods

practiced in the developed world, it is hoped that it may find use in remote and developing regions where access to laboratories or hospitals is unavailable.

Experimental section

Preparation of antibody impregnated thread

Polyester thread was obtained from the School of Fashion and Textiles, RMIT University, Melbourne, Australia. The selection of polyester thread as the substrate was due to its excellent colour display properties, which aid in the identification of the separation of sample components in capillary channels. The thread used was given an initial plasma treatment as described by Li et al. to remove surface contaminants which greatly increased its ability to be wetted [17]. Epiclone™ anti-A, anti-B and anti-D monoclonal grouping reagents were sourced from CSL Australia. Anti-A and anti-B are a transparent cyan and a yellow solution respectively, whilst anti-D is a clear solution. Threads were treated with antibody via soaking in the grouping reagent followed by blotting with standard blotting paper (Drink Coaster Blotting, 280 gm^{-2}) to remove any surplus of antibody solution from the thread. After drying under a fume hood for 10 min, treated thread were ready to be used for ABO and Rh blood typing. In this work, “thread A”, “thread B” and “thread D” are used as abbreviations for the three types of thread, treated with anti-A, anti-B and anti-D/Rh respectively.

Modification of antibodies for enhanced detection

It was found that the addition of strongly water-soluble dyes to antibody solutions can significantly assist in the visual detection of the agglutination of RBCs. In this study, water-soluble dyes were added to the clear anti-D solution to achieve this enhancement to result interpretation. Ink solutions (cyan and magenta) for visual indication of successful separation were prepared by diluting commercial Canon ink jet inks (CLI Y-M-C-BK, PGBK (<http://www.canon.com.au>)) with Millipore filtered water. Diluted inks were then mixed with antibody solution in the ratio of 1:25 ($V:V$) ink to antibody solution. Thread was soaked in the coloured anti-D solutions and then dried under a fume hood. Abbreviations of “thread MD” and “thread CD” were adopted for threads treated with magenta and cyan modified anti-D solutions.

Blood sample tests using the thread-based platform

Blood samples (A+, B+ and O−) were sourced from donors of known blood type, with samples being drawn by a trained nurse, and stored in Vacutainer® test tubes contain-

ing lithium-heparin anticoagulant. All blood samples were stored at 4 °C, and used within 5 days of withdrawal. For the primary investigation of the feasibility of using antibody-treated thread as a blood typing system, three treated threads (thread A, B, D) were immobilised in folded polypropylene films with lodging slits to aid testing, and a micropipette (Eppendorf research® 0.1–2.5 µL) was used to dose a 1 µL blood sample onto each thread. Threads MD and CD were tested in a similar fashion to evaluate whether coloured anti-D enhanced the visibility of separation. For positive results showing separation of agglutinated RBCs and serum, the separation distance between the edge of RBCs and serum was measured using a Vernier calliper.

Confirmation of donor blood type using the glass slide method

Donor blood types were confirmed using the conventional glass slide technique to provide a control for the thread-based platform. Testing procedure was provided by CSL, Australia. This established method was also used to confirm that the dyes added to anti-D solutions did not affect the results by inhibiting agglutination (in the positive case where the blood contains the corresponding antigen) or by causing agglutination when none should occur (by mixing ink solution and blood with no antibody present).

Results and discussion

Separation of agglutinated RBCs from blood serum on thread

Identifying the agglutination of RBCs using porous media has a unique advantage: large and discrete particles in a suspension system undergo a phase separation from the continuous liquid phase in the capillary channels. As the whole-blood sample wicks through the inter-fibre gaps of the antibody-treated threads, blood serum will dissolve the antibody molecules deposited on the surface of the fibres. Therefore, if RBC agglutination occurs as a result of a haemagglutination reaction it is expected to take place at the blood wicking front first. Haemagglutination reactions occur when antibodies (immunoglobulin molecules, IgG and IgM) bond to the specific binding sites on the antigens of adjacent RBCs [17]. The aggregation of the RBCs by the antibody molecules leads to the formation of significantly larger particles that cannot be stably suspended in the serum phase. As the sample wicks along the thread, the size of the agglutinated particles increases. Since the agglutinated RBCs form discrete particles, they cannot contribute to the capillary driving force required for the blood sample to continue wicking forward. Instead, the agglutinated RBC

particles can only be carried by the serum to move forward. In this situation agglutinated particles will be gradually left behind from the serum wicking front. Furthermore, the agglutinated particles in the inter-fibre channels may act as a “filter” which permits serum to pass, but prevents other agglutinated RBC particles from passing. This causes the separation of the agglutinated RBCs from the serum phase. This reaction is visually identifiable by the appearance of a pale pink coloured band between the RBCs and dry antibody residue, as seen in Fig. 1(a, c, e, f). In the case where the deposited antibody does not react with the antigens of the RBCs, no separation is visually detectable (as seen for type O– blood in Fig. 1g–i).

Figure 2 displays collected data quantifying the average length of separation distance for different types of antibody-treated thread. Although there is a small difference in separation distance between differing antibodies, a distance of approximately 3 mm was typical and easily visible by the human eye, being of similar length to a standard “stitch” found on a shirt cuff. Typically, results became easily visible within 1 min of sample dosing, making the test quite rapid compared to existing techniques.

Identifying a person’s ABO and Rh blood type requires three tests, two for the A and B antigens to determine ABO grouping, and a further test for the D antigen to determine Rh grouping. A results-matrix is shown in Table 1 which aids in the interpretation of results. Due to the serious consequences of blood transfusion incompatibility, it is recommended that a serum cross check be performed to ensure a safe transfusion, as is standard with all existing blood grouping methods.

Effect of adding colouring agents to antibody solutions

As the detection of separation is performed visually, it is more difficult to identify the separation of the blood components on thread B and D compared to thread A, due to the similar colour of the anti-B and anti-D solutions and the blood plasma on thread. The addition of dyes to the antibody solutions can assist interpretation of such results. The antibodies purchased are coloured for the purpose of identification, with anti-A being cyan coloured, anti-B, light yellow whilst anti-D/Rh is colourless. It is from this colouring that the enhancement effect was first noticed on thread, with positive results for thread A being much easier to interpret due to the presence of a light coloured band formed between the agglutinated RBCs and the cyan antibody solution. This band is caused by the migration of the blood plasma.

The cyan and yellow dyes in the commercial anti-A and anti-B solutions are patent blue V and tartrazine, respectively. Patent blue V is an acid dye with two sulphonic groups; it dissociates in aqueous solutions and is negatively charged. This dye therefore has a weak affinity towards

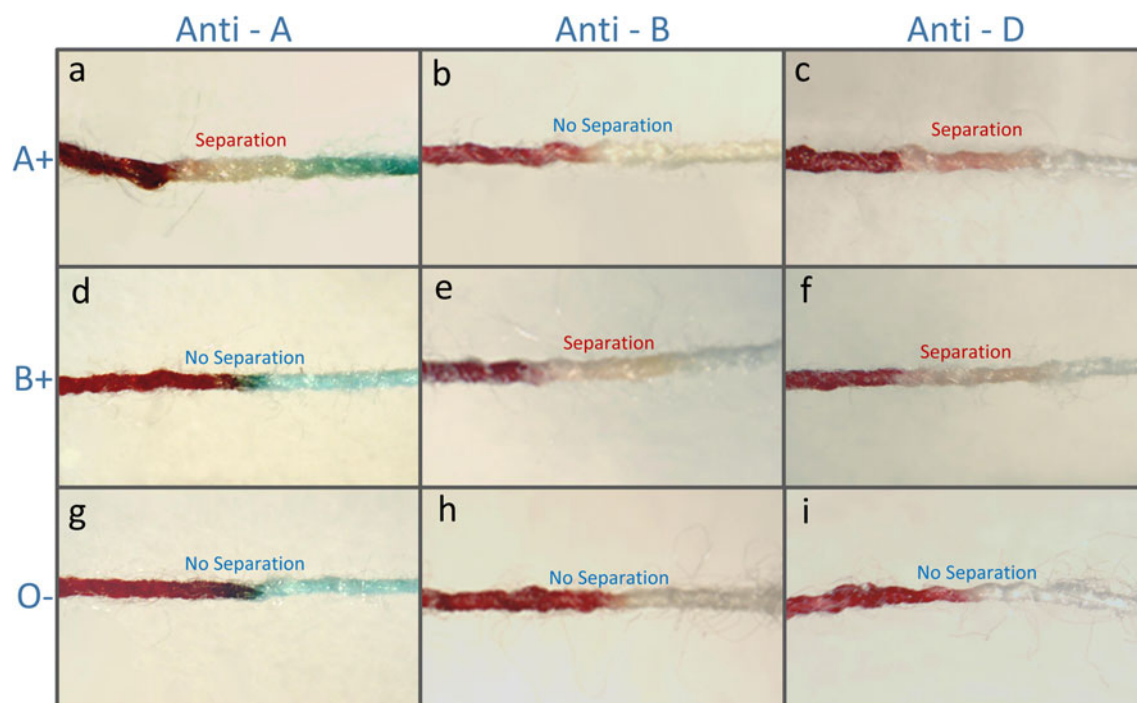


Fig. 1 Proof of concept testing with samples of whole blood of type A+, B+ and O− on antibody-treated polyester threads. *Columns* show results on threads A, B and D from *left to right*, whilst *rows* show the results for the different blood types as labelled on the left

cellulose and polyester fibre surfaces, which also carry a weak negative charge in aqueous solutions [19]. Tartrazine is an azo dye with three dissociable acidic groups—two sulphonic and one carboxylic. Its negatively charged character in aqueous solutions indicates that it also has weak affinity towards cellulose and polyester. When these dyes are deposited onto thread together with antibodies, they can be readily dissolved and carried forward along the thread by the wicking blood sample. When anti-A binds the

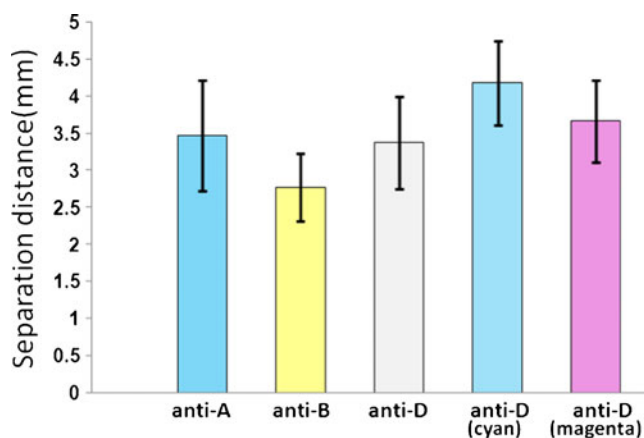


Fig. 2 Graph of separation distance due to agglutination for positive reactions with the different antibody solutions: anti-A, anti-B and anti-D, including cyan and magenta ink jet ink modified anti-D solutions. *Error bars* represent one standard deviation from the arithmetic mean (ten repetitions)

RBCs and causes their agglutination, the agglutinated RBCs will be left further and further behind the wicking front of the plasma. The dissolved dye molecules, in contrast to RBCs, will be carried by the plasma and remain in the wicking front of the plasma phase until it stops. The different migration behaviour of the agglutinated RBCs and these dyes allows a gap to develop between the RBCs and the dye as the plasma wicks along the antibody-treated thread. This gap results in the formation of a band of very light colour in contrast to the agglutinated RBCs and the colour of the dye in the plasma wicking front. The length of the band is comparable to the separation length previously mentioned for unmodified anti-D (Fig. 2), but the contrasting colours make separation more easily visible, enhancing the ability of the user to detect agglutination. This effect is minimal for the Tartrazine doped Anti-B due to its light yellow colouring which is similar to that of plasma. In

Table 1 Results-matrix for aiding interpretation

	AB+	AB−	A+	A−	B+	B−	O+	O−
Anti-A	✓	✓	✓	✓	×	×	×	×
Anti-B	✓	✓	×	×	✓	✓	×	×
Anti-D	✓	×	✓	×	✓	×	✓	×

Ticks indicate a positive result (separation has occurred) whilst crosses indicate a negative result (no separation). The user simply identifies which column matches their result to find their blood type

situations where agglutination does not occur, this band does not develop.

In this study, diluted ink jet printing inks were used as colouring agents to modify antibody solutions. Despite detailed information about the dyes used in the ink formulations being unavailable, it is expected that the dyes must have excellent solubility in aqueous solutions (a basic requirement for ink-formulation dyes) [18]. Since all dyes for ink jet ink-formulation carry negative charges for reasons of safety [18] (positively charged dyes may possess mutagenic properties), ink jet ink dyes also have a poor affinity with the fibres used. Although this poor affinity has a well-known and unwanted effect upon ink jet printing [18], it makes these ink solutions well suited for the doping of antibody solutions.

The enhanced visual identification effect can be achieved for threads B and D by adding ink to the antibody solution before thread treatment. Figure 3 illustrates the effect, showing threads (CD and MD) which have been treated with anti-D solution modified to include cyan and magenta inkjet inks. When compared to earlier results for thread D, one can see that the separation of plasma and RBCs is much clearer with the modified antibody. Figure 2 shows the mean separation distance between agglutinated RBCs and serum on threads CD and MD from ten repeated measurements to be 4.2 and 3.6 mm, respectively. It is expected that the use of suitable dyes to enhance visual

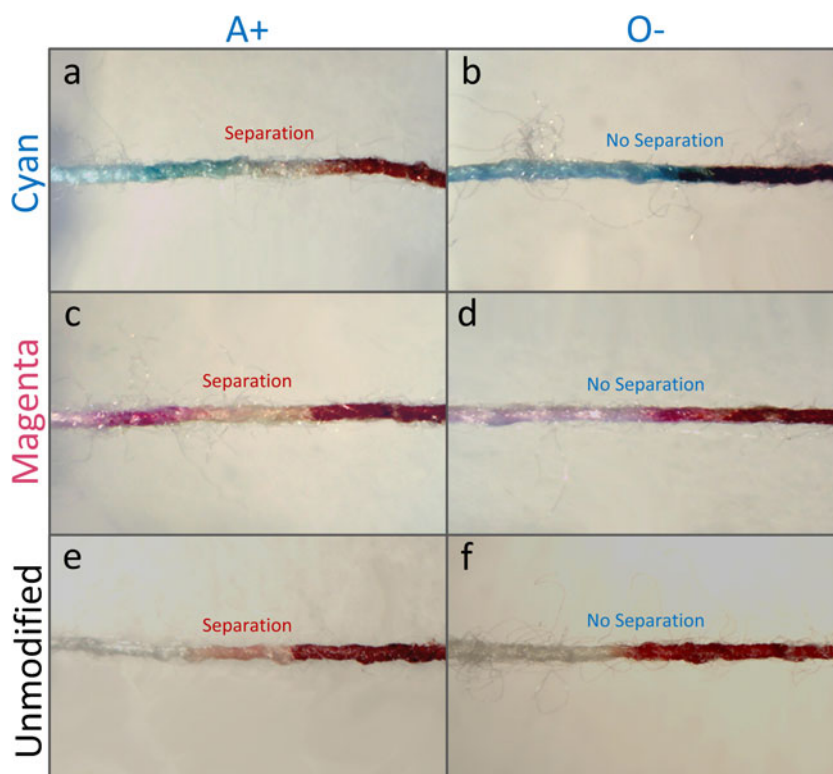
identification of blood typing results is applicable for other porous substrates.

Low-cost dosing device

Blood samples of 1 μL were deposited by micropipette for the previously discussed study. However, no necessity exists for maintaining the sample volume at exactly 1 μL to achieve accurate results. Blood samples (A+) of different volume (0.6, 1, 2 and 4 μL) were deposited onto portions of thread A (six repetitions per volume) to validate this. All threads showed positive results, with separation of agglutinated RBCs and plasma occurring. This result indicates that the use of a simple and low-cost dosing device to deliver blood samples is feasible if sample volumes fall within the range of 0.6 to 4 μL . Various tools for dosing blood into the thread-based system were investigated, with cost, consistency of sample volume delivered and disposability/recyclability being of primary importance. These tools remove the requirement for more precise and expensive tools (e.g. micropipettes) which are not universally available in under-developed areas or for general users.

Among these tools, the use of a sewing needle eye for sample dosing was exemplary as it was (1) able to deliver relatively consistent whole-blood sample volumes (2) easily cleaned and sterilised using a flame (3) inexpensive to

Fig. 3 Blood testing on threads CD, MD and D (for comparison) **a** A+ sample applied to thread CD, a light band can be seen between the RBCs and cyan antibody solution indicating separation of plasma and RBCs; **b** O- sample applied to thread CD, no separation visible. **c** A+ sample applied to thread MD; a positive result is indicated by a light band; **d** O- sample applied to thread MD, no separation visible. **e** A positive result on unmodified thread D for comparison; **f** a negative result on unmodified thread D for comparison



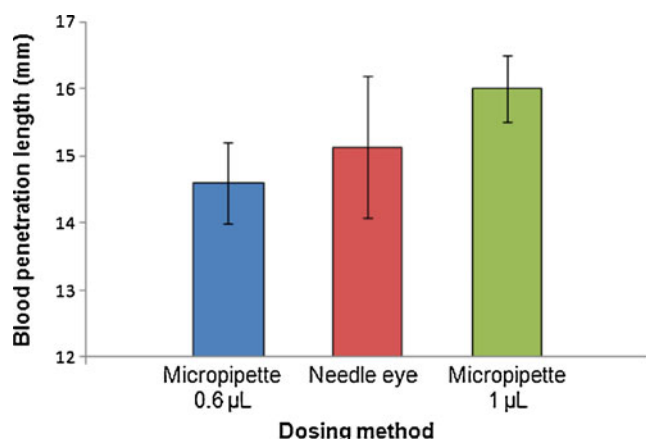


Fig. 4 Graph of penetration length on thread for blood samples dosed with micropipette and needle eye techniques

obtain (4) easily transported and extremely portable and (5) commonplace globally. The procedure simply involves dipping the needle eye into a drop of whole blood from a pricked finger. Blood is drawn into the needle eye and can then be transferred by pressing the needle eye to the thread, which has finer capillary channels and therefore stronger liquid absorption ability.

The repeatability of this technique was assessed by measuring whole-blood penetration length into untreated thread. If the thread is considered relatively uniform then penetration distance is proportional to delivered sample volume. Samples were dosed using a needle eye (of aperture dimensions 0.6 mm \times 4.1 mm) yielding an average penetration of 15.1 mm with a standard deviation (s.d.) of 1.1 mm from six repetitions. In comparison, the micropipette yielded 16.0 \pm 0.5 mm (average \pm s.d.) for 1 μ L blood sample and 14.6 \pm 0.5 mm for 0.6 μ L (see Fig. 4). This result suggests that although the needle eye method does

not achieve consistency of the same degree as the expensive micropipette, it is still capable of delivering samples within the range necessary for the test. Although the metal needles used are recyclable and easily sanitised, a disposable plastic device could be made which operates upon the same principal, albeit at lower cost.

Single-step prototype

In order to further simplify the testing process a single-step device was investigated which can perform the three different antibody tests simultaneously. By immobilising a sample of threads A, B and D in a small square of polymer film in a criss-cross arrangement, it is possible to determine a person's ABO and Rh blood groups with a single dose of whole-blood. A sample of 2 μ L was proven to be sufficient for the test, and could easily be delivered using the needle eye technique previously described (albeit with a larger needle eye) to the centre of the device where the threads intersect. As the sample wicks along each thread, antibody is chromatographically eluted along the length of the threads and away from their intersection much quicker than between different threads; hence any migration of antibody between threads is greatly reduced preventing interference to correct grouping. Figure 5 displays one possible prototype; Fig. 5b is an enlarged image of the right half of the device, the separation achieved indicates the sample is of type A+. The prototype shown in Fig. 5a was constructed simply by wedging the threads in small slits in the polymer film, but it should be noted that a sturdier device could easily be constructed by sewing or gluing the threads to the film. This device is simple to use and produce, compact and portable. A generous cost estimate of only \$0.009 USD per device suggests suitability for use in regions which are economically under-developed.

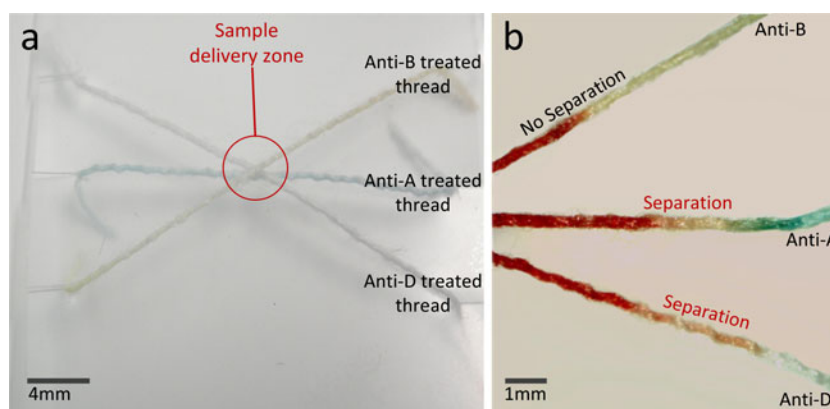


Fig. 5 A single-step blood grouping test prototype for proof of concept, composed of thread A, B and D wedged in a square of polymer film and sharing an intersecting sample delivery zone **a** the unused device with sample delivery zone indicated within a red circle

b an enlargement of the right-hand side of the device after whole blood has been introduced into the delivery zone in the centre via needle eye. The separation occurring on threads A and D indicates that the blood is of type A+

Expiry study

A study was performed investigating the efficacy of the thread-based platform after a 4-week storage period. Two sets of samples were stored in micro-tubes wrapped in foil; one at 4 °C the other at ambient temperature. After storage testing gave good results for all antibody-treated thread types, suggesting that the devices could be transported and stored for a moderate period of time without degrading if sealed in airtight and light-proof packaging.

Conclusions

The results of this study show that the use of thread as a porous substrate for ABO and Rh blood typing is viable; and reduces the volume of blood required (to ~2 µL) compared to conventional methods. The technique is rapid, requires only whole blood and eliminates the need for the end user to either handle other testing reagents or perform sample dilutions. The addition of dye to the antibody solution chromatographically enhances the visibility of the separation of agglutinated RBCs and plasma, making it easier for the user to identify a positive reaction. The simple and recyclable (or disposable) metering device explored enhances the simplicity of the test and further reduces the need for complicated or expensive equipment.

Although only ABO and Rh/D blood groups were tested in this study, it is expected that the platform could easily be extended to identify other groups of interest that follow similar antibody/antigen interactions.

The thread-based blood grouping device prototyped is simple and robust enough to be employed by the end user without assistance. It is portable, disposable, can be easily preserved and maintains a low cost of construction, making it attractive for diagnostics and point of care testing especially in remote and developing regions.

Acknowledgments This work is supported by the Australian Research Council Grant (DP1094179). The authors would like to thank the kind blood donors; Mr. Scot Sharman, Mr. Henri Kröling and Mr. Junfei Tian whose donations have made this work possible as well as Ms. Lisa Collison of the Monash University Health Service for collecting blood donations. The authors also thank Dr. Lijing Wang of the School of Fashion and Textiles, RMIT University, for kindly providing thread and textile samples. The research scholarships of Monash University and the Department of Chemical Engineering are gratefully acknowledged.

References

1. Daniels G, Bromilow I (2007) Essential guide to blood groups. Blackwell, Oxford, UK
2. Joshi et al VDJ (2006) Anatomy and physiology for nursing and health care. BI
3. Daniels G, Reid ME (2010) Transfusion 50(2):281–289
4. Dean L (2005) Blood groups and red cell antigens. National Center for Biotechnology Information (NCBI), Bethesda, MD, US
5. Malomgré W, Neumeister B (2009) Anal Bioanal Chem 393 (5):1443–1451
6. Storry JR, Olsson ML, Reid ME (2007) Transfusion 47:73S–78S
7. Pramanik D (2010) Principles of physiology, 3rd edn. Academic, Kolkata
8. Estridge BH, Reynolds AP, Walters NJ (2000) Basic medical laboratory techniques. Delmar Cengage Learning, Albany, NY, USA
9. Llopis F, Carbonell-Uberos F, Montero MC, Bonanad S, Planelles MD, Plasencia I, Riols C, Planells T, Carrillo C, De Miguel A (1999) Vox Sang 77(3):143–148
10. Llopis F, Carbonell-Uberos F, Planelles M, Montero M, Puig N, Atienza T, Alba E, Montoro J (1997) Vox Sang 72(1):26–30
11. Spindler JH, ter Kl H, Kerowgan M (2001) Transfusion 41:627–632
12. Langston MM, Procter JL, Cipolone KM, Stroncek DF (1999) Transfusion 39(3):300–305
13. Lapiere Y, Rigal D, Adam J, Josef D, Meyer F, Greber S, Drot C (1990) Transfusion 30(2305438):109–113
14. Plapp F, Rachel J, Sinor L (1986) Lancet 327(8496):1465–1466
15. Giebel F, Picker SM, Gathof BS (2008) Transfus Med Hemoth 35 (1):33–36
16. Khan MS, Thouas G, Shen W, Whyte G, Garnier G (2010) Anal Chem 82(10):4158–4164
17. Li X, Tian J, Shen W (2009) ACS Appl Mater Interfaces 2(1):1–6
18. Gregory P (1991) High-technology applications of organic colorants. Plenum, New York, NY, USA
19. Scott WE (1996) Principles of wet end chemistry. TAPPI, Atlanta

Flow control concepts for thread-based microfluidic devices

David R. Ballerini,^{a)} Xu Li,^{a)} and Wei Shen^{b)}

*Department of Chemical Engineering, Australian Pulp and Paper Institute,
Monash University, Clayton Campus, Victoria 3800, Australia*

(Received 3 December 2010; accepted 7 February 2011; published online 14 March 2011)

The emerging concept of thread-based microfluidics has shown great promise for application to inexpensive disease detection and environmental monitoring. To allow the creation of more sophisticated and functional thread-based sensor designs, the ability to better control and understand the flow of fluids in the devices is required. To meet this end, various mechanisms for controlling the flow of reagents and samples in thread-based microfluidic devices are investigated in this study. A study of fluid penetration in single threads and in twined threads provides greater practical understanding of fluid velocity and ultimate penetration for the design of devices. “Switches” which control when or where flow can occur, or allow the mixing of multiple fluids, have been successfully prototyped from multifilament threads, plastic films, and household adhesive. This advancement allows the fabrication of more functional sensory devices which can incorporate more complex detection chemistries, while maintaining low production cost and simplicity of construction. © 2011 American Institute of Physics. [doi:10.1063/1.3567094]

I. INTRODUCTION

Developments in field-based diagnostic technologies have garnered great interest for their potential application to medical and environmental sensing, particularly in impoverished regions where specialist laboratory access is unavailable.^{1–5} A demand for simple, inexpensive diagnostic devices has been publicized by a significant amount of research interest being displayed in microfluidic paper-based analytical devices (μ PADs).^{6–16} A strong demand exists for sensors which can detect biomarkers of disease in blood or urine or environmental contaminants in waterways but are also inexpensive and disposable.

Recent studies from our group and others have further shown that multifilament threads are a viable and inexpensive alternative for the production of low-cost microfluidic devices.^{17–19} These microfluidic thread-based analytical devices (μ TADs) can be produced by relatively unskilled persons quickly and cheaply using simple tools. These devices have shown great potential for use as medical and environmental sensors. Three dimensional μ TADs can also be easily fabricated due to the flexibility and strength of thread.

The flow of the fluid along the thread is driven by capillarity without the need of external forces, following the analogous concept of fluid flow in μ PADs. Although the chemical nature of thread and paper is the same, many other material properties are significantly different. These differences include the length of the fibers, the interfiber bonding, as well as differences in the characteristic porous channel structures. Recent research has highlighted a necessity for characterizing fluid flow in low-cost microfluidic sensors, beginning with μ PADs in order to expand

^{a)}D. R. Ballerini and X. Li contributed equally as co-first authors.

^{b)}Author to whom correspondence should be addressed. Tel.: +61-3-99053447. Electronic mail: wei.shen@eng.monash.edu.au.

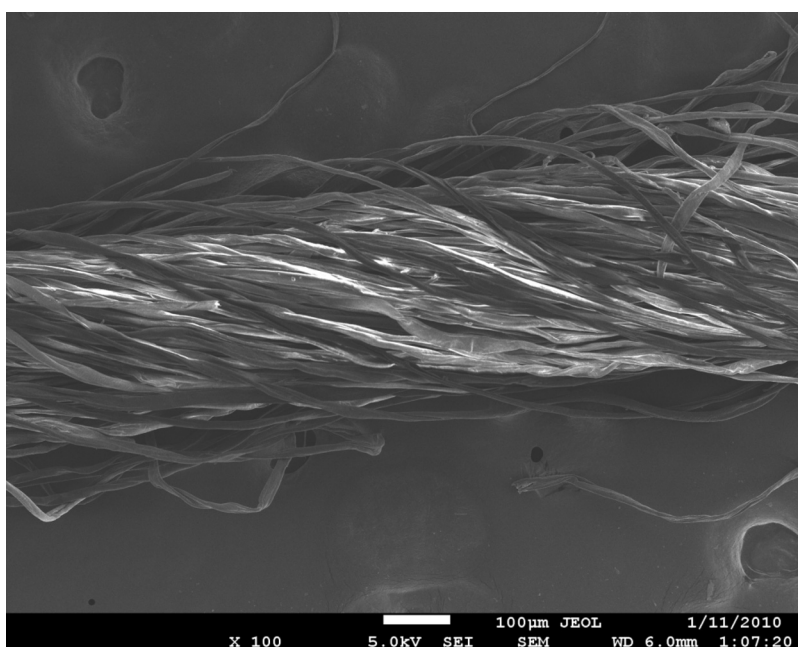


FIG. 1. A SEM image of a polyester thread, showing the individual fibers which comprise the overall structure. Capillary channels are formed by the gaps between fibers, enabling the thread to conduct flow.

their diagnostic capabilities.^{9,13,20–23} It is therefore logical that the next step in the progression of thread-based sensors is an investigation of liquid transport and control on μ TADs to optimize device design and functionality.

In order to design μ TADs which have a reasonable result-reporting time under ambient conditions, it is necessary to characterize the fluid penetration along the thread to estimate the time required for sample fluid transportation. In particular, the ultimate distance of the fluid penetration and the linear range (i.e., distance versus square root of time) of fluid penetration with no external intervention are important parameters to assist device design. Another desirable feature for μ TADs is the ability to control the fluid penetration in a thread by means of external intervention. This involves the design of mechanisms using thread and other low-cost materials to enable control of the timing or the direction of the fluid penetration in μ TADs. The research on these mechanisms, at its preliminary stage, allows the user to design devices which can control the flow of fluids and the timing of reactions in an on/off fashion by designing switches. The on/off switches can further be used to develop microselectors to selectively direct flow to a desired location, or micromixers to mix multiple fluids together.

The SEM image in Fig. 1 shows that a polyester thread is formed by many fibers; the gaps between fibers form capillary channels which enable the penetration of a wetting fluid. In μ TADs, threads must function as fluid transport channels and detection sites. It is possible to divide a piece of thread into different segments, making these segments fulfill different functions. Such division can be made by applying liquid adhesive or wax onto the thread to occupy the interfiber gaps in a thread, eliminating the capillary channels. In such a way, a piece of thread can be divided into a fluid transport channel and a detection site. Sample fluid in the transport channel cannot enter the detection site without external intervention (i.e., activation by a switch). In many applications, the detection zone requires treatment with indicators that should be localized within the detection zone.¹⁷ Segmenting a piece of thread into a transporting channel and detection zone is therefore a necessary fabrication consideration. The sample transporting channel and the detection zone can only be connected when an on/off switch is activated and the two segments are bridged to enable sample flow across the blockage.

Other control mechanisms can further enhance the functions of μ TADs. For example, mi-

croselectors can be built into μ TADs which allow users to direct the samples or reagents they desire to a specific location given multiple options. Moreover, μ TADs can be used as controllable micromixers which are useful when a requirement to mix samples and reagents together at a specific time exists. Micro-TADs incorporating all of these new and simple mechanisms are inexpensive and easily fabricated without specialist equipment, and therefore suitable for use in underdeveloped areas, remote regions, or potentially as point-of-care products globally. We expect that by understanding fluid penetration distance and flow rate as well as exploiting a variety of mechanisms for flow control on μ TADs, we have provided a means to create more sophisticated and functional μ TADs, allowing their further development and expansion of their potential applications.

II. EXPERIMENTAL

A. Threads and textile

Polyester thread was kindly provided by the School of Fashion and Textiles, RMIT University, Melbourne, Australia. Untreated polyester thread can be wetted by aqueous solutions, albeit with a slow penetration rate. Plasma oxidation was used to improve fluid penetration along the polyester thread, since such treatment increases the fiber surface polarity by removing surface contamination by low surface energy materials and also oxidizing the fiber surface. Our previous study showed that cotton thread is also a suitable material for fabricating μ TADs.¹⁷

B. Measurement of fluid capillary rise on threads

Synthetic food dye solution (Queen Food Coloring, Pillar box red) was used to track the penetration of fluids within thread. The surface tension of the dye solution was measured by the capillary rise method²⁴ using a glass capillary (i.d.=0.9 mm) and cathetometer. The kinematic viscosity of the solution was measured with a U-tube viscometer (BS/U tube) using Millipore-purified water as the standard solution. Measurement was conducted in a water bath with temperature held at 30 ± 0.1 °C.

A schematic of the apparatus for measurement of fluid penetration on threads is shown in Fig. 2. A laboratory jack was used to hoist the fluid reservoir containing the dye solution to the appropriate height; a ruler was used to measure the fluid penetration distance on thread. The surface tension and kinematic viscosity of the food dye solution in the reservoir (i.e., beaker) were 65.1 mN/m and 0.883 cS, respectively (at 30 °C). Fluid penetration was recorded using a camcorder (JVC GZ-MG530) and a snapshot program was used to record time-lapse images. Data acquisition began when threads were dipped into the penetration fluid, with penetration distance recorded for 15 min. Each measurement was repeated six times to give the average penetration distance and standard deviation data. Contact between the polymer film and the threads was restricted by bending the film and fixing only the two ends of the thread to the film, which also served to eliminate the untwisting of the threads.

C. Functional elements on μ TADs for flow control

In order to selectively inhibit fluid flow along the thread, interfiber channels were blocked using commercially available cyanoacrylate-based fast acting adhesive (Selleys Quick Fix Supa Glue). With the application of glue (0.5 μ L, 10 min cure under fume hood), no fluid penetration past the glue-sealed segment is possible, suggesting the complete blockage of the interfiber channels within the thread. Glue can also be employed to fix thread onto polymer film for support. These blocking and adhesive characteristics provide the opportunity to build functional elements into μ TADs for more sophisticated fluid flow control.

The first functional element demonstrated for thread-based microfluidics is the binary (on/off) fluid flow control switch. One simple concept is a “knot style” switch built with only thread itself and glue. The device was made by tying an overhand knot in a polyester thread, and then a small segment of the thread located on the loop is completely blocked to stop fluid flow using glue. Polymer film was also incorporated for some other on/off flow control designs, polypropylene

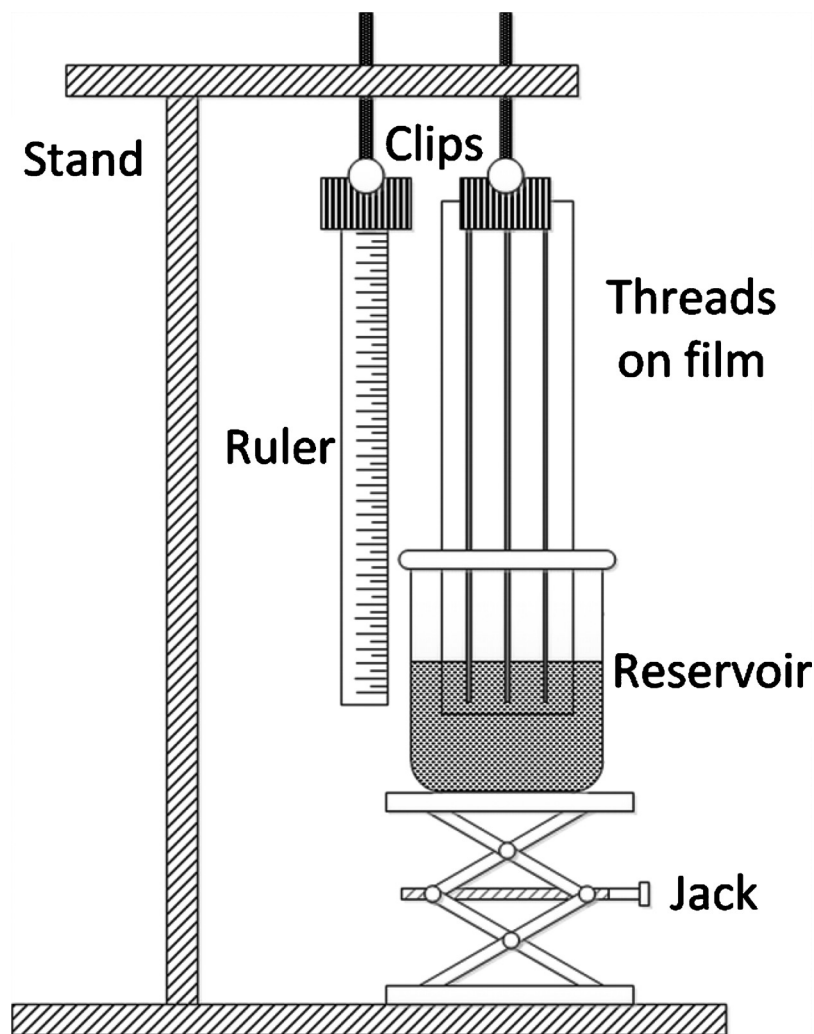


FIG. 2. A schematic of the apparatus employed for the fluid penetration measurements on thread. Threads were fixed to a polymer supporting film and wet with dye solutions from a fluid reservoir.

polymer was selected as the film material due to its hydrophobic nature which eliminates any flow from occurring in the small gap between the thread and the film surface.

The second functional element is the flow selector. The proof-of-concept design shown consists of two inlets (one thread was separated into two parts by blocking the middle part with glue) and one outlet (one thread was capable of being dragged along the first thread to select the flow from the two inlets).

The third functional element is the micromixer; it is composed of two binary switches which are activated at the same time, enabling a μ TAD to mix two solutions from two separate inlets into one outlet by twisting the inlet threads.

D. Testing solutions

Millipore-purified water was used to prepare all aqueous samples required. Ink solutions (cyan, magenta, and yellow) for visual indication of successful flow control used during experiments were prepared by diluting commercial Canon inkjet inks [CLI Y-M-C-BK, PGBK (<http://www.canon.com.au>)] with water.

Sample solutions containing analytes of glucose and protein [bovine serum albumin (BSA), ~66 kDa] were prepared with the artificial urine. Sample solution 1 was a solution of 30 μM BSA and 10 mM glucose in artificial urine.²⁵ The glucose and protein indicator solutions were prepared and applied to the thread using micropipette.²⁵ All reagents were purchased from Sigma-Aldrich.

Sample solutions for micromixer mixing effect tests were HCl (0.01M, solution 2) and NaOH (0.01M, solution 3) solutions which were introduced into two inlets of the micromixer and mixed within a common outlet after folding the μTADs . The commercial pH paper (Advantec, whole range pH test paper) was used to test the pH values of the two inlets and one outlet to show the mixing effect by means of a neutralization reaction.

III. RESULTS AND DISCUSSION

A. Fluid penetration along threads

The fluid penetration distance along threads as a function of time was investigated experimentally by the observation of the capillary rise of the testing fluid against gravity. In general modeling of fluid penetration within a porous media, the Washburn equation is used. In the present study, however, since the capillary rising of fluid in threads was investigated against gravity, the capillary driving force must be reconsidered to include gravity.²⁶ The capillary rising model in the literature was adapted in this study to provide an understanding of fluid penetration along threads. Another factor under ambient conditions is fluid evaporation, which will also be discussed qualitatively below.

Wang *et al.*²⁶ studied the vertical capillary rise and made a derivation using Hagen–Poiseuille’s law [Eq. (1)]. In this derivation the authors assumed that the cross section of the interfiber channels in a yarn has an equivalent radius r and the capillary driving force comprises two opposite pressures, the Laplace pressure and the hydraulic pressure due to gravity [Eq. (2)],

$$\frac{dh}{dt} = \frac{r^2 \Delta P}{8 \eta h}, \quad (1)$$

$$\Delta P = \frac{2\gamma \cos \theta}{r} - \rho g h, \quad (2)$$

where h is the fluid penetration distance along the thread, γ , η , and ρ are the fluid surface tension, viscosity, and density, ΔP is the pressure that provides the fluid penetration driving force, and g is the gravitational constant.

Since the helical nature of the interfiber channels (Fig. 1) is not considered, this model will provide a qualitative trend-prediction of the capillary rise in a thread. The helical pathways of the channels have greater length than the actual length of the thread, therefore the fluid rising rate observed experimentally along the thread would be lower than the modeling prediction. Despite this, the qualitative understanding will still provide practical information of fluid penetration along a thread, which is useful for the design of μTADs .

In the original Washburn derivation²⁷ horizontal capillaries were considered and the driving force comprised of only the Laplace pressure. By substituting the Laplace pressure into Eq. (1), the original form of the Washburn equation can be obtained [Eq. (3)],

$$\frac{dh}{dt} = \frac{\gamma r \cos \theta}{4 \eta h} = \frac{r^2}{8 \eta h} \left(\frac{2\gamma \cos \theta}{r} \right). \quad (3)$$

Integrating Eq. (3) with the initial condition of $h=0$ at $t=0$ will yield the Washburn equation²⁷

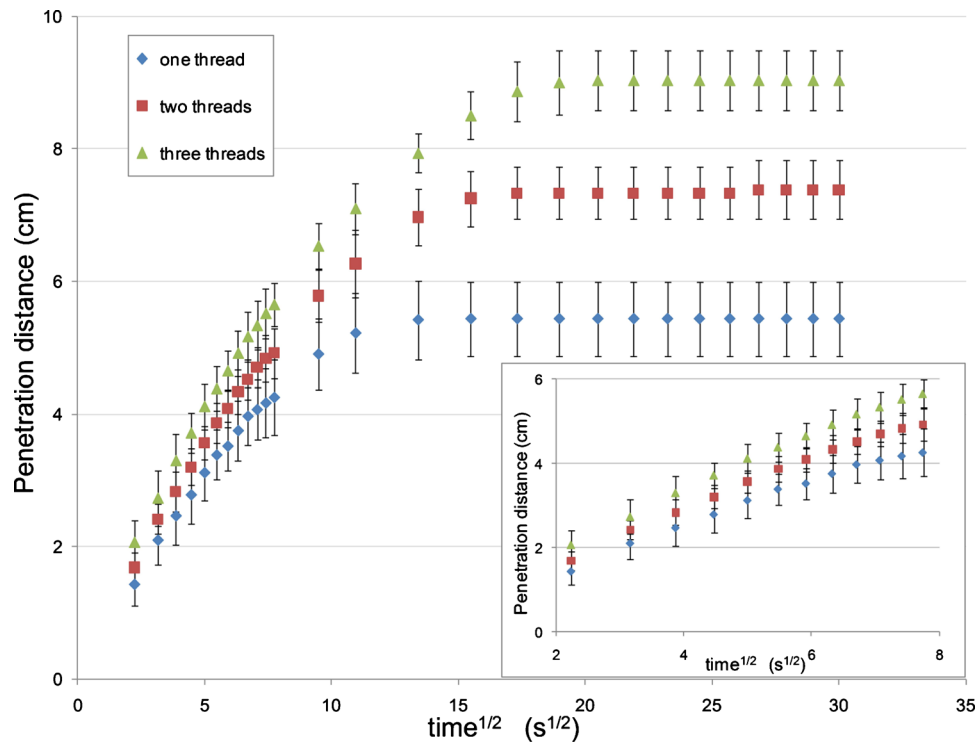


FIG. 3. A graph of penetration distance vs the square root of time for (i) a single thread, (ii) twisted pair, or (iii) twisted triple. The graph highlights a linear relationship between penetration distance and the square root of time over the first minute ($\sim 8\sqrt{s}$), concordant with the Washburn equation. After this the curve flattens out and reaches an ultimate penetration distance due to the effects of evaporation and gravity.

$$h = \sqrt{\frac{\gamma r \cos \theta}{2\eta} t}. \quad (4)$$

When the capillary height is plotted against the square root of time, a straight line will be obtained.

However, when a vertical capillary is modeled, the gravitational force needs to be considered [Eq. (2)]. The fluid penetration kinetics can be written as follows:²⁷

$$\frac{dh}{dt} = \frac{r^2}{8\eta h} \left(\frac{2\gamma \cos \theta}{r} - \rho g h \right). \quad (5)$$

Comparing Eqs. (3) and (5), the capillary driving force (bracketed section) in the case of vertical capillary rise decreases as the height of capillary rise increases. Such a height-dependent loss of driving force will cause the plot of capillary rise height against the square root of time to deviate from the straight line of the horizontal capillary penetration model [Eq. (4)] at longer penetration time. This study provides the basic experimental data and understanding which will be used as general guidance for the design of functional elements.

Our experimental data of capillary rise height and the square root of time show a linear relationship when the height is relatively small (Fig. 3), but a gradual deviation from this linear trend as the time of wetting exceeds ~ 1 min. Such fluid penetration behavior is in an apparent agreement with the loss of capillary driving force (partially) due to gravity. It can be expected that this deviation from linearity would be delayed if threads were orientated horizontally.

Another factor that causes the loss of capillary force is fluid evaporation during the penetration process. This factor is not considered in the modeling above, but is likely to have a dominant effect over longer times, since fluid evaporation will become more and more substantial as the time and the area of fluid on the thread surface exposed to air increase. Fluid evaporation leaves

less free fluid in the capillary channels between fibers, reducing the driving force for the fluid flow through fluid starvation. The complete halting of the fluid penetration front as the penetration distance reached 5.4 cm along a single thread is most likely due to the establishment of an equilibrium between fluid evaporation from the wetted thread surface and the capillary fluid uptake from the reservoir. This conclusion is supported by a further observation that the equilibrium height of capillary rise in a single thread is higher if fluid evaporation is reduced by covering the thread with film. The understanding of fluid penetration behavior along a single thread enables a basic degree of prediction which can be used in the design of μ TADs.

The effect of twisting multiple threads together was investigated by comparing the fluid penetration on a single thread, double-twisted threads, and triple-twisted threads (the twisting frequency is around 200 twists/m). The major geometric feature of the twisted threads is the generation of interthread gaps; these gaps are much larger than interfiber gaps in a thread. The shape of an interthread gap may be crudely viewed as analogous to a “V-groove.” Rye *et al.*²⁸ modeled fluid flow in a V-groove driven by capillary force and found that fluid penetration rate in a V-groove driven by capillary force can be described by a pseudo-Washburn relationship (i.e., penetration distance \propto square root of time). These authors also showed that fluid penetration rate in V-grooves is proportional to the cross sectional width of the groove, and is sensitive to the groove apex angle (the angle between the two walls of the V-groove). Our experimental data show that fluid penetration rates along double-twisted threads are greater than that of a single thread. The fluid shows even higher penetration rate along triple-twisted threads than double-twisted threads, since the former have more interthread gaps. These observations agree with the general trend of the V-groove model and this model can be used to provide a qualitative description of the twisted threads. Furthermore, gravitational and fluid evaporation effects can also be seen from the penetration results for twisted threads. Since the interthread V-grooves increase fluid uptake from the reservoir, the equilibrium of the fluid uptake and fluid evaporation occurs at a higher capillary rise (Fig. 3).

The experimental study of fluid penetration along threads mentioned above suggests that only moderate lengths are appropriate for building functional elements for control of fluid transport. Also, twisted threads can be used for the design of a fluid splitter or a mixer where a sufficient fluid supply needs to be provided to suffice two split flows and vice versa. Moreover, variation of fluid flow rate on μ TADs can be easily achieved by twisting threads together, useful knowledge for the design of devices.

B. Building functional elements on μ TADs for controlled fluid transport

For traditional microfluidic devices, some useful features such as flow control microvalves and fluid micromixers have been successfully built into devices for sophisticated fluid control. However, similar techniques are still unavailable for μ TADs. It is expected that achieving better control over flow connection/disconnection, fluid selection and mixing on μ TADs will accelerate the development of μ TADs and widen the applicability of thread-based microfluidics.

1. Binary type (on/off) switches

The binary type switch works on the principle of using a blocking point to disable fluid transport between two segments of a piece of thread (off), but enable fluid transport when activated by by-passing the blocking point (on). As mentioned earlier, the isolation of the detection zone from the sample introduction channel is necessary for the device fabrication and function. Another desired feature in some analyses is to stop the back flow of the indicator from the detection zone to the channel after the sample delivery.¹⁷ With the switch, this can be done by “turning off” the switch after the sample introduction. The advantage of using glue to form blocking points in thread over using reactive chemical hydrophobization methods is that the blocking points can be formed over a short stretch of thread, and even withstand surfactant solutions with a depressed surface tension as the capillary channels have been effectively eliminated over the range of the blockage.

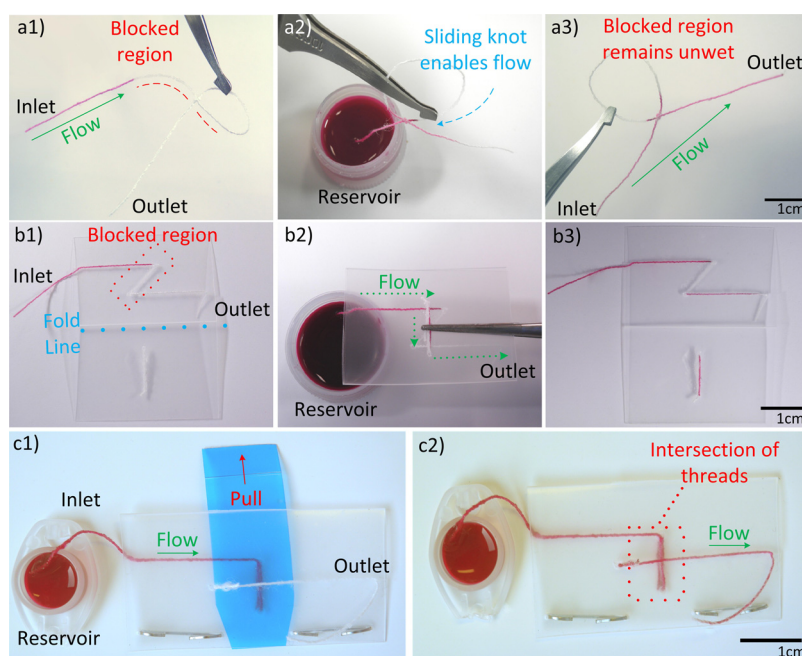


FIG. 4. (a) The simplest of the “on/off” flow control switches is comprised of a thread which incorporates a knot and a loop with an adhesive-blocked segment, sliding the knot over the blocked segment in the loop enables flow to occur along the length of the thread. (a1) The knot device with the inlet fully wet by ink solution, the blockage caused by the glue is indicated by the red dashed line. (a2) The partially wetted device with the inlet in an ink reservoir after being actuated by sliding the knot past the blocked region. (a3) The device after being removed from the reservoir after conducting flow from inlet to outlet. (b) The folding style switch makes use of a polymer film supporting material to function. (b1) The fold type switch in the open position with the inlet wet by ink. The fold line and blocked region are labeled. (b2) The folded device allowing flow from an ink reservoir at its inlet. (b3) The fully wetted device after being used to transport fluid (device having been reopened). (c) Folding style switches can be modified to be pull-tab actuated. (c1) The pull-tab switch with inlet connected to an ink reservoir. (c2) The pull-tab switch with tab removed, allowing flow across the device.

The simplest of the designs presented here uses a knot in a single piece of thread to create a basic on/off flow control mechanism, as shown in Fig. 4(a). Diluted inkjet magenta ink was used to examine the on/off flow along the knotted switch. An overhand knot with a draw loop²⁹ was tied loosely in a thread such that it could slide along the length of the thread. A section of the draw loop was then blocked against fluid flow using glue, and the knot slid and placed over this blocked region so that the switch was in the “off” position and the ink was unable to penetrate through this region [Fig. 4(a)(1)]. After sliding the knot away from the blocked region, the ink can flow across the knot and through the length of the thread [Fig. 4(a)(2)], while the blocked region remains unwet by the fluid.

When polymer film is used as a supporting material for μ TADs design, on/off flow control can be easily achieved in a variety of ways. In this study, we demonstrated different mechanisms of on/off control in μ TADs. These mechanisms included folding the polymer film or removing a temporary obstruction such as a pull-tab.

A simple folding style switch is shown in Fig. 4(b). The device was constructed by folding the polymer film into two smaller rectangles of equal area. On one side of the fold, a thread was stitched into the film running parallel with the crease line of the fold, but with a “z” shaped kink in the center. The diagonal section of the z shape was then blocked using adhesive to prevent the flow. On the opposing side of the film, a small bridge was sewn which was perpendicular to the fold line and directly opposite the center of the z shape. The device is activated by folding the film and bringing threads on opposing sides into contact with each other. The small thread section on

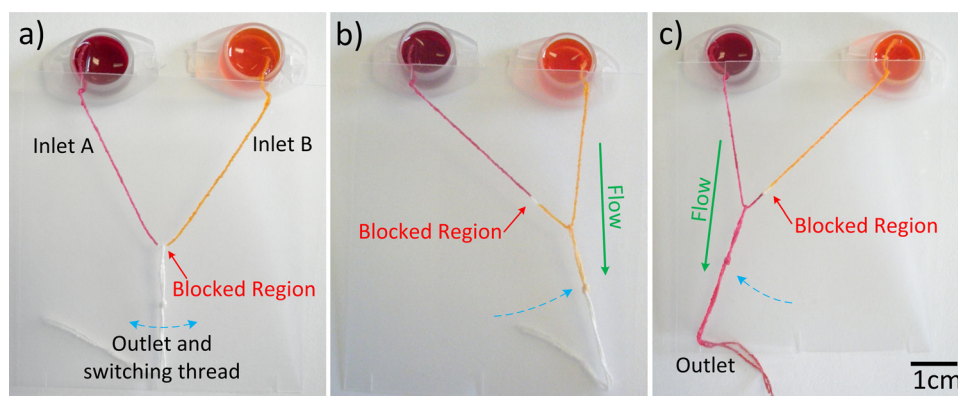


FIG. 5. A microselector, with two inlets and a single outlet, allows a user to select between which one of two samples they wish to transport. Ink solutions are used for visualization of the concept. (a) The unused selector switch set in the off position. The blocked region is indicated and the inlets are connected to ink solution reservoirs. (b) The selector switch after sliding to the right, allowing flow of the yellow ink to the outlet. (c) The selector switch after sliding left, allowing flow of magenta ink.

the left acts as a bridge allowing flow to jump between different sections of the partially blocked thread on the right. Additionally, other porous materials such as textile and paper can be used to act as bridges to allow on/off flow control on thread.

In a pull-tab activated on/off flow control mechanism, a small removable section of polymer film [blue film in Fig. 4(c)] was inserted into the device to form a barrier to flow between opposing threads sewn to the top and bottom films of the device. When the tab is removed by the user pulling upon it, threads on opposing sides of the device are brought into contact with each other and the switch is activated. An advantage of this actuation method is its ease of use, as it eliminates the need for users to hold the device folded shut, and minimizes user contact with the internals of the device. Should an application require the incorporation of hazardous reagents, designers could enclose them entirely within plastic films, reducing the risk of user contact.

An important future application of on-off switches will be to fabricate thread-based microreactors, which allow different reagents to be introduced into reaction zones simultaneously or separately in multistep reactions, or provide controllable reaction time for detection chemistries which require multiple steps, e.g., in blood and urine testing, an analyte may need to be converted into a more detectable form using an enzyme before final detection.

2. Microselectors for flow control

The two-way microselector device shown in Fig. 5 allows a user to choose between samples or reagents (magenta and yellow inks as example solutions here) at two inlets and direct flow down a particular outlet channel at the time the user desires. Alternatively the device can function in reverse, with a single sample or reagent directed to a desired outlet selected from two or more options. Such a device could be useful in complex systems which possess multiple reaction or detection sites, enabling users to selectively perform different types of analyses with the same device.

To illustrate the thread-based microselector applicability to bioassays, a sample solution containing both glucose and protein (sample solution 1) was used to show one possibility for directing sample flow into different outlet channels (Fig. 6). The glucose and protein indicators ($0.1 \mu\text{L}$) were deposited onto the upper left and right threads (i.e., the left and right outlet channels), respectively. The indicators were then allowed to dry under ambient conditions for 15 min. The sample solution was introduced from the lower thread (i.e., the inlet channel). When the sample solution was selected to flow into the right outlet channel by moving the loop to the right, the color change of protein indicator from yellow to blue-green showed that the sample solution had arrived at the desired channel. The loop was then moved to the left to direct the sample flow into the left

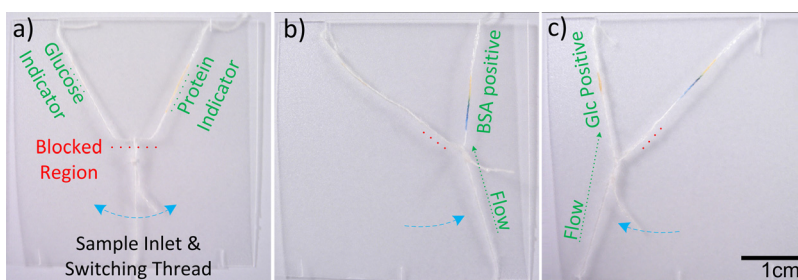


FIG. 6. The microselector allows a user to select between which analyte they wish to analyze. (a) The unused selector switch set in the off position. The blocked region is indicated by a red dashed line, and indicator locations are noted. (b) The selector switch allowing flow to the right, resulting in a color change indicating the presence of protein. (c) The selector switch allowing flow to the left, the presence of glucose is indicated.

outlet channel, which was shown by the development of a yellowish brown color caused by the glucose indicator present. The results showed that the transport of multiple fluid flows can be controlled with the sequential delivery of fluids within μ TADs, thus extending the capabilities and performance of μ TADs while still at low manufacturing cost.

3. Micromixers

Mixing is an important feature in microfluidic devices, required for various chemical functions. The ability to mix reagents and samples gives a designer of μ TADs access to a suite of detection chemistries not available when using only “single step” functionality. This could include sensing systems where an analyte can only be detected after it has been chemically converted to a different form or instances where a colorimetric indicator compound requires a second reaction to produce its visual effect. The flexibility of thread makes it a suitable material for mixing fluids, simply by twisting threads together (i.e., coupling multiple inlets to a single outlet). High twist level maximizes the contact areas between threads (two or more) and therefore increases the diffusion interface and enables fluid mixing. The device shown in Fig. 7 achieved the desired mixing of two colored inks when the device was folded to bring the two wet thread sections in contact with a mixing zone. Thread-based micromixers can also be fabricated with “pull-tab” activation mechanisms.

The efficacy of the thread-based micromixer was shown by testing an acid-base neutralization reaction (Fig. 8). HCl and NaOH solutions (solutions 2 and 3) with equivalent molarity (0.01M) were used as sample solutions in this test. The ends of two inlets of the μ TAD were immersed into two reservoirs filled with solutions 2 and 3, respectively. After the solutions had fully wet the two inlets, the device was folded (by hand, tweezers, or clippers) to direct two solutions into the twisted threads simultaneously for mixing [Fig. 8(b)]. Universal pH test paper was used to test the pH values for three points: (i) middle of inlet transporting solution 2, (ii) middle of inlet transporting solution 3, and (iii) 1 cm from the intersection of the twisted threads (outlet) [Fig. 8(c)]. The theoretical pH values of solutions 2 and 3 are 2 and 12, respectively, which are concordant with the testing values of the first and second test points (at the inlets) from the 12 repeated measurements. For the third test point (i.e., the outlet or reaction product point), readings were recorded at 1 and 3 min after the device being folded. All measurements were repeated 12 times and the results showed that for this test point, the pH value varied between 6 and 8. Compared with the theoretically expected pH value of 7 for the reaction product, the measured values indicated that the unneutralized reagent concentration is at most $10^{-6}M$ (i.e., $\geq 99.99\%$ conversion), showing the intended neutralization and hence mixing capability of the thread-based micromixer.

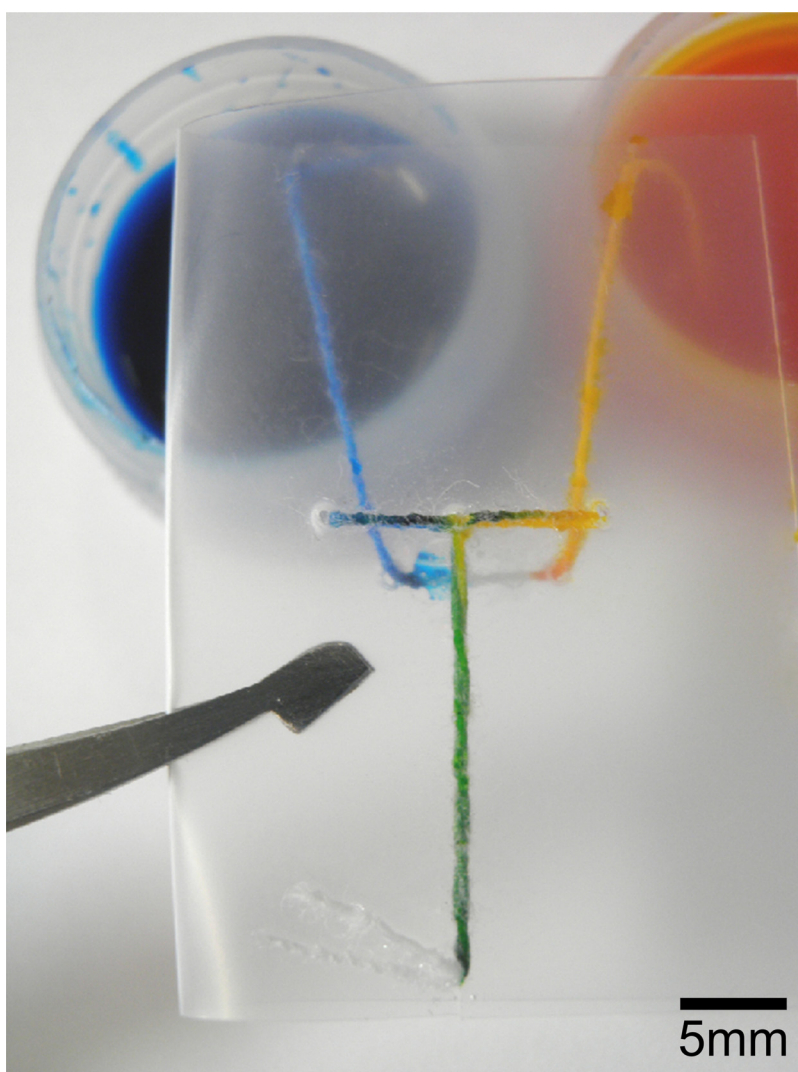


FIG. 7. A micromixer device used to mix two colored inks together. The green color produced illustrates the efficacy of the device.

The concept of building thread-based functional elements (e.g., switches, microselectors, and micromixers) into low-cost μ TADs is valuable for more advanced fluid flow control and provides possibilities for performing multistep reactions on μ TADs without compromising the low fabrication cost and ease of use.

IV. CONCLUSIONS

This study shows that the ability to control flow on thread allows for more sophisticated functions to be built into μ TADs. The measurement of fluid penetration distances and flow rates on thread is an important consideration for the design of μ TADs and understanding fluid transport in these devices. The capacity to mix and select between reagents enables the user to create devices with higher functionality, and facilitates the incorporation of more complex chemistries. The results of this work show that such devices can be made simply and cheaply by relatively unskilled persons using inexpensive materials.

Various mechanisms of flow control (i.e., functional elements) have been demonstrated in this study, with the most basic being the binary on/off style switch which is useful for controlling the

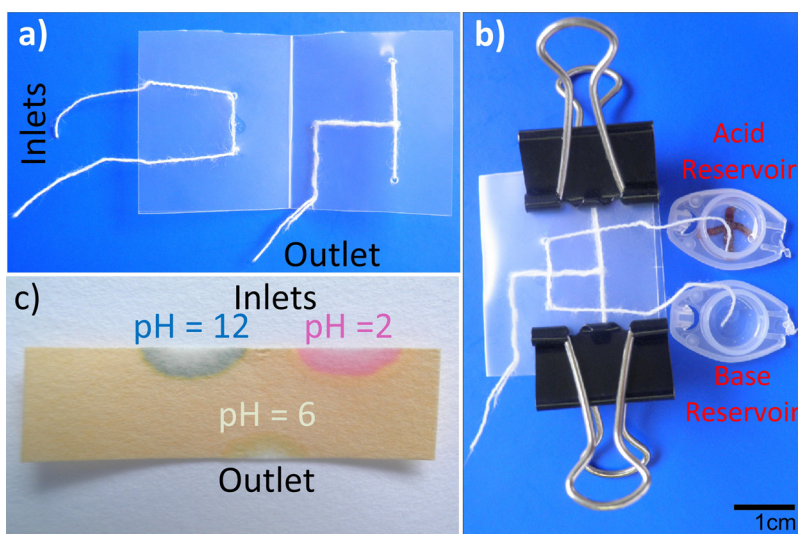


FIG. 8. A micromixer used to neutralize acid and base solutions to demonstrate the possibility of high quality mixing. (a) The unused mixer with inlets on the left and outlet on the lower right. (b) The device in use with one acid inlet (0.01M HCl), one base inlet (0.01M NaOH), and reservoirs. The device is held shut by bulldog clips. (c) pH paper showing measurements from the inlets (pH 2 and 12) and outlet (pH 6), suggesting that 99.99% of the acid was neutralized by the base.

timing of fluid introduction to reactors or other channels. More sophisticated designs included microselectors which give the user the ability to direct flow to one specific outlet given multiple choices. It was also shown that microselectors could function in reverse, with the user selecting one of several samples to be directed into a single outlet. Micromixers which could effectively mix multiple fluids together at a desired time were also developed, allowing the inclusion of multiple-step chemistries into thread-based microfluidics. For these functional elements of thread microfluidic systems, actuation can also be achieved by incorporating external elements (e.g., magnetic or electronic elements) to trigger folding or tab pulling and prolonged closure of the devices.

Concepts presented in this study have provided more flexibility for the design of μ TADs by giving designers new mechanisms for the control of fluid flows without compromising the distinctive properties of μ TADs, such as low cost and ease of use. It is hoped that this addition to knowledge in the field can be utilized to create more functional devices for the detection of disease, environmental contamination, or other novel applications.

ACKNOWLEDGMENTS

The research scholarships of Monash University and the Department of Chemical Engineering are gratefully acknowledged. The authors thank Dr. L. Wang of the School of Fashion and Textiles, RMIT University, for kindly providing us with thread and textile samples, Ms. Y. H. Ngo for assistance in obtaining SEM images, and Mr. K. Wu for assistance in generating fluid penetration data.

- ¹D. Mabey, R. W. Peeling, A. Ustianowski, and M. D. Perkins, *Nat. Rev. Microbiol.* **2**, 231 (2004).
- ²P. von Lode, *Clin. Biochem.* **38**, 591 (2005).
- ³W. G. Lee, Y.-G. Kim, B. G. Chung, U. Demirci, and A. Khademhosseini, *Adv. Drug Delivery Rev.* **62**, 449 (2010).
- ⁴P. Yager, G. J. Domingo, and J. Gerdes, *Annu. Rev. Biomed. Eng.* **10**, 107 (2008).
- ⁵P. Yager, T. Edwards, E. Fu, K. Helton, K. Nelson, M. R. Tam, and B. H. Weigl, *Nature (London)* **442**, 412 (2006).
- ⁶E. M. Fenton, M. R. Mascarenas, G. P. López, and S. S. Sibbett, *ACS Applied Materials & Interfaces* **1**, 124 (2009).
- ⁷X. Li, J. Tian, G. Garnier, and W. Shen, *Colloids Surf., B* **76**, 564 (2010).
- ⁸A. W. Martinez, S. T. Phillips, G. M. Whitesides, and E. Carrilho, *Anal. Chem.* **82**, 3 (2010).
- ⁹X. Li, J. Tian, T. Nguyen, and W. Shen, *Anal. Chem.* **80**, 9131 (2008).
- ¹⁰A. Qi, L. Yeo, J. Friend, and J. Ho, *Lab Chip* **10**, 470 (2010).
- ¹¹Y. Lu, W. Shi, L. Jiang, J. Qin, and B. Lin, *Electrophoresis* **30**, 1497 (2009).

- ¹²K. Abe, K. Suzuki, and D. Citterio, *Anal. Chem.* **80**, 6928 (2008).
- ¹³H. Noh and S. T. Phillips, *Anal. Chem.* **82**, 4181 (2010).
- ¹⁴R. Pelton, *TrAC, Trends Anal. Chem.* **28**, 925 (2009).
- ¹⁵M. S. Khan, G. Thouas, W. Shen, G. Whyte, and G. Garnier, *Anal. Chem.* **82**, 4158 (2010).
- ¹⁶A. W. Martinez, S. T. Phillips, M. J. Butte, and G. M. Whitesides, *Angew. Chem., Int. Ed.* **46**, 1318 (2007).
- ¹⁷X. Li, J. Tian, and W. Shen, *ACS Applied Materials & Interfaces* **2**, 1 (2010).
- ¹⁸R. Safavieh, M. Mirzaei, M. A. Qasaimeh, and D. Juncker, *Proceedings of MicroTAS 2009, The 13th International Conference on Miniaturized Systems for Chemistry and Life Sciences*, ICC Jeju, Jeju, South Korea, 1–5 November 2009.
- ¹⁹M. Reches, K. A. Mirica, R. Dasgupta, M. D. Dickey, M. J. Butte, and G. M. Whitesides, *ACS Applied Materials & Interfaces* **2**, 1722 (2010).
- ²⁰J. L. Osborn, B. Lutz, E. Fu, P. Kauffman, D. Y. Stevens, and P. Yager, *Lab Chip* **10**, 2659 (2010).
- ²¹E. Fu, S. Ramsey, P. Kauffman, B. Lutz, and P. Yager, *Microfluid. Nanofluid.* **10**, 29 (2011).
- ²²E. Fu, B. Lutz, P. Kauffman, and P. Yager, *Lab Chip* **10**, 918 (2010).
- ²³E. Fu, P. Kauffman, B. Lutz, and P. Yager, *Sens. Actuators B* **149**, 325 (2010).
- ²⁴D. J. Shaw, *Introduction to Colloid and Surface Chemistry* (Butterworth-Heinemann, Ann Arbor, 1992).
- ²⁵A. W. Martinez, S. T. Phillips, and G. M. Whitesides, *Proc. Natl. Acad. Sci. U.S.A.* **105**, 19606 (2008).
- ²⁶N. Wang, A. Zha, and J. Wang, *Fibers Polym.* **9**, 97 (2008).
- ²⁷E. W. Washburn, *Phys. Rev.* **17**, 273 (1921).
- ²⁸R. R. Rye, F. G. Yost, and J. A. Mann, *Langmuir* **12**, 4625 (1996).
- ²⁹G. Budworth, *Essential Knots & Basic Ropework* (Lorenz, New York, 2000).



Appendix II: Related Co-Authored Papers Not Included in the Main Body of This Thesis

This page is intentionally blank

Cite this: *Lab Chip*, 2011, **11**, 2869www.rsc.org/loc

PAPER

Printed two-dimensional micro-zone plates for chemical analysis and ELISA†

Junfei Tian, Xu Li and Wei Shen*

Received 3rd May 2011, Accepted 3rd June 2011

DOI: 10.1039/c1lc20374f

In this study we report a new concept of printing low-cost two-dimensional micro-zone plates for chemical and biochemical assays and ELISA. It is different from the concept of forming multi-zone micro-zones on paper by hydrophobic barriers first reported by Yagoda. Instead, the desired multi-zone micro-zone pattern was first printed using a UV-curable varnish onto a polymer film; then fine powders of cellulose or other materials were applied onto the uncured varnish, allowing the powder to stick to the varnish layer. After UV-curing, the powder particles were fixed by the cured varnish, leading to the formation of porous, water absorbing micro-zones on the polymer film. This type of micro-zone plate has the required liquid handling capacity for a variety of low-volume and portable two-dimensional plates for chemical, biochemical assays and ELISA. By suitably spacing porous micro-zones on a non-porous substrate, this type of plate eliminates inter-zone sample leaking. Rapid colorimetric analysis of the results can be performed using a portable battery-powered colour densitometer or a desktop scanner. By introducing a refractive-index-matching liquid into the micro-zones, the plate can be easily analyzed using transmission instruments. A major advantage of this plate fabrication method is that it enables the printing of different powders or functionalized powders to form micro-zones on a same plate, potentially allowing certain more difficult functionalization of materials to be performed before printing. We demonstrate the assaying performance of the plates using an analytical system that aims to clarify the analytical interference between NO_2^- and uric acid (UA) in the analysis of samples where both chemical species are present. We also show that ELISA assays can be performed using this type of plates.

Introduction

Spot testing is a widely used methodology for many biochemical and diagnostic assays. Many qualitative and semi-quantitative spot assays are still in use in chemical and environmental analysis (e.g. nitrogen analysis) and clinical diagnostics (e.g. enzyme-linked immunosorbent assay, or ELISA). The simplicity of many spot assays makes them difficult to be phased out, even though more sophisticated, but much more expensive technologies have become available. A unique advantage of spot assays is that they can test a large sample set using colorimetric or fluorescent detecting techniques and obtain rapid semi-quantitative results *via* either visual detection or simple instrumental detection such as a plate reader. In other applications, spot assays can be used to optimize the assaying conditions of a specific test through a systematical variation of reaction parameters that can influence the test result; these parameters may be pH, reagent concentration or the presence of interferent chemical species. To achieve these tasks, multi-zone micro-zone plates are frequently used, and they become the basic testing devices for spot assays.

The costs of the current mainstream multi- micro-zone plates for spot assays are relatively high. Although a substantial cost goes into the biological reagents used to functionalize the micro-zones, the costs of the multi-well plate structure are still significant, compared to the printable 2D plate. The fabrication of multi-well plates requires polymer molding, which consumes a relatively large quantity of raw polymer materials, therefore, the commercial prices of such plates are also quite high.¹ For laboratory applications, the molded polymer plates typically require around 10 μL of several liquids to be added into a single zone. Such sampling volumes, although not large when compared to many conventional analytical methods, can still be further reduced if 2D micro-zone plates are used. Whilst these mainstream polymer molded multi- micro-zone plates enable a wide range of biochemical and ELISA assays to be performed with the accepted level of reliability, they are, however, reliant upon well-equipped laboratories.

Simple and portable micro-zone plates are therefore necessary, as they will not only reduce the fabrication cost, but also enable the analytical tests to be performed under a laboratory or non-laboratory condition with simple and portable equipment for result reading using either reflective signal recording modes (e.g. a portable colour reader, a desk-top scanner or a camera phone) or transmission signal recording modes (e.g. a portable

Department of Chemical Engineering, Monash University, Wellington Rd, Clayton, Vic, 3800, Australia. E-mail: wei.shen@eng.monash.edu.au

† Electronic supplementary information (ESI) available. See DOI: 10.1039/c1lc20374f

photospectrometer), thus easing the reliance on the availability of well-equipped laboratories. The implication of shifting spot assays from laboratory-based assays to non-laboratory-based assays is clear; such a shift will potentially allow many environmental assays and the diagnosis of some malicious diseases, such as AIDS and tuberculosis,^{2,3} to be performed in developing regions of the world where well-equipped laboratory facilities may not always be available.

Portable and two-dimensional multi-zone micro-zone plates have been explored previously on paper substrate. In 1937, Yagoda⁴ reported a method for making micro-zone plates using filter paper as a substrate. He used a heated brass die with a pattern of an engraved micro-zone design to press on a paraffin loaded paper on top of a plain filter paper, the melted paraffin was then transferred from the paraffin loaded paper into the filter paper, forming hydrophobic barriers that enclosed a series of hydrophilic circles on filter paper where the engraved area of the brass die could not melt and transfer paraffin onto filter paper. Yagoda used this approach to create a series of hydrophilic zones on a filter paper; he then used the micro-zone filter paper for spot tests. Recently, Carrilho *et al.*⁵ used the same principle reported by Yagoda, but employed more advanced technology, including photolithography, to fabricate paper-based micro-zone plate. The micro-zones of hydrophilic filter paper were created by means of a barrier of photoresist. Cheng *et al.*⁶ reported that micro-zone plates made using a more sophisticated approach can perform ELISA.

In this work, we present an alternative fabrication concept of two-dimensional multi-zone micro-zone plates to that pioneered by Yagoda.⁴ Our fabrication concept is to print porous micro-zones onto a polymer film. A significant advantage of our fabrication concept over the reported methods⁴⁻⁶ is that it offers much more flexibility in forming micro-zones of different materials or functionalized micro-zones on one plate. Powders or other forms of materials can be biochemically functionalized before being printed on the plate. This approach offers an easy solution for more difficult micro-zone functionalizations to be first conducted using high-efficiency *ex situ* methods and the functionalized particles to be then printed to form the micro-zone plate. For surface functionalizations of micro-zones involving multi-step biochemical reactions, this approach is easier than conducting *in situ* local functionalization on a paper surface. We demonstrate this advantage by printing cellulose and Teflon powders on one micro-zone plate with two steps of printing. Another advantage is that it is easy to transform a powder-printed micro-zone plate from the reflective to the transmission signal recording mode using a refractive index matching fluid. Using fluid to match the refractive index of paper for transmission analysis has been reported by Müller and Clegg.⁷ Recently Ellerbee *et al.*⁸ reported the use of oil as the refractive index matching fluid for paper-based sensors. The advantage of our design is that a fluid, such as oil, will be restricted only on one surface of the polymer film, significantly improving the ease of plate handling for transmission analysis.

To demonstrate the performance of the plate we carried out a semi-quantitative two-component colorimetric assay and a ferritin ELISA. The two-component colorimetric assay aims to evaluate the analytical interference of two human health biomarkers, the NO_2^- and uric acid (UA). These biomarkers co-

exist in human body fluids, such as in blood and saliva and can be used to evaluate the conditions of renal and lung disease patients.^{9,10} Successful quantification of those chemical species in human samples relies on the non-interference of these species under the assay conditions. We also show that by printing the micro-zones with a protein-binding substrate, the plate can be used for ELISA assays. A battery-operated press room colour densitometer was used to read the plate to obtain the assay results.

Our study shows that the low-cost multi-zone micro-zone plates fabricated using this new approach are capable of delivering quantitative analytical results within the relevant concentration range of the biomarker analysis.

Experimental

Chemicals, materials and solution preparation

The stock solution of NO_2^- (10.0 mmol L^{-1}) was prepared by dissolving 69.0 mg sodium nitrite ($\geq 99\%$, Sigma-Aldrich) in 100 mL water. This stock solution was then diluted with water to make serially diluted NO_2^- solutions of 2000, 1000, 500, 250, 125 and 0 $\mu\text{mol L}^{-1}$. The UA stock solution (12.8 mmol L^{-1}) was prepared by dissolving 215.0 mg uric acid ($\geq 99\%$, Sigma-Aldrich) in 100 mL of 0.2 mol L^{-1} NaOH solution. This stock solution was then diluted with 0.2 mol L^{-1} NaOH solution to make serially diluted UA solutions of 2000, 1000, 500, 250, 125 and 0 $\mu\text{mol L}^{-1}$.

The serially diluted NO_2^- solutions were then mixed with equal volumes of UA solutions of 0, 200, 1000 and 2000 $\mu\text{mol L}^{-1}$ to form the final NO_2^- solution series for the interference study. The NO_2^- concentrations of the final solution series are 1000, 500, 250, 125, 62.5 and 0 $\mu\text{mol L}^{-1}$, and with four levels of UA (1000, 500, 100, 0 $\mu\text{mol L}^{-1}$) as the interferent species. The same procedure was used to prepare the final solution of UA for the interferent study against NO_2^- . A detailed plan of sample and interferent solution introduction to the printed 2D multi-zone plate can be found in Fig. S1 and S2 of the ESI†.

The Griess reaction was used for NO_2^- detection. The indicator solution for NO_2^- contains 50 mmol L^{-1} sulfanilamide ($\geq 99\%$, Sigma-Aldrich), 330 mmol L^{-1} citric acid ($\geq 99.5\%$, Sigma-Aldrich), and 10 mmol L^{-1} *N*-(1-naphthyl) ethylenediamine ($\geq 98\%$, Sigma-Aldrich).⁹

The indicator solution for UA consists of the 1 : 1 mixture of solution A (2.56% (w/v) 2,2'-biquinoline-4,4'-dicarboxylic acid disodium salt hydrate, $\geq 98\%$, Sigma-Aldrich) and solution B (20 mmol L^{-1} sodium citrate and 0.08% (w/v) copper (II) sulfate, $\geq 99\%$, Sigma-Aldrich).⁹

For ferritin ELISA tests, all reagents, except for the ferritin antibody, were obtained from Sigma-Aldrich. Ferritin mitochondrial antibody (AB7334) conjugated with horseradish peroxidase (HRP) was obtained from Abcam. The stock solution of ferritin, which was isolated from human liver (Type IV, 10 $\mu\text{g mL}^{-1}$), was diluted with phosphate-buffered saline (PBS, pH 7.4) to 1 $\mu\text{g mL}^{-1}$. The stock solution of antibody for ferritin (10 mg mL^{-1}) was diluted to the final concentration of 2 $\mu\text{g mL}^{-1}$ before use. A 1% bovine serum albumin (BSA) solution was prepared by dissolving BSA powder in PBS solution. A liquid substrate for HRP, 3,3',5,5'-tetramethylbenzidine (TMB), was used to generate colorimetric signal for analysis.

Cellulose powder (Sigma-Cell, average particle size = 20 μm) and Teflon powder (average particle size 35 μm) were obtained from Sigma-Aldrich. The cellulose powder was used to print the 96-zone plate for the interference study of nitrite ion and uric acid. The polymer film used in this study was a commercial overhead transparency (Xerox). A UV curable flexographic post-print varnish (UV 412) was received as a gift from Flint Inks (Flint Group Australia). Nitrocellulose film (Hybond—C Extra, GE Healthcare) was used for printing of nitrocellulose micro-zone plate for ELISA. Teflon powder was used for printing plates that contain Teflon and cellulose micro-zones.

A portable, battery-operated colour reflection densitometer (X-Rite 404, X-Rite Inc., USA) was used to quantify the colour density changes of the assays in the micro-zones. The X-Rite densitometer has a measurement aperture of 4 mm and it can be calibrated against different substrates. The densitometer measures the major reflected spectral components and gives the average colour density of the measured area (with $D = -\log(I/I_0)$), where D is the measured optical density, I_0 and I are the incident and measured reflected light intensities. A transmission spectrometer (Screen DM-500, Dainippon Screen MFG. Co. Ltd, Kyoto, Japan) was used to measure the light absorbance in transmission mode. These spectrometers are standard instruments in printing industry for colour measurements of printed papers and transparent films.

Fabrication of multi-zone micro-zone plate

A rubber relief printing master (similar to a flexographic printing plate) with the designed printing patterns was used to transfer a thin layer of UV curable varnish onto the transparency film. Cellulose powder was then dusted onto the printed transparency film. Powder particles landed onto the printed but uncured varnish pattern and adhered to the varnish. The UV curable varnish with the stuck cellulose powder was then cured by passing the printed film through a UV curing station; the cured varnish pattern on the transparency film provides good bonding to cellulose powder, which formed porous micro-zones. To suit the use of the X-Rite densitometer in our work, 3 mm diameter micro-zones were designed for all plates. Fig. 1 shows a printed 96-zone plate.

For the ELISA plate, where nitrocellulose film cannot be exposed to UV light, a pattern of a printable air-drying glue was printed on the transparency film to which the nitrocellulose film

was adhered. After the glue became dried, the nitrocellulose film was peeled off, leaving the micro-zones covered with the nitrocellulose film.

Serially diluted Canon ink jet printing inks¹¹ with MilliQ water (undiluted original, 50%, 25%, 12.5% and 6.25%) were used to investigate the colour display abilities of the porous zones of cellulose powders. The original ink was taken as 100%. To characterize the colour display ability of the printing micro-zone plate, an aliquot of 0.3 μL of the ink solutions was added into each zone, the resultant colour was measured using an X-Rite colour spectrometer (X-Rite 404) after the ink dried under ambient conditions. Details of the colour display characterization of the printed micro-zone plate are presented in the ESI†.

Analytical strategy using multi-zone micro-zone plates

The printed cellulose 96-zone plate was used to investigate the interference of UA to the analysis of NO_2^- (and also the interference of NO_2^- to the analysis of UA). To accommodate all combinations of the test conditions, the plate was divided into 4 regions. For the analysis of NO_2^- , a calibration series of six NO_2^- concentrations (0, 62.5, 125, 250, 500, 1000 $\mu\text{mol L}^{-1}$) were used. Four different concentrations of UA (0, 100, 500, 1000 $\mu\text{mol L}^{-1}$) were used as four levels of interferent species. Similarly, for the analysis of UA, a calibration series of six UA concentrations (0, 62.5, 125, 250, 500, 1000 $\mu\text{mol L}^{-1}$) were used. Four different concentrations of NO_2^- were used as four different levels of interferent species. Two microlitres of sample-interferent mixture solution (equal-volume mixture as described above) were added to each zone for analysis. The division of the plate into four regions allows the six-point sample series to be analysed in four repeats, and under four different concentrations of interferent species. This combinatorial arrangement therefore allows the interference study to be carried out by this 96 (*i.e.*, $6 \times 4 \times 4$) spot assay. A detailed division of the four regions is presented pictorially in Fig. S1 and S2 of the ESI†.

In the NO_2^- analysis, a 1 μL aliquot of NO_2^- indicator solution was added to each of the 96 zones. Colour changes in the micro-zones were measured using the X-Rite densitometer. A similar approach was taken for the analysis of UA. A 1 μL aliquot of indicator solution for UA was added to all 96 zones, and colour changes were measured using the X-Rite densitometer.

The protocol of the direct ELISA of ferritin is as follows: ferritin standards were made by diluting the stock solution with PBS solution to 0, 80, 250, 500 and 1000 ng mL^{-1} . Then a four-step procedure is followed: Step 1, a 4 μL aliquot of each of the five ferritin solutions of different concentrations was added into five zones and incubated until dry. Step 2, the dried plate was then dipped into a 1% BSA blocking buffer and incubated for 20 minutes. Step 3, the BSA blocked plate was washed with PBS solution twice, then 2 μL of 2 $\mu\text{g mL}^{-1}$ AB7334 was added into each zone and incubated for 20 minutes. Step 4, the plate was then washed for 3 times with PBS solution, then 2 μL TMB substrate was added into each zone and incubated for 2 minutes in the dark. A pictorial description of the protocol is presented in Fig. S3 of the ESI†. In order to maintain the micro-zones under moist conditions, the plate was kept inside a covered Petri dish in step 3. This is necessary as drying of the micro-zone affects the colour

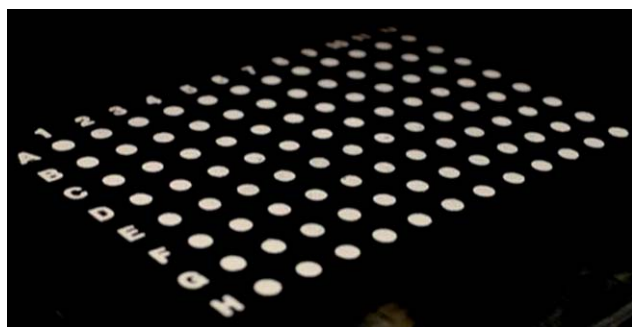


Fig. 1 A 96-zone plate printed with UV-curable varnish and cellulose powder on a polymer transparency film.

development of the substrate (TMB). This method can keep these zones moist for up to 24 hours or even longer. The X-Rite densitometer was used to quantify the colour density changes.

Results and discussion

Characterization of the printed micro-zones

Since the printable UV varnish used in this study was a commercial printing material for films, it has excellent printability on a polymer transparency. To form the required thickness of the varnish film on the polymer film for micro-zones, 0.9 g m^{-2} was required (only the printed area is considered). This gave the printed varnish layer thickness of $0.8 \mu\text{m}$, taking the supplier provided density of the varnish of 1.1 g cm^{-3} . The cellulose powder adhered to each of the micro-zone was gravimetrically determined to be 0.1 mg per zone. Cellulose powder uniformly covered each and every micro-zone, making all micro-zones opaque. Detailed characterization for Teflon powder printed micro-zones was not conducted, but it is expected to be similar to the cellulose powder micro-zones.

The liquid handling capacity and colour display ability of the printed micro-zone plate are presented in detail in Fig. S4 and S5 of the ESI†.

Analytical interference studies of mixed biomarkers using the printed 96-zone plate

Uric acid (UA) and NO_2^- are two important biomarkers of several human health conditions. They have been used jointly to evaluate the condition of renal and lung disease sufferers.⁹ They are present in human body fluids such as blood and saliva. Although detection methods for UA and NO_2^- are available in the literature,¹⁰ their detection interference must be investigated. This is because these two biological species co-exist in human samples.

The first interferent study takes NO_2^- as the analyte and UA as the interferent chemical species. (Fig. S1 in the ESI† describes the analytical strategy of the sample. Regions 1, 2, 3 and 4 of the printed plate were used for analyzing NO_2^- samples containing different levels of UA from 0 to $1000 \mu\text{mol L}^{-1}$.)

One microlitre of the indicator solution for NO_2^- was added to each and every micro-zone and the resultant colour changes in all zones were measured using the X-Rite densitometer. Fig. 2(a) presents a photo for visual appreciation of the micro-zone plate after indicator solution was added to all zones. Fig. 2(b) shows the calibration curves of colour density vs. NO_2^- concentration for each interferent concentration.

The curves of colour density against NO_2^- concentration with the four different concentrations of UA show very little difference and are almost coincident. This suggests that the presence of UA at the concentrations studied does not interfere with the Griess reaction.

The second interferent study takes UA as the analyte and NO_2^- as the interferent chemical species. (Fig. S2 in the ESI† describes the analytical strategy of the samples. Regions 1, 2, 3 and 4 of the printed plate were used for analyzing UA samples containing different levels of NO_2^- from 0 to $1000 \mu\text{mol L}^{-1}$.)

One microlitre of the indicator solution for UA was added to each micro-zone and the resultant colour changes in all zones

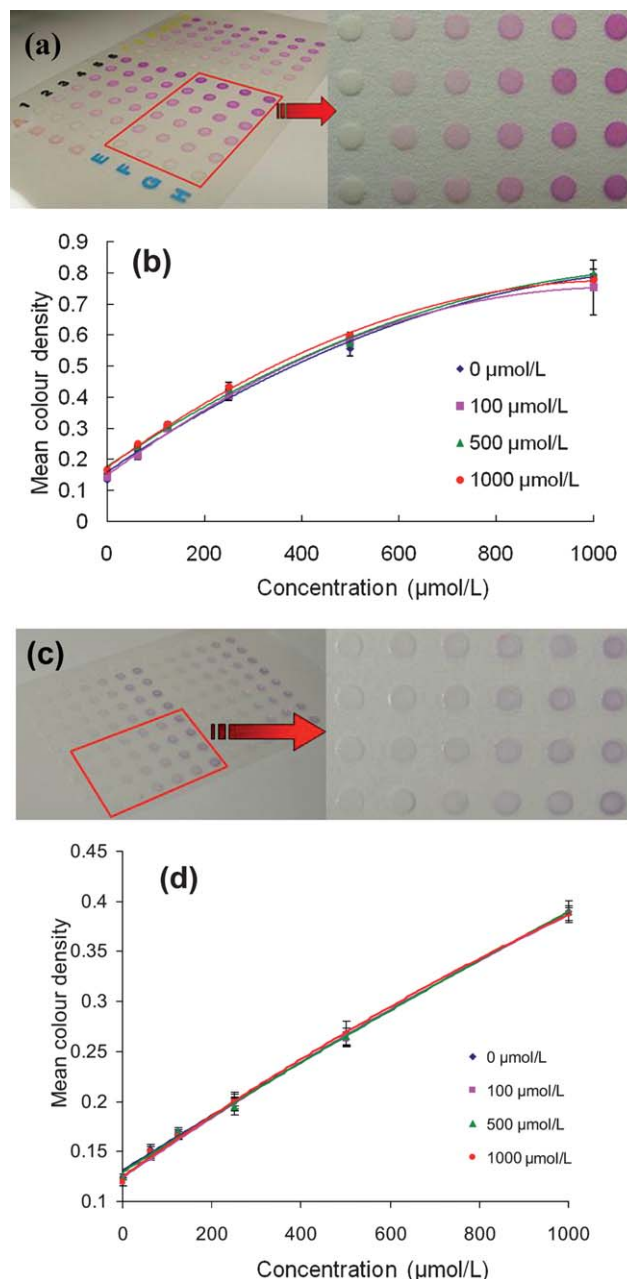


Fig. 2 (a) A photo of a micro-zone plate loaded with NO_2^- sample and UA as the interferent species; one microlitre of indicator solution to NO_2^- was added to all zones. (b) The mean optical density readings of NO_2^- in micro-zones as a function of NO_2^- concentration: the four curves represent data obtained from four regions; each curve has six data points related to six NO_2^- concentrations along each row in a region; the error bars are the standard deviation of the four readings from the four repeated measurements along each column in a region. (c) A photo of a micro-zone plate loaded with UA sample and NO_2^- as the interferent species; one microlitre of indicator solution to UA was added to all zones. (d) The mean optical density readings of UA in micro-zones as functions of UA concentrations: the four curves represent data obtained from four regions; each curve has six data points related to six UA concentrations along each row in a region; the error bars of the data points are the standard deviations of the four readings from the four repeat measurements along each column in a region.

were measured using the X-Rite densitometer. Fig. 2(c) presents the photo for visual appreciation of the micro-zone plate after indicator solution was added to all zones. Fig. 2(d) shows the calibration curves of colour density against UA concentration for each interferent concentration. The results show that the presence of NO_2^- in UA sample solutions does not interfere with the UA assays. UA samples registered lower colour density than NO_2^- assay samples, therefore, their calibration curves are almost linear in the range of 0–1000 $\mu\text{mol L}^{-1}$.

The results of the interference study show that there is no discernible chemical interference from UA in a semi-quantitative analysis of NO_2^- . The analyte and interferent levels of NO_2^- and UA analyzed in this study cover the clinically relevant ranges of the two biomarkers.⁹ This conclusion is in agreement with a recent study by Nagler¹⁰ who used a different approach. It shows that semi-quantitative assays for these two biomarkers do not require separation or special pre-assay chemical treatments. The use of a printed cellulose powder multi-zone micro-zone plate allows simple management of analyte/interferent species and rapid multiple measurements. The printed multi-zone micro-zone plate therefore offers a simple and low-cost alternative tool for multiplex biomarker assaying.

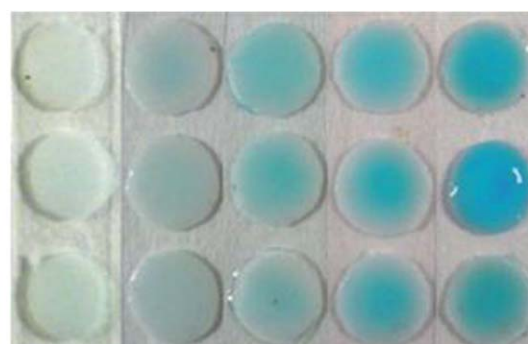
Ferritin ELISA using multi-zone micro-zone plates

To ensure strong ferritin bonding, the micro-zones were printed using nitrocellulose film. Four microlitres of diluted ferritin solutions of 0, 80, 250, 500 and 1000 ng mL^{-1} were added into the micro-zones (as described in the ferritin ELISA protocol in the Experimental section, see also Fig. S3 in the ESI†). The plate was then dipped in a 1% BSA solution for 20 minutes for blocking. After the BSA blocking, a 1.5 μL aliquot of 2 $\mu\text{g mL}^{-1}$ ferritin mitochondrial antibody (AB7334) conjugated with horseradish peroxidase (HRP) was added to each zone. To remove the unbound antibody, the plates were dipped into a small vial of fresh PBS solution 3 times, and then gently blotted with a piece of blotting paper to remove the washing solution from the surface of the plate. After adding liquid substrate to each zone and allowing for 2 minutes of incubation under dark conditions, a colour gradient developed; Fig. 3(a) shows three parallel assays. Reflective colour density readings of the micro-zones with the X-rite densitometer generated the standard curve (Fig. 3(b)), where data points were the mean of the three density readings and the error bar was the standard deviation.

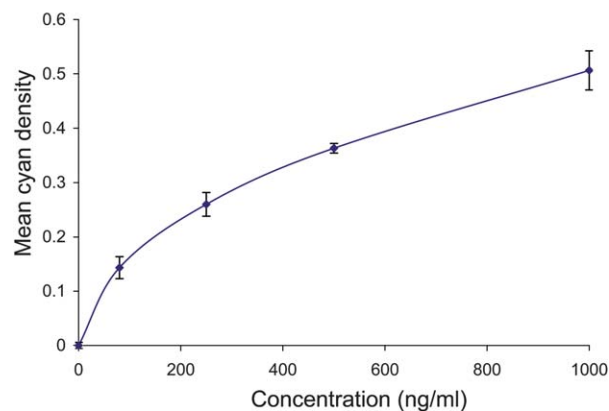
While using nitrocellulose film to perform ELISA has been demonstrated before, the purpose of our study is to demonstrate the ability to print different materials to form micro-zones. An advantage of printed polymer film micro-zone plates is that the plate can easily withstand washing without dimensional distortion. Combined with a portable colour density reading device, the printed plate enables the ELISA testing under non-laboratory conditions where only basic facilities are available.

Printing of different powders on the same micro-zone plate

The most significant advantage of our new fabrication concept is that it offers an easy means to print different powders or a powder that has received different biochemical functionalization treatments on a same plate. Whereas cellulose powder



(a)



(b)

Fig. 3 Results of ferritin ELISA assays obtained from printed micro-zone plates: (a) a photo for visual appreciation, columns are presented electronically closer to show detail; (b) the calibration curve of the ferritin concentration and the measured colour density on.

makes general purpose micro-zones, other powders may also be printed for more specific diagnostic or analytical uses. In certain situations where micro-zones require more complicated bio-functionalization, it is more economical to first functionalize the powder surface using highly efficient methods and apparatus *ex situ* and then form micro-zone plates with the functionalized powders by printing than to perform the *in situ* local surface functionalization on a paper micro-zone plate. We believe the ability to print micro-zones of different materials on the same plate with the already functionalized powder materials is a valuable new feature of our fabrication concept. It offers an easy and low-cost means to fabricate 2D micro-zone plates that can accommodate single or multiple groups of micro-zones to perform different analytical tasks.

Fig. 4 shows the printing of cellulose and Teflon powders onto the same micro-zone plate; columns 1 to 6 were printed with cellulose powder and columns 7 to 12 with Teflon powder. One microlitre of ink jet ink solution was added to the cellulose micro-zones, whilst 8 μL of ink solution was added to the Teflon micro-zones to demonstrate the difference.

Printed powder micro-zone plate for transmission analysis

Refractive index matching using oil and other organic solvents was used to transform the printed powder micro-zone plate for

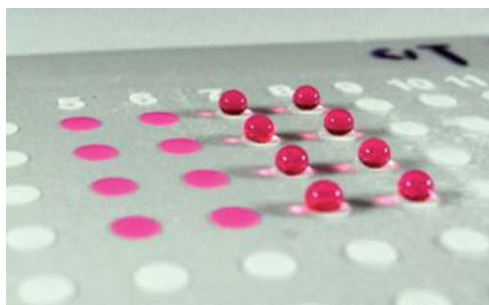


Fig. 4 A micro-zone plate printed with cellulose (columns 1 to 6) and Teflon (columns 7 to 12) powders. One microlitre of an ink jet ink solution was added to zones printed with cellulose powder; 8 μL of ink solution was added to zones printed with Teflon powder.

transmissional analysis. Since the quantity of powder in each zone is small, only a small amount of oil is required to convert the opaque zone into a transparent zone. Fig. 5 shows photos of printed cellulose powder micro-zones being transformed from opaque (Fig. 5(a)) to transparent (Fig. 5(b)) by adding 1.5 μL of microscope oil lens immersion oil to each zone. Cellulose has a refractive index of 1.55;¹² it is reasonably well-matched by the oil lens immersion oil (refractive index = 1.516) and the micro-zones became nearly transparent (compare Fig. 5(a) and (b) for micro-zones in row E). Refractive index matching of the Teflon micro-zones was made using ethanol. The refractive indices of Teflon and ethanol are 1.31–1.33¹³ and 1.36, respectively. The low surface tension of ethanol allows it to penetrate into the pores of the Teflon micro-zones, making the zones transparent. Fig. 5(c) shows micro-zones (A9, A10, A11) printed with Teflon

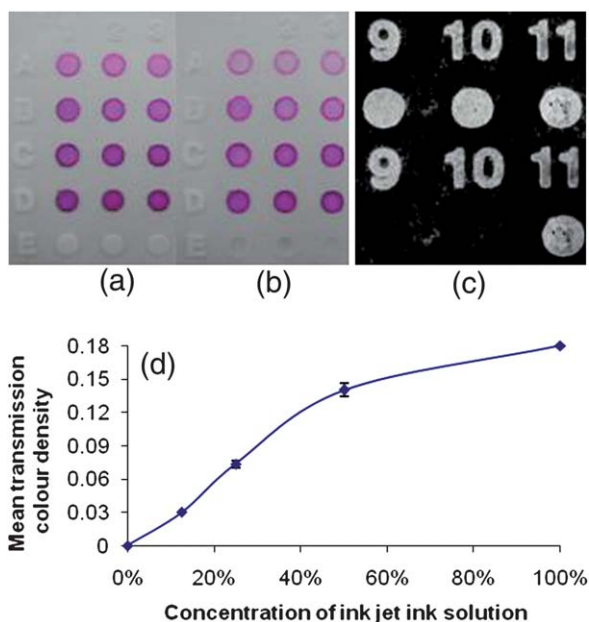


Fig. 5 (a) Micro-zones printed with cellulose powder; (b) microscope lens immersion oil (1.5 μL) added to each cellulose powder zone, all zones became transparent; (c) top: zones A9, A10, A11 printed with Teflon powder, bottom: ethanol was added to zones A9 and A10 to match the refractive index of Teflon and these zones became transparent; (d) ink jet ink colour absorption measurement by a transmission spectrometer.

powder; when ethanol was added to zones A9 and A10 they became transparent.

A transmission spectrometer (Screen DM-500) was used to measure the colour absorption of the micro-zones; results are presented in Fig. 5(d).

Fig. 5 shows that it is possible and easy to use refractive index matching fluids to transform the printed powder micro-zones on polymer film for transmission analysis. The easy handling of the polymer film micro-zone plate provides it with more flexibility for designing 2D plates for low-cost laboratory use or for diagnostic analysis with portable signal readers in remote locations under non-laboratory conditions.

Conclusions

In this study we show a new concept and fabrication method for making low-cost, portable, low-volume and easy-to-use two dimensional micro-zone plates. Since the printed micro-zones are porous whereas the substrate is non-porous, the micro-zone plate eliminates sample leaking between zones.

The micro-zone plates show suitable liquid handling ability required for biochemical assays and ELISA; they also show a strong and consistent colour displaying ability. The polymer film offers the plate a high dimensional stability when the plate is wetted by aqueous solutions, making washing of the micro-zones (in ELISA) very easy. The colour of the micro-zones can be easily analyzed using a portable, battery-driven densitometer or a scanner. The ability of these micro-zone plates to perform chemical assays and ELISA has been demonstrated. Also, the micro-zones can be measured by reflective or transmission spectrometers. The polymer film substrate makes the refractive index matching using an appropriate plate more easy to handle.

A significant advancement of this new fabrication concept is that it allows different powder materials to be printed on the same plate to form different micro-zones. This advancement also allows the printing of the already functionalized powders; it fulfills the necessity that in certain situations where surface functionalization of the micro-zones needs to be performed separately. This fabrication approach will therefore be able to take advantage of the well-developed laboratory-based bio-functionalization and the flexibility of the printing operation.

This new fabrication approach has the potential to mass produce micro-zone plates using high throughput equipment. This is because most materials used in this study, such as film and UV-curable varnish, are printing materials; their printing compatibility is well-established. The functionalized powders can be printed on desired substrates, *i.e.*, transparent, white opaque or black, dependent on specific requirements.

Acknowledgements

Funding received from the Australian Research Council through DP1094179 is acknowledged. Professor David Finkelstein of the Centre for Neuroscience, Melbourne University is gratefully acknowledged for kindly providing us with the ferritin and the ferritin mitochondrial antibody (AB7334) for this work. JT and XL would like to thank Monash University Research and Graduate School and the Faculty of Engineering for their post-graduate research scholarships.

Notes and references

- 1 Sigma-Aldrich catalogue, <http://www.sigmaaldrich.com/australia.html>, accessed 15 September, 2010.
- 2 L. Goldman and D. Ausiello, *Cecil Medicine*, Saunders Elsevier, Philadelphia, 23rd edn, 2007, sect XXIV.
- 3 K. Lyashchenko, R. Colangeli, M. Houde, H. Jahdali, D. Menzies and M. Gennaro, *Infect. Immun.*, 1998, **66**, 3936.
- 4 H. Yagoda, *Ind. Eng. Chem., Anal. Ed.*, 1937, **9**, 79.
- 5 E. Carrilho, S. Phillips, B. Vella, A. Martinez and G. Whitesides, *Anal. Chem.*, 2009, **81**, 5990.
- 6 C. Cheng, A. Martinez, J. Gong, C. Mace, S. Phillips, E. Carrilho, K. Mirica and G. M. Whitesides, *Angew. Chem., Int. Ed.*, 2010, **49**, 4771.
- 7 R. H. Müller and D. L. Clegg, *Anal. Chem.*, 1949, **21**, 1123.
- 8 A. K. Ellerbee, S. T. Phillips, A. C. Siegel, K. A. Mirica, A. W. Martinez, P. Striehl, N. Jain, M. Prentiss and G. M. Whitesides, *Anal. Chem.*, 2009, **81**, 8447.
- 9 Blicharz, D. Rissin, M. Bowden, R. Hayman, C. DiCesare, J. Bhatia, N. Grand-Pierre, W. Siqueira, E. Helmerhorst, J. Loscalzo, F. Oppenheim and D. Walt, *Clin. Chem.*, 2008, **54**, 1473.
- 10 R. Nagler, *Clin. Chem.*, 2008, **54**, 1415.
- 11 Canon ink jet printing inks, <http://www.canon.com.au/>.
- 12 E. Lehtinen, *Pigment Coating and Surface Sizing of Paper*, Fapet Oy, Helsinki, Finland, 2000, p. 124.
- 13 R. Altkorn, I. Koev, R. P. Van Duyne and M. Litorja, *Appl. Opt.*, 1997, **36**, 8992.

Capillary driven low-cost V-groove microfluidic device with high sample transport efficiency†

Junfei Tian,^a Dushmantha Kannangara,^{ab} Xu Li^a and Wei Shen^{*a}

Received 1st March 2010, Accepted 12th May 2010

DOI: 10.1039/c003728a

In this study we investigate the liquid sample delivery speed and the efficiency of microfluidic channels for low-cost and low-volume diagnostic devices driven only by capillary forces. We select open, non-porous surface grooves with a V-shaped cross section for modeling study and for sensor design. Our experimental data of liquid wicking in V-grooves show an excellent agreement with the theoretical data from the V-groove model of Rye *et al.* This agreement allows us to quantitatively analyze the liquid wicking speed in V-grooves. This analysis is used to generate data for the design of sensors. By combining V-groove channels and printable paper-like porous detection zones, microfluidic diagnostic sensors can be formed. Non-porous V-grooves can be fabricated easily on polymer film. Suitably long surface V-grooves allow short liquid transport time (< 500 ms), thus reducing the evaporation loss of the sample during transport. Non-porous V-grooves also significantly reduce chromatographic loss of the sample during transport, therefore increasing the sample delivering efficiency. Sensors of such design are capable of conducting semi-quantitative chemical and biochemical analysis (*i.e.* with a calibration curve) with less than 1000 nL of sample and indicator solution in total.

Introduction

The concept and application of low-cost, portable and field-based diagnostic technologies have become an area attracting much research interest. The potential of these technologies in providing affordable healthcare and environmental monitoring in developing countries strongly drives new innovation for those applications. The use of patterned paper has been recently proposed as a platform technology for low-cost and portable diagnostics.¹ Based on this concept, there have been a number of recent studies into paper-based microfluidic sensors.^{2–6} The use of paper as a base material to fabricate microfluidic sensors exploits its low cost and desirable properties as a wettable, porous medium for liquid transportation and as a white display medium for colorimetric measurement of assays. The basic concept of using paper to fabricate low-cost bioassays has been extended to the use of other low-cost materials and fabrication processes, this could also lead to a new approach to the design of rapid and portable diagnostic devices. A recent report on using cotton thread to fabricate low-cost microfluidic sensors is one of such examples.⁷

In this paper we report the fabrication of low-cost microfluidic diagnostics for performing chemical analyses using small quantities of fluids (<1000 nL in total). The paper microfluidic sensors reported up to the end of 2009 require 2–4 μL ^{1,3,4} of liquid (*i.e.* sample and indicator solutions). This is because liquid transportation in paper requires the liquid to saturate the sample

dosing sites and the channel in order to reach the detection zones. The sample delivery efficiency of these paper microfluidic devices, *i.e.* the volume that reaches the detection sites verses the total volume, is typically less than 50%.^{3,4} For some samples, the sample delivery efficiency may be further reduced by the chromatographic effect. Although under normal circumstances the sampling volume and the delivery efficiency of paper microfluidic systems are adequate or acceptable, in situations where the sample quantity is very small, low-volume sensors with high sample delivery efficiency are desirable.

To reduce the ineffective sample consumption in transport channels of paper sensors, different channel designs are required. While it is desirable to use paper or paper-like materials to make detection zones in sensors, it is advantageous to use non-porous capillary channels to transport liquid samples from the sample inlet site to the detection zones. This is because a non-porous capillary channel can significantly reduce sample retention compared to the porous paper channel. The low surface area of non-porous capillary channels will also cause less chromatographic separation of the analytes in liquid samples, thus further increasing the sample delivery efficiency.

Another important advantage of a non-porous capillary channel is that it can increase the liquid transport speed. Liquid penetration speed in a porous medium can be modeled using the Washburn equation⁸ (eqn (1)), which was initially proposed to study liquid penetration dynamics in a single cylindrical capillary:

$$l = \sqrt{\frac{\gamma r \cos \theta}{2\eta} t} \quad (1)$$

where l is the liquid penetration distance in paper, r is the equivalent capillary pore radius of paper, γ and η are the surface tension and viscosity of the liquid, θ is the contact angle and t is the time of penetration. Yamasaki and Munakata⁹ proposed a more sophisticated model for liquid penetration in paper. In

^aAustralian Pulp and Paper institute, Department of Chemical Engineering, Monash University, Wellington Rd, Clayton, Vic. 3800, Australia. E-mail: wei.shen@eng.monash.edu.au

^bAMCOR Technical Services – Paper and Products, 626 Heidelberg Rd, Fairfield, VIC. 3078, Australia

† Electronic supplementary information (ESI) available: Details of V-groove channels and schematic of the experimental setup. See DOI: 10.1039/c003728a

their model, Yamasaki and Munakata used an average radius to describe the pore sizes in paper; they defined the number of pores in paper to be its porosity divided by the average pore cross section area. They considered that all pores exposed to water would contribute to water penetration. They further considered the porosity and the tortuosity of the capillary channel in paper, and reached a mathematical model showing that liquid penetration process in paper has the \sqrt{t} relationship similar to the Washburn equation.

Although the Washburn equation has been used as the first order estimation of the liquid penetration in paper,¹⁰ the water lateral wicking speed observed in paper is much slower than the value estimated using eqn (1).¹¹ If the average pore radius in a paper sheet is assumed to be 10 μm ,¹¹ and water has a contact angle of 10° with cellulose fibres, the Washburn model predicts that water can wick for a distance of 24 mm in paper in 1 s. However, experimental data of water wicking in filter paper strips show that the wicking speed is almost an order of magnitude slower. This is because water encounters non-cylindrical and irregular capillary passageways which slow down its wicking speed. Cellulose fibres in paper sheet swell rapidly when they are in contact with aqueous liquids; liquid absorption by the fibre wall further slows down the liquid penetration speed in paper. The aim of this work is to design and fabricate low-cost microfluidic devices with high sample delivery efficiency ($> 80\%$), which require a small quantity of liquid to conduct semi-quantitative analysis using a multi-point calibration curve. We used surface V-grooves as capillary channels to transport sample liquids and cellulose powder to formulate a printable paste to “print” porous liquid absorbing zones to form the detection zones of a sensor. A clear advantage of V-grooves is that they can be fabricated very easily on the surface of polymer films. Sensors made by combining liquid absorbing detection zones and non-absorbing liquid transport channels show a substantial improvement of sample delivery efficiency compared to sensors using porous sample transport channels. The V-groove sensors require small quantities of samples and indicator to conduct semi-quantitative analysis (< 1000 nL, *i.e.* sample and indicator solutions in total).

Sensor design concept and V-groove wicking data confirmation

Liquid retention in V-groove channel

In this study a single non-porous surface V-groove channel is used to transport a liquid sample into a porous detection zone which is printed over the channel. The porous detection zone was made of cellulose powder (20 μm). The capillary pressure for liquid penetration in the porous detection zone can be described using the Laplace equation by replacing the radius of curvature with the equivalent cylindrical pore radius of the porous detection zone.

$$\Delta P = \frac{2\gamma \cos \theta_p}{r_e} \quad (2)$$

Where ΔP is the Laplace pressure, r_e is the equivalent cylindrical pore radius of porous detection zone made of cellulose powder, γ is the liquid surface tension and θ_p is the contact angle between the liquid and the porous material that forms the detection zone.

Whilst the liquid wicking in V-groove channels has been investigated by Gerdes *et al.*,^{12–14} Rye *et al.*¹⁵ and Romero and Yost,¹⁶ the driving force was analysed in more detail by Rye *et al.*¹⁵ and Romero and Yost.¹⁶ In this study the Rye’s model is applied to confirm our liquid wicking data. In this model the Laplace pressure can be related to the geometry of V-groove to yield.¹⁵

$$\Delta P = \gamma \frac{\sin(\alpha - \theta) \tan \alpha}{h(l)} \quad (3)$$

where θ is the liquid contact angle between water and the groove wall, and α is the model variable angle (Fig. 1a and 1b). The $h(l)$ is the height of the liquid of the wicking front; it varies along the wicking front. When a liquid drop is placed over the groove, the Laplace pressure (eqn (3)) will drive the liquid to wick along the groove. As the liquid reaches the porous zone, the liquid will be driven by the capillary pressure of the porous zone. In the end, the porous zone absorbs most of the liquid from the groove; liquid left in the channel not absorbed can be estimated by equating eqn (2) and eqn (3):

$$h = \frac{\sin(\alpha - \theta) \tan \alpha}{2 \cos \theta_p} r_e \quad (4)$$

If $\alpha = 60^\circ$, $\theta = 30^\circ$ and $\theta_p = 30^\circ$ the liquid depth in the groove h will be $0.5r_e$. This estimation means that the liquid retention in a V-groove is very low (Fig. 2).

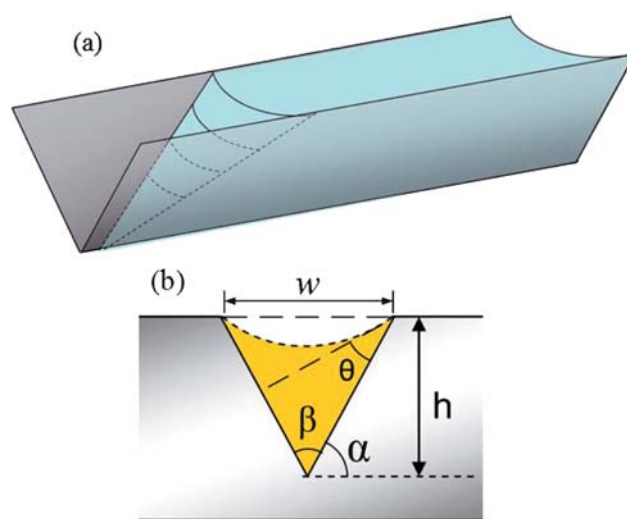


Fig. 1 (a) A schematic showing the geometry of a liquid wicking front in a V-groove; (b) modeling parameters of capillary flow in a V-groove.

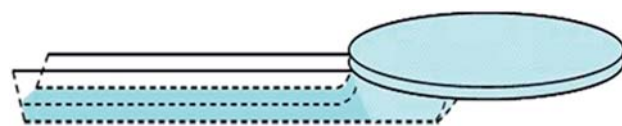


Fig. 2 A schematic of liquid retention in a V-groove which is in contact with a porous material.

Liquid transport speed in V-grooves

Rye *et al.*¹⁵ have proposed a wicking dynamics model which shows that liquid wicking in a V-groove follows a pseudo Washburn relation, *i.e.* liquid wicking distance in a V-groove is proportional to the square root of time (eqn (5)). The model was established based on the principle of an (interfacial) energy balance, and at the same time considered the balance of a capillary driving force and the Poiseuille type liquid flow resistance force in a V-groove channel. By applying the boundary conditions that the V-groove is connected to a large liquid reservoir with no external pressure, Rye *et al.* arrived at a model (eqn (5)). Rye's model shows a strong dependence of liquid wicking rate upon V-groove geometry (*i.e.* the groove depth, h_0 and the apex angle α).

$$l = \sqrt{\frac{[\cos(\theta) - \cos(\alpha)]}{2\pi\sin(\alpha)} \frac{\gamma h_0}{\eta} t} \quad (5)$$

Where l is the wicking distance, t is time, α is the modeling variable angle related to the groove apex angle β ($\beta = \pi/2 - \alpha$, Fig. 1b), θ is the liquid contact angle with the solid surface, γ and η are the liquid surface tension and viscosity, respectively. Compared with the Washburn equation (eqn (1)), Rye's model has a more restricted wetting condition, *i.e.* the liquid contact angle with the solid must be lower than α in order for wicking to occur in the groove. Rye *et al.* tested their model using liquids with surface tension/viscosity ratio (γ/η) of 60–1000 cm/s and found their model agreed reasonably well with some of their experimental data, but also with some exceptions.¹⁵

In order to use open V-grooves as liquid transport channels in microfluidic sensors, it is necessary to understand the wicking dynamics of liquids of much higher γ/η ratio. This is because most diluted aqueous indicator solutions and some human samples, such as urine sample,¹⁷ have relatively high γ/η ratios in the range of 5600–7300 cm/s (with that of water being 7300 cm/s). Samples in open capillaries are prone to evaporation loss, therefore, transport speed must be high enough so as to minimize such loss. In this study, Rye's model was used to model water wicking in V-grooves to provide quantitative guidance to channel design for sensors made on polymer films. We used V-grooves manufactured on a quartz surface and water to experimentally confirm the Rye's model, but we used V-grooves cut on polymer films to fabricate sensors of low cost.

A printable paste made of cellulose powder and starch binder was used to print zones of paste over the V-groove on polymer films. After drying, the porous zones of cellulose powder and binder provide the capillary force to absorb liquid from the V-groove channel into the zones (see supporting information). This design allows a small liquid drop delivered over a V-groove to be rapidly absorbed into the porous zone of cellulose powder and binder. The small size of the non-porous V-groove channel means that it retains much less sample and the sample transport efficiency of this sensor design is higher than sensors made of porous channels.

Experimental

Materials and methods

V-groove samples were obtained from Hatakensaku Pty Ltd, Japan. A single V-groove was manufactured on each 20 mm × 50

Table 1 V-groove geometry from different techniques

Supplier's Specification	SEM		Profilometry		Microscopy w_0 (μm)
	w_0 (μm)	β (°)	w_0 (μm)	β (°)	
90°, 200 μm	204	89.8	203	90.1	202
90°, 500 μm	497	90.1	499	90.2	501
60°, 200 μm	201	60.5	202	59.9	204
60°, 500 μm	496	61.0	499	60.3	497

mm rectangular quartz slab. V-groove samples of two apex angles (60° and 90°) with two widths (200 μm and 500 μm) were obtained. Details of V-groove samples can be found in the supporting information.

The V-groove width and apex angle were independently measured in this study using an SEM (JSM-6300F, JEOL, Japan) and a profilometry (COTEC-Altisurf© 500).

Very good agreements were found between our measurements and the supplier's specifications (Table. 1). We chose V-grooves made on quartz slab for the modeling study because these grooves were fabricated with high precision. Another reason is that the V-groove apex angle fabricated on a quartz slab does not change during sample handling, because of its rigidity.

The V-groove samples were first cleaned with laboratory detergent solution (RBS 35) followed by exhaustive rinsing with Millipore water. The samples were then soaked in a 5% HNO₃ solution overnight and rinsed thoroughly with water. Finally, the samples were dried at 70 °C in an oven filled with nitrogen gas for at least 8 h and allowed to cool down in a desiccator before use. The effectiveness of this cleaning procedure was verified by the batch contact angle comparison and the uniformity of the wetting area on the sample surface. Cleaned samples were used for the wicking experiment within 24 h after the cleaning procedure was completed.

Polymer transparency film (3M, Laser Transparency Film, CG3300) was used to fabricate V-grooves to form liquid transport channels. A computer controlled plotter cutter was used to cut the groove on the film surface. The water contact angle for the transparency film was reduced to 8° after the plasma treatment. The cut grooves were then analyzed using a microscope.

Millipore water (18MΩ) was used for contact angle measurement and for all sample dilutions.

Canon inkjet printing inks were diluted with water and used as colour liquids to show liquid transport in the sensors. The colorimetric reaction for alkaline phosphatase (ALP) quantification was used in this study to demonstrate the capability of the new sensor design. Alkaline phosphatase (10–30 DEA units/mg of solid) was obtained from Sigma-Aldrich. The enzyme was in the form of lyophilized powder. An alkaline phosphatase stock solution (1 mg/ml) was prepared using a buffer solution (pH = 9.8) which contains 1.0 M diethanolamine ($\geq 98\%$, Sigma Aldrich) and 0.5 mM MgCl₂·6H₂O ($\geq 99\%$, Sigma-Aldrich). This stock solution was further diluted with the buffer solution to make serially diluted ALP standard solutions with concentrations of 0.20, 0.04 and 0.008 and 0 mg/ml. A BCIP®/NBT substrate system (Sigma-Aldrich) was used to indicate the activity of the enzyme through colour change. In the demonstration of an enzyme activity calibration curve, 100 nL of each

of the serially diluted ALP solutions was introduced into four porous detection zones of a sensor; 300 nL of BCIP®/NBT liquid substrate was added into the sensor from the V-groove channel cross in the middle of the sensor. The sensor was then scanned using a desktop scanner (Epson Perfection 2450, color photo setting, 1200 dpi resolution), average colour densities of the detection zones were analyzed using Adobe Photoshop.¹⁸

Experimental setup for V-groove wicking modeling

The experimental setup consists of two high-speed cameras, a drop dispensing system and two specially designed back light illumination units.¹² A schematic representation of the experimental configuration can be found in supporting information.

Liquid drop generation. The syringe pump of the OCAH-230 contact angle device (Dataphysics, Filderstadt, Germany) was used to generate water drops. A stainless steel flat-tipped needle of 0.21 mm outer diameter was fitted to the syringe pump, which was programmed to dispense liquid at a speed of 0.11 $\mu\text{L/s}$. The needle was positioned at known heights above the V-groove to dispense drop on the surface to ensure the drop impact to the groove was controlled (*i.e.* 2.4 mm height corresponds to an impact velocity of ~ 0.00 m/s and 15 mm height to ~ 0.44 m/s).

Image capturing system and image analysis. Fastcam Super10KC high-speed camera (Photron USA, Inc., San Diego) was used to capture images of wicking of the drop in the V-grooves at 500 frames per second (fps). The camera was triggered manually in the endless loop mode. The data file was then analyzed using Image-Pro Plus software (Mediacybernetics, Bethesda, US) to calculate wetting and wicking distances.¹²

A second camera (CV- M30 from JAI-Copenhagen, Denmark), capable of recording at 360 fps, was used at a horizontal angle as a support to the top-view camera to calculate the exact time, t_{impact} , at which the liquid drop touches the surface. Both cameras were triggered together at about 2 s prior to drop detachment from the needle. The frame (from JAI camera) just prior to impact was used to determine the pixel distance between the edge of the falling drop and the point of impact.

Groove fabrication on polymer surfaces. V-grooves were fabricated on a transparency film using a computer driven plotter cutter (HYIV-900, Chengdu Da Hua Sheng Yi Science & Technology Development CO., LTD). The cutting force was set at 300 g.

“Printing” of porous cellulose zones. To print the porous cellulose dots, a mixture of the binder solution and the cellulose powder was prepared. The starch solution was prepared in water at 90 °C. Five grams of starch was mixed with water and heated under constant stirring until the starch suspension became clear. This solution was used as the binder. Then, 250 mg cellulose powder was mixed into 600 μL binder solution to form a paste at the room temperature. A syringe was used to deliver 1.5 μL of the paste onto the transparency film over the end of the V-groove. After drying, the paste became porous cellulose dots which served as both a capillary reservoir to absorb liquid samples and a display unit to show colorimetric change of an assay.

Results and discussion

Liquid wicking in V-grooves

The model by Rye *et al.*¹⁵ suggested the liquid wicking in V-grooves is sensitive to the groove geometry, *i.e.* the groove width and the apex angle. These authors have tested their model with wicking experiments of the time scale of 1–50 s.¹⁵ The purpose of our study is to confirm the liquid wicking data prediction using the Rye’s model of liquids that have much higher γ/η ratio than those reported by Rye *et al.*¹⁵ so that the V-groove wicking model can be used to assist the fabrication of sensor channels with high sample delivery rate and efficiency.

We are particularly interested in sensor channels that can deliver liquid in a much shorter time scale, such as tens to hundreds of milliseconds. The liquid wicking results using water will then be directly used to design sensor channels.

Fig. 3 shows video clips of the landing and the subsequent wicking of a water drop in a V-groove. Two observations can be made. First, as the drop was delivered on the surface, the water wicking front in the V-groove is ahead of the water drop/quartz surface contact line on the smooth quartz surface. A slight V-groove wicking asymmetry is observed in the very beginning of the drop contact with the groove (*e.g.* at 1 ms and 3 ms). By the time it reaches 5 ms both wicking fronts are ahead of the spreading fronts. The initial asymmetry in the V-groove wicking could be caused by the slight surface chemical asymmetry along the groove. Second, the shape of the water-quartz surface contact area in the presence of the V-groove is not circularly symmetric compared with the water-quartz contact line on the smooth areas of the quartz. When a V-groove is present the water-quartz contact line has a curved section. The curvature of the contact line diminishes as the contact line converges to the V-groove. Such an asymmetric spreading behaviour on V-groove surfaces starts from the beginning of the impact and is maintained throughout the entire experimental duration. It indicates that surface physical features such as V-grooves influence the spreading of liquid drops on solid surface. The observation of this behaviour from the beginning of the drop contact with the V-groove suggests that the effect of V-groove on wicking shows no time delay.

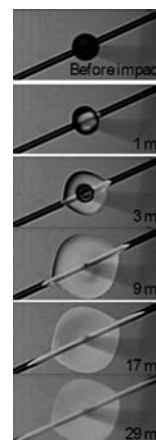


Fig. 3 Video clips of the landing and the subsequent wicking of a water drop in a V-groove.

The experimental results of water drop wicking distances (l) in V-grooves are presented as functions of the square root of time (Fig. 4). Fig. 4 shows the experimental results for water wicking in several V-grooves. The apex angle and the groove width are used to identify the V-groove (*i.e.*, “apex angle (°)–groove width (mm)”). The highest wicking rate is observed in V-groove of 60°–0.5mm, followed by 60°–0.2mm, 90°–0.5mm and 90°–0.2mm (Fig. 4). The trend of water wicking speeds in V-grooves of different widths bears a similarity to that in cylindrical capillaries of different radii; wicking speeds in wider V-grooves are faster than in narrow ones. It suggests that in narrow grooves the flow resistance is high. The shape (*i.e.* the apex angle) of V-grooves also strongly affects the liquid wicking speed. This is because the Laplace pressure that drives the liquid wicking in V-groove reduces as the apex angle becomes larger (or α becomes smaller, see eqn (3)). All experimental data can be extrapolated to the origin (Fig. 4). The theoretical predictions using the Rye’s model¹⁵ are in excellent agreement with the experimental results. This study therefore shows that the Rye’s model can also effectively predict V-groove wicking of liquids of high surface tension to viscosity ratio. The model predictions can, therefore, be transferred to microfluidic sensor channel design.

Our experimental wicking data show that water wicks along the 60°–0.5mm groove for 8 mm in just less than 30 ms. Such a wicking speed is two orders of magnitude greater than the water wicking speed in a paper channel. We can predict using the Rye’s model that for a 50 μm width channel with an apex angle equal to 60°, water ($\gamma = 72 \text{ mN/m}$, $\eta = 0.001 \text{ Pa s}$) can wick for 1 cm in about 660 ms, if the water-groove wall contact angle $\theta = 10^\circ$. The V-groove channels of such width and shape can, therefore, provide much higher liquid transport speed than paper channels. In addition, since the volume of 1 cm length of 60°–50 μm V-groove channel is only 11 nL, channels of this size and shape can transport 100 nL liquid with a sample retention in the channel of much less than 11% based on the calculation using eqn (4).

Sensors made using open capillary channel

V-groove channel and porous detection zones. V-groove channels of different widths were cut on the polymer film surface;

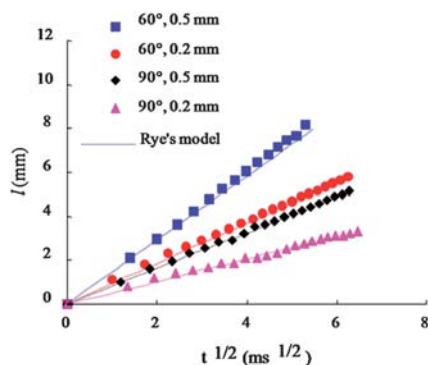


Fig. 4 Comparison of average wicking distance of the water front (z) along the V-groove vs. square root of time (\sqrt{t}) on different V-grooves at the impact velocity of $\sim 0.0 \text{ m/s}$. Experimental data are presented as dots of different shapes and the predictions of the Rye’s model are presented by the dotted lines.

microscope images of the channels are presented in Fig. 5. The cross section image of the groove (Fig. 5 (c)) shows the apex angle of the groove. Image analysis shows that grooves fabricated on polymer films using this method have consistent widths and well-defined apex angle; enabling the mathematical modeling data to be used to aid the channel design to control/predict liquid wicking. Printable cellulose powder paste was printed to the end of the channel to form porous zone to absorb liquid from the V-groove channel (Fig. 6).

As soon as the liquid reaches the porous zone *via* the V-groove channel, the channel will no longer provide penetration driving force. Sample transport from this point will be driven by the porous zone. Based on the liquid absorption model by Yamasaki and Munakata,⁹ when a large number of pores of a porous media are exposed to a liquid, then the liquid absorption rate by the porous media is high. Yamasaki and Munakata studied the penetration of fully wetting liquids (*i.e.* $\theta = 0$) and proposed that

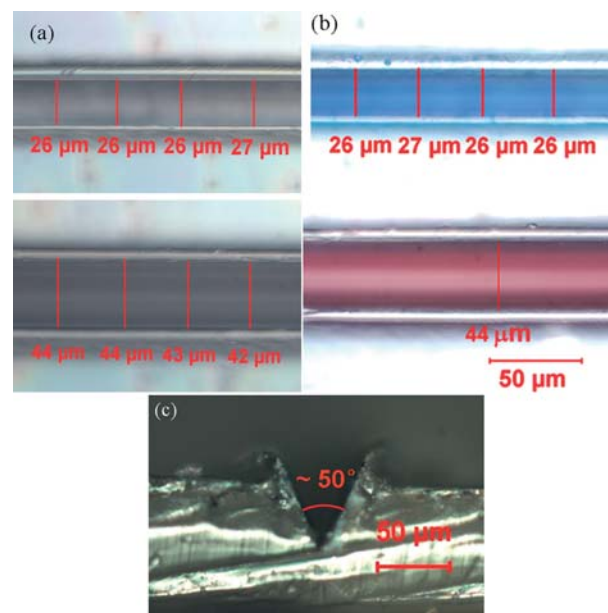


Fig. 5 Micrographs of V-grooves of different widths before (a) and after (b) taking ink solutions as testing liquids, and the cross section view of a V-groove (c).

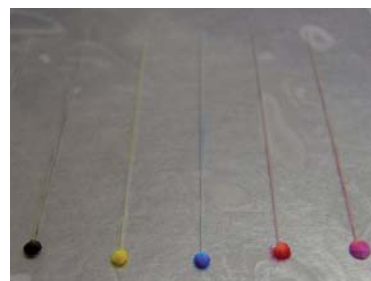


Fig. 6 The ink solution transport in $\sim 80 \mu\text{m}$ wide and 30 mm long V-grooves on a polymer film. Ink solutions were deposited over the grooves at the upper ends of the grooves. The ink solution transportation was further “pumped” by the porous cellulose powder dots at the lower ends of the grooves and transported with only low retention in the grooves.

the volumetric liquid absorption rate by the porous media (paper) can be written as:⁹

$$V(t) = V_r + k \sqrt{\frac{r_{ave} \gamma}{2\eta} t} \quad (6)$$

where $V(t)$ is the time dependent liquid absorption volume, V_r is the surface property of the paper related to the specific testing method they employed, r_{ave} is the average pore radius of the pores in paper, k is a proportional constant related to the paper porosity, and γ and η are the liquid surface tension and viscosity.⁹ They experimentally showed that a fully wetting liquid can be absorbed by paper in several hundreds of milliseconds before the paper became saturated. The absorption rate slows down only after the paper became saturated.⁹ Results by Ymasaki and Munakata suggest that, in our sensor design, the liquid absorption rate of porous cellulose zones is compatible to the liquid transport rate through the V-groove before the zone is saturated. The size of the porous zones can be tailor made to suit the expected liquid sample volume. In this study, porous zones capable of absorbing 100 nL of liquid were designed to form sensors. Ink solution transport in the grooves was rapid and had only a very small fraction retained in the grooves after the transportation was completed.

Multi-detection zone sensors. Sensors with more than one detection zones can be designed by cutting V-groove channels that cross one another. Fig. 7 shows a sensor that has four detection zones; liquid sample can be introduced from the channel cross point in the centre of the sensor.

With the 5 mm channel length, liquid sample can be delivered into the detection zones rapidly and the four detection zones require only 300 nL to completely fill. The inset of Fig. 7 shows the enlarged image of a sensor when filled with the first 100 nL of the black ink solution. Visual examination shows that ink retention in V-groove channels is low. Microfluidic sensors of low volume with multi-sampling capability can, therefore, be fabricated at low cost.

Sample enrichment using V-groove channels and sensors. Sample enrichment is an essential step for analyzing low concentration biological and environmental samples. It is desirable that a sensor can provide the capability of allowing *in situ* sample enrichment. Non-porous channels have a significant advantage over porous channels in that they have negligible chromatographic effect, therefore, allowing a high efficiency transfer of samples for enrichment. Sample can be enriched through a V-groove channel into the printed porous zone by several sample introductions. When a liquid sample transferred

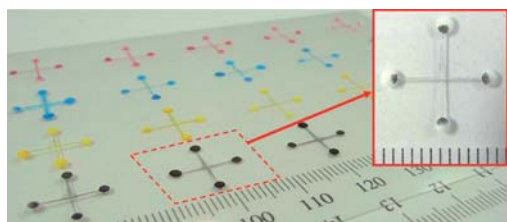


Fig. 7 The performance of 4-zone sensors shown using ink solutions.

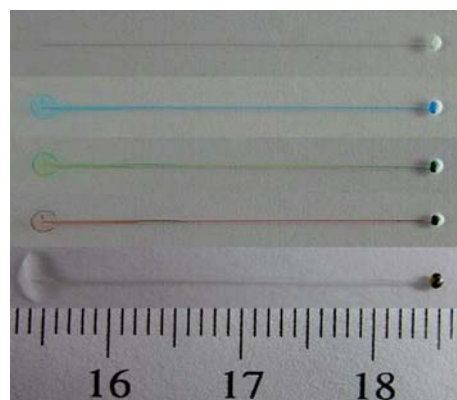


Fig. 8 Photos of a sample enrichment demonstration using one V-groove. A 100 nL aliquot of cyan ink solution was introduced into the V-groove. The porous cellulose zone shows cyan colour as the cyan ink solution reached to the zone. Then 100 nL of yellow ink solution and 100 nL of magenta ink solution were added into the same V-groove sequentially; the porous cellulose zone changed into green and then into black as these ink solutions reached to the porous zone one after another. A 300 nL of water was then introduced to wash the inks into the porous zone.

into the porous zone dries out by evaporation, the second sample introduction can be made. Repeated cycles of sample introduction and evaporation enrich the sample concentration in the porous zone. We demonstrate sample enrichment capability of the V-groove channel sensor by introducing inkjet ink solutions into the porous zone. Fig. 8 shows the step-wise introduction of 100 nL aliquots of cyan, yellow and magenta ink solutions through a 3 cm long V-groove channel into the porous zone. Drying was allowed after the introduction of each of the ink solutions. This was followed by an addition of a 300 nL aliquot of water. Retained inks after each step of ink solution introduction in the V-groove channel were washed into the porous zone by water. There is no noticeable ink retention due to chromatographic effect after the water wash. V-groove channel sensors can therefore, be used as a device to enrich low concentration samples for analytical purposes.

Low-volume, rapid semi-quantitative analysis. V-groove channels combined with porous detection zones can be designed as rapid and low-volume sensors for semi-quantitative chemical and biochemical analysis.

Fig. 9 shows a semi-quantitative analysis of ALP using a four-zone sensor. One hundred nanolitres of ALP solutions of 0, 0.008, 0.04 and 0.20 mg/ml were added into the four detection zones. After 20 s, the ALP solutions in the detection zones dried out by evaporation. Three hundred nanolitres of BCIP®/NBT substrate solution was then introduced from the central point of the sensor; the substrate solution penetrated into all detection zones in less than 0.5 s. The sensor was then placed into a dark box for 5 min to allow colour changes of the substrate to fully develop. Scanning of the sensor and measuring colour intensity lead to the formation of the calibration curve (Fig. 10). The measurement was repeated five times using five sensors to generate the error bars. These results show that sensors with V-groove channels are capable of providing high sample delivery efficiency and performing rapid, low-volume semi-quantitative analysis.

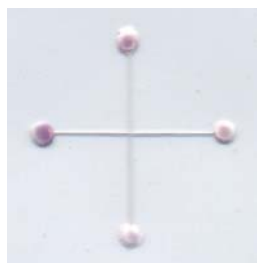


Fig. 9 Semi-quantitative measurement of an ALP using the BCIP®/NBT substrate with a 4-zone V-groove sensor. One hundred nanolitres of ALP solutions of 0, 0.008, 0.04 and 0.20 mg/ml were added into the four detection zones. Three hundred nanolitres of BCIP®/NBT substrate solution was then introduced from the central point of the sensor.

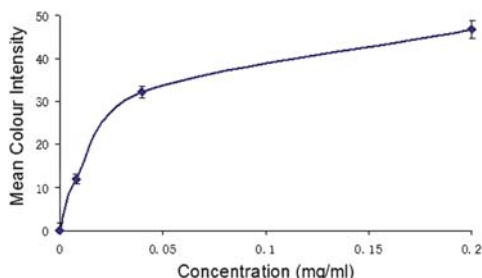


Fig. 10 A calibration curve constructed using the colour intensity readings of the four zones (the solid line serves as a visual guide). Five repeated measurements using five sensors gave the error bars.

Patterns in Fig. 7 and the results in Fig. 9 and 10 show that microfluidic devices with the V-groove design can be used as multi-zone microzone plates for ELISA tests; patterns in Fig. 7 can substantially reduce the labour involved in sample addition and also errors associated to sample additions, since only one addition of the colour developing agent (or anti-body for ELISA) is required.

Conclusions

In this study we investigated the use of V-groove capillary channels as microfluidic channels for fabrication of low-cost microfluidic sensors for chemical and biochemical analysis. Our study shows that V-groove capillary channels made of non-porous materials provide a much higher liquid wicking speed than porous capillary channels such as paper channels. Connecting the V-groove channels to porous materials such as dots of cellulose powder (or paper) as the sample detection zones provides capillary suction force to liquid when the liquid reaches the detection zones. Therefore, liquids transported by the V-groove can be rapidly absorbed by these porous materials, leaving a very small quantity of liquids in the V-groove. The

sampling efficiency (*i.e.* the liquid reaching the detection zone *vs.* the liquid introduced into the sensor) of this sensor design is in the order of 80–90%, significantly higher than some of the paper-based sensors that use paper channels to transport liquid. In addition, the non-porous channels show negligible chromatographic loss of the sample during sample transport compared to the porous channels. This makes their sampling efficiency even higher than channels made of porous materials, including paper.

Sensors with V-groove channels are easy to fabricate and the fabrication of these sensors does not require any solvent, which is required in most fabrication methods of paper-based microfluidic sensors for channel development.^{1,3,4} Sensors with non-porous V-groove channels are capable of conducting semi-quantitative analysis with less than 1000 nL of liquid (*i.e.* standards, samples and indicator solution in total). The performance of the sensors *vs.* their fabrication cost makes paper and paper-like sensors with non-porous sample transport channels a highly relevant candidate for the future development of low-cost, non-powered point-of-care and environmental monitoring devices.

Acknowledgements

This work is supported by the Australian Research Council (ARC). Funding received from ARC through DP1094179 is gratefully acknowledged. JT, DK, XL would like to thank Monash University Research and Graduate School and the Faculty of Engineering for their postgraduate research scholarships.

Notes and references

- 1 A. Martinez, S. Phillips, M. Butte and G. Whitesides, *Angew. Chem., Int. Ed.*, 2007, **46**, 1318.
- 2 A. Martinez, S. Phillips, E. Carrilho, S. Thomas, H. Sindi and G. Whitesides, *Anal. Chem.*, 2008, **80**, 3699.
- 3 K. Abe, K. Suzuki and D. Citterio, *Anal. Chem.*, 2008, **80**, 6928.
- 4 X. Li, J. Tian, T. Nguyen and W. Shen, *Anal. Chem.*, 2008, **80**, 9131.
- 5 Y. Lu, W. Shi, L. Jiang, J. Qin and B. Lin, *Electrophoresis*, 2009, **30**, 1497.
- 6 J. Tian, X. Li, G. Garnier and W. Shen, *Colloids Surf., B*, 2010, **76**, 564.
- 7 X. Li, J. Tian and W. Shen, *ACS Appl. Mater. Interfaces*, 2010, **2**, 1.
- 8 E. Washburn, *Phys. Rev.*, 1921, **17**, 273.
- 9 H. Yamazaki and U. Munakata, *Proceedings of the 10th Fundamental Research Symposium*, Oxford, 1993.
- 10 K. Hodgson and J. Berg, *J. Colloid Interface Sci.*, 1988, **121**, 22.
- 11 R. Roberts, T. Senden, M. Knackstedt and M. Lyne, *J. Pulp Paper Sci.*, 2003, **29**, 123.
- 12 S. Gerdes, A. M. Cazabat and G. Ström, *Langmuir*, 1997, **13**, 7258.
- 13 S. Gerdes, A. M. Cazabat, G. Ström and F. Tiberg, *Langmuir*, 1998, **14**, 7052.
- 14 S. Gerdes and G. Ström, *Colloids Surf., A*, 1996, **116**, 135.
- 15 R. Rye, J. Mann and F. Yost, *Langmuir*, 1996, **12**, 555.
- 16 L. Romero and F. Yost, *J. Fluid Mech.*, 1996, **322**, 109.
- 17 P. W. Perryman and C. F. Selous, *J. Physiol.*, 1935, **85**, 128.
- 18 X. Li, J. Tian and W. Shen, *Anal. Bioanal. Chem.*, 2010, **396**, 495.



Biosurface engineering through ink jet printing

Mohidus Samad Khan^a, Deniece Fon^b, Xu Li^a, Junfei Tian^a, John Forsythe^b, Gil Garnier^{a,*}, Wei Shen^{a,*}

^a Australian Pulp and Paper Institute, Department of Chemical Engineering, Monash University, Clayton, VIC 3800, Australia

^b Department of Materials Engineering, Monash University, Clayton, VIC 3800, Australia

ARTICLE INFO

Article history:

Received 15 May 2009

Received in revised form 28 August 2009

Accepted 15 September 2009

Available online 30 September 2009

Keywords:

Ink jet printing

Microfluidic manufacturing

Bioassays

Tissue scaffold

Protein

Enzyme

ABSTRACT

The feasibility of thermal ink jet printing as a robust process for biosurface engineering was demonstrated. The strategy investigated was to reconstruct a commercial printer and take advantage of its colour management interface. High printing resolution was achieved by formulating bio-inks of viscosity and surface tension similar to those of commercial inks. Protein and enzyme denaturation during thermal ink jet printing was shown to be insignificant. This is because the time spent by the biomolecules in the heating zone of the printer is negligible; in addition, the air and substrate of high heat capacity absorb any residual heat from the droplet.

Gradients of trophic/tropic factors can serve as driving force for cell growth or migration for tissue regeneration. Concentration gradients of proteins were printed on scaffolds to show the capability of ink jet printing. The printed proteins did not desorb upon prolonged immersion in aqueous solutions, thus allowing printed scaffold to be used under in vitro and in vivo conditions. Our group portrait was ink jet printed with a protein on paper, illustrating that complex biopatterns can be printed on large area. Finally, patterns of enzymes were ink jet printed within the detection and reaction zones of a paper diagnostic.

Crown Copyright © 2009 Published by Elsevier B.V. All rights reserved.

1. Introduction

The ability to generate accurate patterns of biomolecules on surfaces and to maintain the functionality of the immobilized biomolecules are two critical requirements to engineer biosurfaces. Recent developments in bio-interface engineering have shown printing as a promising method to create biomolecular patterns onto surfaces [1–4]. Among the multitude of applications, two are of special interest. The first is in scaffolds for tissue engineering. Polymeric scaffolds can be functionalized with proteins for controlling cell growth such as directed neuron outgrowth for neural regeneration applications. The second main application is paper-based diagnostics. These two applications require biomolecules to be very precisely printed in fine patterns, concentration gradients or within fluidic channels. Digital ink jet printing is attractive as manufacturing process for the precision, speed and flexibility it offers. The suitability of ink jet printing to large scale of biosurface manufacturing and the effective engineering of bio-inks are two critical issues to address.

Nerve regeneration is a complex biological process with many biochemical and biomechanical variables affecting the outgrowth

of neuronal axons [3,5,6]. Advances in tissue engineering for nerve regeneration promises solutions to degenerative illnesses like Parkinson and Alzheimer diseases. The effective control of neuron outgrowth and direction can potentially be achieved with signalling molecules, such as nerve growth factor (NGF) immobilized onto scaffolds to produce a local concentration gradient [7–9]. Bio-printing has the capability to become a rapid and accurate process of generating NGF concentration gradient patterns for controlling neuron growth. The challenge is to produce continuous concentration gradient patterns that are smooth enough to be perceived as an effective guidance cue by growing axons. Ink jet printing can become invaluable in tissue engineering to create such controlled concentration gradients.

Recent work by Martinez et al. [10,11] has highlighted paper as a low-cost substrate for microfluidic diagnostics. These devices have tremendous potential for telemedicine when used in conjunction with communication hardware such as camera phones and internet. These devices also show potential in general health and environmental monitoring applications [10–12]. The major challenges are to ensure precision and integrity of biomolecular patterns within the device and to preserve the activity of the immobilized biomolecules.

Among the many printing processes, digital ink jet printing is becoming a technique of choice for biosurface functionalization thanks to its non-contact operation and reduced cross-contamination between samples [13–18]. This technique has been

* Corresponding authors. Tel.: +61 3 9905 9180; fax: +61 3 9905 3413.

E-mail addresses: gil.garnier@eng.monash.edu.au (G. Garnier), wei.shen@eng.monash.edu.au (W. Shen).

used to print arrays or patterns of proteins and nucleic acids [1,17,19–23]. The current drop-on-demand (DOD) ink jet printing technology is capable of delivering ink droplets of a few picolitres [24,25], therefore, satisfying many requirements for bio-surface modification. The two main types of ink jet printers used in biomolecular printing are thermal and piezoelectric [26]. In piezoelectric ink jet printing, a voltage signal is applied to a piezoelectric element fixed to the printing head; the deformation of the piezoelectric element caused by the voltage signal pressurizes the ink in the nozzle and ejects ink droplets from the nozzle [25]. In the thermal ink jet printing, an electric current pulse heats a micro-resistor, causing rapid formation of ink vapour bubbles, which creates a pressure pulse ejecting an ink droplet from a nozzle. The electric current pulse lasts microseconds ($\sim 10 \mu\text{s}^{-1}$) and it was estimated that the resistor surface temperature can increase to 200–300 °C [1,22]. It is not certain if biomolecules can sustain such high temperatures [27].

The availability of robust and affordable bio-ink jet printer is currently restricting the development of biosurface engineering. An alternative and cost effective strategy is to reconstruct commercial ink jet printers; a further advantage is to benefit from the built-in highly developed ink management systems and computer-based user interfaces currently available. Compared to piezoelectric printers, thermal ink jet printers offer a simpler printing head design, more robust and easier to reconstruct for bio-printing applications. Several research groups have pursued this approach [16,19,22,28]. Xu et al. and Prado et al. redesigned their bio-ink compatible printers using HP printers [21,23]. Allain et al. reported a partial modification of a HP printer to print very small quantities of inks (60 μL) for each refilling [19]. However, frequent refilling of bio-inks increases the probability of contamination of the ink supply system, thus compromising the bio-fabrication quality. Another critical issue for printing biomolecules using thermal ink jet printing is to understand the effect of the printing action on the activity of biomolecules. Allain et al. reported that DNA can be spotted with thermal ink jet printers and remained intact. However, proteins are more fragile molecules, the activity of printed protein patterns by a thermal printer needs to be assessed [19].

This study investigates the flexibility of modifying a standard commercial thermal ink jet printer to engineer biosurfaces. The strategy investigated is to ensure good printability by identifying the critical parameters of commercial inks and to formulate bio-inks of similar properties. Two critical requirements must be satisfied. First, the printing resolution with bio-inks must be good and preferably similar to that achieved with regular inks. Second, the printed molecules must be able to sustain the heat and shear generated by ink jet printing. The versatility of thermal ink jet printing for biosurface engineering is analyzed.

2. Experimental

2.1. Materials

Fluorescein isothiocyanate-conjugated bovine albumin (albumin-FITC) and horseradish peroxidase (HRP) (Sigma–Aldrich) solutions were used to formulate bio-inks. The tagged fluorescent dye (FITC) allows the protein (albumin) to be tracked by UV-light or by confocal microscope. Albumin-FITC solutions of a wide range of concentrations (0.2–1.0 mg/mL) were prepared; a protein buffer, 10 mM Tris(hydroxymethyl) amine (Aldrich), was used to maintain the pH of the albumin solution at ≥ 7.0 . HRP was dissolved in 100 mM sodium-phosphate buffer solution to maintain the pH at 6.0 to a concentration of 1.0 mg/mL. A liquid substrate system, 3,3'-diaminobenzidine (DAB) (Aldrich), was used to identify the enzymatic activity of the printed HRP. Water (Millipore, 18 M Ω) was used for making all solutions in the study. The bio-inks were

stored at a temperature below 4 °C. Polymer solutions for electro-spinning were prepared from poly(ϵ -caprolactone) (PCL) (Lactel Absorbable Polymers), which was dissolved in a solvent mixture consisting of chloroform and methanol (Merck Chemicals Ltd.), and a cationic surfactant, dodecyltrimethylammonium bromide (DTAB) (Sigma Aldrich). Whatman filter paper #4 was selected as the paper base for sensor fabrication.

2.2. Methods

2.2.1. Characterization of ink properties

To assist the formulation of bio-inks, ink jet inks of three major brands were surveyed. First two inks were thermal ink jet ink and the third one was piezo ink jet ink. Density (ρ), surface tension (γ) and viscosity (μ) of the commercial inks were measured (Section 3.2). Surface tensions of commercial ink jet inks were measured with a Wilhelmy balance (Cahn Instrument, DCA 322); shear viscosities of the inks were measured using a Rheometrics Fluids Spectrometer (RFSII, USA). Surface tensions of the bio-ink solutions were measured using OCAH-230 (Contact Angle Measuring Device; Dataphysics, Germany) with the pendant drop method. The densities of the inks were measured with a Mettler Toledo Densito 30Px (Switzerland). All the physico-chemical properties of bio-ink were measured at 23 °C. Glass capillary viscometer (BS/U Tube; Standard: ASTM D 445, D446/ISO3104) was used to measure the kinematic viscosity of bio-ink solutions.

2.2.2. Printing bio-ink on porous substrate

A Canon ink jet printer (Pixma ip4500) and ink cartridges (CLI, Y-M-C-BK, PGBK model) were reconstructed for bio-printing. The sponges inside the ink cartridges were removed and cleaned. The ink tanks were cleaned and the sponges were restored. This printer is of the bubble jet design which offers a resolution of 9600 \times 2400 dot per inches (dpi). The printer was controlled by a personal computer which supplies page-data to the printer using MS Office 2003 and IrfanView v4.24 software. Filter paper was the printing substrate. A paper-based microfluidic pattern was created using the method described elsewhere [29]. HRP was printed inside the fluidic channels of the pattern. Albumin-FITC was also ink jet printed onto porous biodegradable electrospun PCL scaffold. The scaffold was electrospun from a solution consisting of 12% (w/v) PCL dissolved in a 3:1 chloroform:methanol with 1 mM DTAB. Electrospun PCL scaffolds were sputter coated with gold (25 mA for 90 s; Balzers SCD005 Sputter coater), and analyzed via scanning electron microscopy (acceleration voltage = 15 kV; Hitachi S570 SEM). Electrospun PCL had average fibre diameter of 240 ± 60 nm (Fig. 1).

2.2.3. Printing analysis

The albumin-FITC printed images were analyzed by laser-scanning krypton confocal microscope and UV-light (Spectroline, ENF-240C/F). The biochemical reaction of HRP and DAB substrate generates the characteristic brown colour on paper [30]. A digital SLR camera (SONY-DSLR-A100) with additional close-up lenses was used to capture images of printed and reacted patterns.

3. Results and discussion

3.1. Control of ink supply and colour management

The reconstruction of the Canon ink jet printer was detailed elsewhere [31,32]. Controlling the colour management of the printer and the operating software interface is necessary to prevent cross-contamination of the printed bio-inks. The colour management system of a desktop ink jet printer reproduces a colour defined using a combination of different proportions of primary CMYK standards: cyan (C), magenta (M), yellow (Y) and black (K). To reproduce

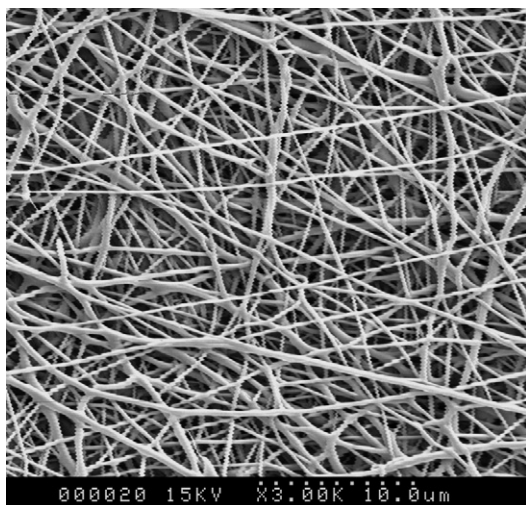


Fig. 1. Scanning electron microscopic (SEM) image of the electrospun PCL nanofibres scaffold.

a colour from the computer screen onto a substrate using the control software, the printer may need to dispense two or more inks from different ink cartridges to print a colour on the substrate that matches that on the screen. Such colour management system is not ideal for bio-printing, as it prevents the printer from dispensing a single protein from a single cartridge. However, simple modifications of the colour settings of MS Office 2003 can prevent the printing of the second bio-ink when unwanted [31,32].

3.2. Bio-inks

Surface tension and viscosity are the two critical parameters of inks, which affect the ink droplet formation in ink jet printing [24]. In the first step, the surface tension, density and viscosity of a series of commercial ink jet inks were measured. In a second step, bio-inks having characteristics (γ , ρ , μ) similar to that of these commercial inks were formulated. Finally, bio-inks were thermal ink jet printed and the pattern resolution was compared to that achieved with the commercial inks.

Table 1 shows the viscosity, surface tension and density of commercial inks of different colours (C, M, Y, K) and three different manufacturers (1, 2, 3). The properties of two bio-inks, albumin-FITC and HRP, are also shown.

The surface tension of C, M, Y inks were found to be consistently in the range of 28.5–32.0 mN/m, whereas the range of black inks (K)

is much wider: 28.6–46.2 mN/m. The densities of inks were similar to that of water (Table 1). The range of viscosity of the inks was found to be 2–9 cP.

The average surface tension of albumin-FITC and HRP were of 56.6 mN/m and 49.1 mN/m, respectively. The densities of the bio-inks were similar to that of water: 997–1000 kg/m³. The viscosity of the bio-inks was also adjusted to that of water. The dynamic viscosity of water at 23 °C is 0.935 cP [33] and the dynamic viscosity of the bio-inks varies from 0.935–0.970 cP, which was similar to the lower limit of the commercial ink viscosity.

To evaluate the effects of the physical properties of inks on their printing performance, commercial inks and the bio-ink (albumin-FITC) were printed using the same printer onto a polymer scaffold and the definition of printed ink dots was analyzed by optical and confocal microscopy.

The diameter d (in μm) of a dispensed droplet through ink jet nozzle can be expressed as

$$d = \sqrt[3]{\left(\frac{6}{\pi} V\right)} = 12.4V^{1/3} \quad (1)$$

where V is the volume (in pL) of the dispensed droplet. According to the manufacturer, the bubble jet printer used in our study generates droplet of 1 pL. The minimum dispensed droplet diameter is then 12.4 μm (Eq. (1)). Asai et al. reported that the diameter of impacted (but non-splashing) droplet delivered by ink jet printing on paper is 1.42 times larger than that of the dispensed droplet [34]. Therefore, the corresponding impacted droplet diameter is 17.6 μm . This calculated value is in good agreement with our experimental results: the impacted droplet diameter corresponding to the smallest single droplet dispensed by our printer nozzle was $18.3 \pm 1.4 \mu\text{m}$ ($n=8$) for commercial ink jet ink (Canon, Cyan ink) and $18.8 \pm 1.8 \mu\text{m}$ ($n=8$) for bio-ink, albumin-FITC. These measured data correspond to a 1% increase in the dispensed ink drop diameter of the bio-ink compared with the commercial ink, and a 3% increase in the ink spot diameter on the substrate. This shows that the changes in ink physical properties within the ranges specified in our study have little impact on the ink droplet size dispensed.

3.3. Printing bio-ink on porous substrate

Fig. 2a is the photograph of text printed with albumin-FITC using two different cartridges (black and magenta cartridges). The fluorescent protein was visible under UV light. The top two lines were printed using Times New Roman, Font 5pt and the bottom two lines were in Font 10pt. The left hand-side text was printed using the black ink cartridge and the right hand-side with the magenta

Table 1
Physical properties of commercial ink jet inks and bio-inks at 23 °C.

Description		Surface tension (mN/m)	Viscosity (cP)	Density (kg/m ³)
Commercial ink jet ink-1 (Canon)	C	28.5	2–5	1007–1089
	M	29.1		
	Y	30.5		
	K	28.6		
Commercial ink jet ink-2 (HP)	C	30.3	2–9	
	M	29.7		
	Y	31.2		
	K	46.2		
Commercial ink jet ink-3 (Epson)	C	30.7	2–3	
	M	30.5		
	Y	32		
	K	38.8		
Bio-ink-1 (albumin-FITC)		54.4–56.4	0.935–0.97	996–999
Bio-ink-2 (HRP)		49.1	0.935 ^a	997–1000

^a Assumed to be the same as for water.

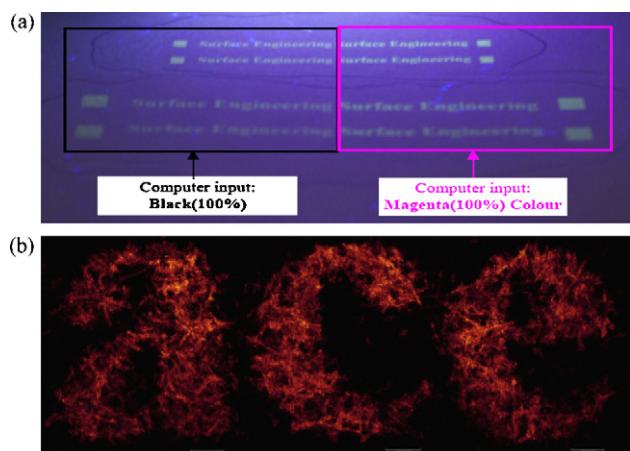


Fig. 2. Text printed using albumin-FITC on paper (Times New Roman, 5pt and 10pt): (a) printing from two different cartridges viewed under UV-light and (b) magnified printed letters under a confocal microscope (Krypton, 5x)

cartridge. The bottom of the photo is blurred because the photo was taken at an angle to accommodate the UV lamp. As a result, the bottom of the image was slightly out of focus. The printing resolution is shown by the confocal image of the Font 5pt text in Fig. 2b.

Good printing resolution was achieved with different proteins using either one or more ink cartridges. Reconstructed ink jet printer can print very sophisticated patterns involving many bio-inks.

The digital picture of our research group was printed on paper (modified size) with albumin-FITC as bio-ink (Fig. 3). Since only albumin-FITC was used, the monochromatic printing mode was selected. The original photo was first converted into grey-scale; albumin-FITC was printed from the black ink cartridge. Since albumin-FITC fluoresces under UV light, the printed image (Fig. 3a) was actually the negative image of the original photo when viewed under UV light. To visually appreciate the printing result, a positive image is required. Fig. 3a was converted into its negative using a graphics software (IrfanView); this operation brought the printed

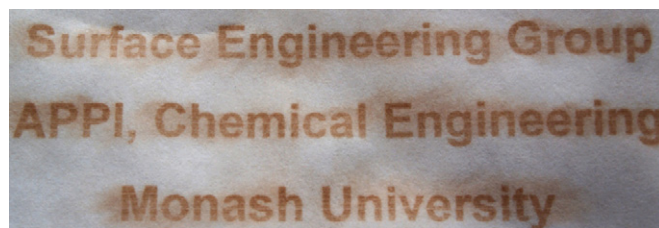


Fig. 4. Text printed with of HRP enzyme on paper (Times New Roman, 14Bpt). The application of DAB liquid substrate reveals the characteristic brown-coloured precipitate of the oxidized DAB, indicating HRP enzyme activity.

negative (Fig. 3a) into a positive form (Fig. 3b). Good tone variation was reproduced.

3.4. Activity of printed biomolecules

To test the activity of the printed biomolecules, a text pattern was printed on paper using the bio-ink formulated with an enzyme, horseradish peroxidase (HRP). The enzymatic activity of the peroxidase was determined by spraying the DAB liquid substrate onto the printed patterns. The oxidation of 3,3'-diaminobenzidine by H_2O_2 in the liquid substrate catalyzed by the printed horseradish peroxidase produces the characteristic brown colour observed in Fig. 4. This indicates that the enzyme was active after being printed.

Risio and Yan have shown that horseradish peroxidase printed using a piezoelectric ink jet printer retained its enzymatic activity [17]. Piezoelectric printer ejects ink droplets by pulses generated by deformation of the crystal from the piezoelectric element. This printing action does not increase temperature. Therefore, piezoelectric printer has had a perceived advantage for bio-printing.

Fig. 4 clearly shows that thermal ink jet printer can also retain the activity of the printed protein molecules. Although it was estimated that the electric pulses could increase the surface temperature of the micro resistor to 200–300 °C [1,26], the duration of the pulse is less than 10 μ s. As soon as the ink droplet is ejected from the nozzle, it is again exposed to room temperature. Since the usual distance between the printer head and the substrate surface is 2 mm, the ink droplet reaches the surface of the substrate in 200 μ s, assuming of flight speed of ink droplet of 10 m/s [25]. Due to inertia, the ink droplet rapidly forms a thin circular pancake upon impacting on the substrate [34,35], which resides at ambient temperature. The printed ink droplet rapidly equilibrates its temperature with the substrate having high heat capacity, in an exaggerated estimation, the ink droplet experiences the boiling temperature for a maximum 250 μ s.

Chang et al. studied the thermal stability of HRP heated in aqueous solutions and found that the enzymatic activity of HRP decreased by 50% in 20 s under near-boiling condition (93 °C) [36]. Assuming similar trend, the expected loss of activity for the HRP enzyme induced by printing is of 0.001%. This estimation shows that thermal deactivation of HRP during thermal ink jet printing is negligible. This confirms thermal ink jet printer for biomolecular printing application as protein denaturing by thermal printing is insignificant. The quantification of the thermal stability of enzyme printed patterns on paper can be found elsewhere [37].

3.5. Printing concentration gradients

Confocal microscopy was used to characterize the resolution of protein patterns printed on scaffolds. The first question to answer is whether printed protein pattern can be fixed on the scaffold surface simply by physisorption of the proteins. If physisorbed protein patterns are unstable and change with time when immersed in a liquid, a printed protein concentration gradient will gradually

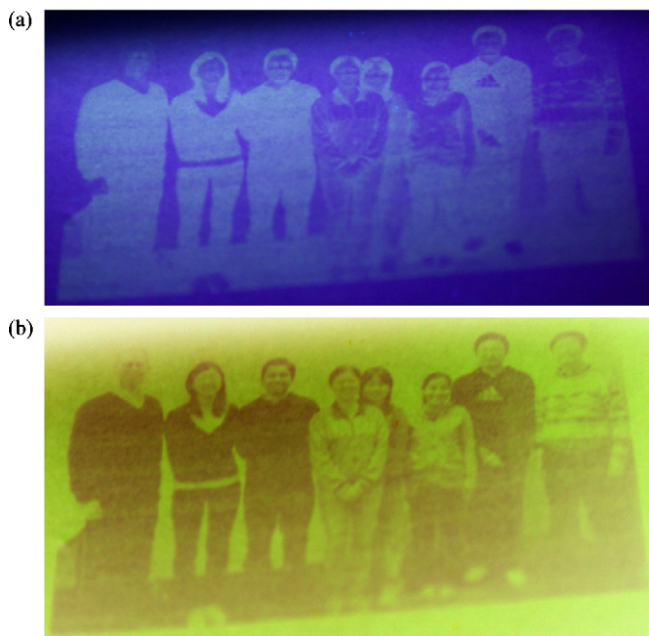


Fig. 3. (a) Printed digital photo using albumin-FITC on paper surface. (b) Negative image of the photo.

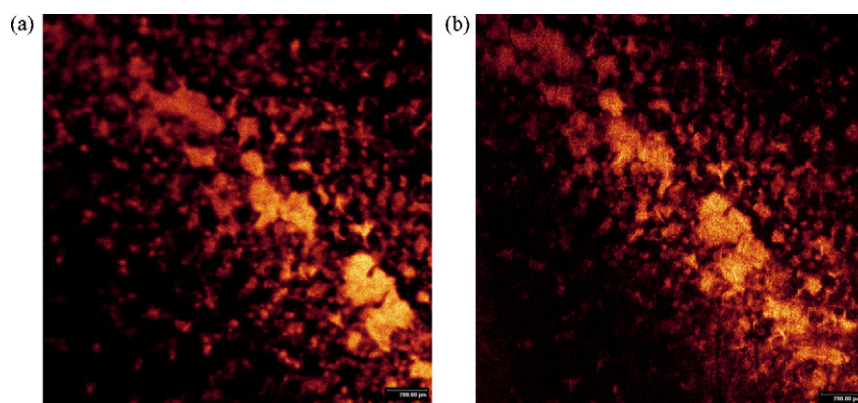


Fig. 5. Confocal Images (Krypton, 5x) of ink jet printed patterns on electrospun PCL Scaffold using albumin-FITC; biomolecules physically adsorbed on the surface (a) before, and (b) after immersing into aqueous buffer (2 days in Phosphate Buffer Solution, PBS); (bar length = 200 μm).

loose its ability to guide neurons. To address this issue, albumin-FITC was printed on electrospun PCL scaffold; the printed pattern was immersed in an aqueous buffer solution for 2 days. The confocal images taken before and after this treatment are shown in Fig. 5a and b, respectively. The adhesion of protein molecules to the substrate surface was sufficiently strong to maintain the printed protein pattern.

An albumin-FITC concentration gradient was also printed using a single ink cartridge; an electronically generated grey-scale pattern was used as image file. Fig. 6a shows the confocal microscopic image of the concentration gradient achieved (bar length = 200 μm). The grey-scale is obtained with the printing algorithm by varying the surface density of the printed dots. Fig. 6a illustrates that the printed protein dots form discrete islands of diameter smaller than 100 μm in the low concentration end of the gradient.

In an attempt to improve the smoothness of the concentration gradient, a novel printing strategy was engineered. Two ink cartridges were used to print two bio-inks. An ascending grey-scale was printed from the albumin-FITC cartridge. Simultaneously, a

descending grey-scale was printed from another nozzle using the blank tris buffer stored in a different cartridge. The overlapping of protein dots with the buffer solution dots provided beneficial mixing of the two bio-inks before drying and fixation on the surface. Printing the two combined and opposite grey-scales of the two bio-inks resulted in a more continuous concentration gradient of the protein (Fig. 6b). Smoother concentration gradients can be generated with multiple cartridges and controlling the elution of inks prior to adsorption and drying onto the substrate.

3.6. Printing microfluidic paper diagnostics

Ink jet printing was also used to fabricate a complete paper-based bioassays and diagnostic devices. Paper-based microfluidic patterns have been reported as the structure for making diagnostic devices for health care [10,11]. Martinez et al. [10,11] have fabricated paper-based microfluidic bioassays by photolithography. Li et al. [12] have recently reported different approach to fabricate paper-based microfluidic patterns by plasma treatment. Plasma treatment generates a hydrophilic pattern on hydrophobic

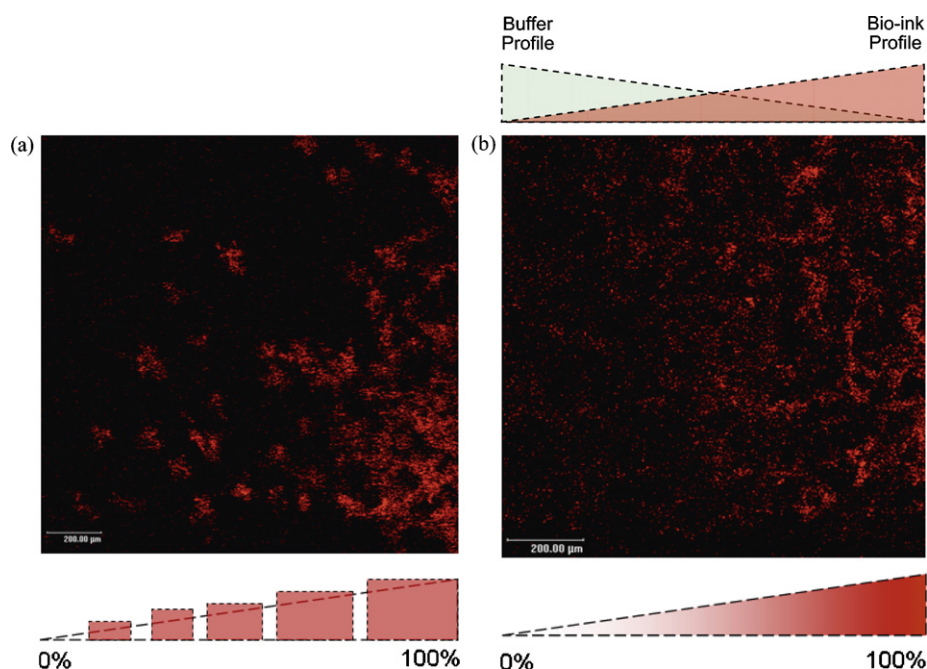


Fig. 6. Confocal Images (Krypton, 5x) of albumin-FITC concentration gradient: (a) concentration gradient printed using mono-bio-ink (protein solution), and (b) concentration gradient printed using two bio-inks printed from two cartridges (protein solution and buffer solution).

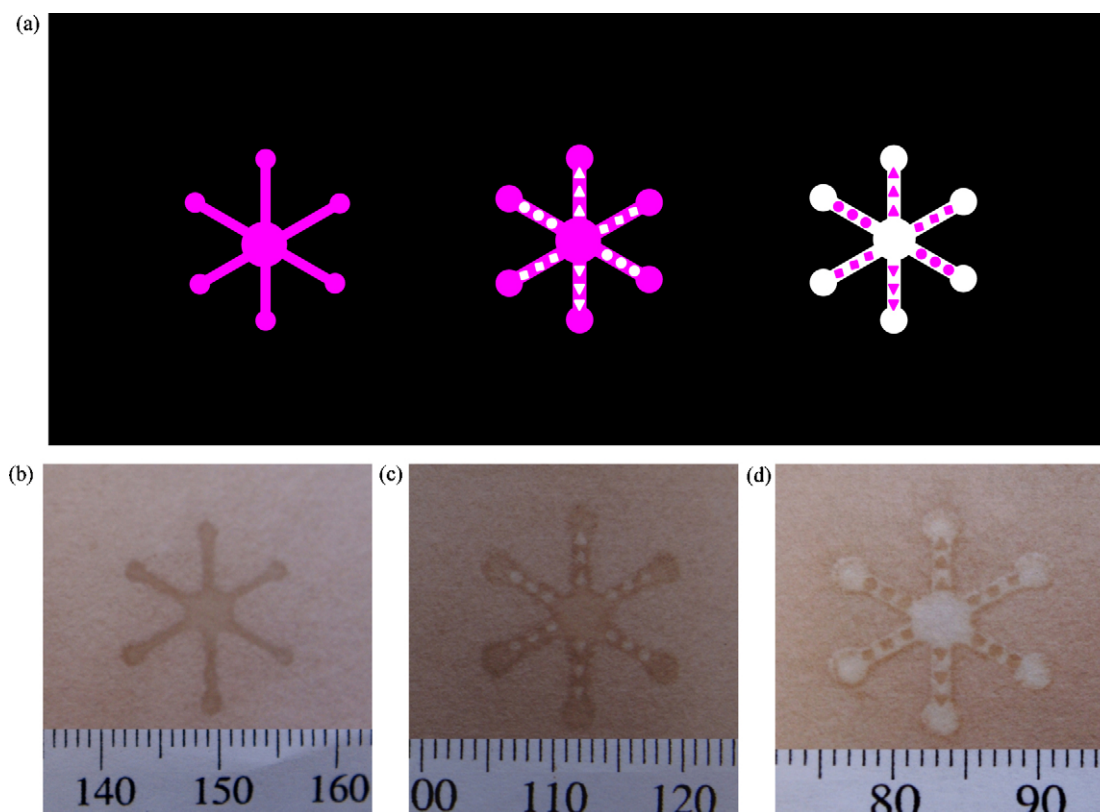


Fig. 7. Paper-based microfluidic devices. (a) Microfluidic paper with three different designs of biomolecular patterns (magenta shades represent intended printing patterns); (b)–(d) the three different printed patterns. The scales are in mm. (For interpretation of the references to color in this figure legend, the reader is referred to the web version of the article.)

paper, providing capillary penetration pathways for liquid samples. Shen et al. [29] and Li et al. [38] later showed that hydrophilic–hydrophobic contrast can be created by ink jet printing. In the present study, we demonstrate that ink jet printing can deliver chemical and biochemical reagents inside channel patterns to form functional devices.

Ink jet printing was first used to print hydrophobic patterns on paper, forming a series of six-channel hydrophilic systems [38] (Fig. 7). The three different digital patterns used for printing the biomolecules and the channels are represented in Fig. 7a; colour represents the biomolecules. HRP enzyme was printed inside the hydrophilic channels (Fig. 7). A few drops of DAB, the liquid enzyme substrate, were deposited in the collector at the centre of the hydrophilic pattern into the device using a micropipette. As the DAB solution penetrates along all channels, the brown colour was formed, revealing the exact position and the activity of the printed HRP. Fig. 7b represents the photo of the bio-diagnostics achieved.

Ink jet printing can be a competitive technique to fabricate paper-based microfluidic bioassays and diagnostic devices. The ability to simultaneously print multiple bio-inks enables the fabrication of more advanced paper-based bioassays and diagnostic devices. Ink jet printing offers the resolution and the on-demand pattern variations required for micro-manufacturing. Moreover, the ability to simultaneously print multiple bio-inks opens the possibility to fabricate advanced paper-based bioassays and diagnostic devices using ink jet printing technique.

4. Conclusion

The feasibility of thermal ink jet printing as a convenient and up-scalable process for biosurface engineering was demonstrated. The strategy investigated was to reconstruct a commercial printer

to take full advantage of the modern colour management interfaces already available; these printers are also low-cost. High printing resolution was achieved by formulating bio-inks. Protein and enzyme denaturation during thermal ink jet printing was experimentally and theoretically proven to be insignificant. The printed enzymes remained active. This is because the retention time spent by the biomolecules in the heating zone of the printer is very short (less than 250 μ s), and thanks to the important heat capacity of air and the printing substrate absorbing any potential residual heat from the bio-ink droplet.

Discrete and continuous concentration gradients of proteins on polymeric scaffolds were achieved by ink jet printing; these protein concentration gradients serve as potential guidance cues for cell growth generation for tissue engineering application. A novel strategy was developed to engineer very smooth, continuous concentration gradients of biomolecules by ink jet printing. It consists of simultaneously printing an increasing concentration gradient of the biomolecule on a porous surface combined with a decreasing concentration gradient of a buffer/eluent/solvent. Gradient uniformity is promoted by controlling the bio-ink dilution and elution with its solvent/buffer prior to absorption into the surface. The printed proteins thus retained by physisorption were shown not to desorb upon prolong immersion in aqueous solutions, allowing printed scaffold to be used for *in vitro* and *in vivo* conditions. Our group portrait was ink jet printed with a protein on paper, illustrating that complex biopatterns can be printed on large area. Finally, patterns of enzymes were specifically ink jet printed within the detection and reaction zones integrated in the fluidic system of a paper diagnostic.

Ink jet printing offers precision and speed for the commercial production of sensors. Reconstructing a commercial ink jet printer can be an economical option that further benefits from highly

developed control software which offer flexibility for biosurface engineering.

Acknowledgements

Monash University is acknowledged for the postgraduate scholarships (MSK, DF, XL, JT). Many thanks to Drs G. Thouas, N. Cowieson, D. Kannangara for discussion.

References

- [1] P. Calvert, Inkjet printing for materials and devices, *Chemistry of Materials* 13 (2001) 3299–3305.
- [2] P. Molnar, M. Hirsch-Kuchma, J.W. Rumsey, K. Wilson, J.J. Hickman, Biosurface engineering, in: J.G. Webster (Ed.), *Encyclopedia of Medical Devices and Instrumentation*, John Wiley & Sons, 2006.
- [3] D.R. Nisbet, S. Pattanawong, N.E. Ritchie, W. Shen, D.I. Finkelstein, M.K. Horne, J.S. Forsythe, Interaction of embryonic cortical neurons on nanofibrous scaffolds for neural tissue engineering, *Journal of Neural Engineering* 4 (2007) 35–41.
- [4] A. Offenhausser, S. Bocker-Meffert, T. Decker, R. Helpenstein, P. Gasteier, J. Groll, M. Moller, A. Reska, S. Schafer, P. Schultea, A. Vogt-Eisele, Microcontact printing of proteins for neuronal cell guidance, *Soft Matter* 3 (2007) 290–298.
- [5] C.J. Flaim, S. Chien, S.N. Bhatia, An extracellular matrix microarray for probing cellular differentiation, *Nature Methods* 2 (2005) 119–125.
- [6] L. Lauer, S. Ingebrandt, M. Scholl, A. Offenhausser, Aligned microcontact printing of biomolecules on microelectronic device surfaces, *IEEE Transactions on Biomedical Engineering* 48 (2001) 838–842.
- [7] S. Ilkhanizadeh, A.I. Teixeira, O. Hermanson, Inkjet printing of macromolecules on hydrogels to steer neural stem cell differentiation, *Biomaterials* 28 (2007) 3936–3943.
- [8] T.M. Keenan, A. Folch, Biomolecular gradients in cell culture systems, *Lab on a Chip* 8 (2008) 34–57.
- [9] E.D. Miller, G.W. Fisher, L.E. Weiss, L.M. Walker, P.G. Campbell, Dose-dependent cell growth in response to concentration modulated patterns of FGF-2 printed on fibrin, *Biomaterials* 27 (2006) 2213–2221.
- [10] A.W. Martinez, S.T. Phillips, M.J. Butte, G.M. Whitesides, Patterned paper as a platform for inexpensive, low-volume, portable bioassays, *Angewandte Chemie International Edition* 46 (2007) 1318–1320.
- [11] A.W. Martinez, S.T. Phillips, E. Carrihe, S.W. Thomas III, H. Sindi, G.M. Whitesides, Simple telemedicine for developing regions: camera phones and paper-based microfluidic devices for real-time, off-site diagnosis, *Analytical Chemistry* 80 (2008) 3699–3707.
- [12] X. Li, J. Tian, T. Nguyen, W. Shen, Paper-based microfluidic devices by plasma treatment, *Analytical Chemistry* 80 (2008) 9131–9134.
- [13] A.V. Lemmo, D.J. Rose, T.C. Tisone, Inkjet dispensing technology: applications in drug discovery, *Current Opinion in Biotechnology* 9 (1998) 615–617.
- [14] M. Nakamura, A. Kobayashi, F. Takagi, A. Watanabe, Y. Hiruma, K. Ohuchi, Y. Iwasaki, M. Horie, I. Morita, S. Takatani, Biocompatible inkjet printing technique for designed seeding of individual living cells, *Tissue Engineering* 11 (2005) 1658–1666.
- [15] J.D. Newman, A.P.F. Turner, Ink-jet printing for the fabrication of amperometric glucose biosensors, *Biosensors and Bioelectronics* 20 (2005) 2019–2026.
- [16] B.R. Ringeisen, C.M. Othon, J.A. Barron, D. Young, B.J. Spargo, Jet-based methods to print living cells, *Biotechnology Journal* 1 (2006) 930–948.
- [17] S.D. Risio, N. Yan, Piezoelectric ink-jet printing of horseradish peroxidase: effect of ink viscosity modifiers on activity, *Molecular Rapid Communications* 28 (2007) 1934–1940.
- [18] E.A. Roth, T. Xu, M. Das, C. Gregory, J.J. Hickman, T. Boland, Inkjet printing for high-throughput cell patterning, *Biomaterials* 25 (2004) 3707–3715.
- [19] L.R. Allain, M. Askari, D.L. Stokes, T. Vo-Dinh, Microarray sampling-platform fabrication using bubble-jet technology for a biochip system, *Fresenius Journal of Analytical Chemistry* 371 (2001) 146–150.
- [20] T. Goldmann, J.S. Gonzalez, DNA-printing: Utilization of a standard inkjet printer for the transfer of nucleic acids to solid supports, *Journal of Biochemical and Biophysical Methods* 42 (2000) 105–110.
- [21] L. Pardo, J.W. Cris Wilson, T. Boland, Characterization of patterned self-assembled monolayers and protein arrays generated by the ink-jet method, *Langmuir* 19 (2003) 1462–1466.
- [22] L. Setti, C. Piana, S. Bonazzi, B. Ballarin, D. Frascaro, A. Fraleoni-Morgera, S. Giuliani, Thermal inkjet technology for the microdeposition of biological molecules as a viable route for the realization of biosensors, *Analytical Letters* 37 (2004) 1559–1570.
- [23] T. Xu, J. Jin, C. Gregory, J.J. Hickman, T. Boland, Inkjet printing of viable mammalian cells, *Biomaterials* 26 (2005) 93–99.
- [24] H. Kipphan, *Handbook of Print Media*, Springer, 2001.
- [25] H.P. Le, Progress and trends in ink-jet printing technology, *The Journal of Imaging Science and Technology* 42 (1998) 49–62.
- [26] I. Barbulovic-Nad, M. Lucente, Y. Sun, M. Zhang, A.R. Wheeler, M. Bussmann, Bio-microarray fabrication techniques—a review, *Critical Reviews in Biotechnology* 26 (2006) 237–259.
- [27] K. Chattopadhyay, S. Mazumdar, Structural and conformational stability of horseradish peroxidase: effect of temperature and pH, *Biochemistry* 39 (2000) 263–270.
- [28] H. Cho, M.A. Parameswaran, H.-Z. Yu, Fabrication of microsensors using unmodified office inkjet printers, *Sensors and Actuators B: Chemical* 123 (2007) 749–756.
- [29] W. Shen, T. Junfei, X. Li, M. Khan, G. Garnier, Method of Fabricating Paper-Based Microfluidic Systems by Printing, Australian Provisional Patent, 2008905776, November 7 (2008), Australia, 2008.
- [30] N.C. Veitch, Horseradish Peroxidase: a modern view of a classic enzyme, *Phytochemistry* 65 (2004) 249–259.
- [31] M.S. Khan, D. Fon, X. Li, J. Forsythe, G. Thouas, G. Garnier, W. Shen, Printing biomolecules part-1: achieving total control of biomolecule delivery using ink jet printing, in: D. Chen (Ed.), *Chemeca 2008, Engineers Australia, IChemE in Australia, City Hall, Newcastle, NSW, 2008*, pp. 744–753.
- [32] M.S. Khan, D. Fon, X. Li, J.S. Forsythe, G. Garnier, W. Shen, Ink jet printing of biomolecules on porous surfaces, in: N. Ahmed (Ed.), *International Conference on Chemical Engineering (ICChE) 2008, Bangladesh University of Engineering and Technology (BUET), Dhaka, Bangladesh, 2008*, pp. 171–176.
- [33] D.R. Lide, *CRC Handbook of Chemistry and Physics*, 84 ed., CRC Press, Inc., 2003–2004.
- [34] A. Asai, M. Shioya, S. Hirasawa, T. Okazaki, Impact of an ink drop on paper, *Journal of Imaging Science and Technology* 37 (1993) 205–207.
- [35] M.S. Khan, D. Kannangara, W. Shen, G. Garnier, Isothermal noncoalescence of liquid droplets at the air-liquid interface, *Langmuir* 24 (2008) 3199–3204.
- [36] B.S. Chang, K.H. Park, D.B. Lund, Thermal inactivation kinetics of horseradish peroxidase, *Journal of Food Science* 53 (1988) 920–923.
- [37] M.S. Khan, W. Shen, G. Garnier, Thermal stability of horseradish peroxidase enzymatic papers, in: R. Coghill (Ed.), *Proceedings of the 63rd Appita Annual Conference and Exhibition, APPITA, Melbourne, Australia, 2009*, pp. 273–280.
- [38] X. Li, J. Tian, W. Shen, Paper as low-cost base material for diagnostic and environmental sensing applications, in: R. Coghill (Ed.), *Proceedings of the 63rd Appita Annual Conference and Exhibition, APPITA, Melbourne, Australia, 2009*, pp. 267–271.



Thermal stability of bioactive enzymatic papers

Mohidus Samad Khan, Xu Li, Wei Shen, Gil Garnier*

Australian Pulp and Paper Institute, Department of Chemical Engineering, Monash University, Clayton, VIC 3800, Australia

ARTICLE INFO

Article history:

Received 11 May 2009

Received in revised form 25 August 2009

Accepted 26 August 2009

Available online 3 September 2009

Keywords:

Bioactive papers

Thermal stability

Enzyme

Deactivation

Kinetics

ABSTRACT

The thermal stability of two enzymes adsorbed on paper, alkaline phosphatase (ALP) and horseradish peroxidase (HRP), was measured using a colorimetric technique quantifying the intensity of the product complex. The enzymes adsorbed on paper retained their functionality and selectivity. Adsorption on paper increased the enzyme thermal stability by 2–3 orders of magnitude compared to the same enzyme in solution. ALP and HRP enzymatic papers had half-lives of 533 h and 239 h at 23 °C, respectively. The thermal degradation of adsorbed enzyme was found to follow two sequential first-order reactions, indication of a reaction system. A complex pattern of enzyme was printed on paper using a thermal inkjet printer. Paper and inkjet printing are ideal material and process to manufacture low-cost-high volume bioactive surfaces.

Crown Copyright © 2009 Published by Elsevier B.V. All rights reserved.

1. Introduction

The benefits of many breakthroughs in biotechnology, medicine and environmental science have often been restricted by the high cost and the limited availability of tests and application devices. Most methods developed in the laboratory are difficult to scale up for mass production. There is a need for low-cost bioassays for health and environmental diagnostics. Disposable routine bioassays for the early detection of cancers and genetic conditions, for daily tests to monitor diabetes, and for instant water analyses of heavy metals and microbial activity are a few of the potential applications. Bioactive papers can also have industrial applications. Enzymes immobilized on paper for the catalytic production of biofuels, antibody immobilized on paper for the high selectivity separation of antigen in blood or fermentation streams, and antimicrobial papers are some examples.

Low-cost is a critical requirement for the successful commercialization of bioassays and bioactive surfaces; this is best achieved through high volume manufacturing and with commodity materials. Printing is a high speed technology, highly adaptive and able to deliver patterns of materials such as functional fluids at an exceptional accuracy. Paper, a non-woven made of cellulosic fibres, is highly wettable when untreated, easy to functionalise and engineer, biodegradable, sterilisable, biocompatible and cheap. It has long been used for analysis in chromatography [1,2]. Liquid flow in paper proceeds through capillarity action which is affected by paper

structure and chemical treatment. Also, thin coatings of polymers and inorganics can easily be achieved through standard wet-end addition, surface sizing, coating and other surface treatments common to the industries. This suggests that paper is a natural material of choice for the production of disposable bioassay devices and bioactive surfaces. However, the biotechnology industry has a limited understanding of the effect of paper structure and chemical composition on fluid transport or biomolecule functionality.

The concept of paper bioassays is to rely on paper for the transport of fluids samples, biomolecule detection/reaction, and the communication of the event in a single step process. Whitesides pioneered paper microfluidic systems by developing hydrophobic barriers on paper with photolithography technique or using an x,y-plotter [3–5]. The pattern accuracy and manufacturing efficiency of microfluidic papers can be improved with plasma treatments or inkjet printing [6]. Peptides, enzymes and cells have also been printed under laboratory conditions using a variety of technologies including inkjet printing [7–20].

Few scientific studies have described the immobilization of enzymes on paper. Among those are paper strip indicators for sea food freshness using two enzymes (xanthine oxidase and nucleoside phosphorylase) [21], and bioactive paper to monitor alcohol content in the breath using alkaline oxidase (AOD) [22]. However, there is little fundamental understanding on the effect of surface property on biofunctionality. Chen et al. investigated by AFM the effect of surface wettability on enzyme loading (*Candida antarctica* lipase B CALB) [23]. As surface wettability increased, the number of immobilized CALB molecules decreased, and enzyme aggregation increased. Changes in protein conformation and orientation were attributed to the protein-surface and protein-protein

* Corresponding author. Tel.: +61 3 9905 9180; fax: +61 3 9905 3413.

E-mail address: Gil.Garnier@eng.monash.edu.au (G. Garnier).

interactions. The enzyme activity was found to decrease with the surface hydrophobicity.

The first requirement of a bioactive paper is to retain the functionality, reaction rate and selectivity of its immobilized biomolecules. The second is to provide good biomolecule stability. Bioactive paper must not only uphold the shear and temperature of the printing and roll to roll manufacturing process, but also sustain the transport and storage conditions while insuring a reasonable shelf-life. The objective of this study is to measure the potential of paper as stable support for the immobilization of enzymes required for catalytic and diagnostic applications. Alkaline phosphatase (ALP) and horseradish peroxidase (HRP) were the enzymes selected for their stability and their wide range of applications.

In the first part of the study, the thermal stability of ALP and HRP adsorbed on paper is measured and modelled. In the second, a complete enzymatic pattern is printed by ink jet printing on paper. Last, the requirements and potentials of bioactive paper for diagnostic and industrial surfaces are analysed. It is the objective of the study to engineer fully bioactive and stable enzymatic papers.

2. Experimentals

2.1. Materials

The two enzymes, horseradish peroxidase (HRP) and alkaline phosphatase (ALP, from bovine intestinal mucosa), were purchased from Aldrich and used as received. HRP and ALP were immobilized on paper to study deactivation of enzymatic papers. HRP was also used to formulate bio-ink deposited on paper by inkjet printing. HRP was dissolved in 100 mM sodium–phosphate buffer solution (pH 6.0) to a concentration of 1.0 mg/mL to print on paper. A liquid substrate system, 3,3'-diaminobenzidine (DAB), from Aldrich, was used to identify the enzymatic activity of HRP. The biochemical reaction of HRP and DAB generates the brown stain on paper.

ALP was dissolved to a concentration of 0.1 mg/mL in 1 M diethanolamine buffer with 0.50 mM magnesium chloride and 5 M HCl to maintain pH at 9.7. Water (Millipore, 18 M Ω) was used for making all dilutions. The 5-bromo-4-chloro-3-indolyl phosphate/nitroblue tetrazolium (BCIP/NBT) liquid substrate system, purchased from Aldrich, was selected to quantify the enzymatic activity of ALP on paper. The biochemical reaction of ALP with BCIP/NBT results in a blue–purple complex; it is very stable and does not fade upon exposure to light [24].

A filter paper (Whatman #4) was chosen as paper substrate for printing and to immobilize biomolecules.

3. Methods

3.1. Printing HRP-enzyme on paper

A basic Canon inkjet printer (Pixma ip4500) and ink cartridges (CLI, Y-M-C-BK, PGBK model) were reconstructed to print the HRP-enzyme solution on paper. This bubble jet printer offers a resolution of 9600 \times 2400 dpi and is controlled by a personal computer which supplies page-data using MS Office 2003 software.

3.2. Immobilization of enzyme on paper

Enzyme aqueous solutions were homogeneously applied onto paper following TAPPI standard (T 205 sp-95). Basically, circular paper samples (16 cm) were immersed into the enzymatic solution contained in a large Petri-dish. To ensure uniform enzyme concentration on paper, the samples were carefully kept horizontal while

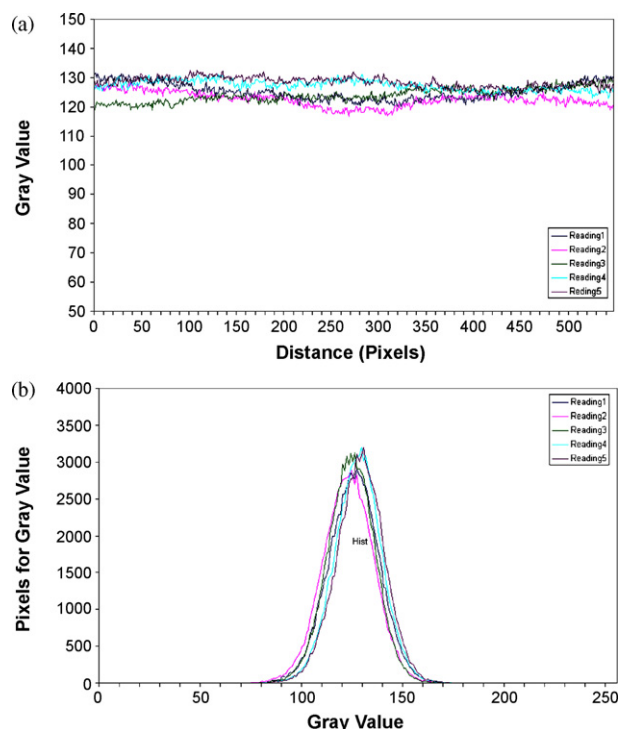


Fig. 1. Dye concentration distribution on paper measured by image analysis (ImageJ 1.41o). (a) Surface profile and (b) histogram of gray values.

being removed from the stock solution. The well-soaked paper samples were then blotted using one set of standard blotting papers (Drink Coster Blotting, 280 GSM) to remove any extra solution. A polyethylene sheet (3 M, PP2500) ($d = 16$ cm) was placed underneath each blotted sample. Paper and polyethylene sheet were placed into a drying ring assembled so that each sample bioactive paper-sheet is uppermost and in contact with the rubber seat of the next ring. The samples were left to dry in a dark chamber at 23 °C and 50% relative humidity for 24 h. The enzymatic paper samples were then used for further deactivation experiment and this time was set as $t = 0$.

To visualize the uniformity of enzyme distribution on paper, a diluted ink jet solution (cyan) was applied on the paper surface using the same procedure. Analyses of the surface profiles (Fig. 1a) and histogram distribution of gray values (Fig. 1b) of five replicates of dyed papers revealed a uniform distribution of ink on paper. The statistics of these tests are summarized in Table 1.

3.3. Thermal stability of enzymatic papers

The enzymatic papers were cut into small samples (6 cm \times 2 cm) and aged at different temperatures in an oven. The ALP and HRP enzymatic paper samples were treated at three different temperatures: 23 °C, 60 °C or 90 °C for various periods. For 23 °C, the samples were treated in a temperature and humidity controlled lab (23 °C and 50% relative humidity). Two ovens (Mettler Universal Oven, Schwabach, Germany) were used to treat samples at 60 °C and 90 °C.

Table 1

Concentration distribution parameters of gray values for adsorbed ink on paper.

Reading	Area (pixels)	Mean	Standard deviation
1	87,132	125.4	12.5
2	87,132	122.6	12.4
3	87,132	124.1	11.4
4	87,132	127.3	11.6
5	87,132	128.4	11.8

A digital humidity and temperature indicator (VAISALA Humidity and Temperature Indicator, Finland; operating range: -20°C to $+60^{\circ}\text{C}$) was used to measure the relative humidity (RH) in the ovens. At 60°C , the RH was in range of 6.5–7.0%. For the second oven, the limiting RH reading was 5–5.5% for 65°C , which indicates even dryer condition at 90°C .

Each enzymatic paper was exposed to its specific liquid substrate after the aging treatment. This was done as follows: small droplets of freshly prepared liquid substrate were applied onto the aged enzymatic papers using a 1.0 mL syringe equipped with a stainless steel flat-tipped needle (0.21 mm outer diameter). The enzyme–substrate reaction was allowed to proceed in a dark chamber for 2 h at 23°C and 50% relative humidity; this treatment insures complete enzymatic reaction [25–27]. From the colour intensity of enzyme–substrate reaction, the relative activity of the enzymatic paper was measured. Each measurement reported results from the average of 6–8 full replicates.

3.4. Image analysis and activity measurement

The colour intensity resulting from the enzyme–substrate reaction of enzymatic papers was measured at 1200 dpi using a standard scanner (EPSON PERFECTION 2450 PHOTO). The scanned images were analysed using ImageJ software (ImageJ 1.41o). ImageJ calculates the gray values of RGB images. RGB pixels are converted to gray values using the built in formula ($\text{gray} = (\text{red} + \text{green} + \text{blue})/3$). For any selected area, the ImageJ software calculates the weighted average gray value within the selection, which can be related to the enzymatic activity of enzymatic paper. Thus the average gray value is the sum of the gray values of all the pixels in the selection divided by the number of pixels. From the gray value analysis, the relative activity of enzymatic papers was measured. Activity corresponding to the gray value at $t=0$ h was considered as 100%. The relative activity at different time intervals was measured and normalized by the activity at $t=0$ h, i.e., relative activity, $[E_a]_t/[E_a]_0 = I/I_0$. The log value of relative activity is defined as the residual activity, $\log(I \times 100/I_0) = \log([E_a]_t \times 100/[E_a]_0)$.

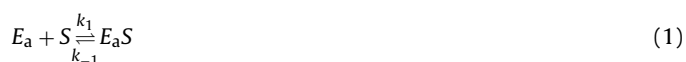
3.5. Calibration curve

Two calibration curves, one for ALP (Fig. 2a) and the other for HRP (Fig. 2b), were built to qualify the extent of enzymatic reaction on paper from the intensity colorimetric sample produced. The colour intensity increases non-linearly with enzyme concentration on paper. Colour results from the product of the enzyme–substrate reaction on papers using different enzyme concentrations.

4. Theory

4.1. Kinetics

The kinetics of enzyme–substrate reaction can be expressed with the two-steps Michaelis–Menten model [28]:



where E_a , S , P and ES represent the enzyme, substrate, product and enzyme complex concentration, respectively. However, enzyme activity is known to decrease as a function of time as some enzyme molecules become inactive when removed from their native environment [28]. The simplest enzymatic deactivation model consists

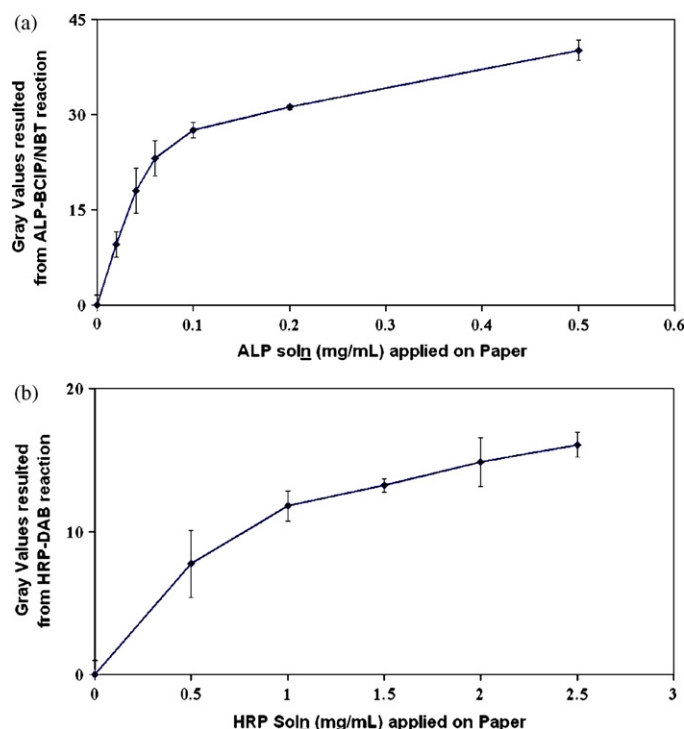


Fig. 2. Calibration curve of gray values of the enzymatic products resulting from enzyme–substrate reaction on paper. (a) ALP enzymatic paper and (b) HRP enzymatic paper.

of an active enzyme (E_a) molecule undergoing an irreversible structural or chemical change to some inactive form (E_i^*) [28]:



The enzyme deactivation rate (r_d) can be written as being proportional to the active enzyme concentration:

$$r_d = -\frac{d[E_a]}{dt} = k_d[E_a] \quad (4)$$

where, k_d is the deactivation rate constant. By integrating:

$$\ln \frac{[E_a]_{t=t}}{[E_a]_{t=0}} = -k_d t \quad (5)$$

from which the half-life ($t_{1/2}$) of enzymatic deactivation can be calculated. At time $t_{1/2}$, the residual enzymatic activity decreases to half of its initial value: $[E_a]_{t=t_{1/2}} = 0.5[E_a]_{t=t_0}$ or:

$$t_{1/2} = \frac{0.693}{k_d} \quad (6)$$

The temperature dependency of rate constant k_d can be correlated using Arrhenius equation [29]:

$$\log k_d = \log A - \frac{E}{2.303R} \left(\frac{1}{T} \right) \quad (7)$$

where, A , E , R and T represent the pre-exponential factor, activation energy of the deactivation process (kJ/mol), gas constant (8.314 J/mol K) and absolute temperature (K), respectively. Reactions with high activation energies are rather temperature sensitive, whereas, reactions with low activation energies are relatively temperature insensitive [30].

4.2. Enzymes

The alkaline phosphatase (ALP) enzyme is responsible for removing phosphate groups from different substrates including

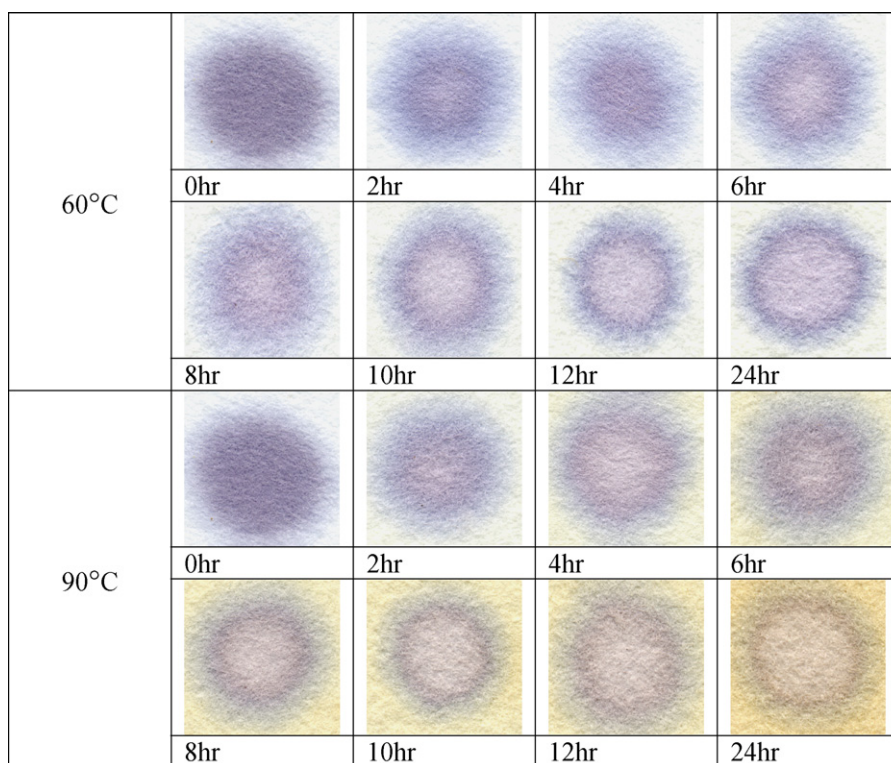
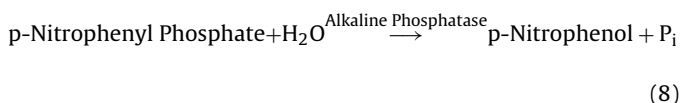


Fig. 3. Aging of ALP enzymatic paper treated at 60 °C and 90 °C for various periods. The blue purple colour reveals the enzyme (ALP)–substrates (BCIP/NBT) reaction.

proteins and alkaloids. It is most effective in an alkaline environment. An example of the reaction can be described as [31]



where P_i = inorganic phosphate.

ALP is present in the liver, intestine, placenta, bone, and kidney of mammals [32]. It can also be obtained from *Escherichia coli*, which has similar catalytic properties, similar pH-rate profile, and forms the same phosphoseryl intermediate as the intestinal enzyme [33]. The molecular weight is 89 kDa for *E. coli* ALP [34] and 126–140 kDa for bovine intestinal ALP [32–35]. ALP exists as a dimer comprising two very similar or identical subunits each containing 429 amino acids [33].

Horseradish peroxidase (HRP) is a single chain polypeptide enzyme containing four disulfide bridges. It is isolated from horseradish roots (*Amoracia rusticana*) and belongs to the ferroporphyrin group of peroxidase [36]. It has a molecular weight of 44 kDa and is reported to be very stable [11]. HRP readily combines with hydrogen peroxide (H_2O_2) and the resultant, HRP– H_2O_2 complex, can oxidize a wide variety of chromogenic hydrogen donors [36]. Most reactions catalyzed by HRP can be expressed by [37]



where, AH_2 and AH^* represent the reducing substrate and its radical product, respectively.

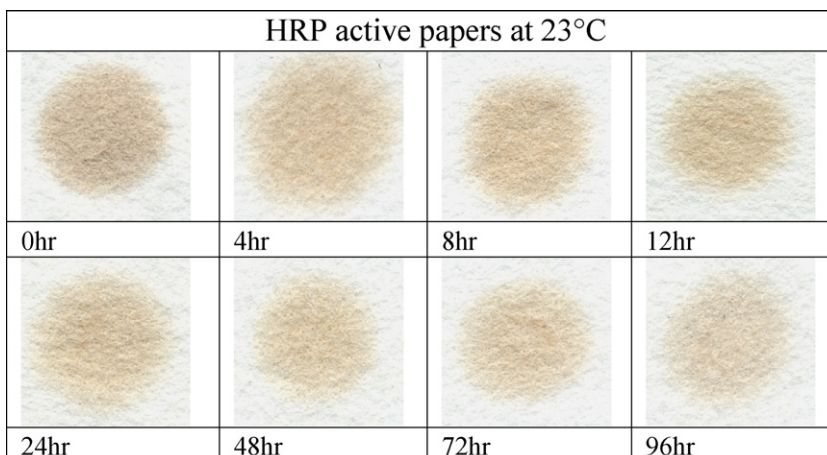


Fig. 4. Aging of HRP enzymatic paper treated at 23 °C for various periods. The brownish colour reveals the enzyme (HRP)–substrates (DAB) reaction.

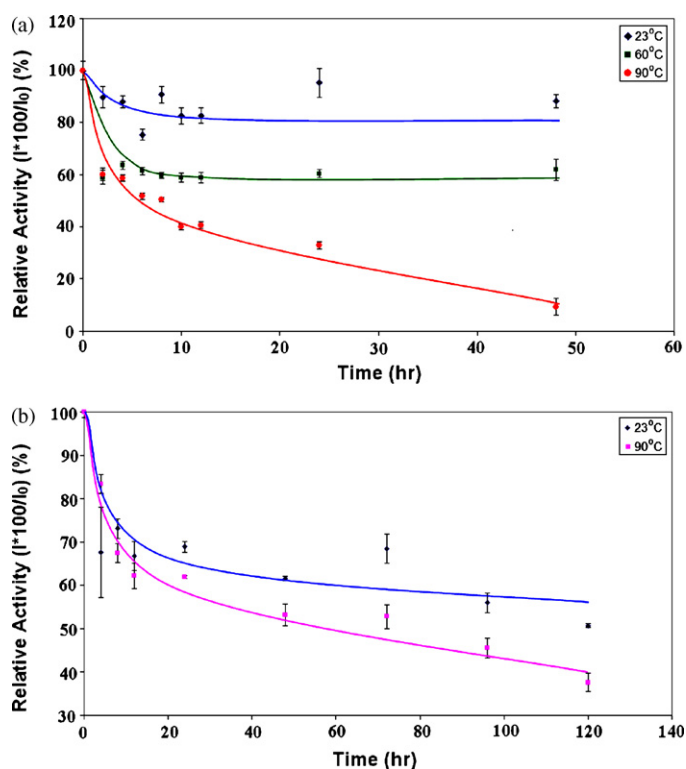


Fig. 5. Effect of time and temperature on the activity of enzymatic paper: (a) ALP paper and (b) HRP paper (I_0 = gray value at 0 hr and I = gray value at 't' h).

5. Results

5.1. Thermal stability of enzymatic papers

Enzymatic paper samples were aged at different temperatures for various periods. After applying the liquid substrate to the aged enzymatic paper and letting the enzyme–substrate reaction proceed to completion, the paper samples were scanned. The relative activities of enzymatic papers were calculated from the weighted mean gray value of the scan images. Figs. 3 and 4 show the colorimetric evolution of the two types of enzymatic paper aged at different temperatures as a function of time. Pictures of ALP enzymatic papers heated at 60 °C and 90 °C for periods up to 24 h are shown in Fig. 3. Fig. 4 illustrates the effect of aging HRP enzymatic papers up to 4 days at room temperature on their bioactivity. Paper yellowing is becoming visible for papers treated at the higher temperature and longer periods (≥ 4 h).

The effect of aging temperature and time on the relative activity of bioactive enzymatic papers is illustrated in Fig. 5. The enzymatic activity quickly fell within the initial hours of thermal treatment and then gradually decreased at a slower rate. The deactivation of enzymatic papers is faster at the higher temperatures. ALP enzymatic papers nicely retain their activity at 23 °C and exhibit only a moderate loss of activity when exposed at 60 °C (Fig. 5a). For HRP papers, the enzyme activity strongly decreased at 90 °C. For lower temperature (23 °C), the HRP enzymatic activity quickly fell within the first hours of thermal treatment and gradually decreased at a slower rate thereafter.

5.2. Bio-printing

The HRP-enzyme solution was ink jet printed on paper. The enzymatic paper was exposed, under standard conditions (23 °C, 50% relative humidity), to a solution containing its specific liquid substrate 3,3'-diaminobenzidine (DAB). The enzyme–substrate



Fig. 6. APPI surface engineering group photo (14.5 cm \times 10.5 cm) inkjet printed using HRP-enzyme ink solution onto Whatman #4 and exposed to its liquid substrate (DAB).

reaction yielded a brownish colour. The colour intensity was proportional to the concentration of the product resulting from the enzymatic activity. Fig. 6 is a picture of our research group obtained by inkjet printing the HRP-enzyme followed by reaction with DAB. Nice concentration profiles were achieved.

6. Discussion

6.1. Immobilized enzymes on paper

Enzymes randomly adsorbed from solution on paper retained their activities and selectivity upon immobilization on paper. This means that the active sites retained their structural integrity and remained available to the substrate. This was expected because of the low molecular weight of the substrates: phosphate ($M_w = 95$ Da) for ALP and peroxide ($M_w = 36$ Da) for HRP. These small molecules can easily diffuse through the cellulosic fibres of paper. The reaction rate of these adsorbed enzymes was not measured in this study. Mass transfer limitations and potential steric hindrance due to the orientation of the immobilized enzyme deserve further attention.

6.2. Enzymatic activity measurement

The intensity of the colour complex was found to vary with the enzymatic product concentration for the range studied; simple measurement of colour intensity can therefore quantify relative enzymatic activity.

The paper substrate was initially white and its background did not contribute any gray value to the enzymatic activity measurement. After prolong exposure to high temperatures, paper can turn yellow, which adds an extra gray value to the image analysis intensity measurement. This is especially catalysed by the alkaline conditions required for the ALP enzyme. To normalize the yellowing of paper from its enzymatic activity, the gray value of the paper control was measured and subtracted from the gray value of enzyme–substrate paper.

6.3. Deactivation of enzymes adsorbed on paper

Protein and enzyme are known to denature and become deactivated once removed from their biological surroundings and exposed to perturbations such as temperature, mechanical forces, radiation, chemicals and transition metals [28]. It is of interest to quantify the effect of enzyme immobilization on paper on its stability.

Yang and Kim [27] quantified the aging of ALP enzyme in aqueous medium; at 50 °C the activity of ALP reduced to around 10% of its initial rate within 30 min (Fig. 7). Chang et al. [25] and Machado and Saraiva [26] measured the aging of HRP-enzyme in aqueous

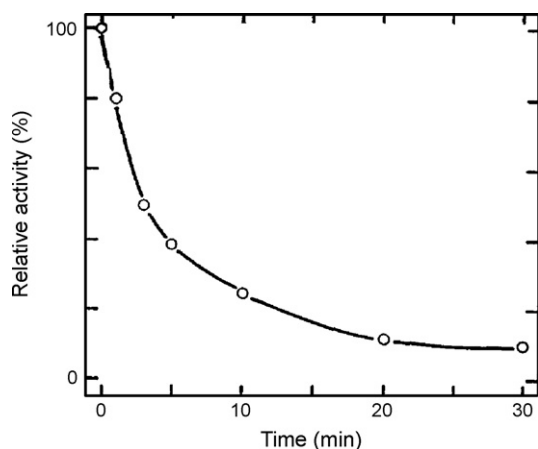


Fig. 7. Relative activity curve of alkaline phosphatase (ALP) heated at 50 °C in a buffer solution for various periods [27].

medium at different temperatures. They reported that in water the activity of HRP reduced to around 5% of its initial rate within 30 min at 90 °C (Fig. 8) [25]. The increased stability of the HRP and ALP enzymes adsorbed on paper is not exclusive to paper as substrate; Pelton et al. also reported that the stability of HRP immobilized in porous silica nanoparticle increases by over an order of magnitude compared to the molecule in solution [38]. OH containing molecules, such as alcohol, were also reported to stabilize HRP in solution [16,25].

Heat deactivates and denatures enzymes by modifying their conformation due to increased thermal movement and decreased solvent stabilization [28,39]. Proteins can also aggregate when heated which can restrict accessibility of their active sites. We believe that immobilization of enzyme on paper prevents protein aggregation and retards the conformation disorder by stabilizing the secondary and tertiary structures of enzyme through the establishment of a network of hydrogen bonds protein–cellulose. The effect of surface chemistry and morphology on enzyme stability deserves further investigation.

6.4. Deactivation kinetics of enzymatic paper

In its simplest form, enzyme deactivation can follow a first-order kinetics with respect to enzyme concentration (Eq. (5)). Enzyme activity plotted on a logarithmic scale is expected to vary linearly with time. That was not the case for enzymes immobilized on paper (Fig. 9), where two first-order kinetic regimes were

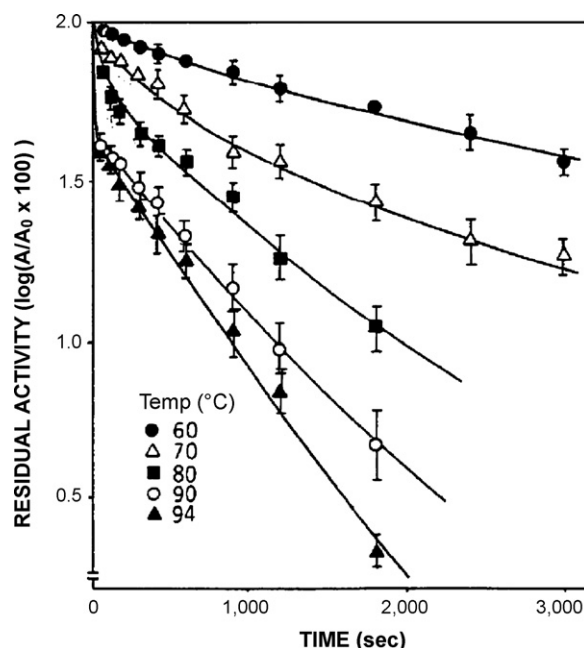


Fig. 8. Residual activity of peroxidase in 0.05 M phosphate buffer (pH 7.0, A_0 : initial activity, A : residual activity) [25] (with permission).

observed (Table 2). Bailey and Ollis [28] also reported that the decay of enzyme activity with time does not always follow the first-order model; kinetics with two distinct rates have been reported. Machado and Saraiva [26] also described that enzymatic deactivation pattern in aqueous medium comprised two distinct first-order phases (semi-logarithmic plot of the activity vs. time). Two sequential first-order reactions might be an indication of a reaction system in which different enzyme molecules denature by two distinct reaction pathways during different time frames. Subscript 1 refers to the deactivation rate constant of the steeper region and subscript 2 describes the pseudo-plateau.

Replotting Fig. 7 in logarithmic scale shows that the deactivation of ALP in aqueous medium projects two different linear regions (Fig. 10). Fig. 8 also indicates two different regions for HRP deactivation in aqueous medium.

The deactivation rate constants for the two regions of ALP deactivation in water (buffer) were calculated at 50 °C, to be 12.9 h^{-1} and 3.4 h^{-1} , respectively (Fig. 10). In contrast, the deactivation rate constants of ALP on paper varied from $229.5 \times 10^{-3} \text{ h}^{-1}$ (phase-1, at 90 °C) to $1.3 \times 10^{-3} \text{ h}^{-1}$ (phase-2, at 23 °C), which are 2–3

Table 2
Deactivation rate constants for bioactive enzymatic papers.

Temperature	ALP active paper			HRP active paper		
	$k_{d1}(\text{h}^{-1})$	$k_{d2}(\text{h}^{-1})$	$(t_{1/2})_2(\text{h}^{-1})$	$k_{d1}(\text{h}^{-1})$	$k_{d2}(\text{h}^{-1})$	$(t_{1/2})_2(\text{h})$
23 °C	62.8×10^{-3}	1.3×10^{-3}	533	59.8×10^{-3}	2.9×10^{-3}	239
60 °C	102.1×10^{-3}	6.05×10^{-3}	114.5			
90 °C	229.5×10^{-3}	32.2×10^{-3}	21.5	92×10^{-3}	4×10^{-3}	173
Activation energy of enzyme deactivation, E						
	E_1 (kJ/mol)		E_2 (kJ/mol)	E_1 (kJ/mol)		
On paper	16.74		42.09	5.74 ^a		
Activation energy of enzyme deactivation, E						
	E (kJ/mol)		E_1 (kJ/mol)	E_2 (kJ/mol)		
In buffer [28,40]	97.2 ± 7.2		177	146		

^a Values are calculated from the slope of two points.

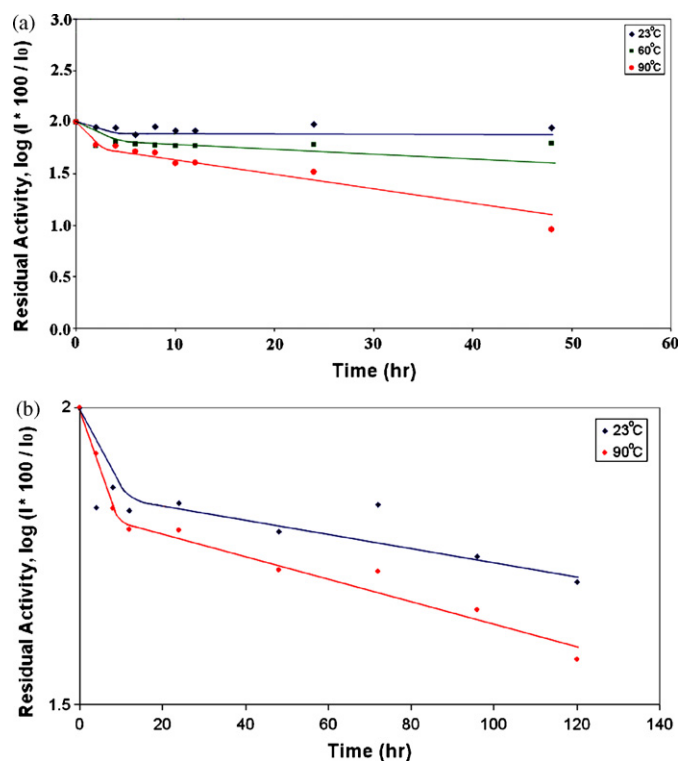


Fig. 9. Residual activity of enzyme active papers heated at different temperatures: (a) ALP enzymatic paper and (b) HRP enzymatic paper (I_0 = gray value at 0 h and I = gray value at t h).

orders of magnitude smaller than in water. The activation energies of ALP deactivation process on paper surface were found to be 16.74 kJ/mol for phase-1 and 42.09 kJ/mol for phase-2 (Table 2).

Machado and Saraiva [26] reported that at 85 °C the deactivation rate constants for both phases of HRP deactivation in solution were 48 h^{-1} and 2.52 h^{-1} . Whereas, at 90 °C, the deactivation rate constants of HRP on paper varied from $92 \times 10^{-3} \text{ h}^{-1}$ to $4 \times 10^{-3} \text{ h}^{-1}$, respectively for phase-1 and 2 (Fig. 9 and Table 2), which are 2–3 orders of magnitude smaller than that in aqueous medium.

Fadiloglu et al. [40] reported the activation energy of ALP deactivation in buffer is 97.2 kJ/mol. The activation energies for HRP deactivation in buffer found by Machado and Saraiva [26] were 177 kJ/mol for phase-1 and 146 kJ/mol for phase-2. The activation energy (E) for the denaturation of enzymatic papers was calcu-

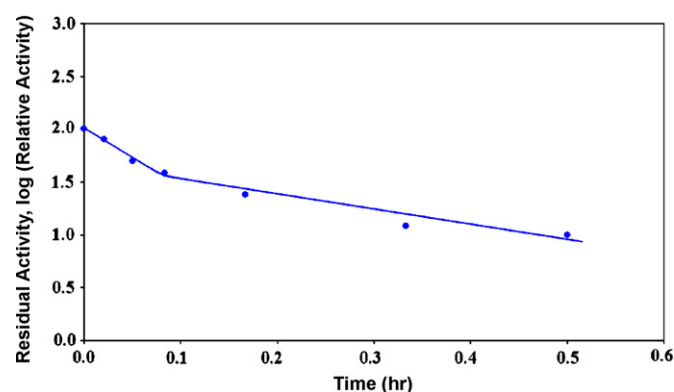


Fig. 10. Residual activity of alkaline phosphatase heated in buffer at 50 °C for various periods (calculated from Ref. [27]).

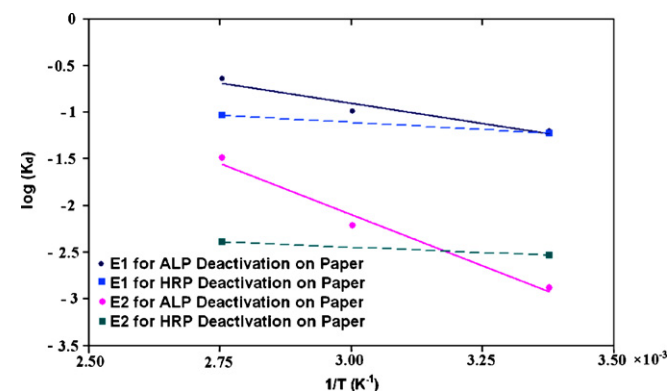


Fig. 11. Arrhenius plot for the thermal deactivation of bioactive enzymatic papers.

lated with the Arrhenius plot (Fig. 11). ' E ' of enzyme deactivation on paper is much smaller than in buffer: 2–5 times smaller for ALP and 30–35 times smaller for HRP (Fig. 12 and Table 2). This indicates that enzyme deactivation in solution is more temperature sensitive than that on paper.

6.5. Bioactive enzymatic papers

The deactivation half-life ($t_{1/2}$) of enzymatic papers can be calculated from the corresponding deactivation rate constants (Eq. (6)). For both enzymatic papers, the phase-1 ended within a few hours (2–12 h) and half-life is considered as a constant negligible

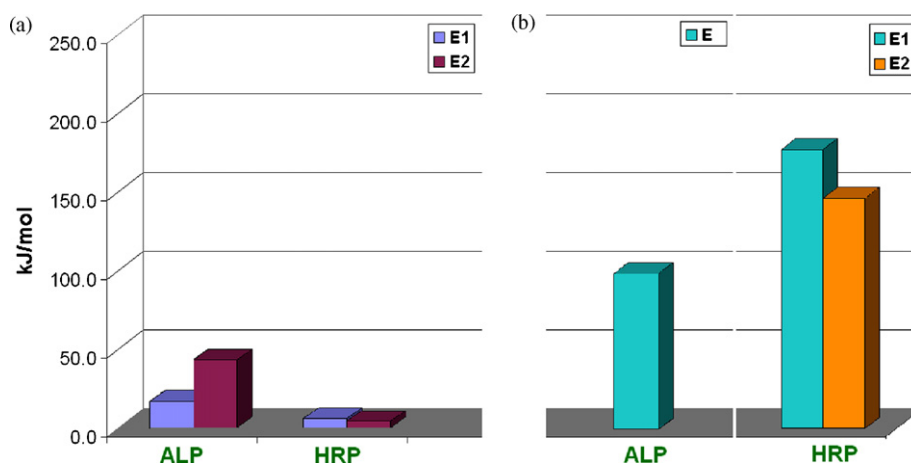


Fig. 12. Activation energy of enzymatic deactivation: (a) enzymes adsorbed on paper and (b) enzymes in buffer solution [26,40] (E_1 and E_2 are the activation energies of enzyme deactivation for phase-1 and 2, respectively).

compared to phase-2. Phase-2 is more stable; its half-life is rather significant and dominates the process. As an approximation, we therefore neglect phase-1 and assume that thermal deactivation is solely described by phase-2. ALP enzymatic paper had a half-life of 533 h, 114.5 h and 21.5 h, at 23 °C, 60 °C and 90 °C, respectively. HRP enzymatic papers half-lives are 239 h at 23 °C and 173 h at 90 °C. From the model, we calculate the deactivation rate constant (k_d) and the half-life of ALP enzymatic paper at 0 °C, to be $0.24 \times 10^{-3} \text{ h}^{-1}$ and 2932 h, respectively. This means that ALP enzymatic paper remains bioactive 22 days at room temperature or 4 months refrigerated. After 14 days at 23 °C, the kinetic model predicts the ALP enzymatic paper to retain 65% of its initial activity; 63% was measured experimentally. This confirms the validity of the model.

7. Conclusion

The activity and thermal stability of two enzymatic papers were quantified using a colorimetric technique measuring the colour intensity of the product complex. Enzymes such as alkaline phosphatase (ALP) and horseradish peroxidase (HRP) adsorbed from solution onto paper and dried remain functional and exhibit strong activity and selectivity. Adsorption onto paper increases the enzyme thermal stability by 2–3 orders of magnitude compared to the enzyme in solution. As an example, ALP enzymatic paper retained 60% of its initial activity after 48 h at 60 °C; this compares to less than 20% activity after 30 min at 50 °C for ALP enzyme in its buffer. The thermal degradation of ALP and HRP enzymes adsorbed on paper follows two sequential first-order reactions, this might indicate two distinct enzyme degradation reactions having different time frames. From the Arrhenius plot, the energies of enzyme deactivation on paper were much smaller than in solution. This simply means that enzyme deactivation on paper is much less temperature sensitive than in solution. From the model, we calculated that ALP enzymatic paper remains bioactive for 22 days if stored at room temperature and 4 months if refrigerated.

A complex pattern of HRP-enzyme was printed on paper by modifying a common thermal inkjet printer. Enzyme sustained the printing thermal and shear stress and remained bioactive. This demonstrates that bioactive paper has exceptional potential for low-cost, high flexibility diagnostic and industrial application.

Acknowledgments

Many thanks to Dr. Nathan Cowieson for discussion and Monash University for postgraduate scholarships (MSK, XL).

References

- [1] L. Lepri, A. Cincinelli, TLC sorbents, in: J. Cazes (Ed.), *Encyclopedia of Chromatography*, CRC Press, 2004, pp. 1–5.
- [2] K. Macek, *Pharmaceutical Application of Thin-Layer and Paper Chromatography*, Elsevier, 1972.
- [3] D.A. Bruzewicz, M. Reches, G.M. Whitesides, Low-cost printing of poly(dimethylsiloxane) barriers to define microchannels in paper, *Analytical Chemistry* 80 (2008) 3387–3392.
- [4] A.W. Martinez, S.T. Phillips, M.J. Butte, G.M. Whitesides, Patterned paper as a platform for inexpensive, low-volume, portable bioassays, *Angewandte Chemie International Edition* 46 (2007) 1318–1320.
- [5] A.W. Martinez, S.T. Phillips, E. Carrihe, S.W. Thomas III, H. Sindi, G.M. Whitesides, Simple telemedicine for developing regions: camera phones and paper-based microfluidic devices for real-time, off-site diagnosis, *Analytical Chemistry* 80 (2008) 3699–3707.
- [6] X. Li, J. Tian, T. Nguyen, W. Shen, Paper-based microfluidic devices by plasma treatment, *Analytical Chemistry* 80 (2008) 9131–9134.
- [7] L.R. Allain, M. Askari, D.L. Stokes, T. Vo-Dinh, Microarray sampling-platform fabrication using bubble-jet technology for a biochip system, *Fresenius Journal of Analytical Chemistry* 371 (2001) 146–150.
- [8] S.M.Z. Hossain, R.E. Luckham, A.M. Smith, J.M. Lebert, L.M. Davies, R.H. Pelton, C.D.M. Filipe, J.D. Brennan, Development of a bioactive paper sensor for detection of neurotoxins using piezoelectric inkjet printing of sol-gel-derived bioinks, *Analytical Chemistry* 81 (2009) 5474–5483.
- [9] S. Ilkhanizadeh, A.I. Teixeira, O. Hermanson, Inkjet printing of macromolecules on hydrogels to steer neural stem cell differentiation, *Biomaterials* 28 (2007) 3936–3943.
- [10] T. Jabrane, J. Jaïdi, M. Dube, P.J. Mangin, in: Iarigai (Ed.), *Gravure Printing of Enzymes and Phages*, *Advances in Printing and Media Technology*, 2008, pp. 279–288.
- [11] T.M. Keenan, A. Folch, Biomolecular gradients in cell culture systems, *Lab on a Chip* 8 (2008) 34–57.
- [12] E.D. Miller, G.W. Fisher, L.E. Weiss, L.M. Walker, P.G. Campbell, Dose-dependent cell growth in response to concentration modulated patterns of FGF-2 printed on fibrin, *Biomaterials* 27 (2006) 2213–2221.
- [13] M. Nakamura, A. Kobayashi, F. Takagi, A. Watanabe, Y. Hiruma, K. Ohuchi, Y. Iwasaki, M. Horie, I. Morita, S. Takatani, Biocompatible inkjet printing technique for designed seeding of individual living cells, *Tissue Engineering* 11 (2005) 1658–1666.
- [14] J.D. Newman, A.P.F. Turner, Ink-jet printing for the fabrication of amperometric glucose biosensors, *Biosensors and Bioelectronics* 20 (2005) 2019–2026.
- [15] B.R. Ringeisen, C.M. Othon, J.A. Barron, D. Young, B.J. Spargo, Jet-based methods to print living cells, *Biotechnology Journal* 1 (2006) 930–948.
- [16] S.D. Risio, N. Yan, Piezoelectric ink-jet printing of horseradish peroxidase: effect of ink viscosity modifiers on activity, *Molecular Rapid Communications* 28 (2007) 1934–1940.
- [17] E.A. Roth, T. Xu, M. Das, C. Gregory, J.J. Hickman, T. Boland, Inkjet printing for high-throughput cell patterning, *Biomaterials* 25 (2004) 3707–3715.
- [18] T. Xu, C.A. Gregory, P. Molnar, X. Cui, S. Jalota, S.B. Bhaduri, T. Boland, Viability, Electrophysiology of neural cell structures generated by the inkjet printing method, *Biomaterials* 27 (2006) 3580–3588.
- [19] T. Xu, J. Jin, C. Gregory, J.J. Hickman, T. Boland, Inkjet printing of viable mammalian cells, *Biomaterials* 26 (2005) 93–99.
- [20] W. Zhao, A.V.D. Berg, Lab on paper, *Lab on a Chip* 8 (2008) 1988–1991.
- [21] G. Masao, Preparation of enzyme-immobilized filter paper for determination of freshness of fish meat, *Jpn Kokai Tokkyo Koho*, Japan (1989).
- [22] Y. Akahori, H. Yamazaki, G. Nishio, H. Matsunaga, K. Mitsubayashi, An alcohol gas-sensor using an enzyme immobilized paper, *Chemical Sensors* 20 (2004) 468–469.
- [23] B. Chen, N. Pernodet, M.H. Rafailovich, A. Bakhtina, R.A. Gross, Protein immobilization on epoxy-activated thin polymer films: effect of surface wettability and enzyme loading, *Langmuir* 24 (2008) 13457–13464.
- [24] BCIP/NBT Liquid Substrate System, Product Information, Sigma Aldrich (web: <http://www.sigmaaldrich.com>), 2009.
- [25] B.S. Chang, K.H. Park, D.B. Lund, Thermal inactivation kinetics of horseradish peroxidase, *Journal of Food Science* 53 (1988) 920–923.
- [26] M.F. Machado, J.M. Saraiva, Thermal stability and activity regain of horseradish peroxidase in aqueous mixtures of imidazolium-based ionic liquids, *Biotechnology Letters* 27 (2005) 1233–1239.
- [27] W.-J. Yang, K.-W. Kim, Kinetic properties of rat intestinal phytase/alkaline phosphatase, *Korean Biochemistry Journal* 27 (1994) 342–345.
- [28] J.E. Bailey, D.F. Ollis, *Biochemical Engineering Fundamentals*, 2nd ed., McGraw-Hill, New York, 1986.
- [29] H.S. Fogler, *Elements of Chemical Reaction Engineering*, Prentice-Hall, Englewood Cliffs, NJ, 1986.
- [30] O. Levenspiel, *Chemical Reaction Engineering*, 3rd ed., John Wiley & Sons, New York, USA, 1999.
- [31] Enzymatic Assay of Phosphatase, Alkaline, Product Information, Sigma Aldrich (web: <http://www.sigmaaldrich.com>), 1995.
- [32] M. Besman, J.E. Coleman, Isozymes of bovine intestinal alkaline phosphatase, *The Journal of Biological Chemistry* 260 (1985) 11190–11193.
- [33] J.E. Coleman, Structure and mechanism of alkaline phosphatase, *Annual Review of Biophysics and Biomolecular Structure* 21 (1992) 441–483.
- [34] R.A. Anderson, B.L. Vallee, Cobal (III), a probe of metal binding sites of *Escherichia coli* alkaline phosphatase, in: *Proceedings of the National Academy of Sciences of the United States of America*, 72, 1975, pp. 394–397.
- [35] M. Fosset, D. Chappet-Tordo, M. Lazdunski, Intestinal alkaline phosphatase. Physical properties and quaternary structure, *Biochemistry* 13 (1974) 1783–1788.
- [36] Peroxidase from Horseradish (HRP), Product Information, Sigma Aldrich (web: <http://www.sigmaaldrich.com>), 1999.
- [37] N.C. Veitch, Horseradish peroxidase: a modern view of a classic enzyme, *Phytochemistry* 65 (2004) 249–259.
- [38] R. Voss, M.A. Brook, J. Thompson, Y. Chen, R.H. Pelton, J.D. Brennan, Non-destructive horseradish peroxidase immobilization in porous silica nanoparticles, *Journal of Materials Chemistry* 17 (2007) 4854–4863.
- [39] R.D. Schmid, Stabilized soluble enzymes, in: T.K. Ghose, A. Fiechter, N. Blakebrough (Eds.), *Advances in Biochemical Engineering*, Springer-Verlag, Berlin Heidelberg, 1979, pp. 41–118.
- [40] S. Fadiloglu, O. Erkmén, G. Sekeroglu, Thermal inactivation kinetics of alkaline phosphatase in buffer and milk, *Journal of Food Processing and Preservation* 30 (2006) 258–268.



Porous liquid marble shell offers possibilities for gas detection and gas reactions

Junfei Tian, Tina Arbatan, Xu Li, Wei Shen*

Department of Chemical Engineering, Monash University, Wellington Rd, Clayton, Vic. 3800, Australia

ARTICLE INFO

Article history:

Received 18 March 2010
Received in revised form 18 June 2010
Accepted 26 June 2010

Keywords:

Liquid marble
Superhydrophobic
Porous layer
Gas sensing
Gas reaction

ABSTRACT

The hydrophobic shell of a liquid marble prevents direct contact of the liquid core of the marble with any condensed phases (i.e. solid or liquid) outside the marble, but allows gas and vapour to diffuse across the shell. This property of a liquid marble naturally enables it to discriminately absorb or emit gaseous and vaporous compounds across its shell while denying contact or transport of liquids. Liquid marbles can, therefore, be used to form micro-gas reactors for gas detection application when loaded with an indicator solution. Liquid marble can also be used as a gas emitter; the relatively thin liquid marble shell enables the gas dissolved in the liquid marble core to be emitted to the supporting surface from a very close range, making it possible to carry out chemical sensing using the emitted gas as an indicator. In this study we show the potential of liquid marbles as gas sensors in different arrangements, i.e. with dissolved indicator in the liquid core to sense gases diffusing into the liquid marble from outside, or with soluble gas in the liquid core that is emitted out of the liquid marble where it is sensed (or used to indicate chemical species outside of the liquid marble). An important implication of this study is that other types of superhydrophobic surfaces may also be used to design sensors for sensing gases and vapours, or to use emitted gases and vapours as indicators for chemical sensing.

Crown Copyright © 2010 Published by Elsevier B.V. All rights reserved.

1. Introduction

Liquid marble is a natural phenomenon generally associated to the phenomenon of the lotus leaf; dust particles on the lotus leaf adhere to the surface of rolling water droplets on the lotus leaf and are removed from the leaf surface. Quéré and Aussillous [1] have reported the phenomenon of liquid marble based on his laboratory studies. Since then a number of research articles have appeared in the literature [2–5], providing a fuller understanding of the fundamental physics and the physical chemistry criteria of the formation of liquid marbles. Hydrophobic particles of regular or irregular shapes have been used to make liquid marbles by rolling liquid drops over a particle bed [5,6]. The hydrophobic particles, therefore, form a porous shell, covering the liquid core, preventing direct contact between the liquid core and any condensed material (i.e. solid or liquid non-wetting to the shell) outside the marble. Recently, Dandan and Erbil have shown that liquid marble can also be formed using solid particles that have $<90^\circ$ contact angle with the liquid. They also reported that the water evaporation rate from the liquid marble is slower than that of the bare water droplet [7]. Quéré and Aussillous [1] and Eshtiaghi et al. [8] have shown, using optical microscopy, that the particle shell of liquid marbles are porous. Hapgood et al. [9] showed that the shell of a stable marble

has a structure consisting of multilayers of hydrophobic particles. Such a structure enables the liquid marble to withstand certain levels of mechanical impacts and deformation, since the porous shell is stretchable.

Recently, Nguyen et al. [10] used confocal microscopy technique to investigate the structure of the liquid marble shell using hydrophobic nano-silica particles, silica R974, and an aqueous rhodamine B solution. The confocal images reported by these authors showed that silica R974 particles formed a loosely packed multilayer shell consisting of small and relatively large lumps of primary particles [10]. The multilayer marble shell thickness varied from 50 to $\sim 150 \mu\text{m}$ and the shell was porous.

The liquid marble phenomenon has attracted an increasing number of application studies exploiting the properties of the liquid marble. Hapgood et al. [9] investigated the hollow structure of dried liquid marbles and showed that such a structure can have useful properties in pharmaceutical applications. Zhang et al. [11] studied the use of liquid marble for DNA amplification using PCR microfluidic devices. Their work took advantage of the contamination-free liquid transport and the low transport friction offered by liquid marbles. Bormashenko et al. studied the floating of liquid marbles in terms of critical density, shape, response to vibration, and surface tension [2,12]. This group also formed liquid marbles with hydrophobic magnetic powder and demonstrated that such liquid marbles can be maneuvered by magnetic forces [13]. These researchers also reported comprehensive studies on the mechanisms of the floating and sliding of liquid marbles for manipulation

* Corresponding author. Tel.: +61 3 99053447.

E-mail address: Wei.shen@eng.monash.edu.au (W. Shen).

purposes [3]. Fujii et al. [14] used pH responsible polymer to control the stability of liquid marbles. Zhao et al. [15] have shown that liquid marbles formed using hydrophobic Fe_3O_4 nanoparticles can be manipulated and transported using magnetic fields. Kim et al. [16] used Janus microspheres to form liquid marbles with highly flexible and superhydrophobic shell; such marbles can withstand mechanical manipulation with tweezers. Gao and McCarthy [4] reported the formation of liquid marbles with ionic liquids. These authors carefully considered the surface chemistry criteria of marble formation and showed that a liquid with surface tension as low as 40 mN/m can form marbles with fine oligomeric tetrafluoroethylene particles.

An interesting property of the liquid marble we are addressing in this study is its hydrophobic and porous shell structure. The porous liquid marble shell prevents direct contact between the liquid core and any surface outside the marble, but does not prevent the transport of gas or vapour. Tian et al. [17] proposed that, since the porous liquid marble shell allows gas or vapour to freely transport across the shell, liquid marble therefore has potential to detect gas when it diffuses from outside of the liquid marble into the liquid core of the marble. It is further realized that porous liquid marble shell also enables liquid marbles to be used as micro-reactors which can selectively react to gas component transported between liquid marbles. When a liquid marble is formed with an appropriate indicator solution and placed onto the surface of a gas/vapour-emitting solid or liquid, the indicator solution is at a very close distance from the gas/vapour-emitting source, but has no direct contact with the source. This makes the liquid marble an efficient sensor for the gas/vapour of interest. If the gas/vapour-emitting body is a liquid, liquid marbles can be placed onto the liquid surface and, after sensing, be recovered from the liquid surface. If the gas/vapour-emitting body is a solid, a suitable liquid vapour pressure may be required to slow down liquid evaporation from the marble in order to enable long-term sensing. Liquid marbles therefore allow the use of liquid indicators to detect or sense gas components from a liquid phase without the need to add the indicator into the liquid phase. Liquid marbles can also be used as a gas/vapour emitter; gases/vapours emitted by the liquid marble can either be sensed by some other detection mechanisms or be used as a gas/vapour indicator to indicate chemical species outside of the liquid marble. Following the same train of thoughts, gas transport between two liquid marbles is also possible. The gas transport between liquid marbles can be used for analysis purposes with very little preparation required. Proper selection of the hydrophobic powder and indicator means that the liquid marble system for gas or vapour detection can further improve the detection sensitive. In this paper we report an investigation of using liquid marbles as colorimetric and fluorescent gas detectors for ammonia and hydrochloric acid gases. The quantitative capabilities of the liquid marble sensors are also studied using conventional UV–vis spectrophotometry and paper-based colorimetry measurements.

2. Experimental

2.1. Materials

Polytetrafluoroethylene powder (100 μm) was obtained from Aldrich and was used to form liquid marble sensors. NaOH (AR), $\text{CuCl}_2 \cdot 2\text{H}_2\text{O}$ (AR), $\text{CoCl}_2 \cdot 2\text{H}_2\text{O}$ (AR) and Ammonia solution (AR, 25%) were obtained from Analar. Phenolphthalein (AR) was obtained from BDH. A fluorescent dye, 8-hydroxypyrene-1,3,6-trisulfonic acid trisodium salt (HPTS), was obtained from Sigma–Aldrich. Another fluorescent dye, rhodamine B, was obtained from Ciba, Switzerland. Millipore water (18 M Ω) was used to prepare all solutions.

An acrylic-based water-borne flexographic printing ink was used as a real emission source of ammonia and amines. This ink was obtained from TMI, USA; it was formulated for printing of packaging polymer films and contained ammonia and low molecular weight amines [18].

Whatman filter paper #4 was used as the base to make indicator paper. Liquid marble of consistent size were generated using a 1 ml syringe with a Gauge 30 needle. A digital camera was used to capture photos of colorimetric changes of liquid marbles during vapour detection. An UV–vis spectrophotometer was used to quantify vapour detection.

2.2. UV–vis spectrophotometric measurement

A Shimadzu UV-1601 UV–vis spectrophotometer was used to quantify colour changes of the indicator solution caused by the absorption and dissolution of gaseous analytes. The maximum absorption wavelength of the indicator solution was first determined; light absorption data were then collected at this wavelength. Triplicate measurements were carried out for each sample.

2.3. Paper-based gas sensors

Circular paper discs ($\varnothing = 2$ mm) were produced from Whatman No. 4 filter paper using a disc punching device (Facit 4070, Sweden). A 600 nL aliquot of 0.1 M CuCl_2 solution was introduced onto each paper disc and allowed to dry. Five so-treated paper discs were then fixed onto a piece of sticky tape, which was placed in a Petri dish to form one gas sensing device. The five indicator-loaded paper discs allowed for five replicate colorimetric measurements to be made. Colour changes of the paper discs were quantified using a desktop scanner (EPSON perfection 2450 PHOTO) and the image analysis software (Adobe PhotoShop 7.0) following the procedure we reported previously [19].

3. Results

3.1. Qualitative NH_3 sensing using liquid marble

When a liquid marble, made using a phenolphthalein indicator solution and Teflon powder, was placed onto the surface of an ammonia solution, ammonia gas penetrated through the liquid marble shell and dissolved into the indicator solution. The phenolphthalein indicator changed colour and the liquid marble became pink. Since the indicator solution in the liquid marble was in very close proximity to the NH_3 solution and the volume of the liquid marble was small (4 μL), the colour change was rapid.

To confirm the colour change of the indicator was caused by the ammonia gas diffused across the marble shell and not by any direct liquid–liquid contact between the indicator solution and the ammonia solution, we reversed the experimental arrangement by placing two liquid marbles containing an ammonia solution and a sodium hydroxide solution, respectively, onto the surface of a phenolphthalein indicator solution contained in two separate Petri dishes (Fig. 1). While the NH_3 -OH liquid marble caused immediate colour change of the indicator solution (Fig. 1(a) and (b)), the NaOH liquid marble does not cause any colour change (Fig. 1(c)). It was therefore confirmed that the indicator colour change was caused by ammonia gas transport across the marble shell and not by liquid contact.

Ammonia detection in this experiment is caused by pH change of the indicator solution. Ammonia sensing using pH indicators has a problem of colour fading; the colour gradually faded and eventually disappeared by the end of the experiment (2 h) as the NH_3 dissolved in the indicator solution evaporated. To overcome

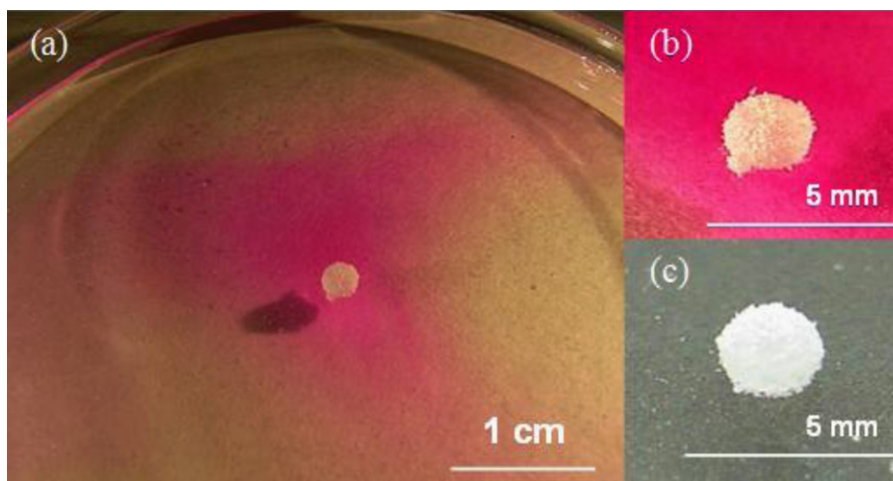


Fig. 1. (a) A liquid marble made using a diluted NH_4OH solution was placed onto the surface of a phenolphthalein indicator solution. The diffusion of NH_3 gas through the marble shell into the indicator solution was detected by the colour change of the phenolphthalein indicator; (b) a close-up view of (a); (c) a close-up view of a liquid marble made using a diluted NaOH solution placed on the surface of water containing phenolphthalein indicator. The lack of any colour change indicates that the liquid core of the marble has no contact with the indicator solution outside of the marble. (For interpretation of the references to color in this figure legend, the reader is referred to the web version of the article.)

this problem, indicators with more permanent colour changes were used. Fig. 2(a) shows liquid marbles made using water, phenolphthalein, 0.1 M of CoCl_2 , 0.1 M of CuCl_2 solutions and Teflon powder. When these liquid marbles were exposed to ammonia gas, the transition metal salts showed strong and sustained colour changes (Fig. 2(b)).

Ammonia can act as a σ -donor to form metal complexes with transition metals such as copper (II). In aqueous solutions, ammonia exists as ammonium and hydroxide ions. Cu(II) in the form of hexaaquacopper(II) ions reacts with hydroxide ions to form a pale blue Cu(II) hydroxide precipitate; the precipitate further reacts with ammonia molecules to form tetraamminediaquacopper(II) ions to give a deep blue colour. Cobalt chloride reacts with NH_3 in a similar way to that of CuCl_2 ; the only difference is that the final cobalt complex with ammonia contains six NH_3 ligands. When NH_3 concentration is low, the pH increase of the solution first leads to the precipitation of $[\text{Co}(\text{H}_2\text{O})_6]^{2+}$ to $[\text{Co}(\text{H}_2\text{O})_4(\text{OH})_2](\text{s})$, which has a bluish green colour. Further exposure to sufficient NH_3 will lead to the formation of the purple hexaammincobalt(II) complex. The reactions of copper and cobalt solutions are summarized below

(schemes (1)–(6)).

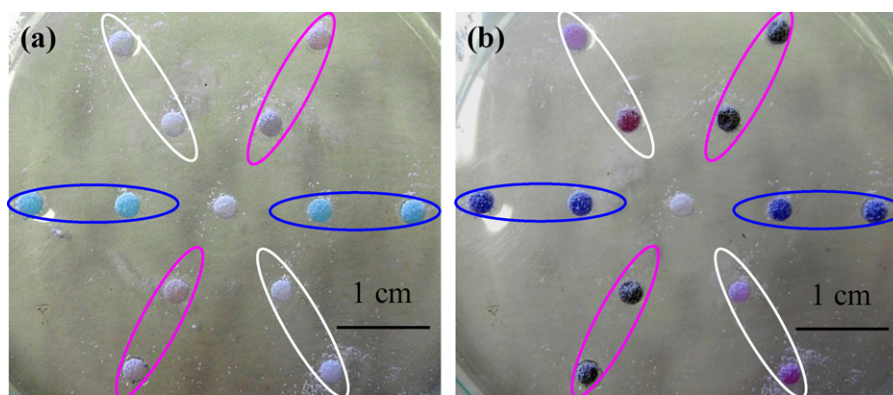
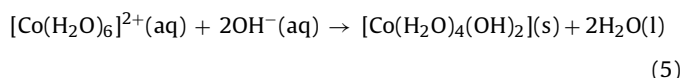
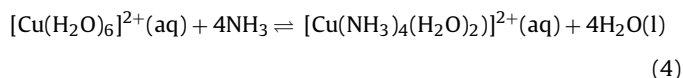
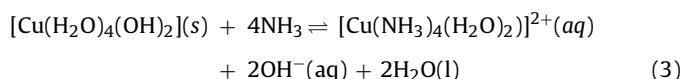
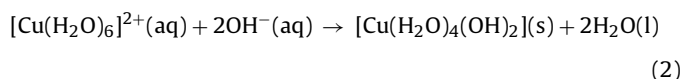
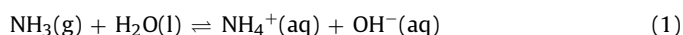


Fig. 2. (a) Four groups of liquid marbles containing water (center), phenolphthalein, CoCl_2 , CuCl_2 solutions, indicated by white, blue, purple circles, respectively. (b) The colour changes of those liquid marbles after exposing to the ammonia gas. (For interpretation of the references to color in this figure legend, the reader is referred to the web version of the article.)

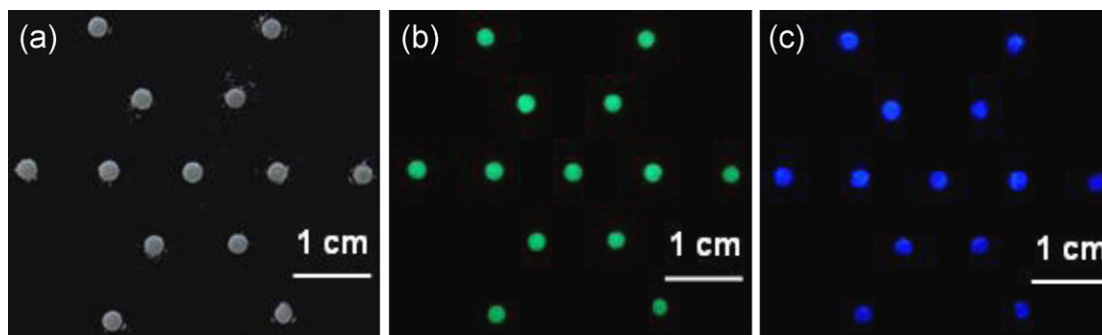
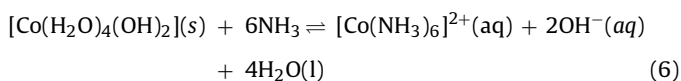


Fig. 3. (a) Liquid marbles containing the HPTS indicator under ambient lighting before and after exposing to HCl vapour; (b) liquid marbles containing the HPTS indicator under UV light before exposing to HCl vapour; (c) liquid marbles containing HPTS under UV light after exposing to HCl vapour.



Since transition metal ammonia complexes are very stable (e.g. for reaction scheme (4), $\lg K_{\text{stab.}} = 12$ [20]), these transition complexes did not fade within the time of the experiment (4 h).

The different colour changes of those transition metal salts triggered by NH_3 suggest that liquid marbles containing different but chemically specific indicators can potentially be used to detect different gaseous species. Conversely, this phenomenon also promises the possible use of liquid marbles to detect chemical species in aqueous media using gas(es) as an indicator(s).

3.2. Qualitative HCl sensing using liquid marble and fluorescent detection mechanism

Fluorescent pH indicator can be used as the core solution of liquid marbles for gas sensing. We use liquid marbles made of an aqueous fluorescent solution of 8-hydroxypyrene-1,3,6-trisulfonic acid trisodium salt (HPTS) (10 mg/L) and Teflon powder to elucidate the gas detection. HPTS is a strongly water soluble and pH dependent fluorescent dye with the pK_a of ~ 7.3 [21]. HPTS has a pH dependent fluorescent colour change from blue (405 nm) at $\text{pH} \leq 6$ to green (centered at 450 nm) at $\text{pH} \geq 8$ [21]. The transition of the colour change occurs between pH 6.6 and 7.4.

HPTS liquid marbles show no specific colour under ambient lighting before and after exposing to HCl vapour (Fig. 3(a)), but show a green fluorescence under UV light before exposing to HCl vapour (Fig. 3(b)). This property of the fluorescent indicator allows it to be distinguished from colorimetric indicators. When HPTS liquid marbles were exposed to HCl vapour, HPTS showed a clear fluorescent colour change which can be observed under UV light (Fig. 3(c)). This result has an implication that different detection mechanisms (e.g. colorimetry and fluorescence) can be employed to carry out simultaneous detections of different vapours or gases.

3.3. Practical work-place gas emission sensing with liquid marble

Liquid marble can potentially be used as a practical gas emission indicator in the work-place and in the environment. In this study we present an application of monitoring ammonia and amine emission in the printing industry. Flexography is a major printing process for production of a wide range of packaging materials including corrugated boxes and polymer films [22,23]. Water-based ink formulations for flexographic printing are widely used for polymer film printing. A current commercial water-based formulation is based on the acrylic resin system; inks formulated using the acrylic resin system are pigment suspensions stabilized by an elevated pH ($\text{pH} = 8.0\text{--}9.5$) which is provided by the hydrolysis of ammonia and low molecular weight amines. Ink drying after printing is triggered

by the evaporation of ammonia and low molecular weight amines. The acrylic resin suspension system coagulates as the pH decreases to below 7.0 [18], allowing the coagulated ink to adhere to the substrate. However, the release of ammonia and low molecular weight amine during ink drying is a serious source of air pollution in the printing industry, since some printing presses have unsealed inking systems and the printed products also emits these gases during the drying process.

Liquid marbles made of a CuCl_2 (0.1 M, $\text{CuCl}_2 \cdot 2\text{H}_2\text{O}$) solution and Teflon powder were used to detect the ammonia and amine release from the flexographic ink. Since the low molecular weight primary, secondary and some tertiary amines can form stable complexes with $\text{Cu}(\text{II})$ ion [24], CuCl_2 can be used as an indicator to detect ammonia and amine vapours in the air. Half a millilitre of acrylic resin based flexographic ink ($\text{pH} = 9.4$) was placed into a Petri dish ($\phi = 10$ cm); a smaller Petri dish ($\phi = 5$ cm) carrying two CuCl_2 liquid marbles was also placed into the larger Petri dish which was then capped. The liquid marbles changed colour within 15 min.

To visually compare the colour change, two fresh CuCl_2 liquid marbles were placed near the liquid marbles that had been exposed to the ink vapour (Fig. 4). The unambiguous colour development of the liquid marbles exposed to the ink vapour, therefore, demonstrates the potential to use liquid marbles for the practical vapour emission detection.

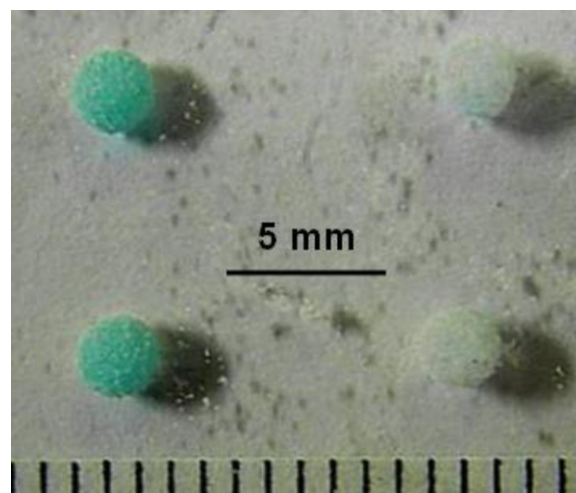


Fig. 4. Liquid marbles of CuCl_2 shelled with Teflon powder changes colour after being exposed to vapour of the water-based flexographic ink. Two fresh liquid CuCl_2 liquid marbles (right) were placed in the same Petri dish for comparison. (For interpretation of the references to color in this figure legend, the reader is referred to the web version of the article.)

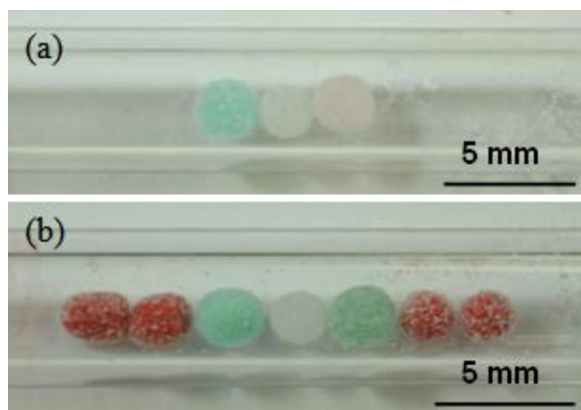


Fig. 5. (a) Liquid marbles made using Teflon powder and CuCl_2 solution (left), water (middle) and CoCl_2 solution (right) were placed in a glass tube; (b) four liquid marbles made using flexographic inks were placed from both sides into the glass tube, which was then sealed. CuCl_2 marble changed from light blue to greenish; CoCl_2 marble changed from light pink to green. Water does not show colour change. (For interpretation of the references to color in this figure legend, the reader is referred to the web version of the article.)

3.4. Gas transport and sensing between liquid marbles

In the above experiments we have shown the transport of gas/vapour across a single liquid marble shell. It is obvious that gases and vapours can also transport through two layers of liquid marble shells, as long as they both are porous. This enables gas transport between individual or separate liquid marbles; an application of this concept would be to perform gas sensing between liquid marbles. An easily perceivable experiment may be to use one liquid marble containing a liquid sample and a desirable number of liquid marbles that contain indicator solutions and then house all marbles in a small space such as within a small beaker or a glass tube that can be easily sealed.

Fig. 5 shows four liquid marbles containing flexographic ink (red) and three other liquid marbles containing the indicator solutions, CuCl_2 (light blue), CoCl_2 (light pink) and water (white), all placed inside a sealed glass tube. All liquid marbles were made using the Teflon powder. Colour changes of CuCl_2 and CoCl_2 solutions after exposing to the ink liquid marbles were caused by reactions (2) and (5), respectively. Colour changes of the indicator liquid marbles confirm that gas transport and sensing between liquid marbles is viable and can be further developed for practical applications.

3.5. Quantitative monitoring of gas emission from liquid marble

The potential to use the gas transport property of the liquid marble shell to quantitatively determine gaseous and vaporous analytes was explored. Our aim in this study was to establish correlations between the sensing signal of the gaseous analyte and its concentration in aqueous samples so as to prove the concept of the quantitative gas sensing using liquid marbles. Ammonia was used as the gaseous chemical species of interest. The experimental arrangement was made so that the solution with dissolved NH_3 gas was encapsulated inside the liquid marbles and a quantitative ammonia signal was collected from outside the liquid marbles.

Ammonia solutions of different concentrations (25%, 12.5%, 6.25%, 3.13% and 1.56%) were used to form liquid marbles. Two colorimetric detection methods, i.e. the UV–vis spectrophotometry and a paper-based gas sensing method, were used to each obtain a calibration curve for signal quantification. For the UV–vis spectrophotometric method, CuCl_2 solution (800 μl of 0.1 M) was introduced onto a watch glass. Eight liquid marbles of NH_3 solution

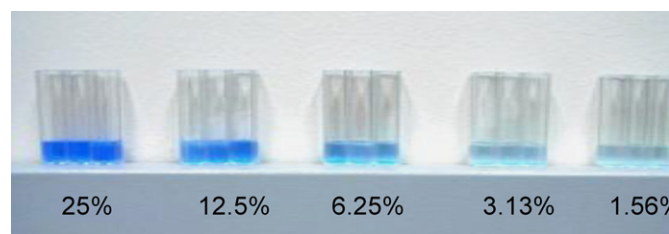


Fig. 6. Visual appreciation of colour changes of the CuCl_2 indicator solutions after the controlled exposure to NH_3 . (For interpretation of the references to color in this figure legend, the reader is referred to the web version of the article.)

were then placed onto the watch glass and in contact with the CuCl_2 solution. The volume of the liquid marbles was controlled to be 4 μl . The watch glass was then sealed to allow controlled exposure of the CuCl_2 solution to the NH_3 gas released from the liquid marbles for 10 min. After the controlled NH_3 release, the CuCl_2 indicator solution was removed from the watch glass into UV–vis cells with a micropipette; the solution was further diluted with 200 μl of water to make 1 ml solution for UV–vis measurement. Three repeated measurements were performed for each ammonia solution. Fig. 6 visually shows the colour change of the indicator solutions after exposure to the ammonia released from the liquid marbles. Fig. 7 shows the UV–vis calibration curve of the CuCl_2 indicator solutions after reaction with ammonia.

For the paper-based gas sensing method, five liquid marbles containing NH_3 solution of the same concentration were introduced into each paper-based gas sensing device. The device was then capped to allow the controlled exposure of the indicator-loading paper discs to NH_3 for 10 min. Circular movement of the sensing device was provided to allow the free rolling motion of the liquid marbles around the paper discs. At the end of the 10 min period the liquid marbles were removed from the Petri dish. Fig. 8 shows the visual appreciation of colour changes of the paper discs; Fig. 9 shows the colorimetric measurements using the scanner and the colour analysis software Adobe Photoshop 7.0.

Comparing the two quantitative methods, the UV–vis method provides an almost straight line calibration curve for high gas exposure levels, but the first two low concentration points show large deviation from the trend line (not shown) that passes the origin. There may be two contributing reasons for the error: First, when hexaaquacopper(II) ions react with hydroxide ions, the product is a pale blue precipitate (scheme (2)); this product may contribute to light absorption, giving a higher absorption reading. Second, the fine particles form stable colloidal suspended when NH_3 con-

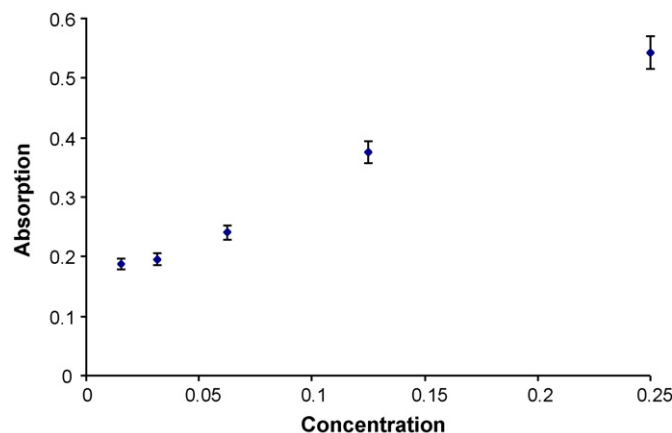


Fig. 7. UV–vis calibration curve of the absorption of CuCl_2 indicator after reaction NH_3 exposure versus the NH_3 concentration of the liquid marble core solution.

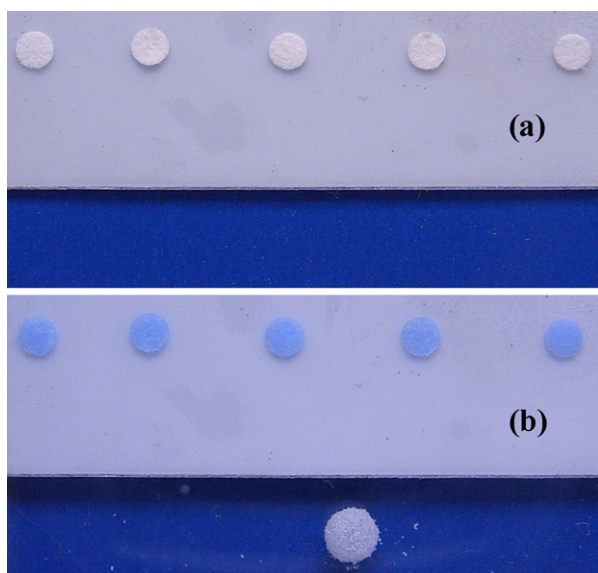


Fig. 8. (a) Paper discs loaded with CuCl_2 indicator; (b) colour change of the indicator paper discs after the controlled exposure to NH_3 . (For interpretation of the references to color in this figure legend, the reader is referred to the web version of the article.)

centration is low; the scattering of light by these particles may contribute to the loss of light intensity; this scattering is stronger in shorter wavelength range. The scattered light is interpreted by the spectrometer as “light absorption”. The scattering of light by colloidal particles is not as significant at higher NH_3 concentrations, due to the formation of the final tetraamminediaquacopper(II) ions (scheme (3)). The UV–vis method can, however, differentiate higher levels of NH_3 release. The paper-based gas sensing device gives a smooth calibration curve for low NH_3 release. Since this method does not rely on the Beer’s law, it effectively avoids the interference of colloidal suspension of $[\text{Cu}(\text{H}_2\text{O})_4(\text{OH})_2](\text{s})$, and it is therefore more suitable for sensing vapour emitted from low concentration solutions. These quantitative gas sensing experiments show that the gas permeable and liquid impermeable characteristics of the liquid marble shell (and also other porous and superhydrophobic materials) can be used to design sensors to obtain quantitative gas sensing data. It should be noted that in this sensing design the gas released by the liquid marble can also be used as an indicator for the presence of the chemical species of interest on the supporting surfaces.

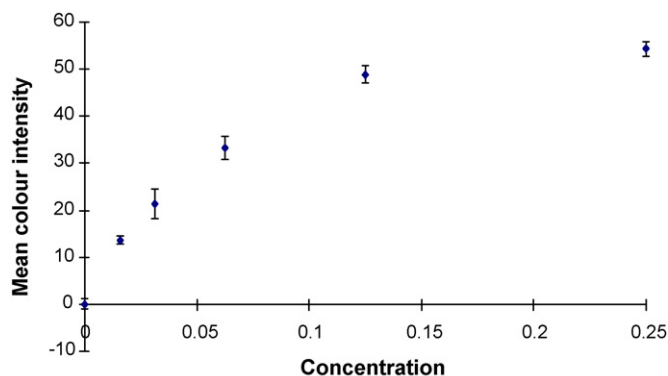


Fig. 9. Colour intensity verses the concentration of the aqueous solutions of NH_3 . Colour intensity values were obtained using the software Adobe PhotoShop 7.0.

4. Discussion

The porous structure of the liquid marble shell and its hydrophobic nature offer a realistic means to use liquid marbles to sense gaseous and vaporous components in the environment. The rough outer layer of the liquid marble shell generate a Cassie condition which completely prevents any contact between the liquid inside the marble and the liquid (or solid) outside the marble, while allowing the free transport of gases and vapours across the shell. The relatively small shell thickness of liquid marbles allows the core indicator solution to be in very close proximity of a gas/vapour-emitting liquid or solid. The close proximity of the indicator solution to the gas/vapour-emitting source, together with the high porosity of the marble shell, minimizes the gas diffusion resistance, therefore allowing the sensitive detection of the gaseous and vaporous species of interest.

The careful selection of hydrophobic powder materials to form liquid marbles may reduce the adsorption of gas and vapour by the liquid marble shell, therefore reducing chemical interference to gas and vapour sensing. We used Teflon powder to form liquid marbles for NH_3 and HCl sensing because that Teflon has excellent chemical resistance to these gases and therefore, any chemical interference is negligible [25].

Liquid marble enable several chemical sensing possibilities to be exploited. While a liquid marble loaded with an indicator solution can be used as a gas or vapour sensor, a liquid marble loaded with one (or several) water dissolvable gases can be used as a gas emitter. The close range gas emission of the liquid marble to a solid or a liquid phase containing chemical species that are reactive to the emitted gases can be used as the detection chemistry. In this sensing design, the gas is used as an indicator. Liquid marbles loaded with different indicator solutions can be used to simultaneously detect different gases and vapours emitted from the same source. Fluorescent and colorimetric reactions can be used to further enhance the capabilities of gas sensing. Liquid marbles therefore provide flexible and versatile designs for chemical sensing.

Combining liquid marbles with appropriate detection methods, it is possible to gain quantitative signals which correlate to the concentrations of gases and vapours in their emitting sources. The ability of liquid marble to produce quantitative chemical sensing is particularly attractive and worth pursuing.

It is expected that, liquid marbles with strengthened shell mechanical properties will significantly widen the capability of this novel type of sensor for field sensing applications, including water and soil gas emission evaluation. This study shows that it is also possible to use other types of porous superhydrophobic surfaces to fabricate low-cost gas and vapour sensors for various applications, particularly as novel packaging materials that have the ability of monitoring the content of the package.

5. Conclusion

In this work, we focused on the gas permeability property of the liquid marble shell and exploited this property for gas sensing applications. The superhydrophobic liquid marble shell completely prevents any contact between the core liquid and the liquid or solid outside of the marble, but allows gas transport across the shell. Liquid marble offers flexibility to achieve different designs for chemical sensing. These include gas sensing, and to use gas as an indicator for chemical sensing. It is possible to use liquid marbles loaded with different indicators to sense different gases from the same emission source. The use of colorimetric and fluorescent indicators further enhances the sensing capability of liquid marbles. Our future investigations will focus on the kinetic details of gas transport through the marble shell; this will enable liquid mar-

ble to be used for more practical engineering purposes. A further important implication of this study is that superhydrophobic surfaces of other kinds can also be used to design low-cost gas sensing devices provided that they are porous and inert to the gas to be sensed.

Acknowledgements

The authors would like to gratefully acknowledge Monash University for postgraduate research scholarships (JT, TA, XL) and Australian Research Council Discovery Grant and DP1094179. The authors would like to specially thank Dr E. Perkins of the Department of Chemical Engineering, Monash University, for proof reading the manuscript.

References

- [1] P. Aussillous, D. Quéré, Liquid Marbles, *Nature* 411 (2001) 924–927.
- [2] E. Bormashenko, Y. Bormashenko, A. Musin, Water rolling and floating upon water: marbles supported by a water/marble interface, *J. Colloid Interface Sci.* 333 (2009) 419–421.
- [3] E. Bormashenko, Y. Bormashenko, A. Musin, Z. Barkay, On the mechanism of floating and sliding of liquid marbles, *ChemPhysChem* 10 (2009) 654–656.
- [4] L. Gao, T.J. McCarthy, Ionic liquid marbles, *Langmuir* 23 (2007) 10445–10447.
- [5] P. Aussillous, D. Quéré, Properties of liquid marbles, *Proc. R. Soc.* 462 (2006) 973–999.
- [6] P. McEleney, G.M. Walker, I.A. Larmour, S.E.J. Bell, Liquid marble formation using hydrophobic and super-hydrophobic powders, *Chem. Eng. J.* 147 (2009) 373–382.
- [7] M. Dandan, H.Y. Erbil, Evaporation rate of graphite liquid marbles: comparison with water droplets, *Langmuir* 25 (2009) 8362–8367.
- [8] N. Eshtiaghi, J.S. Liu, W. Shen, K.P. Hapgood, Liquid marble formation: spreading coefficients or kinetic energy? *Powder Technol.* 196 (2009) 126–132.
- [9] K.P. Hapgood, L. Farber, J.N. Michaels, Agglomeration of hydrophobic powders via solid spreading nucleation, *Powder Technol.* 188 (2009) 248–254.
- [10] T.H. Nguyen, K. Hapgood, W. Shen, Observation of the liquid marble morphology using confocal microscopy, *Chem. Eng. J.* 162 (2010) 396–405.
- [11] C. Zhang, J. Xu, W. Ma, W. Zheng, PCR microfluidic devices for DNA amplification, *Biotechnol. Adv.* 24 (2006) 243–284.
- [12] E. Bormashenko, R. Pogreb, G. Whyman, A. Musin, Y. Bormashenko, Z. Barkay, Shape, vibration, and effective surface tension of water marbles, *Langmuir* 25 (2009) 1893–1896.
- [13] E. Bormashenko, R. Pogreb, Y. Bormashenko, A. Musin, T. Stein, New investigation on ferrofluidics; ferrofluidic marbles and magnetic field driven drops on superhydrophobic surfaces, *Langmuir* 24 (2008) 12119–12122.
- [14] S. Fujii, S. Kameyama, S.P. Armes, D. Dupin, M. Suzuki, Y. Nakamura, pH-responsive liquid marbles stabilized with poly(2-vinylpyridine) particles, *Soft Matter* 6 (2010) 635–640.
- [15] Y. Zhao, J. Fang, H. Wang, X. Wang, T. Lin, Magnetic liquid marbles: manipulation of liquid droplets using highly hydrophobic Fe_3O_4 nanoparticles, *Adv. Mater.* 22 (2010) 707–710.
- [16] S.-H. Kim, S.Y. Lee, S.-M. Yang, Janus microspheres for a highly flexible and impregnable water-repelling interface, *Angew. Chem.* 49 (2010) 2535–2538.
- [17] J. Tian, T. Arbatan, X. Li, W. Shen, Liquid marble for gas sensing, *Chem. Commun.* 46 (2010) 4734–4736.
- [18] P. Laden, *Chemistry and Technology of Water Based Inks*, Chapman & Hall, London, 1997.
- [19] X. Li, J. Tian, W. Shen, Quantitative biomarker assay with microfluidic paper-based analytical devices *Anal. Bioanal. Chem.* 396 (2010) 495–501.
- [20] T. Jackson, *Chemistry Ideas*, 2nd edn, Heinemann Education Publishers, Bath, 2000.
- [21] C.C. Overly, K.D. Lee, E. Berthiaume, P.J. Hollenbeck, Quantitative measurement of intraorganelle pH in the endosomal-lysosomal pathway in neurons by using ratiometric imaging with pyranine, *Proc. Natl. Acad. Sci. U.S.A.* 92 (1995) 3156–3160.
- [22] J.M. Adams, P.A. Dolin, *Printing Technology*, 5th ed., Delmar, New York, 2002.
- [23] R.H. Leach, R.J. Pierce, *The Printing Ink Manual*, 5th ed., Kluwer Academic Publishers, Dordrecht, 1999.
- [24] A.G. Kumbhar, K. Kishore, Redox reactions of Cu(II) -amine complexes in aqueous solutions, *Radiat. Phys. Chem.* 66 (2003) 275–280.
- [25] <http://www.vp-scientific.com/Chemical.Resistance.Chart.htm>.

Liquid marble for gas sensing

Junfei Tian, Tina Arbatan, Xu Li and Wei Shen*

Received 20th January 2010, Accepted 5th May 2010

First published as an Advance Article on the web 20th May 2010

DOI: 10.1039/c001317j

The porous and superhydrophobic shell of a liquid marble prevents contact of its liquid core with outside surfaces, but allows gas transport. Liquid marble can therefore be used to sense gas or emit gas. Liquid marbles loaded with different indicators can simultaneously sense different gases *via* different mechanisms.

Since the phenomenon of liquid marble was reported by Quéré and Aussillous,¹ there has been a flourish of studies of this phenomenon on the fundamental physics and physical chemistry criteria of marble formation.^{2–5} The liquid marble phenomenon is generally understood as being a manifestation of superhydrophobicity; hydrophobic particles are in contact with a liquid which does not wet the particles; liquid marble may be made by rolling a liquid drop over a hydrophobic powder bed, and particles picked up by the liquid drop form a loosely packed and porous shell encapsulating the drop.⁵ The hydrophobic liquid marble shell prevents any direct contact between the liquid core and surfaces outside the marble shell, allowing liquid marbles to assume a near spherical shape and sit stably on a supporting surface, solid or liquid. Recently, liquid marble made using solid particles that have a $<90^\circ$ contact angle with the liquid has been reported.⁶ Nguyen⁷ studied the shell morphology of liquid marbles using confocal microscopy and obtained a more detailed picture of the porous and multilayer structure of the liquid marble shell: smaller particles tend to be in direct contact with the liquid core and larger particles make up the outer layers, which are more porous and rough. Such a structure makes the liquid marble shell stretchable; it enables a liquid marble to withstand a certain level of mechanical impact and deformation.

The interesting phenomenon of liquid marble has attracted a growing number of application studies exploiting the properties of the system. Hapgood *et al.*⁸ reported X-ray tomography images showing the hollow structure of dried liquid marbles. Their study explored the drying of the liquid core of a liquid marble to create hollow marble shells for pharmaceutical applications. Zhang *et al.* reported the use of liquid marble for DNA amplification using PCR microfluidic devices.⁹ This application took advantage of the low liquid transport friction and non-contamination nature of liquid marble. Zhao *et al.*¹⁰ have also shown that liquid marbles formed using hydrophobic Fe_3O_4 nanoparticles can be manipulated and transported using magnetic fields.

Among the many properties of liquid marble, its porous shell structure attracts our attention. The porous and

superhydrophobic marble shell prevents direct contact between the marble liquid core and any surface outside of the marble, but allows the transport of gas or vapour. This property intuitively enables liquid marble to be used as a gas or vapour sensor. When a liquid marble is formed with an appropriate indicator solution and placed onto the surface of a gas or vapour emitting solid or liquid, the indicator solution is at an intimately close distance from the gas or vapour emitting source while having no direct contact with the source. This makes the liquid marble an efficient sensor for gases or vapours of interest. In this communication we describe the use of liquid marbles as colorimetric and fluorescent gas sensors for ammonia and hydrochloric acid gases. The quantitative aspects of the liquid marble sensors are also studied using paper-based colorimetric measurements.

In a qualitative NH_3 sensing experiment, four groups of liquid marbles were made using water (MilliQ, 18 M Ω), a phenolphthalein solution (AR, BDH), a 0.1 M $\text{CoCl}_2 \cdot 2\text{H}_2\text{O}$ solution (AR, Analar) and a 0.1 M $\text{CuCl}_2 \cdot 2\text{H}_2\text{O}$ solution (AR, Analar); they were all shelled with Teflon powder (Sigma-Aldrich). When those liquid marbles were exposed to NH_3 gas emitted from an NH_4OH solution (6.25%, diluted from 25% ammonia solution (AR, Analar)), the colour changes of the liquid marbles rapidly developed (Fig. 1). The rapid colour change of the indicators inside the liquid marbles is an indication that the porous liquid marble shell presents low resistance to gas transport through the shell; liquid marbles can, therefore, be used as effective gas sensors with appropriate indicators.

Ammonia sensing from an aqueous NH_3 emitting source using liquid marbles was also carried out. A liquid marble loaded with phenolphthalein indicator was placed onto the surface of an NH_4OH solution; rapid colour changes of liquid marbles were observed as expected. To confirm that the colour change of the indicator is caused by the ammonia gas transport across the marble shell and not by any direct liquid contact between the indicator solution and the ammonia



Fig. 1 (a) Four groups of liquid marbles containing water, phenolphthalein, CoCl_2 , and CuCl_2 solutions, respectively, were placed from left to right in an "M" pattern. (b) The colour changes of the indicators in these liquid marbles after exposure to ammonia gas.

Australian Pulp and Paper Institute, Department of Chemical Engineering, Monash University, Wellington Rd, Clayton, Vic. 3800, Australia. E-mail: wei.shen@eng.monash.edu.au; Tel: +61 3 99053447

solution, we further made two liquid marbles, one contained NH_4OH solution and the other contained NaOH solution. These two liquid marbles were placed onto two Petri dishes filled with the phenolphthalein indicator solution. Whilst the NH_4OH liquid marble caused immediate colour change of the indicator solution, the NaOH liquid marble did not cause any colour change, therefore confirming that the indicator colour change was caused by ammonia gas transport across the marble shell and not by liquid contact.

Among the liquid marbles made of the three different indicators, the colour change of the phenolphthalein indicator gradually faded and disappeared in 2 h as the NH_3 dissolved in the indicator solution evaporated. On the other hand, the transition metal salt indicators provided more permanent colour changes after reacting with NH_3 and forming stable complexes¹¹ (Fig. 1). The complex tetraamminediaquacopper(II) ions, for example, have a stability constant of $K_{\text{stab}} = 10^{12}$.¹¹ The use of different indicators to achieve different colour changes also implies that liquid marbles made using different but chemically specific indicators can potentially be used to detect different gaseous species. Conversely, this phenomenon also promises the possible use of liquid marbles to detect chemical species in aqueous media using gas(es) as an indicator(s).

Fluorescent pH indicator was found to have a special advantage when used as the core solution of liquid marbles for gas sensing. We used liquid marbles made of an aqueous solution of 8-hydroxypyrene-1,3,6-trisulfonic acid trisodium salt (HPTS) (10 mg L^{-1} , Sigma-Aldrich) and Teflon powder to elucidate the gas detection using fluorescent indicator. HPTS is a strongly water soluble and pH dependent fluorescent dye with a $\text{p}K_{\text{a}}$ of ~ 7.3 .¹² HPTS has a pH dependent fluorescent colour change from blue (405 nm) at $\text{pH} \leq 6$ to green (centered at 450 nm) at $\text{pH} \geq 8$.¹² HPTS liquid marbles show no specific colour under ambient lighting before and after exposure to HCl vapour (Fig. 2(a)), but show a green fluorescence under UV light (Fig. 2(b)).

This property of the fluorescent indicator allows it to be distinguished from colorimetric indicators. When HPTS liquid marbles were exposed to HCl vapour, HPTS showed a clear fluorescent colour change which could be observed under UV light (Fig. 2(c)). This result has an implication that different detection mechanisms (e.g. colorimetry and fluorescence) can be employed to carry out simultaneous detections of different vapours or gases. Liquid marble shells provide a super-hydrophobic separating layer which effectively prevents the indicator solutions in different marbles from contacting one another, allowing the indicators to report independent colour changes.

Here we further present an application of gas sensing using liquid marble in the work-place in the printing industry. Flexography is a dominant process in the printing of a wide range of packaging materials, including corrugated boxes and polymer films.^{13,14} Water-based ink formulations for flexographic printing are widely used for the polymer film printing. A successful commercial water-based formulation is based on the acrylic resin system; inks formulated using the acrylic resin system are a stable pigment suspension under elevated pH (8.0–9.5) which is provided by the dissociation of water in the

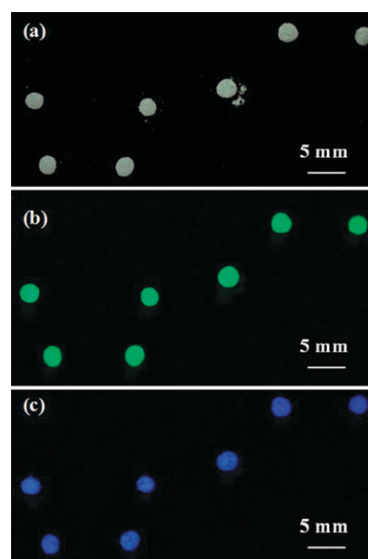


Fig. 2 (a) Liquid marbles containing HPTS indicator under ambient lighting before and after exposure to HCl vapour; (b) liquid marbles containing the HPTS indicator under UV light before exposure to HCl vapour; (c) liquid marbles containing HPTS under UV light after exposure to HCl vapour.

presence of ammonia and low molecular weight amines. The drying of the ink after printing is triggered by the evaporation of ammonia and low molecular weight amines. The acrylic resin suspension system coagulates as the pH decreases to below 7,¹⁵ providing adhesion of the dried ink to the substrate. However, the release of ammonia and low molecular weight amine during ink drying is a serious source of air pollution in the printing industry.

Liquid marble made of a CoCl_2 solution and Teflon powder was used to detect the ammonia and amine released from the flexographic ink, since Co(II) ion¹⁷ can form stable complexes with low molecular weight primary, secondary and some tertiary amines. Five hundred micrograms of acrylic resin based flexographic ink (TMI, USA) was placed into a Petri dish ($\phi = 10 \text{ cm}$); a smaller Petri dish ($\phi = 5 \text{ cm}$) carrying a CoCl_2 liquid marble (formed with 0.1 M CoCl_2 solution) was also placed into the larger Petri dish which was then capped. The liquid marble changed colour (Fig. 3) within 7 min.

To visually compare the colour change, a fresh CoCl_2 liquid marble was placed near the liquid marble that had been exposed to the ink vapour (Fig. 3). The unambiguous colour development of the liquid marble exposed to the ink vapour,



Fig. 3 A liquid marble of CoCl_2 shelled with Teflon powder changed colour after being exposed to the vapour of water-based flexographic ink (left). A fresh CoCl_2 liquid marble (right) was placed in the same Petri dish for comparison.

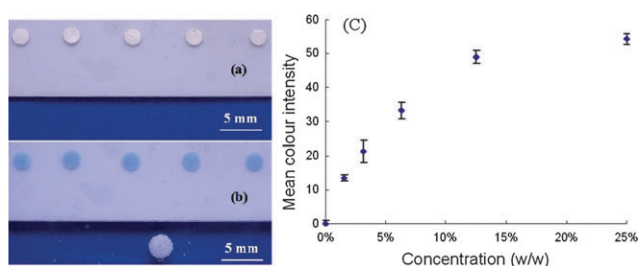


Fig. 4 (a) Paper discs loaded with the CuCl_2 indicator; (b) colour change of the indicator-treated paper discs after the controlled exposure to NH_3 ; (c) color intensity vs. concentration of the NH_4OH solutions. Colour intensity values were obtained using the software Adobe PhotoShop 7.0.

therefore, demonstrates the potential of using liquid marble for practical vapour emission detection.

The potential to use liquid marble for quantitative gas sensing was also explored. Our aim in this study was to establish correlations between the colorimetric sensing signal of a gaseous analyte and its concentration in aqueous samples so as to prove the concept of quantitative gas sensing using liquid marble. Ammonia was used as the gaseous chemical species of interest. The experimental arrangement was made so that a NH_4OH solution was encapsulated inside liquid marbles and a quantitative colorimetric signal was collected from outside the liquid marbles.

Ammonia solutions of different concentrations (25%, 12.5%, 6.25%, 3.13% and 1.56%) were used to form liquid marbles. Liquid drops of the same size (4 μL) were generated using a Hamilton syringe and a gauge 30 needle to form liquid marbles. A paper-based gas sensing method was used to detect NH_3 released from the marbles. Circular paper discs ($\phi = 2$ mm) were produced from Whatman No. 4 filter paper using a disc punching device (Facit 4070, Sweden). A 600 nL aliquot of 0.1 M CuCl_2 solution was introduced onto each paper disc and allowed to dry. Five so-treated paper discs were then fixed onto sticky tape, which was placed in a Petri dish to form one gas sensing device. The five indicator-loaded paper discs allowed five replicate colorimetric measurements to be made. Five liquid marbles containing NH_4OH solution of a specific concentration were introduced into each of the above paper-based gas sensing devices. The device was then capped to allow the controlled exposure of the indicator-loaded paper discs to NH_3 for 10 min. Circular movement of the sensing device was provided to allow the free rolling of the liquid marbles in the Petri dish. At the end of the 10 min period, liquid marbles were removed from the Petri dish.

Colour changes of the paper discs were quantified using a desktop scanner (EPSON perfection 2450 PHOTO) and the software (Adobe PhotoShop 7.0) following the procedure we reported previously.¹⁶ Fig. 4(a) and (b) show the visual appreciation of the colour changes of the paper discs; Fig. 4(c) shows the calibration curve of the colorimetric measurements. The quantitative results so obtained are encouraging.

In conclusion, the porous structure of the liquid marble shell offers a realistic means to use liquid marble to sense gaseous

and vaporous components in an environment. The careful selection of hydrophobic powdered materials to form liquid marbles may eliminate chemical reactions of gas and vapour with the liquid marble shell. We used Teflon powder to form liquid marble for NH_3 and HCl sensing; Teflon has an excellent chemical resistance to these gases, any chemical interference by Teflon is, therefore, negligible.¹⁸

Liquid marble enables several chemical sensing design possibilities to be exploited. While a liquid marble loaded with an indicator solution can be used as a gas or vapour sensor, a liquid marble loaded with one (or several) water dissolvable gas(es) can be used as a gas emitter. In this sensor design, the gas is used as an indicator to indicate the presence of the chemical species of interest in the environment. Fluorescent and colorimetric reactions can be used to further enhance the capabilities of gas sensing.

The ability to use liquid marble to produce quantitative chemical sensing is particularly attractive and worth pursuing. It offers a less expensive and more flexible gas sensing option to the current main stream gas sensing instruments which use a hydrophobic and gas permeable polymeric membrane to separate gas for indirect electrochemical detection.¹⁹

Australian Research Council funding through projects DP1094179 and LP0989823 is gratefully acknowledged. JT, TA, XL would like to thank Monash University and the Faculty of Engineering for their postgraduate scholarships.

Notes and references

- 1 P. Aussillous and D. Quéré, *Nature*, 2001, **411**, 924.
- 2 E. Bormashenko, Y. Bormashenko and A. Musin, *J. Colloid Interface Sci.*, 2009, **333**, 419.
- 3 E. Bormashenko, Y. Bormashenko, A. Musin and Z. Barkay, *ChemPhysChem*, 2009, **10**, 654.
- 4 L. Gao and T. J. McCarthy, *Langmuir*, 2007, **23**, 10445.
- 5 P. Aussillous and D. Quéré, *Proc. R. Soc. London, Ser. A*, 2006, **462**, 973.
- 6 M. Dandan and H. Y. Erbil, *Langmuir*, 2009, **25**, 8362.
- 7 T. H. Nguyen, *Masters Thesis*, Monash University, 2009.
- 8 K. P. Hapgood, L. Farber and J. N. Michaels, *Powder Technol.*, 2009, **188**, 248.
- 9 C. Zhang, J. Xu, W. Ma and W. Zheng, *Biotechnol. Adv.*, 2006, **24**, 243.
- 10 Y. Zhao, J. Fang, H. Wang, X. Wang and T. Lin, *Adv. Mater.*, 2010, **22**, 707.
- 11 T. Jackson, *Chemistry Ideas*, Heinemann Education Publishers, Bath, 2nd edn, 2000, p. 296.
- 12 C. C. Overly, K. D. Lee, E. Berthiaume and P. J. Hollenbeck, *Proc. Natl. Acad. Sci. U. S. A.*, 1995, **92**, 3156.
- 13 J. M. Adams and P. A. Dolin, *Printing Technology*, Delmar, New York, 5th edn, 2002, p. 352.
- 14 R. H. Leach and R. J. Pierce, *The Printing Ink Manual*, Kluwer Academic Publishers, Dordrecht, 5th edn, 1999, p. 547.
- 15 P. Laden, *Chemistry and Technology of Water Based Inks*, Chapman & Hall, London, 1997, p. 198.
- 16 X. Li, J. Tian and W. Shen, *Anal. Bioanal. Chem.*, 2010, **396**, 495.
- 17 G. J. Van Driel, W. L. Driessen and J. Reedijk, *Inorg. Chem.*, 1985, **24**, 2919.
- 18 http://www.vp-scientific.com/Chemical_Resistance_Chart.htm.
- 19 D. A. Skoog, F. J. Holler and T. A. Nieman, *Principle of Instrumental Analysis*, Harcourt Brace & Co., Orlando, 5th edn, 1998, 607.



Appendix III: Patents Generated from This Thesis

This page is intentionally blank

(19) World Intellectual Property Organization
International Bureau



(43) International Publication Date
14 January 2010 (14.01.2010)

PCT

(10) International Publication Number
WO 2010/003188 A1

(51) International Patent Classification:
B01L 3/00 (2006.01) *D21H 25/00* (2006.01)
B81C 1/00 (2006.01)

(74) Agent: **WATERMARK PATENT AND TRADE MARK ATTORNEYS**; Level 2, 302 Burwood Road, Hawthorn, Victoria 3122 (AU).

(21) International Application Number:
PCT/AU2009/000889

(81) Designated States (*unless otherwise indicated, for every kind of national protection available*): AE, AG, AL, AM, AO, AT, AU, AZ, BA, BB, BG, BH, BR, BW, BY, BZ, CA, CH, CL, CN, CO, CR, CU, CZ, DE, DK, DM, DO, DZ, EC, EE, EG, ES, FI, GB, GD, GE, GH, GM, GT, HN, HR, HU, ID, IL, IN, IS, JP, KE, KG, KM, KN, KP, KR, KZ, LA, LC, LK, LR, LS, LT, LU, LY, MA, MD, ME, MG, MK, MN, MW, MX, MY, MZ, NA, NG, NI, NO, NZ, OM, PE, PG, PH, PL, PT, RO, RS, RU, SC, SD, SE, SG, SK, SL, SM, ST, SV, SY, TJ, TM, TN, TR, TT, TZ, UA, UG, US, UZ, VC, VN, ZA, ZM, ZW.

(22) International Filing Date:
10 July 2009 (10.07.2009)

(25) Filing Language: English

(26) Publication Language: English

(30) Priority Data:
2008903553 11 July 2008 (11.07.2008) AU
2008905776 7 November 2008 (07.11.2008) AU

(71) Applicant (*for all designated States except US*): **MONASH UNIVERSITY** [AU/AU]; Wellington Road, Clayton, Victoria 3168 (AU).

(84) Designated States (*unless otherwise indicated, for every kind of regional protection available*): ARIPO (BW, GH, GM, KE, LS, MW, MZ, NA, SD, SL, SZ, TZ, UG, ZM, ZW), Eurasian (AM, AZ, BY, KG, KZ, MD, RU, TJ, TM), European (AT, BE, BG, CH, CY, CZ, DE, DK, EE, ES, FI, FR, GB, GR, HR, HU, IE, IS, IT, LT, LU, LV, MC, MK, MT, NL, NO, PL, PT, RO, SE, SI, SK, SM, TR), OAPI (BF, BJ, CF, CG, CI, CM, GA, GN, GQ, GW, ML, MR, NE, SN, TD, TG).

(72) Inventors; and

(75) Inventors/Applicants (*for US only*): **SHEN, Wei** [AU/AU]; 1 Landen Avenue, Glen Waverley, Victoria 3150 (AU). **LI, Xu** [CN/AU]; 49 Townsend Street, Glen Waverley, Victoria 3150 (AU). **TIAN, Junfei** [CN/AU]; Unit 3/20 Dover Street, Oakleigh East, Victoria 3166 (AU). **KHAN, Mohidus Samad** [—/AU]; 1486 North Road, Clayton, Victoria 3168 (AU). **GARNIER, Gil** [AU/AU]; 31A Bangalay Avenue, Frankston South, Victoria 3199 (AU).

Published:

— with international search report (Art. 21(3))

(54) Title: METHOD OF FABRICATING MICROFLUIDIC SYSTEMS

(57) Abstract: A method of fabricating a microfluidic system having microfluidic channels on a surface of a hydrophilic substrate, the method including the steps of: hydrophobizing the substrate surface; locating a mask defining the substrate surface, the mask having open areas defining the periphery of the microfluidic channels; and applying an irradiation treatment to areas of the substrate surface exposed by the open areas of the mask, said exposed areas becoming hydrophilic to therefore form said microfluidic channels.

METHOD OF FABRICATING MICROFLUIDIC SYSTEMS

TECHNICAL FIELD

The present invention is generally directed to microfluidic systems, and
5 fabrication of such systems on low cost substrates such as paper, woven fabric
and non-woven cellulosic material.

BACKGROUND TO THE INVENTION

The concept of making inexpensive microfluidic channels on paper and
10 other woven and non-woven fibrous and porous surfaces has been successfully
proven. The aim of building such systems has been to fabricate low-cost bio-
analytical and indicator devices, with direct envisaged applications in detecting
waterborne bacteria and metals ions in drinking water, the presence of some
specific proteins or biomarkers in body fluid (cancer test), the level of glucose and
15 other bio-chemical substances in human or animal blood and urine samples.
Developments of low-cost paper-based bio-analytical and environmental
analytical devices have so far allowed quick and single step reaction to detect
analytes in a fluid sample.

Researchers in Harvard University led by Whitesides (see Martinez, A.W.,
20 Phillips, S.T., Butte, M.J. and Whitesides G.M., and "Patterned Paper as a
platform for Inexpensive, Low-Volume, Portable Bioassays", Angew. Chem. Int.
Ed. 46, 1318-1320 (2007)) have recently created channels on paper by printing
patterns of conventional photoresists polymers (PMMA). Paper provides the
capillary channels, while the photoresist polymers form the barrier which defines
25 the channel. More recently, the Harvard group further developed their photoresist
technique in making fine channels in paper. They used an ink jet printer to print
patterns on transparent polymer films, which were used as masks for photo
lithography to generate photoresist patterns in paper following their published
approach (Martinez, A.W., Phillips, S.T., Wiley, B.J., Gupta, M. and Whitesides,
30 G.M. Lab on a Chip, (2008) DOI: 10.1039/b811135a). They showed that fine
microfluidic channels can be generated in paper using the photoresist barrier
approach and these channels have comparable resolution to the microfluidic
channels made using other substrates such as silicon wafer. A problem

associated with the use of such photolithography techniques is that they result in rigid and brittle barriers which can be easily damaged if the paper is creased or crumpled.

In another published paper, the Harvard group used an x-y plotter to draw channels on paper surface (see Bruzewicz, D.A., Reches, M. and Whitesides, G.M., "Low-Cost Printing of Poly(dimethylsiloxane) Barriers to Define Microchannels in Paper", Anal Chem. 80, 3387-3392 (2008)). The plotter's pens were filled with a hydrophobic solution of polydimethyl siloxane (PDMS) in hexane, and a plethora of patterns several centimetres long with channel 1cm to 2 mm wide were created. Their second micro-channels system created on paper surface overcame a major drawback of the first one, *ie* the rigid and brittle barrier material of conventional photoresist polymers. Their second system, however, has a poor channel resolution and definition, since the penetration of PDMS solution in paper sheet cannot be controlled. The use of silicones to define the walls of the microchannels would also require FDA approval in view of the potential health related issues. Both fabrication approaches result in physical barriers which define the periphery of the micro-channels.

Abe *et al.* (Abe, K; Suzuki, K; Citterio, D. "Inkjet-printed microfluidic multianalyte chemical sensing paper", Anal. Chem. (2008) 6928-6934) presented a method of using a solution of hydrophobic polymer (PS) to impregnate paper. After the polymer physically covered the fibre surface and dried, they used a Microdrop dispensing device to deliver solvent droplets to dissolve the polymer from the fibre surface, thus forming microfluidic channels by restoring the hydrophilicity of the paper. These authors also used the Microdrop dispensing device to deliver chemical sensing agents into their pattern to form a functional device for biomedical detection.

In US 7125639, Molecular Transfer lithography, the inventor Charles Daniel Schaper (class 430/253, 430/258) describes a process for patterning a substrate comprising the steps of: 1) coating a carrier with a photosensitive material, 2) exposing the photosensitive material to a pattern of radiation, and 3) physically transferring the exposed material to the substrate.

In US 6518168, Self-assembled monolayers direct patterning of surfaces, by Paul G Clem *et al* (filing date 11/02/1998), A technique for creating patterns of

material deposited on a surface involves forming a self-assembled monolayer in a pattern on the surface and depositing, via chemical vapor deposition or via sol-gel processing, a material on the surface in a pattern complementary to the self-assembled monolayer pattern. The material can be a metal, metal oxide, or the like.

In WO/2008/060449 MICROFLUIDIC DETECTOR, by BUTTE, Manish, J. *et al* (Application date 9-11/2007), articles and methods for determining an analyte indicative of a disease condition are provided. In some embodiments, articles and methods described herein can be used for determining a presence, qualitatively or quantitatively, of a component, such as a particular type of cell, in a fluid sample. In one particular embodiment, a low-cost microfluidic system for rapid detection of T cells is provided. The microfluidic system may use immobilized antibodies and adhesion molecules in a channel to capture T cells from a fluid sample such as a small volume of blood. The captured T cells may be labelled with a metal colloid (eg, gold nanoparticles) using an antibody specific for the T Cell Receptor (TCR), and metallic silver can be catalytically precipitated onto the cells. The number of T cells captured can be counted and may indicate a disease condition of a patient such as severe combined immune deficiency or human immunodeficiency virus.

Those patent applications and research papers proposed methods to make microfluidic systems and devices using a variety of materials, including using paper and other non-woven or porous materials as substrates. Microfluidic channels can be fabricated using paper and other non-woven or porous materials in batch operations. However all of the above-noted systems utilise complex and time consuming processes that cannot be readily adapted to allow for low cost, high speed industrial production. Furthermore, all these earlier systems rely on a physical barrier to define the microfluidic channels.

It is an object of the present invention to provide a method of fabricating a microfluidic system which overcomes at least one of the disadvantages of prior art methods.

SUMMARY OF THE INVENTION

With this in mind, according to one aspect of the present invention, there is provided a method of fabricating a microfluidic system having microfluidic channels on a surface of a hydrophilic substrate, the method including the steps of:

- a) hydrophobizing the substrate surface;
- b) locating a mask defining the substrate surface, the mask having open areas defining the periphery of the microfluidic channels; and
- c) applying an irradiation treatment to areas of the substrate surface exposed by the open areas of the mask, said exposed areas becoming hydrophilic to therefore form said microfluidic channels.

According to another aspect of the present invention, there is provided a microfluidic system fabricated according to the above described method.

The method according to the present invention provides a hydrophilic hydrophobic contrast within the substrate. This allows the substrate material to retain its original flexibility, unlike the prior art methods which utilise a physical barrier.

The hydrophilic substrate may be provided by a cellulosic material including paper, woven fabric and non-woven materials. The paper products can include filter paper, office paper, chromatography paper, tissues (towel, facial, bath wipes), newspaper, packaging paper, specialty papers, and so on. The preferential alignment of the fibres of the paper can be controlled or aligned using any technique known in the art. The paper can be surface treated with any of the usual techniques involving coating, surface sizing, spraying and the like.

The hydrophilic treatment acts to reduce the surface energy of the substrate surface. Various methods can be selected to hydrophobize the surface/substrate. An embodiment of the invention consists of absorbing or adsorbing a solution of hydrophobic substance dissolved in a volatile solvent. Hydrophobic substance include, but are not restricted to, alkyl ketene dimer (AKD), alkenyl succinic anhydride (ASA), rosin, latex, silicones, fluorochemicals, polyolefin emulsions, resin and fatty acids, natural and synthetic waxes and any hydrophobic substance known in the art. Another application is through vapour deposition of a hydrophobic substance.

The irradiation treatment acts to significantly increase the surface energy of the substrate surface rendering the treated areas with greater wettability by water and aqueous liquids. The wettability of the porous material by liquids then provides capillary driving force and allows the penetration of liquids within and
5 along the channels created by the irradiation treatment.

The irradiation treatment may include plasma, corona and other irradiation treatments.

The microfluidic channels may preferably be in a pattern transporting a fluid to analyse in parallel to different detection zones. The typical channel
10 dimensions vary in length from 10 cm to 1 mm and in width from 2 cm to 100 μm . The fluidic system has typically the same rigidity, mechanical, properties and softness as those of the original substrate.

It would also be advantageous to fabricate microfluidic systems using high volume, high speed and continuous printing methods which are able to provide
15 on-demand microfluidic channel pattern variations.

With this in mind, according to a further aspect of the present invention, there is provided a method of fabricating a microfluidic system having microfluidic channels on a surface of a hydrophilic substrate, the method including the step of printing a hydrophobic agent on the substrate surface to thereby provide a
20 hydrophobic/hydrophilic contrast thereon to define a peripheral edge of the microfluidic channels.

According to yet another aspect of the present invention, there is provided a microfluidic system fabricated according to the above described method.

The printing of the hydrophobic agent provides a hydrophobic/hydrophilic
25 contrast between the peripheral edge of the microfluidic channels and the channels themselves. This is distinguished from prior art printing methods that seek to provide a physical barrier along the peripheral edge of the microfluidic channels.

The advantages of the present invention are the low manufacturing cost,
30 the high processing speed and the exceptional pattern accuracy achievable. In one form of the invention a hydrophobic chemical (wax, polymer, oligomer or molecule) is dissolved in an organic solvent and printed. In another, a stable aqueous emulsion of the hydrophobic chemical is printed. The printed substrate

can further be activated to fully develop the hydrophobicity via molecular rearrangement including the creation of covalent bonds. Of special interest are the hydrophobic materials used in the paper industry such as the internal sizing agents (AKD, ASA, rosin) and the surface sizing agents (polymers, latex). Our invention offers, for the first time, the possibility to manufacture at high speed, low cost and high quality micro-fluidic systems.

A possible manufacturing arrangement includes: 1) an unwinder, 2) a first printing station for the hydrophobic barrier, 3) an infra-red oven, (to activate) and 4) a rewinder, all arranged in series. Optional are 5) a cooling unit and 6) a second printing unit printing for the active system (biomolecule, reactive system). Should digital printers be selected (inkjet printers), on-demand pattern variations can be achieved. The invention is ideally suited to manufacture paper based diagnostic devices for health or environment analysis and control. The complete fluidic can be manufactured by printing, using a single line or even a single printer.

An ink may be formed with the hydrophobizing agent. A first option is to dissolve the hydrophobizing agent in an organic solvent for printing using common technology. A second option is to emulsify the hydrophobic agent into a stable aqueous ink. The advantage of this later option is that no volatile organic compounds (VOC) are emitted. VOC are to avoid under manufacturing conditions because of their important health and fire hazards.

After printing, the hydrophobic pattern can further be activated to fully develop the hydrophobicity via molecular rearrangement including the creation of covalent bonds. This is achieved by aging, heat, reaction or radiation. This treatment will also improve the permanency of the pattern.

While all hydrophobic compounds can be used as ink, the internal and surface sizing agents common in the Paper industry are especially attractive for their effectiveness, low cost, and low toxicity. Further they fulfil many health and safety requirements. Of special interest are alkyl ketene dimmers (AKD), alkenyl succinic anhydride (ASA), rosin, and the latex and polymers used in surface sizing

The printing fluids can be printed on paper to fabricate microfluidic systems and devices using contact and non-contact printing processes and equipments,

such as gravure, flexography, screen printing, ink jet printing, etc. In this application the applicants used digital ink jet printing to demonstrate the fabrication of microfluidic systems on paper.

5 Compared with the previous physical barrier fabrication methods, the new fabrication method according to the present invention enables the manufacturing of paper-based microfluidic devices in commercial scales and at low cost. Creation of hydrophilic-hydrophobic contrast is a simpler approach to define liquid penetration channels in paper than the physical barrier approach.

10 The use of digital printing technology to selectively deliver cellulose hydrophobization chemicals on paper surface to form the hydrophilic-hydrophobic contrast has some other advantages. Digital printing offers electronic pattern variation which allows fast change over for fabrication of different devices. Since the hydrophilic-hydrophobic contrast fabrication concept can retain the original flexibility of the paper, it offers natural bending and folding resistance, which
15 fundamentally overcomes the poor bending and folding resistance often encountered with devices fabricated with other methods. These attributes are particularly attractive for personal care device applications such as in a diaper indicator application for example.

20 **BRIEF DESCRIPTION OF THE DRAWINGS**

It will be convenient to further describe the invention with respect to the accompanying drawings which illustrate preferred embodiments of the microfluidic system according to the present invention. Other embodiments of the invention are possible, and consequently, the particularity of the accompanying
25 drawings is not to be understood as superseding the description of the invention.

In the drawings:

Figure 1 shows a single microfluidic channel fabricated according to a first embodiment of the invention;

30 Figure 2 shows a capillary channel pattern on filter paper fabricated according to the first embodiment of the invention;

Figure 3 shows a capillary channel pattern fabricated on two ply tissue paper according to the first embodiment of the present invention;

Figure 4 shows a capillary channel pattern fabricated on a kitchen paper towel according to the first embodiment of the present invention;

Figure 5 shows a capillary channel pattern fabricated on photocopy paper according to the first embodiment of the present invention;

5 Figure 6 shows a capillary channel pattern fabricated on news print paper according to the first embodiment of the present invention;

Figure 7 shows printed microfluidic patterns fabricated according to a second embodiment of the present invention;

10 Figures 8 and 9 show different microfluidic patterns printed using a desktop digital ink jet printer on filter paper according to the second embodiment of the invention.

Figure 10 shows the benching and folding resistance of the microfluidic patterns printed according to the second embodiment of the invention; and

15 Figures 11 and 12 show the pattern of a microfluidic channel and an immunohistochemical staining enzyme printed according to the second embodiment of the invention.

DETAILED DESCRIPTION OF THE INVENTION

20 The invention will now be described with reference to the following Examples describing different possible utilisations of the present invention. It is however to be appreciated that the invention is not restricted to these examples.

Example 1

25 In one embodiment of the invention as shown in Figure 1, a filter paper was hydrophobized by immersion in a solution of AKD dissolved in heptane and the solvent was allowed to evaporate. A heat treatment of the treated paper in an oven at 100°C for 30 - 50 minutes was applied. In the second step, a solid mask was applied to the paper substrate and the system was exposed to a plasma reactor (K1050X plasma asher (Quorum Emitech, UK) for 10-100 seconds at the intensity of 12 - 50 W). The plasma treatment left no visible mark on the sample
30 and the sample retained its original softness and flexibility. The treated channel becomes wettable by aqueous solutions and allows the capillary transport of the solutions. The width of the channel can be well controlled. Figure 1 shows a

single channel treated with a mask of 1 mm in width on filter paper, and shows the channel before and after wetting by water.

The treated channel can have any geometrical pattern as shown in Figure 2. First, a pattern includes a sample dosing zone (A) and one or multiple channels that lead to detection or reaction wells (B). Second, a pattern includes one or multiple sample dosing zones that are connected to one or multiple detection or reaction wells. In this example, a pattern of one sample dosing zone connected to multiple detection/reaction zones via capillary channels was created by plasma treatment.

A few drops of water were added to the sample dosing zone and the water was rapidly and accurately delivered to all detection/reaction wells where indicators were to be added as shown in Figure 2.

Example 2

In a second embodiment of the invention as shown in Figure 3, micro-channels were formed onto composites cellulosic materials. A two-ply Kleenex mainline facial tissue was treated similarly to example 1. Figure 3 represents the liquid filled micro-channels on Kleenex two-ply tissue.

Example 3

In a third embodiment of the invention as shown in Figure 4, micro-channels were formed onto a layered and molded paper basesheet. A three-layer molded paper towel (Kimberly-Clark Viva) was treated similarly to example 1. Figure 4 represents the liquid filled micro-channels on three-layer Kimberly-Clark Viva towel.

Example 4

In the fourth embodiment of the invention as shown in Figure 5, micro-channels were created on non-woven materials containing nano- and micro-fillers. Reflex copy paper (80 gsm) contains 15% calcium carbonate fillers of the particle size typically 1 – 2 μm . Reflex copy paper is sized and does not require hydrophobic treatment. A plasma treatment created the micro-channel pattern on to the copy paper as shown in Figure 5.

Example 5

In the fourth embodiment of the invention as shown in Figure 6, micro-channels were created on non-woven materials containing nano- and micro-fillers, lignocellulosic fibres and recycled paper fibres. Norstar newsprint paper (55 gsm) contains >50% recycle fibres, lignocellulosic fibres, calcium carbonate and clay fillers of the particle size typically 1 -2 μm . A plasma treatment created the micro-channel pattern on the Norstar newsprinting paper.

The remaining examples illustrate a second embodiment of the present invention that utilises ink jet printing technology to define the microfluidic channels.

Example 6

Alkenyl ketene dimer (liquid AKD) was used to formulate printing fluids which were solvent-based and water-based. Any method known in the art can be selected to hydrophobize the surface/substrate. An embodiment of the invention consists of absorbing or adsorbing a solution of hydrophobic substance dissolved in a volatile solvent or suspended in emulsion form. Hydrophobic substance include, but are not restricted to, AKD, ASA, rosin, latex, silicones, fluorochemicals, polyolefin emulsions, resin and fatty acids, natural and synthetic waxes and any hydrophobic substance known in the art. Solvent-based printing fluids were formulated using solvents in which AKD can dissolve. These typically include, but are not restricted to, chloroform, dichloromethane, toluene, hexane, heptane and their mixtures. A solvent soluble dye can also be added into the printing fluid if visibility of the printed pattern is required. Water-based printing fluid can be formulated using one or a mixture of polar solvents and water. These include, but are not restricted to, acetone, alcohols and esters. AKD can be first dissolved into polar solvent or their mixture and then mix with water. The concentration of hydrophobic agents in printing fluids was 0.5% - 8% v/v.

In this example digital ink jet printing method was used to print the printing fluids on paper. Microfluidic patterns were printed on Whatman #4 filter paper. Printing fluids show good penetration into the paper sheets and dry quickly. The printed patterns were subjected to a high temperature treatment to cure AKD so that it reacts with cellulose and develops strong hydrophobicity.

Figure 7 shows a printed microfluidic patterns in which liquid penetration channels are confined by the printed hydrophobic areas.

Example 7

In this example as shown in Figures 8 and 9, the applicants show the use of printing method to fabricate microfluidic systems in a continuous manner, massive quantity, on-demand variation of patterns and very low cost.

Figure 8 shows different microfluidic patterns printed using a desktop digital ink jet printer on a large filter paper sheet. Ink jet printing can print on A4 sheets in a continuous manner.

Figure 8 and Figure 9 show different microfluidic patterns can be designed and form the page-data. Digital ink jet printing can print different patterns in any desirable sequence and in any quantity required.

Example 8

In this example as shown in Figure 10, the applicants show that the microfluidic devices fabricated by printing of hydrophobization agents on paper are able to retain the flexibility of the papersheet and overcome the problem associated with an early design by Martinez et al. (Angew. Chem. Int. Ed. 46 (2007) 1318 -1320).

Figure 10 shows the bending and folding resistance of the printed microfluidic patterns. A printed paper microfluidic pattern was crumbled, but it still functioned well after the paper was opened up.

Example 9

The applicants show in Figures 11 and 12 that printing methods can be used to fabricate devices for biomedical tests. The unique advantage of printing methods is that they can transfer several fluids onto paper or other non-woven materials to form a pattern consisting of a microfluidic system and biomedical/chemical agents for testing purposes. Modern printing methods are capable of providing accurate registration for biomedical/chemical agents to be printed inside the microfluidic systems for the designed purposes. Therefore modern printing processes can fabricate devices consisting of microfluidic channels and biomedical/chemical detection mechanisms in a single process.

Figure 11 shows the pattern of a microfluidic channel in which an immunohistochemical staining enzyme (horseradish peroxidase) was then printed. After a colour substrate (3,3'-diaminobenzidine tetrahydrochloride) was introduced into the microfluidic system via the central sample dosing site, it penetrated into channels. A colour change was obtained which confirmed that printed immunohistochemical staining enzyme was active after printing. Figure 12 shows the colour change after the microfluidic system was allowed to dry.

CLAIMS:

1. A method of fabricating a microfluidic system having microfluidic channels on a surface of a hydrophilic substrate, the method including the steps of:
 - hydrophobizing the substrate surface;
 - 5 locating a mask defining the substrate surface, the mask having open areas defining the periphery of the microfluidic channels; and
 - applying an irradiation treatment to areas of the substrate surface exposed by the open areas of the mask, said exposed areas becoming hydrophilic to therefore form said microfluidic channels.
- 10 2. A method according to claim 1, wherein the hydrophilic substrate is formed of cellulosic material including paper, woven and non-woven materials.
3. A method according to claim 1 or 2, wherein the surface is hydrophobized using a solution including a hydrophobic substance dissolved in a volatile solvent, the hydrophobic substance being selected from an alkyl ketene dimer (AKD),
15 alkenyl succinic anhydride (ASA), rosin, latex, silicones, fluorchemicals, polyolefin emulsions, resin and fatty acids, natural and synthetic waxes.
4. A method according to any one of the preceding claims wherein the irradiation treatment includes plasma and corona treatments.
5. A microfluidic system fabricated by the method as claimed in any one of
20 the preceding claims.
6. A method of fabricating a microfluidic system having microfluidic channels on a surface of a hydrophilic substrate, the method including the step of printing a hydrophobic agent on the substrate surface to thereby provide a hydrophilic-hydrophobic contrast thereon to define a peripheral edge of the microfluidic
25 channels.
7. A method according to claim 6 wherein the hydrophobic agent is a hydrophobic molecule, oligomer or polymer dissolved in a solvent.

8. A method according to claim 6 wherein the hydrophobic agent is a hydrophobic molecule, oligomer or polymer emulsified or in suspension in water, forming a water based ink.
9. A method according to claim 6 wherein the hydrophobic agent is an internal size (AKD, ASA, rosin, silicone, fluorochemicals, polyolefin emulsions, resin and fatty acid, natural and synthetic waxes and the like) or a surface sizing material (Styrene maleic anhydride (SMA), latex).
10. A method according to claim 9, wherein the hydrophobic agent is dissolved in an organic solvent or emulsified.
- 10 11. A method according to claim 6 further including an activation step following printing to activate the hydrophobic agent, including the development of covalent bond with the substrate.
12. A method according to claim 11 wherein the activation step includes aging, heat treatment or radiation.
- 15 13. A method according to any one of claims 6 to 12, wherein the hydrophilic substrate is formed of cellulosic material including paper, woven and non-woven materials.
14. A method according to any one of claims 6 to 12 wherein the printing is by an inkjet or other contact and non-contact process printing applications.
- 20 15. A microfluidic system fabricated by the method as claimed in any one of claims 6 to 14.

1/5

Figure 1

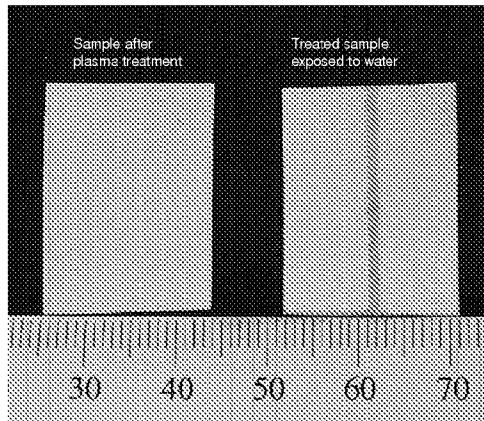


Figure 2

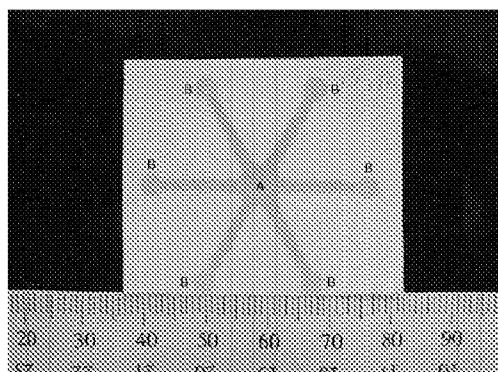
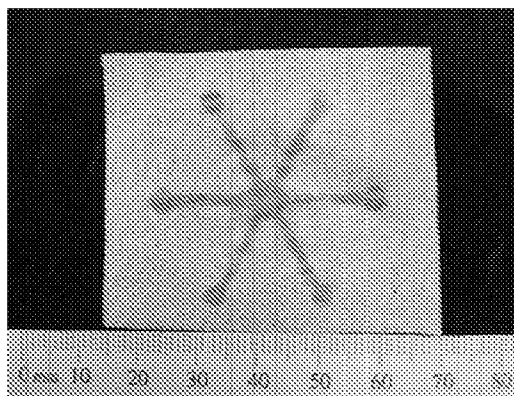


Figure 3



2/5

Figure 4

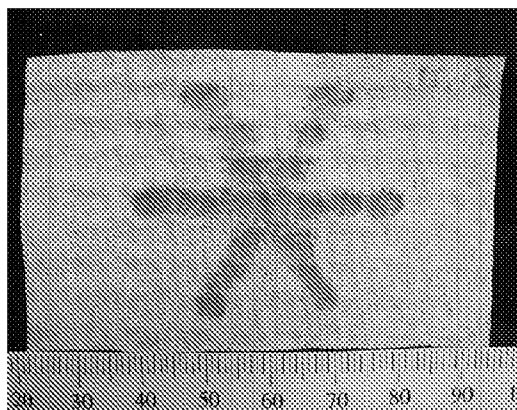


Figure 5

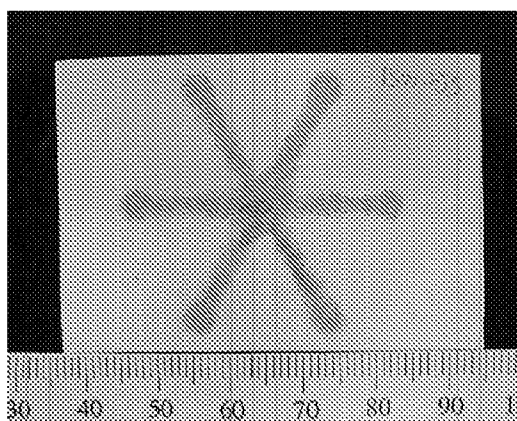
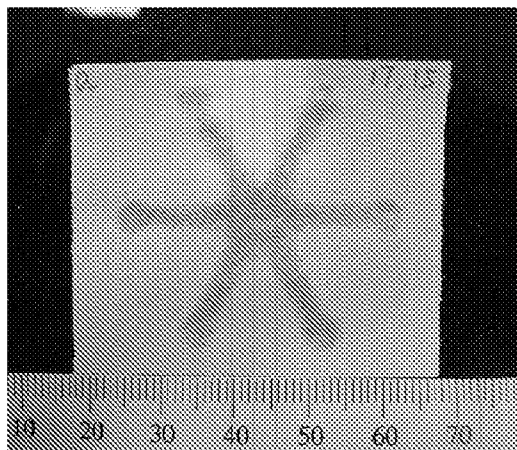


Figure 6



3/5

Figure 7

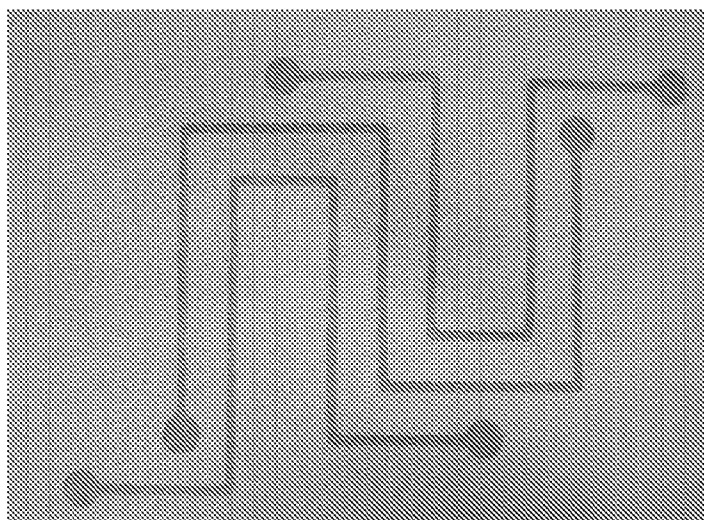
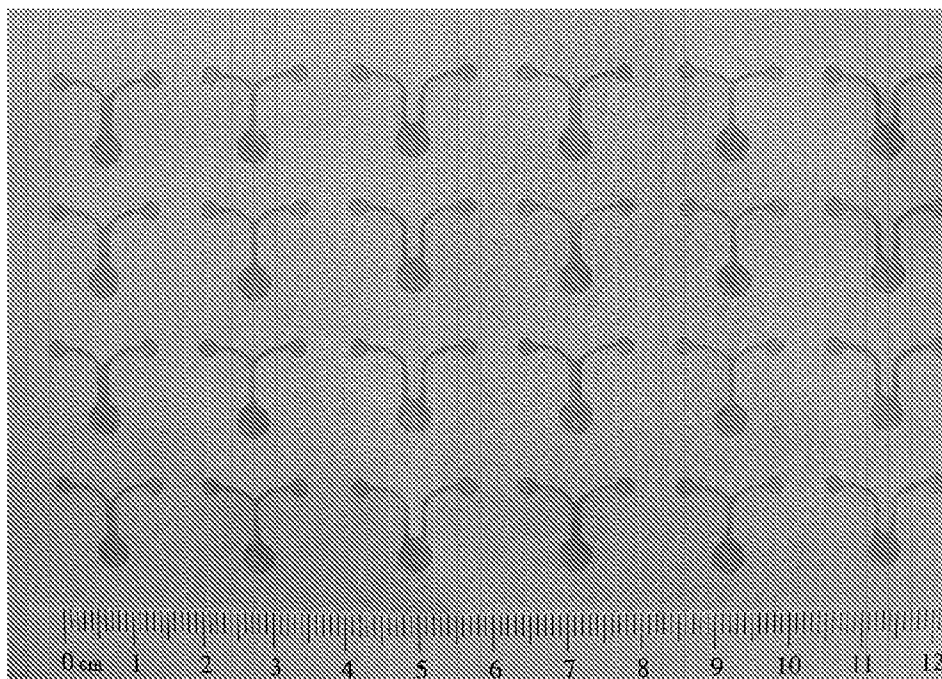


Figure 8



4/5

Figure 9

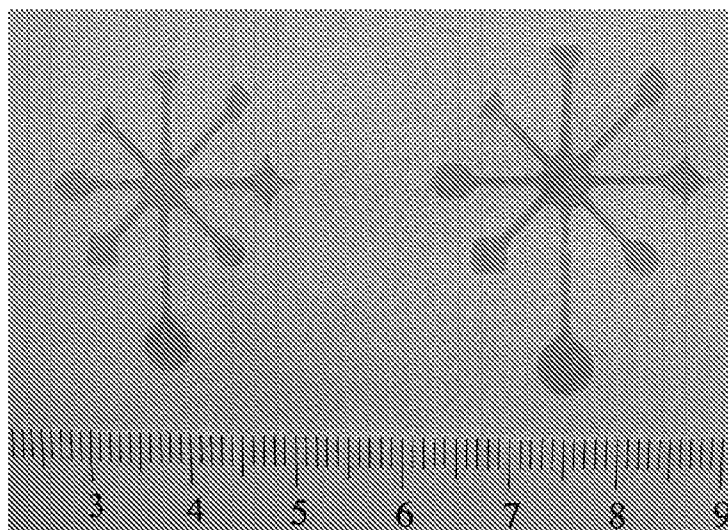
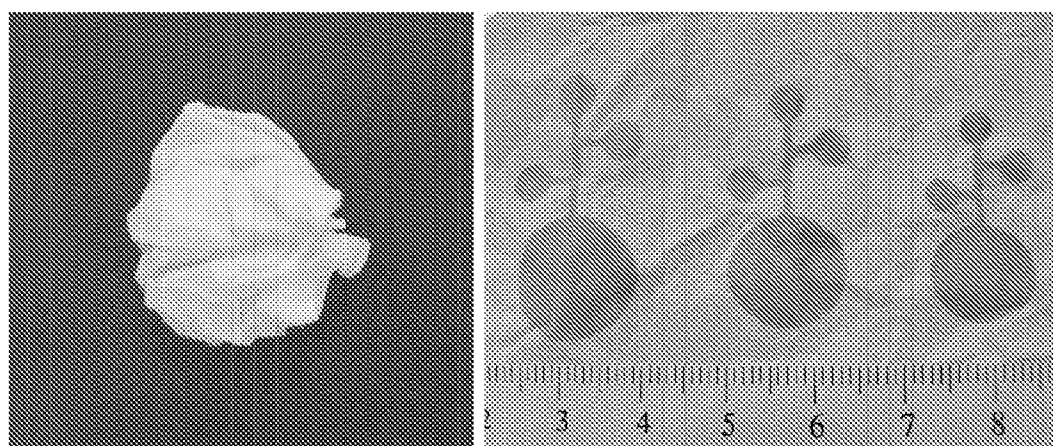


Figure 10



5/5

Figure 11

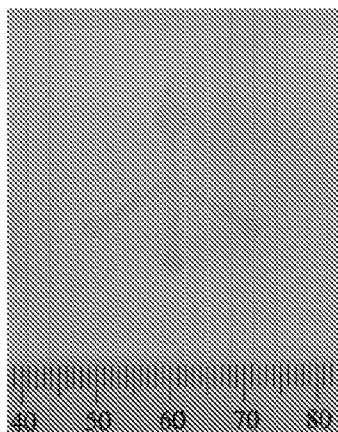
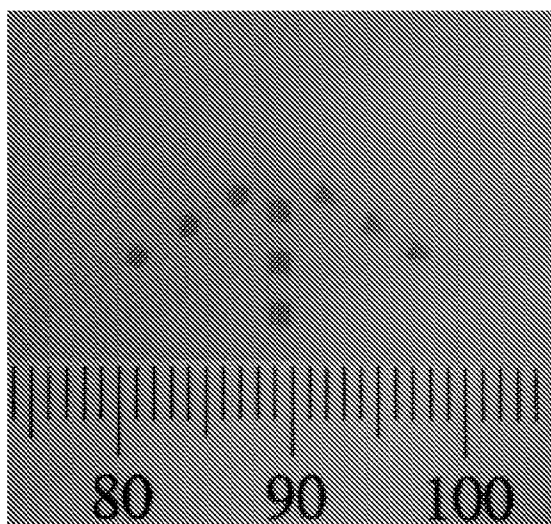


Figure 12





(51) International Patent Classification:
B81B 5/00 (2006.01) **B01L 99/00** (2010.01)
B32B 29/06 (2006.01) **B81C 1/00** (2006.01)
G01N 33/00 (2006.01)

(21) International Application Number:
PCT/AU2009/001009

(22) International Filing Date:
10 August 2009 (10.08.2009)

(25) Filing Language: English

(26) Publication Language: English

(30) Priority Data:
2008904179 14 August 2008 (14.08.2008) AU

(71) Applicant (for all designated States except US):
MONASH UNIVERSITY [AU/AU]; Wellington Road,
Clayton, Victoria 3168 (AU).

(72) Inventors; and

(75) Inventors/Applicants (for US only): **SHEN, Wei**
[AU/AU]; 1 Landen Avenue, Glen Waverley, Victoria
3150 (AU). **LI, Xu** [CN/AU]; 49 Townsend Street, Glen
Waverley, Victoria 3150 (AU). **TIAN, Junfei** [CN/AU];
Unit 3/20 Dover Street, Oakleigh East, Victoria 3166
(AU). **NGUYEN, Thanh Huynh** [AU/AU]; Unit 6, 99A
Athol Road, Springvale South, Victoria 3172 (AU).
GARNIER, Gil [AU/AU]; 31A Bangalay Avenue,
Frankston South, Victoria 3199 (AU).

(74) Agent: **WATERMARK PATENT AND TRADE
MARK ATTORNEYS**; Level 2, 302 Burwood Road,
Hawthorn, Victoria 3122 (AU).

(81) Designated States (unless otherwise indicated, for every
kind of national protection available): AE, AG, AL, AM,
AO, AT, AU, AZ, BA, BB, BG, BH, BR, BW, BY, BZ,
CA, CH, CL, CN, CO, CR, CU, CZ, DE, DK, DM, DO,
DZ, EC, EE, EG, ES, FI, GB, GD, GE, GH, GM, GT,
HN, HR, HU, ID, IL, IN, IS, JP, KE, KG, KM, KN, KP,
KR, KZ, LA, LC, LK, LR, LS, LT, LU, LY, MA, MD,
ME, MG, MK, MN, MW, MX, MY, MZ, NA, NG, NI,
NO, NZ, OM, PE, PG, PH, PL, PT, RO, RS, RU, SC, SD,
SE, SG, SK, SL, SM, ST, SV, SY, TJ, TM, TN, TR, TT,
TZ, UA, UG, US, UZ, VC, VN, ZA, ZM, ZW.

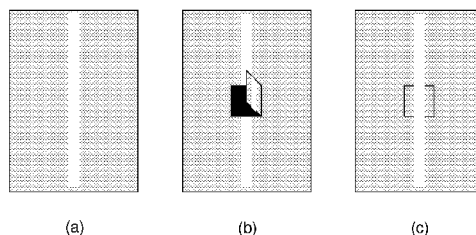
(84) Designated States (unless otherwise indicated, for every
kind of regional protection available): ARIPO (BW, GH,
GM, KE, LS, MW, MZ, NA, SD, SL, SZ, TZ, UG, ZM,
ZW), Eurasian (AM, AZ, BY, KG, KZ, MD, RU, TJ,
TM), European (AT, BE, BG, CH, CY, CZ, DE, DK, EE,
ES, FI, FR, GB, GR, HR, HU, IE, IS, IT, LT, LU, LV,
MC, MK, MT, NL, NO, PL, PT, RO, SE, SI, SK, SM,
TR), OAPI (BF, BJ, CF, CG, CI, CM, GA, GN, GQ, GW,
ML, MR, NE, SN, TD, TG).

Published:

— with international search report (Art. 21(3))

(54) Title: SWITCHES FOR MICROFLUIDIC SYSTEMS

Figure 1.



(57) Abstract: A microfluidic system including a substrate in sheet form, at least one hydrophilic microfluidic channel supported on a surface of the substrate, and at least one function component formed as part of the substrate for providing a functional component for the microfluidic channel wherein the functional component comprises at least one cut within the substrate for providing a switch or filter component for the microfluidic channel.

SWITCHES FOR MICROFLUIDIC SYSTEMS

TECHNICAL FIELD

5 The present invention is generally directed to microfluidic systems; and is in particular directed to switches, filters and other functional components used in such systems. While the invention will be described with respect to paper based substrates in sheet form, it will be appreciated that the invention is not restricted to substrates made of this material and may be used on substrates of other
10 materials such as, for example, hydrophilic polymer substrates.

BACKGROUND OF THE INVENTION

 The concept of making inexpensive microfluidic channels on paper and other woven and non-woven fibrous and porous surfaces to produce a
15 microfluidic system been successfully proven. Paper in sheet form is readily obtainable and can produce a very low cost substrate for such a microfluidic system. One aim of building such systems has been to fabricate low-cost bio-analytical and indicator devices, with direct envisaged applications in detecting waterborne bacteria in drinking water, the presence of some specific protein or
20 biomarkers in body fluid (cancer test), the level of glucose and other bio-chemical substances in human or animal blood and urine samples. Development of low-cost paper-based bio-analytical and environmental analytical devices have so far allowed quick and single step reaction to detect analytes in a fluid sample. Researchers in Harvard University led by Whitesides (see Martinez, A.W.,
25 Phillips, S.T., Butte, M.J. and Whitesides G.M., and "Platform for Inexpensive, Low-Volume, Portable Bioassays", Angew. Chem. Int. Ed. 46, 1318-1320 (2007)) have recently created channels on paper by printing patterns of conventional photoresists polymers (PDMS). Paper provides the capillary channels, while the photoresist polymers form the barrier which defines the channel. More recently,
30 the Harvard group used an x-y plotter to draw channels on paper surface (see Bruzewicz, D.A., Reches, M. and Whitesides, G.M., "Low-Cost Printing of Poly(dimethylsiloxane) Barriers to Define Microchannels in Paper, Anal Chem. 80, 3387-3392 (2008) and Martinez, A.W.; Phillips, S.T.; Carrilho, E.; Thomas III,

S.W.; Sindi, H.; Whitesides, G.M., "Simple telemedicine for developing regions: camera phones and paper-based microfluidic devices for real-time, off-site diagnosis". Anal. Chem. 80 (2008) 3699 – 3707)). The plotter's pens were filled with a hydrophobic solution of polydimethyl siloxane (PDMS) in hexane, and a
5 plethora of patterns 10cm long with channel 1cm to 2 mm wide were created. Their second micro-channels system created on paper surface overcame a major drawback of the first one, *ie* the rigid and brittle barrier material of conventional photoresist polymers. Their second system, however, has a poor channel resolution and definition, since the penetration of PDMS solution in paper sheet
10 cannot be controlled.

In US 7125639, Molecular Transfer lithography, the inventor Charles Daniel Schaper (class 430/253, 430/258) describes a process for patterning a substrate comprising the steps of: 1) coating a carrier with a photosensitive material, 2) exposing the photosensitive material to a pattern of radiation, and 3)
15 physically transferring the exposed material to the substrate.

In US 6518168, Self-assembled monolayers direct patterning of surfaces, by Paul G Clem et al (filing date 11/02/1998), A technique for creating patterns of material deposited on a surface involves forming a self-assembled monolayer in a pattern on the surface and depositing, via chemical vapor deposition or via sol-gel
20 processing, a material on the surface in a pattern complementary to the self-assembled monolayer pattern. The material can be a metal, metal oxide, or the like.

In WO/2008/060449 MICROFLUIDIC DETECTOR, by BUTTE, Manish, J. *et al* (Application date 9-11/2007), Articles and methods for determining an
25 analyte indicative of a disease condition are provided. In some embodiments, articles and methods described herein can be used for determining a presence, qualitatively or quantitatively, of a component, such as a particular type of cell, in a fluid sample. In one particular embodiment, a low-cost microfluidic system for rapid detection of T cells is provided. The microfluidic system may use
30 immobilized antibodies and adhesion molecules in a channel to capture T cells from a fluid sample such as a small volume of blood. The captured T cells may be labelled with a metal colloid (eg, gold nanoparticles) using an antibody specific for the T Cell Receptor (TCR), and metallic silver can be catalytically precipitated

onto the cells. The number of T cells captured can be counted and may indicate a disease condition of a patient such as severe combined immune deficiency or human immunodeficiency virus.

None of the above noted patents describe any functional components for controlling the movement of fluids or otherwise influencing the fluid within the microfluidic system. Furthermore, multiple-step reactions cannot be performed by the above described systems.

It is therefore an object of the present invention to provide a microfluidic system incorporating such functional components.

It is another preferred object to provide a microfluidic system allowing multiple-step reactions or functions to be performed.

DESCRIPTION OF THE INVENTION

According to one aspect of the present invention, there is provided a microfluidic system including a substrate in sheet form, at least one hydrophilic microfluidic channel supported on a surface of the substrate, and at least one functional component formed as part of the substrate for providing a function for the microfluidic channel.

According to one preferred embodiment, the functional component is formed by at least one cut provided within the substrate for defining a portion of the substrate displaceable relative to the remainder of the substrate, the substrate portion supporting at least part of the microfluidic channel. According to another preferred embodiment, the function component is formed by at least one cut provided within the substrate and a strip of material passing through the cut to form a sliding switch, the strip being formed of the same or similar material to the substrate, wherein at least part of the microfluidic channel is supported on the strip.

The functional component may provide a switch for controlling fluid flow along the microfluidic channel. Preferably, a plurality of said switches may be provided, the switches controlling the flow of a reactant from a dosing zone to at least one detection zone. A said detection zone may be provided on each switch. Alternatively, the switches may control the flow of a plurality of reactants from a plurality of dosing zones to at least one reactant zone. According to another

preferred embodiment, a single said switch may control fluid flow along a plurality of microfluidic channels.

According to a further preferred embodiment, at least one hydrophilic channel and (or) at least one functional component described above are formed on two or more sheets of the same or different substrates. By activating at least one functional component on at least one sheet, fluid is allowed to wick from one sheet to another, thus providing a functional component capable of controlling fluid movement in a three dimensional paper-based microfluidic device.

According to another preferred embodiment of the invention, the part of the microfluidic channel supported by the functional component may provide a filter for fluid within the microfluidic channel.

The present invention preferably provides switches and other function components that can be activated on microfluidic systems fabricated on substrates in sheet form. The switch activation system can rely on different mechanisms of activation including: 1) mechanical, 2) electromagnetic, 3) chemical, 4) optical.

The applicant has developed a novel two-step method of fabricating microfluidic channels on non-woven porous material. This novel method consists of a two-step process. In the first, a hydrophobic treatment is applied to the surface to reduce the surface energy of the substrate (for hydrophobic porous materials, this step is not required). In the second, precise channels of the chosen pattern are etched on the treated surface. Plasma treatment significantly increases the surface energy of the porous substrates, rendering them wettable by water and aqueous liquids. The wettability of the porous material by liquids then provides capillary driving force and allows the penetration of liquids within and along the channels created by the plasma treatment. Various patterns can be generated; the plasma treatment leaves no visible marks on the substrate surface and does not change the flexibility or stiffness of the materials by more than 5%.

The applicant has also developed a method of fabricating a microfluidic system where a hydrophobic agent is printed onto a hydrophilic substrate to form a hydrophobic/hydrophilic contrast that defines the microfluidic channels. Both of

the above referenced fabrication methods are described in more detail in the Applicant's International patent application no. PCT/AU2009/000889.

Mechanical modes of switch activation to modify fluid flow can result from any force mechanically affecting the system. The force may be applied directly,
5 indirectly, by vacuum or by pressure to the system.

Electromagnetic modes of fluid activation triggering can result from any electric field, magnetic effect or combination thereof allowing a change in fluid flow.

Chemical modes of triggering a microfluidic system switch include any type
10 of chemical principles. These include reaction, dissolution, precipitation, and changes in hydrophobicity, viscosity, photoreactions and the like. These involve mono or multiple reactants, surfactant, polymers, colloids.

The present invention also preferably provides a method to make microfluidic patterns on non-woven materials with filters or reagent releasing sites
15 that can be activated by a triggering action.

The present invention further preferably provides a method to make micro-reactors on paper surface which have controlled inputs of reactants.

The present invention also preferably provides a method to facilitate multi-step reactions and tests that require time delays between each step of the
20 reaction.

According to another aspect of the present invention, there is provided a method of producing a microfluidic system having a substrate in sheet form, at least one hydrophilic microfluidic channel supported on a surface of the substrate, and at least one functional component formed as part of the substrate for
25 providing a function for the microfluidic channel; including forming the functional component by making at least one cut within the substrate for defining a portion of the substrate displaceable relative to the remainder of the substrate, the substrate portion supporting at least part of the microfluidic channel.

According to a further aspect of the present invention, there is provided a
30 method of producing a microfluidic system having a substrate in sheet form, at least one hydrophilic microfluidic channel supported on a surface of the substrate, and at least one functional component formed as part of the substrate for providing a function for the microfluidic channel; including forming the function

component by making at least one cut within the substrate and passing a strip of material through the cut to form a sliding switch, the strip being formed of the same or similar material to the substrate, at least part of the microfluidic channel being supported on the strip.

5 Plasma treatment significantly increases the surface energy of the porous substrates, rendering them wettable by water and aqueous liquids. The wettability of the porous material by liquids then provides capillary driving force and allows the penetration of liquids within and along the channels created by the plasma treatment.

10 The printing of hydrophobizing agents onto hydrophilic papers defines microfluidic patterns on paper. The easiness of using electronically generated printing pattern onto paper surface to make paper-based microfluidic patterns makes printing a highly desirable efficient alternative approach to fabricate channels on paper.

15 The materials that can be made into such devices include, but are not restricted to, non-wovens, woven fabrics, foams, composites, films and membranes. Of special interest are the materials made of cellulosic materials, including papers and non-woven, and fabrics. The paper products of interest include filter paper, office paper, chromatography paper, tissues (towel, facial, bath, wipes), newsprint, packaging paper, non-woven polymer scaffolds, etc.

20 Any method known in the art can be selected to hydrophobize the surface/substrate. An embodiment of the invention consists of absorbing or adsorbing a solution of hydrophobic substance dissolved in a volatile solvent. Hydrophobic substance include, but are not restricted to, AKD, ASA, rosin, latex, silicones, fluorochemicals, polyolefin emulsions, resin and fatty acids, natural and synthetic waxes and any hydrophobic substance known in the art. Another application is through vapour deposition of a hydrophobic substance.

25 The invention may preferably provide a fluidic pattern for transporting a fluid to analyse in parallel to different detection zones. The typical channel dimensions may vary in length from 1 mm to 10 cm and in width from 2 cm to 100 μm . The fluidic system has typically the same rigidity, mechanical, properties and softness as those of the original substrate.

Alternatively, the invention may provide switches which can be activated by, but not restricted to, contact mechanical force, non-contact mechanical forces such as vacuum and pneumatic air jets, electrostatic and electromagnetic triggering mechanisms.

5 The present invention may also provide filters, ion exchange sites and reagent releasing reservoirs for a microfluidic system that can be switched into the microfluidic channels on demand.

10 The present invention therefore provides simple and versatile techniques to manufacture inexpensive microfluidic patterns systems on substrates, including flexible substrates such as paper, non-woven, foam and porous media with functional components, such as switches, micro-reactors and filters. Applications include low-cost bio-assays and indicators to monitor specific health or environmental conditions. These functional components strongly enhance the capabilities of the paper microfluidic systems, enable tests consist of more than
15 one reaction to be carried out on low-cost microfluidic systems. A preferred embodiment of the invention consists of fabricating microfluidic devices on porous, non-woven and woven substrates that have functional and intelligent component using plasma treatment with a mask and digital or contact printing methods.

20 Furthermore, this invention identifies the potential of microfluidic systems built on paper and other porous materials to enable multiple-step reactions and to be used as indicators and micro-reactors. To fulfil this potential, switches, filters and reaction sites can be designed and built in the microfluidic channels to control the flow and reaction of analytes and indicators.

25

BRIEF DESCRIPTION OF THE DRAWINGS

It will be convenient to further describe the invention with reference to the accompanying drawings which illustrate examples of the present invention. Other examples are possible, and consequently the particularity of the accompanying
30 drawings is not be understood as superseding the generality of the preceding description of the invention.

In the drawings:

Figure 1(a) to (c) are schematic views showing a first example of the present invention;

Figure 2(a) to (c) are schematic views showing a second example of the present invention;

5 Figure 3(a) to (c) are photos showing the operation of a switch according to the present invention;

Figure 4 is a schematic view of a third example of the present invention;

Figure 5 is a schematic view of a fourth example of the present invention;

10 Figure 6 is a schematic view of the example of Figure 5 showing its operation;

Figure 7 is a photo showing the filter of Figure 5 in operation;

Figure 8 is a schematic view of a further example of the present invention;

Figure 9(a) to (e) are photos showing the operation of the example of Figure 8; and

15 Figure 10 is a schematic drawing of a control switch for a three dimensional paper-based microfluidic system.

DETAILED DESCRIPTION OF THE INVENTION

20 The following description describes various examples of microfluidic systems incorporating a functional component according to the present invention.

Example 1

Referring initially to Figures 1 to 4, there is shown arrangements where a functional component according to the present invention is integrally formed from the same material as the substrate supporting the microfluidic system.

25 In one example of the invention, a filter paper was hydrophobized by immersion in a solution of AKD dissolved in heptane and the solvent was allowed to evaporate. A heat treatment of the treated paper in an oven at 100°C for 30 – 50 minutes was applied. In the second step, a solid mask was applied to the paper substrate and the system was exposed to a plasma reactor (K1050X
30 plasma asher (Quorum Emitech, UK) for 10 – 100 seconds at the intensity of 12 – 50 W). The plasma treatment left no visible mark on the sample and the sample retained its original softness and flexibility. The treated channel becomes

wettable by aqueous solutions and allows the capillary transport of the solutions (Figure 1(a)). In the third step, a cut was made across the channel in the way shown in Figure 1(b), but not restricted to it, to form the functional component according to the present invention. When this channel was folded in an angle to the paper sheet, capillary flow in the channel stopped at the point of the cut (Figure 1(b)). When the cut section was folded back into the paper sheet, the plasma treated area was made to contact the fluidic channel, enabling the capillary flow through the cut paper (Figure 1(c)). The capillary flow continues on. The functional component is therefore in the form of a mechanical switch. The activation of the switch can also be achieved by various means using contact and non-contact actions as claimed above.

Another way is to make a functional component in the form of a mechanical switch is to make two parallel cuttings across the capillary flow channel (Figure 2). The switch can be activated by a pulling action. The switch can also be activated by various means using contact and non-contact actions as claimed above.

Figure 3 shows the operation of a switch made using the design in Figure 2(a) to (c), and shows (a) Introduction of liquid onto the device; (b) switch in off (0) position; (c) switch is triggered by mechanical contact force and is in on (1) position.

The functional component as shown in Figures 1 to 3 can be easily incorporated in a paper-based microfluidic system. Figure 4 shows one of the many possibilities which shows a design of a microfluidic system consisting of one sample dosing zone (centre) and six detection zones; sample can be directed to any detection zone by operating switches. (0) is off and (1) is on.

Using this design, a fluid doped into any of the sample doping zones can be directed, via the use of switches, into any other part of the fluidic circuit, with any time delay required.

Example 2

Figures 5 to 7 show arrangements where a functional component according to the present invention is formed using material that is the same as or

similar to the material of the substrate of the microfluidic system, where the functional component is formed separately from that substrate.

In this example more than one piece of paper was plasma treated in the way shown in Figure 5(a). The lighter areas indicate the treated areas. The fluidic channel on the paper was not treated all way through the paper, but has a gap equal to or larger than 0.5 mm. Two cuts were made parallel to the channel and on both sides of the untreated gap. A paper strip wider than the gap in the fluidic channel was given a plasma treatment across it as shown in Figure 5(a).

The two pieces of paper can be assembled to form a functional component in the form of a sliding switch as shown in Figure 5(b). Figure 5(b) shows the "off" position of the switch, since the treated areas on the paper strip does not match with capillary flow channel. When the strip is pulled, the sliding switch was activated and allowed liquid to penetrate through and across the sliding switch. Figure 5(c) shows the sliding switch in the "on" position.

Example 3

In the example of the invention as shown in Figure 6, the "sliding switch" arrangement shown in Figure 5(a) to (c) is used in a different application to provide a microfluidic filter. These filters and reagent releasing sites can also be built in the microfluidic systems made of paper and other non-woven materials. Ion-exchange resins, high specific surface area functionalized and not functionalized nano particles, antibodies and antigens, can be deposited or printed onto any of the above filters. When a complex sample solution is delivered into sample doping zone, it can be sent to a detection or reaction zone via a filter, which can immobilize the interference ions and molecules in the sample before it reaches the detection and reaction zone. As, a sample liquid flow through the filter via capillary wicking, specific ions, specific molecules, virus and specific biomolecules will be bond and immobilized by the materials in the filter (Figure 6(c)).

Figure 7 shows the filter of Figures 6(a) to (c) in operation. The sample used was a diluted ink jet ink, the filter was a piece of matt ink jet paper which has a dye capture coating layer. For the purpose of showing the concept, the size of the coating area was not controlled. A diluted ink jet ink solution was introduced

from the right end of the device. Most dye was immobilized by the dye capturing coating layer on the filter. The sample liquid penetrated passing the filter to the left side of the device was free of dye.

5 A reagent releasing site can be designed in a similar way as a filter. The paper strip (Figure 5(a)) does not require plasma treatment. A narrow band of coating of water soluble reagent supported by hydrophilic coating media is deposited on the paper strip. When the paper strip is activated, the sample will leach the reagent off the coating media on the paper strip and carry it forward.

Example 4

10 This example shows an application of the present invention which allows a microfluidic system to be used for multiple-step restrictions or functions to be performed.

Well controlled microfluidic reactors can be made on paper- and other non-woven- based materials using micro-channels and functional components according to the present invention such as filters and switches. Figure 8 shows the concept of a simple reactor that has two inlets.

The concept of microfluidic reactors built on low-cost microfluidic detectors, indicators, diagnostic devices uniquely facilitate multi-step reactions.

20 This microfluidic reactor consists of two sample dosing zones (A1 and A2), one reaction zone (B) and two switches (S1 and S2). Two reactants can be introduced into the reactor B in a controlled manner with any time delay required.

Figure 9 shows the microfluidic reactor in operation. A small quantity of phenolphthalein indicator was placed into the reaction zone (B) to demonstrate an acid-base neutralization reaction. A microfluidic reactor of the design of Figure 8 was built for demonstration (Figure 9(a)). A NaOH and a HCl solution were introduced into samples dosing zones A2 and A1, respectively (Figure 9(b)). Both switches were in "off" position. Switch S2 was then switched on to allow the NaOH solution to enter the reaction zone. As the NaOH solution entered the reaction zone, a change of indicator colour was observed (Figure 9(c)). Then S1 was switched on to allow the HCl solution to enter the reaction zone (Figure 9(d)). As the HCl solution entered the reaction zone, neutralization reaction occurred.

Figure 9(e) shows the expected fading of indicator colour as the neutralization reaction completed.

Figure 10 is a schematic drawing of a control switch for a three dimensional paper-based microfluidic system. The three dimensional paper-based microfluidic device can be built as shown in Figure 10. Hydrophilic channels are formed on both the top and bottom sheets of papers. On the top paper sheet the hydrophilic channel is cut as shown in Figure 10 so that it can be moved (S1). A hydrophobic medium in sheet or film form with a cut notch (or a hole, not shown) is sandwiched in between the two sheets. By aligning the channels on the paper sheets with the notch in the hydrophobic medium, a switch can be formed. The operation of the switch involves pushing the switch (S1) down to make contact with the hydrophilic channel in the bottom paper sheet through the notch in the hydrophobic film.

CLAIMS:

1. A microfluidic system including a substrate in sheet form, at least one hydrophilic microfluidic channel supported on a surface of the substrate, and at least one functional component formed as part of the substrate for providing a function for the microfluidic channel.
5
2. A microfluidic system according to claim 1, wherein the functional component is formed by at least one cut provided within the substrate for defining a portion of the substrate displaceable relative to the remainder of the substrate, the substrate portion supporting at least part of the microfluidic channel.
- 10 3. A microfluidic system according to claim 1, wherein the function component is formed by at least one cut provided within the substrate and a strip of material passing through the cut to form a sliding switch, the strip being formed of the same or similar material to the substrate, wherein at least part of the microfluidic channel is supported on the strip.
- 15 4. A microfluidic system according to claim 2 or 3 wherein the functional component provides a switch for controlling fluid flow along the microfluidic channel.
5. A microfluidic system according to claim 4, including a plurality of said switches, the switches controlling the flow of a reactant from a dosing zone to at least one detection zone.
20
6. A microfluidic system according to claim 5, wherein the detection zone is provided on the switch.
7. A microfluidic system according to claim 4, including a plurality of said switches, the switches controlling the flow of a plurality of reactants from a plurality of dosing zones to at least one reactant zone.
25

8. A microfluidic system according to claim 4, wherein a single said switch controls fluid flow along a plurality of microfluidic channels.

9. A microfluidic system according to claim 2 or 3 wherein the part of the microfluidic channel supported by the functional component provides a filter for
5 fluid within the microfluidic channel.

10. A microfluidic system according to claim 2 or 3, including a plurality of said substrates, wherein the functional component is provided on one said substrate, and the microfluidic channel are provided on another said substrate.

11. A method of producing a microfluidic system having a substrate in sheet
10 form, at least one hydrophilic microfluidic channel supported on a surface of the substrate, and at least one functional component formed as part of the substrate for providing a function for the microfluidic channel; including forming the functional component by making at least one cut within the substrate for defining a portion of the substrate displaceable relative to the remainder of the substrate,
15 the substrate portion supporting at least part of the microfluidic channel.

12. A method of producing a microfluidic system having a substrate in sheet form, at least one hydrophilic microfluidic channel supported on a surface of the substrate, and at least one functional component formed as part of the substrate for providing a function for the microfluidic channel; including forming the function
20 component by making at least one cut within the substrate and passing a strip of material through the cut to form a sliding switch, the strip being formed of the same or similar material to the substrate, at least part of the microfluidic channel being supported on the strip.

Figure 1.

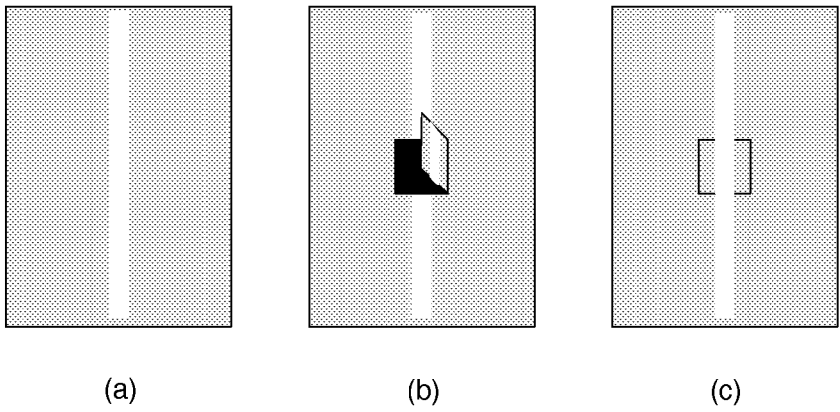
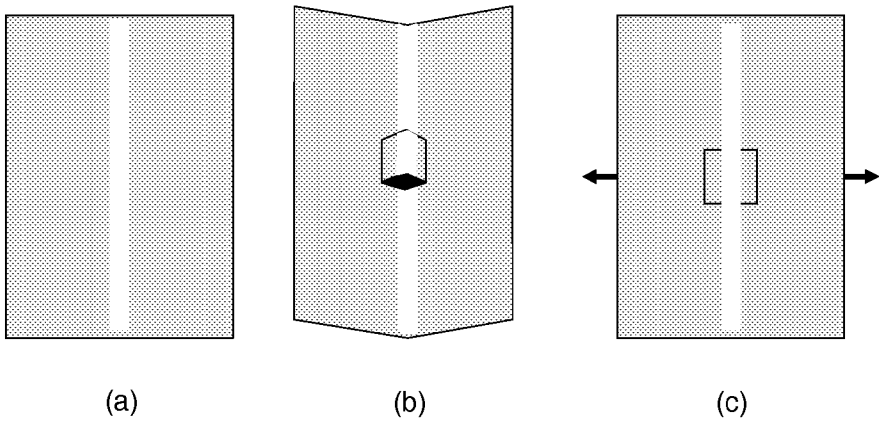


Figure 2.



2/5

Figure 3.

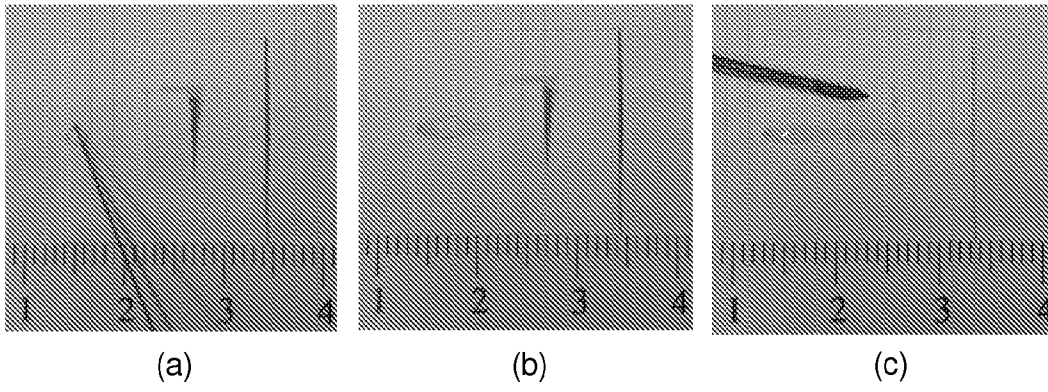


Figure 4.

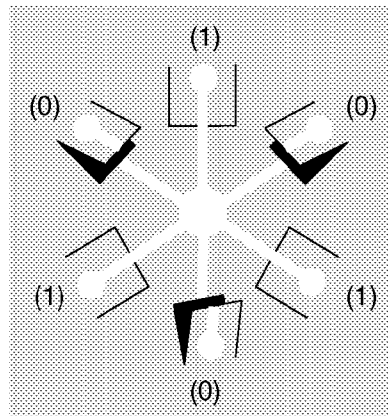


Figure 5

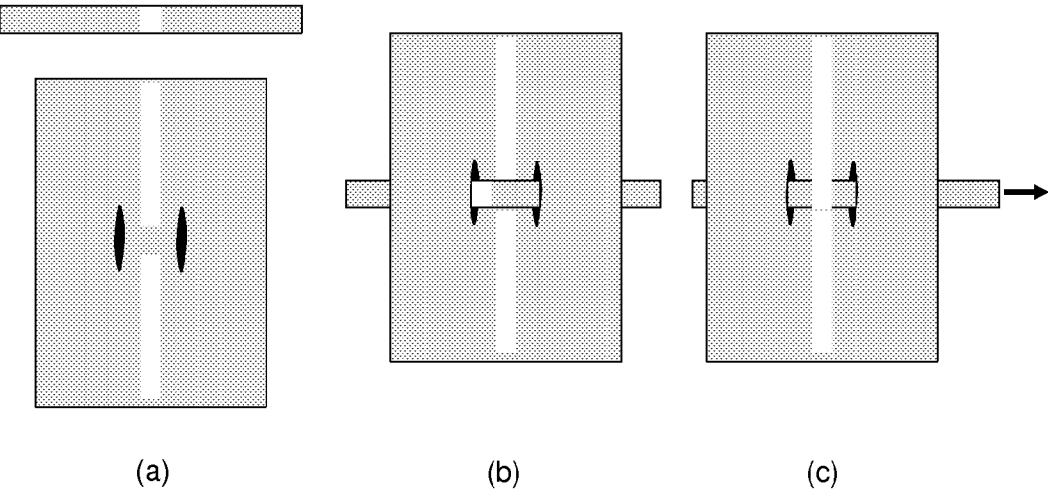
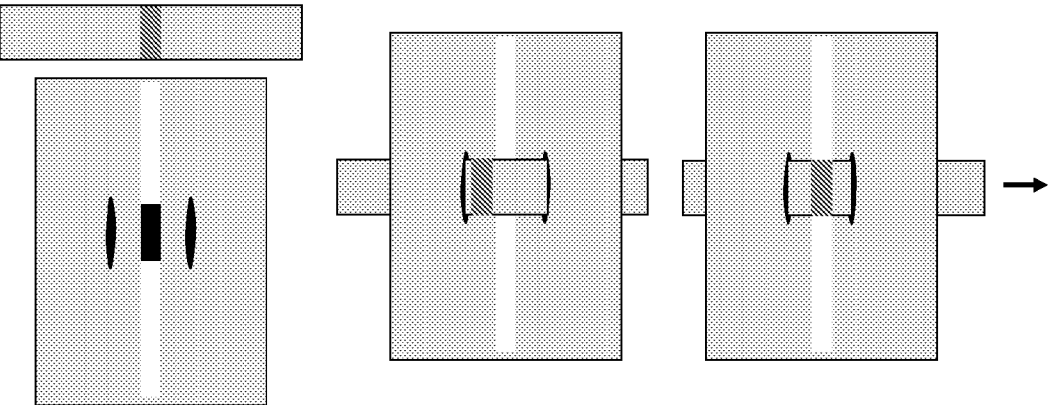


Figure 6



4/5

Figure 7

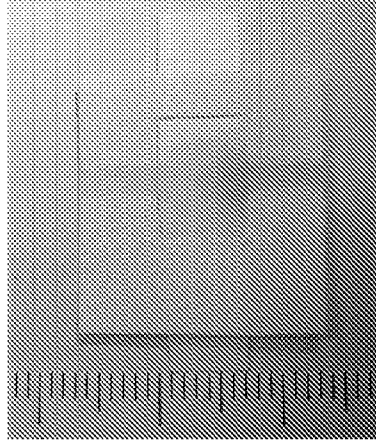


Figure 8

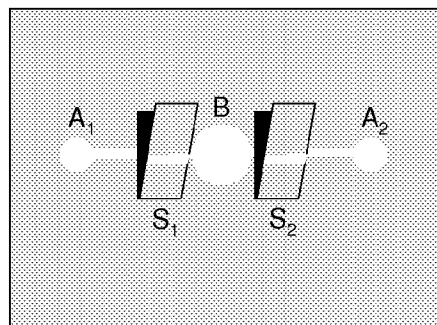
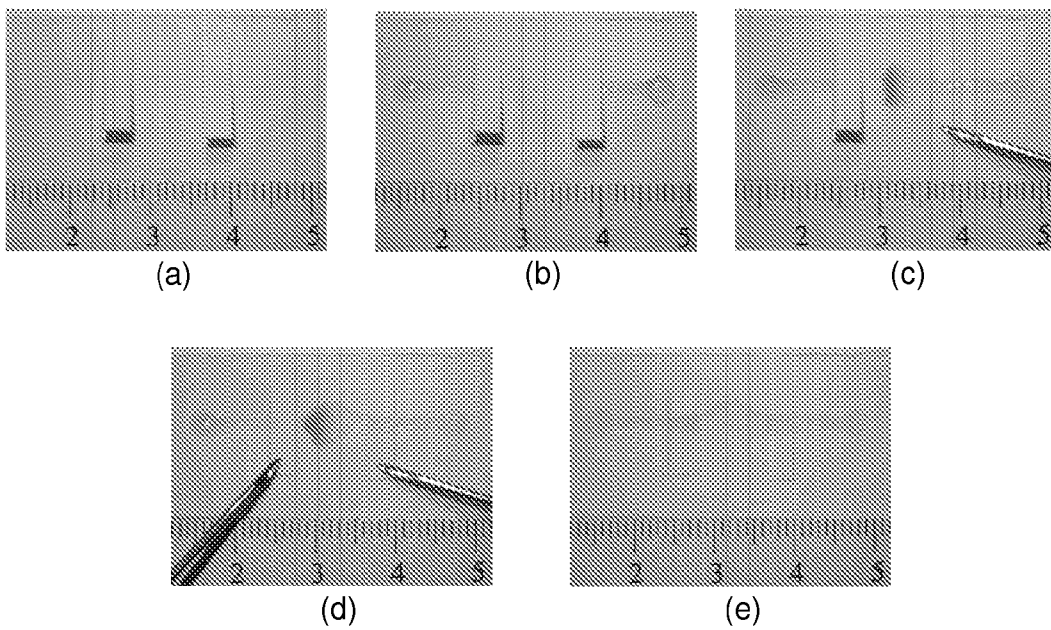
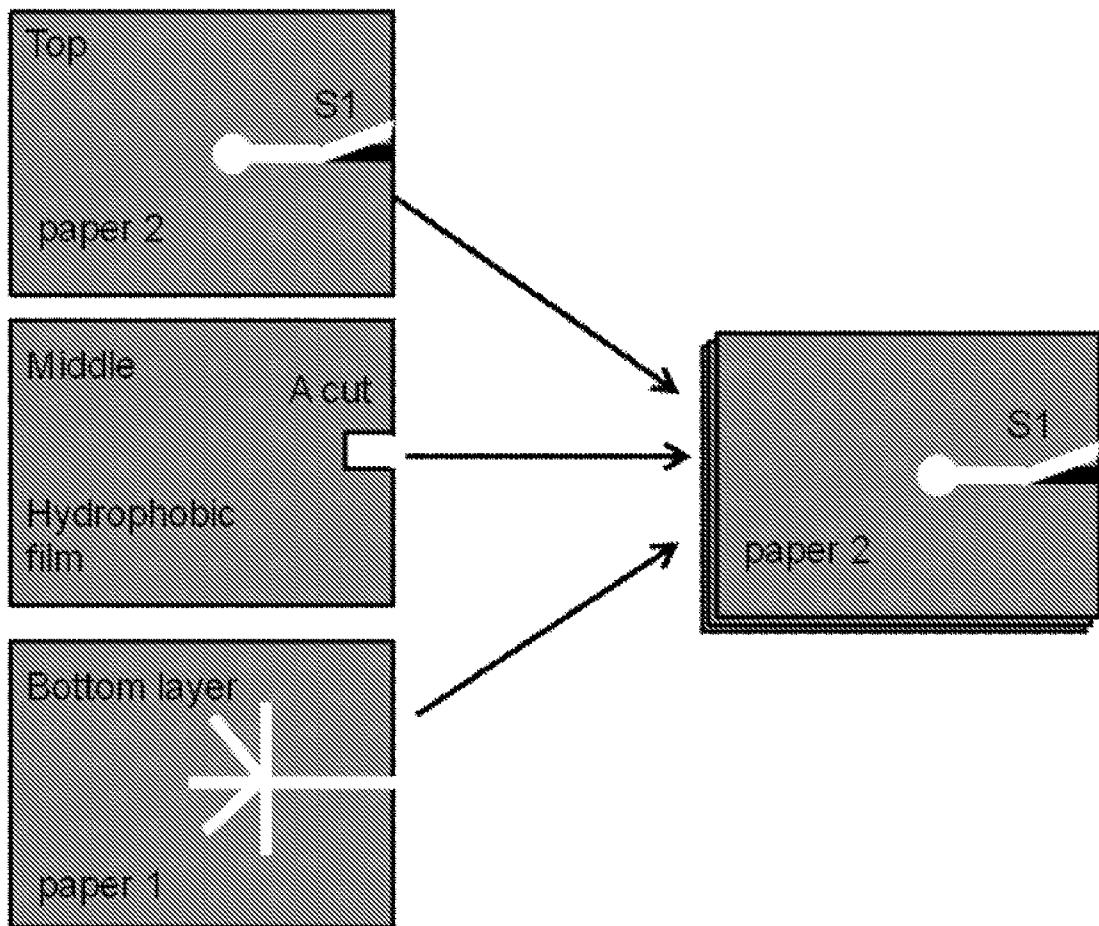


Figure 9



5/5

Figure 10.



(19) World Intellectual Property Organization
International Bureau



(43) International Publication Date
6 January 2011 (06.01.2011)

(10) International Publication Number
WO 2011/000047 A1

PCT

(51) International Patent Classification:
G01N 33/52 (2006.01) *G01N 33/48* (2006.01)

(21) International Application Number:
PCT/AU2010/000837

(22) International Filing Date:
30 June 2010 (30.06.2010)

(25) Filing Language: English

(26) Publication Language: English

(30) Priority Data:
2009903024 30 June 2009 (30.06.2009) AU

(71) Applicant (for all designated States except US):
MONASH UNIVERSITY [AU/AU]; Wellington Road,
Clayton, Victoria 3168 (AU).

(72) Inventors; and

(75) Inventors/Applicants (for US only): **SHEN, Wei**
[AU/AU]; 1 Landen Avenue, Glen Waverley, Victoria
3150 (AU). **LI, Xu** [CN/AU]; 49 Townsend Street, Glen
Waverley, Victoria 3150 (AU). **TIAN, Junfei** [CN/AU];
3/18 Dover Street, Oakleigh East, Victoria 3166 (AU).
GARNIER, Gil [AU/AU]; 31A Bangalay Avenue,
Frankston South, Victoria 3199 (AU).

(74) Agent: **WATERMARK PATENT AND TRADE
MARK ATTORNEYS**; Level 2, 302 Burwood Road,
Hawthorn, Victoria 3122 (AU).

(81) Designated States (unless otherwise indicated, for every
kind of national protection available): AE, AG, AL, AM,
AO, AT, AU, AZ, BA, BB, BG, BH, BR, BW, BY, BZ,
CA, CH, CL, CN, CO, CR, CU, CZ, DE, DK, DM, DO,
DZ, EC, EE, EG, ES, FI, GB, GD, GE, GH, GM, GT,
HN, HR, HU, ID, IL, IN, IS, JP, KE, KG, KM, KN, KP,
KR, KZ, LA, LC, LK, LR, LS, LT, LU, LY, MA, MD,
ME, MG, MK, MN, MW, MX, MY, MZ, NA, NG, NI,
NO, NZ, OM, PE, PG, PH, PL, PT, RO, RS, RU, SC, SD,
SE, SG, SK, SL, SM, ST, SV, SY, TH, TJ, TM, TN, TR,
TT, TZ, UA, UG, US, UZ, VC, VN, ZA, ZM, ZW.

(84) Designated States (unless otherwise indicated, for every
kind of regional protection available): ARIPO (BW, GH,
GM, KE, LR, LS, MW, MZ, NA, SD, SL, SZ, TZ, UG,
ZM, ZW), Eurasian (AM, AZ, BY, KG, KZ, MD, RU, TJ,
TM), European (AL, AT, BE, BG, CH, CY, CZ, DE, DK,
EE, ES, FI, FR, GB, GR, HR, HU, IE, IS, IT, LT, LU,
LV, MC, MK, MT, NL, NO, PL, PT, RO, SE, SI, SK,
SM, TR), OAPI (BF, BJ, CF, CG, CI, CM, GA, GN, GQ,
GW, ML, MR, NE, SN, TD, TG).

Published:

— with international search report (Art. 21(3))

(54) Title: QUANTITATIVE AND SELF-CALIBRATING CHEMICAL ANALYSIS USING PAPER-BASED MICROFLUIDIC SYSTEMS

(57) Abstract: A method of determining the concentration of a test fluid sample using a paper-based microfluidic system having a plurality of hydrophilic testing zones, including: a) depositing said test fluid sample on at least one said testing zone; b) depositing a plurality of standard fluid samples or reactives of differing known concentrations on other said testing zones; c) introducing an indicator solution to each said test zone to thereby react with the deposited fluid sample and result in a colour intensity change which is a function of the fluid sample concentration; and d) comparing the differences in colour intensity between the test fluid sample and the standard fluid samples or reactives to thereby determine the concentration of said test fluid sample.

**QUANTITATIVE AND SELF-CALIBRATING CHEMICAL ANALYSIS USING
PAPER-BASED MICROFLUIDIC SYSTEMS**

FIELD OF THE INVENTION

The present invention is generally directed at quantitative chemical analysis systems, and in particular to chemical analysis using paper-based microfluidic systems.

BACKGROUND OF THE INVENTION

The conventional approach for obtaining accurate quantitative measurements of analyte concentration requires the use of equipment intensive analysis. This approach for determining the concentration of an analyte in a solution requires the use of expensive equipment using spectroscopy, chromatography, NMR, atomic absorption or other analytical procedures that can also be difficult and time consuming to use. Also, a relatively large volume of the solution may be required for the tests.

The use of paper-based microfluidic systems for use in a variety of applications including chemical analysis was first proposed in Martinez, A.W.; Phillips, S.T.; Butte, M.; Whitesides, G.M., Patterned Paper as a Platform for Inexpensive, Low-volume, Portable Bioassays, Angew. Chem. Int. Ed., 2007, 46, 1318-1320. The advantages of using such systems are their low cost and portability. Furthermore, the sample volume amount can be significantly reduced which is helpful when the obtained sample amount is limited (example a biological sample from a hospital patient). It should be noted that the term "paper" is used in the application to refer to cellulosic material including woven fabrics and non-woven material in addition to paper.

Further developments of such paper-based microfluidic systems are described in the applicant's Australian provisional patent application nos. 2008903553 and 2008905776. In the applicant's microfluidic systems, a hydrophobic/hydrophilic contrast is provided on the surface of the paper substrate to thereby define microfluidic channels for controlling the transport of aqueous solutions due to capillary action without the need of external pumping.

The concentration of a test sample may be determined by using colourmetric methods with such microfluidic systems by reacting the test sample with an indicator solution. The accuracy of the results are however influenced by

many external factors including environmental conditions such as the ambient temperature and relative humidity, the quality and age of the paper, the quality and the settings of the scanner or camera used to record the results, or the means to transmit the results electronically. This can lead to significant errors in the colorimetric analytical results. Therefore, the same test sample measured using different paper substrates, using different scanners or cameras, or transmitted using different electronic transmission systems with different software could result in significant variations in the result.

The same principle can be used with ELISA-type of analysis based on paper, where bioconjugates are fixed on paper.

SUMMARY OF THE INVENTION

It is therefore an object of the present invention to more accurately determine the concentration of a test sample using paper-based microfluidic systems.

With this in mind, there is provided a method of determining the concentration of a test fluid sample using a paper-based microfluidic system having a plurality of hydrophilic testing zones, including:

- a) depositing said test fluid sample on at least one said testing zone;
- b) depositing a plurality of standard fluid samples or reactives of differing known concentrations on other said testing zones;
- c) introducing an indicator solution to each said test zone to thereby react with the deposited fluid sample and result in a colour intensity change which is a function of the fluid sample concentration; and
- d) comparing the differences in colour intensity between the test fluid sample and the standard fluid samples or reactives to thereby determine the concentration of said test fluid sample.

The deposition of the standard fluid samples or reactives can be done prior to or during the deposition of the test sample.

The use of a plurality of standard fluid samples or reactives of different known concentrations provides an internal self-calibration for the method according to the present invention. This can lead to more accurate results being obtained notwithstanding the various external factors that refer to previously. This is because the test results are determined on the basis of the relative

differences between the test fluid sample and the standard fluid samples or reactivities, thereby avoiding the influences associated with the external factors referred to previously.

The results may therefore be recorded using a variety of equipment including a desktop scanner or even a phone camera. The image may therefore be imported into a graphics program such as Adobe Photoshop®, and converted into greyscale mode. The main colour intensities can then be modified using the histogram function of the software. The ultimate mean intensity value of each test zone may preferably then be obtained by subtracting the measured average intensity from the mean intensity of a blank control zone and converted as a graph to obtain a calibration curve, the graph plotting mean intensity against solution concentration.

ELISA is an enzyme-linked immunosorbent assay. Paper-based microfluidic device may be designed to perform ELISA-like assay. In this assay certain amounts of antigen are fixed on the paper surface, a specific antibody is applied over the paper surface so that it can bind to the antigen. This antibody is bonded to an enzyme. In the last step of ELISA a substance is added to convert the enzyme to some detectable signal.

There is also provided a system for determining the concentration of a test fluid sample, said system including:

- a) a paper-based microfluidic system having a plurality of hydrophilic testing zones, said test fluid sample being depositable on at least one testing zone;
- b) a plurality of standard fluid samples or reactivities of differing known concentration for depositing on other said testing zones;
- c) an indicator solution for introducing to each test zone to thereby react with the fluid samples and result in a colour intensity change which is a function of the fluid sample concentration,

wherein by comparing differences in colour intensity between the test fluid sample and the standard fluid samples or reactivities the concentration of the test fluid sample can be determined.

BRIEF DESCRIPTION OF THE DRAWINGS

It will be convenient to further describe the invention with respect to the accompanying drawings which illustrate the method according to the present invention. Other embodiments of the invention are possible, and consequently, the particularity of the accompanying drawings is not to be understood as superseding the description of the invention.

In the drawings:

Figure 1 shows a paper-based microfluidic system for creating an NO_2^- calibration curve according to the present invention;

Figure 2 shows an NO_2^- calibration curve obtained from the test results from the microfluidic system as shown in figure 1;

Figure 3 shows a paper-based microfluidic system for determining the NO_2^- concentration of an unknown sample according to the present invention;

Figure 4 shows a calibration curve obtained from the test results from the microfluidic system as shown in figure 3;

Figure 5 shows a paper-based microfluidic system for measuring the Uric Acid (UA) concentration of an unknown sample according to the present invention;

Figure 6 shows a calibration curve obtained from the test results from the microfluidic system as shown in figure 5.

DETAILED DESCRIPTION OF THE INVENTION

The invention will now be described with reference to the following examples describing different possible utilisations of the present invention. It is however to be appreciated that the invention does not restrict to these examples.

The fabrications of the paper-based microfluidic systems were achieved using the techniques as described in the applicant's above noted provisional applications.

Whatman filter paper (No. 4) was selected as the substrate to prepare the microfluidic systems. Two methods were used for fabrication - plasma treatment and ink jet printing. The former patterning method was based on the principle of using a vacuum plasma reactor (K1050X plasma asher (Quorum Emitech, UK)) and premade masks to selectively dehydrophobize filter paper samples which have already been hydrophobized by alkyl ketene dimer (Wax 88 konz, BASF)

beforehand. The latter one was using a commercial desktop ink jet printer to selectively deposit alkenyl ketene dimer (Precis 900, Hercules Australia Pty Ltd) onto filter paper. The microfluidic systems, were fabricated with a pattern consisting of six detection zones and one central inlet zone.

5 Millipore-purified water was used to prepare all liquid samples required for testing the performance of microfluidic systems. Serially diluted nitrite and uric acid standard solutions were prepared with sodium nitrite ($\geq 99\%$, Sigma-Aldrich) dissolved in water and uric acid ($\geq 99\%$, Sigma-Aldrich) dissolved in sodium hydroxide solution (0.2 mol/L), respectively.

10 The indicator solution for NO_2^- contains 50 mmol/L sulfanilamide ($\geq 99\%$, Sigma-Aldrich), 330 mmol/L, citric acid ($\geq 99.5\%$, Sigma-Aldrich), and 10 mmol/L N-(1-naphthyl) ethylenediamine, $\geq 98\%$, Sigma-Aldrich).

The indicator solution for UA consists of the 1:1 mixture of solution A (2.56% (w/v) 2,2'-biquinoline-4,4'-dicarboxylic acid disodium salt hydrate, $\geq 98\%$,
15 Sigma-Aldrich) and solution B (20 mmol/L sodium citrate and 0.08% (w/v) copper (II) sulfate, $\geq 99\%$, Sigma-Aldrich).

For creating a nitrite calibration curve, one blank control (water, 0.5 μL) and five serially diluted nitrite standard solution samples (with concentration ranging from 78 $\mu\text{mol/L}$ to 1250 $\mu\text{mol/L}$, 0.5 μL) were deposited onto six detection
20 zones in sequence using the eppendorf research® pipette (0.1-2.5 μL).

A nitrite solution (500 $\mu\text{mol/L}$ NO_2^-) was assumed as the sample solution of unknown concentration. This sample solution (0.5 μL) was spotted onto one detection zone with serially diluted nitrite standard solution samples (156 $\mu\text{mol/L}$ to 2500 $\mu\text{mol/L}$, 0.5 μL) on the other detection zones in sequence. In this assay,
25 water (0.5 μL) was added onto the central inlet zone as the blank control.

For uric acid assay, a uric acid solution (500 $\mu\text{mol/L}$ UA) was assumed as unknown sample solution and successively loaded with five serially diluted UA standard solution samples (100 $\mu\text{mol/L}$ to 1600 $\mu\text{mol/L}$) onto each detection zone of the μPAD . NaOH solution (0.2 mol/L) was used as the blank control in this assay.

30 In all the above assays, corresponding indicator solutions (5 μL) were introduced into detection zones from the inlet zone with the eppendorf research® pipette (0.5-10 μL) owing to the capillary penetration. For each assay, six independent measurements have been taken with six devices.

The results of the colorimetric assays were imaged with a desktop scanner (Epson Perfection 2450, color photo setting, 1200 dpi resolution), then imported into Adobe Photoshop® and converted into grayscale mode. The mean color intensities were quantified using the histogram function of Adobe Photoshop®.

- 5 The ultimate mean intensity value of each detection zone was obtained by subtracting the measured average intensity from the mean intensity of blank control and transferred to Microsoft Excel® to obtain calibration curve data.

Example 1

In this example, an NO_2^- calibration curve was created as shown in Figures 10 1 and 2. The colorimetric testing of NO_2^- was based on the principle of the Griess reaction which is a common quantification measurement method for NO_2^- . In this assay, serially diluted NO_2^- standard solutions (78, 156, 312, 625, 1250 $\mu\text{mol/L}$) were deposited into each detection zone 1-5 in sequence, while the blank control solution was spotted on the detection zone 0. Then the indicator solution for NO_2^- was 15 introduced into the device via inlet zone. When the indicator solution penetrated into testing zones by capillary action and contacted with the analyte, the citric acid within the indicator solution converted NO_2^- to HNO_2 . The nitrous acid then transformed sulfanilamide into diazotized sulfanilamide which coupled with N-(1-naphthyl)-ethylenediamine to form a pink azo compound. The resulting color developed in each 20 detection zone changes from almost colorless (zone 0) to pink (zone 5) due to the different concentration of standard solution samples (Figure 1). In Figure 2, the value of mean color intensity of each standard sample is the average of six independent measurements which were taken using six microfluidic systems, measured and calculated with software. The error bar is the relative standard deviation.

25 Linear least-squares fitting of the nitrite data gave coefficient of determination (R^2) of 0.9902. The mean color intensity is proportional to the NO_2^- concentration. This assay certified that we can use paper-based microfluidic systems (six-channel pattern as an example) to create calibration curves for quantitative analysis.

30 Example 2

In this example, the NO_2^- concentration of an unknown sample was measured. To measure the nitrite concentration of an unknown sample using

paper-based microfluidic systems, we prepared a blank control solution ($0 \mu\text{mol/L NO}_2^-$, deposited on zone 0), five standard solutions ($156, 312, 625, 1250, 2500 \mu\text{mol/L NO}_2^-$, deposited on zone 1-5), and a $500 \mu\text{mol/L NO}_2^-$ solution (deposited on zone x) as an assumed unknown sample solution. The indicator solution was still introduced into the system from central inlet zone which developed different color in different testing zones (Figure 3). In this assay, six microfluidic systems were used to run six independent tests which provided the mean color intensity and error bar for every standard solution to create the calibration curve (Figure 4) which gave a quadratic regression equation for calculating the unknown sample concentration. As long as the measured concentration is close to the real value, the paper-based microfluidic systems are deemed to be efficient tools to quantitatively analyze the analyte concentration of an unknown sample solution. The result obtained from software analyses showed that the measured average color intensity for the unknown sample is 12.684, thus the NO_2^- concentration of unknown sample from calculation is $507 \mu\text{mol/L}$ (1.4% relative error compared with the real concentration of $500 \mu\text{mol/L}$).

Example 3

In this example, the UA concentration of an unknown sample was measured as shown in Figures 5 and 6.

The colorimetric assay of uric acid was based on a bicinchoninate chelate method. When the indicator solution for UA came into the detection zone, Cu (II) in the indicator solution was reduced to Cu (I) by UA which has been loaded on the testing zone beforehand, then the cuprous ion formed a purple chelate product with sodium bicinchoninate. The resulting color developed in testing zones 0-5 gradually became darker from light purple to purple corresponding to different UA concentrations ($0, 100, 200, 400, 800, 1600 \mu\text{mol/L}$) (Figure 6). The data and error bars in Figure 7 are the mean and relative standard deviation, respectively, from 6 independent measurements taken using six devices. We prepared the sample solution with $500 \mu\text{mol/L}$ uric acid and assumed this solution as the unknown sample which was also deposited on the testing zone x. With software analyses, the average of six measured values of color intensity is 12.492 for unknown sample; hence the mean UA concentration of six unknown samples can

be calculated from the regression equation, which was 502 $\mu\text{mol/L}$. The relative error is 0.4% compared with the real concentration value (500 $\mu\text{mol/L}$).

The result from all assays illustrated that the paper-based microfluidic systems are sufficient to operate parallel tests on different detection zones simultaneously. The amount of tests ran with one system correlates with the number of testing zones which is changeable according to different predesigned patterns. In the described examples, the six-channel pattern is capable of detecting up to seven samples at one time, thereby creating a calibration curve and providing a regression equation for unknown sample concentration measurement. This method is a low-cost, rapid and simple concentration detection method by virtue of colorimetric chemistry of the tested analyte.

Microfluidic paper-based multifluidic systems, combined with the colorimetric reaction of analyte and the existing computer software (e.g. Adobe Photoshop®), can provide a cheap and easy-to-use tool for the quantitative detection of unknown sample concentration. The raw material for these microfluidic systems – paper – is relatively economical and the fabrication method of these systems is quite simple. Therefore, the paper-based microfluidic system can be a useful tool when measurements performed in less-industrialized area or remote region with limited resources. Moreover, this method substantially reduces the sample volume, which is helpful when the obtainable sample amount is limited (e.g. the biological sample from patients).

CLAIMS:

1. A method of determining the concentration of a test fluid sample using a paper-based microfluidic system having a plurality of hydrophilic testing zones, including:
 - 5 a) depositing said test fluid sample on at least one said testing zone;
 - b) depositing a plurality of standard fluid samples or reactives of differing known concentrations on other said testing zones;
 - c) introducing an indicator solution to each said test zone to thereby react with the deposited fluid sample and result in a colour intensity change which
 - 10 is a function of the fluid sample concentration; and
 - d) comparing the differences in colour intensity between the test fluid sample and the standard fluid samples or reactives to thereby determine the concentration of said test fluid sample.
2. A method according to claim 1 including quantifying the colour intensity in
- 15 each said test zone as a function of the known fluid sample concentrations to thereby produce a calibration curve from which the concentration of the test fluid sample can be obtained.
3. A method according to claim 1 or 2, wherein one said test zone is deposited with water or a standard solution to provide a blank control zone.
- 20 4. A method according to claim 1, wherein the standard fluid samples or reactives are deposited prior to the deposition of the test fluid sample.
5. A method according to claim 1, wherein a ELISA-type of bio analysis is performed using bioconjugation.
6. A system for determining the concentration of a test fluid sample, said
- 25 system including:
 - a) a paper-based microfluidic system having a plurality of hydrophilic testing zones, said test fluid sample being depositable on at least one testing zone;

10

b) a plurality of standard fluid samples or reactivities of differing known concentration for depositing on other said testing zones;

c) an indicator solution for introducing to each test zone to thereby react with the fluid samples and result in a colour intensity change which is a
5 function of the fluid sample concentration,

wherein by comparing differences in colour intensity between the test fluid sample and the standard fluid samples or reactivities the concentration of the test fluid sample can be determined.

7. A paper-based microfluidic system adapted to carry out the method
10 according to any one of claims 1 to 5.

1/3

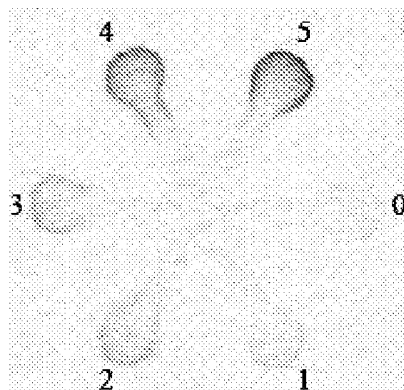


Figure 1

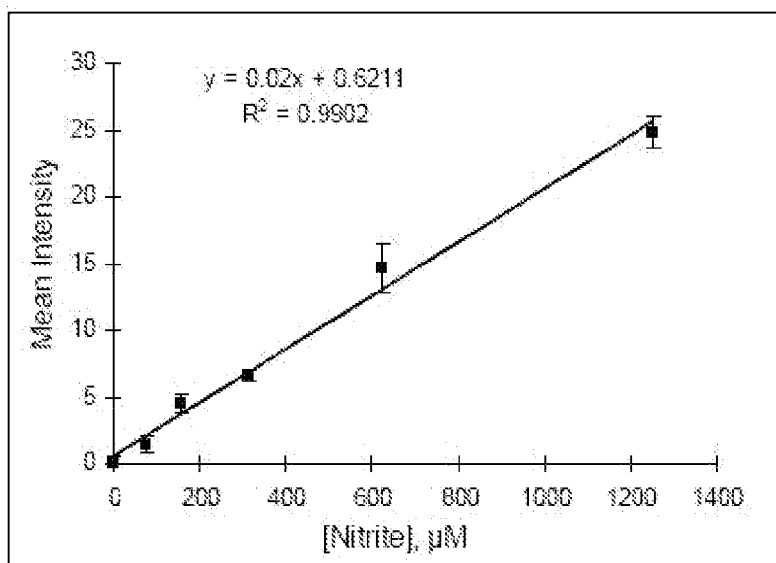


Figure 2

2/3

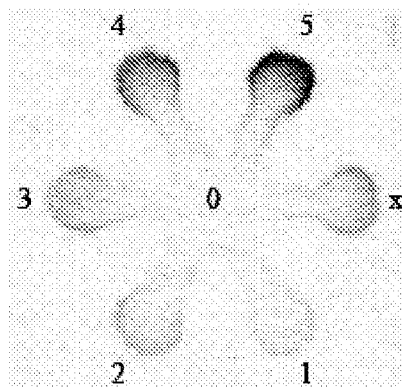


Figure 3

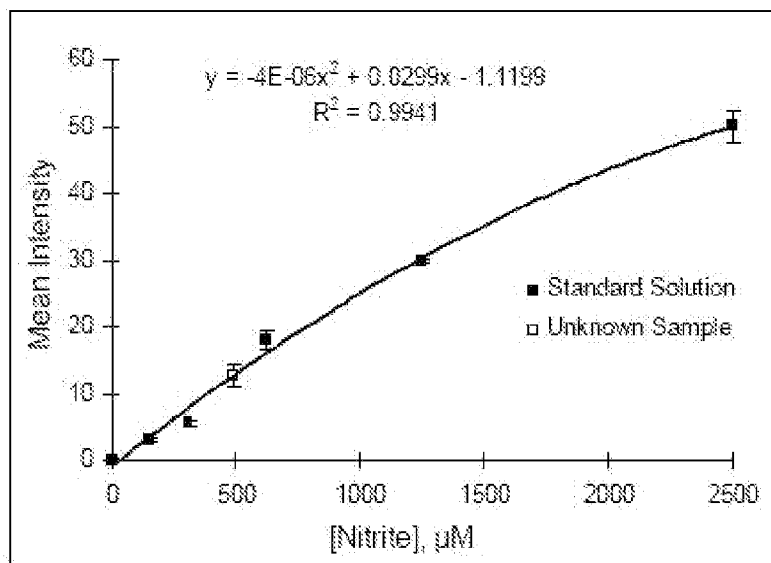


Figure 4

3/3

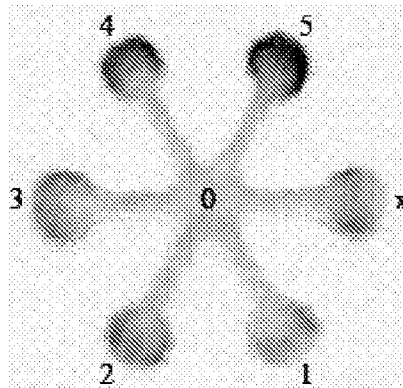


Figure 5

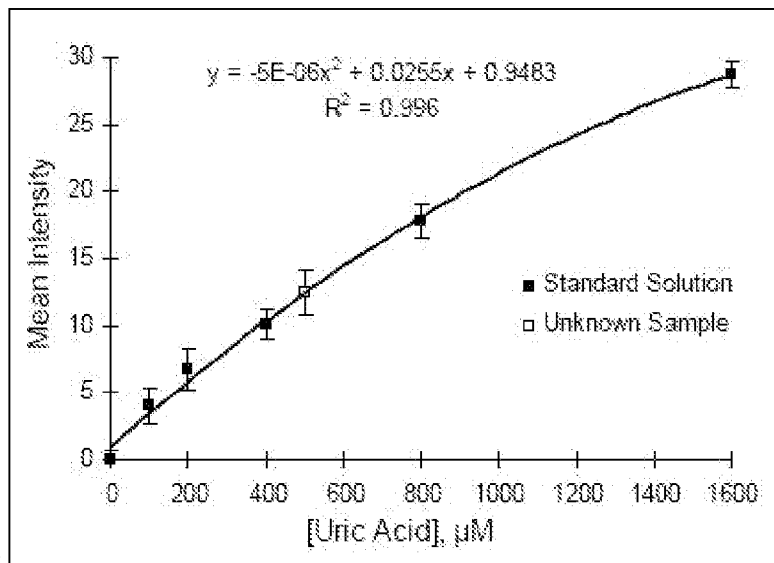


Figure 6

(19) World Intellectual Property Organization
International Bureau



(43) International Publication Date
27 January 2011 (27.01.2011)

PCT

(10) International Publication Number
WO 2011/009164 A1

(51) International Patent Classification:

B81B 1/00 (2006.01) **B01L 3/00** (2006.01)
B01F 3/08 (2006.01) **B81B 3/00** (2006.01)

(21) International Application Number:

PCT/AU2010/000922

(22) International Filing Date:

20 July 2010 (20.07.2010)

(25) Filing Language:

English

(26) Publication Language:

English

(30) Priority Data:

2009903382 20 July 2009 (20.07.2009) AU

(71) Applicant (for all designated States except US):
MONASH UNIVERSITY [AU/AU]; Wellington Road,
Clayton, Victoria 3168 (AU).

(72) Inventors; and

(75) Inventors/Applicants (for US only): **SHEN, Wei**
[AU/AU]; 1 Landen Avenue, Glen Waverley, Victoria
3150 (AU). **LI, Xu** [CN/AU]; 49 Townsend Street, Glen
Waverley, Victoria 3150 (AU). **BALLERINI, David**
Robert [AU/AU]; 23 Ward Avenue, Oakleigh South,
Victoria 3167 (AU). **TIAN, Junfei** [CN/AU]; 3/18 Dover
Street, Oakleigh East, Victoria 3166 (AU).

(74) Agent: **WATERMARK PATENT AND TRADE**
MARK ATTORNEYS; Level 2, 302 Burwood Road,
Hawthorn, Victoria 3122 (AU).

(81) Designated States (unless otherwise indicated, for every
kind of national protection available): AE, AG, AL, AM,
AO, AT, AU, AZ, BA, BB, BG, BH, BR, BW, BY, BZ,
CA, CH, CL, CN, CO, CR, CU, CZ, DE, DK, DM, DO,
DZ, EC, EE, EG, ES, FI, GB, GD, GE, GH, GM, GT,
HN, HR, HU, ID, IL, IN, IS, JP, KE, KG, KM, KN, KP,
KR, KZ, LA, LC, LK, LR, LS, LT, LU, LY, MA, MD,
ME, MG, MK, MN, MW, MX, MY, MZ, NA, NG, NI,
NO, NZ, OM, PE, PG, PH, PL, PT, RO, RS, RU, SC, SD,
SE, SG, SK, SL, SM, ST, SV, SY, TH, TJ, TM, TN, TR,
TT, TZ, UA, UG, US, UZ, VC, VN, ZA, ZM, ZW.

(84) Designated States (unless otherwise indicated, for every
kind of regional protection available): ARIPO (BW, GH,
GM, KE, LR, LS, MW, MZ, NA, SD, SL, SZ, TZ, UG,
ZM, ZW), Eurasian (AM, AZ, BY, KG, KZ, MD, RU, TJ,
TM), European (AL, AT, BE, BG, CH, CY, CZ, DE, DK,
EE, ES, FI, FR, GB, GR, HR, HU, IE, IS, IT, LT, LU,
LV, MC, MK, MT, NL, NO, PL, PT, RO, SE, SI, SK,
SM, TR), OAPI (BF, BJ, CF, CG, CI, CM, GA, GN, GQ,
GW, ML, MR, NE, SN, TD, TG).

Published:

— with international search report (Art. 21(3))

(54) Title: THREE-DIMENSIONAL MICROFLUIDIC SYSTEMS

(57) Abstract: A three-dimensional microfluidic system including: at least one hydrophilic thread along which fluid can be transported through capillary wicking; and at least one hydrophobic substrate for supporting the hydrophilic thread. A method of transporting and mixing a plurality of fluids within a microfluidic system including at least two hydrophilic threads and a hydrophobic substrate having at least two zones, each of the hydrophilic threads supported on a different hydrophobic substrate zone, including: delivering each said fluid to a different hydrophilic thread; and bringing the at least two hydrophilic threads into contact to cause mixing of the fluids.

THREE-DIMENSIONAL MICROFLUIDIC SYSTEMS

FIELD OF THE INVENTION

The present invention is directed to three-dimensional microfluidic systems.

BACKGROUND OF THE INVENTION

Microfluidic systems utilising microfluidic channels are generally limited to fluid flows in two dimensions along the plane of the surface of the substrate supporting the channels. The concept and design of the microfluidic systems is to use capillary channels defined by the physical or chemical barriers to control the flow path of fluids. There are however advantages in being able to have microfluidic channels running in three dimensions, since three dimensional microfluidic systems can substantially reduce the size of microfluidic devices. Also, there is a great advantage of taking a different approach of fabricating microfluidic channels to form microfluidic devices without having to put physical and chemical barriers on the surface of the substrate supporting the channels.

In Honkai Wu, Teri W. Odom, Daniel T. Thui and George M. Whitesides, J. Am. Chem. Soc. 2003, 125, 554 – 559 “Fabrication of complex three-dimensional microchannel systems in PDMS”, such a three-dimensional microfluidic system is described. This paper described a system which utilises channels formed from polydimethylsiloxane (PDMS) which can be fabricated into complex geometries thereby allowing the flow of fluids in more than one plane. The fabrication of such systems is however, complex, and the use of PDMS limits the types of solution that can be passed through the channels. In Martinez A.W.; Phillips S.T. and Whitesides GM. PNAS, 2008, 105, 19606 – 19611 “Three-dimensional microfluidic devices fabricated in layered paper and tape”, a three-dimensional paper-based microfluidic device is described. This paper described the fabrication of the three-dimensional device using a laminated structure of paper and tape. The microfluidic channel pattern was fabricated using photolithography and PDMS. The device fabricated in this manner utilizes the principle of defining physical barrier in a porous substrate; the devices are therefore rigid. For long fluidic channels, a relatively large volume of liquid is required, since the three-dimensional channels must be filled with fluid.

SUMMARY OF THE PRESENT INVENTION

It is therefore an object of the present invention to provide a three dimensional microfluidic system that provides a novel barrier-free fluid transportation concept and overcomes at least one of the disadvantages of
5 known systems.

With this in mind, according to one aspect of the present invention, there is provided a three dimensional microfluidic system including at least one hydrophilic thread along which fluid can be transported through capillary wicking, at least one hydrophobic substrate for supporting the hydrophilic thread. The
10 thread may for example be sewn into or wound around or braided with the hydrophobic substrate depending on the physical characteristics of the substrate. It is envisaged that more than one hydrophilic thread be utilised. Alternatively or in addition, more than one hydrophobic substrate may be used.

According to a preferred embodiment, a plurality of hydrophilic threads
15 may be supported on the at least one hydrophobic substrate, wherein said threads are separate from each other. This enables different fluids to be transported along different threads without any mixing occurring, even though the threads may overlap without contacting. Alternatively, a plurality of hydrophilic threads may be supported on the at least one hydrophobic substrate, wherein at
20 least one pair of said threads are in contact with each other. This allows for a degree of mixing to occur between fluids transported on the different threads that are in contact.

The hydrophobic substrate may be made from any one of a variety of different materials including, but not limited to, polymer, metal ceramic or
25 composites of these materials.

The hydrophobic substrate may preferably be a continuous film through which the hydrophilic thread is woven. Alternatively, the hydrophobic substrate may be a woven sheet through which the hydrophilic thread is interwoven. In another preferred embodiment, the hydrophobic substrate may be a hydrophobic thread
30 about which a said hydrophilic thread is twisted. It is envisaged that the hydrophobic substrate may be a gel or wax for supporting the hydrophilic thread passing therethrough.

The hydrophilic thread may be formed from any hydrophilic material. According to a preferred embodiment of the invention, the hydrophilic thread may be formed from cellulose material. The hydrophilic thread is preferably formed from a continuous filament of hydrophilic material. Alternatively, the hydrophilic thread may be formed from a discontinuous line of hydrophilic powder. The hydrophilic thread may have a diameter of between 1mm and 1nm. Alternatively, the hydrophilic thread may have a cross-section of variable diameter to thereby allow control of the fluid flow rate of the fluid transported along the thread.

According to another aspect of the present invention, there may be provided a three-dimensional microfluidic system including at least one hydrophobic thread supported on a hydrophilic substrate, wherein said fluid is transportable along the thread by capillary wicking. The fluids that can be transported along a hydrophobic thread include non-aqueous fluids such as hydrocarbon fluids, oils and other low surface tension organic fluids.

Preferably the system further includes a switch means for allowing or preventing fluid flow along the at least one hydrophilic thread. The switch means may include at least one hydrophobic segment on the at least one hydrophilic thread and means for bypassing the hydrophobic segment and allowing fluid flow. The bypass means may include a looped hydrophilic thread. Alternatively the bypass means may include a bridging hydrophilic thread.

According to a further aspect of the present invention, there is provided a method of transporting at least one fluid within a microfluidic system including at least one hydrophilic thread, including delivering the fluid to an end of the hydrophilic thread, the fluid being transported along the thread through capillary wicking. Preferably, a plurality of fluids may be transported without mixing through the microfluidic system, as each said fluid is delivered to a different hydrophilic thread, the threads being separate from each other. Alternatively, a plurality of fluids may be transported and mixed through the microfluidic system, by delivering each said fluid to a different hydrophilic thread, the threads being in contact with each other.

According to yet another aspect of the present invention, there is provided a method of detecting a fluid sample within a microfluidic system including at least one hydrophilic thread, including delivering said fluid sample to an end of the

hydrophilic thread for transportation by capillary wicking therealong, at least part of the thread forming a sample detection zone.

According to yet another aspect of the present invention, there is provided a method of transporting and mixing a plurality of fluids within a microfluidic system including at least two hydrophilic threads and a hydrophobic substrate having at least two zones, each of the hydrophilic threads supported on a different hydrophobic substrate zone, including: delivering each said fluid to a different hydrophilic thread; and bringing the at least two hydrophilic threads into contact to cause mixing of the fluids. Preferably the hydrophobic substrate zones are folded together bringing the at least two hydrophilic threads into contact.

The three dimensional microfluidic system according to the present invention may be used in a large number of different applications. The invention may be built within other materials such as woven, non-woven, powder, gel, wax and so on to form microfluidic sensors utilizing colorimetric and non-colorimetric detection principles. The present invention can for example be used to perform Enzyme-linked immunosorbent assay (ELISA) like tests, electrophoresis and chromatographic analyses as well as other more complex reactions and tests. The hydrophilic threads may be used to transport and detect a wide range of liquids including hydrocarbons.

The present invention can therefore be used in applications in bio-assays of different bio-fluids, or in environmental testing of, for example, water quality. Because the microfluidic system can be built into other materials, it has many personal care and military applications as an integrated detection system within, for example, the fabric of the clothes of the civilian or military wearer. The present invention can be used in isolated or combined with any other analytical instrument.

The three-dimensional microfluidic systems according to the present invention have many advantages. It preferably allows for a variety of different fluids to be transported unlike previous systems based on PDMS and other physical barriers where the fluid being transported can physically or chemically react with or swell the barrier. It preferably only requires a relatively small volume of sample fluid, unlike other diagnostic or detection devices. It has been found for example that fluid volumes of as low as 0.1 micro litres can provide usable

results. The systems can preferably be made very compact thereby allowing a high density of circuitry in the devices using the present invention. The production costs may be relatively low due to ease of manufacture and has high design flexibility. These systems could therefore be made as part of a disposable product. A variety of different fluids may be transported, and the fluid flow can preferably be controlled to allow for mixing of fluids or controlling the fluid flow rate by, for example, varying the cross-section of the thread. The present invention can also preferably be readily integrated to operate with different switches and flow control devices.

10 In addition to the requirement for control of flow in microfluidic devices, a need exists for the mixing of reagents and samples. Complex detection chemistries often involve multiple steps and chemical intermediates, and this calls for the ability to mix liquids together onboard lab-on-a-chip devices. For example, rapid mixing is necessary in many microfluidic systems used for biochemical
15 analyses, such as those involving enzymatic reactions.

BRIEF DESCRIPTION OF THE DRAWINGS:

It will be convenient to further describe the invention with respect to the accompanying figures which illustrate preferred embodiments of the three dimensional microfluidic system according to the present invention. Other
20 embodiments of the invention are possible, and consequently, the particularity of the accompanying figures is not to be understood as superseding the generality of the preceding description of the invention.

In the drawings:

Figure 1 shows a first example of three-dimensional microfluidic system
25 according to the present invention;

Figure 2 shows a second example of the three-dimensional microfluidic system according to the present invention;

Figure 3 shows a third example of the three-dimensional microfluidic system according to the present invention;

30 Figure 4 shows a fourth example of the three-dimensional microfluidic system according to the present invention; and

Figure 5 shows a fifth example of the three-dimensional microfluidic system according to the present invention.

Figure 6 shows a sixth example of the three-dimensional microfluidic system according to the present invention.

Figure 7 shows a seventh example of the three-dimensional microfluidic system according to the present invention.

5 Figure 8 shows an eighth example of the three-dimensional microfluidic system according to the present invention.

Figure 9 shows a ninth example of the three-dimensional microfluidic system according to the present invention.

10 Figure 10 shows a tenth example of the three-dimensional microfluidic system according to the present invention.

Figure 11 shows an eleventh example of the three-dimensional microfluidic system according to the present invention.

Figure 12 shows a twelfth example of the three-dimensional microfluidic system according to the present invention.

15 Figure 13 shows a thirteenth example of the three-dimensional microfluidic system according to the present invention.

Figure 14 shows a fourteenth example of the three-dimensional microfluidic system according to the present invention.

20 Figure 15 shows a fifteenth example of the three-dimensional microfluidic system according to the present invention.

Figure 16 shows a sixteenth example of the three-dimensional microfluidic system according to the present invention.

DETAILED DESCRIPTION OF THE PRESENT INVENTION:

25 Thread conducts the flow of liquids via capillary action, with the space between the cellulose fibres of the thread forming capillary channels. Blockage of these channels with glues or waxes can be used strategically to disable the capillary flow of liquids past a certain point in a thread. Using this effect it is possible to simply create flow control devices with thread.

30 As shown in the following examples, thread can be used to construct on/off functional switches which allow the user to enable or disable liquid flow in thread-based microfluidic devices, thus enhancing the possibilities for the fabrication of low-cost thread-based reactors. Different reagents in multi-step reactions can be

introduced into reaction zones simultaneously or separately by simply activating or deactivating switches.

Thread-based devices can also be built as selectors which allow users to direct the samples or reagents they desire to a required location. Moreover, thread can be used as a controllable mixer which is useful when a requirement to mix samples and reagents together at a specific time exists. All of these new and simple types of thread-based microfluidic device components are very low cost and can be easily fabricated without special laboratory equipment, and are therefore suitable for use in underdeveloped areas, remote regions or potentially as point-of-care products globally.

Thread channels can be blocked using commercially available cyanoacrylate-based fast acting adhesive to selectively inhibit liquid flow along a thread. With the application of adhesive or glue, no fluid penetration past the glue-sealed segment is possible. The glue completely blocks the inter-fibre channels within the thread. Also, the glue can be employed to firmly fix thread onto polymer film. These blocking and adhesive characteristics allow switches to be built into thread-based microfluidic devices.

Polypropylene polymer films can be used to support threads and fabricate fold, wedge and pull tab type switches (all of which are detailed below).

The following examples illustrate the operation of the three dimensional microfluidic system in a variety of different situations. The initial five examples illustrate the principles of operation of the three-dimensional microfluidic systems according to the present invention. The remaining examples illustrate embodiments of the invention having flow control arrangements.

Example 1

In one embodiment of the invention as shown in Figure 1, a thread 3 of cotton fibre was treated with a plasma (K1050X) plasma asher (Quorum Emitech, UK) for 5 – 50 seconds at the intensity of 10 – 50 W) to increase its hydrophilicity. The treated thread 3 showed no visible mark or colour change. Several pieces of treated thread 3 were then sewn through a polymer film 5 in a pattern shown in Figure 1 where there are several overlapping circles. This is a three-dimensional pattern where several pieces of thread cross one another, their stitches passing

each other from above and below the polymer film; they therefore do not have contact. These threads define the capillary passageways without the need of a barrier. When fluids were introduced on to different threads, they travel along the thread by capillary effect. Because of the three-dimensional structure, the
5 microfluidic system device allowed the fluids to travel independently without mixing. Such a microfluidic system can be built in multilayers to form a complex fluid transport device. Such a microfluidic system can be used to transport a wide range of fluids, including hydrocarbons, which cannot be transported by microfluidic systems with PDMS barriers.

10 **Example 2**

The second embodiment of the invention as shown in Figure 2, illustrates how a hydrophilic thread can transport a fluid sample without being woven or sewn into a supporting substrate. When one hydrophilic thread 6 forms a braid with a hydrophobic thread 7, the fluid only travels along the hydrophilic thread 6.
15 Figure 2 shows a braid of two cotton threads with one treated with plasma 6 and the other not treated 7. Hydrophilic characteristics of the thread are provided by the plasma treatment. Fluid introduced onto the treated thread 6, only travelled along that hydrophilic thread 6. This has a practical benefit in that the present invention can be incorporated within textiles used for clothing as well as other
20 applications.

When using a sewing machine to sew thread through textile, some machines use two threads, one which goes with the needle, and the other which comes from the bottom. If one of these threads is hydrophilic and the other hydrophobic, liquid will only transport through the hydrophilic thread. Or, a
25 pattern can be sewn where one thread (hydrophobic) holds the other (hydrophilic), but with only hydrophilic thread transporting fluid. The hydrophobic thread that holds the hydrophilic thread will not transport fluid. Alternatively, a hydrophilic thread in a rope can be used to transport or detect a fluid sample, but other threads in the rope will merely be used to provide strength, not transporting
30 fluid samples.

Example 3

The third embodiment of the invention as shown in Figure 3, illustrates how a microfluidic system according to the present invention can be made using hydrophilic threads to mix different fluids during fluid transport along the threads.

- 5 Figure 3 shows, on the left, three plasma treated threads B, Y, M taking fluids of three different colours; with the uppermost thread transporting a blue fluid B, the middle thread transporting a yellow fluid Y, and the lowermost thread transporting a magenta fluid M. The uppermost and middle threads were braided at a central mixing area C whereas the lowermost thread is not. The fluids of the two braided
- 10 threads B, Y mixed to form green fluid G to the right of the central mixing area C, whereas the magenta fluid transported in the lowermost thread M did not undergo mixing as it was not braided with the other threads.

Example 4

- The fourth embodiment of the invention as shown in Figure 4, illustrates
- 15 how a hydrophilic thread can be used to make a sample detector. The amount (in volume) of the liquid introduced onto a thread results in a length of wicking that is proportional to the volume added. The colour change on a single stitch of thread due to the passage of fluid along its length is sufficient to deliver visual detection. Figure 4 shows a series of hydrophilic threads where 0.1, 0.2, 0.4 and 0.8 micro
- 20 Litres of colour fluid were respectively introduced onto each plasma treated thread, from the topmost to lowermost thread. The lengths of the thread that have changed colour due to the transportation of the fluid along the thread are almost proportional to the fluid volumes introduced. The point where the fluid was introduced on each thread is labelled 10 in Figure 4. The uppermost thread had
- 25 0.1 micro Litre of fluid introduced into it. The fluid travelled to the point marked 11 in Figure 4. The point marked 12 corresponds to the point where 0.2 microLitre of fluid was transported. Similarly, point 13 indicates where 0.4 micro Litre of fluid travelled to and point 14 indicates where 0.8 micro Litre of fluid travelled to. This proportionality means that the colour density of the liquid on the thread is not
- 30 affected by how much volume of each sample is added onto a thread. The colour density of the stain will be the same, since the amount of dye per unit length of

the stained thread is the same. Therefore even without an accurate liquid handling device, good analytical results can be obtained.

Example 5

The fifth embodiment of the invention as shown in Figure 5, illustrates how
5 a hydrophilic thread can be used to construct microfluidic sensors with other materials including, but not restricted by, paper, textile and other woven, non-woven material, powdery, gel, wax and a wide range of other materials. In Figure 5 there is shown fluid transported through an aluminium foil substrate 20, with a piece of paper 21 being used as a detector to show the arrival of the fluid. In this
10 arrangement, the hydrophilic thread 23 is used as the liquid transport path and paper 21 is used as the colour-revealing detector. Colour change on the paper can occur on a larger area than on a single stitch of thread and can therefore offer a stronger signal. To do so, the indicator or the sample can be deposited on the piece of paper 21, and the thread 23 can then be used to transport said
15 sample or indicator. Therefore, when the sample travelling along the thread sees the indicator on paper (or when the indicator travelling along the thread sees the sample on the paper), a detectable signal can be collected.

Example 6 - Knot style switch

The sixth embodiment illustrates how a knot on a single piece of thread
20 can be used to create a basic on/off flow control mechanism, referred to as a switch. This is shown in Figures 6 and 9.

The insert to Figure 6 illustrates how to tie a simple overhand knot. An overhand knot with a draw loop is tied in a thread loosely such that it can slide along the length of the thread. A section of the draw loop has a small
25 hydrophobic region created by wetting the thread with a small amount of fast drying adhesive (eg "Supa Glue") which effectively blocks the capillary channels between the cellulose fibres of the thread thus blocking fluid flow in the thread. The knot is then slid and placed over this region so that flow can not occur. The switch is now in the "off" position. When the knot is slid away from the blocked
30 region, fluid is allowed to flow through the length of the thread. The blocked channel area 61 remains unstained despite the movement of magenta ink along the rest of the thread.

In Figure 9, diluted inkjet magenta ink was used to examine the on/off flow along the knotted switch. The switch can be placed in the “off” position by placing the knot over the adhesive-blocked region, causing the ink to stop penetrating when it reaches the blocked region. As illustrated in Figure 9C, after sliding the
5 knot away from the blocked region 61, the ink flows across the knot and through the length of the thread, while the blocked region remains unwet by the fluid. The principal advantage of such a design is in its simplicity. No films or supports are required for this type of switch, it can be produced from a single piece of thread.

Example 7 - Wedge style switch

10 A “wedge” film enabled switching device for binary style flow control is shown in Figures 10A1, 10A2 and 10A3. The device is constructed by cutting two small slits (~5 mm) directly opposite each other and centrally located on opposing edges of a rectangular polymer film. A third slit is then cut in between and perpendicular to the first two and also centrally on the rectangles edge,
15 penetrating inwards approximately half of its width. A thread of the desired length can then be wedged into each of the two outer slits. The free end of one of these two threads can then be tightly wedged into the central slit, while the other thread is only loosely placed in the central slit above the first.

Figure 10A1 shows the unused wedge type switch in the open/off position.
20 The partly wetted wedge switch in Figure 10A2 remains open and disables ink flow. Figure 10A3 shows a closed switch conducting ink flow. Flow is conducted between two threads simply by pulling the thread on the right down 100 and wedging it within a slit in the polymer film 102, where it is locked in contact with the thread on the left 104. Liquid (diluted magenta ink) flows can now easily jump
25 between these threads, creating a continuous flow path. This design can be constructed without much equipment, for example, only thread, scissors and a piece of plastic film is necessary.

Example 8 - Folding style switch with bridge

A fold enabled device is shown in Figure 10B1, 10B2 and 10B3. The
30 device is constructed from a rectangular polymer film, folded into two smaller rectangles of equal area. On one side of the fold, a thread 106 was stitched into the film 102 running parallel with the crease line of the fold, but with a “z” shaped

kink in the centre, its ends fixed to the film by being wedged into small slits. The diagonal section of the “z” shape, which is on the exterior surface of the folded device, was then blocked using adhesive to prevent flow. On the opposing side of the film, a small bridge 108 was sewn which was perpendicular to the fold line and directly opposite the centre of the “z” shape.

Figure 10B1 shows the unused fold type switch in the open/off position. The partially wetted fold switch in Figure 10B2 remains open and disables ink flow. Figure 10B3 shows a reopened fully wetted fold switch after it was used to transport ink flow. This microfluidic switch device is activated by the film being folded onto itself. This brings threads 106, 108 on opposing sides into contact with each other. The small thread section 108 on the left acts as a bridge allowing fluid to jump between different sections of a partially blocked thread 106 on the right. Additionally, other porous materials such as textile and paper can be used to act as bridges to allow on/off flow control on the thread.

15 **Example 9 - Pull-tab activated style switches**

Figure 11 shows a pull tab style switch adapted from a folding style switch. The pull-tab activated device is a simple adaptation of the folding style of on/off functional switches. Any device which is actuated by folding can be adapted to function by a pull tab.

The fold type switch detailed in example 8 above can be adapted to function with “pull-tab” style activation mechanisms. This is achieved by placing a small removable section of polymer film within the device, and then sealing the device permanently folded using adhesive, heat sealing or stapling. When the tab is removed by the user pulling upon it, threads on opposing sides of the device are brought into contact with each other and the switch is activated. An advantage of this method of actuation is its ease of use, as it eliminates the need for the user to hold the device folded shut, and minimises user contact with the internals of the device. Should an application require the incorporation of hazardous reagents, this switch enables them to be entirely enclosed within plastic films reducing the risk of user contact.

Figure 11A shows an unused pull-tab switch before activation. The tab 111 can be identified by the arrow drawn on its end. The pull-tab switch shown in

Figure 11B has an inlet zone 112 loaded with ink solution. The pull-tab switch in Figure 11C has had its tab removed to allow the flow of ink across the device.

The folding type switch can be adapted to a pull-tab switch by sizing a thin piece of polymer film to act as the tab. The tab needs to be large enough to cover
5 the region where the opposing threads contacted each other, but small enough to allow staples or other items to seal the folded device permanently shut. The tab is then inserted into the device which is folded. Staples are driven through both sides of the far edge of the folded device parallel to the crease line, but do not penetrate the tab. Alternatively adhesive or heat sealing could be used as an
10 alternative to stapling.

Example 10 - Selective flow control device

A selective flow control device according to an embodiment of the present invention can be made using only thread and adhesive. The device shown in Figure 12 consists of two threads 121, 123 for conducting fluids and two support
15 threads 122, 124 which are hydrophobic to allow handling. One of the hydrophilic threads 121 was tied to support threads at both ends using simple overhand knots, the topology of which is shown in Figure 7. The centre of this conducting thread is then selectively blocked using adhesive, creating a 5 mm zone where ink flow can not penetrate. The second conducting thread 123 is then tied to the
20 first 121 using a noose knot. The second conducting thread 123 can then be dragged along the first thread 121, and placed on the hydrophobic zone to render the device in the "off" position, also shown in Figure 7.

The two way selector switch device shown in Figure 12 allows a user to choose between two available samples or reagents, giving the ability to direct
25 flow down a particular outlet channel at the time the user desires. Figure 12A shows an unused selector switch set in the off position. Figure 12B shows the selector switch in the off position but loaded with yellow 120 and cyan 125 inks. Figure 12C shows the selector switch conducting ink flow of the yellow ink. When the user selects the flow of yellow ink, the yellow ink flows from the switch to the
30 thread at the base of Figure 12C. Similarly, when the user selects the flow of cyan ink, the cyan ink flows from the switch to the thread at the base of the switch

as indicated in Figure 12D. Figure 12D shows the selector switch in the off position having previously carried the cyan ink.

Alternatively the device can function in reverse, with a single sample or reagent introduced to the lower channel, and the user selecting into which outlet
5 they desire flow to be directed. Such a device is useful in complex systems which possess multiple reactor or detection sites, enabling users to selectively perform different types of analyses with the same device. An alternative design uses a combination of thread and a folding polymer film support. The user can select between different outlets by folding in different directions, or conversely select
10 between different inlets with a single outlet.

Example 11 - Flow mixing device

The ability to mix liquids is important for many applications. A flow mixer requires the most complicated construction process of the embodiments described. Beginning with a folded rectangular film identical to that described for
15 the folding style switch above (example 8), five holes are punched through the film using a sewing needle. Figure 8 describes the location of the holes and can be used as a template. The inlet thread 81 is then sewn into the two holes on the left, and the centre 82 blocked from flow with a small amount of adhesive, the ends of the thread are then secured in small slits 84 as shown. A second thread
20 83 is then sewn into the opposing side and tied as described by step 3 of Figure 8. The final step (step 4) is twisting the two loose ends of the knot into one outlet channel, and securing the twisted threads into another small slit 85. Care must be taken during construction to ensure that the inlet and outlet threads are on the same side of the film.

25 The embodiment of the present invention shown in Figure 13 achieves excellent mixing of two coloured inks at the specific time desired by the user. Mixing occurs when the device 130 is folded bringing the two wet thread sections 131, 132 in contact with the mixing zone 133. In this case, the effectiveness of the mixer is illustrated in Figure 13C by the vibrant green colour 133 which results
30 from the mixing of cyan 132 and yellow 131 inkjet inks. This type of mixing switch is valuable for detection chemistries requiring two or more steps, with a sample being mixed with and then reacting with an initial reagent in a mixer, followed by

further reactions with other reagents in subsequent mixers. Thread-based mixers can also be fabricated with “pull tab” or “sliding bead” activation mechanisms discussed in example 9.

Applications

- 5 The above embodiments of the present invention can be used in various applications. Three examples of applications for the thread-based microfluidic devices are described below. Three sample solutions containing protein, glucose and a mixture of the two analytes were created.

Reactor

- 10 Single switches can be built into the thread-based microfluidic devices to control the sequence and timing of fluid flow into the reaction zones. These devices can be used as low-cost and easy-to-use microfluidic reactors which are suitable for two/multi-step reactions. It is important to choose suitable materials as the reaction zone. Paper, threaded knots or cellulose powder have been
15 shown to be viable options because of their porous structure and absorbent properties. In this application, textile was used as the reaction zone. Textile sheets can simply be cut into the desired shape to achieve well-defined reaction zones using scissors or a fabric guillotine.

- Figure 14 displays a microfluidic reactor which uses a combination of two
20 folding switches 141, 142 and a textile reaction zone (3 × 3 mm, secured using double sided tape). In this case a protein indicator was introduced first by activating the right switch, followed by a sample containing the protein analyte, in the left switch 141, being added to the reaction zone 143, resulting in the colour change shown in Figure 14C. This design allows the user to “load” their own
25 detection chemistries to create functional detectors, as well as execute multi-step reactions. The ends of the two inlet threads can be made to fixed lengths to control the intake quantities of the sample and indicator solutions.

Two-way selector

- In another application of one of the embodiments of the present invention,
30 thread can be fabricated into microfluidic devices which give selective control of liquid flow direction. With different device designs, two or more samples can be

directed into one specified output port, or a single sample can be driven into different outlet channels. For example, a sample solution containing both glucose and protein was used to show one possibility of directing sample flow into different outlet channels, shown in Figure 15. The glucose and protein indicators
5 (0.1 μ L) were deposited onto the upper left 151 and right 152 threads (i.e., the left and right outlet channels) respectively. The indicators were then allowed to dry under ambient conditions for 15 minutes. The sample solution was introduced from the lower thread 153 (i.e., the inlet channel). Figure 15B shows that when the sample solution is selected to flow into the right outlet channel 152, by moving
10 the loop to the right, the colour of the protein indicator changes from yellow to blue-green 155. This shows that the sample solution contained protein and had arrived at the desired channel. The loop is then moved to the left (Figure 15C) to direct the sample flow into the left outlet channel 151. This is illustrated by the development of a yellowish brown colour 156 caused by the glucose indicator
15 present. The results show that thread-based selectors are well suited for practical applications.

Mixer

In yet another application of one of the embodiments of the present invention, the device shown in Figure 16 mixed together two samples. The
20 device then detects the two different biomarker analytes present (glucose and protein) in separate detection zones with the pre-loaded indicators to illustrate the mixing achieved. The two reagents entered the device on the left on different ends of a single thread 161, 162 which had a blocked region 163 to prevent premature mixing. Then the device was folded along the crease 164 to introduce
25 the two sample solutions into the twisted threads 165 for mixing. Finally the mixed solution was split to two streams 166, 167 by dividing the twisted two threads. The protein and glucose indicator had already been deposited onto each end of the split left 166 and right 167 threads respectively. Figure 16B shows samples containing protein and glucose being successfully mixed, with the two
30 components detected separately after mixing, shown by colour change 168, 169.

CLAIMS:

1. A three-dimensional microfluidic system including:
at least one hydrophilic thread along which fluid can be transported through capillary wicking; and
5 at least one hydrophobic substrate for supporting the hydrophilic thread.
2. A three-dimensional microfluidic system according to claim 1 including a plurality of hydrophilic threads supported on the at least one hydrophobic substrate, wherein said threads are separate from each other.
3. A three-dimensional microfluidic system according to claim 1 including a
10 plurality of hydrophilic threads supported on the at least one hydrophobic substrate, wherein at least one pair of said threads are in contact with each other.
4. A three-dimensional microfluidic system according to claim 1, wherein the hydrophobic substrate is a continuous film through which the hydrophilic thread is woven.
- 15 5. A three-dimensional microfluidic system according to claim 1, wherein the hydrophobic substrate is a woven sheet through which the hydrophilic thread is interwoven.
6. A three-dimensional microfluidic system according to claim 1, wherein the hydrophobic substrate is a hydrophobic thread about which a said hydrophilic
20 thread is twisted.
7. A three-dimensional microfluidic system according to claim 1, wherein the hydrophobic substrate is a gel or wax for supporting the hydrophilic thread passing therethrough.
8. A three-dimensional microfluidic system according to any one of the
25 preceding claims, wherein the hydrophilic thread is formed from cellulose material.

9. A three-dimensional microfluidic system according to any one of claims 1 to 7, wherein the hydrophilic thread is a formed from a continuous filament of hydrophilic material.
10. A three-dimensional microfluidic system according to any one of claims 1 to 8, wherein the hydrophilic thread is a formed from a line of hydrophilic powder.
11. A three-dimensional microfluidic system according to any one of the preceding claims, wherein the thread has a diameter of between 1mm and 1nm.
12. A three-dimensional microfluidic system according to any one of claims 1 to 10, wherein the thread has a cross-section of variable diameter.
13. A three-dimensional microfluidic system including at least one hydrophobic thread supported on a hydrophilic substrate, wherein fluid is transported along the thread by capillary wicking.
14. A three-dimensional microfluidic system according to any one of claims 1 to 10, further including a switch means for allowing or preventing fluid flow along the at least one hydrophilic thread.
15. A three-dimensional microfluidic system according to claim 14 wherein the switch means includes at least one hydrophobic segment on the at least one hydrophilic thread and means for bypassing the hydrophobic segment and allowing fluid flow.
16. A three-dimensional microfluidic system according to claim 15 wherein the bypass means includes a looped hydrophilic thread.
17. A three-dimensional microfluidic system according to claim 15 wherein the bypass means includes a bridging hydrophilic thread.
18. A three-dimensional microfluidic system according to any one of claims 14-17 wherein the system includes a pair of hydrophilic threads, and means for

separating the threads and bringing the threads into contact to allow fluid flow from one said thread to the other said thread.

19. A method of transporting at least one fluid within a microfluidic system including at least one hydrophilic thread, including delivering the fluid to an end of the hydrophilic thread, the fluid being transported along the thread through capillary wicking.

20. A method according to claim 19 including transporting a plurality of fluids without mixing through the microfluidic system, including delivering each said fluid to a different hydrophilic thread, the threads being separate from each other.

21. A method according to claim 20 including transporting and mixing a plurality of fluids through the microfluidic system, including delivering each said fluid to a different hydrophilic thread, the threads being in contact with each other.

22. A method of detecting a fluid sample within a microfluidic system including at least one hydrophilic thread, including delivering said fluid sample to an end of the hydrophilic thread for transportation by capillary wicking therealong, at least part of the thread forming a sample detection zone.

23. A method of transporting and mixing a plurality of fluids within a microfluidic system including at least two hydrophilic threads and a hydrophobic substrate having at least two zones, each of the hydrophilic threads supported on a different hydrophobic substrate zone, including:
delivering each said fluid to a different hydrophilic thread; and
bringing the at least two hydrophilic threads into contact to cause mixing of the fluids.

24. A method according to claim 23 wherein the hydrophobic substrate zones are folded together bringing the at least two hydrophilic threads into contact.

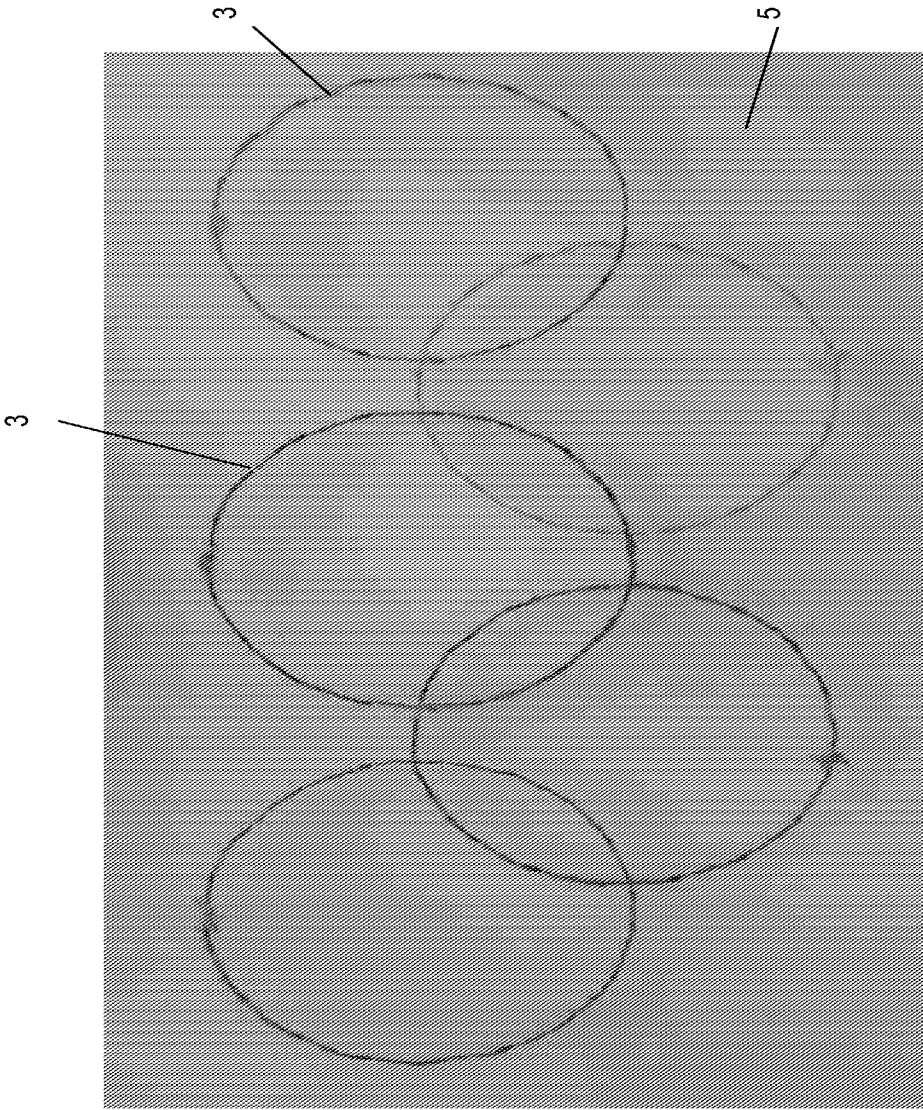


Figure 1

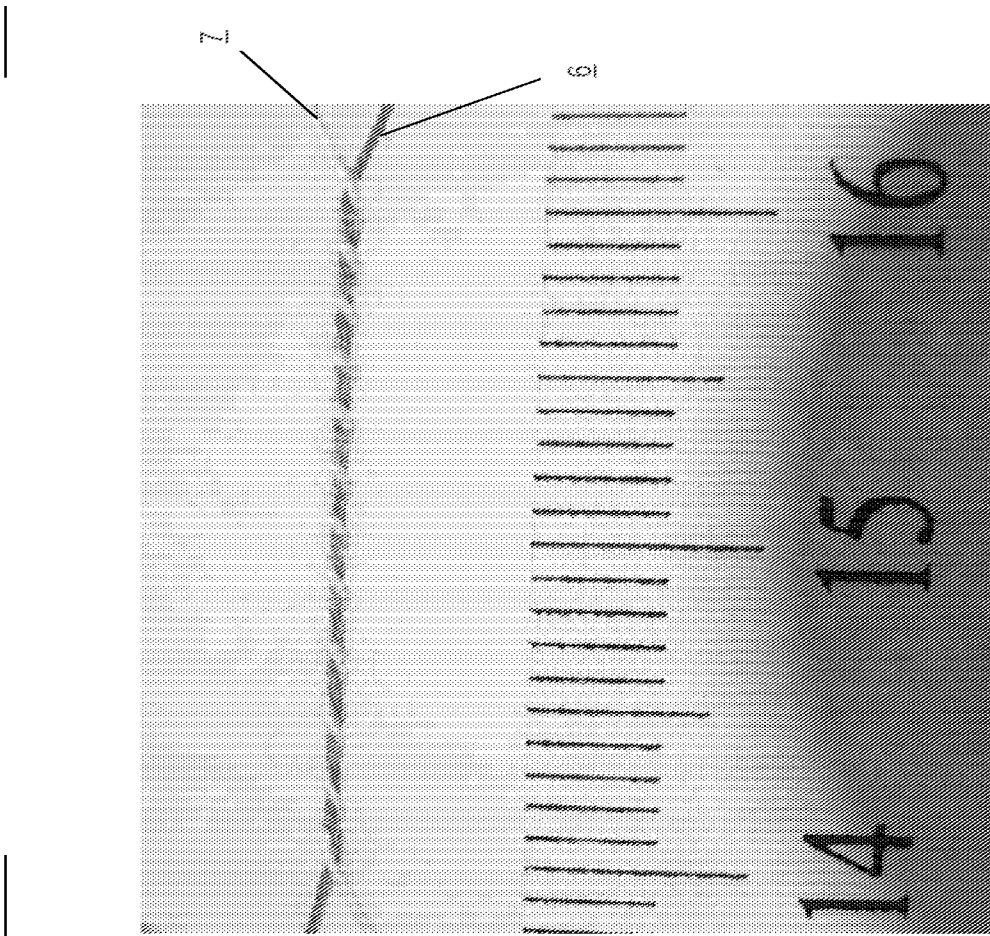


Figure 2

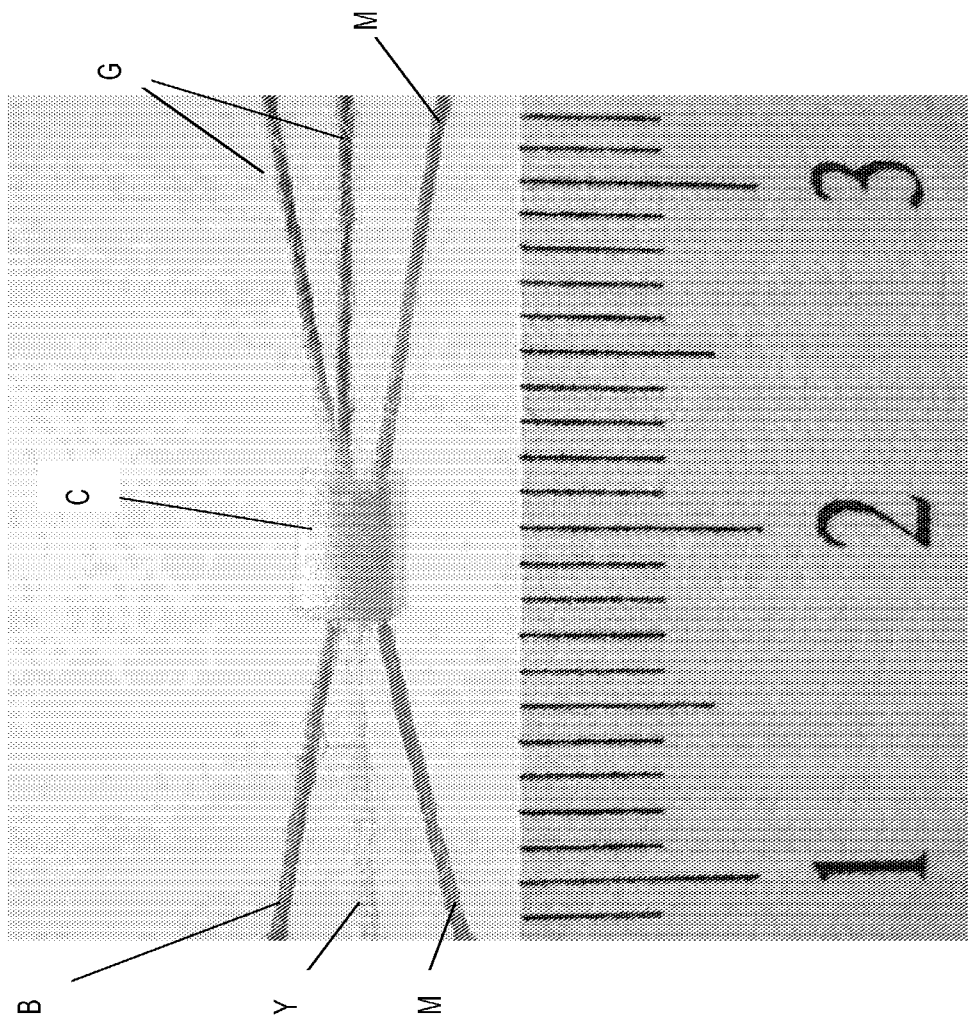


Figure 3

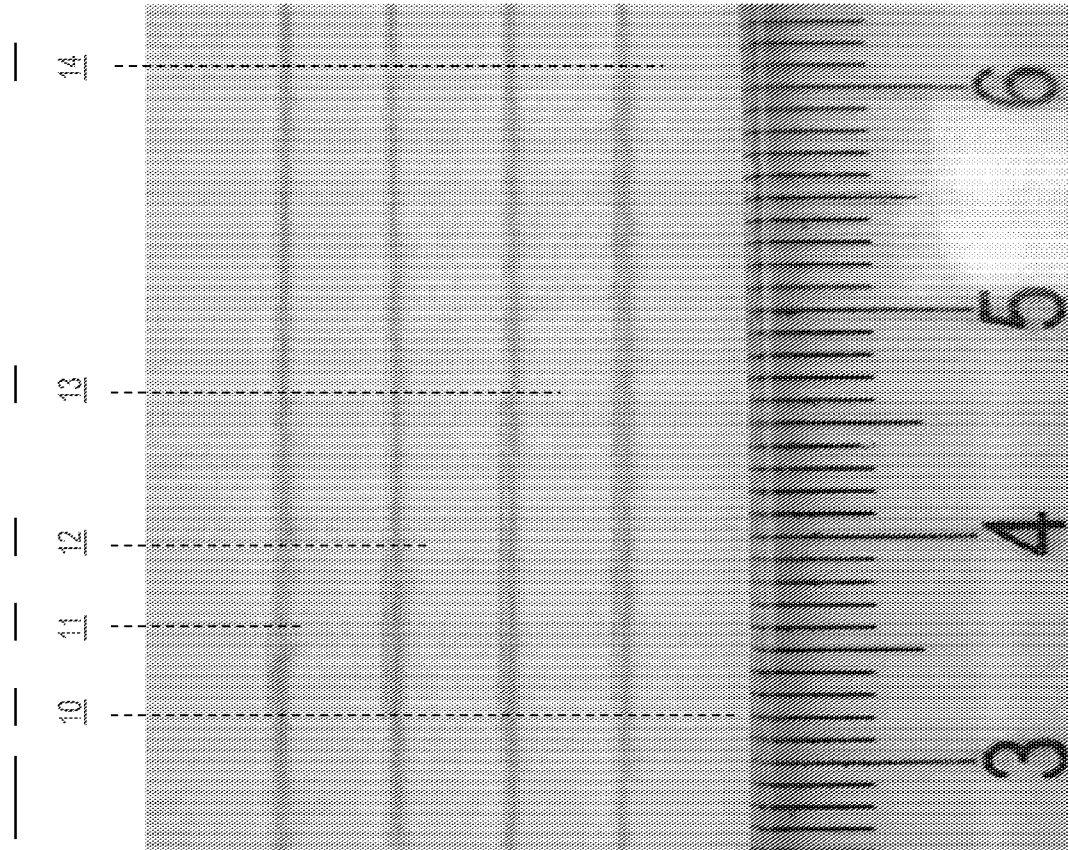


Figure 4

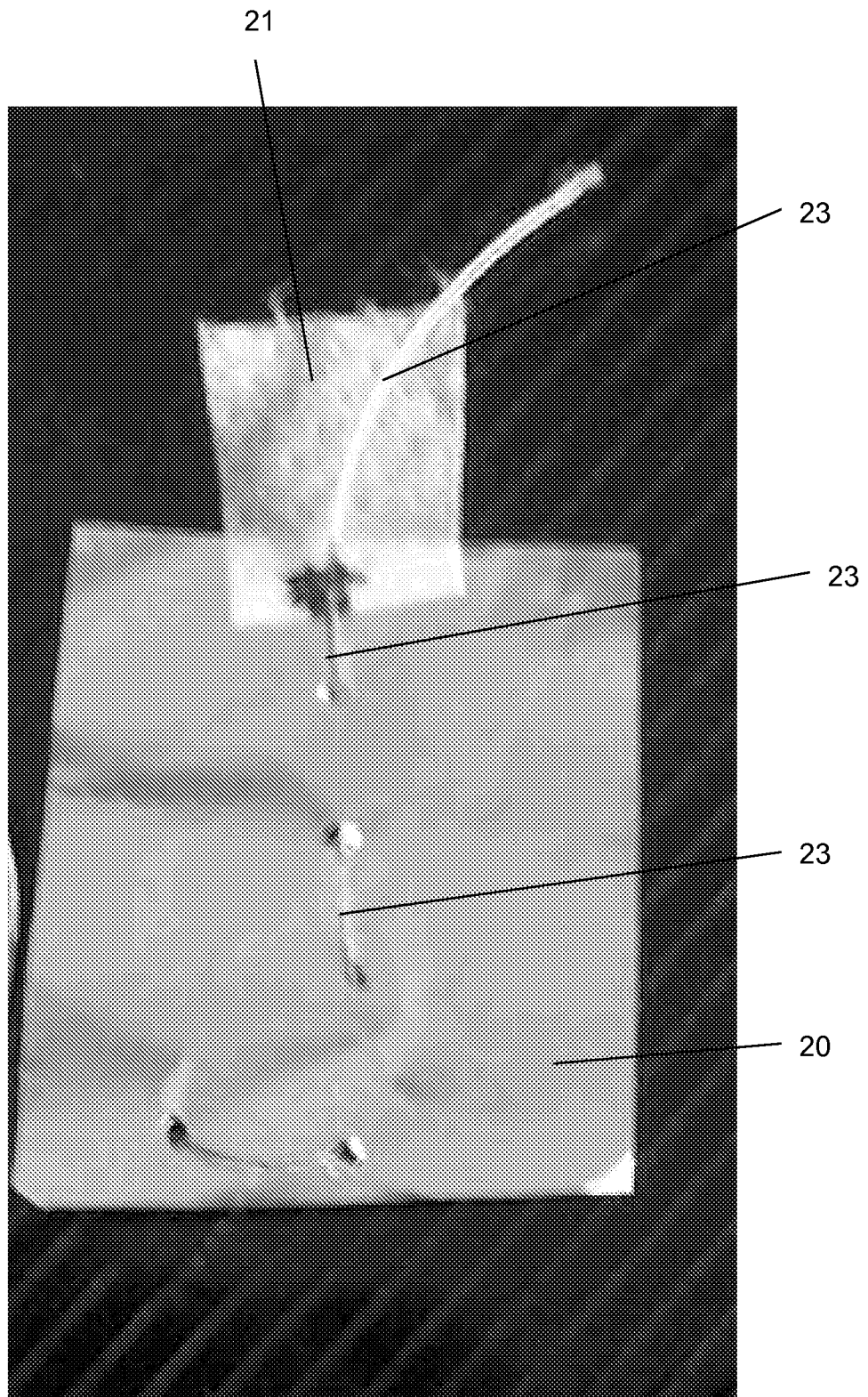


Figure 5

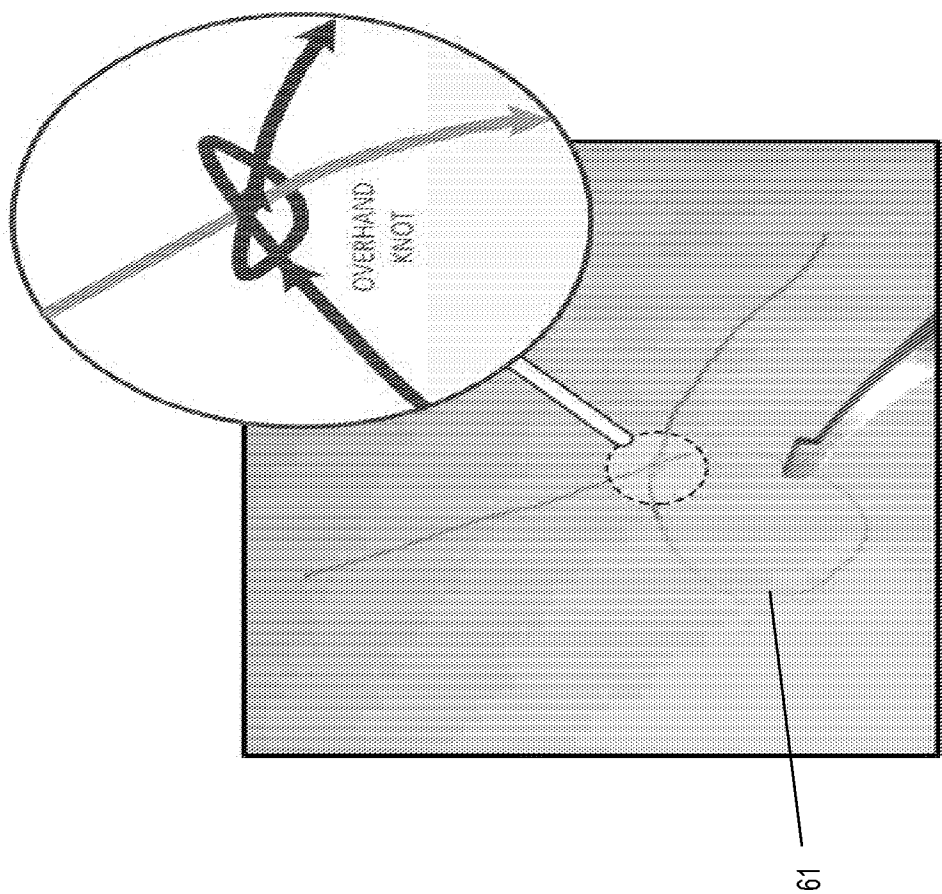
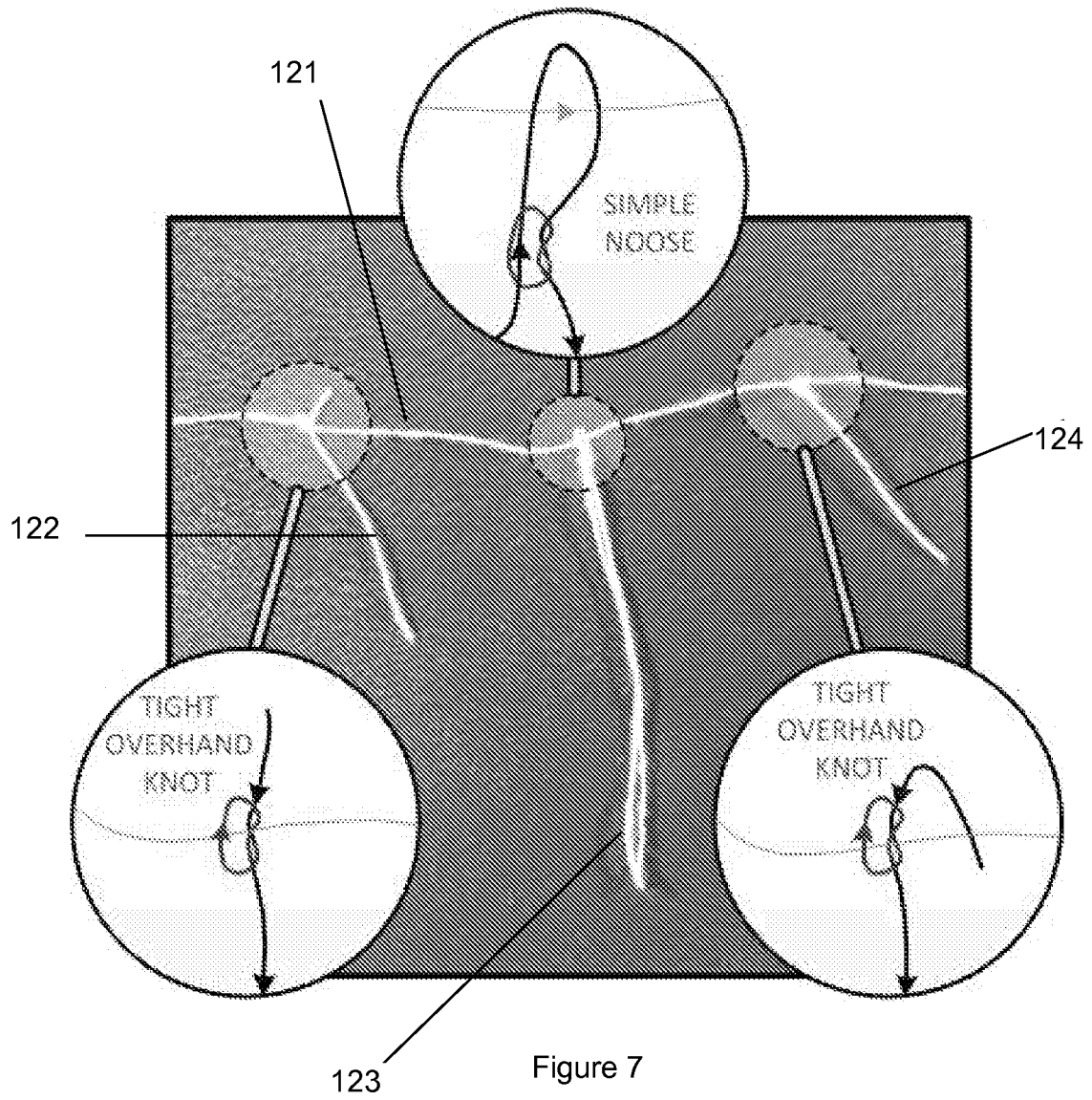
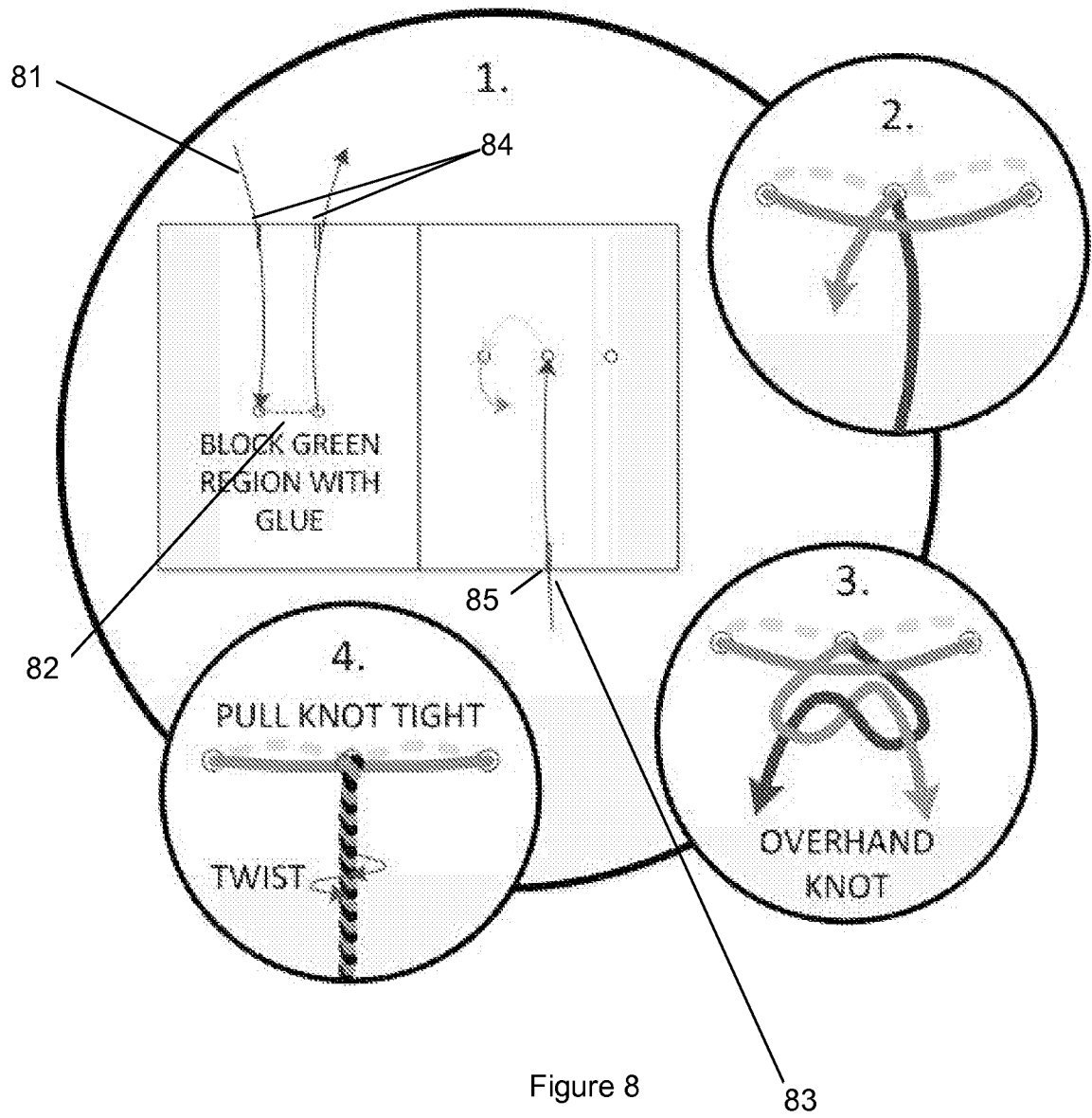
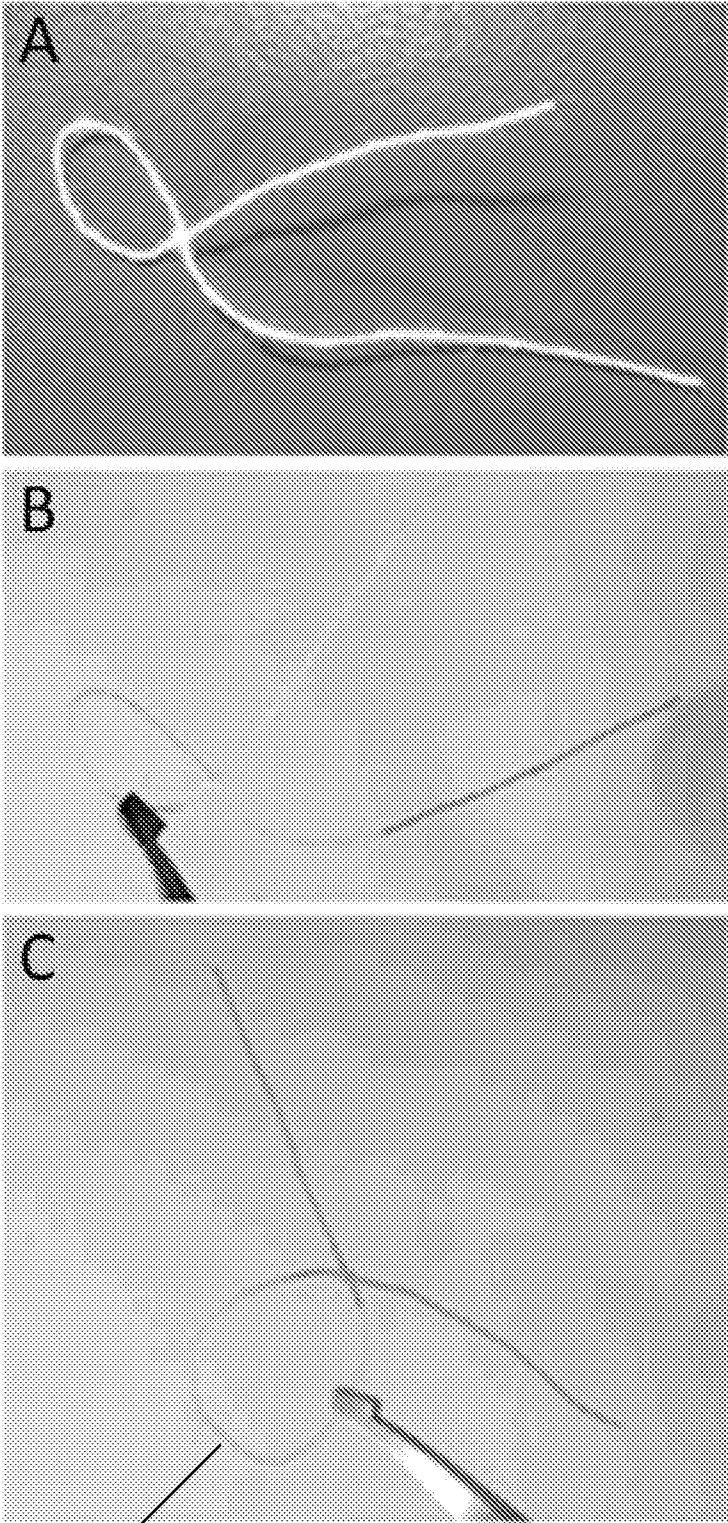


Figure 6







61

Figure 9

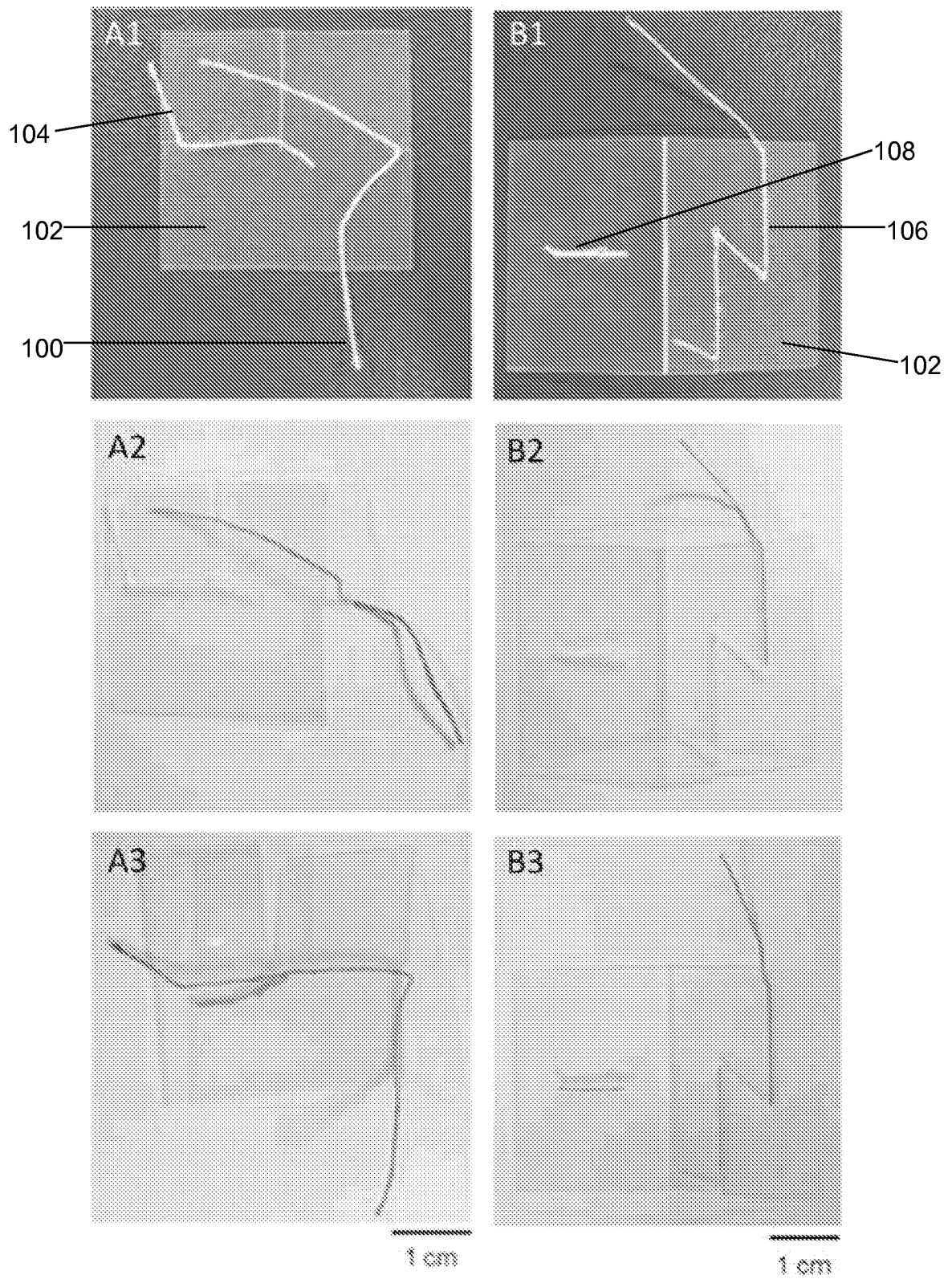


Figure 10

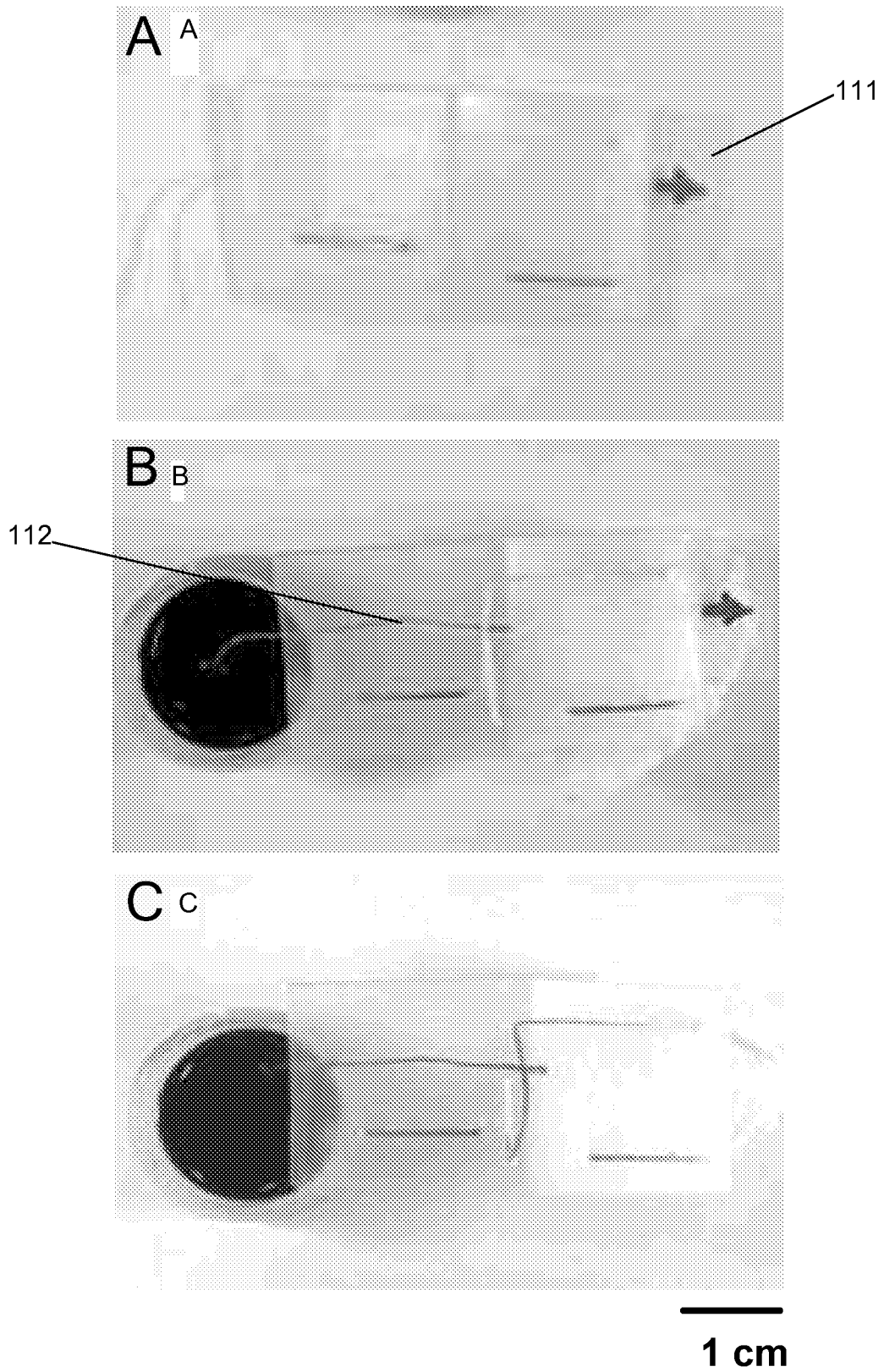


Figure 11

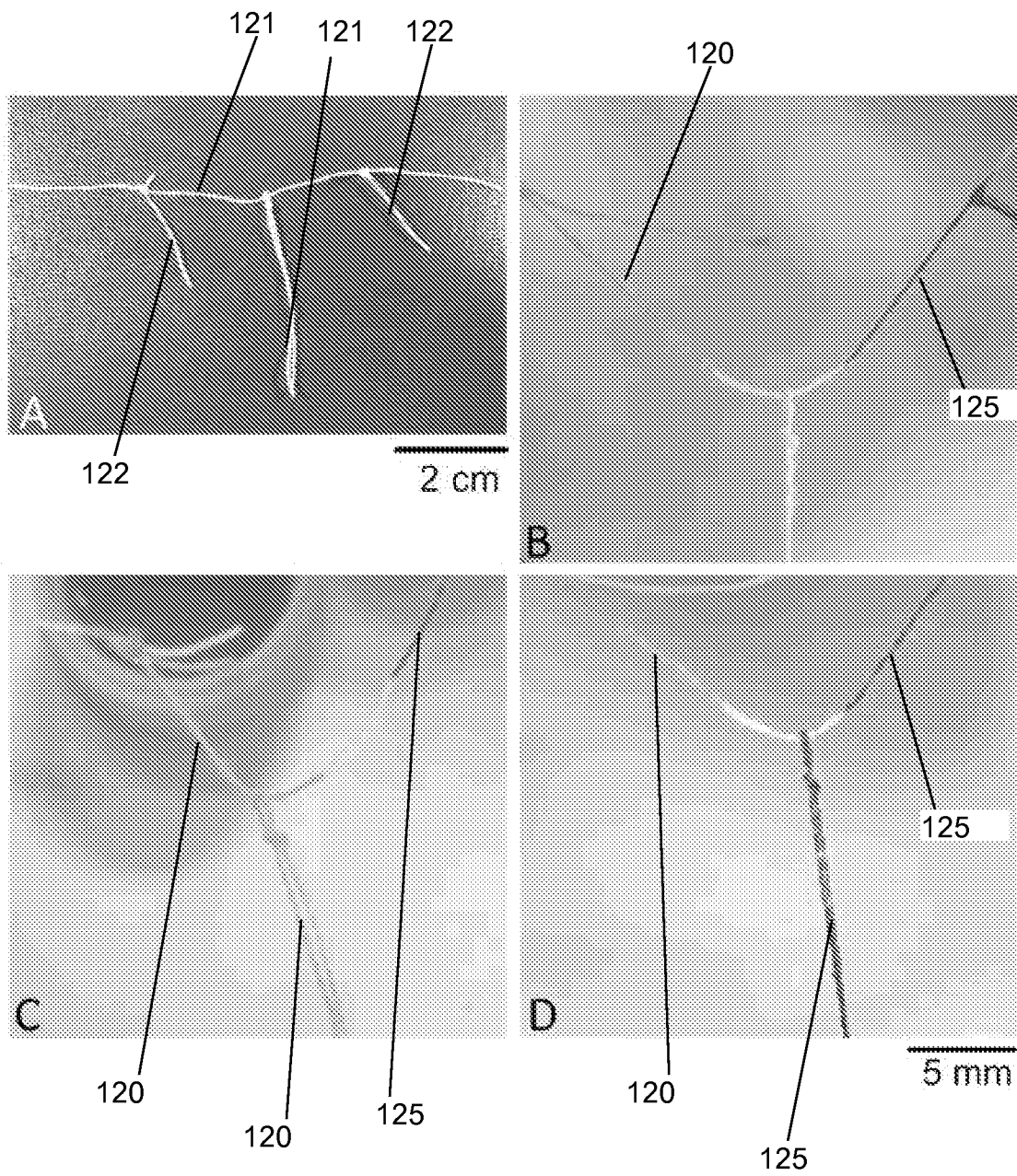


Figure 12

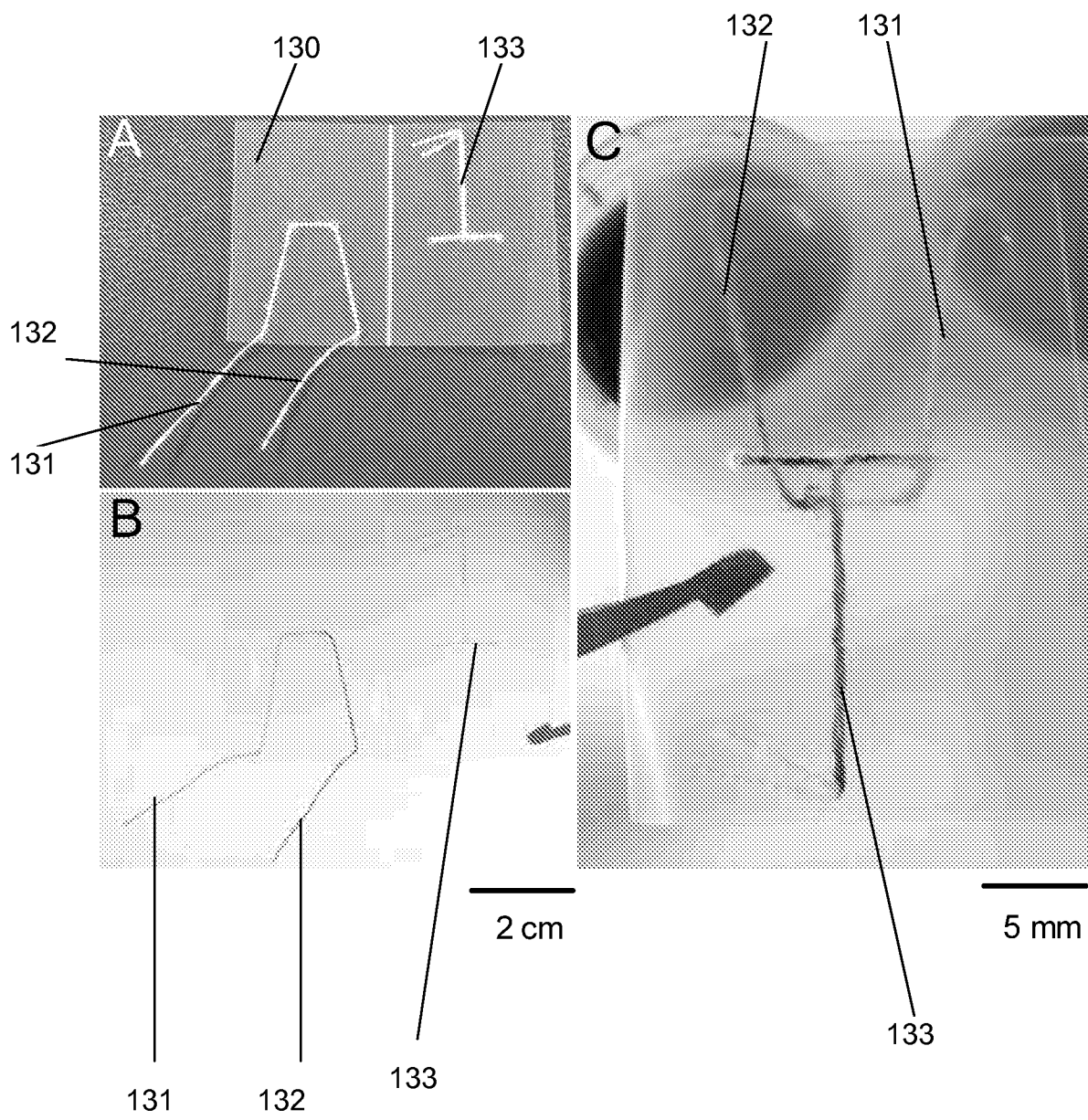


Figure 13

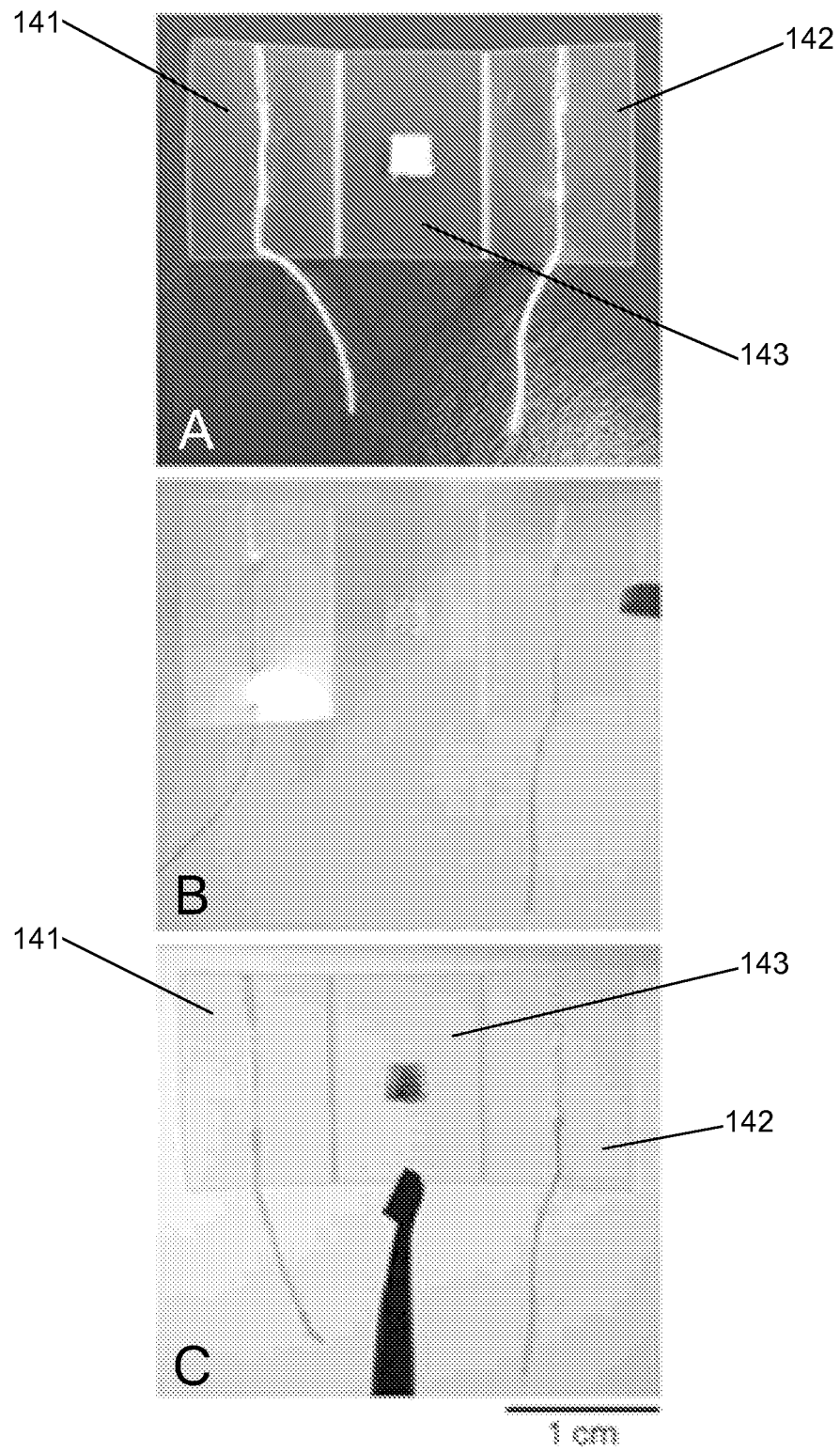


Figure 14

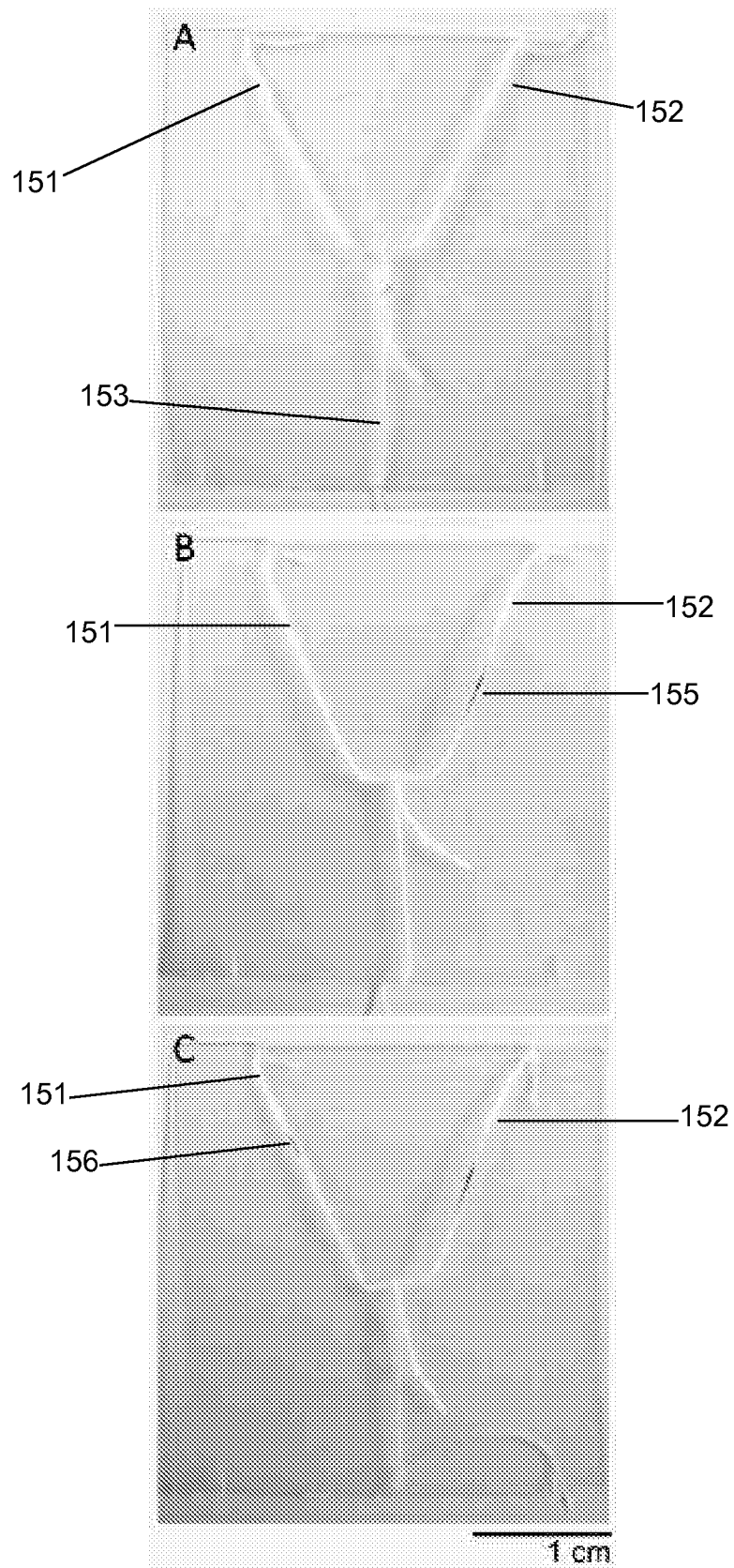


Figure 15

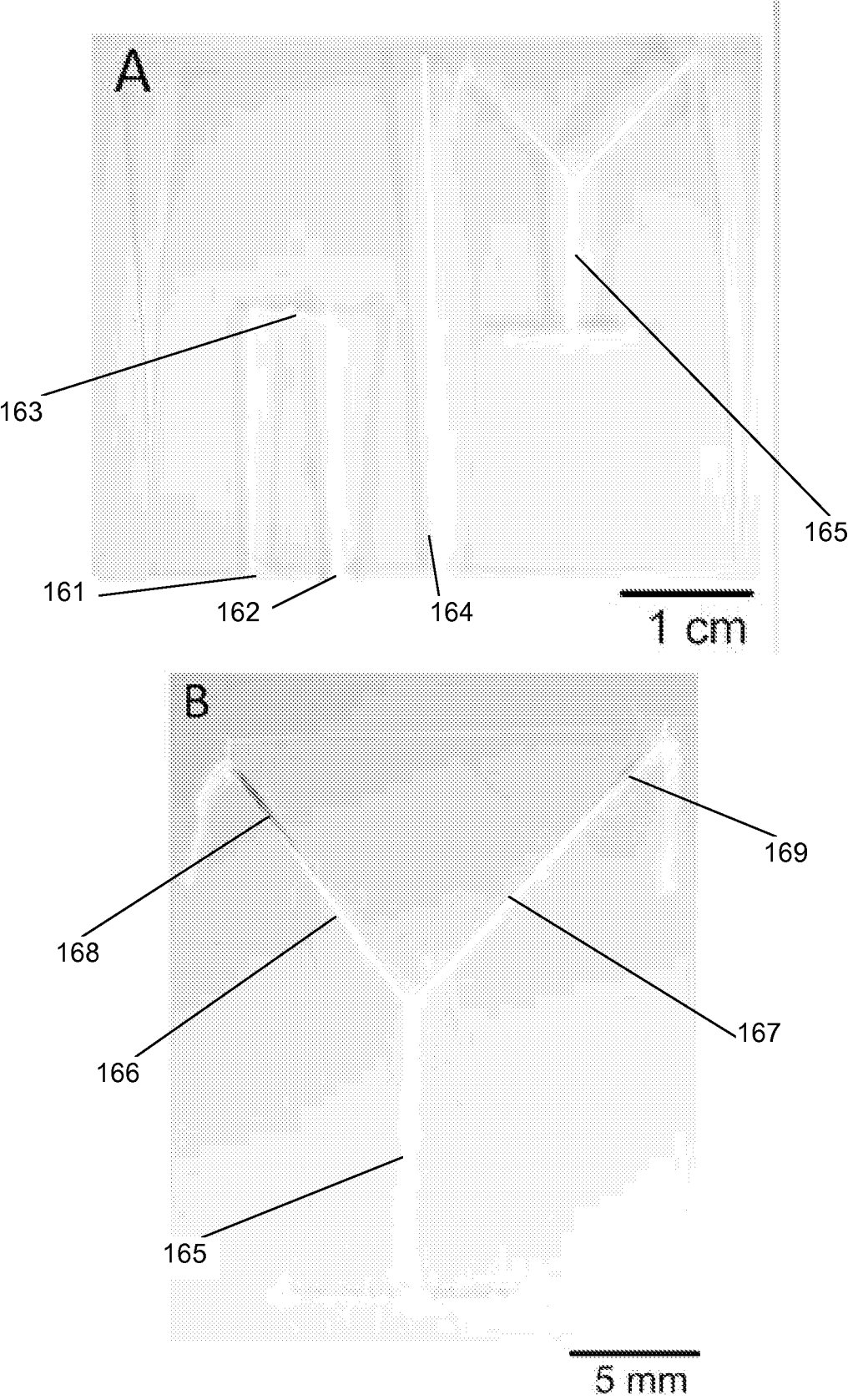


Figure 16

(19) World Intellectual Property Organization
International Bureau



(43) International Publication Date
31 March 2011 (31.03.2011)

(10) International Publication Number
WO 2011/035385 A1

PCT

(51) International Patent Classification:

G01N 33/53 (2006.01) *A61B 5/00* (2006.01)
D21H 25/00 (2006.01) *G01N 30/91* (2006.01)
G01N 33/80 (2006.01)

(21) International Application Number:

PCT/AU2010/001255

(22) International Filing Date:

24 September 2010 (24.09.2010)

(25) Filing Language:

English

(26) Publication Language:

English

(30) Priority Data:

2009904643 24 September 2009 (24.09.2009) AU

(71) Applicant (*for all designated States except US*):
MONASH UNIVERSITY [AU/AU]; Wellington Road,
Clayton, Victoria 3168 (AU).

(72) Inventors; and

(75) Inventors/Applicants (*for US only*): **GARNIER, Gil**
[AU/AU]; 31A Bangalay Avenue, Frankston South, Vic-
toria 3199 (AU). **SHEN, Wei** [AU/AU]; 1 Landen Av-
enue, Glen Waverley, Victoria 3150 (AU). **KHAN, Mo-
hidus Samad** [—/AU]; 1486 North Road, Clayton, Vic-
toria 3168 (AU). **LI, Xu** [CN/AU]; 49 Townsend Street,
Glen Waverley, Victoria 3150 (AU). **THOUAS, George**
[AU/AU]; 2(b) Asquith Street, Box Hill, Victoria 3128
(AU).

(74) Agent: **WATERMARK PATENT AND TRADE
MARK ATTORNEYS**; Level 2, 302 Burwood Road,
Hawthorn, Victoria 3122 (AU).

(81) Designated States (*unless otherwise indicated, for every
kind of national protection available*): AE, AG, AL, AM,
AO, AT, AU, AZ, BA, BB, BG, BH, BR, BW, BY, BZ,
CA, CH, CL, CN, CO, CR, CU, CZ, DE, DK, DM, DO,
DZ, EC, EE, EG, ES, FI, GB, GD, GE, GH, GM, GT,
HN, HR, HU, ID, IL, IN, IS, JP, KE, KG, KM, KN, KP,
KR, KZ, LA, LC, LK, LR, LS, LT, LU, LY, MA, MD,
ME, MG, MK, MN, MW, MX, MY, MZ, NA, NG, NI,
NO, NZ, OM, PE, PG, PH, PL, PT, RO, RS, RU, SC, SD,
SE, SG, SK, SL, SM, ST, SV, SY, TH, TJ, TM, TN, TR,
TT, TZ, UA, UG, US, UZ, VC, VN, ZA, ZM, ZW.

(84) Designated States (*unless otherwise indicated, for every
kind of regional protection available*): ARIPO (BW, GH,
GM, KE, LR, LS, MW, MZ, NA, SD, SL, SZ, TZ, UG,
ZM, ZW), Eurasian (AM, AZ, BY, KG, KZ, MD, RU, TJ,
TM), European (AL, AT, BE, BG, CH, CY, CZ, DE, DK,
EE, ES, FI, FR, GB, GR, HR, HU, IE, IS, IT, LT, LU,
LV, MC, MK, MT, NL, NO, PL, PT, RO, SE, SI, SK,
SM, TR), OAPI (BF, BJ, CF, CG, CI, CM, GA, GN, GQ,
GW, ML, MR, NE, SN, TD, TG).

Published:

— with international search report (Art. 21(3))

(54) Title: TESTING DEVICE FOR IDENTIFYING ANTIGENS AND ANTIBODIES IN BIOFLUIDS

(57) Abstract: A testing device for identifying an antigen or antibody within a biofluid sample including: a substrate having a hydrophilic surface thereon; the surface including a collection zone, and at least one detection zone extending therefrom; wherein the biofluid sample can be mixed with a specific antigen or antibody, and deposited on the collection zone and transferred by capillary action to the detection zone; the antigen or antibody in the biofluid sample reacting with an appropriate said antibody or antigen thereby resulting in a visual indication within the detection zone.

**TESTING DEVICE FOR IDENTIFYING ANTIGENS AND ANTIBODIES IN
BIOFLUIDS**

FIELD OF THE INVENTION

The present invention is directed to the identification of antigens and antibodies within a biofluid. While the invention will be described with specific reference to its use in determining a person's blood type, it is to be appreciated that other applications of the invention are also envisaged.

BACKGROUND TO THE INVENTION

Blood is essential for sustaining living tissue, with the most important roles of supplying oxygen and other soluble nutrients, immune protection and metabolic turnover. While it is a tissue in its own right, blood in a chemical sense can be considered as a stable, highly packed colloid suspension made of red blood cells (erythrocytes, 4-6 million/mL, 6-8 μ m), white cells (leukocytes, 4000-6000 /mL, 10-21 μ m), platelets (150,000-400,000 /mL, 2-5 μ m) carried within a fluid solution (serum) containing a host of biomolecules (eg albumins, fatty acids, hormones), metabolites and electrolytes. A subset of these biomolecules, such as the binding proteins responsible for tissue immunity (antigens) and blood type, are directly adsorbed onto the surface of blood cells. Common portable testing methods for blood include analysis of glucose content, cholesterol, metabolic panel (sodium, potassium, bicarbonate, blood urea nitrogen, magnesium, creatine, calcium, triglycerides), microbial and disease markers and protein molecular profile (liver, prostate). Surprisingly, and in spite of its vital importance, there are no convenient low cost disposable tests available for "on the spot" analysis of blood type. Blood samples are typically outsourced to an analytical laboratory. Reliable low cost tests which are able to instantaneously and reliably provide critical blood analysis without the requirement of sophisticated laboratory analytical instrumentation such as chromatographic and spectroscopic methods, would be invaluable for improving human health in developing countries, where economic resources are limited. Blood analysis is also important in non-human applications, such as veterinary medicine, where there is a demand for low cost and versatile devices suitable for field use.

DESCRIPTION OF INVENTION

With this in mind, according to one aspect of the present invention, there is provided a testing device for identifying an antigen or antibody within a biofluid sample including;

- 5 a substrate having a hydrophilic surface thereon;
 the surface including a collection zone, and at least one detection zone extending therefrom;
 wherein the biofluid sample can be mixed with a specific antigen or antibody, and deposited on the collection zone and transferred by capillary action
10 to the detection zone;
 the antigen or antibody in the biofluid sample reacting with an appropriate said antibody or antigen thereby resulting in a visual indication within the detection zone.

According to another aspect of the present invention there is provided a
15 testing device for identifying an antigen or antibody within a biofluid sample including;

- a substrate having a hydrophilic surface thereon;
 the surface including a collection zone, and at least one detection zone extending therefrom;
20 the detection zone having an antibody or antigen immobilised therein;
 wherein the biofluid sample can be deposited on the collection zone and transferred by capillary action to the detection zone;
 the antigen or antibody in the biofluid sample reacting with an appropriate said antibody or antigen within the detection zone thereby resulting in a visual
25 indication therein.

The substrate may be formed from paper or other cellulosic materials. Alternatively, the substrate may include a chromographic layer thereon or may be a wettable porous medium.

The biofluid sample being tested may preferably be blood, and the visual
30 indication may be due to an agglutination of the blood upon reaction with a specific antibody resulting in reduced wicking and/or separation of the blood in the detection zone.

The substrate surface may have a hydrophilic microfluidic channel pattern thereon defining the collection zone and the detection zone. Preferably, a plurality of detection zones may extend from the collection zone.

It has been found that red blood cell agglutination, triggered by specific antigen interaction, drastically decreases blood wicking and dispersion on paper or chromatographic media. The agglutination process also considerably enhances the chromatographic separation (elution) of the individual blood components, especially the red blood cells from the serum. The testing device according to the present invention can allow direct analysis of blood cells because of this visual indication. This can be performed instantaneously, either with a detection/reporting system built-in to the device or in conjunction with other off-line analytical equipment. The testing device may also allow for the identification and quantification of specific biomolecules (*eg* antigens and antibodies) based on induced coagulation, followed by the wicking and elution (separation) of the soluble protein fraction from the blood sample onto the porous substrate. The blood colloids, whose coagulation directly affects their wicking/separation, can either be present in the fluid of interest, such as the red blood cells of blood, or introduced as nanoparticles (gold, silver, micro-silica, zeolite, titanium dioxide and the like). In the latter case, the nanoparticle is typically covered with the specific counter-biomolecule or molecule of interest used as sensitive reporter component. The colloid particles may be of a size ranging from 1 nm to 100 μ m and may be introduced into the biofluid being analysed.

In the application of the present invention for determining the type of blood group, the present invention may determine the antigens present within a blood sample, the antigens determining whether the blood type is type A, B, O, AB and Rhesus +/- . Antibodies A, B and D (Rhesus) are deposited into separate detection zones. It may also be preferable to include an untreated control zone in one of the detection zones. A drop of blood is then deposited on the central collection zone, the blood sample being transferred by capillary action to each of the detection zones. When the blood sample contacts an appropriate antibody, the reaction of the red blood cells antigen with its corresponding antibody results in agglutination or coagulation of the red cells. This agglutination results in a drop in velocity of the movement of the blood sample along the microfluidic channel

providing the detection zone and separation of the red blood cells from the serum. The velocity of the blood samples travelling along other detection zones with non-specific antibodies is unaffected. This visual contrast facilitates easy and rapid identification of the blood type of the blood sample.

5 The applicant has developed a low cost paper based microfluidic system which is described in International patent application no. PCT/AU2009/000889 details of which are incorporated herein by reference. The microfluidic systems described in this application utilise a paper based substrate, with the described fabrication methods producing hydrophilic microfluidic channels on the paper
10 based substrates. It should be noted that the term paper is used in this application to refer to all cellulosic materials including woven fabrics and non-woven cellulosic material as well as paper. The microfluidic systems described in these applications can be readily adapted for the purpose of the present invention.

15 The testing device according to the present invention may also be used to detect illness as a result of blood cell malfunction on the blood cells being of abnormal shape as is the case with malaria. Alternatively, the testing device according to the present invention may be used to detect illness by identifying the presence of an antigen, antibody, virus (such as HIV, influenza) or protein.

20 In the International application, the microfluidic channels are fabricated by printing a hydrophobic agent on the substrate surface to define a peripheral edge of the microfluidic channels. According to the present invention, the antibody or antigen may also be printed within the microfluidic channels. The technology used, namely ink jet printing technology, may also be used to print the antigen or
25 antibody within the microfluidic channels.

According to a further aspect of the present invention, there is provided a method for identifying an antigen or antibody within a biofluid sample, including:

mixing the biofluid sample with a specific antigen or antibody,

depositing the mixed biofluid sample on a collection zone of a testing
30 device including a substrate having a hydrophilic surface thereon, the surface including said collection zone and at least one detection zone extending therefrom, the biofluid sample being transferred by capillary action to the detection zone; and

identifying the antigen or antibody by a resultant visual indication within the detection zone arising where the antigen or antibody in the biofluid sample reacts with an appropriate said antibody or antigen.

According to yet another aspect of the present invention, there is provided
5 a method for identifying an antigen or antibody within a biofluid sample, including:

depositing the biofluid sample on a collection zone of a testing device including a substrate having a hydrophilic surface thereon, the surface including said collection zone and at least one detection zone extending therefrom, the detection zone having an antibody or antigen immobilised therein, the biofluid
10 sample being transferred by capillary action to the detection zone; and

identifying the antigen or antibody by a resultant visual indication arising where the antigen or antibody in the biofluid sample reacts with an appropriate said antibody or antigen within the detection zone.

BRIEF DESCRIPTION OF THE DRAWINGS

15 It will be convenient to further describe the invention with respect to the accompanying drawings which illustrate preferred embodiments of the testing device according to the present invention. Other embodiments of the invention are possible, and consequently, the particularity of the accompanying drawings is not to be understood as superseding the preceding description of the invention.

20 In the drawings:

Figure 1 shows a testing device according to the present invention used to determine B+ blood;

Figure 2 shows a testing device according to the present invention used to determine O+ blood;

25 Figure 3 shows the testing device according to the present invention using AB+ and B+ blood;

Figure 4 is the testing device according to the present invention showing blood wicking and blood separation as a function of time;

Figure 5 shows a testing device according to the present invention
30 incorporating a valve;

Figure 6 A-F shows the operation of a testing device according to the present invention incorporating valves and switches;

Figure 7 are schematic representations of testing devices according to the present invention adapted for testing different blood types; and

Figure 8 shows the testing device of Figure 7 showing the separation of red blood cells from the blood serum.

5 DETAILED DESCRIPTION OF THE INVENTION

The applicants have discovered that blood agglutination mediated by specific antibody-antigen interactions drastically affects its separation behaviour on contact with paper or any thin layer chromatographic surface. The invention relies on this biochemical phenomenon to control the rate of wicking and
10 separation, which enables (i) identification and quantitative assessment of a specific antibody/antigen, (ii) blood typing, and potentially (iii) identification of blood-borne pathogens as a disease diagnostic. The present invention is intended predominantly for applications in human and veterinary medicine and biotechnology.

15 Standard techniques for detection of blood agglutination are traditionally manual, involve dispensing of antibodies on a glass slide and microscopic visualization. However, the visualisation of agglutination is often subjective, and its automation requires a bank of sophisticated analytical equipment. The present invention provides a single-step blood test that simplifies and circumvents these
20 difficulties.

One application of the invention involves a two step process in which the blood sample is first coagulated/agglutinated by combining it with the specific antibody/antigen of interest, followed by its deposition on the analytical substrate (eg Non-woven paper or porous mesh) on which the sample wicking and
25 separation by elution/chromatography is measured, directly or indirectly. These two mixing steps can be enhanced and more accurately performed by mixing on paper substrates using built-in valving and channelling control features.

A second application of the invention involves a single-step process in which the biofluid/sample is deposited directly on the substrate/device which has
30 previously been treated with the specific antigen/antibody. For this process, the analyte samples simultaneously coagulate and elude on the same substrate. The measured elution velocity and the extent of sample separation are directly related

to the extent of coagulation, enabling the concentration of the biomolecule to be detected and quantified at the same time.

Both applications of the invention can be applied to a test device made of paper or any non-woven chromatographic surface, which are relatively cost effective. These substrates are also able to be modified with the use of advanced printing techniques to create microfluidic features composed of hydrophobic materials, as previously described in the applicant's International application no. PCT/AU2009/000889. Combined with methods of direct antibody deposition using printing, manufacture and placement of antibody reagent can enable very accurate spatial control of blood flow within the paper substrate.

EXAMPLES

Example 1: Sequential agglutination/coagulation of blood followed by wicking on paper: B+ (two step process) (See Figure 1)

Antibody A and B (Epiclone™ Anti-A, Anti-B, and Anti-D; CSL, Australia) solutions were used. Anti-A and Anti-B come as blue and yellow colour reagents, respectively. 'B+' blood was used in this study. The blood sample was supplied into plastic vials with anti-coagulant. 'B+' blood was separately mixed with pure Anti-A and Anti-B (as received) to prepare 100µL solution. Paper strips (70mm×2mm) were made from Whatman#4 filter paper on which 2 mm unit marks were printed. The paper strips were soaked into phosphate buffer saline (PBS). Excess PBS was removed from the paper strips using standard blotting papers (Drink Coster Blotting, 280 GSM). The paper strips were then placed on Reflex Paper (80 GSM). 20 µL of every mixed solution was dispensed at the centre of paper strip using a calibrated micro-pipette. Pictures were taken after 4 minutes wicking.

It can be seen that:

B+ blood mixed with the solution of antibody A wicked and did not separate upon mixing and paper elution/wicking.

B+ blood mixed with the solution of antibody B wicked and STRONGLY separated (red cells from serum) and showed wicking.

B+ blood mixed with the solution of antibody D (Rhesus +) wicked and STRONGLY separated (red cells from serum).

A blood sample agglutinated/coagulated upon contact with its specific antibodies separated/eluded upon contact with paper (here Blood B+ with Anti-B
5 and Anti-D antibodies).

A blood sample upon contact with non-specific antibody (here Blood B+ with Anti-A) does not agglutinate and does not separate/elute upon contact with paper.

This dramatic difference in elution/separation of blood/antibody mixing can
10 be used to communicate specific agglutination and therefore can be used to identify blood typing.

Example 2: Sequential agglutination/coagulation of blood followed by wicking on paper: O+ (two step process) (See Figure 2)

Antibody A and B (Epiclone™ Anti-A, Anti-B and Anti-D; CSL, Australia)
15 solutions were used. Anti-A and Anti-B come as blue and yellow colour reagents, respectively. 'O+' blood was used in this study. The blood sample was supplied into plastic vials with anti-coagulant. 'O+' blood was separately mixed with Anti-A and Anti-B to prepare 100µL solution. Paper strips (70mm×2mm) were made from Whatman#4 filter paper on which 2 mm unit marks were printed. The paper
20 strips were soaked into phosphate buffer saline (PBS). Excess PBS was removed from the paper strips using standard blotting papers (Drink Coster Blotting, 280 GSM). The paper strips were then placed on Reflex Paper (80 GSM). 20 µL of every mixed solution was dispensed at the centre of paper strip using a calibrated micro-pipette. Pictures were taken after 4 minutes wicking.

25 It can be seen that:

O+ blood mixed with the solution of antibody A wicked and did not separate upon mixing and paper elution/wicking.

O+ blood mixed with the solution of antibody B wicked and did not separate (red cells from serum) and showed wicking.

30 O+ blood mixed with the solution of antibody D (Rhesus +) wicked and STRONGLY separated (red cells from serum).

A blood sample agglutinated/coagulated upon contact with its specific antibodies separated/eluded upon contact with paper (here Blood O+ with Anti-D antibodies).

5 A blood sample upon contact with non-specific antibody (here Blood O+ with Anti-A and Anti-B) does not agglutinate and does not separate/elute upon contact with paper.

This dramatic difference in elution/separation of blood/antibody mixing can be used to communicate specific agglutination and therefore can be used to identify blood typing.

10 Example 3: Simultaneous agglutination/coagulation of blood followed by wicking on paper: Effect of antigen concentration (one step process) (See Figure 3)

In another embodiment of the invention, the paper is first treated with specific antibodies, dried or conditioned before been exposed to a sample of pure blood. This example provides a single step treatment in which the only
15 requirement is to deposit a drop of blood on the paper. This example also illustrates the effect of diluting the antibody solution on the wicking and separation performance of blood on paper. Antibody dilution affects the ratio blood (with its antigen) antibody.

Antibody A and B (Epiclone™ Anti-A and Anti-B; CSL, Australia) solutions
20 were used. Anti-A and Anti-B come as blue and yellow colour reagents, respectively. "AB+" and 'B+' blood were used in this study. The blood sample was supplied into plastic vials with anti-coagulant. Paper strips (70mm×2mm) were made from Whatman#4 filter paper on which 2 mm unit marks were printed. Paper strips were soaked into antibody solutions of different concentrations
25 (Anti-A@1.0x, 0.8x, 0.6x, 0.4x, 0.2x and 0.0x); phosphate buffer saline (PBS) was used as diluent. Excess antibody was removed from the paper strips with blotting papers. The antibody (Anti-A) active paper strips were then placed on Reflex Paper. Blood drops of 20µL were dispensed at the centre of paper strip using a calibrated micro-pipette. The wicking distance was measured from centre to
30 either direction. Pictures were taken after 10 minutes.

The results are shown in Figure 3. It can be seen that:

Blood separates upon wicking with its specific antibody treated paper.

Blood separation is a non-linear function of the antibody concentration on the treated paper. The higher the antibody concentration, the more abrupt is the cell separation from the serum.

There is an optimum concentration to maximize
5 wicking/separation/visualization.

Coagulation of red cell upon contact with its specific antibody drastically reduces its wicking/diffusion speed on the chromatographic surface, which promotes separation of cells from the serum. This drastic reduction and differentiation of elution speeds can serve as direct indicator of the type of blood.

10 Example 4: Effect of time on the wicking/separation of blood on bioactive antibody paper (see Figure 4)

In another embodiment of the invention, the paper is first treated with specific antibodies, dried or conditioned before been exposed to a sample of pure blood. This example illustrates the effect of contact time blood-antibody treated
15 paper on the wicking and separation performance of blood on paper.

Antibody A and B (Epiclone™ Anti-A; CSL, Australia) solutions were used. Anti-A comes as a blue colour reagent. "AB+" blood was used in this study. The blood sample was supplied into plastic vials with anti-coagulant. Paper strips (70mm×2mm) were made from Whatman#4 filter paper on which 2 mm unit
20 marks were printed. Paper strips were soaked into antibody solutions (Anti-A@); phosphate buffer saline (PBS) was used as diluent. Excess antibody was removed from the paper strips with blotting papers. The antibody (Anti-A) active paper strips were then placed on Reflex Paper. Blood drops of 20µL were dispensed at the centre of paper strip using a calibrated micro-pipette. The
25 wicking distance was measured from centre to either direction. Pictures were taken after different intervals of time.

It can be seen that:

blood wicking/separation levels off after about 4 minutes.

There is a minimum time of contact of antibody-blood required to allow
30 proper blood coagulation/agglutination and wicking/separation.

There is an optimum time of contact of blood-antibody-paper. Too short, the blood does not properly coagulate; too long, the separation of red cell and serum can lose some of its sharpness.

Example 5: Paper microfluidic system to control flow, reaction and dilution (see Figure 5)

In the embodiment of the invention, paper-based microfluidic reactors can be used to conduct blood type tests. Specific antibodies are printed into the reactor designed on paper. Then blood cell suspension is introduced into the same reactor. The required period of time is allowed so that the antibodies and cell suspension can contact and mix. After a preset period of time, the valve of the reactor is closed to facilitate penetration of blood across the valve. If only the penetration of serum is observed, the test is positive because of agglutination of blood during the mixing time. If the penetration of blood is observed, the test is negative. Thus paper-based microfluidic reactor can provide a rapid visual test of blood type.

Example 6: Microfluidic system with valves (see Figure 6)

Paper microfluidic devices can be designed to increase the ratio of blood/antibody and to provide the required time delay to allow blood and antibody interactions before the test. This example shows that all these steps can be performed using a paper device. Figure 6 shows the design of the paper device. (A) A filter paper sheet is printed and cut as shown, and specific antibodies are either printed or deposited in the circled region. A paper switch is made on the right hand side of the device. (B) Blood sample is introduced onto the indicated region. (C) The cut paper is folded towards the blood sample as shown. (D) Blood sample is allowed to stay in contact with the antibody loaded paper for a set time. (E) After a short period of contact time, the switch is closed as shown. If the test is positive, blood will agglomerate and only serum will wick out along the switch. (F) After a short period of contact, the switch is closed as shown. If the test is negative, blood will not agglomerate and will wick out along the switch.

Example 7: Paper microfluidic system for blood typing (See Figure 7)

In another embodiment of the invention, a microfluidic system is printed on paper or a chromatographic medium and antibodies A, B and D (Rhesus) are printed into each of the 3 detection arms. Blood typing is analysed by placing a blood droplet in the middle reservoir and reading the results. All the different combinations of blood type and their representations are represented in Figure 7.

Example 8: Chromatographic Separation of RBC/Blood Serum on Paper (See Figure 8)

Figure 8 illustrates blood group detection using chromatographic separation of red blood cells (RBC) and blood serum on antibody active paper surface; (a) schematic of chromatographic separation on paper bioassay; (b) and (c)(I) are trial 1 and 2 using A+ blood sample, respectively; (b)(II), (c)(II) are the converted images of (b)(I), (c)(I) (RGB colour to BRG colour), respectively, for better resolution.

Modifications and variations as would be deemed obvious to the person skilled in the art are included within the ambit of the present invention as claimed in the appended claims.

CLAIMS:

1. A testing device for identifying an antigen or antibody within a biofluid sample including:
 - a substrate having a hydrophilic surface thereon;
 - 5 the surface including a collection zone, and at least one detection zone extending therefrom;
 - wherein the biofluid sample can be mixed with a specific antigen or antibody, and deposited on the collection zone and transferred by capillary action to the detection zone;
 - 10 the antigen or antibody in the biofluid sample reacting with an appropriate said antibody or antigen thereby resulting in a visual indication within the detection zone.
2. A testing device for identifying an antigen or antibody within a biofluid sample including:
 - 15 a substrate having a hydrophilic surface thereon;
 - the surface including a collection zone, and at least one detection zone extending therefrom;
 - the detection zone having an antibody or antigen immobilised therein;
 - wherein the biofluid sample can be deposited on the collection zone and
 - 20 transferred by capillary action to the detection zone;
 - the antigen or antibody in the biofluid sample reacting with an appropriate said antibody or antigen within the detection zone thereby resulting in a visual indication therein.
3. A testing device according to claim 1 or 2, wherein the substrate is formed
- 25 from paper or other cellulosic materials.
4. A testing device according to claim 1 or 2, wherein the substrate includes a chromatographic layer thereon or other wettable porous media.

5. A testing device according to claim 1 or 2, wherein the substrate surface has a hydrophilic microfluidic channel pattern thereon defining the collection zone and the detection zone.
6. A testing device according to claim 5, including a plurality of detection zones extending from the collection zone.
7. A testing device according to claim 1 or 2, wherein biofluid sample being tested is blood, and the visual indication is due to an agglutination of the blood upon reaction with a specific antibody resulting in reduced wicking and/or separation of the blood in the detection zone.
8. A testing device according to claim 7, wherein the testing device includes at least one valve for controlling the wicking of biofluid to the detection zone from the collection zone.
9. A testing device according to claim 7, wherein the testing device includes a switch for controlling the contact of the biofluid with the antibody or antigen.
10. A method for identifying an antigen or antibody within a biofluid sample, including:
- mixing the biofluid sample with a specific antigen or antibody;
 - depositing the mixed biofluid sample on a collection zone of a testing device including a substrate having a hydrophilic surface thereon, the surface including said collection zone and at least one detection zone extending therefrom, the biofluid sample being transferred by capillary action to the detection zone; and
 - identifying the antigen or antibody by a resultant visual indication within the detection zone arising where the antigen or antibody in the biofluid sample reacts with an appropriate said antibody or antigen.
11. A method for identifying an antigen or antibody within a biofluid sample, including:

depositing the biofluid sample on a collection zone of a testing device including a substrate having a hydrophilic surface thereon, the surface including said collection zone and at least one detection zone extending therefrom, the detection zone having an antibody or antigen immobilised therein, the biofluid
5 sample being transferred by capillary action to the detection zone; and

identifying the antigen or antibody by a resultant visual indication arising where the antibody or antigen in the biofluid sample reacts with an appropriate said antigen or antibody within the detection zone.

12. A method as claimed in claim 10 or 11, including mixing nanoparticles
10 within the biofluids sample to facilitate said reaction in the detection zone.

13. A method according to any one of claims 10 to 12, wherein biofluid sample being tested is blood, and the visual indication is due to an agglutination of the blood upon reaction with a specific antibody resulting in reduced wicking and/or separation of the blood in the detection zone.

15 14. A method according to claim 13, including detecting blood type from the visual indication.

15. A method according to claim 13 including detecting illness from the visual indication.

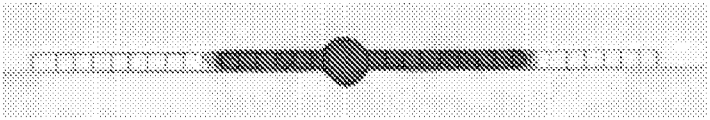
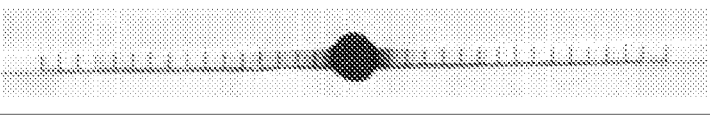
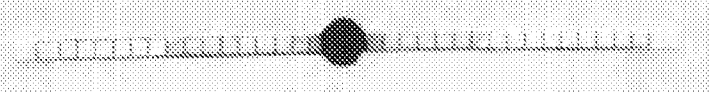
Blood sample mixed with antibody solutions	Blood Sample -B+
Anti-A	
Anti-B	
Anti-D	

Figure 1

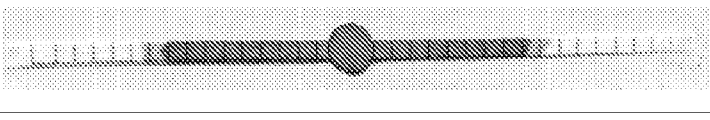

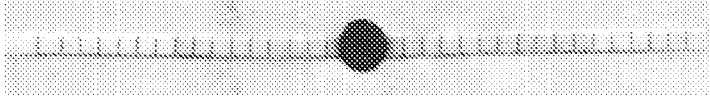
Blood sample mixed with antibody solutions	Blood Sample O+
Anti-A	
Anti-B	
Anti-D	

Figure 2

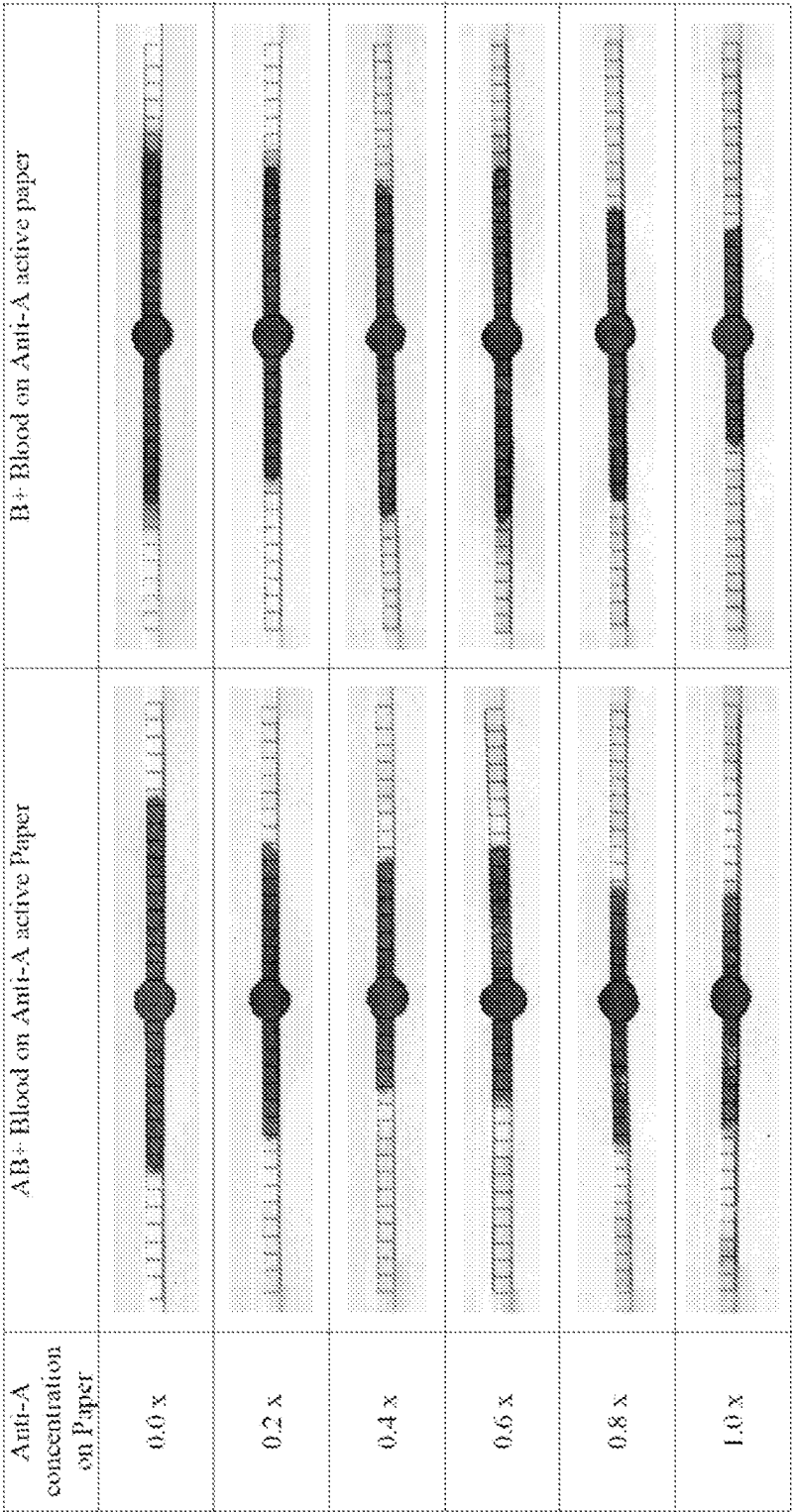


Figure 3

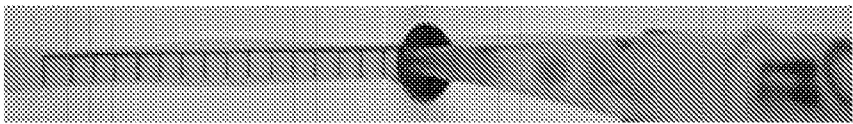
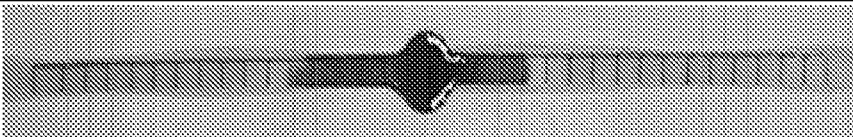
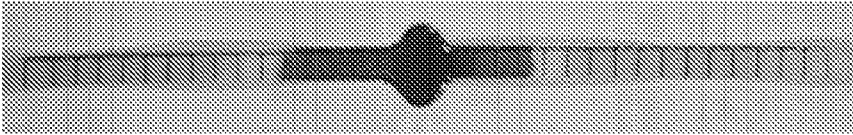
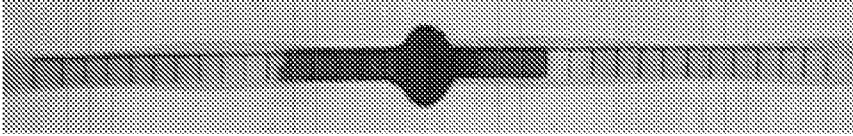

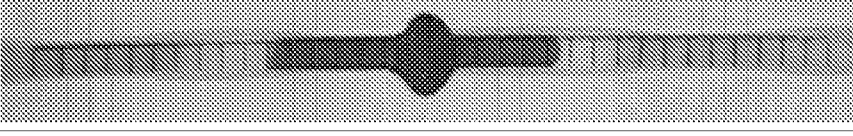
Time, t (min)	AB+ Blood wicking on Anti-A (1.0x) active paper
0.0	
1.0	
2.0	
3.0	
4.0	
5.0	

Figure 4

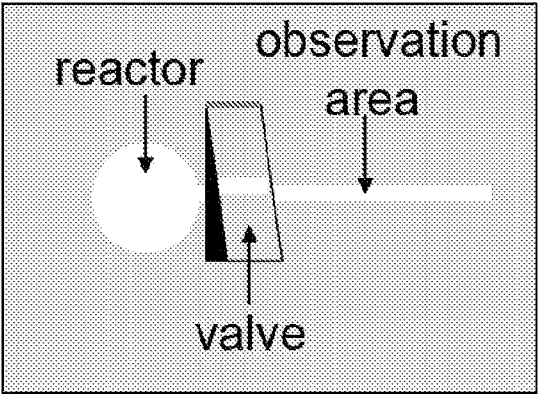


Figure 5

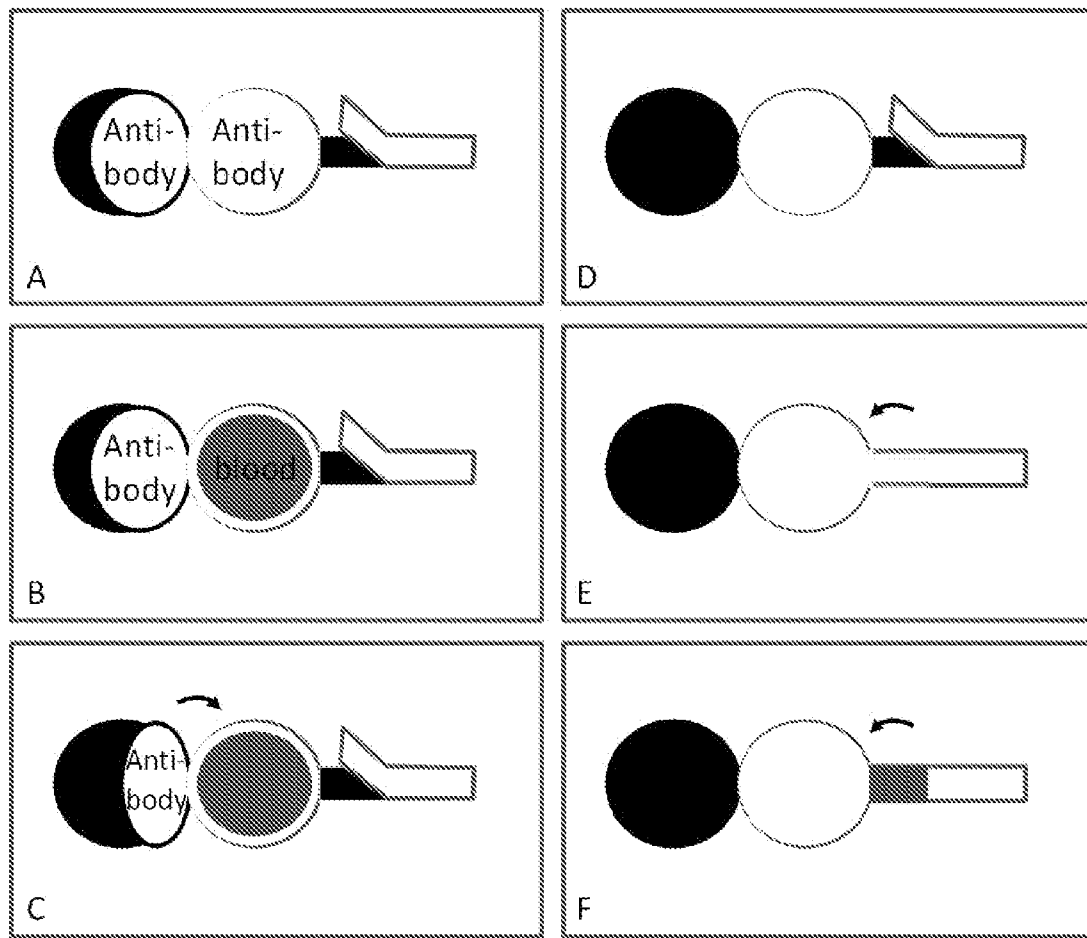
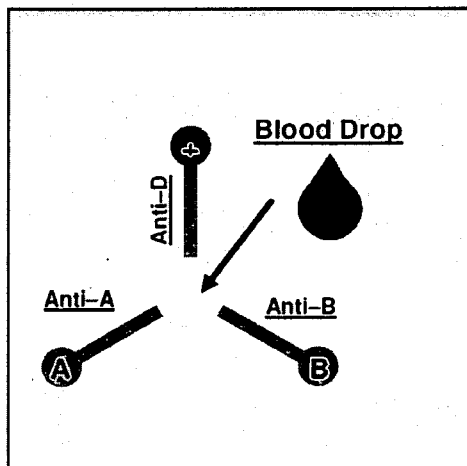
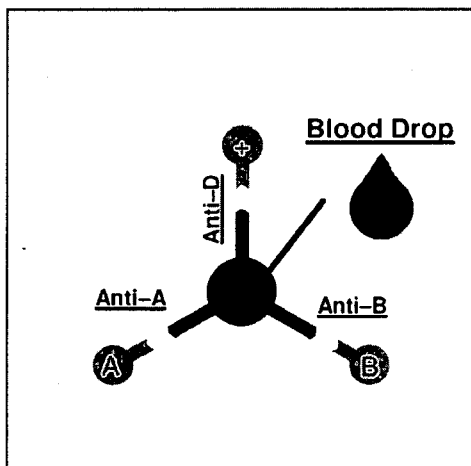


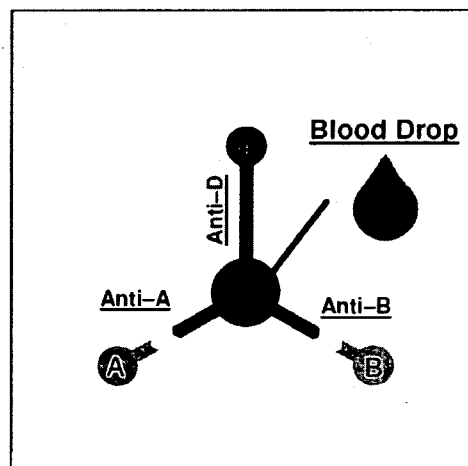
Figure 6



(a) Paper based (ABO) blood type detection device



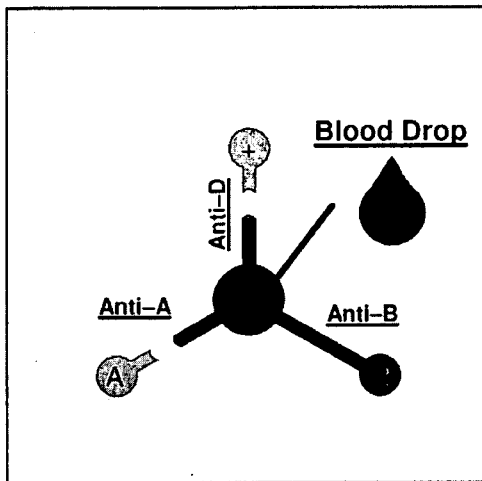
(b) Detection of AB+ blood



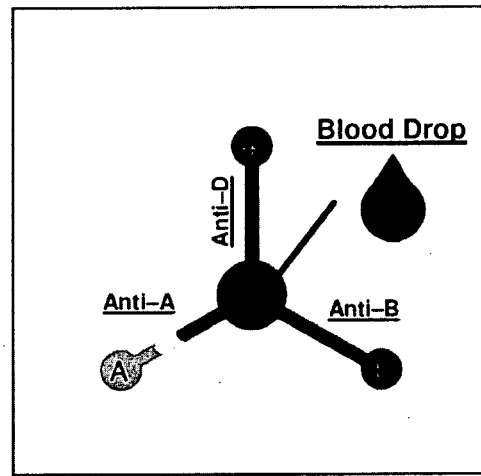
(c) Detection of AB- blood

Figure 7

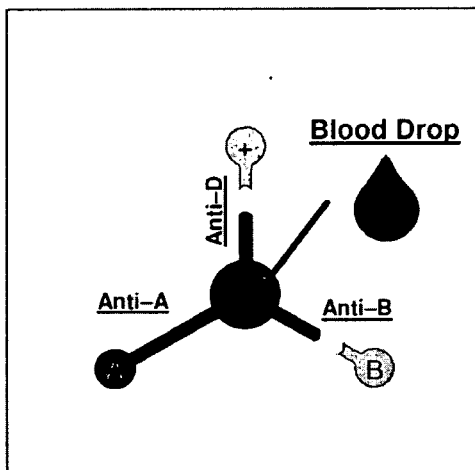
Figure 7 (cont.)



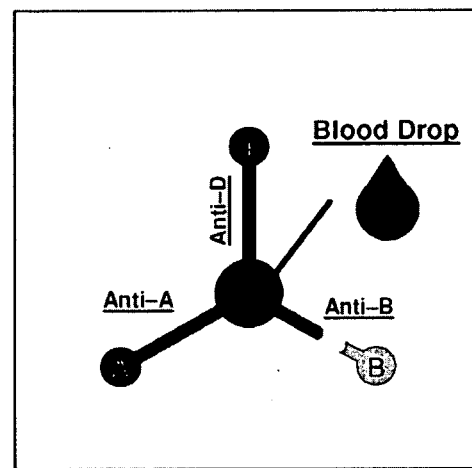
(d) Detection of A+ blood



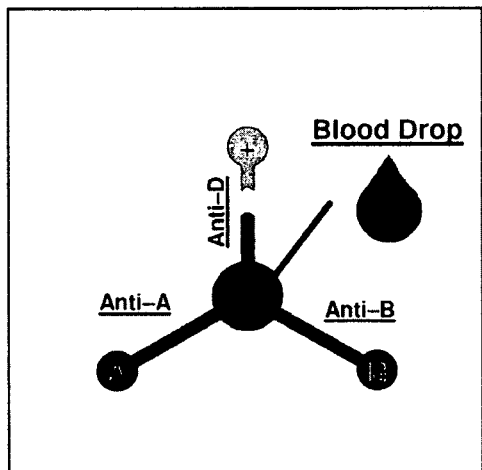
(e) Detection of A- blood



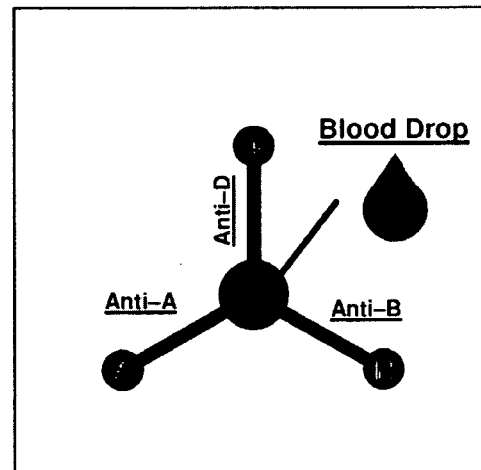
(f) Detection of B+ blood



(g) Detection of B- blood



(h) Detection of O+ blood



(i) Detection of O- blood

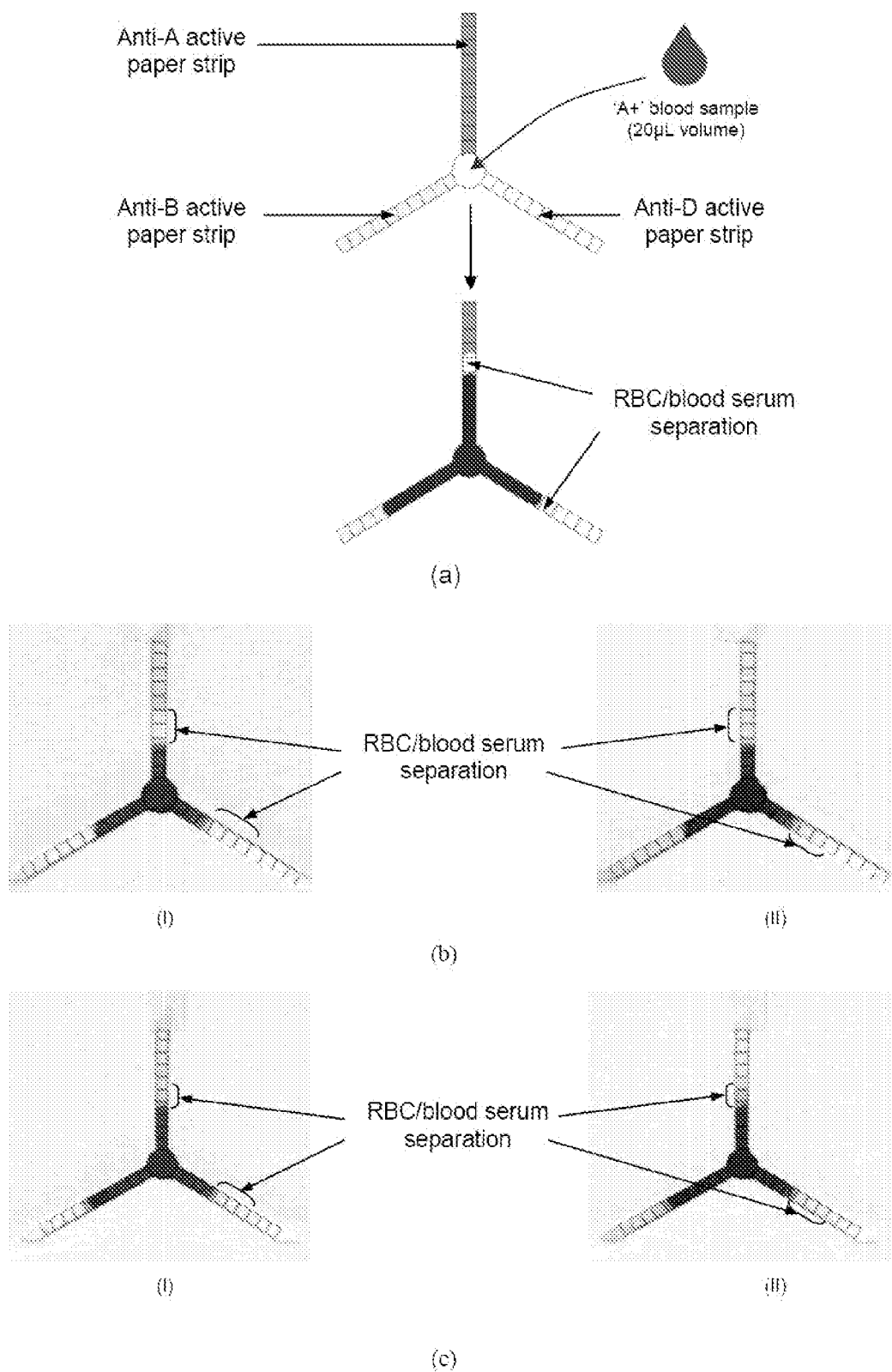


Figure 8